UNIVERSITY OF CALIFORNIA,
IRVINE

Stereoselective Strategies for the Construction of Cyclic Peptides, Depsipeptides, Sugars, and Alkenes

DISSERTATION

submitted in partial satisfaction of the requirements
for the degree of

DOCTOR OF PHILOSOPHY

in Chemistry

by

Diane Nguyen Le

Dissertation Committee:
Professor Vy M. Dong, Chair
Professor Larry E. Overman
Professor Christopher D. Vanderwal

2017

DEDICATION

To

my family and friends

in recognition of their steadfast love, patience, and support

TABLE OF CONTENTS

LIST OF FIGURES……v

LIST OF TABLES……viii

ACKNOWLEDGMENTS……x

CURRICULUM VITAE……xii

ABSTRACT OF THE DISSERTATION……xv

CHAPTER 1: Construction of Cyclic Peptides using Dehydrophenylalanine as a Traceless Turn Inducer……1

1.1 Application of Dehydrophenylalanine as a Turn Inducer in the Synthesis of Dichotomin E

1.1.1 Introduction……1

1.1.2 Retrosynthetic Analysis of Dichotomin E……3

1.1.3 Synthesis of Cyclic Dehydropeptides……4

1.1.4 Macrocyclization to Form Cyclic Dehydropeptides……5

1.1.5 Hydrogenation of Cyclic Dehydropeptides……6

1.1.6 Mechanistic Studies of Dehydrophenylalanine……7

1.1.7 Conclusion……11

1.2 Molecular Recognition of Peptides in Rh-Catalyzed Hydrogenation: Evidence for a Unidirectional Reduction

1.2.1 Introduction……12

1.2.2 Synthesis of Cyclic Dehydropeptides……14

1.2.3 Diastereoselective Hydrogenation of Cyclic Dehydropeptides……15

1.2.4 Mechanistic Support for a Unidirectional Reduction……17

1.2.5 Conclusion……22

1.3 Experimental Data

1.3.1 Experimental Details for Application of Dehydrophenylalanine as a Turn Inducer in the Synthesis of Dichotomin E……23

1.3.2 Experimental Details for Molecular Recognition of Peptides in Rh-Catalyzed Hydrogenation: Evidence for a Unidirectional Reduction……58

1.3.3 NMR Spectra……101

CHAPTER 2: Enantioselective, Rh(I)-Catalyzed Intermolecular Hydroacylation of *α*-Ketoamides……161

2.1 Rh(I)-Catalyzed Intermolecular Hydroacylation of *α*-Ketoamides

2.1.1 Introduction……161

2.1.2 Development of Rh(I)-Catalyzed Intermolecular Hydroacylation…164

2.1.3 Substrate Scope Evaluation……165

2.1.4 Mechanistic Investigation of Intermolecular Hydroacylation……168

2.1.5 Conclusion……171

2.2 Experimental Data

2.2.1 Experimental Details……171

2.2.2 NMR Spectra……187
2.2.3 Chiral HPLC Data……200
CHAPTER 3: Regioselective Functionalization of Carbohydrates……209
3.1 Cu(II)-Catalyzed Regioselective Functionalization of Monosaccharides
3.1.1 Introduction……209
3.1.2 Development of Cu(II)-Catalyzed Regioselective Functionalization……211
3.1.3 Expansion of Methodology to Furanosides……214
3.1.4 Expansion of Methodology to Regioselective Alkylation……219
3.1.5 Conclusion……221
3.2 Experimental Data
3.2.1 Experimental Details……221
3.2.2 NMR Spectra……229
CHAPTER 4: Approach to Stereodefined All-Carbon Tetrasubstituted Alkenes Mediated by Lithium Hexamethyldisilazide……235
4.1 Synthesis of All-Carbon Tetrasubstituted Alkenes Mediated by Lithium Hexamethyldisilazide
4.1.1 Introduction……235
4.1.2 Development of Stereoselective Enolate Formation and Tosylation……238
4.1.3 Substrate Scope Evaluation……240
4.1.4 Stereospecific Suzuki-Miyaura Cross-Coupling……243
4.1.5 Conclusion……244
4.2 Experimental Data
4.2.1 Experimental Details……244
4.2.2 NMR Spectra……257

REFERENCES……282

LIST OF FIGURES

Page

Figure 1.1 Cyclic peptide therapeutics……1

Figure 1.2 Proline as turn inducer in cyclic peptide synthesis……...2

Figure 1.3 a) Crystal structure of tetrapeptide containing dehydrophenylalanine. b) Proposed strategy using dehydrophenylalanine as a traceless turn inducer……..……..3

Figure 1.4 Synthesis of unsaturated pentapeptide **1.3**……4

Figure 1.5 Effect of dehydroamino acid on macrocyclization. (n = number of dehydroamino acid residues)……..…6

Figure 1.6 Asymmetric hydrogenation affords dichotomin E……7

Figure 1.7 CD spectra of pentapeptides **1.11**, **1.3**, and **1.2**……..……8

Figure 1.8 Minimized energy conformation **1.15** of unsaturated peptide **1.3** consistent with NMR analysis……9

Figure 1.9 Temperature coefficients (Δδ/ΔT) of unsaturated pentapeptide **1.3** and saturated pentapeptide **1.11**……...10

Figure 1.10 Mimicking features of the ribosome using a simplified model system……13

Figure 1.11 a) Solid phase peptide synthesis. b) Modified version Bergmann's peptide synthesis……14

Figure 1.12 Synthesis of linear pentapeptide **1.19**……...15

Figure 1.13 Hydrogenation of cyclic dehydropeptides……16

Figure 1.14 Mechanistic support for unidirectional hydrogenation……17

.

Figure 1.15 Transition structures **1.26$_a$‡** for *anti* (left) and **1.26$_s$‡** for *syn* (right) hydrogenation at site ΔPhe$_2$. Non-reacting hydrogens have been hidden and phenyls on the ligand are shown transparent for clarity……19

Figure 1.16 Hydrogen bonding in pro-*anti* **1R2S3R^{TS}** (left) and pro-*syn* **1R2S3S^{TS}** (right)……..20

Figure 1.17 Hydrogen bonding in pro-*syn* **1R2S3R4*R*^{TS}** (left) and pro-*anti* **1R2S3R4S^{TS}** (right)……20

Figure 1.18 Synthesis of linear pentapeptide **1.12**……...34

Figure 1.19 Synthesis of linear precursor **S14**……..39

Figure 1.20 ^{1}H NMR (DMSO–*d*^{6}, 298 K) of synthetic sample of dichotomin E made via SPPS……...51

Figure 1.21 ^{1}H NMR (DMSO–*d*^{6}, 298 K) of synthetic sample of dichotomin E made via hydrogenation……..……..51

Figure 1.22 ^{1}H NMR spectrum (Pyr–*d*^{5}, 298 K) of synthetic sample of dichotomin E after debenzylation spiked with authentic material…….55

Figure 1.23 Variable temperature data comparing tyrosine N–H for unsaturated peptide **1.3** and saturated peptide **1.11**……..……56

Figure 1.24 Variable temperature data comparing internal alanine N–H for unsaturated peptide **1.3** and saturated peptide **1.11**……..57

Figure 1.25 Variable temperature data comparing phenylalanine N–H for unsaturated peptide **1.3** and saturated peptide **1.11**.....57

Figure 1.26 Variable temperature data comparing terminal alanine N–H for unsaturated peptide **1.3** and saturated peptide **1.11**……...58

Figure 1.27 ^{19}F-NMR after Pd/C hydrogenation……....96

Figure 1.28 ^{1}H-NMR of cyclic pentapeptide **1.27** after hydrogenation using (*R,R',S,S'*)-Duanphos……99

Figure 1.29 ^{1}H-NMR of cyclic pentapeptide **S29** made via SPPS……99

Figure 2.1 Undesired decarbonylation pathway for hydroacylation……162

Figure 2.2 Ketone hydroacylation affords medium sized rings……162

Figure 2.3 Design of a transition metal-catalyzed hydroacylation……...164

Figure 2.4 a) Plot of initial rates (k_{obs}) with respect to [α-ketoamide **3d**] showing first order dependence. b) Plot of initial rates (k_{obs}) with respect to [aldehyde **2d**] showing first order dependence……169

Figure 2.5 Plot of initial rates (k_{obs}) with respect to [catalyst] showing second order dependence……..…….169

Figure 2.6 Kinetic isotope effect study using method of initial rates……...170

Figure 2.7 Proposed catalytic cycle……..171

Figure 2.8 Plot of initial rates with various aldehyde concentrations…….....183

Figure 2.9 Plot of initial rates with various ketone concentrations. (An induction period is observed when a large excess of ketone **3d** was used (orange line, Figure 2.9). This data was not used in determination of the kinetic order)…….184

Figure 2.10 Plot of initial rates with various catalyst concentrations……185

Figure 3.1 Catalytic advances to functionalize carbohydrate derivatives……..209

Figure 3.2 Inspiration from lectin……..210

Figure 3.3 Proposed ligand-controlled site-selective binding with Cu(II) Complexes…….211

Figure 3.4 Copper(II) activation of *cis*-diol motifs……...214

Figure 3.5 Interconversion between C2 and C3 endo……...218

Figure 3.6 Site selective alkylation of carbohydrate derivatives……..220

Figure 3.7 Application of Sr-catalyzed benzylation and efforts towards building block synthesis…….220

Figure 4.1 Synthesizing tetrasubstituted alkenes……..236

Figure 4.2 Drug therapeutics containing all-carbon tetrasubstituted alkenes……236

Figure 4.3 Synthetic route toward GDC-0810…….237

Figure 4.4 Lithium enolates using LiHMDS and trialkylamine additives…….238

Figure 4.5 Proposed route to all-carbon tetrasubstituted alkenes……...238

LIST OF TABLES

Page

Table 1.1 Subjecting synthesized intermediates to hydrogenation conditions……..18

Table 1.2 ^{1}H NMR data for dichotomin E, cyclo(Gly-Tyr-Ala$_1$-Phe-Ala$_2$)…….49

Table 1.3 ^{13}C NMR data for dichotomin E, cyclo(Gly-Tyr-Ala$_1$-Phe-Ala$_2$)……..….50

Table 1.4 Variable temperature data for unsaturated pentapeptide **1.3**……..……56

Table 1.5 Variable temperature data for saturated pentapeptide **1.11**……..…..56

Table 1.6 Ligand evaluation……..….97

Table 2.1 New Josiphos ligand enables high reactivity and enantioselectivity……165

Table 2.2 Substrate scope of non-chelating aldehydes with *α*-ketoamides…….166

Table 2.3 Substrate scope of non-chelating aldehydes with *α*-ketomorpholine amides……168

Table 3.1 Selective acylation of *α*-glucopyranosides……...212

Table 3.2 Substrate scope evaluation for selective acylation of *α*-glucopyranosides……..213

Table 3.3 Benzoylation of β-ribofuranoside **5**……215

Table 3.4 Copper(II)-catalyzed regioselective tosylation of β-ribofuranoside **5**…...215

Table 3.5 Copper(II)-catalyzed tosylation of β-ribofuranoside **5** using various sulfonyl chloride……216

Table 3.6 Ligand-controlled switch in regioselectivity using copper(II) catalysis….217

Table 3.7 Switch in regioselectivity using Ca(OTf)$_2$……..218

Table 4.1 Reaction optimization……..239

Table 4.2 Optimizing base equivalence……240

Table 4.3 Substrate scope evaluation with variation at R$_1$……..241

Table 4.4 Substrate scope evaluation with variation at R$_2$……..242

Table 4.5 Substrate scope evaluation with variation at R_3……..243

Table 4.6 Stereospecific Suzuki-Miyaura cross-coupling…..……..244

ACKNOWLEDGMENTS

I would like to express my deepest gratitude and appreciation to my advisor, Professor Vy Dong for all the support she has given me over the last five years. Thank you taking me in as a graduate student and giving me the opportunity to grow as a scientist and individual as a member of your lab. Thank you for always supporting me, giving me opportunities, and pushing me to improve myself in every way possible. I would also like to extend my sincere gratitude to Wilmer Alkhas. Thank you for everything you have done for me. Both you and Vy have been there for me in so many ways over the course of my graduate career.

I would like to thank my committee members, Professor Larry Overman and Professor Chris Vanderwal for their time and valuable insight into my research. I would also like to thank Professor Warren Wood for inspiring me to pursue a degree in organic chemistry and for enabling me to do undergraduate research.

In addition, I would also like to thank all the past and current members of the Dong Research Group. My teamily. It's been the greatest honor to be able to do chemistry alongside each one of you. Thank you for your unwavering support for me, especially in the final stretch of my graduate studies. I will cherish all the memories we had with each other – from unlimited super soakings, hot pot parties, and Friday night activities. I will sincerely miss everyone, but I know our paths will cross again in the future. I would also like to extend a special shout out to Daniel Kim, Faben Cruz, Alexander Lu, and Dr. Xiaohui Yang for taking time to edit chapters of my thesis.

Furthermore, I would like to thank the National Science Foundation for a Graduate Research Fellowship and the U.S. Department of Education for a GAANN fellowship. I

also thank the American Chemical Society for permission to include portions of Chapter 1, 2, and 4 and John Wiley & Sons for permission to include portions of Chapter 3 in my dissertation.

Lastly, I would like to thank my biggest supporters in life. Thank you to my sister and brother for putting up with me and for always being there for me. Thank you to my parents for their love, encouragement, and support for me in this entire journey. I know you both have sacrificed a lot for me to get to the point where I am today.

CURRICULUM VITAE

DIANE NGUYEN LE

RESEARCH EXPERIENCE

University of California, Irvine (Irvine, CA)
Ph.D. Organic Chemistry **2012-2017**
Research Advisor: Prof. Vy. M. Dong
Stereoselective strategies for the construction of cyclic peptides, depsipeptides, sugars, and alkenes

Genentech (South San Francisco, CA)
Summer Internship **2016**
Research Advisors: Dr. Andrew McClory and Dr. Haiming Zhang
Developing stereoselective methods in the Small Molecule Process Chemistry department

University of Portland (Portland, OR)
B.S. Chemistry, Magna Cum Laude **2008-2012**
Research Advisor: Prof. Warren. J. L. Wood
Synthesis of bioactive sultam thioureas against West Nile Virus

AWARDS

Intern Day Poster Prize – Runner Up, *Genentech*	**2017**
NSF Graduate Research Fellowship, *UC Irvine*	**2013–2016**
GAANN (Graduate Assistance in Areas of National Need) Fellowship, *UC Irvine*	**2012–2013**
William and Lavina Wilson Award in Chemistry, *UPortland*	**2011–2012**
Walter J. Stott Endowed Scholarship, *UPortland*	**2011–2012**
C.R.C Freshman Chemistry Achievement Award, *UPortland*	**2008–2009**
Dean's List, *UPortland*	**2008–2012**
President's Scholarship, *UPortland*	**2008–2012**

TEACHING EXPERIENCE

Department of Chemistry, University of California, Irvine
Teaching Assistant – CHM 51C – Organic Chemistry Lecture **2017**
Taught discussion sections and gave additional problem sets through a peer-led learning approach

Department of Chemistry, University of California, Irvine
Teaching Assistant – CHM 51LB/M52LB/H52LB/ – General/ Honors/Majors Organic Chemistry Laboratory **2013, 2017**
Instructed organic chemistry laboratory designed for chemistry majors and taught basic synthesis, purification, and separation techniques

Department of Chemistry, University of Portland
Teaching Assistant – CHM 207/208/325/326 – General and Organic Chemistry Lecture **2009–2012**
Taught discussion sections and gave additional problem sets through a peer-led learning approach

Teaching Assistant – CHM 278/375/376/379 – General, Organic, and Analytical Laboratory **2009–2012**

Aided in instructing chemistry laboratories and demonstrating general laboratory techniques

Department of Biology, University of Portland
Teaching Assistant – BIO 206 – General Biology Laboratory **2009**
Taught discussion sections and gave additional problem sets through a peer-led learning approach

PUBLICATIONS

8. **Le, D. N.**; Hansen, E; Khan, H. A.; Kim, B.; Wiest, O.; Dong, V. M. (2017) Cyclic Peptide Synthesis by a Unidirectional Hydrogenation. *Submitted*

7. Li, B. X.; **Le, D. N.**; Mack, K. A.; McClory, A.; Lim, N.-K.; Cravillion, T.; Savage, S.; Han, C.; Collum, D. B.; Zhang, H.; Gosselin, F. (2017) Highly Stereoselective Synthesis of Tetrasubstituted Acyclic All-Carbon Olefins via Enol Tosylation and Suzuki-Miyaura Coupling. *Journal of the American Chemical Society*, **2017**, *139*, 10777.

6. Dong, V. M.; Kou, K. G. M.; **Le, D. N.** (2017) Transition-Metal Catalyzed Hydroacylation. *Organic Reactions*. *In Press.*

5. **Le, D. N.***; Riedel, J.*; Kozlyuk, N.; Martin, R. W.; Dong, V. M. (2017) Cyclizing Pentapeptides: Mechanism and Application of Dehydrophenylalanine as a Traceless Turn-Inducer. *Org. Lett.*, **2017**, *19*, 114.

4. Kou, K. G. M.; **Le, D. N.**; Dong, V. M. (2014) Rh(I)-Catalyzed Intermolecular Hydroacylation: Enantioselective Cross-Coupling of Aldehydes and Ketoamides. *J. Am. Chem. Soc.*, **2014**, *136*, 9471.

3. Chen, I.-H., Kou, K. G. M.; **Le, D. N.**; Rathbun, C. M.; Dong, V. M. (2013) Ligand-Controlled Switch: Regioselective Functionalization of Carbohydrate Derivatives. *Chem. Eur. J.*, **2014**, *20*, 5013.

2. Li, V.; **Le, D. N.**; Valente, E. J.; Wood, W. J. L. (2012) Sultam Thioureas Synthesized via an Alternative Ring-Forming Reaction. *Synthetic Communications*, **2015**, *45*, 1055.

1. Feeny, R. M.; **Le, D. N.**; Parks, J. W.; Epstein, M. G.; Pagano, J. V.; Abbene, A. C.; Graham, E. B.; Farrell, J. R.; McGuire, J. R.; Zoellner, R. W.; Valente, E. J.; Barklis, E.; Wood, W. J. L. (2012) Sultam thioureas: Synthesis and antiviral activity against West Nile virus. *Synlett*, **2012**, *2*, 301.

PRESENTATIONS

Le, D. N.; Dong, V. M. (2017) Molecular recognition of peptides in Rh-catalyzed hydrogenation: Evidence for a Unidirectional Reduction. *Moving Molecules from the Academic Lab to the Clinic*; May 25; Irvine, CA. *Poster presentation.*

Le, D. N.; Dong, V. M. (2017) Molecular recognition of peptides in Rh-catalyzed hydrogenation: Evidence for a Unidirectional Reduction. *UC Chemical Symposium*; March 28; Arrowhead, CA. *Poster presentation.*

Le, D. N.; Riedel, J.; Dong, V. M. (2016) Dehydrophenylalanine as a Traceless Turn Inducer. *Gordon Research Conference: Organic Reactions and Processes*; July 18; Easton, MA. *Poster presentation.*

Le, D. N.; Riedel, J.; Zhu, Y.; Dong, V. M. (2016) Dehydrophenylalanine as a Traceless Turn Inducer. *ISACS19: Challenges in Organic Chemistry*; March 22; Irvine, CA. *Poster presentation.*

Le, D. N.; Kou, K. G. M.; Dong, V. M. (2014) Rh(I)-Catalyzed Enantioselective Ketone Hydroacylation of Ketoamides. *Boston Women in Chemistry Symposium*; October 4; Cambridge, MA. *Poster presentation.*

Le, D. N.; Kou, K. G. M.; Chen, I.-H.; Dong, V. M. (2013) Regioselective functionalization of furanoside derivatives through transition metal catalysis. *246th American Chemical Society (ACS) National Meeting*; September 10; Indianapolis, IN. *Poster presentation.*

Le, D. N.; Feeny, R. M.; Parks, J. W.; Epstein, M. G.; Pagano, J. V.; Abbene, A. C.; Graham, E. B.; Farrell, J. R.; McGuire, J. R.; Zoellner, R. W.; Valente, E. J.; Barklis, E.; Wood, W. J. L (2012) Sultam thioureas: Synthesis and antiviral activity against West Nile virus. *243rd American Chemical Society (ACS) National Meeting*; March 28; San Diego, CA. *Poster presentation.*

ABSTRACT OF THE DISSERTATION

Stereoselective Strategies for the Construction of Cyclic Peptides, Depsipeptides, Sugars, and Alkenes

By

Diane Nguyen Le

Doctor of Philosophy in Chemistry

University of California, Irvine, 2017

Professor Vy M. Dong, Chair

Cyclic peptides have attracted attention due to their promising metabolic stability, conformational rigidity, and potential to mimic protein−protein interactions. We describe a method to access cyclic peptides using dehydrophenylalanine as a traceless turn inducer in the total synthesis of dichotomin E. The enamide facilitates ring-closing at high concentrations, and Rh-catalyzed hydrogenation of the unsaturated cyclic peptide results in selective formation of the natural product or its epimer, depending on our choice of phosphine ligand.

In addition, we demonstrate how a simple amino acid sequence can be recognized by a Rh-catalyst in a process which initiates the sequential reduction of cyclic dehydropeptides. Molecular recognition of amino acid sequences plays a key role in enzyme-substrate specificity, the regulation of genes, and the treatment of diseases. While critical in biological processes, molecular recognition of amino acids using a transition metal catalyst also holds great promise in organic synthesis. We report

experimental and theoretical evidence to support the unidirectional hydrogenation toward the synthesis of cyclic peptides.

Like their peptide counterparts, depsipeptides are valuable therapeutic drug targets. These peptides are characterized by a combination of ester and amide linkages. To this end, we report the first enantioselective, intermolecular ketone hydroacylation of *α*-ketoamides with simple aldehydes for the construction of *α*-acyloxyamides in high yields and enantioselectivities.

Carbohydrates find importance in cellular communication, structural recognition, and cancer treatment. Although many of these oligosaccharides are generated through chemical synthesis, the presence of multiple hydroxyl sites in the carbohydrate presents a synthetic challenge. Toward a solution to this challenge, we have achieved a Cu-catalyzed regioselective functionalization of monosaccharides.

Constructing stereodefined alkenes is a longstanding challenge in organic synthesis. While methods to di- and trisubstituted alkenes have been reported, general protocols toward the synthesis of tetrasubstituted alkenes are underdeveloped. We describe a method toward the synthesis of stereodefined all-carbon tetrasubstituted alkenes from readily accessible ketones, first by a stereoselective enol tosylation followed by a Pd-catalyzed Suzuki-Miyaura cross coupling.

CHAPTER 1 – Construction of Cyclic Peptides using Dehydrophenylalanine as a Traceless Turn Inducer

1.1 Application of Dehydrophenylalanine as a Turn Inducer in the Synthesis of Dichotomin E*

1.1.1 Introduction

Naturally occurring cyclic peptides have inspired the invention of strategies[1-5] for organic synthesis and therapeutics for use as antibiotics[6-8] and immunosuppressants.[9] In comparison to their linear counterparts, these cyclic structures show enhanced metabolic stability,[10] conformational rigidity,[11] and potential to mimic protein-protein interactions (Figure 1.1).[12] While significant progress has been made in the construction of relatively large cyclic peptides, the construction of smaller peptides (*i.e.*, those containing five or fewer amino acids) remains a challenge.[13-17] In addition, cyclizing peptides at high concentrations on an industrial scale is important,[18] thus a turn-inducer is desirable to ensure an efficient and economically feasible process.[19,20] Specific amino acids (*e.g.*, proline, pseudoprolines, D-amino acids, and *N*-methylated amino acids) have been

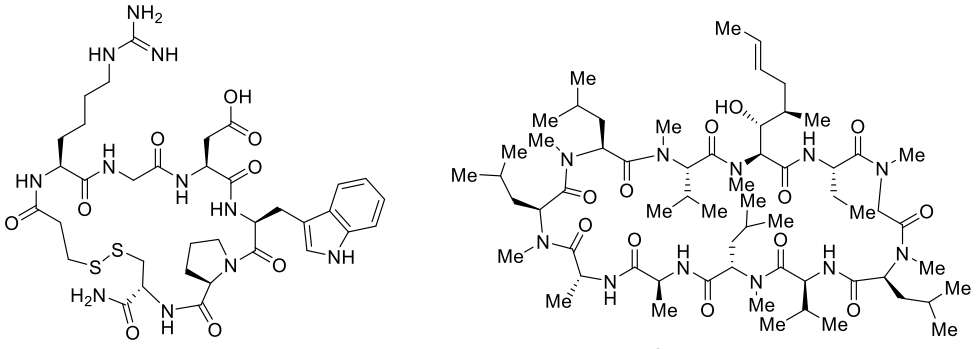

Integrilin
·Isolated from Sistrurus miliarius barbouri
·Anti-platelet drug
·7 amino acids

Cyclosporine A
·Isolated from Tolypocladium inflatum
·Immunosuppressant
·11 amino acids

Figure 1.1 Cyclic peptide therapeutics

* Reproduced in part with permission from Le, D. N.*; Riedel, J.*; Kozlyuk, N.; Martin, R. W.; Dong, V. M. *Org. Lett.* **2017**, *19*, 114. Copyright 2017 American Chemical Society

identified as turn-inducers that can be incorporated into a linear precursor to facilitate macrocyclizations.[21-23]

For example, Mutter has used pseudoproline as a turn inducer in the synthesis of cyclic tripeptides (Figure 1.2). Pseudoprolines are masked threonine- or serine-type residues, which can be unveiled after macrocyclization upon treatment with acid. In addition to using two proline residues in the linear peptide sequence, macrocyclization occurred at various concentrations (0.001 – 0.1 M) using PyBOP in up to 85% yield.[24] Furthermore, Grubbs has used olefin metathesis to generate cyclic peptides mimicking the glutaredoxin active site. Using a proline turn inducer, ring-closing metathesis occurred to afford the desired cyclic peptide in 70% yield at 0.004 M concentration.[1] Despite these advances, the ring-closing of small peptides without such turn-inducers requires dilute concentrations due to competitive dimerization and epimerization.[25,26] Towards a more general solution to this challenge, we proposed the use of dehydroamino acids as *traceless* turn-inducers.

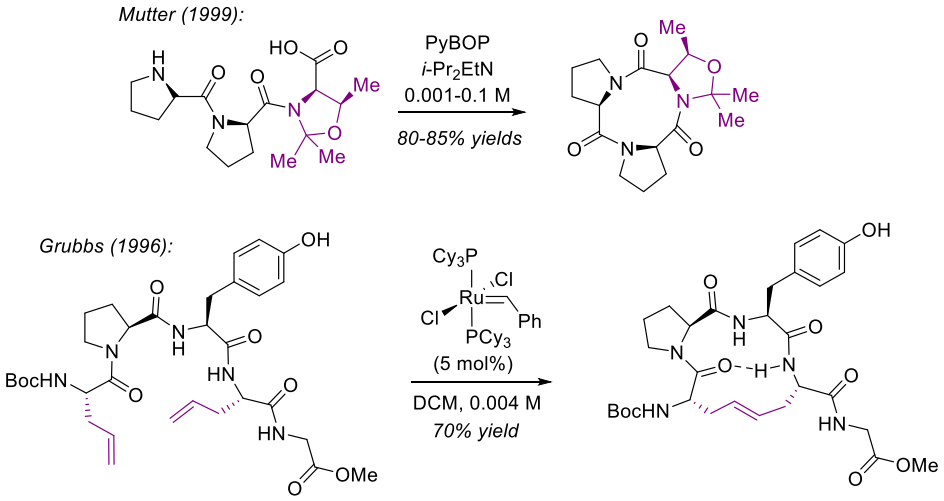

Figure 1.2 Proline as turn inducer in cyclic peptide synthesis

Dehydroamino acids modulate backbone conformations and produce folded structures.[27-30] The impact of dehydrophenylalanine on the conformation of small peptides has been studied extensively over the last decade.[31-34] For example, Singh has shown that dehydrophenylalanines can induce *β*-turns in a linear tetrapeptide on the basis of X-ray crystallography studies (Figure 1.3a).[35] The ability of dehydroamino acids to impart folded conformations has yet to be exploited for achieving efficient ring-closings to gain access to various cyclic peptides. We envisioned that this unsaturated moiety, which has been studied extensively in asymmetric hydrogenation, could serve as a versatile functional handle for further elaboration in the late-stage preparation of natural product derivatives.[36] Moreover, these unsaturated derivatives could serve as analogs in structure-activity relationship (SAR) studies or serve as potential epitope mimetics.[37,38]

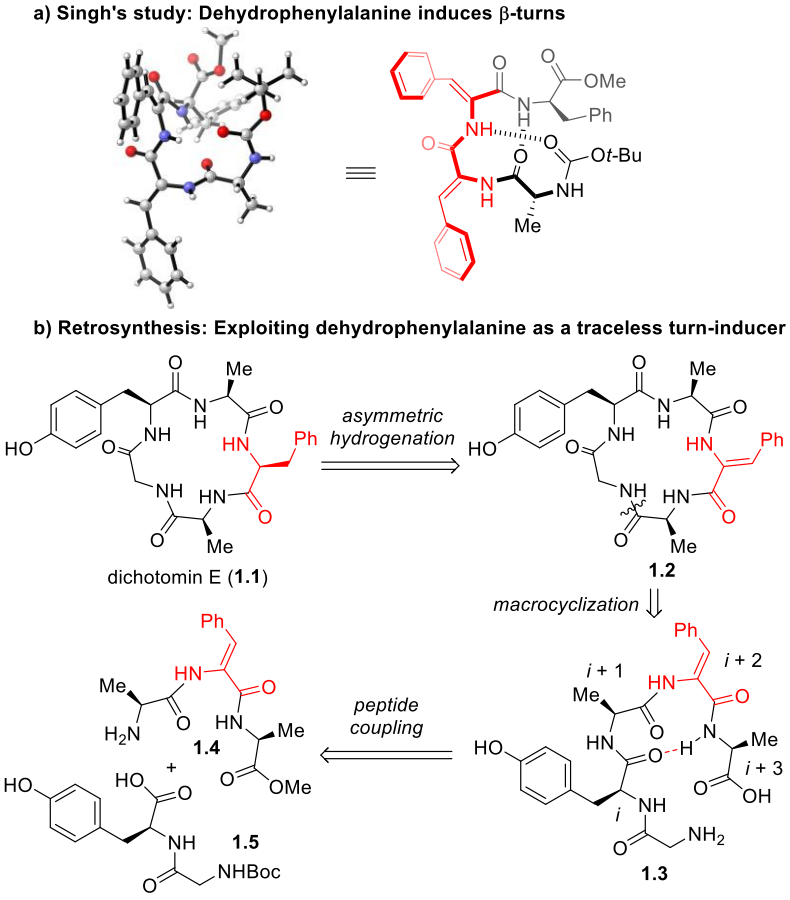

Figure 1.3 a) Crystal structure of tetrapeptide containing dehydrophenylalanine. b) Proposed strategy using dehydrophenylalanine as a traceless turn inducer

1.1.2 Retrosynthetic Analysis of Dichotomin E

We report the first use of dehydrophenylalanine as a traceless turn inducer via application in the synthesis of dichotomin E. Isolated from the chickweed plant, *Stellaria*

dichotoma, dichotomin E (**1.1**) is a cyclic peptide containing five amino acids with cell growth inhibitory activity against leukemia cells.[39] Our retrosynthetic analysis for construction of this small cyclic peptide is summarized in Figure 1.3b. First, we imagined that the natural product could be obtained from cyclic peptide **1.2**, containing a (*Z*)-dehydrophenylalanine,[40] by catalytic hydrogenation. In contrast to the incorporation of other turn-inducers, the dehydrophenylalanine can be easily unveiled to the L- or D- amino acid. Next, we chose to disconnect the glycine-alanine peptide bond to reveal the linear and unsaturated peptide **1.3**. We chose this disconnection to help favor an effective macrocyclization by placing the dehydrophenylalanine at the *i+2* position, where it was previously reported to induce a *β*-turn.[41] A similar disconnection was used in the previous synthesis of dichotomin E by Tam.[42] In general, the macrocyclizations are more favorable using glycine because it is a relatively unhindered nucleophile.[43]

1.1.3 Synthesis of Cyclic Dehydropeptides

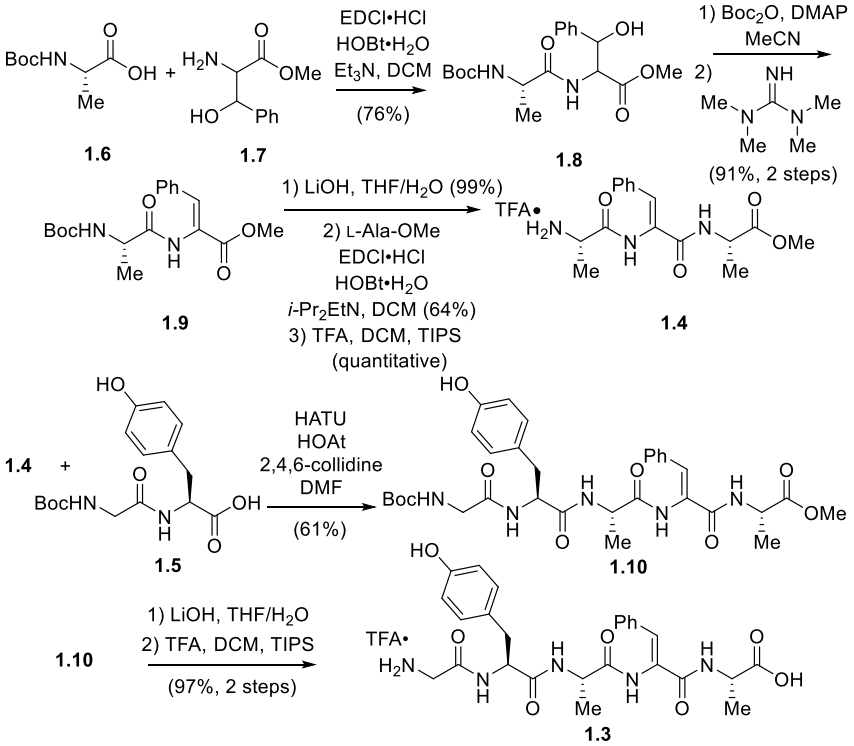

Figure 1.4 Synthesis of unsaturated pentapeptide **1.3**

With this retrosynthetic analysis in mind, we prepared unsaturated pentapeptide **1.3** (Figure 1.4). Boc-L-alanine **1.6** was coupled to DL-(β-OH)–Phe–OMe **1.7** to afford dipeptide **1.8** in 76% yield. Treatment of dipeptide **1.8** with Boc-anhydride and tetramethylguanidine afforded unsaturated dipeptide **1.9** in 91% yield.[44] Subjecting dipeptide **1.9** to hydrolysis, peptide coupling, and TFA deprotection, resulted in tripeptide **1.4** in 63% yield over two steps. Tripeptide **1.4** was then coupled to dipeptide **1.5** in 61% yield to afford pentapeptide **1.10**. After hydrolysis and Boc deprotection of pentapeptide **1.10**, unsaturated pentapeptide **1.3** was afforded in 97% yield over two steps. For comparison, we also prepared saturated linear peptide **1.11** in 64% yield using solid phase peptide synthesis (SPPS).

1.1.4 Macrocyclization to Form Cyclic Dehydropeptides

When saturated linear pentapeptide **1.11** was subjected to macrocyclization at 0.1 M, only 15% yield of dichotomin E (**1.1**) was obtained, with a 1.5:1 selectivity for the desired monomer over cyclodimer (Figure 1.5a). In stark contrast, treatment of unsaturated pentapeptide **1.3** under the same conditions resulted in formation of cyclic pentapeptide **1.2** in 74% yield, improved the selectivity to 39:1. Subsequently, cyclic pentapeptide **1.2** was isolated in 81% yield at 0.05 M (Figure 1.5b). In comparison to Tam's method, where a silver ion-assisted orthogonal cyclization at 0.001 M concentration afforded the macrolactam in 87% yield, our approach circumvents the need for high dilution by using *one-hundred times* less solvent in the macrocyclization.

Next, we prepared pentapeptide **1.12** bearing two-dehydroamino acids and subjected this linear precursor to ring-closing. Under the same cyclization conditions at 0.1 M concentration, cyclic pentapeptide **1.13** was isolated in 84% yield with 26:1

selectivity for the monomer over cyclodimer (cf Figure 1.5b and 1.5c). Together, these results demonstrate that dehydrophenylalanines act as turn-inducers that greatly favor macrocyclization even at high concentrations.

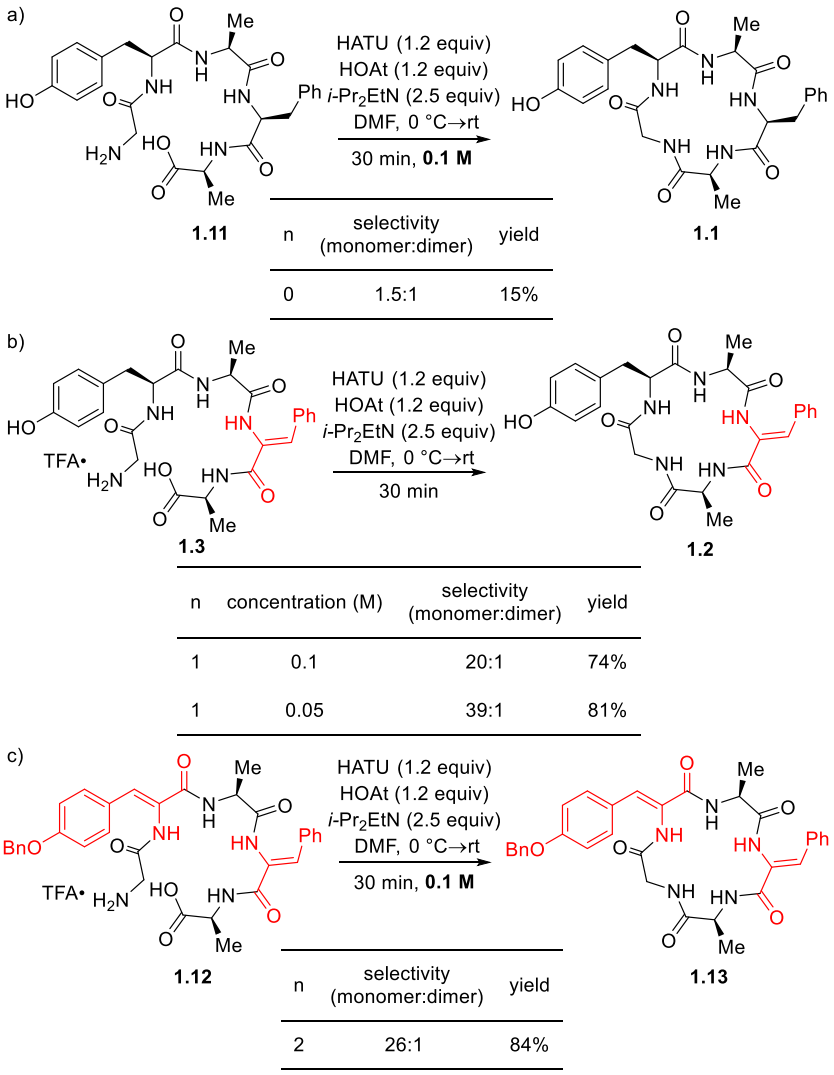

Figure 1.5 Effect of dehydroamino acid on macrocyclization. (n = number of dehydroamino acid residues)

1.1.5 Hydrogenation of Cyclic Dehydropeptides

With the unsaturated cyclic peptides **1.2** and **1.13** in hand, we applied hydrogenation to install the final stereocenters. Hydrogenation of cyclic peptide **1.2** using $Rh(cod)_2BF_4$ and achiral dppp ligand resulted in formation of an 8:1 mixture favoring

epimer **1.1'** of dichotomin E (eq 1). To overcome inherent substrate bias, we turned to asymmetric hydrogenation, which is commonly used in the synthesis of medicines in industry.[45] Zhang and coworkers previously reported the asymmetric hydrogenation of enamides using Rh(I)-catalyst and Duanphos ligand to afford the corresponding amide in 99% *ee*.[46] By using 5 mol% $Rh(cod)_2BF_4$ and 5 mol % (*S*,*S*',*R*,*R*')-Duanphos in THF under 30 atm of hydrogen, we were able to hydrogenate peptide **1.2** and obtain dichotomin E (**1.1**) in 96% yield and >95:5 *dr* (Figure 1.6). Of note, reduction of cyclic peptide **1.2** using (*R*,*R*',*S*,*S*')-Duanphos affords epimer **1.1'** in 82% yield and >95:5 dr. Cyclic peptide **1.13**, bearing two enamides, can also be transformed to dichotomin E by tandem asymmetric reduction followed by debenzylation.

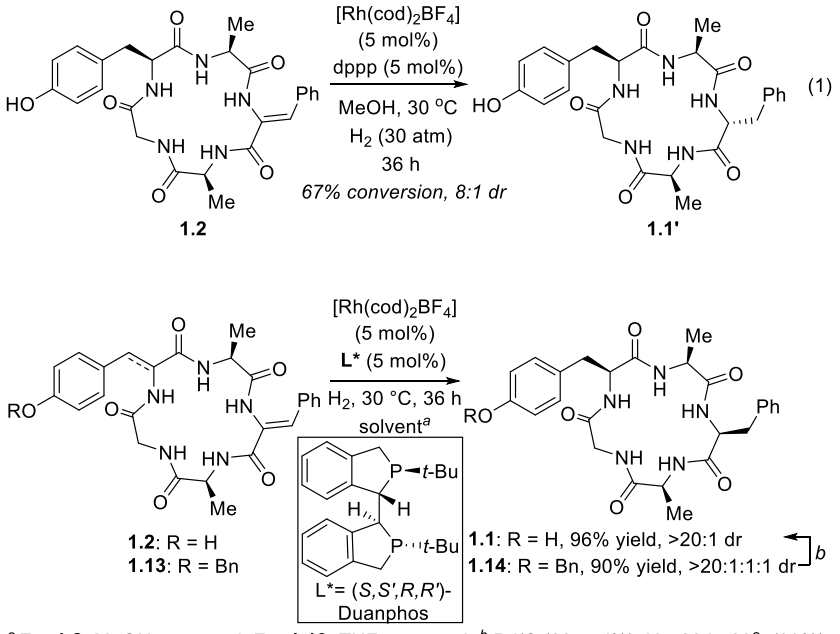

[a] For **1.2**, MeOH was used. For **1.13**, THF was used. [b] Pd/C (20 mol%), H_2, 28 h, 30°, (99%)

Figure 1.6 Asymmetric hydrogenation affords dichotomin E[a,b]

1.1.6 Mechanistic Studies of Dehydrophenylalanine

To better understand the mechanism of macrocyclization, Jan Riedel performed CD spectroscopy experiments for pentapeptides **1.11**, **1.3**, and **1.2** in MeOH (298 K) to

investigate the presence of secondary structure (Figure 1.7).[47] Uncyclized dehydropeptide **1.3** showed absorption patterns consistent with a cyclized structure, similar to cyclic dehydropeptide **1.2**. In contrast, uncyclized, saturated pentapeptide **1.11** showed no absorption patterns indicative of any secondary structural motif. The CD spectrum supports that the presence of dehydrophenylalanine has a pronounced effect on the secondary structure of uncyclized dehydropeptide **1.3**, which helps to facilitate macrocyclization.

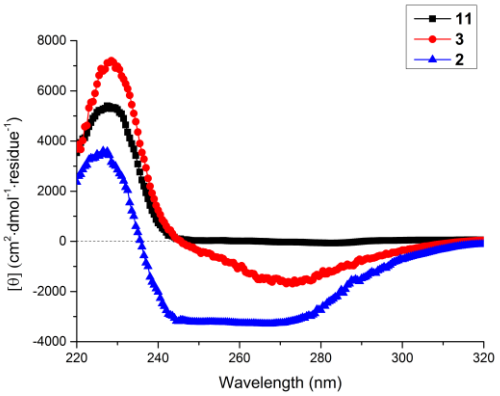

Figure 1.7 CD spectra of pentapeptides **1.11**, **1.3**, and **1.2**

In collaboration with Jan Riedel, Natalia Kozlyuk, and Professor Rachel Martin at UC Irvine, solution-state NMR and molecular modeling were used to elucidate the structure of unsaturated pentapeptide **1.3**. The ^{3}J-couplings for Tyr and two Ala residues were obtained from 2D ^{1}H *J*-resolved NMR spectra.[48] These couplings were used to calculate $H_NH\alpha$ φ dihedral angles via the Karplus relation.[49] Using these dihedral angle and 2D NOESY restraints, we performed molecular modeling studies with Maestro to obtain 20 low-energy conformations that were consistent with our experimental observations. These calculations support lowest energy structure **1.15** containing a left-handed alpha-turn, which is preorganized towards macrocyclization (Figure 1.8).

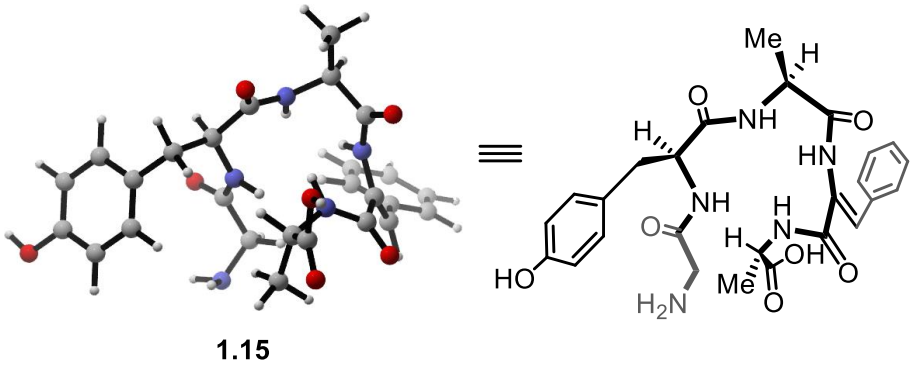

1.15

Figure 1.8 Energy minimized conformation **1.15** of unsaturated peptide **1.3** consistent with NMR analysis

We also investigated intramolecular H-bonding using the temperature coefficients of the N-H chemical shifts (Δδ/ΔT), which can be used as an indicator of intramolecular H-bonding as opposed to H-bonds to solvent.[50] A value of -0.0039 ppm/K was obtained for the internal alanine N–H in dehydropeptide **1.3**, in contrast to the value of -0.0052 ppm/K observed for saturated pentapeptide **1.11**. This difference suggests that there is dynamic intramolecular hydrogen bonding in dehydropeptide **1.3** but not in saturated pentapeptide **1.11**, consistent with the ensemble of structures predicted by the molecular modeling (Figure 1.9). Together, these results demonstrate that a single dehydrophenylalanine residue can induce a left-handed alpha turn.

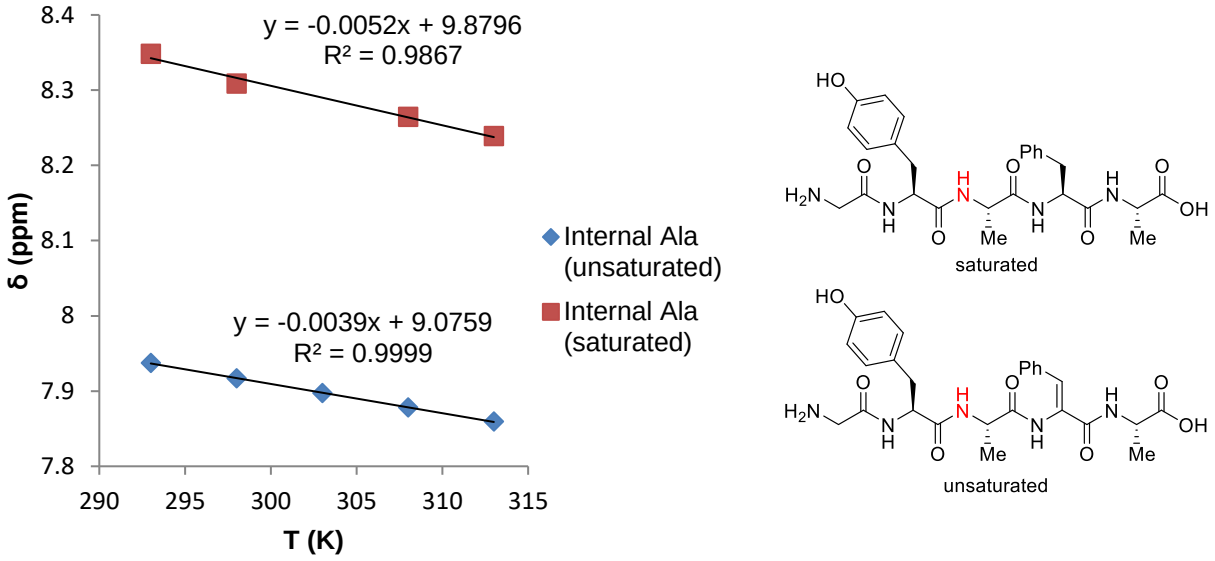

Figure 1.9 Temperature coefficients (Δδ/ΔT) of unsaturated pentapeptide **1.3** and saturated pentapeptide **1.11**

When we replaced the phenyl substituent with a cyclohexyl substituent in **1.3**, cyclic monomer formation was observed in a promising, yet less efficient 54% yield by ^{1}H NMR. This result suggests that the steric impact of the substituent influences cyclization. Given the higher yielding macrocyclizations we observed in Figure 1.5, conjugation between the phenyl substituent and helps promote ring-closing by increasing the steric impact of the phenyl group. Weiss and Lawrence *et al.* used dehydrophenylalanine as a β-breaker to study insulin and showed that extended conjugation of the aromatic π-electrons with the neighboring C=C and C=O electrons enforces a near-planarity.[51] The near-planar conformation of dehydrophenylalanine will result in a greater steric interaction between the phenyl group and the adjacent amide group, as shown in **1.15**, which ultimately restricts the ϕ–angle of the dehydroamino acid.[31] This restriction, through the increased $A_{1,3}$-strain, biases the *N* and the *C* termini towards cyclization. Interestingly, a peptide containing three consecutive dehydroalanine units has been shown to adopt an extended conformation, where all the amide groups show near-planarity.[52] This example

suggests that the steric interactions of the group at the *β*-carbon of the dehydroamino acid correlates to its ability to induce a turn.

1.1.7 Conclusion

In conclusion, we have demonstrated dehydrophenylalanine as an effective and traceless turn-inducer in the synthesis of dichotomin E. NMR analysis reveals that unsaturated pentapeptide **1.3** adopts a cyclic, preorganized structure. The enamide serves as a turn-inducer to facilitate ring-closing, without the need for high dilution. Moreover, it is a convenient functional handle for the late-stage construction of natural products and their derivatives. In SPPS, the overall yield is typically exceptional because each step in this linear approach is driven by exploiting excess reagents.[53] Combined with the need for dilute solvent conditions, the amount of waste generated in this traditional approach to cyclic peptide construction is significant. Our approach aims for a more efficient synthesis of cyclic peptides, especially on a large scale, while SPPS enables a rapid synthesis of peptide libraries on a small scale. Future studies in our laboratory are focused on better understanding (1) the scope and limitations of dehydroamino acids as turn-inducers for macrocyclization and (2) the mechanism of tandem hydrogenations in cyclic enamides. We expect that our simple, yet effective, strategy for ring-closing will be of use to chemists interested in accessing cyclic pentapeptides for use as biological probes and therapeutics.

1.2 Molecular Recognition of Peptides in Rh-Catalyzed Hydrogenation: Evidence for a Unidirectional Reduction

1.2.1 Introduction

Through the art of synthesis, chemists build simplified models to understand our world at the molecular level. Emulating the ribosome, a catalyst key to the central dogma of biology, represents an important and challenging endeavor.[54-56] The ribosome recognizes a specific start codon in the mRNA strand and catalyzes the sequential synthesis of a peptide in the *N* to *C* direction (Figure 1.10a). This flow of sequence-specific information is encoded by sets of nucleic acids.[57] In a pioneering study, Leigh and coworkers synthesized an artificial small-molecule machine that mimics certain aspects of the ribosome.[58] Leigh's machine features a stoichiometric amount of thiol that moves along the rotaxane to construct a hexapeptide in the *C* to *N* direction (Figure 1.10b). Through the elegant design of the mechanically-strained molecular machine, the peptide sequence is governed by the order of pre-installed amino acid building blocks on the rotaxane. Yet, an intriguing challenge in designing a chemical model for ribosomal peptide synthesis is the demonstration of a synthetic catalyst to identify an initial site for a sequential functionalization. Herein, we describe that catalytic amounts of a rhodium-salt can recognize information encoded in a macrocycle containing a sequence of prochiral units to create a cyclic peptide via hydrogenation with high levels of stereocontrol (Figure 1.10c). On the basis of combined experimental and theoretical studies, we provide evidence for a unique mechanism that involves unidirectional reduction to set four stereocenters around a macrocyclic ring. Thus, our ribosome-mimic builds a saturated peptide in the *C* to *N* direction. Our study provides a blueprint for using cascade catalysis [59] in building cyclic peptides.

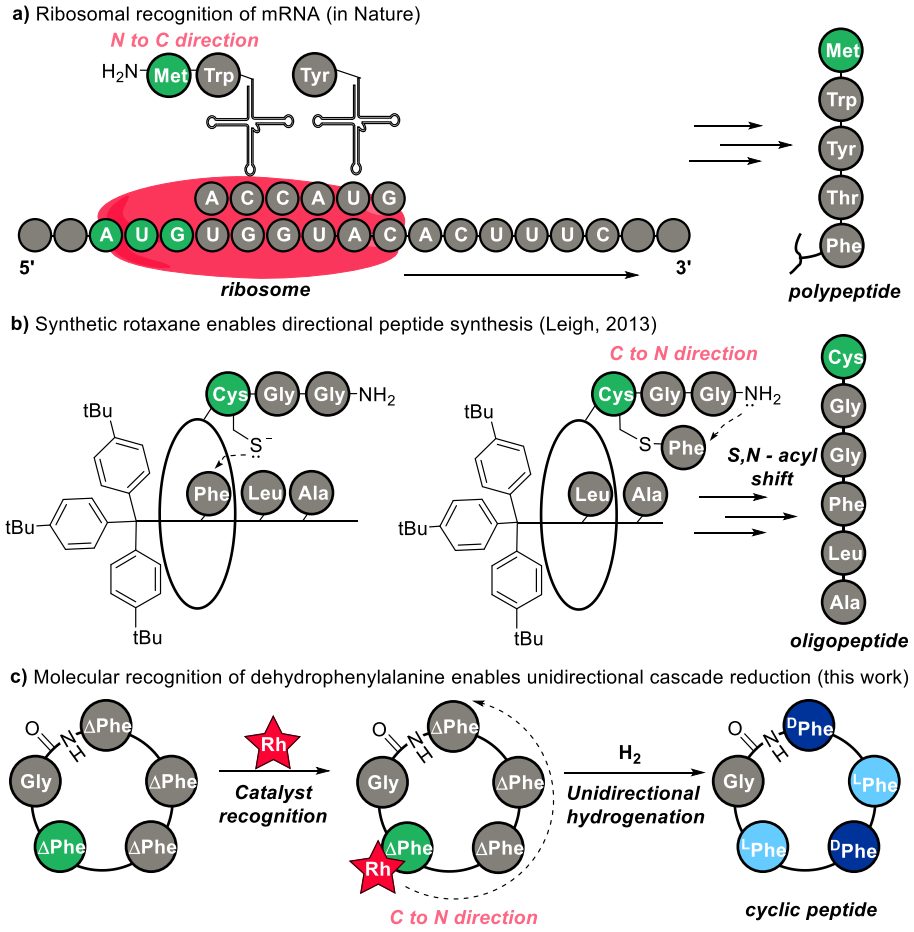

Figure 1.10 Mimicking features of the ribosome with a simplified model system

Cyclic peptides have attracted attention due to their enhanced metabolic stability,[10] conformational rigidity,[60] and potential to mimic protein−protein interactions.[61] As a result, these circular structures continue to inspire the invention of synthetic tools and strategies.[5] The classic approach relies on coupling chiral, enantiopure amino acid building blocks to generate a linear peptide prior to ring-closing.[62] However, valuable enantiopure linear peptides are often affected at the macrocyclization step, suffering from *C* terminal epimerization and competing oligomerization.[63] In contrast, we imagined first constructing a dehydropeptide using achiral building blocks. On the basis of previous studies, this linear dehydropeptide should readily ring-close to generate a macrocycle more efficiently than its saturated counterpart.[64] In addition to the advantage of efficient

ring-closing, a transition metal catalyst could be used to achieve a unidirectional cascade hydrogenation to furnish the requisite stereogenic centers in a single step.

1.2.2 Synthesis of Cyclic Dehydropeptides

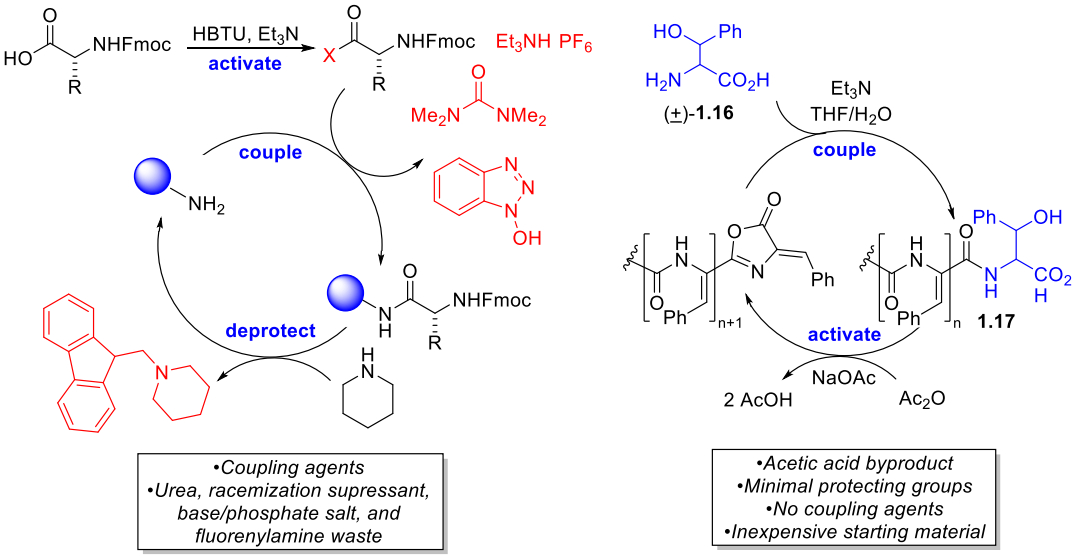

Figure 1.11 a) Solid phase peptide synthesis. b) Modified version Bergmann's peptide synthesis

In accordance with this blueprint, we prepared the linear pentapeptide **1.19** containing four dehydrophenylalanines (ΔPhe) from oxazolone **1.18** using a modified version of Bergmann's peptide synthesis.[65] In contrast to conventional solid phase peptide synthesis (Figure 1.11a), which uses excess of reagents and produces abundant waste byproducts, acetic acid is produced as the only byproduct in his approach (Figure 1.11b). The two-step peptide elongation involves an isolable oxazolone intermediate as an activated form of carboxylic acid, which could ring-open in the presence of an amine nucleophile such as racemic *β*-phenylserine **1.16**. Then, the resulting peptide **1.17** is activated with sodium acetate and acetic anhydride to afford an elongated oxazolone**.** Following these iterations, we obtained the linear pentapeptide **1.19** in 53% yield over six steps (Figure 1.12). After deprotection of linear precursor **1.19** using TFA, DMAP was

added as a nucleophilic catalyst to facilitate aminolysis to afford the corresponding cyclic dehydropeptide **1.20** in 81% yield with no dimerization observed, despite the relatively high concentration (0.1 M) (eq 2).

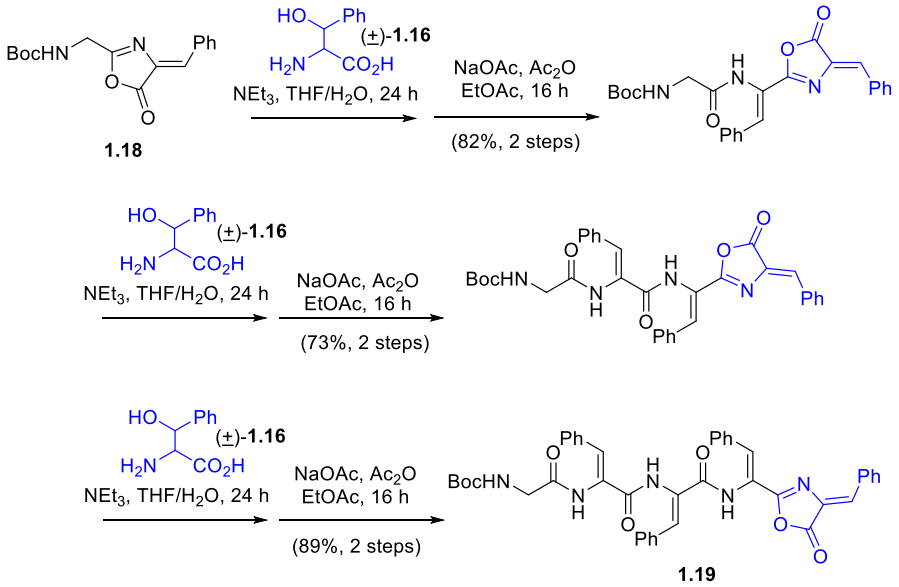

Figure 1.12 Synthesis of linear pentapeptide **1.19**

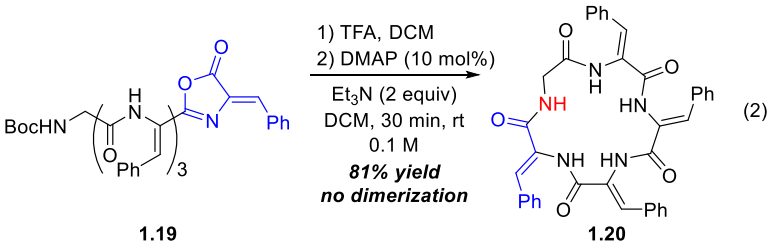

(2)

1.2.3 Diastereoselective Hydrogenation of Cyclic Dehydropeptides

To provide a more convenient handle for NMR analysis, we also prepared fluorinated analogue **1.21**. Considering that there are four dehydroamino acid residues in **1.21**, full reduction could generate a total of sixteen possible stereoisomers. Surprisingly, when a combination of $[Rh(cod)_2]BF_4$ and an achiral ligand (1,3-bis(diphenylphosphino)propane, dppp) was used as a catalyst, one diastereomer was

formed in 88% yield and with excellent diastereocontrol (20:2:1:1:1 *dr)* (Figure 1.13, top right).[66] Through independent synthesis from D- and L-phenylalanine, we confirmed that this isomer was (±) cyclic D,L-*α*-peptide **1.25**. Of note, cyclic D,L-*α*-peptides have been used as therapeutic agents against gram negative and gram positive bacteria.[67,68] In stark contrast, Pd/C produced a racemic mixture of all eight possible diastereomers, which were detected by ^{19}F-NMR spectroscopy and LC-MS analysis (Figure 1.13, left).[69]

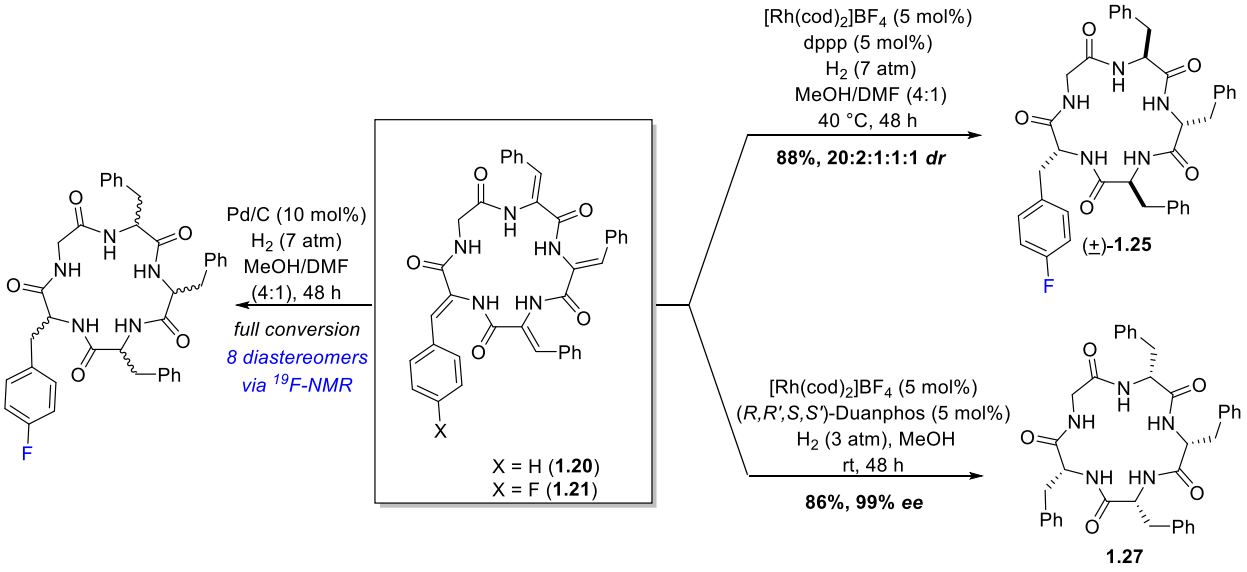

Figure 1.13 Hydrogenation of cyclic dehydropeptides

The essentially complete diastereoselectivity observed in the presence of a simple, achiral ligand (*i.e*. dppp) suggests that this reduction is proceeding in a specific order about the macrocyclic ring and is controlled by the sequence of the substrate. This in turn implies that the hydrogenation is initiated by recognition of the Rh-catalyst to a specific dehydrophenylalanine. To understand the intriguing finding, we performed further experimental and theoretical studies to elucidate the mechanism of the diastereoselective reduction.

1.2.4 Mechanistic Support for a Unidirectional Reduction

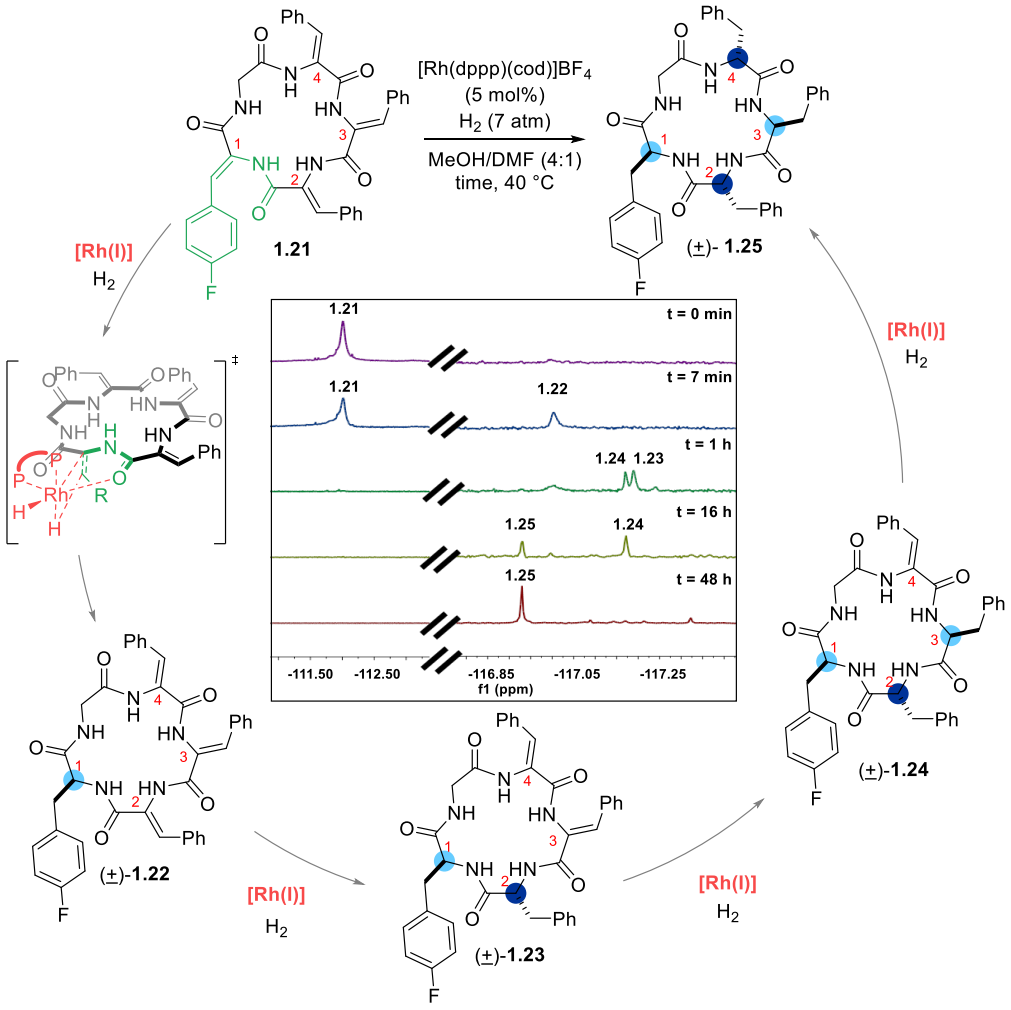

Figure 1.14 Mechanistic support for unidirectional reduction

First, we tested the hypothesis of a strictly sequential reduction. If the hydrogenation proceeds in one direction around the ring starting with a specific dehydrophenylalanine (highlighted in green, Figure 1.14), three intermediate macrocycles would arise (such as **1.22**, **1.23**, and **1.24**). By stopping the reduction of cyclic peptide **1.21** at various time points, three distinct intermediates were observed by ^{19}F-NMR spectroscopy. Next, we independently prepared and characterized cyclic peptides **1.22**, **1.23**, and **1.24**. The spectroscopic data for these three structures matched the structure of the aforementioned intermediates by ^{19}F-NMR (Figure 1.14). Moreover, when intermediate **1.22** was subjected to the Rh-catalyzed hydrogenation conditions, the

corresponding cyclic peptide **1.25** was obtained in 76% yield and 20:<1:<1:<1:<1 *dr* (Table 1.1). Similarly, when we subjected cyclic peptide **1.23** to hydrogenation, we also observed cyclic peptide **1.25** in 99% yield and 20:<1:<1:<1:<1 *dr*. Finally, hydrogenating cyclic peptide **1.24** gave the desired peptide in 99% yield and 20:<1:<1:<1:<1 *dr*. Together, these experiments support the proposed intermediates that arise during a sequential reduction that occurs with high *anti* diastereoselectivity.

Table 1.1 Subjecting synthesized intermediates to hydrogenation conditions

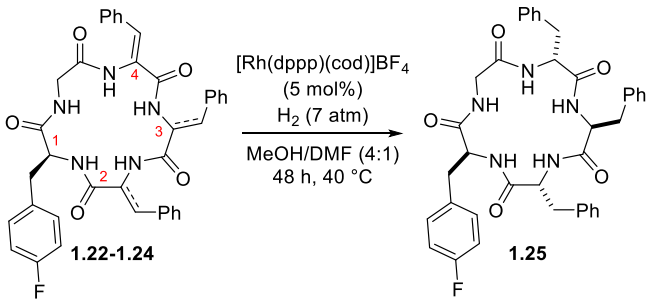

1.22-1.24 **1.25**

entry	cyclic peptide	yield	*dr*
1	L-(4-F)Phe$_1$ΔPhe$_2$ΔPhe$_3$ΔPhe$_4$ (**1.22**)	76%	20:<1:<1:<1:<1
2[a]	L-(4-F)Phe$_1$D-Phe$_2$ΔPhe$_3$ΔPhe$_4$ (**1.23**)	99%	20:<1:<1:<1:<1
3[b]	L-(4-F)Phe$_1$D-Phe$_2$L-Phe$_3$ΔPhe$_4$ (**1.24**)	99%	20:<1:<1:<1:<1

[a] at 60 °C, 20 atm H_2. [b] in THF solvent at 80 °C, 40 atm H_2

Next, we studied the structural origin of the experimentally observed *anti* selectivity through theoretical studies in collaboration with Eric Hansen and Professor Olaf Wiest at the University of Notre Dame. Given the complexity of cyclic dehydropeptide **1.20**, even a minimal conformational analysis of the transition state is not feasible. We therefore used the transition state force field (TSFF) for the Rh-catalyzed hydrogenation of enamides,[70] which we developed previously using the quantum guided molecular mechanics (Q2MM) method.[71] This method was previously shown to allow the rapid exploration of the conformational space at the transition state using Monte Carlo sampling, and by

Boltzmann averaging of the relative energies of the conformational ensembles of the diastereomeric transition structures, to accurately predict the stereochemistry of the hydrogenation.[72]

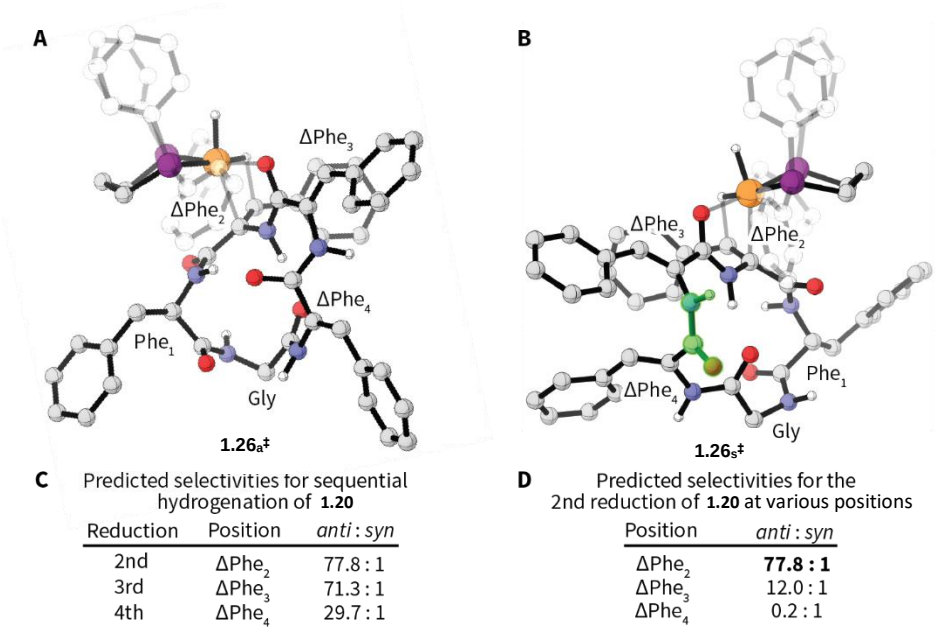

C Predicted selectivities for sequential hydrogenation of **1.20**

Reduction	Position	*anti* : *syn*
2nd	ΔPhe_2	77.8 : 1
3rd	ΔPhe_3	71.3 : 1
4th	ΔPhe_4	29.7 : 1

D Predicted selectivities for the 2nd reduction of **1.20** at various positions

Position	*anti* : *syn*
ΔPhe_2	**77.8 : 1**
ΔPhe_3	12.0 : 1
ΔPhe_4	0.2 : 1

Figure 1.15 Transition structures **1.26$_a$‡** for *anti* (left) and **1.26$_s$‡** for *syn* (right) hydrogenation at site ΔPhe_2. Non-reacting hydrogens have been hidden and phenyls on the ligand are shown transparent for clarity

Figure 1.15 summarizes the results of these simulations for the cyclic dehydropeptide **1.20** using $[Rh(dppp)]^+$. Figure 1.15a and 1.15b shows the lowest energy transition structures **1.26$_a$‡** and **1.26$_s$‡** for the second reduction of cyclic dehydropeptide **1.20** leading to the *anti* (left) and *syn* (right) diastereoselectivity, respectively. The accessible conformational space of the cyclic dehydropeptide is complex, and no single conformation or interaction is solely responsible for the calculated and experimentally observed preference. Nevertheless, analysis of the conformations of **1.26$_a$‡** and **1.26$_s$‡** shows that in order to position the side chains at Phe_1 and ΔPhe_2 in a pseudo-equatorial position to minimize steric repulsion with the dppp ligand, the backbone of the cyclic dehydropeptide is distorted into a strained conformation. As a result, one amide bond in

1.26$_S^‡$ is forced into an energetically unfavorable *cis*[73] conformation (highlighted in green, Figure 1.15b), favoring the transition structure leading to the observed *anti* selective hydrogenation. Clustering of the low-energy transition structures also shows that the transition structures for the hydrogenations at ΔPhe$_3$ and ΔPhe$_4$ leading to the experimentally observed product are stabilized by more intramolecular hydrogen bonds (Figure 1.16 and Figure 1.17).

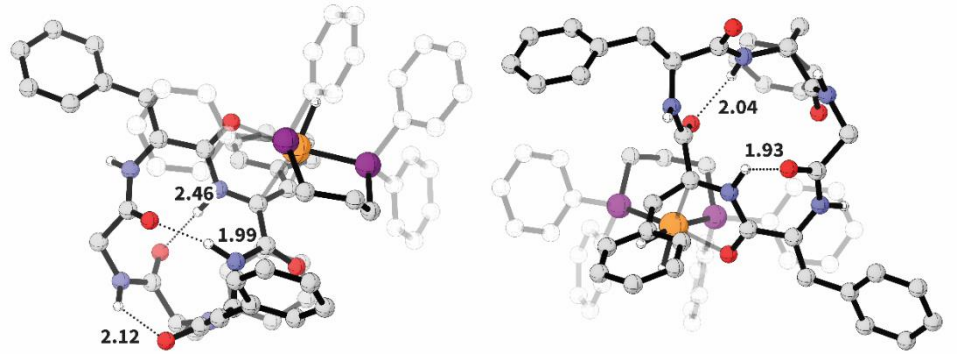

Figure 1.16 Hydrogen bonding in pro-*anti* **1R2S3R**^{TS} (left) and pro-*syn* **1R2S3S**^{TS} (right)

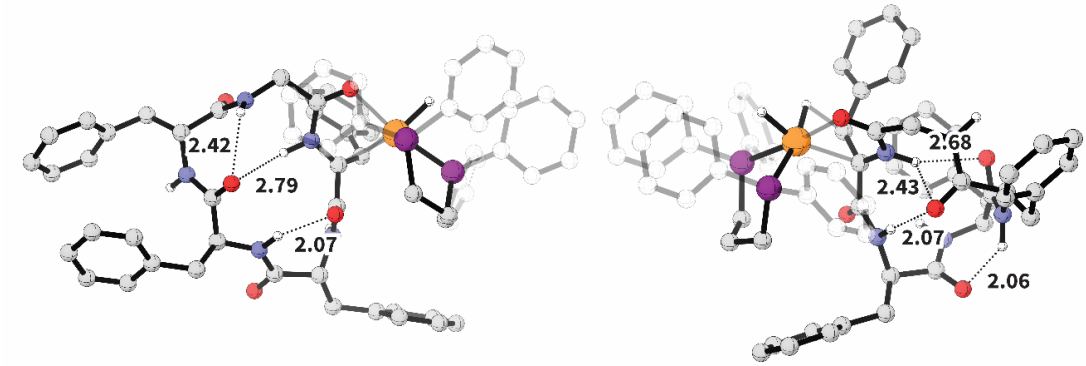

Figure 1.17 Hydrogen bonding in pro-*syn* **1R2S3R4R**^{TS} (left) and pro-*anti* **1R2S3R4S**^{TS} (right).

Moreover, after the first hydrogenation at ΔPhe$_1$ in cyclic dehydropeptide **1.20**, the subsequent reductions occur *anti* with predicted selectivities ranging from 30:1 to 78:1 *dr*

(Figure 1.15c), in good agreement with the experimentally observed diastereoselectivity of 20:<1:<1:<1:<1 (cf Table 1.1). It is noteworthy that the final hydrogenation at ΔPhe_4 is the least selective one, suggesting that the diastereoselectivity is related to the increased flexibility of the cyclic dehydropeptide.

The computational studies also allow us to probe the basic hypothesis of a sequential, unidirectional hydrogenation controlled by the interplay between the substrate and Rh-catalyst. Figure 1.15d shows the results for the expected diastereoselectivity for the second hydrogenation at the three possible centers. Only the simulations for the sequential hydrogenation at ΔPhe_2 leads to the experimentally observed result, while reaction at ΔPhe_3 or ΔPhe_4 would lead to significantly different or even opposing diastereoselectivities. Together, the experimental and computational results demonstrate that the Rh-catalyst preferentially binds to ΔPhe_1 for the initial reduction of cyclic dehydropeptide **1.20**. We hypothesize that the adjacent glycine residue, containing a sp^3-hybridized α-carbon, enables the flexibility for the Rh-catalyst to bind in a reactive conformation to initiate the sequential reduction.[30] As the hydrogenation proceeds in the *C* to *N* direction, the next ΔPhe in the sequence becomes more flexible and is hydrogenated in the next step.

Finally, we studied the question of whether an appropriate chiral ligand can override the diastereoselectivity observed when using the Rh-dppp catalyst. Among the thousands of chiral phosphine ligands developed for asymmetric hydrogenation,[74] Duanphos is the best for reduction of *α*-(acetamido)acrylate derivatives [46]. We previously used Duanphos to access cyclic peptides by overriding substrate bias in the synthesis of the chickweed natural product, dichotomin E.[64] With 5 mol% $[Rh(cod)_2]BF_4$, (*R*,*R*',*S*,*S*')-

Duanphos gave cyclic peptide **1.27** in 86% isolated yield and 99% *ee* (Figure 1.13, bottom right).

1.2.5 Conclusion

Molecular recognition between transition metal catalysts and amino acid sequences is a powerful strategy in organic synthesis.[75] Through our combined experimental and theoretical study, we have demonstrated the first example of a unidirectional hydrogenation controlled by a small synthetic peptide. This catalyst-substrate recognition has further implications in the construction of cyclic peptides using tandem hydrogenation and the study of molecular recognition in synthetic systems.

1.3 Experimental Data

1.3.1 Experimental Details for Application of Dehydrophenylalanine as a Turn Inducer in the Synthesis of Dichotomin E

The data shown Figure 1.7 and Figure 1.8 were obtained by J.R. and N.K., and the reader is directed to the Supporting Information of the published manuscript[64] for the details of those experiments. This experimental section will focus on my contributions to the project.

Typical procedures for synthesis of linear pentapeptides

i) Synthesis of Gly-Tyr-Ala-ΔPhe-Ala **1.3**

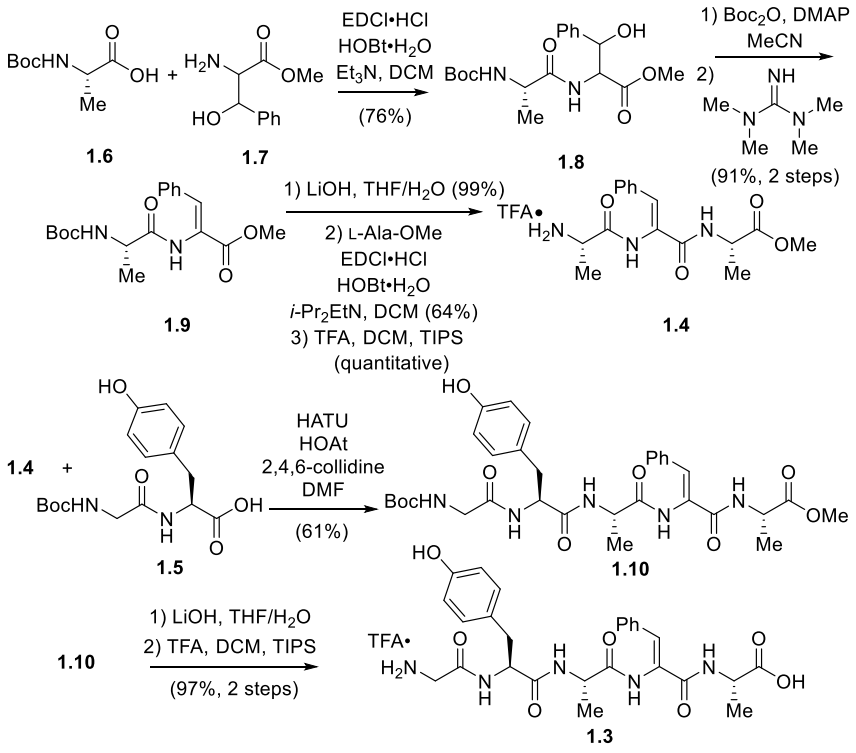

Figure 1.4 Synthesis of unsaturated pentapeptide **1.3**

Representative peptide coupling with EDCI (Method A): To a round bottom flask equipped with a stir bar was added Boc-L-alanine **1.6** (5.00 g, 26.4 mmol), DL-(β-OH)–Phe–OMe **1.7** (6.13 g, 26.4 mmol), HOBt·H_2O (4.29 g, 31.7 mmol), and DCM (100 mL).

The mixture was cooled to 0 °C and Et_3N (9.16 mL, 66.1 mmol) was subsequently added. EDCI·HCl (6.08 g, 31.7 mmol) was added in portions and the reaction gradually warmed to rt and stirred for 22 h. The reaction mixture was transferred to a separatory funnel and was washed with 100 mL sat. $NaHCO_3$ (aq), 100 mL 10% $KHSO_4$ (aq), and 100 mL brine. The organic phase was dried over Na_2SO_4, filtered, and concentrated under reduced pressure. The unpurified reaction mixture was then purified by column chromatography (eluting with 20:1 DCM/MeOH) to afford dipeptide **1.8** as a white solid (7.4 g, 76%).

Representative elimination to form dehydroamino acid (Method B): The procedure was adapted from Suárez.[44] To a round bottom flask equipped with a stir bar was added dipeptide **1.8** (7.40 g, 20.2 mmol), DMAP (244 mg, 2.00 mmol) and MeCN (60 mL). The mixture was cooled to 0 °C and Boc_2O (4.63 g, 21.2 mmol) was quickly added. After disappearance of starting material analyzed via LC-MS, tetramethylguanidine (0.77 mL, 6.1 mmol) was added. After 12 h, the reaction mixture was concentrated under reduced pressure and then purified by column chromatography (eluting with 20:1 DCM/MeOH) to afford the unsaturated dipeptide **1.9** as a white solid (6.4 g, 91%, 2 steps).

Representative hydrolysis procedure (Method C): To a round bottom flask equipped with a stir bar was added methyl ester **1.9** (6.40 g, 18.4 mmol), THF (90 mL), and H_2O (90 mL). The mixture was cooled to 0 °C and 1M LiOH (aq) (19 mL, 19 mmol) was subsequently added. The reaction gradually warmed to rt and stirred for 14 h. The reaction mixture was acidified with 10% $KHSO_4$ (aq), and the THF was concentrated under reduced pressure. The reaction mixture was transferred to a separatory funnel where it was extracted with ethyl acetate (3 x 100 mL). The organic layer was washed

with 100 mL brine, dried over Na_2SO_4, filtered, and concentrated under reduced pressure to afford carboxylic acid **S1** as a colorless oil (6.1 g, 99%).

Representative Boc-deprotection (Method D): To a round bottom flask equipped with a stir bar was added Boc-protected amine **S2** (638 mg, 1.52 mmol), triisopropylsilane (0.33 mL, 1.6 mmol), and DCM (15 mL). The reaction mixture was cooled to 0 °C and TFA (1.17 mL, 15.2 mmol) was slowly added. The reaction slowly warmed to rt and stirred for 24 h. The DCM was concentrated under reduced pressure and to the mixture was added toluene to form a TFA azeotrope, which was subsequently concentrated under reduced pressure. The reaction mixture was further dried on the high vacuum and subsequently triturated with Et_2O to afford amine **1.4** in quantitative yield which was used without further purification.

Preparation of DL-(β-OH)–Phe–OMe 1.7 (Method E):

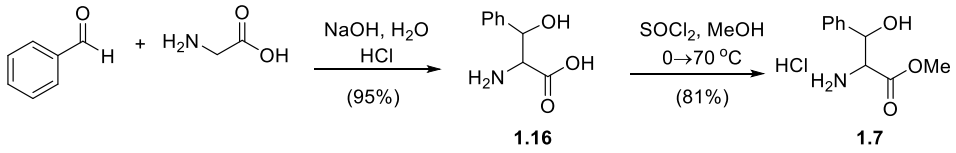

To a stirring solution of NaOH (60 g, 1.5 mol) in water (250 mL) at rt was added glycine (75 g, 1.0 mol). The solution was stirred for 10 min and benzaldehyde (215 mL, 2.1 mol) was added and the solution was stirred for 20 min. The solution became a beige emulsion and the solid was broken apart. Concentrated HCl (aq) (130 mL) was added slowly and the mixture stirred until the beige solid was consumed to give a clear yellow solution. Shortly, beige precipitates were observed and the mixture was cooled to 0 °C. The beige

solid was collected via vacuum filtration and the solid was washed with Et_2O. The solid was dried *in vacuo* to give **1.16** an off-white solid (172 g, 95%). Characterization data was consistent with those previously reported.[76]

To a round bottom flask equipped with a stir bar was added **1.16** (25 g, 138 mmol) and anhydrous MeOH (190 mL) under N_2 and the mixture was cooled to 0 °C. Thionyl chloride (22.5 mL, 310 mmol) was subsequently added dropwise and the reaction stirred overnight for 16 h at 70 °C. The reaction mixture was concentrated under reduced pressure, redissolved in DCM, and subsequently concentrated again (2x). The resulting white solid was washed with Et_2O to afford DL-(β-OH)–Phe–OMe **1.7** was an off-white solid (26.0 g, 81%). Characterization data was consistent with those previously reported.[77]

Methyl 2-((*S*)-2-((tert-butoxycarbonyl)amino)propanamido)-3-hydroxy-3-phenylpropanoate (1.8)

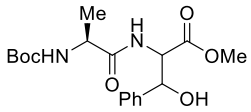

The product was prepared by method A using Boc alanine **1.6** (5.00 g, 26.4 mmol) and purified by column chromatography (eluting with 90:10 DCM/MeOH) to afford a white solid (7.4 g, 61%, 1:1 dr). ^{1}H NMR (499 MHz, DMSO) δ 7.89 (d, *J* = 9.1 Hz, 1H), 7.76 (d, *J* = 8.9 Hz, 1H), 7.45 – 7.32 (m, 4H), 7.31 – 7.24 (m, 4H), 7.25 – 7.19 (m, 2H), 7.00 (d, *J* = 8.0 Hz, 1H), 6.86 (d, *J* = 8.0 Hz, 1H), 5.92 (d, *J* = 4.8 Hz, 2H), 5.14 (dd, *J* = 4.9, 3.2 Hz, 1H), 5.12 – 5.06 (m, 1H), 4.55 (ddd, *J* = 12.7, 9.0, 3.2 Hz, 2H), 4.10 – 3.84 (m, 2H), 3.65 (s, 3H), 3.61 (s, 3H), 1.39 (s, 9H), 1.38 (s, 9H), 1.02 (d, *J* = 7.2 Hz, 3H), 0.94 (d, *J* = 7.2 Hz, 3H). ^{13}C NMR (126 MHz, DMSO) δ 172.96, 172.91, 170.61, 154.88, 154.82, 141.57, 141.47, 127.76, 127.73, 127.25, 127.16, 126.38, 126.14, 109.52, 78.15, 77.97, 72.22, 72.11, 58.05, 52.02, 51.99, 49.78, 49.29, 28.21,

18.30, 17.96. IR (ATR): 3337, 3013, 2978, 1660, 1498, 1365, 1168 cm^{-1}. HRMS (ESI-TOF) *m/z* calc'd for $C_{18}H_{26}N_2O_6Na$ $[M+Na]^+$: 389.1689, found: 389.1687.

Methyl (*S,Z*)-2-(2-((tert-butoxycarbonyl)amino)propanamido)-3-phenylacrylate (1.9)

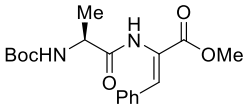

The product was prepared by method B using methyl ester **1.8** (7.40 g, 20.2 mmol) and purified by column chromatography (eluting with 93:7 DCM/MeOH) to afford the product as a white solid (6.4 g, 91%, 2 steps). ^{1}H NMR (400 MHz, DMSO) δ 9.56 (s, 1H), 7.77 – 7.64 (m, 2H), 7.43 – 7.30 (m, 3H), 7.26 (s, 1H), 7.03 (d, *J* = 7.2 Hz, 1H), 4.21 – 4.05 (m, 1H), 3.70 (d, *J* = 1.4 Hz, 3H), 1.41 (s, 9H), 1.26 (d, *J* = 7.2 Hz, 3H). ^{13}C NMR (126 MHz, DMSO) δ 173.13, 165.41, 155.23, 133.31, 132.11, 130.23, 129.47, 128.49, 125.92, 78.05, 52.16, 49.82, 28.24, 17.40. IR (ATR): 3291, 3005, 2979, 1673, 1490, 1249, 1162 cm^{-1}. HRMS (ESI-TOF) *m/z* calc'd for $C_{18}H_{24}N_2O_5Na$ $[M+Na]^+$: 371.1583, found: 371.1588. $[\alpha]^{24}_D$ +66 (*c* = 0.46, MeOH).

(*S,Z*)-2-(2-((tert-butoxycarbonyl)amino)propanamido)-3-phenylacrylic acid (S1)

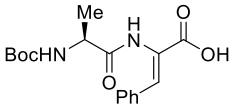

The product was prepared by method C using unsaturated dipeptide **1.9** (6.40 g, 18.4 mmol) and obtained as a white solid (6.0 g, 99%). ^{1}H NMR (500 MHz, DMSO) δ 12.68 (s, 1H), 9.39 (s, 1H), 7.76 – 7.55 (m, 2H), 7.42 – 7.32 (m, 3H), 7.28 (s, 1H), 7.02 (d, *J* = 7.3 Hz, 1H), 4.21 – 4.05 (m, 1H), 1.40 (s, 9H), 1.25 (d, *J* = 7.2 Hz, 3H). ^{13}C NMR (126 MHz, $CDCl_3$) δ 172.66, 166.30, 155.21, 133.68, 131.83, 130.14, 129.19, 128.39, 126.52, 78.03, 49.83, 28.25, 17.52. IR (ATR): 3281, 2980, 1685, 1539, 1162 cm^{-1} HRMS (ESI-TOF) *m/z* calc'd for $C_{17}H_{22}N_2O_5Na$ $[M+Na]^+$: 357.1426, found: 357.1419. $[\alpha]^{25}_D$ +70 (*c* = 0.25, MeOH).

Methyl ((*Z*)-2-((*S*)-2-((tert-butoxycarbonyl)amino)propanamido)-3-phenylacryloyl)-L-alaninate (S2)

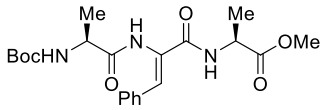

The product was prepared by method A using carboxylic acid **S1** (3.80 g, 11.4 mmol), L-alanine methyl ester (1.60 g, 11.4 mmol), and *i*-Pr$_2$EtN (7.90 mL, 45.6 mmol) and purified by column chromatography (eluting with 85:15 DCM/acetone) to afford the product as a white solid (3.0 g, 64%). ^{1}H NMR (499 MHz, DMSO) δ 9.57 (s, 1H), 7.93 (d, *J* = 6.8 Hz, 1H), 7.65 – 7.49 (m, 2H), 7.42 – 7.31 (m, 3H), 7.25 (s, 1H), 7.21 (m, 1H), 4.44 – 4.34 (m, 1H), 4.08 – 3.99 (m, 1H), 3.64 (s, 3H), 1.39 (s, 9H), 1.34 (d, *J* = 7.2 Hz, 3H), 1.23 (d, *J* = 7.1 Hz, 3H). ^{13}C NMR (126 MHz, DMSO) δ 172.75, 172.71, 164.34, 155.71, 133.83, 130.04, 129.58, 128.84, 128.47, 128.39, 78.35, 51.86, 50.06, 48.23, 28.19, 16.93, 16.71. IR (ATR): 3291, 3017, 2981, 1751, 1685, 1530, 1163 cm^{-1}. HRMS (ESI-TOF) *m/z* calc'd for $C_{21}H_{29}N_3O_6Na$ $[M+Na]^+$: 442.1954, found: 442.1946. $[\alpha]^{25}_D$ –41 (*c* = 0.25, MeOH).

Methyl ((Z)-2-((S)-2-aminopropanamido)-3-phenylacryloyl)-L-alaninate (1.4)

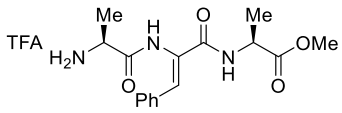

The product was prepared by method D using tripeptide **S2** (5.60 g, 13.3 mmol) and obtained as a white solid in quantitative yield. ^{1}H NMR (499 MHz, DMSO) δ 9.95 (s, 1H), 8.46 (d, *J* = 7.1 Hz, 1H), 8.22 – 8.14 (m, 2H), 7.60 – 7.52 (m, 2H), 7.49 – 7.39 (m, 2H), 7.38 – 7.33 (m, 1H), 7.16 (s, 1H), 4.41 (p, *J* = 7.2 Hz, 1H), 4.11 – 4.01 (m, 1H), 3.65 (s, 3H), 1.44 (d, *J* = 7.0 Hz, 3H), 1.35 (d, *J* = 7.3 Hz, 3H). ^{13}C NMR (126 MHz, DMSO) δ 172.95, 169.08, 164.31, 133.67, 129.40, 129.08, 128.91, 128.55, 128.34, 51.91, 48.47, 48.12, 16.87, 16.42. IR

(ATR): 2996, 1740, 1660, 1519, 1137 cm^{-1}. HRMS (ESI-TOF) *m/z* calc'd for $C_{16}H_{21}N_3O_4H$ $[M+H]^+$: 320.1610, found: 320.1620. $[\alpha]^{26}_D$ +90 (*c* = 0.31, MeOH).

Methyl (tert-butoxycarbonyl)glycyl-L-tyrosinate (S3)

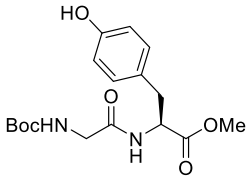

Dipeptide **S3** was prepared according to method A using Boc-Gly-OH (7.10 g, 40.6 mmol), and L-Tyr-OMe (7.20 g, 36.9 mmol) and purified by column chromatography to afford the product as a white solid (11.8 g, 82% yield). The characterization data was in agreement with literature.[78]

(tert-butoxycarbonyl)glycyl-L-tyrosine (1.5)

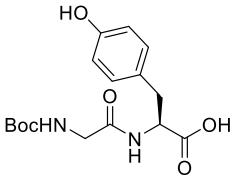

Dipeptide carboxylic acid **1.5** was prepared according to method C using methyl ester **S3** (11.8 g, 33.4 mmol) to afford the product as a white solid (10.9 g, 96%). The characterization data was in agreement with literature.[78]

Methyl ((*Z*)-2-((*S*)-2-((*S*)-2-(2-((tert-butoxycarbonyl)amino)acetamido)-3-(4-hydroxyphenyl)propanamido)propanamido)-3-phenylacryloyl)-L-alaninate (1.10)

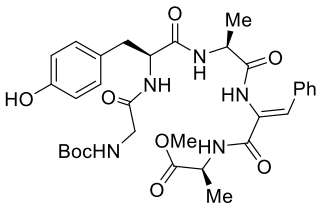

To a round botton flask equipped with a stir bar was added carboxylic acid **1.5** (4.10 g, 12.2 mmol), amine **1.4** (4.80 g, 11.1 mmol), HATU (5.00 g, 13.3 mmol), HOAt (0.452 g, 3.32 mmol) and DMF (42 mL). The reaction mixture was cooled to 0 °C and 2,4,6-collidine (3.70 mL, 27.7 mmol) was added. The reaction warmed to rt and stirred for 24 h. The solvent was removed under reduced pressure and the product was purified by column chromatography (eluting with 90:10 DCM/MeOH, increasing in 0.5% increments)

to afford the product as a white solid (4.32 g, 61%). ^{1}H NMR (500 MHz, DMSO) δ 9.66 (s, 1H), 9.16 (s, 1H), 8.47 (d, *J* = 5.1 Hz, 1H), 8.00 (d, *J* = 6.3 Hz, 1H), 7.65 (d, *J* = 8.2 Hz, 1H), 7.61 – 7.53 (m, 2H), 7.44 – 7.37 (m, 2H), 7.38 – 7.32 (m, 1H), 7.27 (s, 1H), 6.98 (d, *J* = 8.2 Hz, 2H), 6.94 (t, *J* = 6.2 Hz, 1H), 6.60 (d, *J* = 8.4 Hz, 2H), 4.48 (td, *J* = 8.4, 4.3 Hz, 1H), 4.40 – 4.18 (m, 2H), 3.64 (s, 3H), 3.54 (dd, *J* = 16.8, 6.1 Hz, 1H), 3.43 (dd, *J* = 16.8, 6.0 Hz, 1H), 2.88 (dd, *J* = 14.1, 4.3 Hz, 1H), 2.67 (dd, *J* = 14.1, 8.6 Hz, 1H), 1.36 (s, 9H), 1.31 (d, *J* = 7.1 Hz, 3H), 1.26 (d, *J* = 7.3 Hz, 3H). ^{13}C NMR (126 MHz, DMSO) δ 173.10, 172.16, 171.74, 169.06, 164.27, 155.84, 155.80, 133.82, 130.25, 130.22, 129.58, 128.94, 128.51, 128.40, 127.33, 114.84, 78.15, 53.39, 51.86, 49.24, 48.52, 43.26, 36.74, 28.17, 16.66, 16.49. IR (ATR): 3305, 2974, 1656, 1514, 1160 cm^{-1}. HRMS (ESI-TOF) *m/z* calc'd for $C_{32}H_{41}N_5O_9Na$ $[M+Na]^+$: 662.2802, found: 662.2817. $[\alpha]^{26}_D$ –82 (*c* = 0.25, MeOH).

((*Z*)-2-((*S*)-2-((*S*)-2-(2-aminoacetamido)-3-(4-hydroxyphenyl)propanamido)propanamido)-3-phenylacryloyl)-L-alanine (1.3)

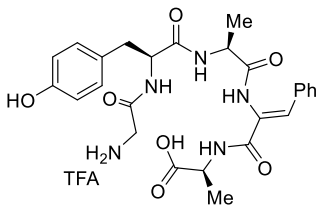

To a round bottom flask equipped with a stir bar was added methyl ester **1.10** (4.20 g, 6.60 mmol), THF (30 mL), and H_2O (30 mL). The mixture was cooled to 0 °C and 1M LiOH (aq) (7.26 mL, 7.26 mmol) was subsequently added. The reaction was allowed to gradually warm to rt and stirred for 48 h. The reaction mixture was acidified with 10% $KHSO_4$ (aq) and the THF was concentrated under reduced pressure. The reaction mixture was transferred to a separatory funnel where it was extracted with ethyl acetate (3 x 100 mL). The organic layer was washed with 100 mL brine, dried over Na_2SO_4, filtered, and concentrated under

reduced pressure to afford carboxylic acid **S4** which was used in the next step without further purification.

To a round bottom flask equipped with a stir bar was added carboxylic acid **S4** (6.60 mmol), and DCM (60 mL). The reaction mixture was cooled to 0 °C and TFA (5.1 mL, 66 mmol) was slowly added. The reaction slowly warmed to rt and stirred for 14 h. The DCM was concentrated under reduced pressure and to the mixture was added toluene to form a TFA azeotrope, which was subsequently concentrated under reduced pressure. The reaction mixture was further dried on the high vacuum and subsequently triturated with Et_2O to afford unsaturated peptide **1.3** (4.0 g, 97% 2 steps). ^{1}H NMR (500 MHz, DMSO) δ 9.62 (s, 1H), 9.22 (s, 1H), 8.56 (d, *J* = 5.7 Hz, 1H, $N–H_{Ala(term)}$), 8.52 (d, *J* = 8.4 Hz, 1H, $N–H_{Tyr}$), 7.91 (d, *J* = 6.9 Hz, 3H, $N–H_{Ala(int)+Gly}$), 7.57 (d, *J* = 7.7 Hz, 2H), 7.42 – 7.30 (m, 3H), 7.22 (s, 1H), 7.04 (d, *J* = 8.1 Hz, 2H), 6.64 (d, *J* = 8.0 Hz, 2H), 4.56 (td, *J* = 9.2, 3.7 Hz, 1H), 4.39 – 4.22 (m, 2H), 3.55 (d, *J* = 16.2 Hz, 1H), 3.43 (d, *J* = 16.2 Hz, 1H), 2.93 (dd, *J* = 14.2, 3.8 Hz, 1H), 2.59 (dd, *J* = 14.1, 10.1 Hz, 1H), 1.36 (d, *J* = 7.3 Hz, 3H), 1.31 (d, *J* = 7.1 Hz, 3H).^{13}C NMR (126 MHz, DMSO) δ 174.22, 172.30, 171.59, 165.91, 164.30, 156.09, 134.02, 130.22, 129.90, 129.71, 129.02, 128.81, 128.64, 127.69, 115.13, 54.36, 49.29, 48.38, 40.19, 36.94, 17.25, 16.84. IR (ATR): 3270, 1656, 1515, 1172 cm^{-1}. HRMS (ESI-TOF) *m/z* calc'd for $C_{26}H_{31}N_5O_7H$ $[M+H]^+$: 526.2302, found: 526.2303. $[\alpha]^{26}_D$ –20 (*c* = 0.23, MeOH).

ii) Synthesis of Gly-Tyr-Ala-Phe-Ala **1.11**

Glycyl-L-tyrosyl-L-alanyl-L-phenylalanyl-L-alanine (1.11)

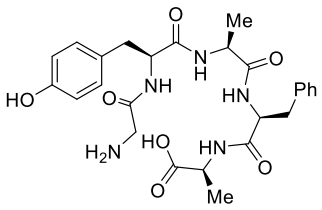

Linear pentapeptide **1.11** was manually synthesized via Fmoc solid phase peptide synthesis (SPPS) using 2-chlorotrityl chloride (CTC) resin (substitution 1.1 mmol/g). The resin (0.360 g, 0.400 mmol) was swelled in anhydrous DCM (20 mL) for 45 min. The beads were washed once with DMF (peptide grade). DMF (10 mL), Fmoc-Ala-OH (500 mg, 1.60 mmol) and *i*-Pr_2EtN (2.5 mL) were added and allowed to mix under N_2 for 15 minutes. The coupling with Fmoc-Ala-OH was repeated again. After the double coupling, the beads were washed with DMF and the Fmoc group was deprotected with 20% 4-methylpiperidine in DMF (20 mL) for 15 minutes. This deprotection was repeated again. The resin was washed three times with DMF (15 mL) and a Kaiser test was performed to determine presence of deprotected amine. The beads were washed once with *N*-methyl-2-pyrrolidone (15 mL). To begin the next coupling, NMP (10 mL), Fmoc-Phe-OH (620 mg, 1.6 mmol), HBTU (610 mg, 1.6 mmol), and *i*-Pr_2EtN (2.5 mL) were added and the resin bubbled under N_2 for 30 min. The completion of the coupling was monitored by the Kaiser test. If incomplete, the coupling step was repeated again. The resin was washed three times with DMF (15 mL). The deprotection of the Fmoc group was repeated as above two times. To elongate the peptide, the coupling and deprotection steps were performed with Fmoc-Ala-OH, Fmoc-Tyr-OH, and Fmoc-Gly-OH. After the last amino acid was deprotected, the beads were washed three times with DMF. To the resin was added 40 mL cleavage solution (95% TFA, 2.5% H_2O, 2.5% TIPS), and the resin bubbled under N_2 for 3 h. A new receiving flask was replaced on the peptide synthesizer

and the TFA was drained into the new flask. The TFA solution was separated into 4 conical vials and cold ether (–20 °C) was added to precipitate the peptide. The vials were centrifuged (3000 rpm, 0–4 °C) for 20 minutes. The remaining TFA and ether solution was decanted from the conical vials and the peptide precipitate was concentrated. The peptide was dissolved in 18 mL (10% MeCN/H_2O), filtered through a 0.20 micron filter, and purified by RP-HPLC on a C_{18} column (eluting with MeCN and H_2O containing 0.1% TFA, linear gradient 10–35% MeCN over 30 min). The pure fractions were combined, concentrated under reduced pressure, and then lyophilized to afford the product as a white powder (136 mg, 64%). ^{1}H NMR (400 MHz, DMSO) δ 9.19 (s, 1H), 8.51 (d, *J* = 8.4 Hz, 1H, N–H_{Tyr}), 8.29 (d, *J* = 2.3 Hz, 1H N–$H_{Ala(int)}$), 8.27 (d, *J* = 2.2 Hz, 1H, N–$H_{Ala(term)}$), 7.86 (d, *J* = 8.2 Hz, 1H, N–H_{Phe}), 7.28 – 7.12 (m, 5H), 7.01 (d, *J* = 8.5 Hz, 2H), 6.63 (d, *J* = 8.5 Hz, 2H), 4.52 (td, *J* = 8.8, 4.4 Hz, 2H), 4.31 – 4.09 (m, 2H), 3.50 (d, *J* = 16.3 Hz, 1H), 3.36 (d, *J* = 16.2 Hz, 2H), 3.05 (dd, *J* = 14.0, 4.2 Hz, 1H), 2.83 (ddd, *J* = 16.4, 12.6, 6.2 Hz, 2H), 2.56 (dd, *J* = 14.1, 10.3 Hz, 1H), 1.28 (d, *J* = 7.3 Hz, 3H), 1.16 (d, *J* = 7.1 Hz, 3H). ^{13}C NMR (126 MHz, $CDCl_3$) δ 174.03, 171.78, 170.58, 165.72, 157.78, 155.87, 137.62, 130.13, 129.32, 128.00, 127.59, 126.24, 114.93, 54.16, 53.40, 48.26, 47.59, 40.08, 37.44, 37.04, 18.23, 17.29. IR (ATR): 3284, 3040, 2928, 1676, 1654, 1636, 1500 cm^{-1}. HRMS (ESI-TOF) *m/z* calc'd for $C_{26}H_{33}N_5O_7Na$ $[M+Na]^+$: 550.2278 found: 550.2266. $[\alpha]^{27}_D$ –35 (*c* = 0.26, MeOH).

iii) Synthesis of Gly-ΔTyr-Ala-ΔPhe-Ala **1.12**

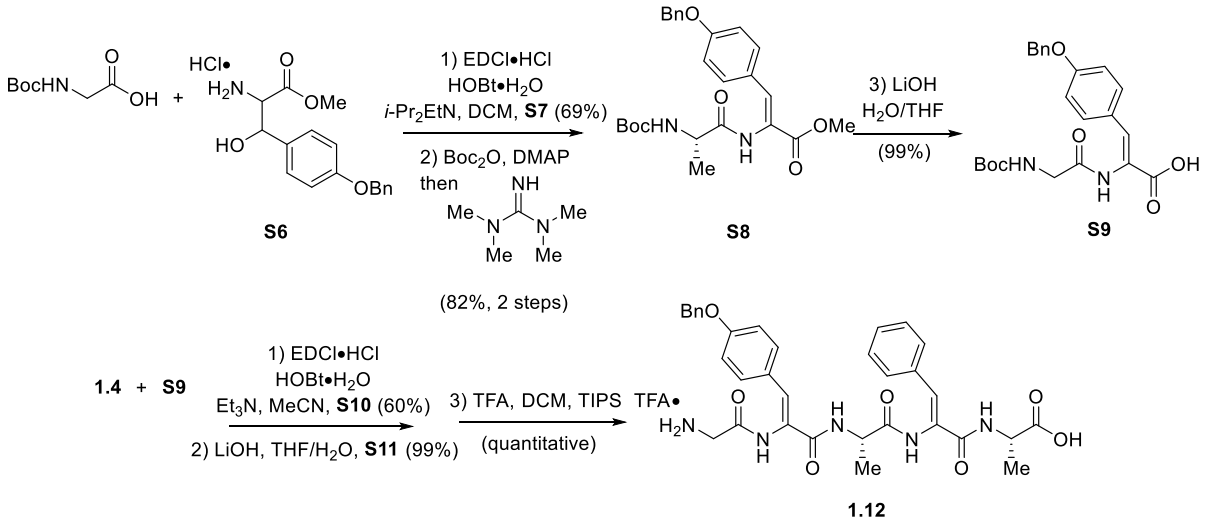

Figure 1.18. Synthesis of linear precursor **1.12**

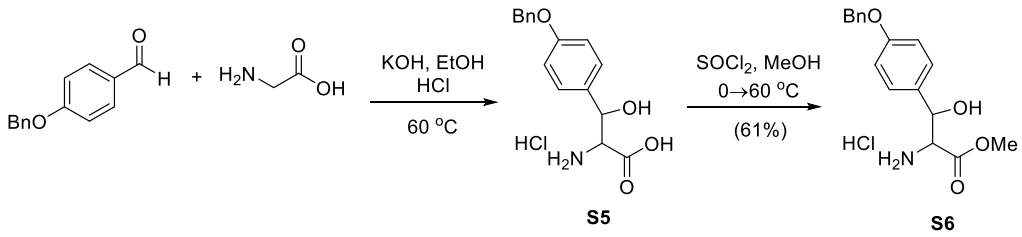

Methyl 2-amino-3-(4-(benzyloxy)phenyl)-3-hydroxypropanoate hydrochloride (S6)

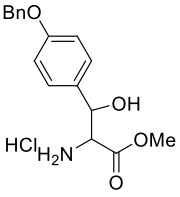

To a round bottom flask equipped with a stir bar was added glycine (3.0 g, 40 mmol), KOH (4.5 g, 80 mmol), and EtOH (100 mL). The reaction mixture stirred for 10 min and changed from a cloudy to clear solution. 4-Benzoxybenzylaldehyde (17 g, 80 mmol) was added followed by additional portion of EtOH (40 mL). The reaction mixture stirred for another 30 min at rt before it was heated to 60 °C and stirred overnight. The resulting solution became vicious. The EtOH was concentrated under reduced pressure and then H_2O (40 mL) followed by concentrated HCl (8 mL) was added. The cloudy mixture was filtered using vacuum filtration and the

solid was washed with DCM and Et_2O to afford **S5** as a light tan solid which was used in the next step without further purification.

To a round bottom flask equipped with a stir bar under N_2 was added **S5** (7.90 g, 24.4 mmol) and 49 mL anhydrous MeOH. The reaction mixture was cooled to 0 °C and $SOCl_2$ (3.54 mL, 48.8 mmol, 2 equiv) was added dropwise. The reaction mixture stirred for 30 min at 0 °C and then at 60 °C for 24 h. The MeOH was concentrated under reduced pressure. DCM was added to redissolve the compound and then concentrated under reduced pressure. This process was repeated once more with DCM. The solid was then triturated with Et_2O to afford the product as a light tan solid (8.3 g, 61%, 2 steps). ^{1}H NMR (500 MHz, DMSO) δ 8.43 (s, 2H), 7.44 (d, *J* = 7.2 Hz, 2H), 7.39 (t, *J* = 7.5 Hz, 2H), 7.33 (d, *J* = 7.2 Hz, 1H), 7.30 (d, *J* = 8.6 Hz, 2H), 7.01 (d, *J* = 8.7 Hz, 2H), 6.46 (d, *J* = 4.3 Hz, 1H), 5.11 (s, 2H), 5.04 – 4.93 (m, 1H), 4.11 (d, *J* = 5.6 Hz, 1H), 3.60 (s, 3H). ^{13}C NMR (126 MHz, $CDCl_3$) δ 167.96, 158.16, 137.05, 131.56, 128.45, 127.84, 127.74, 127.64, 114.64, 70.71, 69.16, 58.61, 52.62. IR (ATR): 3243, 3013, 2955, 2933, 1753, 1504, 1244 cm^{-1}. HRMS (ESI-TOF) *m/z* calc'd for $C_{17}H_{19}NO_4Na$ $[M+Na]^+$: 324.1212, found: 324.1214.

Methyl 3-(4-(benzyloxy)phenyl)-2-(2-((tert-butoxycarbonyl)amino)acetamido)-3-hydroxypropanoate (S7)

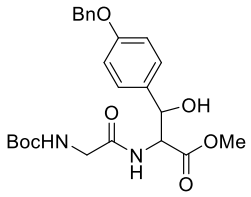

The product was prepared by method A using Boc-Gly-OH (3.00 g, 17.1 mmol) and **S6** (6.37 g, 18.8 mmol) and purified by column chromatography (eluting with 4:1 DCM/acetone) to afford the product as a white solid (5.4 g, 69%). ^{1}H NMR (400 MHz, $CDCl_3$) δ 7.44 – 7.30 (m, 5H), 7.26 (d, 2H), 6.93 (dd, *J* = 10.8, 4.0 Hz, 2H), 5.20 (d, *J* = 3.4 Hz, 1H), 5.13 (s 1H), 5.04 (s, 2H), 4.81 (dd, *J* = 8.8, 3.4 Hz, 1H), 3.84 – 3.73 (m, 2H), 3.72 (s, 3H), 1.45 (s, 9H). ^{13}C NMR

(126 MHz, $CDCl_3$) δ 170.92, 169.84, 158.82, 156.13, 136.95, 131.93, 128.73, 128.15, 127.66, 127.26, 114.96, 80.50, 73.54, 70.11, 58.19, 52.83, 44.26, 28.42. IR (ATR): 3356, 3014, 2978, 1735, 1672, 1509, 1253, 1167 cm^{-1}. HRMS (ESI-TOF) *m/z* calc'd for $C_{24}H_{30}N_2O_7Na$ $[M+Na]^+$: 481.1951, found: 481.1958.

Methyl (*Z*)-3-(4-(benzyloxy)phenyl)-2-(2-((tert-butoxycarbonyl)amino)acetamido)acrylate (S8)

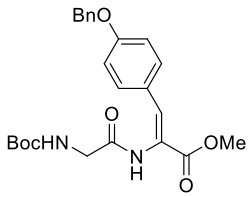

The product was prepared by method B using dipeptide **S7** (4.70 g, 10.3 mmol) and purified by column chromatography (eluting with 7:3 hexanes/ethyl acetate) to afford the product as a white solid (3.7 g, 82%, 2 steps). ^1H NMR (400 MHz, $CDCl_3$) δ 7.61 (s, 1H), 7.50–7.31 (m, 7H), 6.96 (d, *J* = 8.8 Hz, 2H), 5.24 (s, 1H), 5.07 (s, 2H), 3.94 (s, 1H), 3.82 (s, 3H), 1.45 (s, 9H). ^{13}C NMR (126 MHz, $CDCl_3$) δ 168.54, 165.85, 160.07, 156.34, 136.59, 133.89, 132.04, 128.80, 128.29, 127.64, 126.33, 121.33, 115.14, 80.68, 70.14, 52.76, 44.99, 28.45. IR (ATR): 3370, 3248, 3009, 2978, 1757, 1667, 1595, 1504, 1248 cm^{-1}. HRMS (ESI-TOF) *m/z* calc'd for $C_{24}H_{28}N_2O_6Na$ $[M+Na]^+$: 463.1845, found: 463.1850.

(*Z*)-3-(4-(benzyloxy)phenyl)-2-(2-((tert-butoxycarbonyl)amino)acetamido)acrylic acid (S9)

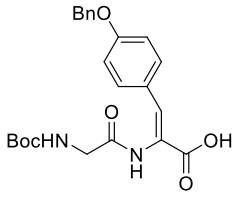

The product prepared by method C using methyl ester **S8** (3.70 g, 8.40 mmol) and was obtained as a white solid (3.5 g, 99%). ^1H NMR (500 MHz, DMSO) δ 9.28 (s, 1H), 7.57 (d, *J* = 8.4 Hz, 2H), 7.44 (m, 2H), 7.39 (m, 2H), 7.33 (m, 1H), 7.22 (s, 1H), 7.08 (t, *J* = 5.6 Hz, 1H), 6.98 (d, *J* = 8.7 Hz, 2H),

5.14 (s, 2H), 3.67 (d, *J* = 5.8 Hz, 2H), 1.39 (s, 9H). ^{13}C NMR (126 MHz, DMSO) δ 168.83, 166.58, 158.82, 155.89, 136.86, 131.78, 128.79, 128.72, 128.49, 127.91, 127.67, 126.74, 114.67, 78.07, 69.21, 43.45, 28.23. IR (ATR): 3256, 3005, 2977, 2927, 1691, 1662, 1506, 1182 cm^{-1}. HRMS (ESI-TOF) *m/z* calc'd for $C_{23}H_{26}N_2O_6Na$ $[M+Na]^+$: 449.1689, found: 449.1691.

Methyl ((*Z*)-2-((*S*)-2-((*Z*)-3-(4-(benzyloxy)phenyl)-2-(2-((tert-butoxycarbonyl)amino)acetamido)acrylamido)propanamido)-3-phenylacryloyl)-L-alaninate (S10)

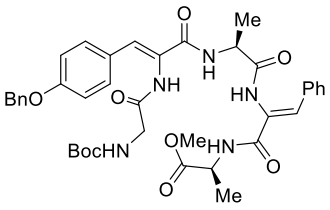

The product was obtained using method A using carboxylic acid **S9** (3.0 g, 7.0 mmol), amine **1.4** (3.0 g, 7.0 mmol), Et_3N (2.90 mL, 21.1 mmol), and MeCN (70 mL) as solvent and purified via column chromatography (eluting with 90:10 DCM/MeOH) to afford the product as a light yellow solid (3.04 g, 60%). ^{1}H NMR (500 MHz, DMSO) δ 9.58 (s, 1H), 9.53 (d, *J* = 11.6 Hz, 1H), 8.18 (d, *J* = 4.9 Hz, 1H), 8.04 (d, *J* = 6.5 Hz, 1H), 7.58 (d, *J* = 6.3 Hz, 2H), 7.55 (d, *J* = 8.7 Hz, 2H), 7.44 (d, *J* = 7.2 Hz, 2H), 7.39 (t, *J* = 7.3 Hz, 4H), 7.37 – 7.30 (m, 3H), 7.19 – 7.13 (m, 2H), 7.01 (d, *J* = 9.1 Hz, 2H), 5.15 (s, 2H), 4.36 (p, *J* = 7.1 Hz, 1H), 4.32 – 4.24 (m, 1H), 3.76 – 3.66 (m, 2H), 3.65 (s, 3H), 1.39 (s, 9H), 1.38 – 1.33 (m, 6H). ^{13}C NMR (126 MHz, DMSO) δ 172.98, 172.35, 169.86, 165.90, 164.08, 158.85, 156.25, 136.82, 133.72, 131.56, 130.74, 129.65, 129.52, 128.98, 128.51, 128.48, 128.20, 127.91, 127.65, 126.39, 126.05, 114.89, 78.38, 69.22, 51.90, 50.15, 48.39, 43.91, 28.21, 16.82, 16.18. IR (ATR): 3261, 3018, 2982, 2942, 1739, 1716, 1654, 1618, 1600, 1505, 1163 cm^{-}

[1]. HRMS (ESI-TOF) *m/z* calc'd for $C_{39}H_{45}N_5O_9Na$ $[M+Na]^+$: 750.3115, found: 750.3097. $[\alpha]^{25}_D$ –32 (*c* = 0.30, MeOH).

((*Z*)-2-((*S*)-2-((*Z*)-3-(4-(benzyloxy)phenyl)-2-(2-((tert-butoxycarbonyl)amino)acetamido)acrylamido)propanamido)-3-phenylacryloyl)-L-alanine (S11)

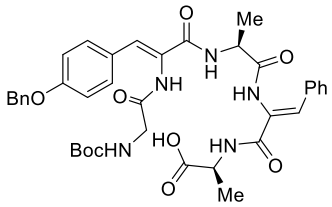

The product was obtained using method C from methyl ester **S10** (2.92 g, 4.01 mmol) as a light yellow solid in quantitative yield. ^{1}H NMR (400 MHz, DMSO) δ 9.58 (s, 1H), 9.55 (s, 1H), 8.14 (d, *J* = 5.3 Hz, 1H), 7.88 (d, *J* = 6.7 Hz, 1H), 7.58 (d, *J* = 7.3 Hz, 2H), 7.55 (d, *J* = 8.8 Hz, 2H), 7.44 (d, *J* = 6.9 Hz, 2H), 7.43 – 7.36 (m, 4H), 7.34 (dd, *J* = 7.1, 1.8 Hz, 2H), 7.30 (s, 1H), 7.21 (t, *J* = 5.3 Hz, 1H), 7.18 (s, 1H), 7.01 (d, *J* = 8.9 Hz, 2H), 5.14 (s, 2H), 4.40 – 4.28 (m, 1H), 4.25 – 4.14 (m, 1H), 3.79 – 3.63 (m, 2H), 1.39 (s, 9H), 1.37 – 1.29 (m, 6H). ^{13}C NMR (101 MHz, DMSO) δ 174.02, 172.29, 169.94, 165.67, 163.74, 158.85, 156.28, 136.86, 133.84, 131.59, 130.33, 129.66, 129.52, 128.88, 128.59, 128.51, 128.44, 127.93, 127.67, 126.50, 126.12, 114.89, 78.37, 69.25, 49.96, 48.69, 43.95, 28.23, 17.37, 16.41. IR (ATR): 3266, 3018, 2982, 2928, 1685, 1654, 1600, 1514, 1244, 1181 cm^{-1}. HRMS (ESI-TOF) *m/z* calc'd for $C_{38}H_{43}N_5O_9Na$ $[M+Na]^+$: 736.2958, found: 736.2947. $[\alpha]^{27}_D$ +18 (*c* = 0.25, MeOH).

((*Z*)-2-((*S*)-2-((*Z*)-2-(2-aminoacetamido)-3-(4-(benzyloxy)phenyl)acrylamido)propanamido)-3-phenylacryloyl)-L-alanine (1.12)

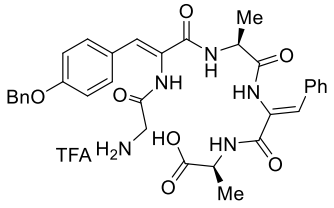

The product was obtained using method D using carboxylic acid **S11** (2.85 g, 3.99 mmol) as a yellow solid in quantitative yield. ^{1}H NMR (400 MHz, DMSO) δ 9.63 (s, 1H), 8.39 (d, *J* = 5.2 Hz, 1H), 7.96 (d, *J* = 6.9 Hz, 1H), 7.59 (d, *J* = 7.3 Hz, 2H), 7.54 (d, *J* = 8.8 Hz, 2H), 7.48 – 7.31 (m, 8H), 7.29 (s, 1H), 7.20 (s, 1H), 7.04 (d, *J* = 8.7 Hz, 2H), 5.16 (s, 2H), 4.44 – 4.16 (m, 2H), 3.80 (dd, *J* = 34.5, 16.3 Hz, 2H), 1.43 – 1.27 (m, 6H). ^{13}C NMR (126 MHz, DMSO) δ 174.00, 172.31, 166.19, 165.23, 164.00, 158.95, 136.77, 133.83, 131.47, 130.10, 129.77, 129.58, 129.50, 128.87, 128.53, 128.48, 127.93, 127.64, 126.11, 125.47, 115.00, 69.26, 50.02, 48.22, 40.71, 17.00, 16.33. IR (ATR): 3261, 3023, 2973, 1689, 1645, 1600, 1509, 1167 cm^{-1}. HRMS (ESI-TOF) *m/z* calc'd for $C_{33}H_{35}N_5O_7Na$ $[M+Na]^+$: 636.2434, found: 636.2422. $[\alpha]^{25}_D$ +39 (*c* = 0.26, MeOH).

iv) Synthesis of Gly-ΔTyr-Ala-Phe-Ala **S14**

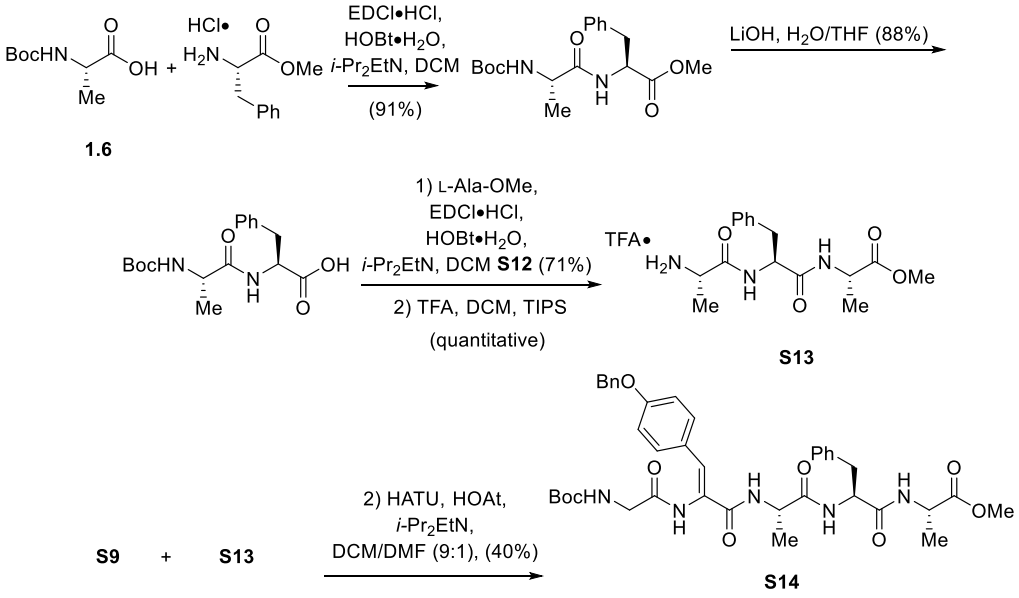

Figure 1.19 Synthesis of linear precursor **S14**.

Methyl (tert-butoxycarbonyl)-L-alanyl-L-phenylalaninate

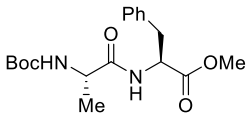

Boc-L-Ala-L-Phe-OMe was prepared according to method A using Boc-Ala-OH (3.00 g, 15.9 mmol), and L-phenylalanine methyl ester (3.76 g, 17.4 mmol) and purified by column chromatography (eluting with 2:1 hexanes/ethyl acetate) to afford the product as a white solid (5.1 g, 91% yield). The characterization data was in agreement with literature.[79]

(tert-butoxycarbonyl)-L-alanyl-L-phenylalanine

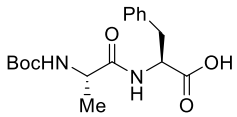

Boc-L-Ala-L-Phe-OH was prepared according to method C using Boc-L-Ala-L-Phe-OMe (5.00 g, 14.3 mmol) to afford the product as a white solid (4.2 g, 88%). The characterization data was in agreement with literature.[80]

Methyl (tert-butoxycarbonyl)-L-alanyl-L-phenylalanyl-L-alaninate (S12)

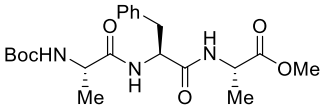

Tripeptide **S12** was prepared according to method A using Boc-L-Ala-L-Phe-OH (4.10 g, 12.5 mmol), and L-Alanine methyl ester (1.90 g, 13.7 mmol) and purified by column chromatography (eluting with 1:1 hexanes/ethyl acetate) to afford the product as a white solid (3.7 g, 71%). The characterization data was in agreement with literature.[80]

Methyl L-alanyl-L-phenylalanyl-L-alaninate (S13)

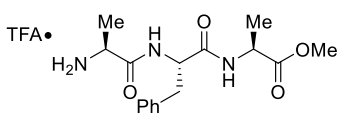

The product was prepared by method D using tripeptide **S12** (1.00 g, 2.37 mmol) and obtained as a white solid in quantitative yield. ^{1}H NMR (400 MHz, DMSO) δ 8.64 – 8.54 (m, 2H), 7.99 (d, *J* = 3.0 Hz, 2H), 7.32 – 7.25 (m, 4H), 7.25 – 7.16 (m, 1H), 4.58 (td, *J* = 9.8, 4.2 Hz, 1H), 4.29 (p, *J* =

7.2 Hz, 1H), 3.83 – 3.71 (m, 1H), 3.62 (s, 3H), 3.05 (dd, *J* = 14.0, 4.2 Hz, 1H), 2.79 (dd, *J* = 14.0, 10.0 Hz, 1H), 1.32 (d, *J* = 7.1 Hz, 3H), 1.30 (d, *J* = 7.3 Hz, 3H). ^{13}C NMR (126 MHz, DMSO) δ 172.86, 170.73, 169.56, 137.56, 129.20, 128.18, 126.46, 54.07, 51.94, 47.95, 47.64, 37.29, 17.23, 16.90. IR (ATR): 3727, 3066, 2947, 1652, 1539, 1200, 1136 cm^{-1}. HRMS (ESI-TOF) *m/z* calc'd for $C_{16}H_{23}N_3O_4H$ $[M+H]^+$: 322.1767, found: 322.1766. $[\alpha]^{24}_D$ –9 (*c* = 0.18, MeOH).

Methyl ((*Z*)-3-(4-(benzyloxy)phenyl)-2-(2-((tert-butoxycarbonyl)amino)acetamido)acryloyl)-L-alanyl-L-phenylalanyl-L-alaninate (S14)

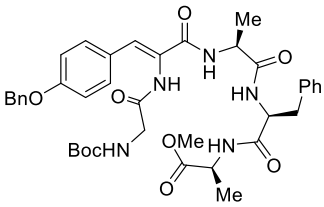

To a round botton flask equipped with a stir bar was added carboxylic acid **S9** (500 mg, 1.17 mmol), amine **S13** (562 mg, 1.29 mmol), HOAt (0.452 g, 3.32 mmol), DCM (13.5 mL) and DMF (1.5 mL). The reaction mixture was cooled to 0 °C and *i*Pr$_2$EtN (0.611 mL, 3.51 mmol) was added. HATU (532 mg, 1.40 mmol) was added in portions and the reaction warmed to rt and stirred for 24 h. The solvent was removed under reduced pressure and the product was purified by column chromatography (eluting with 20:1 DCM/MeOH) to afford the product as a white solid (337 mg, 40%). ^{1}H NMR (500 MHz, DMSO) δ 9.73 (s, 1H), 8.06 (d, *J* = 6.5 Hz, 1H), 8.01 (d, *J* = 6.7 Hz, 1H), 7.82 (d, *J* = 8.6 Hz, 1H), 7.57 (d, *J* = 8.7 Hz, 2H), 7.45 (d, *J* = 7.1 Hz, 2H), 7.40 (t, *J* = 7.4 Hz, 2H), 7.33 (t, *J* = 7.2 Hz, 1H), 7.28 – 7.21 (m, 4H), 7.21 – 7.12 (m, 2H), 7.02 (d, *J* = 9.1 Hz, 3H), 5.16 (s, 2H), 4.42 (td, *J* = 9.8, 4.3 Hz, 1H), 4.23 (m, 1H), 4.16 (m, 1H), 3.76 (qd, *J* = 16.7, 5.7 Hz, 2H), 3.60 (s, 3H), 3.10 (dd, *J* = 13.8, 4.1 Hz, 1H), 2.84 (dd, *J* = 13.8, 10.3 Hz, 1H), 1.37 (s, 9H), 1.27 (d, *J* = 7.3 Hz, 3H), 1.15 (d, *J* = 7.2

Hz, 3H). ^{13}C NMR (126 MHz, $CDCl_3$) δ 172.79, 171.91, 170.77, 170.41, 165.47, 158.73, 156.21, 137.96, 136.86, 131.52, 129.24, 128.49, 128.05, 128.01, 127.92, 127.67, 126.72, 126.43, 126.18, 114.89, 78.35, 69.22, 53.78, 51.84, 49.60, 47.71, 43.84, 36.98, 28.18, 17.12, 16.79. IR (ATR): 3272, 3081, 2984, 1640, 1539, 1515, 1455, 1228, 1173 cm^{-1}. HRMS (ESI-TOF) *m/z* calc'd for $C_{39}H_{47}N_5O_9Na$ $[M+Na]^+$: 752.3271, found: 752.3300. $[\alpha]^{23}_D$ –42 (*c* = 0.17, MeOH).

Typical procedures for macrocyclization

i) Cyclization to Gly-Tyr-Ala-ΔPhe-Ala **1.2**

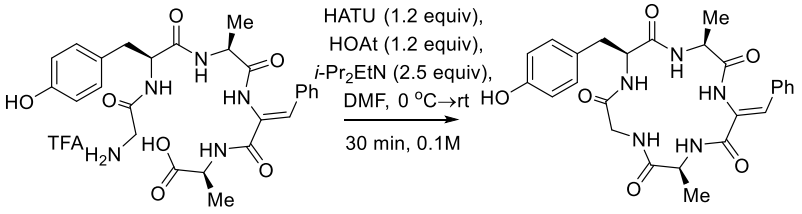

concentration (M)	selectivity (monomer:dimer)	yield
0.1	20:1	74%
0.05	39:1	81%

(3*S*,9*S*,12*S*)-6-((*Z*)-benzylidene)-12-(4-hydroxybenzyl)-3,9-dimethyl-1,4,7,10,13-pentaazacyclopentadecane-2,5,8,11,14-pentaone (1.2)

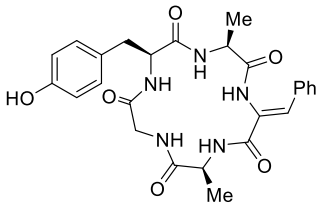

To a round bottom flask equipped with a stir bar was added peptide **1.3** (50 mg, 0.078 mmol), HOAt (13 mg, 0.094 mmol) and DMF (0.780 mL) and the mixture was stirred until homogenous. The reaction mixture was cooled to 0 °C and *i*Pr$_2$EtN (0.034 mL, 0.195 mmol) was added dropwise followed by the addition of HATU (36 mg, 0.094 mmol) and it was subsequently warmed to rt and stirred for 30 min. DMF was then removed under reduced pressure and the product was purified by column chromatography (eluting with 93:7 ethyl acetate/MeOH) to afford the product as a white solid (29.4 mg, 74%) in

20:1 selectivity of monomer over cyclodimer. When the reaction was run on 0.05 M concentration from **1.3** (0.100 g, 0.156 mmol), the product was isolated as a white solid (63.7 mg, 81%) in 39:1 selectivity of monomer over cyclodimer. The selectivity was determined by LC-MS analysis of the unpurified reaction mixture. ^{1}H NMR (500 MHz, DMSO) δ 9.38 (s, 1H), 9.25 (s, 1H), 8.34 (d, *J* = 8.1 Hz, 1H), 8.19 (dd, *J* = 7.6, 3.3 Hz, 1H), 7.95 (t, *J* = 11.0 Hz, 1H), 7.64 (d, *J* = 8.7 Hz, 1H), 7.47 (d, *J* = 7.5 Hz, 2H), 7.37 (t, *J* = 7.5 Hz, 2H), 7.30 (t, *J* = 7.3 Hz, 1H), 7.10 (s, 1H), 6.99 (d, *J* = 8.4 Hz, 2H), 6.66 (d, *J* = 8.4 Hz, 2H), 4.48 – 4.34 (m, 3H), 4.15 (dd, *J* = 15.0, 7.7 Hz, 1H), 3.30 (dd, *J* = 15.1, 3.4 Hz, 1H), 2.81 (m, 2H), 1.27 (d, *J* = 7.0 Hz, 3H), 1.19 (d, *J* = 6.9 Hz, 3H). ^{13}C NMR (126 MHz, DMSO) δ 171.50, 170.88, 169.78, 169.03, 165.27, 156.01, 134.25, 130.05, 129.29, 128.93, 128.71, 128.48, 127.71, 127.03, 115.07, 56.04, 48.44, 48.27, 43.40, 37.45, 16.88, 16.87. IR (ATR): 3257, 3052, 2978, 1635, 1508, 1440, 1240 cm^{-1}. HRMS (ESI-TOF) *m/z* calc'd for $C_{26}H_{29}N_5O_6Na$ $[M+Na]^+$: 530.2015, found: 530.2001. $[\alpha]^{26}_D$ –76 (*c* = 0.30, MeOH).

ii) Cyclization to Gly-Tyr-Ala-Phe-Ala **1.1**

Preparation of authentic material of dichotomin E

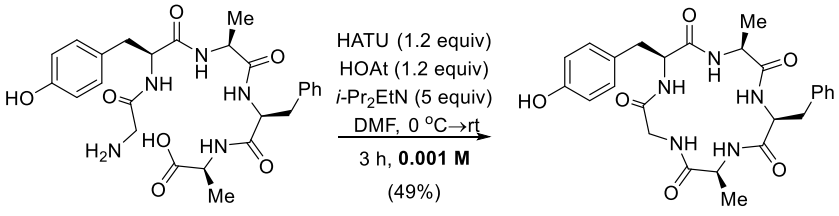

1.11 **1.1**

To a round bottom flask equipped with a stir bar was added peptide **1.11** (100 mg, 0.190 mmol), HOAt (31 mg, 0.228 mmol) and DMF (190 mL) and the mixture was stirred until homogenous. The reaction mixture was cooled to 0 °C and *i*-Pr$_2$EtN (0.166 mL, 0.950 mmol) was added dropwise followed by the addition of HATU (87 mg, 0.228 mmol) and it

was subsequently warmed to rt and stirred for 30 min. DMF was then removed under reduced pressure. The peptide was dissolved in 10 mL 38% MeCN/H_2O, filtered through a 0.20 micron filter, and purified by RP-HPLC on a C_{18} column (eluting with MeCN and H_2O containing 0.1% TFA, linear gradient 20-70% MeCN over 45 min). The pure fractions were combined, and concentrated under reduced pressure to afford dichotomin E **1.1** as a colorless powder (47 mg, 50%). ^{1}H NMR (400 MHz, Pyr, 303 K) δ 9.73 (br t, *J* = 5.6 Hz, 1H), 9.34 (d, *J* = 7.1 Hz, 1H), 9.10 (d, *J* = 8.2 Hz, 1H), 9.06 (d, *J* = 8.0 Hz, 1H), 8.77 (s, 1H), 7.40 (d, *J* = 7.4 Hz, 2H), 7.28 (m, 2H), 7.29 (d, *J* = 8.0 Hz, 2H), 7.23 (m, 1H), 7.09 (d, *J* = 8.2 Hz, 2H), 5.15 (td, *J* = 8.4, 6.8 Hz, 1H), 4.93 – 4.85 (m, 1H), 4.84 – 4.77 (m, 1H), 4.58 (dd, *J* = 14.6, 6.8 Hz, 1H), 4.51 – 4.42 (m, 1H), 3.73 (dd, *J* = 14.4, 4.9 Hz, 1H), 3.54 (m, 2H), 3.40 (dd, *J* = 13.7, 6.8 Hz, 1H), 3.16 (dd, *J* = 13.9, 8.8 Hz, 1H), 1.62 (d, *J* = 6.8 Hz, 3H), 1.58 (d, *J* = 7.1 Hz, 3H). ^{1}H NMR (500 MHz, DMSO, 298 K) δ 9.21 (s, 1H), 8.55 (br t, *J* = 5.7 Hz, 1H), 8.08 (d, *J* = 7.4 Hz, 1H), 8.07 (d, *J* = 7.6 Hz, 1H), 8.04 (d, *J* = 8.4 Hz, 1H), 7.84 (d, *J* = 8.2 Hz, 1H), 7.28 (m, 2H), 7.21 (t, *J* = 7.5 Hz, 3H), 7.01 (d, *J* = 8.4 Hz, 2H), 6.65 (d, *J* = 8.4 Hz, 2H), 4.26 – 4.23 (m, 1H), 4.23 – 4.18 (m, 1H), 4.13 – 4.09 (m, 1H), 4.07 – 4.03 (m, 1H), 3.92 (dd, *J* = 14.4, 6.3 Hz, 1H), 3.28 (dd, *J* = 14.4, 5.2 Hz, 1H), 3.11 (dd, *J* = 13.4, 9.6 Hz, 1H), 3.04 (dd, *J* = 13.2, 5.1 Hz, 1H), 2.93 (dd, *J* = 14.0, 5.3 Hz, 1H), 2.71 (dd, *J* = 13.9, 9.5 Hz, 1H), 1.23 (d, *J* = 6.7 Hz, 3H), 1.21 (d, *J* = 6.8 Hz, 3H). ^{13}C NMR (126 MHz, Pyr, 303 K) δ 174.15, 173.67, 173.20, 172.55, 171.43, 158.14, 138.96, 131.21, 130.17, 129.25, 128.73, 127.45, 116.69, 58.33, 57.13, 52.32, 50.38, 45.04, 37.96, 37.86, 17.81, 17.44. ^{13}C NMR (126 MHz, DMSO, 298 K) δ 172.52, 171.66, 170.81, 170.47, 169.24, 155.88, 137.73, 129.90, 129.12, 128.24, 127.66, 126.47, 115.03, 56.92, 55.72, 49.60, 48.30, 43.33, 36.07, 22.53, 17.46, 17.09. IR (ATR): 3281,

1648, 1512, 1442, 1207, 1160 cm^{-1}. IR (ATR): 3281, 1648, 1512, 1442, 1207, 1160 cm^{-1}. HRMS (ESI-TOF) *m/z* calc'd for $C_{26}H_{31}N_5O_6Na$ $[M+Na]^+$: 532.2172 found: 532.2169. $[\alpha]^{25}_D$ +67 (*c* = 0.24, MeOH). For detailed analysis, see table 1.2 on page 49.

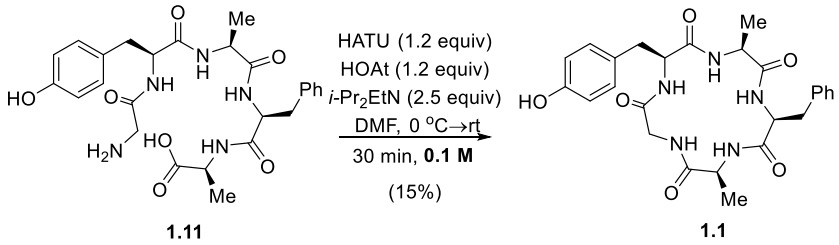

1.11 **1.1**

To a round bottom flask equipped with a stir bar was added peptide **1.11** (50 mg, 0.095 mmol), HOAt (15 mg, 0.11 mmol) and DMF (0.950 mL) and the mixture was stirred until homogenous. The reaction mixture was cooled to 0 °C and *i*-Pr_2EtN (0.042 mL, 0.238 mmol) was added dropwise followed by the addition of HATU (36 mg, 0.094 mmol) and it was subsequently warmed to rt and stirred for 30 min. DMF was then removed under reduced pressure. The peptide was dissolved in 10 mL 20% MeCN/H_2O, filtered through a 0.20 micron filter, and purified by RP-HPLC on a C_{18} column (eluting with MeCN and H_2O containing 0.1% TFA, linear gradient 15-60% MeCN over 45 min). The pure fractions were combined, and concentrated under reduced pressure to afford dichotomin E **1.1** as an off-white solid (7.2 mg, 15%). The cyclic dimer was also obtained as ~2:1 mixture of diastereomers (5.0 mg, 10%). MS (ESI) *m/z* calc'd for $C_{52}H_{62}N_{10}O_{12}H$ $[M+H]^+$: 1019.5 found: 1019.5.

iii) Cyclization to Gly-ΔTyr-Ala-ΔPhe-Ala **1.13**

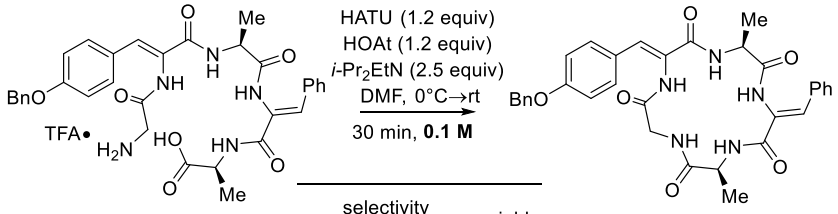

selectivity (monomer:dimer)	yield
26:1	84%

(3*S*,9*S*)-6-((*Z*)-benzylidene)-12-((*Z*)-4-(benzyloxy)benzylidene)-3,9-dimethyl-1,4,7,10,13-pentaazacyclopentadecane-2,5,8,11,14-pentaone (1.13)

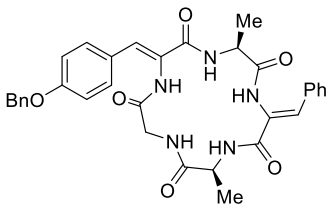

To a round bottom flask equipped with a stir bar was added peptide **1.12** (1.00 g, 1.37 mmol), HOAt (225 mg, 1.65 mmol) and DMF (13.7 mL) and the mixture was stirred until homogenous. The reaction mixture was cooled to 0 °C and *i*-Pr$_2$EtN (0.596 mL, 3.43 mmol) was added dropwise followed by the addition of HATU (627 mg, 1.65 mmol). The reaction mixture was subsequently warmed to rt and stirred for 30 min. DMF was then removed via vacuum distillation and the product was purified by column chromatography (eluting with 93:7 DCM/MeOH) to afford cyclic peptide **1.13** as a light yellow solid (684 mg, 84%) in 26:1 selectivity for the monomer over cyclodimer. The selectivity was determined by LC-MS analysis of the unpurified reaction mixture. ^{1}H NMR (500 MHz, DMSO) δ 9.47 (s, 1H), 9.31 (s, 1H), 8.20 (d, *J* = 7.5 Hz, 1H), 8.13 (s, 1H), 8.02 (d, *J* = 8.3 Hz, 1H), 7.51 (t, *J* = 7.4 Hz, 4H), 7.46 (d, *J* = 7.0 Hz, 2H), 7.43 – 7.37 (m, 4H), 7.33 (dt, *J* = 10.1, 7.2 Hz, 2H), 7.14 (s, 1H), 7.07 – 6.99 (m, 3H), 5.15 (s, 2H), 4.61 – 4.48 (m, 1H), 4.44 – 4.34 (m, 1H), 4.06 (dd, *J* = 15.6, 6.2 Hz, 1H), 3.84 (dd, *J* = 15.3, 4.2 Hz, 1H), 1.28 (d, *J* = 6.8 Hz, 6H).^{13}C NMR (126 MHz, DMSO) δ 172.04, 170.40, 167.97, 165.96, 165.19, 158.76, 136.85, 134.24, 131.41, 129.32, 129.08, 128.68, 128.49, 128.20,

128.11, 127.93, 127.73, 127.66, 126.71, 125.57, 114.76, 69.23, 49.31, 48.80, 43.37, 17.29, 17.10. IR (ATR): 3023, 2969, 2910, 1680, 1644, 1631, 1613, 1500, 1174 cm^{-1}. HRMS (ESI-TOF) *m/z* calc'd for $C_{33}H_{33}N_5O_6Na$ $[M+Na]^+$: 618.2328, found: 618.2327. $[\alpha]^{25}_D$ +123 (*c* = 0.30, MeOH).

General procedure for hydrogenation

i) Hydrogenation of Gly-Tyr-Ala-ΔPhe-Ala **1.2**

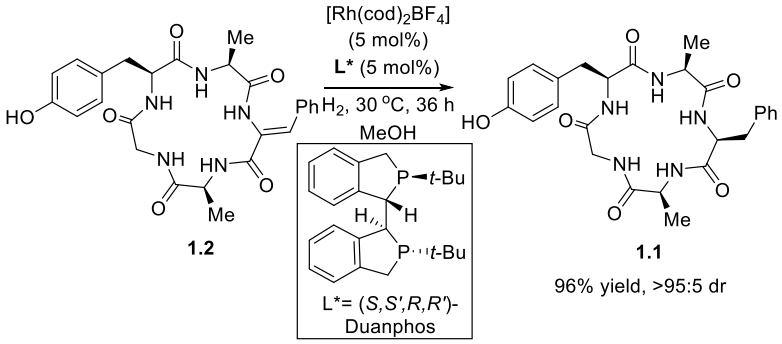

Dichotomin E (**1**)

In a N_2-filled glovebox, $[Rh(cod)_2BF_4]$ (0.40 mg, 0.0010 mmol, 5 mol%) and (*S,S',R,R'*)-Duanphos (0.40 mg, 0.0010 mmol, 5 mol%) were added to a ½ dr vial equipped with a stir bar containing pentapeptide **1.2** (10 mg, 0.020 mmol). MeOH (394 µL) was added and the vial was capped with a screwcap with a slitted rubber septum and taken outside of the glovebox. The vial was sonicated to ensure all contents were dissolved and then placed in the HEL CATalyst block and the head was screwed into place. The block was filled then purged three times with hydrogen, and then pressurized with hydrogen to 30 atm. The reaction stirred at 30 °C and was stopped after 36 h. The solvent was concentrated under reduced pressure and the reaction mixture was triturated with DCM to afford dichotomin E as an off-white solid (9.6 mg, 96%). ^{1}H NMR (400 MHz, Pyr-d_5, 303 K) δ 9.73 (br t, *J* = 5.6 Hz, 1H), 9.34 (d, *J* = 7.1 Hz, 1H), 9.10 (d, *J* = 8.2 Hz, 1H), 9.06

(d, *J* = 8.0 Hz, 1H), 8.77 (s, 1H), 7.40 (d, *J* = 7.4 Hz, 2H), 7.28 (m, 2H), 7.29 (d, *J* = 8.0 Hz, 2H), 7.23 (m, 1H), 7.09 (d, *J* = 8.2 Hz, 2H), 5.15 (td, *J* = 8.4, 6.8 Hz, 1H), 4.93 – 4.85 (m, 1H), 4.84 – 4.77 (m, 1H), 4.58 (dd, *J* = 14.6, 6.8 Hz, 1H), 4.51 – 4.42 (m, 1H), 3.73 (dd, *J* = 14.4, 4.9 Hz, 1H), 3.54 (m, 2H), 3.40 (dd, *J* = 13.7, 6.8 Hz, 1H), 3.16 (dd, *J* = 13.9, 8.8 Hz, 1H), 1.62 (d, *J* = 6.8 Hz, 3H), 1.58 (d, *J* = 7.1 Hz, 3H). ^{1}H NMR (500 MHz, DMSO, 298 K) δ 9.21 (s, 1H), 8.55 (br t, *J* = 5.7 Hz, 1H), 8.08 (d, *J* = 7.4 Hz, 1H), 8.07 (d, *J* = 7.6 Hz, 1H), 8.04 (d, *J* = 8.4 Hz, 1H), 7.84 (d, *J* = 8.2 Hz, 1H), 7.28 (m, 2H), 7.21 (t, *J* = 7.5 Hz, 3H), 7.01 (d, *J* = 8.4 Hz, 2H), 6.65 (d, *J* = 8.4 Hz, 2H), 4.26 – 4.23 (m, 1H), 4.23 – 4.18 (m, 1H), 4.13 – 4.09 (m, 1H), 4.07 – 4.03 (m, 1H), 3.92 (dd, *J* = 14.4, 6.3 Hz, 1H), 3.28 (dd, *J* = 14.4, 5.2 Hz, 1H), 3.11 (dd, *J* = 13.4, 9.6 Hz, 1H), 3.04 (dd, *J* = 13.2, 5.1 Hz, 1H), 2.93 (dd, *J* = 14.0, 5.3 Hz, 1H), 2.71 (dd, *J* = 13.9, 9.5 Hz, 1H), 1.23 (d, *J* = 6.7 Hz, 3H), 1.21 (d, *J* = 6.8 Hz, 3H). ^{13}C NMR (126 MHz, Pyr, 303 K) δ 174.15, 173.67, 173.20, 172.55, 171.43, 158.14, 138.96, 131.21, 130.17, 129.25, 128.73, 127.45, 116.69, 58.33, 57.13, 52.32, 50.38, 45.04, 37.96, 37.86, 17.81, 17.44. ^{13}C NMR (126 MHz, DMSO, 298 K) δ 172.52, 171.66, 170.81, 170.47, 169.24, 155.88, 137.73, 129.90, 129.12, 128.24, 127.66, 126.47, 115.03, 56.92, 55.72, 49.60, 48.30, 43.33, 36.07, 22.53, 17.46, 17.09. IR (ATR): 3281, 1648, 1512, 1442, 1207, 1160 cm^{-1}. IR (ATR): 3281, 1648, 1512, 1442, 1207, 1160 cm^{-1}. HRMS (ESI-TOF) *m/z* calc'd for $C_{26}H_{31}N_5O_6Na$ $[M+Na]^+$: 532.2172 found: 532.2169. $[\alpha]^{25}_D$ +67 (*c* = 0.24, MeOH).

^{1}H NMR comparison of literature,[42] authentic material synthesized via SPPS, and synthetic material after hydrogenation is given below (Table 1.2). (Note: due to rapid proton exchange and other dynamic effects, the ^{1}H NMR spectrum of the synthetic sample of dichotomin E obtained via SPPS in pyridine–d_5 varies slightly with literature values. Therefore, characterization data was also obtained in DMSO–d_6. Dichotomin E has previously been synthesized by Tam,[42] however, no spectral data was reported and characterization of the natural product was confirmed by MALDI-MS).

Table 1.2 ^{1}H NMR data for dichotomin E, cyclo(Gly-Tyr-Ala$_1$-Phe-Ala$_2$)

	^{1}H NMR δ (multiplicity, *J* (Hz), integration)			
Proton	Literature Report (pyridine–d_5)[a] at 303 K	Synthetic Sample via SPPS (pyridine–d_5)[b] at 303 K	Synthetic Sample via SPPS (DMSO–d_6)[c] at 298 K	Synthetic Sample via Hydrogenation (DMSO–d_6)[d] at 298 K
CH_2 (Gly)	4.49 (dd, *J* = 14.5, 6.5 Hz, 1H) 3.82 (dd, *J* = 14.5, 5.1, 1H)	4.58 (dd, *J* = 14.6, 6.8 Hz, 1H) 3.73 (dd, *J* = 14.4, 4.9 Hz, 1H)	3.92 (dd, *J* = 14.4, 6.3 Hz, 1H) 3.28 (dd, *J* = 14.4, 5.3 Hz, 1H)	3.91 (dd, *J* = 14.7, 6.2 Hz, 1H) 3.28 (dd, *J* = 14.4, 5.5 Hz, 1H)
N–H (Gly)	9.74 (br t, 1H)	9.73 (br t, *J* = 5.6 Hz, 1H)	8.55 (br t, *J* = 5.8 Hz, 1H)	8.54 (br t, *J* = 5.7 Hz, 1H)
C_α–H (Tyr)	5.15 (dt, *J* = 8.6, 6.6 Hz, 1H)	5.15 (td, *J* = 8.4, 6.8 Hz, 1H)	4.24 (m, 1H)	4.24 (m, 1H)
CH_2 (Tyr)	3.23 (dd, *J* = 14.0, 8.6 Hz, 1H) 3.43 (dd, *J* = 14.0, 6.6 Hz, 1H)	3.16 (dd, *J* = 13.9, 8.8 Hz, 1H) 3.40 (dd, *J* = 13.7, 6.8 Hz, 1H)	2.71 (dd, *J* = 13.9, 9.5 Hz, 1H) 2.93 (dd, *J* = 14.0, 5.3 Hz, 1H)	2.72 (dd, *J* = 13.6, 9.3 Hz, 1H) 2.92 (dd, *J* = 13.7, 4.9 Hz, 1H)
C_{sp2}–H (Tyr)	7.28 (d, *J* = 8.4 Hz, 2H) 7.07 (d, *J* = 8.4 Hz, 2H)	7.29 (d, *J* = 8.0 Hz, 1H) 7.09 (d, *J* = 8.2 Hz, 2H)	7.01 (d, *J* = 8.4 Hz, 2H) 6.65 (d, *J* = 8.4 Hz, 2H)	7.01 (d, *J* = 8.5 Hz, 2H) 6.65 (d, *J* = 8.5 Hz, 2H)
N–H (Tyr)	9.01 (d, *J* = 8.6 Hz, 1H)	8.76 (1H)	8.04 (d, *J* = 8.4 Hz, 1H)	8.04 (d, *J* = 8.6 Hz, 1H)
C_α–H (Ala$_1$)	4.58 (br t, *J* = 7.0 Hz, 1H)	4.48 (m, 1H)	4.05 (m, 1H)	4.06 (m, 1H)
CH_3 (Ala$_1$)	1.57 (d, *J* = 7.1 Hz, 3H)	1.58 (d, *J* = 7.1 Hz, 1H)	1.21 (d, *J* = 6.8 Hz, 3H)	1.21 (d, *J* = 7.1 Hz, 3H)
N–H (Ala$_1$)	9.47 (d, *J* = 8.1 Hz, 1H)	9.34 (d, *J* = 7.1 Hz, 1H)	7.84 (d, *J* = 8.2 Hz, 1H)	7.89 (br s, 1H)
C_α–H (Phe)	4.87 (m, 1H)	4.82 (m, 1H)	4.10 (m, 1H)	4.11 (m, 1H)
CH_2 (Phe)	3.53 (m, 2H)	3.54 (m, 2H)	3.11 (dd, *J* = 13.4, 9.6 Hz, 1H) 3.04 (dd, *J* = 13.2, 5.1 Hz, 1H)	3.11 (dd, *J* = 13.4, 9.9 Hz, 1H) 3.04 (dd, *J* = 13.5, 5.4 Hz, 1H)
C_{sp2}–H (Phe)	7.39 (d, *J* = 7.3 Hz, 2H) 7.28 (t, *J* = 7.3 Hz, 2H) 7.23 (m, 1H)	7.40 (d, *J* = 7.4 Hz, 2H) 7.28 (m, 2H) 7.23 (m, 1H)	7.28 (m, 2H) 7.21 (m, 3H)	7.28 (m, 2H) 7.20 (m, 3H)
N–H (Phe)	9.30 (br s, 1H)	9.10 (d, *J* = 8.2 Hz, 1H)	8.08 (d, *J* = 7.4 Hz, 1H)	8.11 (br s, 1H)
C_α–H (Ala$_2$)	4.89 (m, 1H)	4.89 (m, 1H)	4.21 (m, 1H)	4.21 (m, 1H)
CH_3 (Ala$_2$)	1.61 (d, *J* = 6.9 Hz, 3H)	1.62 (d, *J* = 6.8 Hz, 1H)	1.23 (d, *J* = 6.7 Hz, 3H)	1.22 (d, *J* = 7.0 Hz, 3H)
N–H (Ala$_2$)	9.30 (br s, 1H)	9.06 (d, *J* = 8.0 Hz, 1H)	8.07 (d, *J* = 7.6 Hz, 1H)	8.09 (br s, 1H)

[a] Data reported by Shiro and recorded on a Bruker AM400 or AM500 spectrometer (not specified). Concentration was 15 mg/0.5 mL pyridine–d_5 [b] Data recorded on a Bruker DRX400 spectrometer. Concentration was 15 mg/0.5 mL pyridine–d_5 [c] Data recorded on a Bruker DRX500 with TCI (three channel inverse) cryoprobe. [d] Data recorded on a Bruker DRX400 spectrometer

Table 1.3 ^{13}C NMR data for dichotomin E, cyclo(Gly-Tyr-Ala_1-Phe-Ala_2)

	^{13}C NMR δ	
Carbon	Literature Report (pyridine–d_5)[a] at 303 K	Synthetic Sample via SPPS (pyridine–d_5)[b] at 303 K
CH_2 (Gly)	44.51	45.04
C=O (Gly)	171.02	171.43
C_α–H (Tyr)	56.83	57.13
C_β–H (Tyr)	37.36	37.86
C_γ-H (Tyr)	128.30	128.73
C_δ-H (Tyr)	130.73	131.21
C_ε-H (Tyr)	116.21	116.69
C_ζ-H (Tyr)	157.57	158.14
C=O (Tyr)	172.65	172.55
C_α–H (Ala_1)	51.75	52.32
CH_3 (Ala_1)	17.34	17.81
C=O (Ala_1)	173.23	173.20
C_α–H (Phe)	57.76	58.33
C_β–H (Phe)	37.63	37.96
C_γ-H (Phe)	138.42	138.96
C_δ-H (Phe)	129.71	130.17
C_ε-H (Phe)	128.76	129.25
C_ζ-H (Phe)	126.95	127.45
C=O (Phe)	173.92	174.15
C_α–H (Ala_2)	50.16	50.38
CH_3 (Ala_2)	17.34	17.44
C=O	173.92	173.67

[a] Data reported by Shiro and recorded on a Bruker AM400 or AM500 spectrometer (not specified). Concentration was 15 mg/0.5 mL pyridine–d_5. [b] Data recorded on a Bruker DRX500 with TCI (three channel inverse) cryoprobe. Concentration was 15 mg/0.5 mL pyridine–d_5.

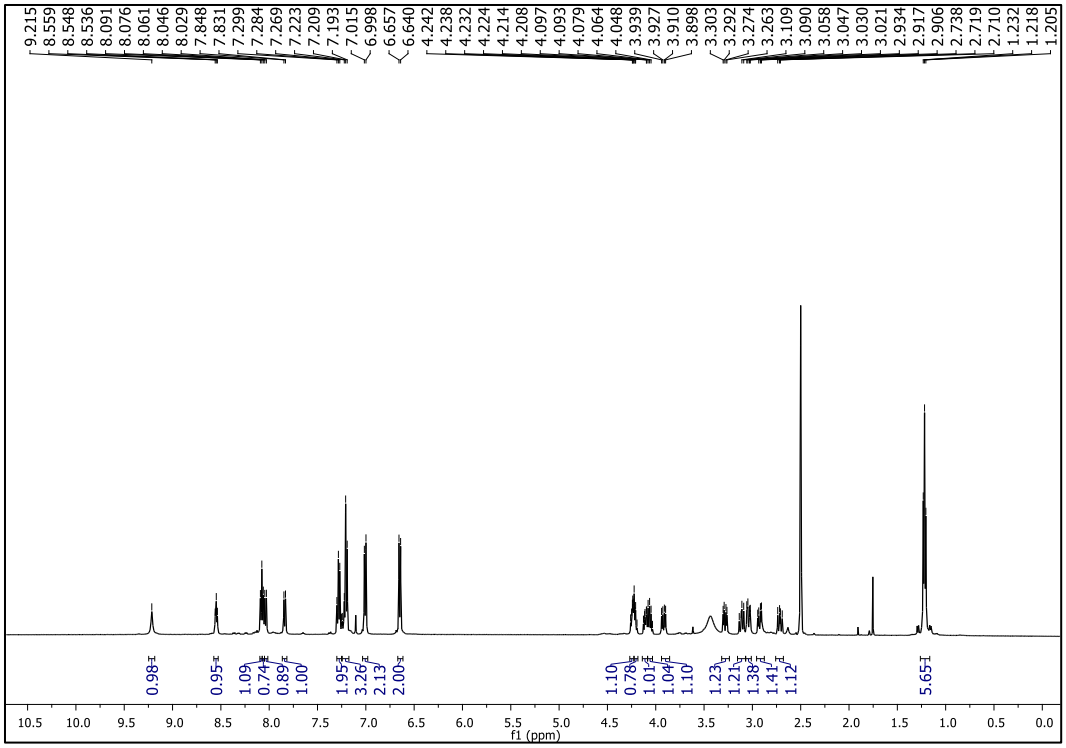

Figure 1.20. ^{1}H NMR (DMSO–d_6, 298 K) of synthetic sample of dichotomin E made via SPPS

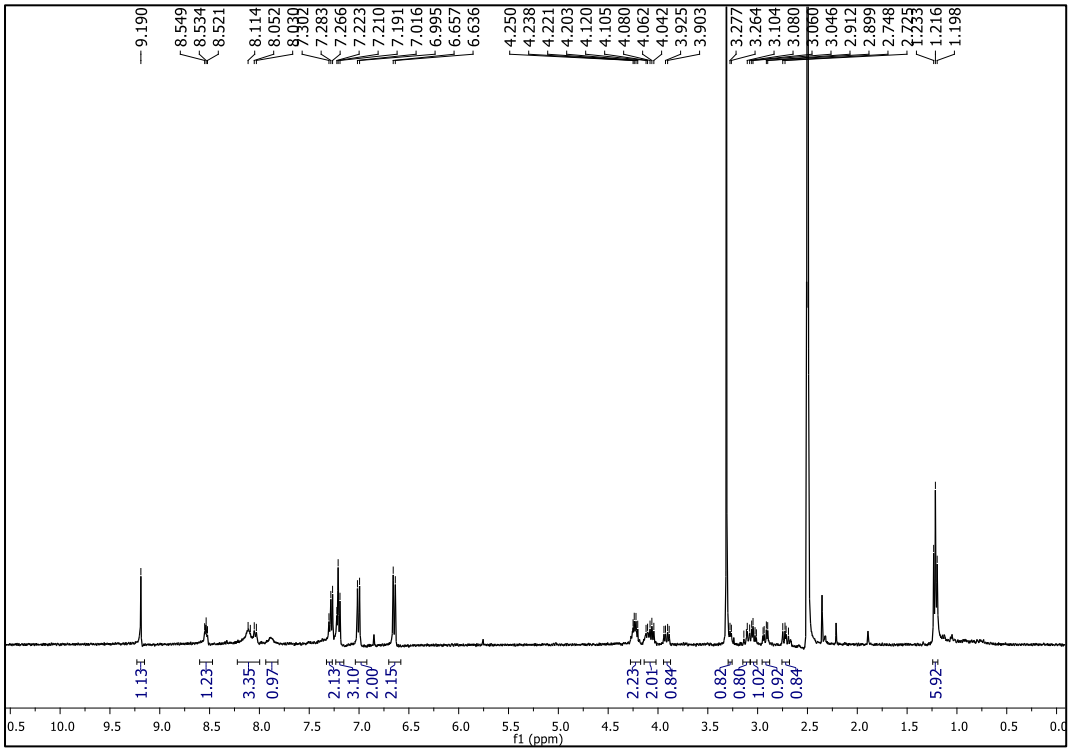

Figure 1.21. ^{1}H NMR (DMSO–d_6, 298 K) of synthetic sample of dichotomin E made via hydrogenation

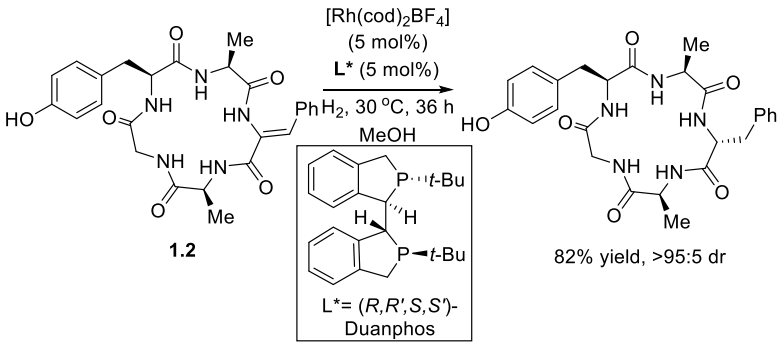

Dichotomin epimer (**1.1'**)

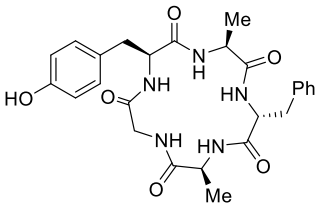

In a N_2-filled glovebox, $[Rh(cod)_2BF_4]$ (0.40 mg, 0.0010 mmol, 5 mol%) and (*R,R',S,S'*)-Duanphos (0.40 mg, 0.0010 mmol, 5 mol%) were added to a ½ dr vial equipped with a stir bar containing pentapeptide **1.2** (10 mg, 0.020 mmol). MeOH (394 µL) was added and the vial was capped with a screwcap with a slitted rubber septum and taken outside of the glovebox. The vial was then placed in the HEL CATalyst block and the head was screwed into place. The block was filled then purged three times with hydrogen, and then pressurized with hydrogen to 30 atm. The reaction stirred at 30 °C. The reaction was stopped after 36 h and the solvent was concentrated under reduced pressure. The reaction mixture was triturated with DCM to afford the product as an off-white solid (8.2 mg, 82%). ^{1}H NMR (500 MHz, DMSO) δ 9.22 (s, 1H), 8.60 (d, *J* = 7.7 Hz, 1H), 8.35 (d, *J* = 7.5 Hz, 1H), 8.09 (d, *J* = 8.4 Hz, 1H), 7.98 (t, *J* = 5.5 Hz, 1H), 7.50 (d, *J* = 7.7 Hz, 1H), 7.25 (dt, *J* = 13.9, 7.1 Hz, 4H), 7.19 (t, *J* = 7.0 Hz, 1H), 7.01 (d, *J* = 8.4 Hz, 2H), 6.65 (d, *J* = 8.4 Hz, 2H), 4.40 (dd, *J* = 14.9, 7.8 Hz, 1H), 4.34 – 4.21 (m, 2H), 4.09 (ddd, *J* = 9.9, 7.5, 5.1 Hz, 1H), 3.73 (dd, *J* = 14.4, 4.9 Hz, 1H), 3.53 (dd, *J* = 14.3, 6.3 Hz, 1H), 2.98 (dd, *J* = 13.7, 6.6 Hz, 1H), 2.88 (dd, *J* = 14.0, 4.9 Hz, 1H), 2.75 (ddd, *J* = 24.1, 13.9, 9.2 Hz, 2H), 1.14 (d, *J* = 7.2 Hz, 3H), 1.06 (d, *J* = 6.7 Hz, 3H). ^{13}C NMR (126 MHz, DMSO) δ

172.47, 171.99, 170.97, 170.84, 169.38, 155.94, 137.81, 129.89, 129.13, 128.12, 127.62, 126.31, 115.04, 56.99, 54.43, 47.91, 47.79, 42.76, 35.85, 35.39, 18.02, 17.16. IR (ATR): 3271, 3086, 2984, 1638, 1539, 1443, 1372, 1233 cm^{-1}. HRMS (ESI-TOF) *m/z* calc'd for $C_{26}H_{31}N_5O_6Na$ $[M+Na]^+$: 532.2172, found: 532.2151. $[\alpha]^{26}_D$ –14 (*c* = 0.39, MeOH).

ii) Hydrogenation of Gly-ΔTyr-Ala-ΔPhe-Ala **1.13**

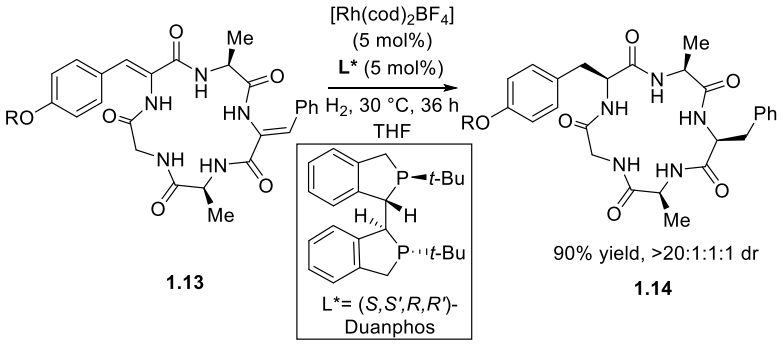

(3*S*,6*S*,9*S*,12*S*)-6-benzyl-12-(4-(benzyloxy)benzyl)-3,9-dimethyl-1,4,7,10,13-pentaazacyclopentadecane-2,5,8,11,14-pentaone (1.14)

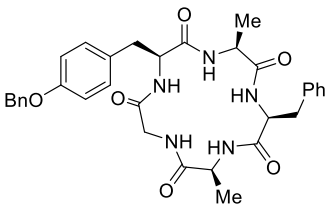

In a N_2-filled glovebox, $[Rh(cod)_2BF_4]$ (2 mg, 0.005 mmol, 5 mol%) and (*S,S',R,R'*)-Duanphos (0.8 mg, 0.002 mmol, 5 mol%) were added to a ½ dr vial equipped with a stir bar containing pentapeptide **1.13** (24 mg, 0.040 mmol). THF (0.8 mL) was added and the vial was capped with a screwcap with a slitted rubber septum and taken outside of the glovebox. The vial was sonicated to ensure all contents were dissolved and then placed in the HEL CATalyst block and the head was screwed into place. The block was filled then purged three times with hydrogen, and then pressurized with hydrogen to 30 atm. The reaction was stopped after 24 h and the solvent was removed under reduced pressure. The compound was then triturated with DCM to afford the product as a light tan solid (21.6

mg, 90%). ^{1}H NMR (400 MHz, DMSO) δ 8.56 (t, *J* = 5.7 Hz, 1H), 8.12 – 8.03 (m, 3H), 7.85 (d, *J* = 8.1 Hz, 1H), 7.44 (d, *J* = 7.0 Hz, 2H), 7.39 (t, *J* = 7.2 Hz, 2H), 7.35 – 7.30 (m, 1H), 7.28 (d, *J* = 6.9 Hz, 2H), 7.21 (t, *J* = 7.1 Hz, 3H), 7.14 (d, *J* = 8.6 Hz, 2H), 6.91 (d, *J* = 8.6 Hz, 2H), 5.06 (s, 2H), 4.31 – 4.17 (m, 2H), 4.14 – 4.02 (m, 2H), 3.92 (dd, *J* = 14.3, 6.4 Hz, 1H), 3.29 – 3.24 (m, 1H), 3.13 (dd, *J* = 13.3, 9.4 Hz, 1H), 3.04 (dd, *J* = 13.7, 5.5 Hz, 1H), 2.99 (dd, *J* = 14.3, 4.7 Hz, 1H), 2.77 (dd, *J* = 13.6, 9.3 Hz, 1H), 1.22 (dd, *J* = 7.0, 4.0 Hz, 6H). ^{13}C NMR (126 MHz, DMSO) δ 172.58, 171.65, 170.83, 170.39, 169.27, 156.99, 137.73, 137.19, 130.00, 129.79, 129.11, 128.43, 128.24, 127.80, 127.70, 126.46, 114.51, 69.11, 56.98, 55.61, 49.57, 48.28, 43.34, 36.02, 35.98, 17.52, 17.08. IR (ATR): 3077, 3014, 2978, 1672, 1658, 1645, 1500, 1239 cm^{-1}. HRMS (ESI-TOF) *m/z* calc'd for $C_{33}H_{37}N_5O_6Na$ $[M+Na]^+$: 622.2642, found: 622.2639. $[\alpha]^{27}_D$ +114 (*c* = 0.19, DMF).

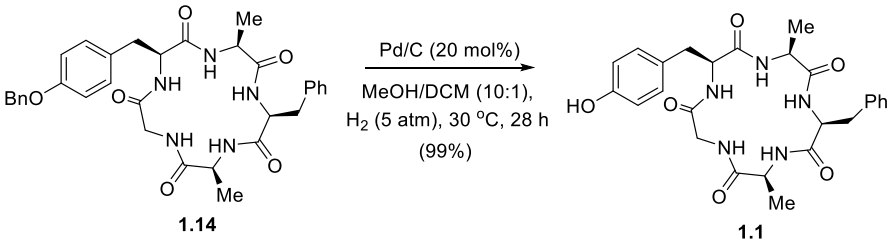

1.14 **1.1**

To a ½ dr vial equipped with a stir bar was added cyclic pentapeptide **1.14** (5 mg, 0.008 mmol) and 10% Pd/C (1.7 mg, 0.0016 mmol, 20 mol%). The contents were dissolved in MeOH (0.600 mL) and DCM (0.060 mL) and the vial was capped with a screwcap with a slitted rubber septum. The vial was sonicated to ensure all contents were dissolved and then placed in the HEL CATalyst block and the head was screwed into place. The block was filled then purged three times with hydrogen, and then pressurized with hydrogen to 5 atm. The reaction was warmed to 30 °C. After 28 h and the reaction mixture was filtered through a plug of celite to afford dichotomin E **1.1** as an off-white solid (4.1 mg, 99%). ^{1}H

NMR of the product after debenzylation showed variation in chemical shift values. The product obtained after debenzylation was then spiked with authentic synthetic sample obtained via SPPS (Table 1.2) to afford the ^{1}H NMR spectrum of dichotomin E (Figure 1.21).

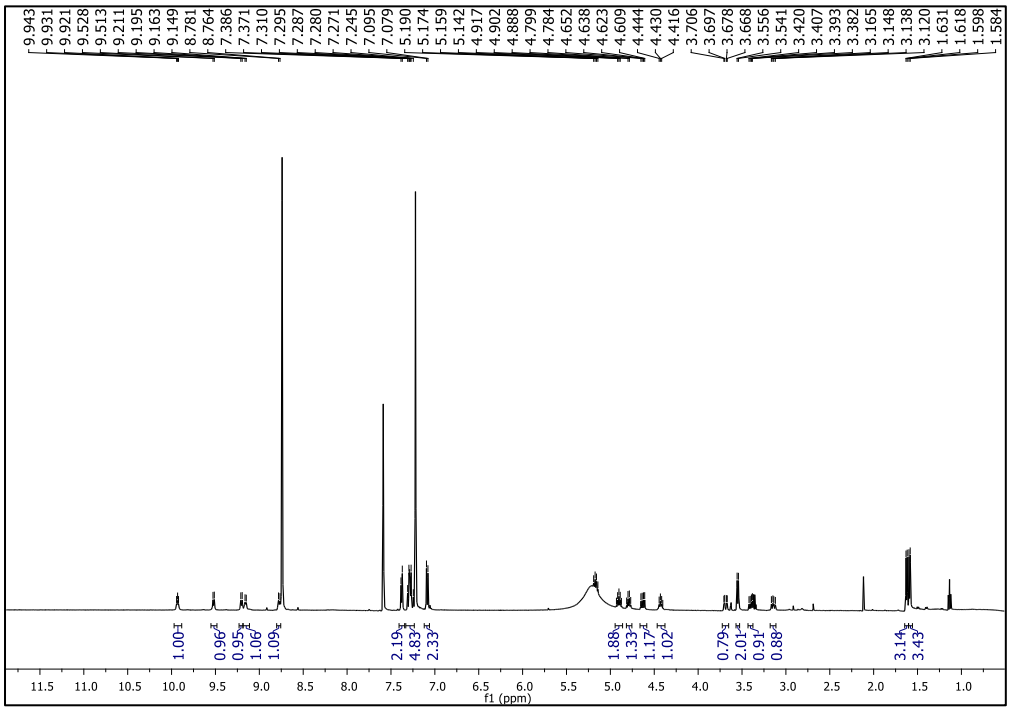

Figure 1.22. ^{1}H NMR spectrum (Pyr–*d*^{5}, 298 K) of synthetic sample of dichotomin E after debenzylation spiked with authentic material.

NMR analysis - Variable temperature NMR experiment

^{1}H-NMR variable temperature experiments[50] were performed on a 500 MHz Bruker DRX500 spectrometer with a TCI cryoprobe. For each experiment, the temperature was increased by 5 K with 10 minute equilibration time between experiments. 8 scans were collected for each data point. The experiments were conducted in DMSO solvent. After obtaining the spectra, the δ (ppm) was plotted vs. T(K), and the Δδ/ ΔT was obtained for each N–H bond.

Table 1.4 Variable temperature data for unsaturated pentapeptide **1.3**

T (K)	δ (ppm) Tyr N–H	δ (ppm) Ala N–H (internal)	δ (ppm) ΔPhe N–H	δ (ppm) Ala N–H (terminal)
293	8.5345	7.9371	9.6430	8.5933
298	8.5144	7.9170	9.6164	8.5649
303	8.4947	7.8974	9.5897	8.5364
308	8.4753	7.8782	9.5633	8.5076
313	8.4562	7.8593	9.5385	8.4780

Table 1.5 Variable temperature data for saturated pentapeptide **1.11**

T (K)	δ (ppm) Tyr N–H	δ (ppm) Ala N–H (internal)	δ (ppm) Phe N–H	δ (ppm) Ala N–H (terminal)
293	8.5562	8.3481	7.8956	8.3254
298	8.5355	8.3086	7.8792	8.2886
303	8.5186	–	7.8458	–
308	8.4997	8.2645	7.8222	8.2436
313	8.4809	8.2390	7.7995	8.2133

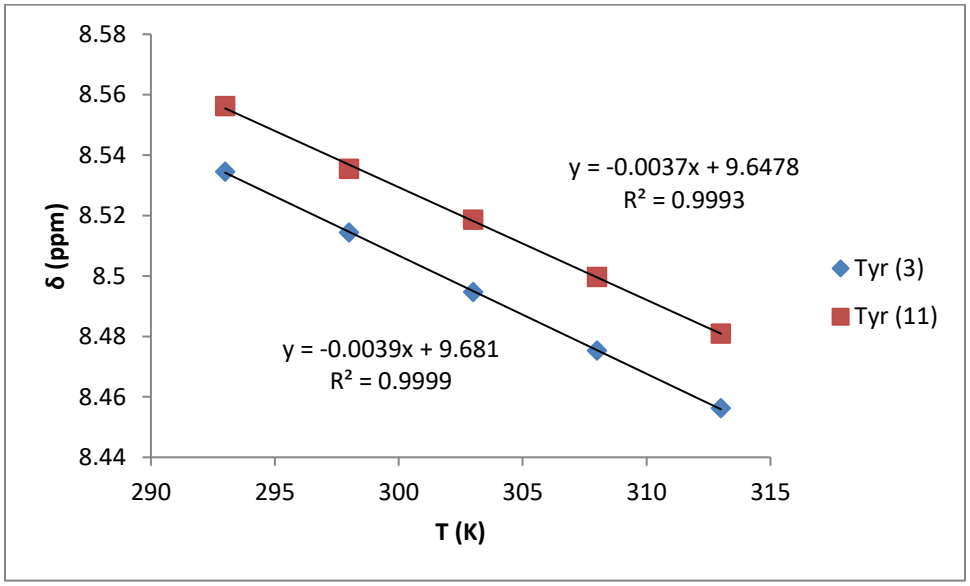

Figure 1.23 Variable temperature data comparing tyrosine N–H for unsaturated peptide **1.3** and saturated peptide **1.11**

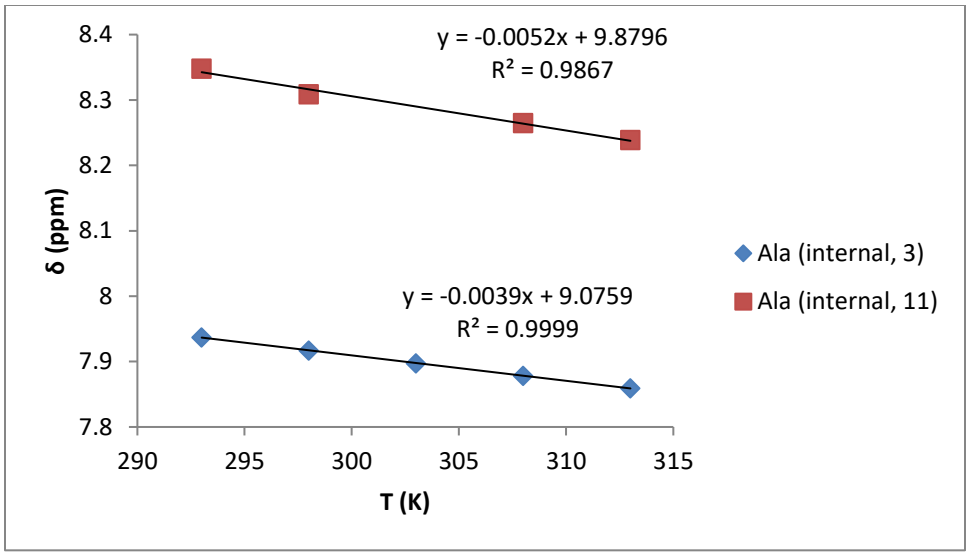

Figure 1.24 Variable temperature data comparing internal alanine N–H for unsaturated peptide **1.3** and saturated peptide **1.11**

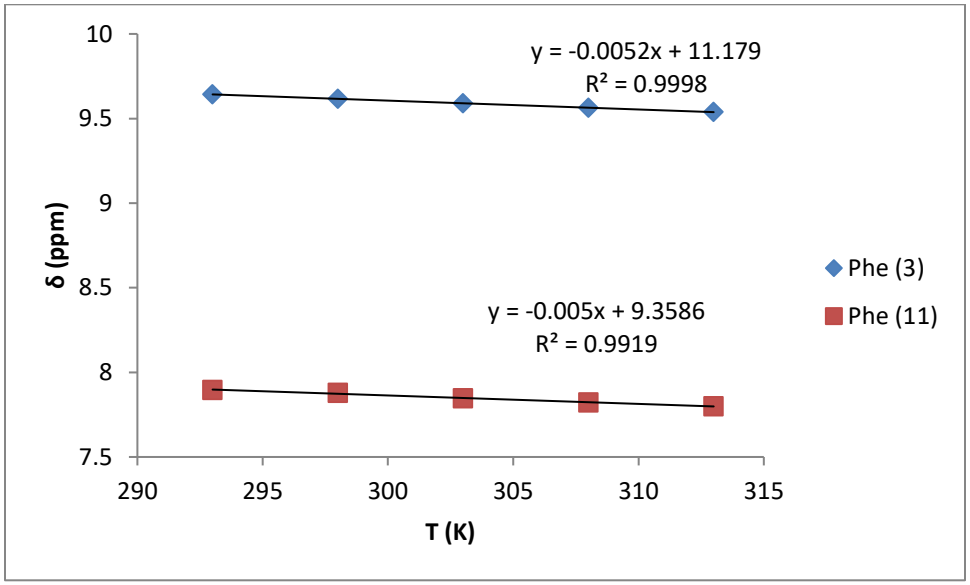

Figure 1.25 Variable temperature data comparing phenylalanine N–H for unsaturated peptide **1.3** and saturated peptide **1.11**

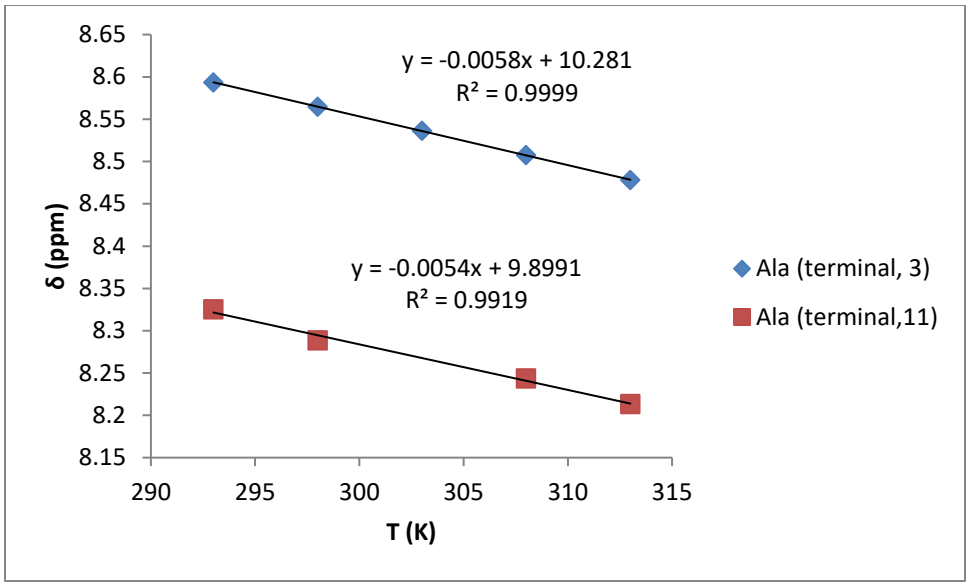

Figure 1.26. Variable temperature data comparing terminal alanine N–H for unsaturated peptide **1.3** and saturated peptide **1.11**

1.3.2 Experimental Details for Molecular Recognition of Peptides in Rh-Catalyzed Hydrogenation: Evidence for a Unidirectional Reduction

The computational data shown Figure 1.15, Figure 1.16, and Figure 1.17 was obtained by E.H. This experimental section will focus on my contributions to the project.

Typical procedures for synthesis of cyclic pentapeptides

i) Synthesis of pentapeptide **1.20**

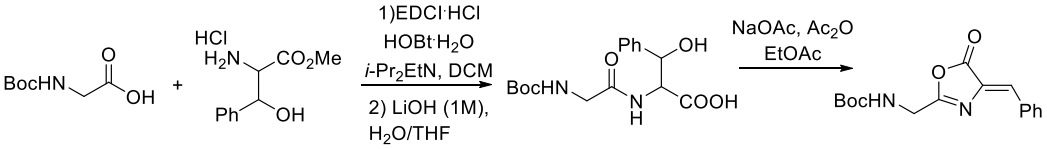

***tert*-butyl (*Z*)-((4-benzylidene-5-oxo-4,5-dihydrooxazol-2-yl)methyl)carbamate (1.18)**

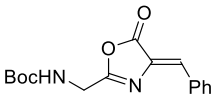

To a round bottom flask equipped with a stir bar was added Boc-Gly-OH (20 g, 114 mmol) and DL-(β-OH)–Phe–OMe **1.7** (29 g, 125 mmol) and

HOBt·H_2O (24 g, 125 mmol) and DCM (400 mL). The mixture was cooled to 0°C and *i*-Pr_2EtN (50 mL, 285 mmol) was subsequently added. EDCI·HCl (24 g, 125 mmol) was added in portions and the reaction gradually warmed to rt and stirred for 16 h. The reaction mixture was transferred to a separatory funnel and washed with sat. $NaHCO_3$ (aq), 10% $KHSO_4$ (aq), H_2O, and brine. The organic phase was dried over Na_2SO_4, filtered, and concentrated under reduced pressure. The crude reaction mixture was purified by column chromatography (eluting with 30:70 hexanes/EtOAc) and obtained as a white solid (21 g, 53% yield). Characterization data was consistent with those previously reported.[81]

To a round bottom flask equipped with a stir bar was added the corresponding methyl ester (17.2 g, 48.8 mmol), THF (244 mL), and H_2O (185 mL). The mixture was cooled to 0°C and 1M LiOH (aq) (58.6 mL, 1.2 equiv) was subsequently added. The reaction gradually warmed to rt and stirred for 16 h. The reaction mixture was quenched with 10% $KHSO_4$ (aq) and the THF was concentrated under reduced pressure. The reaction mixture was transferred to a separatory funnel where it was extracted with EtOAc three times. The organic layer was washed with brine, dried over Na_2SO_4, filtered, and concentrated under reduced pressure to afford the desired carboxylic acid, which was used without further purification.

To a round bottom flask equipped with a stir bar was added carboxylic acid (48.8 mmol) and EtOAc (98 mL). To this solution was added acetic anhydride (46 mL, 488 mmol) and sodium acetate (7.9 g, 96.7 mmol) and the mixture was stirred at rt for 16 h. Sat. $NaHCO_3$ (aq) was added to quench excess acetic anhydride and acetic acid until the reaction mixture stopped bubbling. The mixture was extracted 3x with EtOAc and the combined

organic layer was washed with brine and dried over anhydrous Na_2SO_4. The solution was filtered and solvent was evaporated under reduced pressure to afford the product as a light yellow solid (11.5 g, 79% over two steps). Characterization data was consistent with

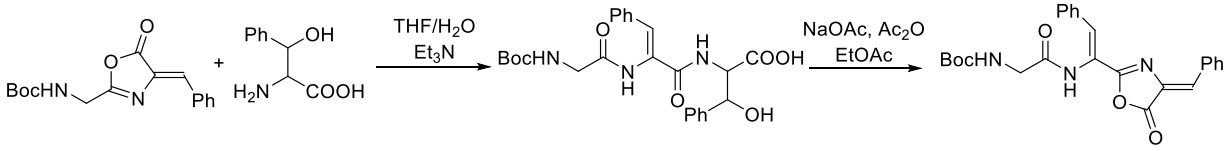

those previously reported.[82]

tert-butyl(2-(((*Z*)-1-(4-((*Z*)-benzylidene)-5-oxo-4,5-dihydrooxazol-2-yl)-2-phenylvinyl)amino)-2-oxoethyl)carbamate (S15)

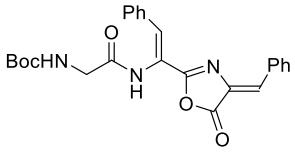

To a solution of (±)-**1.16** (7.41 g, 40.88 mmol) in THF/H_2O (1:1, 0.1 M) was added triethylamine (5.7 mL, 40.88 mmol) and the mixture was sonicated until homogeneous. The mixture was added to a solution of oxazolone **1.18** (10.3 g, 34.07 mmol) in THF (340 mL). The reaction was stirred at rt for 15 h. The mixture was acidified with 10% $KHSO_4$ (aq), extracted with 3x with EtOAc, and the organic layer was washed with brine. The organic layer was dried over anhydrous Na_2SO_4 and concentrated under reduced pressure to afford the desired carboxylic acid which was used without further purification.

To a round bottom flask equipped with a stir bar was added the carboxylic acid (34.07 mmol) and EtOAc (68 mL). To this solution was added acetic anhydride (32 mL, 340.7 mmol) and sodium acetate (5.60 g, 68.14 mmol) and the mixture was stirred at rt for 24 h. Sat. $NaHCO_3$ (aq) was added to quench excess acetic anhydride and acetic acid until the reaction mixture stopped bubbling. The mixture was extracted 3x with EtOAc and the combined organic layer was washed with brine and dried over anhydrous Na_2SO_4. The solution was filtered and solvent was evaporated under reduced pressure. The oil was

dissolved in a minimal amount of DCM and hexanes was added to precipitate the oxazolone **S15**. The solvent was decanted and the solid was washed 2x with hexanes to afford the product as a yellow solid (12.5 g, 82% over two steps). ^{1}H NMR (500 MHz, $CDCl_3$) δ 8.10 (d, *J* = 7.4 Hz, 2H), 7.98 (br s, 1H), 7.57 (br s, 2H), 7.50 (s, 1H), 7.34-7.48 (m, 6H), 7.19 (s, 1H), 5.35 (br s, 1H), 4.04 (d, *J* = 3.68 Hz, 2H), 1.46 (s, 9H). ^{13}C NMR (125 MHz, $CDCl_3$) δ 169.0, 167.1, 162.1, 156.5, 135.3, 133.5, 133.4, 133.0, 132.7, 132.5, 131.5, 130.4, 129.1, 128.9, 119.7, 110.1, 80.9, 45.2, 28.4. IR (ATR): 3268, 1784, 1689, 1650 cm^{-1}. HRMS (ESI-TOF) *m/z* calc'd for $C_{25}H_{26}N_3O_5$ $[M+H]^+$: 448.1866, found 448.1851.

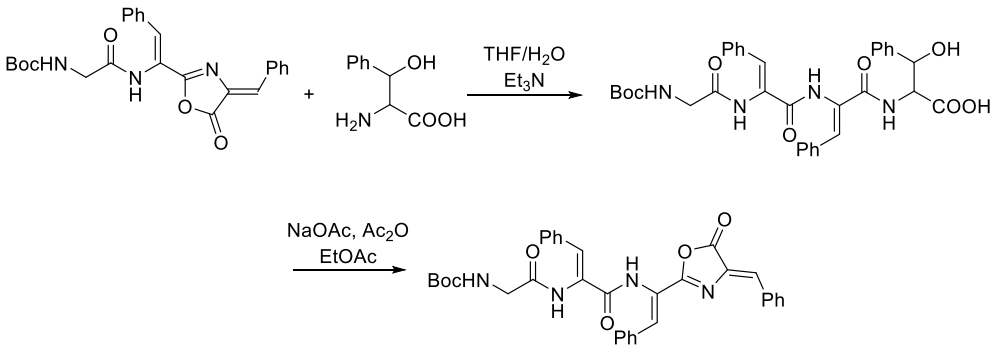

***tert*-butyl (2-(((*Z*)-3-(((*Z*)-1-(4-((*Z*)-benzylidene)-5-oxo-4,5-dihydrooxazol-2-yl)-2-phenylvinyl)amino)-3-oxo-1-phenylprop-1-en-2-yl)amino)-2-oxoethyl)carbamate (S16)**

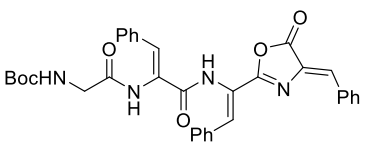

To a solution of (±)-**1.16** (6.0 g, 33.25 mmol) in THF/H_2O (1:1, 0.1 M) was added triethylamine (4.6 mL, 33.25 mmol) and the mixture was sonicated until homogeneous. The mixture was added to a solution of oxazolone **S15** (12.4 g, 27.7 mmol) in THF (270 mL). The reaction was stirred at rt for 21 h. The mixture was acidified with 10% $KHSO_4$ (aq), extracted with

3x with EtOAc, and the organic layer was washed with brine. The organic layer was dried over anhydrous Na_2SO_4 and concentrated under reduced pressure to afford the desired carboxylic acid which was used without further purification.

To a round bottom flask equipped with a stir bar was added the carboxylic acid (27.7 mmol) and EtOAc (55 mL). To this solution was added acetic anhydride (26 mL, 277 mmol) and sodium acetate (4.5 g, 55.4 mmol) and the mixture was stirred at rt for 16 h. Sat. $NaHCO_3$ (aq) was added to quench excess acetic anhydride and acetic acid until the reaction mixture stopped bubbling. The mixture was extracted 3x with EtOAc and the combined organic layer was washed with brine and dried over anhydrous Na_2SO_4. The solution was filtered and solvent was evaporated under reduced pressure. The oil was dissolved in a minimal amount of DCM and hexanes was added to precipitate the oxazolone. The solvent was decanted and the solid was washed 2x with hexanes to afford the product as a yellow solid (12.0 g, 73% over two steps). ^{1}H NMR (499 MHz, DMSO) δ 9.85 (s, 1H), 9.80 (s, 1H), 8.28 (d, *J* = 7.0 Hz, 2H), 7.92 (d, *J* = 5.0 Hz, 2H), 7.69 (d, *J* = 7.4 Hz, 2H), 7.58 (s, 1H), 7.53 – 7.36 (m, 9H), 7.35 (s, 1H), 7.27 (s, 1H), 7.11 (t, *J* = 5.7 Hz, 1H), 3.80 (d, *J* = 5.8 Hz, 2H), 1.38 (s, 9H). ^{13}C NMR (126 MHz, DMSO) δ 169.9, 166.7, 165.5, 162.4, 156.1, 135.0, 133.7, 133.3, 133.3, 133.0, 132.5, 131.3, 131.0, 130.9, 130.2, 129.9, 129.4, 129.3, 129.1, 128.9, 128.7, 128.6, 128.3, 121.9, 78.2, 43.6, 28.2.

IR (ATR): 3372, 3237, 2989, 1806, 1778, 1686, 1660 cm^{-1}. HRMS (ESI-TOF) *m/z* calc'd for $C_{34}H_{33}N_4O_6$ $[M+H]^+$: 593.2394, found 593.2368.

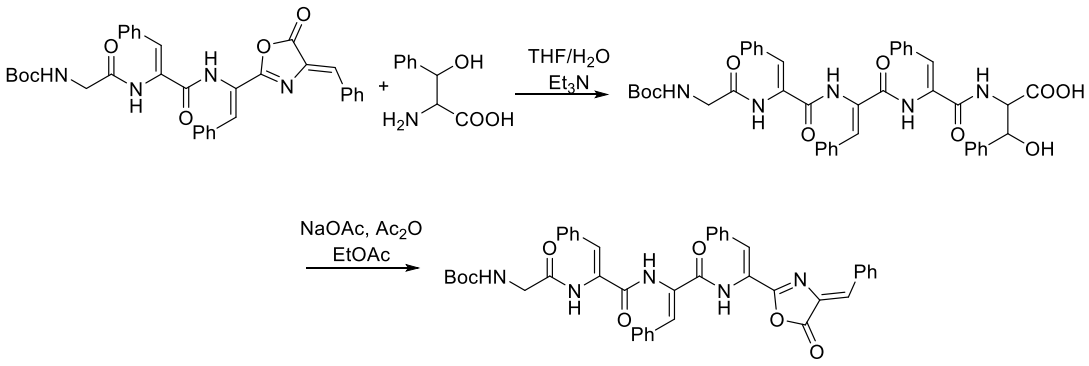

***tert*-butyl (2-(((*Z*)-3-(((Z)-3-(((*Z*)-1-(4-((*Z*)-benzylidene)-5-oxo-4,5-dihydrooxazol-2-yl)-2-phenylvinyl)amino)-3-oxo-1-phenylprop-1-en-2-yl)amino)-3-oxo-1-phenylprop-1-en-2-yl)amino)-2-oxoethyl)carbamate (1.19)**

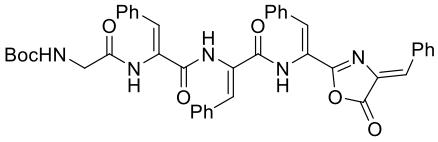

To a solution of (±)-**1.16** (114 mg, 0.628 mmol) in THF/H_2O (1:1, 0.1 M) was added triethylamine (88 µL, 0.628 mmol) and the mixture was sonicated until homogeneous. The mixture was added to a solution of oxazolone **S16** (310 mg, 0.523 mmol) in THF (10 mL). The reaction was stirred at rt for 15 h. The mixture was acidified with 10% $KHSO_4$ (aq), extracted with 3x with EtOAc, and the organic layer was washed with brine. The organic layer was dried over anhydrous Na_2SO_4 and concentrated under reduced pressure to afford the desired carboxylic acid which was used without further purification.

To a round bottom flask equipped with a stir bar was added the carboxylic acid (0.523 mmol) and EtOAc (1 mL). To this solution was added acetic anhydride (0.5 mL, 5.23 mmol) and sodium acetate (86 mg, 1.05 mmol) and the mixture was stirred at rt for 26 h. Sat. $NaHCO_3$ (aq) was added to quench excess acetic anhydride and acetic acid until the

reaction mixture stopped bubbling. The mixture was extracted 3x with EtOAc and the combined organic layer was washed with brine and dried over anhydrous Na_2SO_4. The solution was filtered and solvent was evaporated under reduced pressure. The oil was dissolved in a minimal amount of DCM and hexanes was added to precipitate the oxazolone. The solvent was decanted and the solid was washed 2x with hexanes to afford the product as a yellow solid (343 mg, 89% over two steps). ^{1}H NMR (600 MHz, DMF-d_7) δ 10.09 (s, 1H), 9.89 (s, 1H), 9.68 (s, 1H), 8.39-8.40 (m, 2H), 8.05 (d, *J* = 7.4 Hz, 1H), 7.77 (d, *J* = 7.5 Hz, 1H), 7.74 (d, *J* = 7.4 Hz, 1H), 7.68 (s, 1H), 7.49-7.56 (m, 4H), 7.39-7.48 (m, 9H), 7.35 (s, 1H), 6.93 (br, 1H), 3.96 (d, *J* = 5.4 Hz, 1H), 1.35 (s, 9H). ^{13}C NMR (125 MHz, $CDCl_3$) δ 170.8, 167.8, 164.9, 164.5, 162.6, 156.9, 135.1, 134.6, 133.7, 133.6, 133.1, 132.8, 131.7, 131.2, 131.1, 130.3, 130.1, 129.9, 129.7, 129.6, 129.5, 129.2, 129.0, 128.8, 128.7, 128.6, 127.7, 127.3, 120.7, 81.6, 45.2, 28.3. IR (ATR): 3253, 1779, 1670, 1640 cm^{-1}. HRMS (ESI-TOF) *m/z* calc'd for $C_{43}H_{40}N_5O_7$ $[M+H]^+$: 738.2922, found 738.2886.

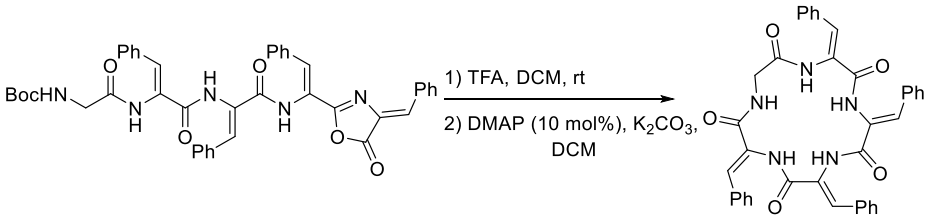

3,6,9,12-tetra((*Z*)-benzylidene)-1,4,7,10,13-pentaazacyclopentadecane-2,5,8,11,14-pentaone **(1.20)**

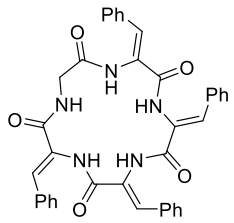

To a round bottom flask equipped with a stir bar under N_2 was added Boc-protected amine **1.19** (346 mg, 0.469 mmol) and anhydrous DCM (5.9 mL). The reaction mixture was cooled to 0 °C and TFA (0.897 mL, 11.7 mmol) was slowly added. The reaction slowly warmed to rt and stirred for 2 h. The DCM was concentrated under reduced pressure and to the mixture was added toluene to form a TFA azeotrope, which was subsequently concentrated under reduced pressure. The crude reaction mixture was further dried on the high vacuum and subsequently triturated with Et_2O to afford TFA·amine salt and was immediately used in the next reaction without further purification.

The amine (0.469 mmol) was then dissolved in anhydrous DCM (4.69 mL, 0.1M) and to this yellow solution was added anhydrous Et_3N (0.131 mL, 0.938 mmol) and DMAP (5.7 mg, 0.0469 mmol). The reaction mixture was stirred at rt for 30 min. The solution was then diluted by addition of 150 mL of DCM. The organic phase was washed four times with 10 mL 1M HCl. The organic phase was then dried with Na_2SO_4 and concentrated under reduced pressure to afford a light yellow solid. This solid was then triturated with Et_2O to afford cyclic pentapeptide **1.20** as a light yellow solid (243 mg, 81%). ^{1}H NMR (499 MHz, DMSO, 373K, d1=5 s) δ 9.63 (s, 1H), 9.38 (s, 1H), 9.34 (s, 1H), 9.23 (s, 1H), 8.05 (t, *J* = 4.4 Hz, 1H), 7.63 – 7.52 (m, 8H), 7.46 – 7.32 (m, 12H), 7.28 (s, 1H), 7.20 (s, 1H), 7.16 (s, 1H), 7.08 (s, 1H), 4.00 (d, *J* = 5.4 Hz, 2H). ^{13}C NMR (126 MHz, DMSO, d1=5 s) δ 169.0, 165.3, 165.2, 164.8, 163.9, 133.9, 133.8, 133.5, 133.3, 131.7, 129.5, 129.3, 129.1, 129.0, 128.7, 128.7, 128.4, 128.4, 128.3, 128.2, 128.1, 128.1, 127.9, 127.9, 127.8,

127.8, 127.7, 127.6, 127.4, 43.3. IR (ATR): 3272, 3050, 2927, 1634, 1500, 1490, 1447, 1363, 1256, 1203, 1075, 1029, 1001, 929 cm^{-1}. HRMS (ESI-TOF) *m/z* calc'd for $C_{38}H_{31}N_5O_5$ $[M+H]^+$: 638.2397, found 638.2379.

ii) Synthesis of pentapeptide **1.21**

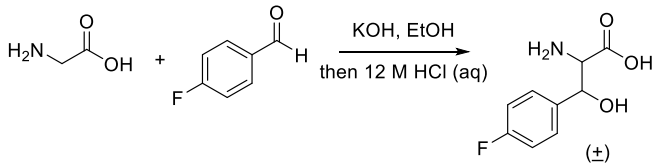

2-amino-3-(4-fluorophenyl)-3-hydroxypropanoic acid (S17)

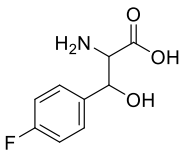

To a 250 mL Erlenmeyer flask equipped with a stir bar was added EtOH (200 mL) and KOH (5.6 g, 100 mmol) and this mixture was stirred at rt until complete dissolution of the KOH was observed. Glycine (3.75 g, 50 mmol) was then added, and this mixture was again stirred until homogeneous. 4-fluorobenzaldehyde (10.7 mL, 100 mmol) was then added with stirring. After 2-4 h of stirring at rt, precipitate formed until the entire reaction mixture became a white solid. This solid was then broken up mechanically and 9 mL of 12M HCl (aq.) was added with stirring. Any remaining large clumps were crushed using a glass rod. The precipitate was filtered off, and the filtrate was concentrated under reduced pressure. To the crude concentrate was added 50 mL of DCM and 80 mL of H_2O. The phases were separated and the aqueous phase was washed twice more with dichloromethane (2 x 50 mL) then concentrated under reduced pressure. The crude solid was then triturated with Et_2O to afford (±) fluoroserine **S17** derivative as a white solid (1.5 g, 17%). ^1H NMR (600 MHz, DMSO) δ 7.40 (dd, *J* = 8.6, 5.7 Hz, 2H), 7.13 (t, *J* = 8.9 Hz, 2H), 5.04 (d, *J* = 4.3 Hz, 1H),

3.39 (d, *J* = 4.4 Hz, 1H). ^{13}C NMR (151 MHz, DMSO) δ 168.7, 161.5 (d, *J* = 242.1 Hz), 138.4 (d, *J* = 2.8 Hz), 128.5 (d, *J* = 8.2 Hz), 114.7 (d, *J* = 21.2 Hz), 70.3, 59.3. ^{19}F NMR (376 MHz, DMSO) δ -116.36. IR (ATR): 3133, 2915, 1635, 1596, 1506, 1484, 1221 cm^{-1}. HRMS (ESI-TOF) *m/z* calc'd for $C_9H_{10}FNO_3Na$ $[M+Na]^+$: 222.0542, found: 222.0542.

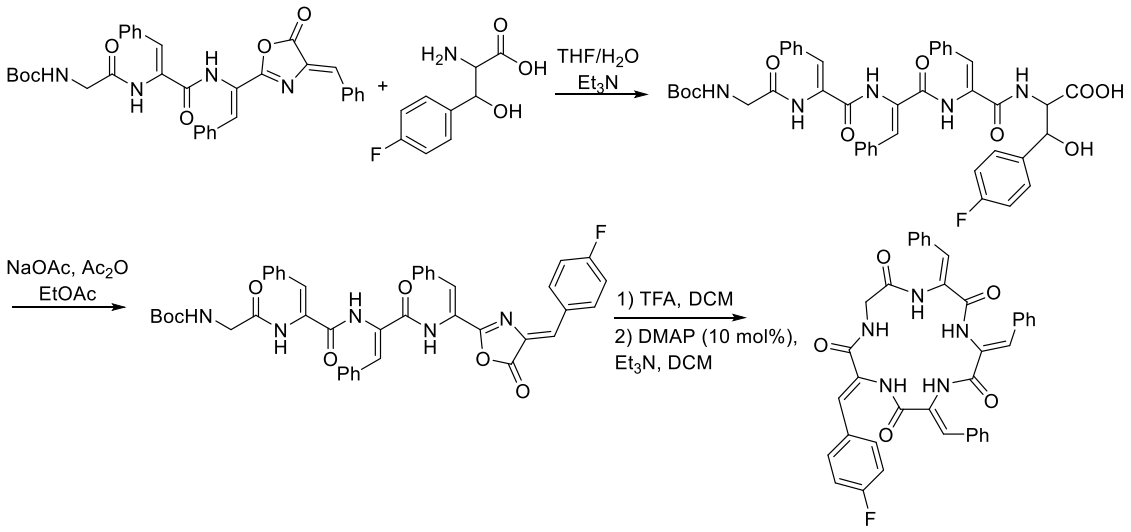

6,9,12-tri((*Z*)-benzylidene)-3-((*Z*)-4-fluorobenzylidene)-1,4,7,10,13-pentaazacyclopentadecane-2,5,8,11,14-pentaone (1.21)

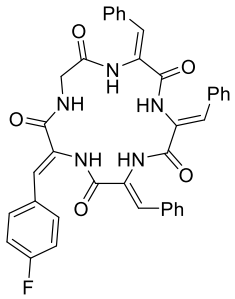

To a solution of fluoroserine **S17** (806 mg, 4.05 mmol) in THF/H_2O (1:1, 0.1 M) was added triethylamine (564 µL, 4.05 mmol) and the mixture was sonicated until homogeneous. The mixture was added to a solution of oxazolone **S16** (2.00 g, 3.37 mmol) in THF (34 mL). The reaction was stirred at rt for 15 h. The mixture was acidified with 10% $KHSO_4$ (aq), extracted with 3x with EtOAc, and the organic layer was washed with brine. The organic layer was dried over anhydrous Na_2SO_4 and concentrated under reduced pressure to afford the desired carboxylic acid which was used without further purification.

To a round bottom flask equipped with a stir bar was added the carboxylic acid (3.37 mmol) and EtOAc (6.7 mL). To this solution was added acetic anhydride (3.18 mL, 33.7 mmol) and sodium acetate (552 mg, 6.74 mmol) and the mixture was stirred at rt for 26 h. Sat. $NaHCO_3$ (aq) was added to quench excess acetic anhydride and acetic acid until the reaction mixture stopped bubbling. The mixture was extracted 3x with EtOAc and the combined organic layer was washed with brine and dried over anhydrous Na_2SO_4. The solution was filtered and solvent was evaporated under reduced pressure. The oil was dissolved in a minimal amount of DCM and hexanes was added to precipitate the oxazolone. The solvent was decanted and the solid was washed 2x with hexanes to afford the desired oxazolone which was used in the next step without further purification.

To a round bottom flask equipped with a stir bar under N_2 was added the resulting oxazolone (3.37 mmol) and anhydrous DCM (34 mL). The reaction mixture was cooled to 0 °C and TFA (5.20 mL, 67.4 mmol) was slowly added. The reaction slowly warmed to rt and stirred for 2 h. The DCM was concentrated under reduced pressure and to the mixture was added toluene to form a TFA azeotrope, which was subsequently concentrated under reduced pressure. The crude reaction mixture was further dried on the high vacuum and subsequently triturated with Et_2O to afford TFA·amine salt and was immediately used in the next reaction without further purification.

TFA·amine salt (3.37 mmol) was dissolved in anhydrous DCM (67 mL, 0.05 M) and to this solution was added anhydrous Et_3N (0.94 mL, 6.74 mmol) and DMAP (41 mg, 0.34 mmol). The reaction mixture was stirred at rt for 3 h and subsequently concentrated under reduced pressure. The crude reaction mixture was then purified via column chromatography (eluting with 25% DCM/acetone) to afford cyclic pentapeptide **1** as a light

yellow solid (235 mg, 12% yield over 4 steps). ^{1}H NMR (499 MHz, DMSO, 373 K, d1=25 s) δ 9.65 (s, 1H), 9.40 (s, 1H), 9.35 (s, 1H), 9.22 (s, 1H), 8.09 (s, 1H), 7.71 – 7.53 (m, 7H), 7.49 – 7.31 (m, 10H), 7.27 (s, 1H), 7.25 – 7.15 (m, 4H), 7.09 (s, 1H), 4.00 (d, *J* = 5.4 Hz, 2H). ^{13}C NMR (151 MHz, DMSO, 373 K, d1=25 s) δ 169.1, 165.3, 165.3, 164.8, 163.9, 161.6 (d, *J* = 247.5 Hz), 133.8, 133.5, 133.3, 131.2 (d, *J* = 8.3 Hz), 130.5 (d, *J* = 3.1 Hz), 129.5, 129.4, 129.4, 129.3, 129.2, 129.1, 128.7, 128.5, 128.4, 128.4, 128.4, 128.3, 127.99, 127.97, 127.8, 127.4, 127.4, 114.7 (d, *J* = 21.6 Hz), 43.4. ^{19}F NMR (376 MHz, DMSO) δ -112.20. IR (ATR): 3050, 1633, 1601, 1509, 1233, 1203 cm^{-1}. HRMS (ESI-TOF) *m/z* calc'd for $C_{38}H_{30}FN_5O_5Na$ $[M+Na]^+$: 678.2129, found: 678.2134.

iii) Synthesis of pentapeptide **1.22**

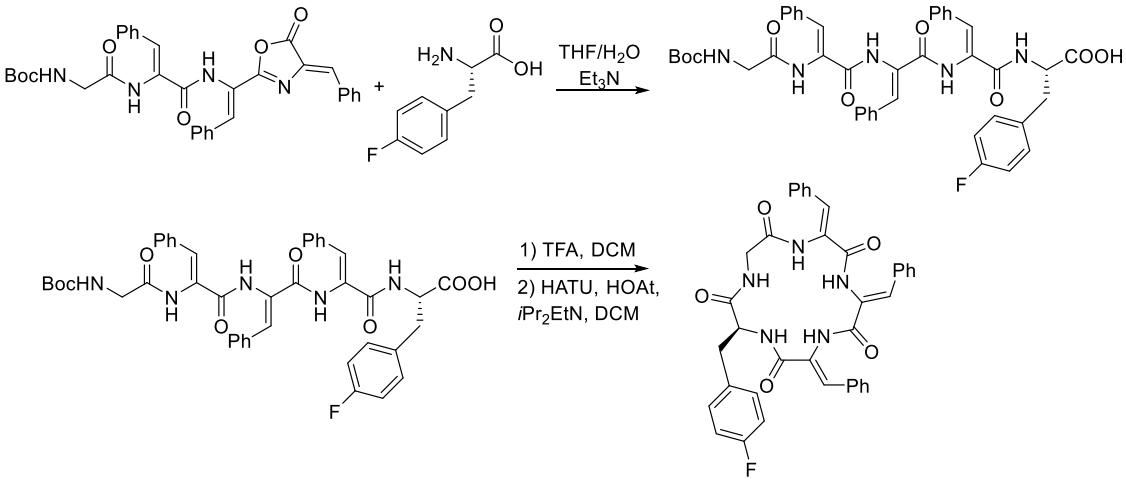

(*S*)-6,9,12-tri((*Z*)-benzylidene)-3-(4-fluorobenzyl)-1,4,7,10,13-pentaazacyclopentadecane-2,5,8,11,14-pentaone (1.22)

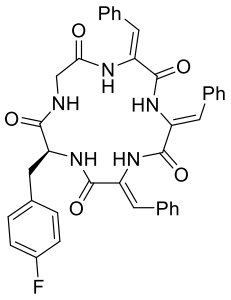

To a solution of L-Phe(4-F)-OH (0.602 g, 3.29 mmol) in THF/H_2O (1:1, 0.1 M) was added Et_3N (459 µL, 3.29 mmol) and the mixture was sonicated until homogeneous. The mixture was added to a solution of

oxazolone **S16** (1.50 g, 2.53 mmol) in THF (25 mL). The reaction was stirred at rt for 11 h. The mixture was acidified with 10% $KHSO_4$ (aq), extracted with 3x with EtOAc, and the organic layer was washed with brine. The organic layer was dried over anhydrous Na_2SO_4 and concentrated under reduced pressure to afford the desired carboxylic acid which was used in the next step without further purification.

To a round bottom flask equipped with a stir bar under N_2 was added the carboxylic acid (2.53 mmol) and anhydrous DCM (32 mL). The reaction mixture was cooled to 0 °C and TFA (2.9 mL, 38.0 mmol) was slowly added. The reaction slowly warmed to rt and stirred for 22 h. The DCM was concentrated under reduced pressure and to the mixture was added toluene to form a TFA azeotrope, which was subsequently concentrated under reduced pressure. The crude reaction mixture was further dried on the high vacuum and subsequently triturated with Et_2O to afford TFA·amine salt and was immediately used in the next reaction without further purification.

To a round botton flask equipped with a stir bar was added the TFA·amine salt (2.53 mmol), HOAt (0.688 g, 5.06 mmol), and anhydrous DCM (51 mL, 0.05 M). The reaction mixture was cooled to 0 °C and *i*-Pr_2EtN (2.2 mL, 12.7 mmol) was added. HATU (2.40 g, 6.33 mmol) was added in portions and the reaction warmed to rt and stirred for 4 h. The solvent was removed under reduced pressure and the product was purified by column chromatography (eluting with hexanes/EtOAc) to afford the product as a yellow solid (365 mg, 22% over 3 steps). ^{1}H NMR (499 MHz, DMSO, 368 K) δ 9.56 (s, 1H), 9.35 (s, 1H), 9.25 (s, 1H), 8.05 (s, 1H), 7.83 (d, *J* = 8.1 Hz, 1H), 7.63 – 7.52 (m, 5H), 7.47 – 7.29 (m, 12H), 7.20 (s, 1H), 7.18 (s, 1H), 7.15 (s, 1H), 7.07 (t, *J* = 8.8 Hz, 2H), 4.71 – 4.63 (m, 1H), 4.20 (dd, *J* = 14.9, 7.1 Hz, 1H), 3.59 (dd, *J* = 14.9, 4.5 Hz, 1H), 3.21 (dd, *J* = 13.9, 7.2 Hz,

1H), 3.00 – 2.96 (m, 1H). ^{13}C NMR (126 MHz, DMSO, 368 K, d1=10 s) δ 171.0, 169.2, 165.0, 164.9, 163.6, 160.6 (d, *J* = 242.0 Hz), 133.8, 133.6 (d, *J* = 3.6 Hz), 133.6, 133.4, 130.3 (d, *J* = 7.9 Hz), 129.2, 129.1, 129.06, 129.01, 128.9, 128.4, 128.3, 128.1, 128.0, 127.9, 127.9, 127.9, 127.8, 127.7, 127.4, 114.2 (d, *J* = 21.1 Hz), 54.8, 43.1, 35.5. ^{19}F NMR (376 MHz, DMSO) δ -117.00. IR (ATR): 3055, 3027, 2910, 1652, 1640, 1501, 1221 cm^{-1}. HRMS (ESI-TOF) *m/z* calc'd for $C_{38}H_{32}FN_5O_5Na$ $[M+Na]^+$: 680.2285, found: 680.2289. $[\alpha]^{25}_D$ +175 (*c* = 0.25, $CHCl_3$).

iv) Synthesis of pentapeptide **1.23**

methyl (*S*)-2-((*R*)-2-((*tert*-butoxycarbonyl)amino)-3-phenylpropanamido)-3-(4-fluorophenyl)propanoate (S18)

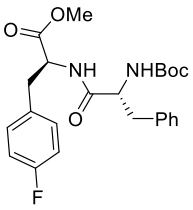

To a round bottom flask equipped with a stir bar was added Boc-D-Phe-OH (2.00 g, 7.50 mmol), 4-fluoro-L-Phe-OMe (1.90 g, 8.25 mmol), HOBt·H_2O (1.50 g, 9.00 mmol), and DCM (94 mL). The mixture was cooled to 0 °C and *i*-Pr_2EtN (4.00 mL, 22.5 mmol) was subsequently added. EDCI·HCl (1.73 g, 9.00 mmol) was added in portions and the reaction gradually warmed to rt and stirred for 22 h. The reaction mixture was transferred to a separatory funnel and was washed with sat. $NaHCO_3$ (aq), 10% $KHSO_4$ (aq), and brine. The organic phase was dried over Na_2SO_4, filtered, and concentrated under reduced pressure. The unpurified reaction mixture was then purified by column chromatography (eluting with 7:3 hexanes/EtOAc) to afford dipeptide **S18** as a white solid (3.1 g, 94%). ^{1}H NMR (600 MHz, $CDCl_3$) δ 7.30 (t, *J* = 7.3 Hz, 2H), 7.25 – 7.23 (m, 1H), 7.20 – 7.17 (m, 2H), 6.97 – 6.83 (m, 4H), 6.39 (br s, 1H), 4.89 (br s, 1H), 4.86 – 4.76 (m, 1H), 4.36 (br s, 1H), 3.67 (s, 3H), 3.08 (dd, *J* =

13.8, 7.1 Hz, 1H), 3.00 (dd, *J* = 14.0, 5.5 Hz, 2H), 2.92 (dd, *J* = 14.0, 5.8 Hz, 1H), 1.38 (s, 9H). ^{13}C NMR (126 MHz, $CDCl_3$) δ 171.5, 171.0, 162.1 (d, *J* = 245.3 Hz), 155.5, 136.7, 131.4 (d, *J* = 2.9 Hz), 130.8 (d, *J* = 7.6 Hz), 129.5, 128.9, 127.2, 115.6 (d, *J* = 21.2 Hz), 80.5, 55.9, 53.2, 52.5, 38.3, 37.2, 28.4. ^{19}F NMR (376 MHz, $CDCl_3$) δ -116.04. IR (ATR): 3044, 2972, 1741, 1674, 1657, 1517, 1232, 1160 cm^{-1}. HRMS (ESI-TOF) *m/z* calc'd for $C_{24}H_{29}FN_2O_5Na$ $[M+Na]^+$: 467.1958, found: 467.1953. $[\alpha]^{26}_D$ –13 (*c* = 0.24, $CHCl_3$).

(*S*)-2-((*R*)-2-amino-3-phenylpropanamido)-3-(4-fluorophenyl)propanoic acid (S19)

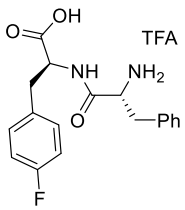

To a round bottom flask equipped with a stir bar was added methyl ester **S18** (1.5 g, 3.4 mmol), THF (16 mL), and H_2O (13 mL). The mixture was cooled to 0 °C and 1M LiOH (aq) (6.1 mL, 6.1 mmol) was subsequently added. The reaction gradually warmed to rt and stirred for 23 h. The reaction mixture was acidified with 10% $KHSO_4$ (aq), and the THF was concentrated under reduced pressure. The reaction mixture was transferred to a separatory funnel where it was extracted with EtOAc (3 x 100 mL). The organic layer was washed with 100 mL brine, dried over Na_2SO_4, filtered, and concentrated under reduced pressure to afford the desired carboxylic acid which was used in the next step without further purification.

To a round bottom flask equipped with a stir bar was added the resulting carboxylic acid (3.4 mmol), triisopropylsilane (0.70 mL, 3.4 mmol), and DCM (42 mL). The reaction mixture was cooled to 0 °C and TFA (3.8 mL, 5.1 mmol) was slowly added. The reaction slowly warmed to rt and stirred for 24 h. The DCM was concentrated under reduced pressure and to the mixture was added toluene to form a TFA azeotrope, which was subsequently concentrated under reduced pressure. The reaction mixture was further

dried on the high vacuum and subsequently triturated with Et_2O to afford amine **S19** as a white solid (1.5 g, 99%). ^{1}H NMR (400 MHz, DMSO) δ 8.92 (d, *J* = 7.7 Hz, 1H), 8.14 (br s, 2H), 7.33 – 7.17 (m, 5H), 7.10 (t, *J* = 8.9 Hz, 2H), 7.04 – 6.98 (m, 2H), 4.54 (td, *J* = 9.1, 4.8 Hz, 1H), 4.12 – 3.98 (m, 1H), 3.06 (dd, *J* = 13.8, 4.7 Hz, 1H), 2.90 (dd, *J* = 14.0, 5.0 Hz, 1H), 2.82 (dd, *J* = 13.8, 9.6 Hz, 1H), 2.69 (dd, *J* = 13.9, 7.9 Hz, 1H). ^{13}C NMR (126 MHz, DMSO) δ 172.3, 167.9, 161.2 (d, *J* = 242.3 Hz), 134.6, 133.3 (d, *J* = 2.8 Hz), 131.2 (d, *J* = 8.0 Hz), 129.5, 128.5, 127.2, 115.0 (d, *J* = 21.1 Hz), 53.6, 53.2, 37.0, 36.3. ^{19}F NMR (376 MHz, $CDCl_3$) δ -116.84. IR (ATR): 3055, 2949, 1730, 1685, 1506, 1199, 1182, 1148 cm^{-1}. HRMS (ESI-TOF) *m/z* calc'd for $C_{18}H_{19}FN_2O_3Na$ $[M+Na]^+$: 353.1277, found: 353.1268. $[\alpha]^{25}_D$ +3 (*c* = 0.29, MeOH).

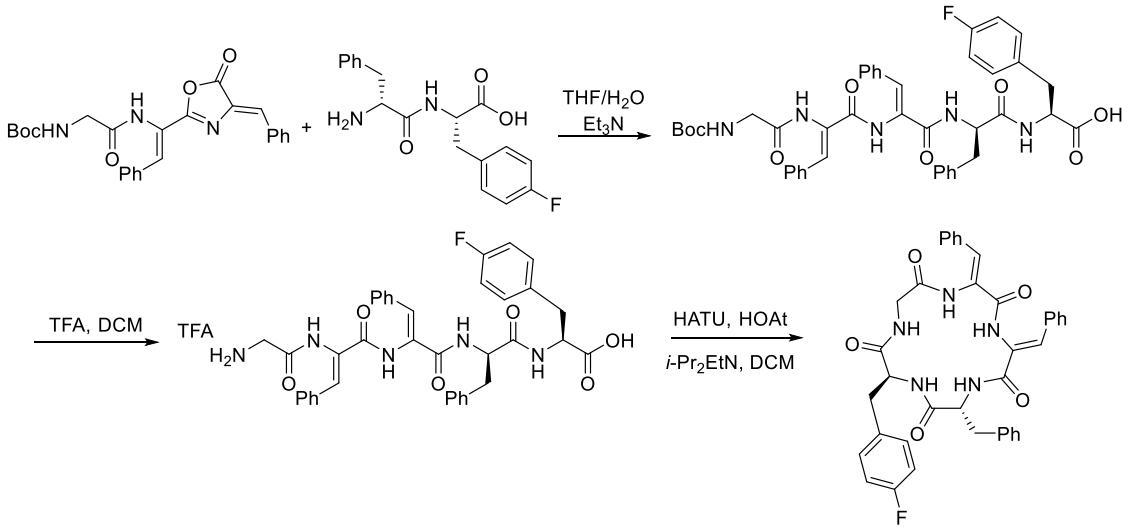

(3*S*,6*R*)-6-benzyl-9,12-di((*Z*)-benzylidene)-3-(4-fluorobenzyl)-1,4,7,10,13-pentaazacyclopentadecane-2,5,8,11,14-pentaone **(1.23)**

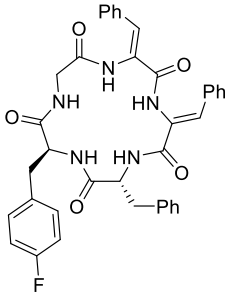

To a solution of dipeptide **S19** (764 mg, 1.72 mmol) in THF/H_2O (1:1, 0.1 M) was added Et_3N (240 µL, 4.05 mmol) and the mixture was sonicated until homogeneous. The mixture was added to a solution of oxazolone **S15** (700 mg, 1.56 mmol) in THF (16 mL). The reaction was

stirred at rt for 15 h. The mixture was acidified with 10% $KHSO_4$ (aq), extracted with 3x with EtOAc, and the organic layer was washed with brine. The organic layer was dried over anhydrous Na_2SO_4 and concentrated under reduced pressure to afford the desired carboxylic acid which was used in the next step without further purification.

To a round bottom flask equipped with a stir bar under N_2 was added the resulting carboxylic acid (1.56 mmol) and anhydrous DCM (20 mL). The reaction mixture was cooled to 0 °C and TFA (1.8 mL, 23.4 mmol) was slowly added. The reaction slowly warmed to rt and stirred for 2 h. The DCM was concentrated under reduced pressure and to the mixture was added toluene to form a TFA azeotrope, which was subsequently concentrated under reduced pressure. The crude reaction mixture was further dried on the high vacuum and subsequently triturated with Et_2O to afford TFA·amine salt and was immediately used in the next reaction without further purification.

To a round botton flask equipped with a stir bar was added the corresponding TFA·amine salt (1.56 mmol), HOAt (0.212 g, 1.56 mmol), and DMF (31 mL, 0.05 M). The reaction mixture was cooled to 0 °C and *i*-Pr_2EtN (0.679 mL, 3.90 mmol) was added. HATU (711 mg, 1.87 mmol) was added in portions and the reaction warmed to rt and stirred for 24 h. The solvent was removed under reduced pressure and the product was purified by column chromatography (eluting with 1:4 hexanes/EtOAc) to afford the product as a white solid (167 mg, 16% over 3 steps). ^{1}H NMR (400 MHz, DMSO, 330 K) δ 9.85 (s, 1H), 9.44 (s, 1H), 8.33 (d, *J* = 6.9 Hz, 1H), 7.84 (d, *J* = 5.5 Hz, 1H), 7.82 – 7.74 (m, 1H), 7.65 – 7.50 (m, 4H), 7.47 – 7.27 (m, 7H), 7.25 – 7.06 (m, *J* = 22.5, 6.2 Hz, 8H), 7.01 (t, *J* = 8.8 Hz, 2H), 6.86 (s, 1H), 4.62 – 4.47 (m, 2H), 4.19 (dd, *J* = 16.7, 6.4 Hz, 1H), 3.75 (dd, *J* = 16.2, 4.5 Hz, 1H), 3.12 – 3.06 (m, 1H), 3.01 (dd, *J* = 14.1, 5.6 Hz, 1H), 2.86 (dd, *J* = 13.5, 5.0

Hz, 1H), 2.79 (dd, *J* = 14.3, 9.1 Hz, 1H). ^{13}C NMR (151 MHz, DMSO, 368 K, d1=10 s) δ 171.4, 170.2, 169.6, 164.4, 163.9, 160.5, (d, *J* = 242.1 Hz), 137.6, 133.9, 133.5 (d, *J* = 2.9 Hz), 133.3, 130.1 (d, *J* = 7.9 Hz), 130.0, 129.04, 128.94, 128.84, 128.4, 128.20, 128.18, 128.0, 127.8, 127.7, 127.5, 126.4, 125.5, 114.2 (d, *J* = 21.1 Hz), 54.7, 54.2, 42.1, 36.4, 34.2. ^{19}F NMR (376 MHz, DMSO) δ -117.19. IR (ATR): 3050, 2910, 1657, 1646, 1545, 1506, 1221 cm^{-1}. HRMS (ESI-TOF) *m/z* calc'd for $C_{38}H_{34}N_5O_5Na$ $[M+Na]^+$: 682.2441, found: 682.2449. $[\alpha]^{26}_D$ +202 (*c* = 0.25, DMF).

v) Synthesis of pentapeptide **1.24**

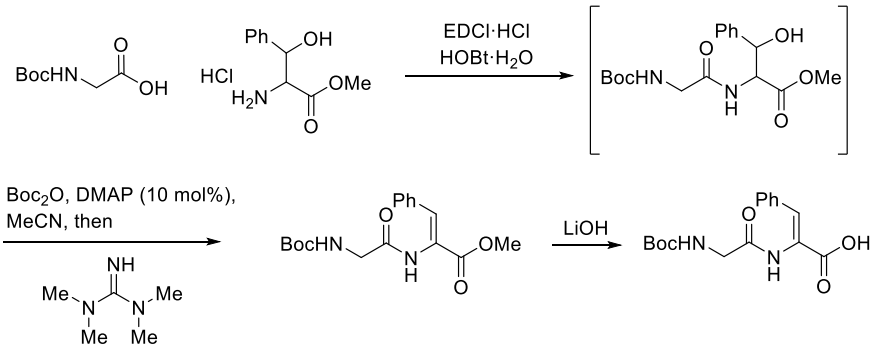

methyl (*Z*)-2-(2-((*tert*-butoxycarbonyl)amino)acetamido)-3-phenylacrylate (S20)

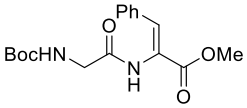

To a round bottom flask equipped with a stir bar was added Boc-Gly-OH (3.00 g, 17.1 mmol), DL-(β-OH)–Phe–OMe **1.7** (4.20 g, 18.0 mmol), HOBt·H_2O (3.50 g, 20.5 mmol), and DCM (214 mL). The mixture was cooled to 0 °C and *i*-Pr_2EtN (8.90 mL, 51.3 mmol) was subsequently added. EDCI·HCl (3.93 g, 20.5 mmol) was added in portions and the reaction gradually warmed to rt and stirred for 22 h. The reaction mixture was transferred to a separatory funnel and was washed with sat. $NaHCO_3$ (aq), 10% $KHSO_4$ (aq), and brine. The organic phase was dried over Na_2SO_4,

filtered, and concentrated under reduced pressure to afford the corresponding dipeptide which was used in the next step without further purification.

The procedure was adapted from Suárez.[44] To a round bottom flask equipped with a stir bar was added the corresponding dipeptide (17.1 mmol), DMAP (209 mg, 1.71 mmol) and MeCN (52 mL). The mixture was cooled to 0 °C and Boc_2O (3.91 g, 18.0 mmol) was quickly added. After disappearance of starting material analyzed via LC-MS, tetramethylguanidine (2.1 mL, 17.1 mmol) was added. After 12 h, the reaction mixture was concentrated under reduced pressure and then purified by column chromatography (eluting with 3:2 hexanes/EtOAc) to afford the unsaturated dipeptide **S20** as a white solid (1.83 g, 32%, 2 steps).

(*Z*)-2-(2-((*tert*-butoxycarbonyl)amino)acetamido)-3-phenylacrylic acid (S21)

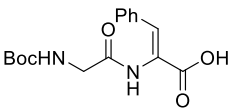

To a round bottom flask equipped with a stir bar was added methyl ester **S20** (1.82 g, 5.44 mmol), THF (26 mL), and H_2O (21 mL). The mixture was cooled to 0 °C and 1M LiOH (aq) (8.2 mL, 8.2 mmol) was subsequently added. The reaction gradually warmed to rt and stirred for 13 h. The reaction mixture was acidified with 10% $KHSO_4$ (aq), and the THF was concentrated under reduced pressure. The reaction mixture was transferred to a separatory funnel where it was extracted with EtOAc (3 x 100 mL). The organic layer was washed with 100 mL brine, dried over Na_2SO_4, filtered, and concentrated under reduced pressure to afford carboxylic acid **S21** as a pale yellow oil (1.6 g, 92%). ^{1}H NMR (400 MHz, DMSO) δ 12.70 (s, 1H), 9.42 (s, 1H), 7.71 – 7.53 (m, 2H), 7.42 – 7.34 (m, 3H), 7.27 (s, 1H), 7.06 (br t, *J* = 5.8 Hz, 1H), 3.69 (d, *J* = 6.0 Hz, 2H), 1.40 (s, 9H). ^{13}C NMR (126 MHz, DMSO) δ 169.3, 166.3, 155.9, 133.6, 131.7,

130.1, 129.2, 128.5, 126.5, 78.1, 43.3, 28.2. IR (ATR): 3256, 3021, 2982, 1705, 1666, 1634, 1510, 1403, 1271, 1263, 1153 cm^{-1}. HRMS (ESI-TOF) *m/z* calc'd for $C_{16}H_{20}N_2O_5Na$ $[M+Na]^+$: 343.1270, found: 343.1277

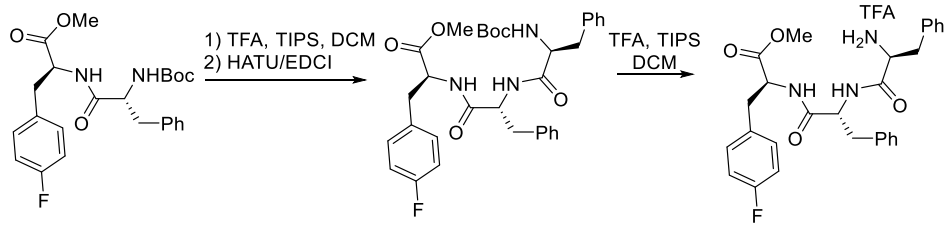

Methyl (6*S*,9*R*,12*S*)-6,9-dibenzyl-12-(4-fluorobenzyl)-2,2-dimethyl-4,7,10-trioxo-3-oxa-5,8,11-triazatridecan-13-oate (S22)

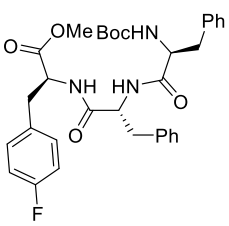

To a round bottom flask equipped with a stir bar was added the Boc-protected dipeptide **S18** (3.5 g, 7.9 mmol), triisopropylsilane (1.62 mL, 7.9 mmol), and DCM (98 mL). The reaction mixture was cooled to 0 °C and TFA (7.7 mL, 101 mmol) was slowly added. The reaction slowly warmed to rt and stirred for 24 h. The DCM was concentrated under reduced pressure and to the mixture was added toluene to form a TFA azeotrope, which was subsequently concentrated under reduced pressure to afford the TFA·amine salt which was used in the next step without further purification.

To a round bottom flask equipped with a stir bar was added the TFA·amine salt (7.9 mmol), Boc-L-Phe-OH (2.1 g, 7.9 mmol), $HOBt·H_2O$ (1.6 g, 9.5 mmol), and DCM (100 mL). The mixture was cooled to 0 °C and *i*-Pr_2EtN (10.3 mL, 59.3 mmol) was subsequently added. EDCI·HCl (1.8 g, 9.5 mmol) was added in portions and the reaction gradually warmed to rt and stirred for 17 h. The reaction mixture was transferred to a separatory funnel and was washed with sat. $NaHCO_3$ (aq), 10% $KHSO_4$ (aq), and brine. The organic

phase was dried over Na_2SO_4, filtered, and concentrated under reduced pressure. The crude reaction mixture was purified via column chromatography (eluting with 55:45 hexanes/EtOAc) to afford tripeptide **S22** as a white solid (4.8 g, >99%). ^{1}H NMR (400 MHz, $CDCl_3$) δ 7.37 – 7.20 (m, 7H), 7.16 – 7.11 (m, 2H), 7.02 – 6.82 (m, 6H), 6.64 (s, 1H), 6.24 (s, 1H), 5.03 – 4.95 (m, 1H), 4.79 – 4.66 (m, 1H), 4.67 – 4.55 (m, 1H), 4.21 – 4.12 (m, 1H), 3.63 (s, 3H), 3.05 – 2.86 (m, 5H), 2.83 – 2.71 (m, 1H), 1.38 (s, 9H). ^{13}C NMR (126 MHz, $CDCl_3$) δ 171.4, 171.3, 170.2, δ 162.1 (d, *J* = 245.5 Hz), 155.59, 155.57, 136.6, 136.2, 131.6 (d, *J* = 1.7 Hz), 130.9 (d, *J* = 7.9 Hz), 129.6, 129.4, 128.89, 128.83, 127.3, 115.5 (d, *J* = 21.3 Hz), 80.6, 56.7, 54.0, 53.6, 52.4, 38.3, 37.4, 37.2, 28.4. ^{19}F NMR (376 MHz, $CDCl_3$) δ -116.04. IR (ATR): 3033, 2915, 1758, 1724, 1629, 1489, 1221, 1160 cm^{-1}. HRMS (ESI-TOF) *m/z* calc'd for $C_{33}H_{38}FN_3O_6Na$ $[M+Na]^+$: 614.2642, found: 614.2623. $[\alpha]^{23}_D$ +38 (*c* = 0.29, $CHCl_3$).

Methyl (*S*)-2-((*R*)-2-((*S*)-2-amino-3-phenylpropanamido)-3-phenylpropanamido)-3-(4-fluorophenyl)propanoate (S23)

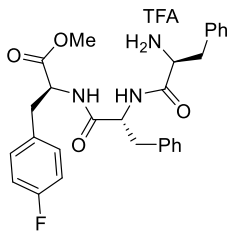

To a round bottom flask equipped with a stir bar was added tripeptide **S22** (3.0 g, 5.1 mmol), triisopropylsilane (1.0 mL, 5.1 mmol), and DCM (98 mL). The reaction mixture was cooled to 0 °C and TFA (5.7 mL, 76.5 mmol) was slowly added. The reaction slowly warmed to rt and stirred for 42 h. The DCM was concentrated under reduced pressure and to the mixture was added toluene to form a TFA azeotrope, which was subsequently concentrated under reduced pressure and triturated with Et_2O to afford tripeptide **S23** as a pale yellow solid (3.3g, >99%). ^{1}H NMR (600 MHz, DMSO) δ 8.89 – 8.86 (d, *J* = 8.3 Hz, 1H), 8.84 (d, *J* =

8.8 Hz, 1H), 8.00 (br s, 2H), 7.34 – 7.28 (m, 2H), 7.25 – 7.19 (m, 5H), 7.19 – 7.14 (m, 1H), 7.14 – 7.07 (m, 4H), 6.95 – 6.87 (m, 2H), 4.71 (m, 1H), 4.54 (m, 1H), 4.00 (br s, 1H), 3.64 (s, 3H), 3.09 (dd, *J* = 13.8, 5.0 Hz, 1H), 2.85 (dd, *J* = 13.7, 10.1 Hz, 1H), 2.78 (dd, *J* = 14.1, 4.5 Hz, 1H), 2.69 (dd, *J* = 13.5, 4.0 Hz, 1H), 2.53 (d, *J* = 14.4, 8.2 Hz, 1H), 2.46 (dd, *J* = 13.6, 10.4 Hz, 1H). ^{13}C NMR (151 MHz, DMSO) δ 171.8, 170.7, 167.7, 161.2 (d, *J* = 242.3 Hz), 137.3, 134.6, 133.2 (d, *J* = 2.9 Hz), 131.2 (d, *J* = 8.1 Hz), 129.5, 129.4, 128.4, 128.1, 127.1, 126.6, 115.0 (d, *J* = 21.1 Hz), 53.8, 53.4, 53.2, 52.1, 38.4, 36.9, 36.2. ^{19}F NMR (376 MHz, DMSO) δ -116.62. IR (ATR): 3061, 2932, 1741, 1652, 1512, 1143 cm^{-1}. HRMS (ESI-TOF) *m/z* calc'd for $C_{28}H_{30}FN_3O_4H$ $[M+H]^+$: 492.2299, found: 492.2282. $[\alpha]^{26}_D$ +3 (*c* = 0.35, MeOH).

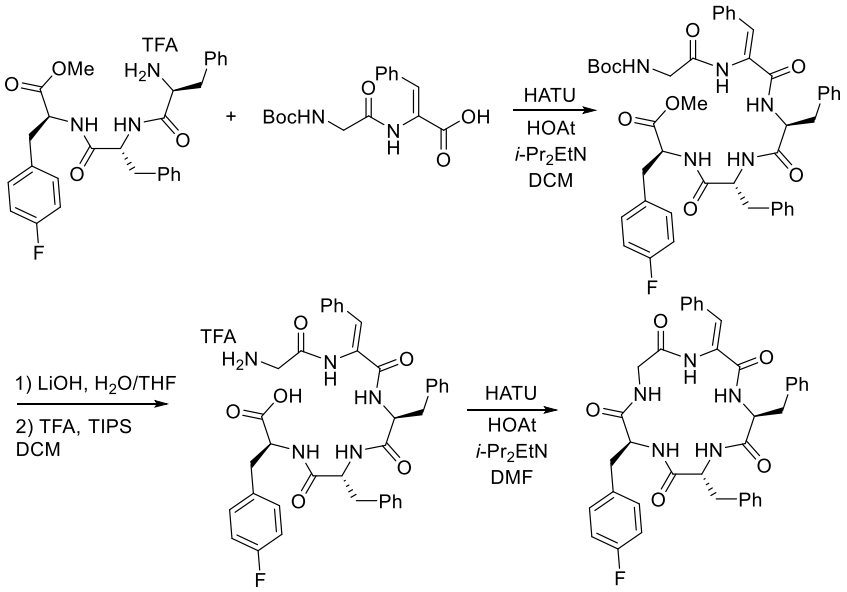

Methyl (12*S*,15*R*,18*S*)-12,15-dibenzyl-9-((*Z*)-benzylidene)-18-(4-fluorobenzyl)-2,2-dimethyl-4,7,10,13,16-pentaoxo-3-oxa-5,8,11,14,17-pentaazanonadecan-19-oate (S24)

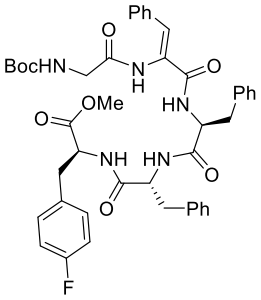

To a round botton flask equipped with a stir bar was added the dipeptide **S21** (1.6 g, 5.0 mmol), tripeptide **S23** (3.0 g, 5.0 mmol), and HOAt (681 mg, 5.0 mmol), and DCM (63 mL). The reaction mixture was cooled to 0 ^{o}C and *i*-Pr_2EtN (4.4 mL, 25 mmol) was added. HATU (2.3 g, 6.0 mmol) was added in portions and the reaction warmed to rt and stirred for 14 h. The reaction mixture was transferred to a separatory funnel and was washed with sat. $NaHCO_3$ (aq), 10% $KHSO_4$ (aq), and brine. The organic phase was dried over Na_2SO_4, filtered, and concentrated under reduced pressure. The crude reaction mixture was purified via column chromatography (eluting with 1:1 hexanes/EtOAc) to afford pentapeptide **S24** as a pale yellow solid (3.3 g, 83%). ^{1}H NMR (400 MHz, DMSO) δ 9.59 (s, 1H), 8.58 (d, *J* = 8.1 Hz, 1H), 8.20 (d, *J* = 8.7 Hz, 1H), 7.97 (d, *J* = 8.1 Hz, 1H), 7.52 (d, *J* = 7.3 Hz, 2H), 7.40 – 7.03 (m, 17H), 7.01 (br t, *J* = 5.8 Hz, 1H), 6.87 (s, 1H), 4.60 – 4.49 (m, 2H), 4.49 – 4.38 (m, 1H), 3.81 – 3.67 (m, *J* = 5.2 Hz, 2H), 3.33 (s, 3H), 3.07 (dd, *J* = 13.7, 5.1 Hz, 1H), 2.90 (dd, *J* = 13.7, 9.7 Hz, 1H), 2.86 – 2.57 (m, 4H), 1.36 (s, 9H). ^{13}C NMR (126 MHz, DMSO) δ 171.8, 171.2, 170.5, 169.8, 164.9, 161.1 (d, *J* = 242.2 Hz), 156.0, 138.0, 137.8, 133.8, 133.2 (d, *J* = 2.8 Hz), 131.2 (d, *J* = 8.0 Hz), 129.6, 129.3, 129.2, 128.9, 128.7, 128.5, 128.0, 127.8, 126.3, 126.1, 114.9 (d, *J* = 21.1 Hz), 78.2, 54.6, 54.0, 53.5, 52.0, 43.6, 37.9, 36.9, 36.1, 28.2. ^{19}F NMR (376 MHz, DMSO) δ -116.89. IR (ATR): 3055, 2966, 1663, 1506, 1216, 1165 cm^{-1}. HRMS (ESI-TOF) *m/z* calc'd for $C_{44}H_{48}FN_5O_8Na$ $[M+Na]^+$: 816.3384, found: 816.3364. $[\alpha]^{24}_D$ +98 (*c* = 0.19, $CHCl_3$).

(2*S*,5*R*,8*S*)-14-amino-5,8-dibenzyl-11-((*Z*)-benzylidene)-2-(4-fluorobenzyl)-4,7,10,13-tetraoxo-3,6,9,12-tetraazatetradecanoic acid (S25)

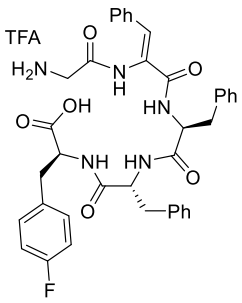

To a round bottom flask equipped with a stir bar was added pentapeptide **S24** (710 mg, 0.93 mmol), THF (4.4 mL), and H_2O (3.6 mL). The mixture was cooled to 0 °C and 1M LiOH (aq) (1.9 mL, 1.9 mmol) was subsequently added. The reaction gradually warmed to rt and stirred for 39 h. The reaction mixture was acidified with 10% $KHSO_4$ (aq), and the THF was concentrated under reduced pressure. The reaction mixture was transferred to a separatory funnel where it was extracted with DCM (3 x 30 mL). The organic layer was washed with 50 mL brine, dried over Na_2SO_4, filtered, and concentrated under reduced pressure to afford the desired carboxylic acid which was then used in the next step without further purification.

To a round bottom flask equipped with a stir bar was added the pentapeptide carboxylic acid (670 mg, 0.86 mmol), triisopropylsilane (0.18 mL, 0.86 mmol), and DCM (11 mL). The reaction mixture was cooled to 0 °C and TFA (1.0 mL, 12.9 mmol) was slowly added. The reaction slowly warmed to rt and stirred for 49 h. The DCM was concentrated under reduced pressure and to the mixture was added toluene to form a TFA azeotrope, which was subsequently concentrated under reduced pressure and triturated with Et_2O to afford pentapeptide **S25** as white solid (839 mg, >99%). ^{1}H NMR (600 MHz, DMSO) δ 9.47 (br s, 2H), 8.50 (d, *J* = 7.6 Hz, 1H), 8.20 (d, *J* = 8.6 Hz, 1H), 8.15 (d, *J* = 8.2 Hz, 1H), 7.50 (d, *J* = 7.4 Hz, 2H), 7.39 (t, *J* = 7.4 Hz, 2H), 7.36 – 7.31 (m, 1H), 7.30 – 7.02 (m, 15H), 6.90 (s, 1H), 4.63 – 4.57 (m, 1H), 4.57 – 4.49 (m, 1H), 4.49 – 4.41 (m, 1H), 3.84 – 3.72 (m,

2H), 3.11 (dd, *J* = 13.6, 4.1 Hz, 1H), 2.85 (dd, *J* = 13.5, 9.8 Hz, 1H), 2.81 (dd, *J* = 13.5, 3.0 Hz, 1H), 2.77 – 2.71 (m, 1H), 2.62 (dd, *J* = 13.4, 10.5 Hz, 1H), 2.57 (dd, *J* = 12.8, 11.4 Hz, 1H). ^{13}C NMR (151 MHz, DMSO) δ 173.0, 171.0, 170.5, 166.5, 164.4, 161.1 (d, *J* = 241.8 Hz), 138.1, 137.8, 133.9 (d, *J* = 2.4 Hz), 133.6, 131.2 (d, *J* = 8.0 Hz), 129.6, 129.3, 129.2, 128.9, 128.7, 128.2, 128.2, 128.00, 127.98, 126.3, 126.2, 114.8 (d, *J* = 21.0 Hz), 54.4, 53.8, 53.7, 40.7, 38.0, 37.1, 36.5. ^{19}F NMR (376 MHz, DMSO) δ -116.99. IR (ATR): 3027, 2932, 1668, 1624, 1534, 1523, 1199, 1132 cm^{-1}. HRMS (ESI-TOF) *m/z* calc'd for $C_{38}H_{38}FN_5O_6Na$ $[M+Na]^+$: 702.2704, found: 702.2684. $[\alpha]^{26}_D$ +114 (*c* = 0.47, MeOH).

(3*S*,6*R*,9*S*)-6,9-dibenzyl-12-((*Z*)-benzylidene)-3-(4-fluorobenzyl)-1,4,7,10,13-pentaazacyclopentadecane-2,5,8,11,14-pentaone (1.24)

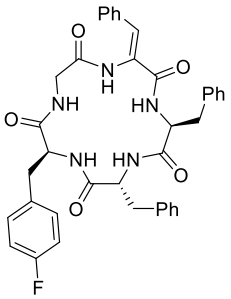

To a round botton flask equipped with a stir bar was added pentapeptide **S25** (1 g, 1.26 mmol), HOAt (343 mg, 2.52 mmol), and DMF (252 mL). The reaction mixture was cooled to 0 ^{o}C and *i*-Pr_2EtN (1.1 mL, 6.3 mmol) was added. HATU (1.2 g, 3.15 mmol) was added in portions and the reaction warmed to rt and stirred for 25 h. The solvent was removed under reduced pressure and the product was filtered and triturated with methanol and DCM to afford the product as a white solid (398 mg, 48%). ^{1}H NMR (499 MHz, DMSO) δ 9.97 (s, 1H), 8.70 (d, *J* = 7.4 Hz, 1H), 8.29 (d, *J* = 8.8 Hz, 1H), 8.20 (t, *J* = 5.0 Hz, 1H), 7.57 (d, *J* = 7.4 Hz, 2H), 7.46 – 7.30 (m, 4H), 7.25 – 7.13 (m, *J* = 21.7, 12.0, 4.6 Hz, 8H), 7.11 – 7.02 (m, 4H), 7.01 – 6.95 (m, 3H), 4.57 (dd, *J* = 13.5, 7.0 Hz, 1H), 4.51 (td, *J* = 9.7, 4.4 Hz, 1H), 4.39 (dd, *J* = 14.6, 7.5 Hz, 1H), 3.90 (dd, *J* = 15.2, 6.6 Hz, 1H), 3.83 (dd, *J* = 15.2, 3.8 Hz, 1H), 3.00 (m, 2H), 2.88 – 2.72 (m, 3H), 2.67 (dd, *J* = 14.1, 8.3 Hz, 1H). ^{13}C NMR (126 MHz,

DMSO, d1=5 s) δ 171.9, 171.2, 170.9, 169.2, 165.0, 160.9 (d, *J* = 241.6 Hz), 137.5, 137.3, 134.0 (d, *J* = 3.0 Hz), 133.6, 130.7 (d, *J* = 8.0 Hz), 129.6, 129.2, 128.9, 128.8, 128.7, 128.6, 128.1, 128.1, 128.0, 126.2, 126.1, 114.8 (d, *J* = 21.0 Hz), 54.4, 54.3, 54.2, 42.4, 37.8, 35.9, 35.0. ^{19}F NMR (376 MHz, DMSO) δ -117.17. IR (ATR): 3089, 2954, 1634, 1551, 1506, 1210 cm^{-1}. HRMS (ESI-TOF) *m/z* calc'd for $C_{38}H_{36}FN_5O_5Na$ $[M+Na]^+$: 684.2598, found: 684.2586. $[\alpha]^{26}_D$ +154 (*c* = 0.27, DMF).

vi) Synthesis of pentapeptide **1.25**

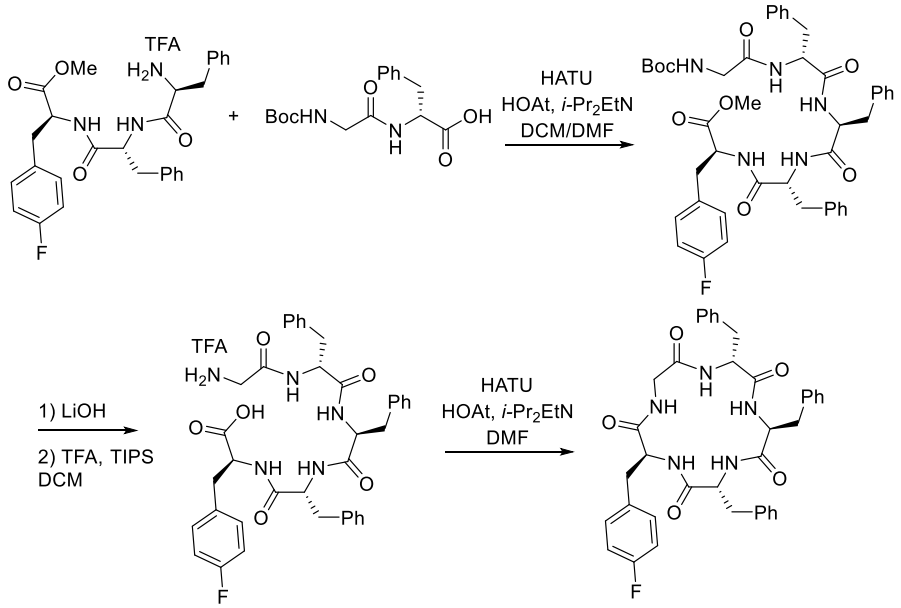

(*tert*-butoxycarbonyl)glycyl-D-phenylalanine **(S26)**

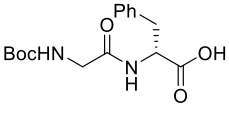

To a round bottom flask equipped with a stir bar was added the Boc-Gly-OH (2 g, 11.4 mmol), Boc-D-Phe-OH (2.7 g, 7.9 mmol), HOBt·H_2O (2.3 g, 13.7 mmol), and DCM (143 mL). The mixture was cooled to 0 °C and *i*-Pr_2EtN (6 mL, 34.2 mmol) was subsequently added. EDCI·HCl (2.6 g, 13.7 mmol) was added in portions and the reaction gradually warmed to rt and stirred for 6 h. The reaction mixture was transferred to a separatory funnel and was washed with sat. $NaHCO_3$ (aq), 10%

$KHSO_4$ (aq), and brine. The organic phase was dried over Na_2SO_4, filtered, and concentrated under reduced pressure. The crude reaction mixture was purified via column chromatography (eluting with 2:3 hexanes/EtOAc) to afford the dipeptide as a colorless oil (3.5 g, 92%). Characterization data was consistent with those previously reported.[83]

To a round bottom flask equipped with a stir bar was added Boc-Gly-Phe-OMe (3.5 g, 10.4 mmol), THF (49 mL), and H_2O (40 mL). The mixture was cooled to 0 °C and 1M LiOH (aq) (18.7 mL, 18.7 mmol) was subsequently added. The reaction gradually warmed to rt and stirred for 31 h. The reaction mixture was acidified with 10% $KHSO_4$ (aq), and the THF was concentrated under reduced pressure. The reaction mixture was transferred to a separatory funnel where it was extracted with DCM (3 x 100 mL). The organic layer was washed with 100 mL brine, dried over Na_2SO_4, filtered, and concentrated under reduced pressure to afford the title compound as a white solid (3.5 g, >99%). Characterization data was consistent with those previously reported.[84]

Methyl (9*R*,12*S*,15*R*,18*S*)-9,12,15-tribenzyl-18-(4-fluorobenzyl)-2,2-dimethyl-4,7,10,13,16-pentaoxo-3-oxa-5,8,11,14,17-pentaazanonadecan-19-oate (S27)

To a round botton flask equipped with a stir bar was added the dipeptide **S26** (536 mg, 1.65 mmol), tripeptide **S23** (1 g, 1.65 mmol), DCM (10 mL), and DMF (2.5 mL). The reaction mixture was cooled to 0 ^oC and *i*-Pr_2EtN (2.0 mL, 11.6 mmol) was added. HATU (743 mg, 1.98 mmol) was added in portions and the reaction warmed to rt and stirred for 12 h. The reaction mixture was washed with sat. $NaHCO_3$ (aq), 10% $KHSO_4$ (aq), and brine. The organic phase was dried over Na_2SO_4, filtered, and concentrated under

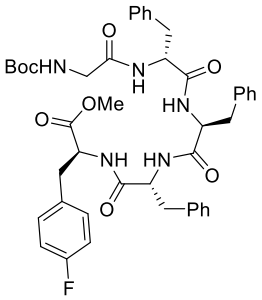

reduced pressure. The crude reaction mixture was dried further on the high vacuum and was purified via column chromatography (eluting with 20:1 DCM/MeOH) to afford a white solid. The solid was further triturated with Et_2O to give pentapeptide **S27** as a white solid (669 mg, 51%). ^{1}H NMR (600 MHz, DMSO) δ 8.69 (d, *J* = 8.2 Hz, 1H), 8.43 (d, *J* = 8.8 Hz, 1H), 8.32 (d, *J* = 8.7 Hz, 1H), 7.65 (d, *J* = 8.3 Hz, 1H), 7.32 – 7.05 (m, 17H), 6.91 – 6.78 (m, 2H), 4.66 – 4.58 (m, 1H), 4.57 – 4.51 (m, 1H), 4.51 – 4.45 (m, 1H), 3.64 (s, 3H), 3.47 (dd, *J* = 16.8, 5.7 Hz, 1H), 3.39 (dd, *J* = 16.9, 6.1 Hz, 1H), 3.07 (dd, *J* = 13.7, 4.9 Hz, 1H), 2.85 (dd, *J* = 13.6, 10.1 Hz, 1H), 2.70 (dd, *J* = 13.1, 3.1 Hz, 1H), 2.59 – 2.52 (m, 1H), 2.40 – 2.27 (m, 1H), 1.33 (s, 9H). ^{13}C NMR (151 MHz, DMSO) δ 171.8, 171.1, 170.8, 170.4, 168.8, 161.1 (d, *J* = 242.2 Hz), 155.6, 137.9, 137.6, 137.4, 133.2 (d, *J* = 2.8 Hz), 131.2 (d, *J* = 8.0 Hz), 129.37, 129.35, 129.2, 127.91, 127.89, 127.8, 126.3, 126.2, 126.0, 114.9 (d, *J* = 21.1 Hz), 78.0, 53.8, 53.5, 53.34, 53.27, 52.0, 43.0, 38.3, 38.04, 37.99, 36.2, 28.1. ^{19}F NMR (376 MHz, DMSO) δ -116.67. IR (ATR): 3083, 3027, 2927, 1629, 1534, 1495, 1227, 1154 cm^{-1}. HRMS (ESI-TOF) *m/z* calc'd for $C_{44}H_{50}FN_5O_8Na$ $[M+Na]^+$: 818.3541, found: 818.3521. $[\alpha]^{24}_D$ +18 (*c* = 0.28, $CHCl_3$).

(2*S*,5*R*,8*S*,11*R*)-14-amino-5,8,11-tribenzyl-2-(4-fluorobenzyl)-4,7,10,13-tetraoxo-3,6,9,12-tetraazatetradecanoic acid (S28)

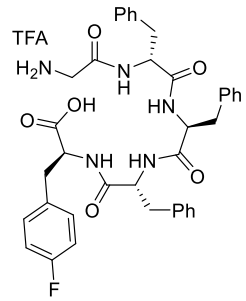

To a round bottom flask equipped with a stir bar was added pentapeptide **S27** (550 mg, 0.69 mmol), THF (7 mL), and H_2O (5 mL). The mixture was cooled to 0 °C and 1M LiOH (aq) (2.3 mL, 2.3 mmol) was subsequently added. The reaction gradually warmed to rt and

stirred for 35 h. The reaction mixture was acidified with 10% $KHSO_4$ (aq), and the THF was concentrated under reduced pressure. The reaction mixture was transferred to a separatory funnel where it was extracted with DCM (3 x 100 mL). The organic layer was washed with 100 mL brine, dried over Na_2SO_4, filtered, and concentrated under reduced pressure to afford the desired carboxylic acid which was then used in the next step without further purification.

To a round bottom flask equipped with a stir bar was added the pentapeptide carboxylic acid (0.69 mmol), triisopropylsilane (0.2 mL, 0.79 mmol), and DCM (9.6 mL). The reaction mixture was cooled to 0 °C and TFA (0.900 mL, 11.9 mmol) was slowly added. The reaction slowly warmed to rt and stirred for 12 h. The DCM was concentrated under reduced pressure and to the mixture was added toluene to form a TFA azeotrope, which was subsequently concentrated under reduced pressure and triturated with Et_2O to afford pentapeptide **S28** as a white solid (621 mg, >99%). ^{1}H NMR (600 MHz, DMSO, 330 K) δ 8.37 – 8.19 (m, 4H), 7.27 – 6.96 (m, 19H), 4.66 – 4.53 (m, 3H), 4.50 – 4.41 (m, 1H), 3.44 (d, *J* = 16.1 Hz, 1H), 3.31 (d, *J* = 16.1 Hz, 1H), 3.09 (dd, *J* = 13.8, 4.7 Hz, 1H), 2.85 (dd, *J* = 13.7, 9.3 Hz, 1H), 2.78 (dd, *J* = 13.7, 4.1 Hz, 1H), 2.68 – 2.59 (m, 1H), 2.53 (dd, *J* = 13.5, 10.6 Hz, 1H), 2.44 – 2.37 (m, 2H). ^{13}C NMR (151 MHz, DMSO, 330 K) δ 173.1, 171.3, 171.1, 170.6, 166.3, 161.6 (d, *J* = 241.9 Hz), 138.23, 138.17, 137.9, 134.2 (d, *J* = 3.1 Hz), 131.6 (d, *J* = 7.9 Hz), 129.78, 129.76, 129.6, 128.4, 128.34, 128.29, 126.69, 126.65, 126.63, 115.2 (d, *J* = 21.2 Hz), 54.2, 54.2, 54.1, 54.0, 40.8, 38.7, 38.6, 38.5, 37.0. ^{19}F NMR (376 MHz, DMSO) δ -117.01. IR (ATR): 3061, 3016, 2910, 1640, 1545, 1501, 1221 cm^{-1}. HRMS (ESI-TOF) *m/z* calc'd for $C_{38}H_{40}FN_5O_6Na$ $[M+Na]^+$: 704.2860, found: 704.2859. $[\alpha]^{26}_D$ +7 (*c* = 0.52, MeOH).

(3*S*,6*R*,9*S*,12*R*)-6,9,12-tribenzyl-3-(4-fluorobenzyl)-1,4,7,10,13-pentaazacyclopentadecane-2,5,8,11,14-pentaone (1.25)

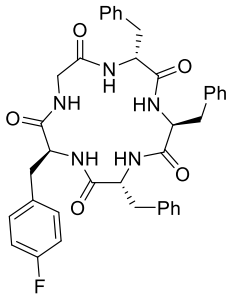

To a round botton flask equipped with a stir bar was added pentapeptide **S28** (200 mg, 0.250 mmol), HOAt (85.1 mg, 0.625 mmol), and DMF (250 mL). The reaction mixture was cooled to 0 ^{o}C and *i*-Pr$_2$EtN (0.22 mL, 1.25 mmol) was added. HATU (238 mg, 0.625 mmol) was added in portions and the reaction warmed to rt and stirred for 12 h. The solvent was removed under reduced pressure and then purified by column chromatography (eluting with 4:1 DCM/EtOH) to afford a solid. This solid was further triturated with MeOH and Et$_2$O to give the title compound as a white solid (20 mg, 12%). ^{1}H NMR (400 MHz, DMSO) δ 8.75 (d, *J* = 6.8 Hz, 1H), 8.54 (d, *J* = 8.3 Hz, 1H), 8.38 (t, *J* = 6 Hz, 1H), 7.85 (d, *J* = 8.5 Hz, 1H), 7.64 (d, *J* = 7.2 Hz, 1H), 7.28 – 6.96 (m, 19H), 4.65 – 4.55 (m, 1H), 4.54 – 4.43 (m, 2H), 4.40 – 4.32 (m, 1H), 4.26 – 4.16 (m, 1H), 3.71 (dd, *J* = 16.2, 6.4 Hz, 1H), 3.47 (dd, *J* = 16.0, 5.2 Hz, 1H), 3.00 – 2.57 (m, 8H). ^{13}C NMR (151 MHz, DMSO) δ 171.3, 170.9, 170.7, 170.1, 168.4, 160.8 (d, *J* = 242.0 Hz), 137.51, 137.50, 136.9, 133.4 (d, *J* = 3.1 Hz), 130.5 (d, *J* = 8.0 Hz), 128.7, 128.43, 128.42, 127.8, 127.8, 127.7, 126.0, 125.80, 125.76, 114.6 (d, *J* = 21.1 Hz), 55.1, 54.0, 53.3, 53.0, 42.9, 37.4, 36.1, 35.0, 34.8. ^{19}F NMR (376 MHz, DMSO) δ -116.93. IR (ATR): 3055, 2927, 1646, 1540, 1204 cm^{-1}. HRMS (ESI-TOF) *m/z* calc'd for $C_{38}H_{38}FN_5O_5Na$ $[M+Na]^+$: 686.2755, found: 686.2742. $[\alpha]^{27}_D$ +6 (*c* = 0.18, DMF).

vii) SPPS Syntheses

(3*S*,6*S*,9*S*,12*S*)-6,9,12-tribenzyl-3-(4-fluorobenzyl)-1,4,7,10,13-pentaazacyclopentadecane-2,5,8,11,14-pentaone (S29)

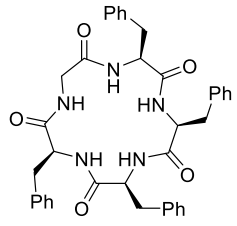

The corresponding linear pentapeptide was manually synthesized via Fmoc solid phase peptide synthesis (SPPS) using 2-chlorotrityl chloride (CTC) resin (substitution 1.1 mmol/g). The resin (0.360 g, 0.400 mmol) was swelled in anhydrous DCM (20 mL) for 45 min. The beads were washed once with DMF (peptide grade). DMF (10 mL), Fmoc-Phe-OH (620 mg, 1.60 mmol) and *i*-Pr_2EtN (2.5 mL) were added and allowed to mix under N_2 for 15 minutes. The coupling with Fmoc-Phe-OH was repeated again. After the double coupling, the beads were washed with DMF and the Fmoc group was deprotected with 20% 4-methylpiperidine in DMF (20 mL) for 15 minutes. This deprotection was repeated again. The resin was washed three times with DMF (15 mL) and a Kaiser test was performed to determine presence of deprotected amine. The beads were washed once with *N*-methyl-2-pyrrolidone (15 mL). To begin the next coupling, NMP (10 mL), Fmoc-Phe-OH (620 mg, 1.6 mmol), HBTU (610 mg, 1.6 mmol), and *i*-Pr_2EtN (2.5 mL) were added and the resin bubbled under N_2 for 30 min. The completion of the coupling was monitored by the Kaiser test. If incomplete, the coupling step was repeated again. The resin was washed three times with DMF (15 mL). The deprotection of the Fmoc group was repeated as above two times. To elongate the peptide, the coupling and deprotection steps were performed with Fmoc-Phe-OH, Fmoc-Phe-OH, and Fmoc-Gly-OH. After the last amino acid was deprotected, the beads were washed three times with DMF. To the resin was added 40 mL cleavage solution (95% TFA, 2.5% H_2O, 2.5% triisopropylsilane), and the resin

bubbled under N_2 for 3 h. A new receiving flask was replaced on the peptide synthesizer and the TFA was drained into the new flask. The TFA solution was separated into 4 conical vials and cold ether (–20 °C) was added to precipitate the peptide. The vials were centrifuged (3000 rpm, 0–4 °C) for 20 minutes. The remaining TFA and ether solution was decanted from the conical vials and the peptide precipitate was concentrated. Then to a round botton flask equipped with a stir bar was added the linear pentapeptide (0.400 mmol), HOAt (136 mg, 1.00 mmol), and DMF (400 mL). The reaction mixture was cooled to 0 ºC and *i*-Pr_2EtN (0.348 mL, 2.00 mmol) was added. HATU (380 mg, 1.00 mmol) was added in portions and the reaction warmed to rt and stirred for 12 h. The solvent was concentrated under reduced pressure and a white solid formed. This solid was then filtered and triturated with DCM, MeOH, and Et_2O to afford the title compound as a white solid (92 mg, 36% overall). The ^{1}H-NMR spectrum was consistent with the cyclic pentapeptide **1.27** obtained after asymmetric hydrogenation (Figure 1.28 and 1.29).

(3*S*,6*S*,9*S*,12*S*)-6,9,12-tribenzyl-3-(4-fluorobenzyl)-1,4,7,10,13-pentaazacyclopentadecane-2,5,8,11,14-pentaone (S30)

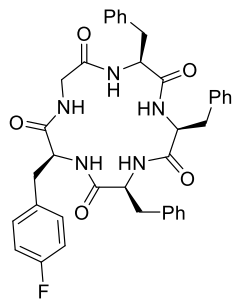

The corresponding linear pentapeptide was manually synthesized via Fmoc solid phase peptide synthesis (SPPS) using 2-chlorotrityl chloride (CTC) resin (substitution 1.1 mmol/g). The resin (0.360 g, 0.400 mmol) was swelled in anhydrous DCM (20 mL) for 45 min. The beads were washed once with DMF (peptide grade). DMF (10 mL), Fmoc-4-fluoro-Phe-OH (649 mg, 1.60 mmol) and *i*-Pr_2EtN (2.5 mL) were added and allowed to mix under N_2 for 15 minutes. The coupling with Fmoc-4-fluoro-Phe-OH was repeated again. After the double coupling, the beads were washed with DMF and the Fmoc group was deprotected

with 20% 4-methylpiperidine in DMF (20 mL) for 15 minutes. This deprotection was repeated again. The resin was washed three times with DMF (15 mL) and a Kaiser test was performed to determine presence of deprotected amine. The beads were washed once with *N*-methyl-2-pyrrolidone (15 mL). To begin the next coupling, NMP (10 mL), Fmoc-Phe-OH (620 mg, 1.6 mmol), HBTU (610 mg, 1.6 mmol), and *i*-Pr_2EtN (2.5 mL) were added and the resin bubbled under N_2 for 30 min. The completion of the coupling was monitored by the Kaiser test. If incomplete, the coupling step was repeated again. The resin was washed three times with DMF (15 mL). The deprotection of the Fmoc group was repeated as above two times. To elongate the peptide, the coupling and deprotection steps were performed with Fmoc-Phe-OH, Fmoc-Phe-OH, and Fmoc-Gly-OH. After the last amino acid was deprotected, the beads were washed three times with DMF. To the resin was added 40 mL cleavage solution (95% TFA, 2.5% H_2O, 2.5% triisopropylsilane), and the resin bubbled under N_2 for 3 h. A new receiving flask was replaced on the peptide synthesizer and the TFA was drained into the new flask. The TFA solution was separated into 4 conical vials and cold ether (–20 °C) was added to precipitate the peptide. The vials were centrifuged (3000 rpm, 0–4 °C) for 20 minutes. The remaining TFA and ether solution was decanted from the conical vials and the peptide precipitate was concentrated. Then to a round botton flask equipped with a stir bar was added the linear pentapeptide (0.400 mmol), HOAt (136 mg, 1.00 mmol), and DMF (400 mL). The reaction mixture was cooled to 0 ^oC and *i*-Pr_2EtN (0.348 mL, 2.00 mmol) was added. HATU (380 mg, 1.00 mmol) was added in portions and the reaction warmed to rt and stirred for 12 h. The solvent was concentrated under reduced pressure and a white solid formed. This solid was then filtered and triturated with DCM, MeOH, and Et_2O to afford the title

compound as a white solid (61 mg, 23% overall). ^{1}H NMR (600 MHz, DMSO) δ 8.52 (br t, *J* = 5.2 Hz, 1H), 8.35 (d, *J* = 7.5 Hz, 1H), 8.32 (d, *J* = 8.1 Hz, 1H), 8.25 (d, *J* = 7.8 Hz, 1H), 7.95 (d, *J* = 8.3 Hz, 1H), 7.32 – 6.98 (m, 19H), 4.37 – 4.29 (m, 1H), 4.29 – 4.19 (m, 2H), 4.08 – 3.97 (m, 1H), 3.92 (dd, *J* = 14.4, 5.8 Hz, 1H), 3.29 (dd, *J* = 14.3, 4.8 Hz, 1H), 3.12 – 2.84 (m, 7H), 2.80 – 2.69 (m, 1H). ^{13}C NMR (151 MHz, DMSO) δ 171.4, 171.1, 170.7, 170.6, 169.2, 161.0 (d, *J* = 241.6 Hz), 137.7, 137.5, 137.4, 134.2 (d, *J* = 2.8 Hz), 130.9 (d, *J* = 8.0 Hz), 129.2, 129.1, 129.0, 128.9, 128.3, 128.2, 126.39, 126.37, 126.35, 114.9 (d, *J* = 21.0 Hz), 57.4, 55.9, 55.8, 54.6, 43.3, 36.9, 36.5, 35.7, 30.7. ^{19}F NMR (376 MHz, DMSO) δ -117.17. IR (ATR): 3083, 3022, 2932, 1640, 1495, 1216 cm^{-1}. HRMS (ESI-TOF) *m/z* calc'd for $C_{38}H_{38}FN_5O_5$ $[M+Na]^+$: 686.2755, found: 686.2736. $[\alpha]^{27}_D$ –97 (*c* = 0.22, DMF).

General procedures for hydrogenation

Representative examples:

Method A – Hydrogenation using Schlenk tube

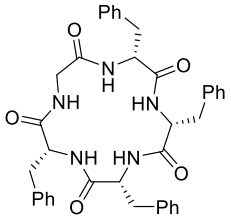

(3*R*,6*R*,9*R*,12*R*)-3,6,9,12-tetrabenzyl-1,4,7,10,13-pentaazacyclopentadecane-2,5,8,11,14-pentaone (1.27)

In a nitrogen-filled glove box, to a Schlenk vial equipped with a stir bar was added (*R,R',S,S'*)-DuanPhos (3 mg, 0.0079 mmol) and $[Rh(cod)_2]BF_4$ (3 mg, 0.0075 mmol) in dry and degassed MeOH (2 mL). This mixture was stirred at rt for 5 min, then cyclic peptide **1.20** (128 mg, 0.2 mmol) in MeOH (4 mL) was added to this mixture. The Schlenk tube was sealed, removed from the nitrogen box, and then connected to a Schlenk line (vacuum gas manifold). The pre-catalyst solution was degassed via three cycles of 'freeze-pump-thaw'. On the last 'thaw' cycle, the Schlenk tube was backfilled

with H_2 gas and subsequently sealed while the reaction mixture was still frozen. The Schlenk tube was allowed to thaw to pressurize the vial and the reaction mixture was stirred at rt for 48 h, over which an off-white solid precipitated from the solution. The heterogeneous mixture was then collected into a scintillation vial and concentrated under reduced pressure. The resulting crude solid was triturated in DCM and MeOH and then filtered to afford an off-white solid (108 mg, 86%, 99% *ee*). ^{1}H NMR (300 MHz, DMSO) δ 8.53 (t, *J* = 5.4 Hz, 1H), 8.34 (d, *J* = 7.4 Hz, 1H), 8.33 (d, *J* = 8.0 Hz, 1H), 8.23 (d, *J* = 8.0 Hz, 1H), 7.98 (d, *J* = 8.4 Hz, 1H), 7.31 – 7.10 (m, 18H), 7.09 - 7.02 (m, 2H), 4.35 (m, 1H), 4.24 (m, 2H), 4.04 (q, *J* = 7.8 Hz, 1H), 3.92 (dd, *J* = 14.5, 6.0 Hz, 1H), 3.28 (dd, *J* = 14.5, 5.1 Hz, 1H), 3.17 (d, *J* = 5.3 Hz, 1H), 3.11 (dd, *J* = 13.8, 5.5 Hz, 1H), 3.02 - 2.85 (m, 6H), 2.74 (dd, *J* = 14.1, 9.2 Hz, 1H). ^{13}C NMR (100 MHz, DMSO) δ 171.5, 171.1, 170.7, 170.6, 169.1, 138.0, 137.7, 137.5, 137.4, 129.1, 129.1, 129.0, 128.8, 128.19, 128.17, 126.3, 57.4, 56.0, 55.8, 54.6, 43.3, 36.9, 36.8, 36.6, 36.5. IR (ATR): 3295, 3028, 2926, 1615, 1528, 1496, 1454, 837 cm^{-1}. HRMS (ESI-TOF) *m/z* calc'd for $C_{38}H_{39}N_5O_5$ $[M+H]^+$: 646.3020, found 646.3023.

(3*R*,6*R*,9*R*,12*R*)-3,6,9,12-tetrabenzyl-1,4,7,10,13-pentaazacyclopentadecane-2,5,8,11,14-pentaone (1.28)

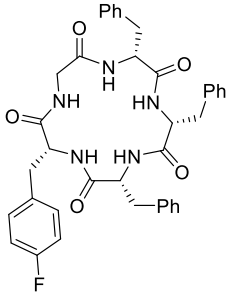

In a nitrogen-filled glove box, to a Schlenk vial equipped with a stir bar was added (*R,R',S,S'*)-DuanPhos (0.29 mg, 0.00076 mmol) and $[Rh(cod)_2]BF_4$ (0.31 mg, 0.00076 mmol) in dry and degassed MeOH (0.350 mL). This mixture was stirred at rt for 5 min, then cyclic peptide **1.21** (10 mg, 0.015 mmol) in MeOH (0.300 mL) was added to this mixture. The Schlenk tube was sealed, removed from the nitrogen box, and then connected to a Schlenk line (vacuum gas

manifold). The pre-catalyst solution was degassed via three cycles of 'freeze-pump-thaw'. On the last 'thaw' cycle, the Schlenk tube was backfilled with H_2 gas and subsequently sealed while the reaction mixture was still frozen. The Schlenk tube was allowed to thaw to pressurize the vial and the reaction mixture was stirred at 50 °C for 48 h, over which an off-white solid precipitated from the solution. The heterogeneous mixture was then collected into a scintillation vial and concentrated under reduced pressure. The resulting crude solid was triturated in DCM and MeOH and then filtered to afford an off-white solid (7.2 mg, 72%, 20:<1 *dr*). The diastereoselectivity was determined by ^{19}F-NMR analysis of the unpurified reaction mixture The ^{1}H-NMR spectrum of **1.28** was consistent with an authentic sample synthesized via SPPS (page 89). ^{1}H NMR (400 MHz, DMSO) δ 8.52 (br t, *J* = 5.4 Hz, 1H), 8.36 (d, *J* = 7.8 Hz, 1H), 8.33 (d, *J* = 7.8 Hz, 1H), 8.25 (d, *J* = 8.1 Hz, 1H), 7.96 (d, *J* = 5.3 Hz, 1H), 7.32 – 6.96 (m, 19H), 4.38 – 4.29 (m, 1H), 4.29 – 4.19 (m, 2H), 4.07 – 3.99 (m, 1H), 3.92 (dd, *J* = 14.1, 5.7 Hz, 1H), 3.30 – 3.24 (m, 1H), 3.14 – 2.81 (m, 7H), 2.81 – 2.63 (m, 1H).

Method B – Hydrogenation using Hel Reactor

(3*S*,6*R*,9*S*,12*R*)-6,9,12-tribenzyl-3-(4-fluorobenzyl)-1,4,7,10,13-pentaazacyclopentadecane-2,5,8,11,14-pentaone (±)**-1.25**

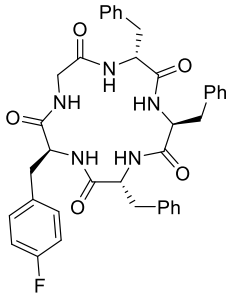

In a N_2-filled glovebox, $[Rh(cod)_2]BF_4$ (0.31 mg, 0.00076 mmol, 5 mol%) and dppp (0.32 mg, 0.00076 mmol, 5 mol%) in MeOH/DMF (4:1, 306 µL, 0.05 M) were added to a ½ dr vial equipped with a stir bar containing pentapeptide **1.21** (10 mg, 0.0153 mmol). The vial was capped with a screwcap with a slitted rubber septum and taken outside

of the glovebox. The vial was sonicated to ensure all contents were dissolved and then placed in the HEL CATalyst block and the head was screwed into place. The block was filled then purged three times with hydrogen, and then pressurized with hydrogen to 7 atm. The reaction stirred at 40 ^{o}C and was stopped after 48 h. The solvent was concentrated under reduced pressure and the reaction mixture was triturated with DCM to afford the title compound as an off-white solid (8.9 mg, 88%, 20:2:1:1:1 *dr*). The diastereoselectivity was determined by ^{19}F-NMR analysis of the unpurified reaction mixture. ^{1}H NMR (400 MHz, DMSO) δ 8.75 (d, *J* = 6.8 Hz, 1H), 8.54 (d, *J* = 8.3 Hz, 1H), 8.38 (t, *J* = 6 Hz, 1H), 7.85 (d, *J* = 8.5 Hz, 1H), 7.64 (d, *J* = 7.2 Hz, 1H), 7.28 – 6.96 (m, 19H), 4.65 – 4.55 (m, 1H), 4.54 – 4.43 (m, 2H), 4.40 – 4.32 (m, 1H), 4.26 – 4.16 (m, 1H), 3.71 (dd, *J* = 16.2, 6.4 Hz, 1H), 3.47 (dd, *J* = 16.0, 5.2 Hz, 1H), 3.00 – 2.57 (m, 8H). ^{13}C NMR (151 MHz, DMSO) δ 171.3, 170.9, 170.7, 170.1, 168.4, 160.8 (d, *J* = 242.0 Hz), 137.5, 137.5, 136.9, 133.4 (d, *J* = 3.1 Hz), 130.5 (d, *J* = 8.0 Hz), 128.7, 128.43, 128.42, 127.81, 127.75, 127.7, 126.0, 125.8, 125.7, 114.6 (d, *J* = 21.1 Hz), 55.1, 54.0, 53.3, 53.0, 42.9, 37.4, 36.1, 35.0, 34.8. ^{19}F NMR (376 MHz, DMSO) δ -116.93. IR (ATR): 3055, 2927, 1646, 1540, 1204 cm^{-1}. HRMS (ESI-TOF) *m/z* calc'd for $C_{38}H_{38}FN_5O_5Na$ $[M+Na]^+$: 686.2755, found: 686.2742.

Table 1.1, entry 1: 1.25 was prepared according to method B using $[Rh(cod)_2]BF_4$ (0.31 mg, 0.00076 mmol, 5 mol%) and dppp (0.32 mg, 0.00076 mmol, 5 mol%) in MeOH/DMF (4:1, 306 µL, 0.05 M), and pentapeptide **1.22** (10 mg, 0.0153 mmol). The diastereoselectivity was determined by ^{19}F-NMR analysis of the unpurified reaction mixture. The product was isolated as an off white solid (7.7 mg, 76%, 20:<1:<1:<1:<1 *dr*).

Table 1.1, entry 2: 1.25 was prepared according to method B using $[Rh(cod)_2]BF_4$ (0.15 mg, 0.00038 mmol, 5 mol%) and dppp (0.16 mg, 0.00038 mmol, 5 mol%) in MeOH/DMF (4:1, 304 µL, 0.025 M), and pentapeptide **1.23** (5 mg, 0.0076 mmol) stirring at 60 °C and H_2 (20 atm). The diastereoselectivity was determined by ^{19}F-NMR analysis of the unpurified reaction mixture. The product was isolated as an off white solid (5.0 mg, 99%, 20:<1:<1:<1:<1 *dr*).

Table 1.1, entry 3: 1.25 was prepared according to method B using $[Rh(cod)_2]BF_4$ (0.31 mg, 0.00076 mmol, 10 mol%) and dppp (0.31 mg, 0.00076 mmol, 10 mol%) in THF (500 µL, 0.015 M), and pentapeptide **1.24** (5 mg, 0.0076 mmol) stirring at 80 °C and H_2 (40 atm). The diastereoselectivity was determined by ^{19}F-NMR analysis of the unpurified reaction mixture. The product was isolated as an off white solid (5.0 mg, 99%, 20:<1:<1:<1:<1 *dr*).

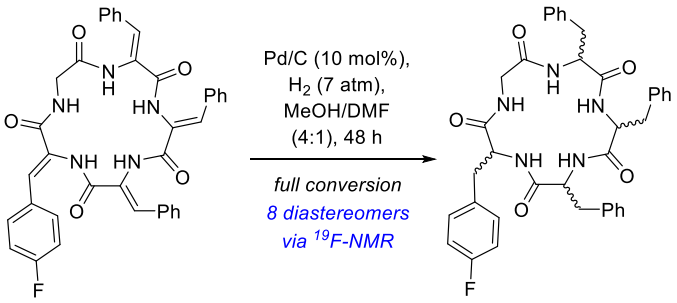

To a ½ dr vial equipped with a stir bar was added cyclic pentapeptide **1.21** (10 mg, 0.0153 mmol) and 10% Pd/C (1.6 mg, 0.00153 mmol, 10 mol%). The contents were dissolved in MeOH/DMF (4:1, 306 µL, 0.05 M) and the vial was capped with a screwcap with a slitted rubber septum. The vial was sonicated to ensure all contents were dissolved and then

placed in the HEL CATalyst block and the head was screwed into place. The block was filled then purged three times with hydrogen, and then pressurized with hydrogen to 7 atm. After 48 h and the reaction mixture was filtered through a plug of celite, eluted with MeOH, concentrated under reduced pressure and then analyzed by ^{19}F-NMR and LC-MS analysis, which showed the presence of 8 diastereomers (Figure 1.27).

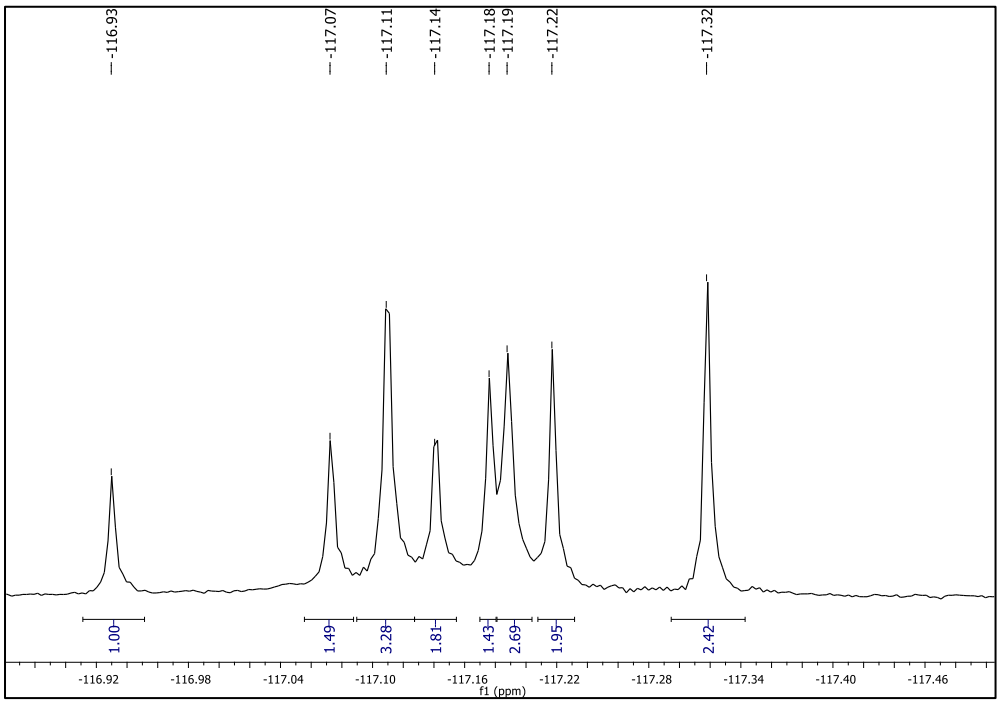

Figure 1.27 ^{19}F-NMR after Pd/C hydrogenation

Ligand evaluation

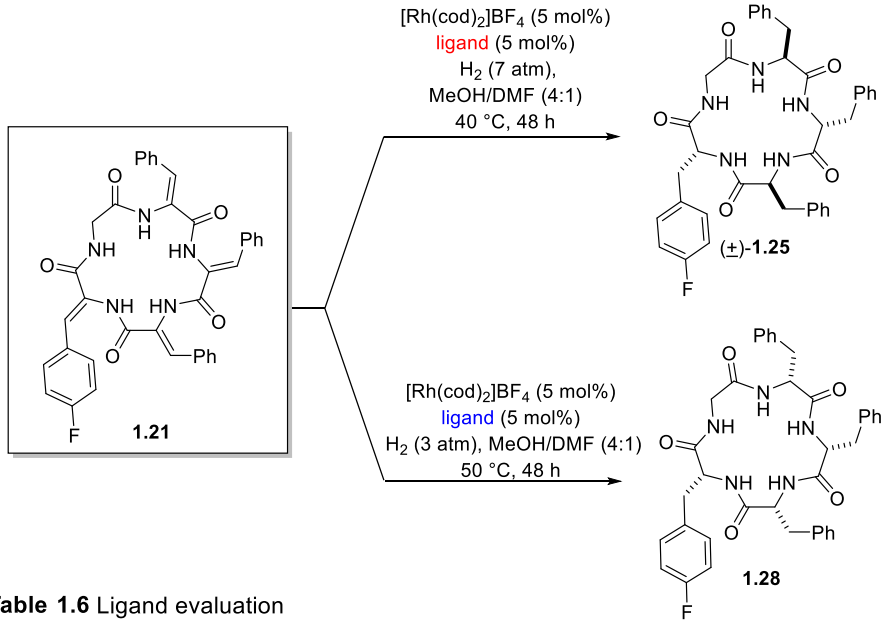

Table 1.6 Ligand evaluation

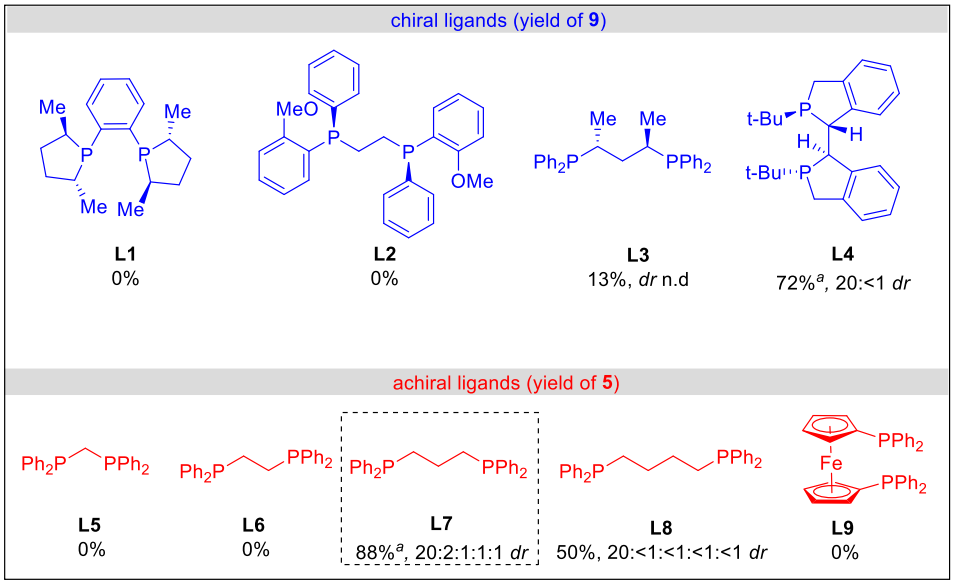

[a] Isolated yield

For the ligand evaluation of cyclic pentapeptide **1.21** to form **1.28**, method A was used for the hydrogenation (Table 1.6). For the reaction of cyclic peptide **1.21** to form (±)-**1.25**, method B was used for the hydrogenation. Yields and diastereoselectivity were determined by ^{19}F-NMR spectroscopy analysis of the unpurified reaction mixture.

NMR time trace

Five independent hydrogenations were set up using general hydrogenation procedure method B. The reaction was quenched at incomplete conversion at t=0 min, 7 min, 1 h, 16 h, and 48 h by opening the reaction to air. ^{19}F-NMR time points in Figure 3 were performed on a 400 MHz Bruker DRX400 spectrometer at 298 K, 8 scans, and 30 s relaxation delay. The NMR spectra was taken in DMSO-d_6 solvent.

Determination of absolute stereochemistry via SFC analysis

Column: IC, 40% MeOH isocratic, thermostat set to 44 ˚C, sample prepared in 1:1 DCM/MeOH

1. Cyclo(Gly-L-Phe-L-Phe-L-Phe-L-Phe) (**S29**) made from authentic (L-Phe)$_4$-OH and **1.27**

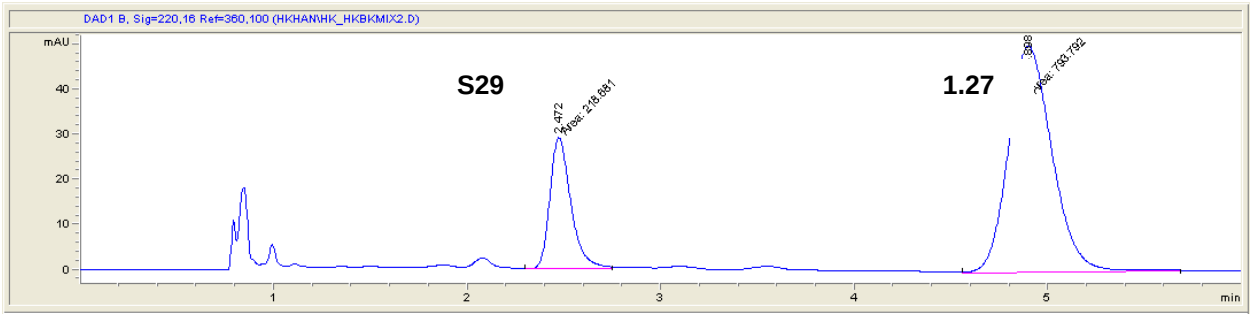

2. **S29** made from hydrogenation of pentapeptide **1.20** with (*S,S',R,R'*)-DuanPhos as the ligand

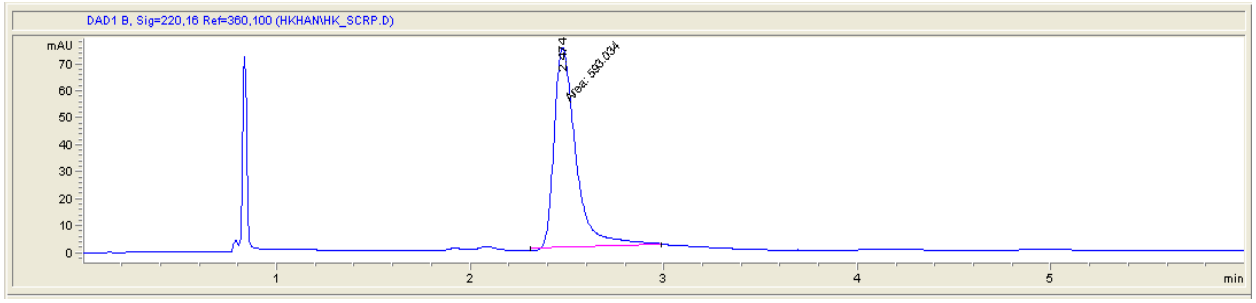

3. **1.27** made from hydrogenation of **1.20** using (*R,R',S,S'*)-Duanphos

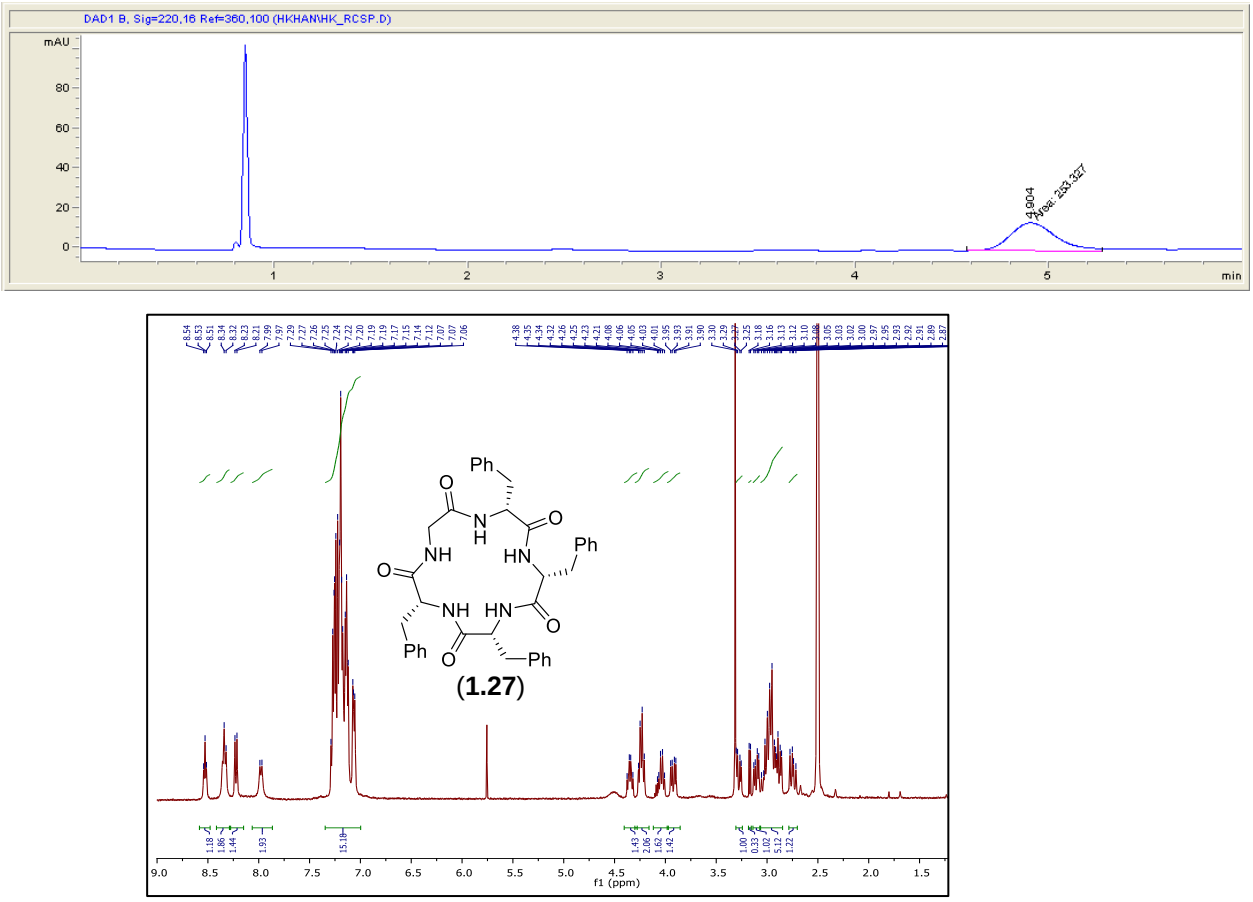

Figure 1.28. ^{1}H-NMR of cyclic pentapeptide **1.27** after hydrogenation using (*R,R',S,S'*)-Duanphos

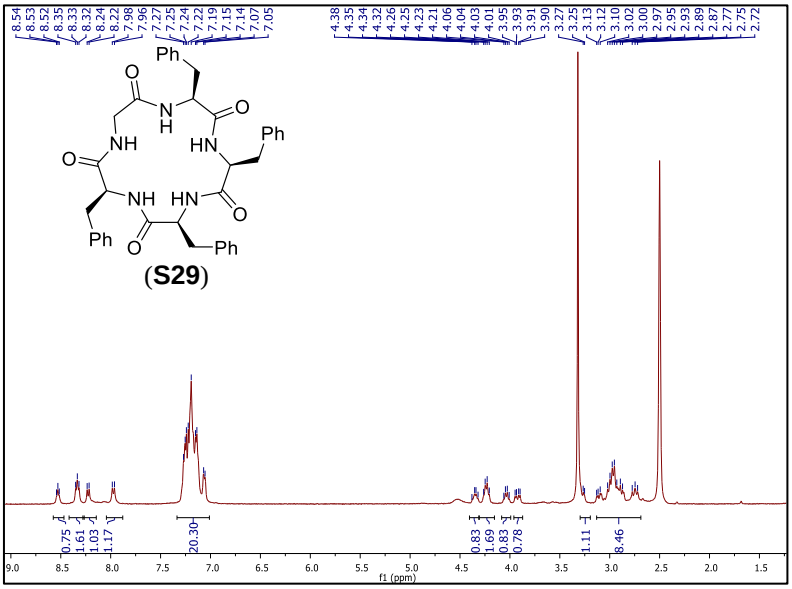

Figure 1.29 ^{1}H-NMR of cyclic pentapeptide **S29** made via SPPS

The absolute stereochemistry of **1.27** when using $Rh(cod)_2BF_4$ and (*R,R',S,S'*)–Duanphos gives the D-amino acid configuration.

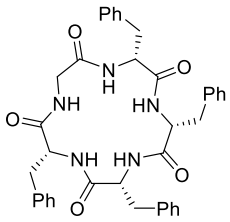

1.3.3 NMR Spectra

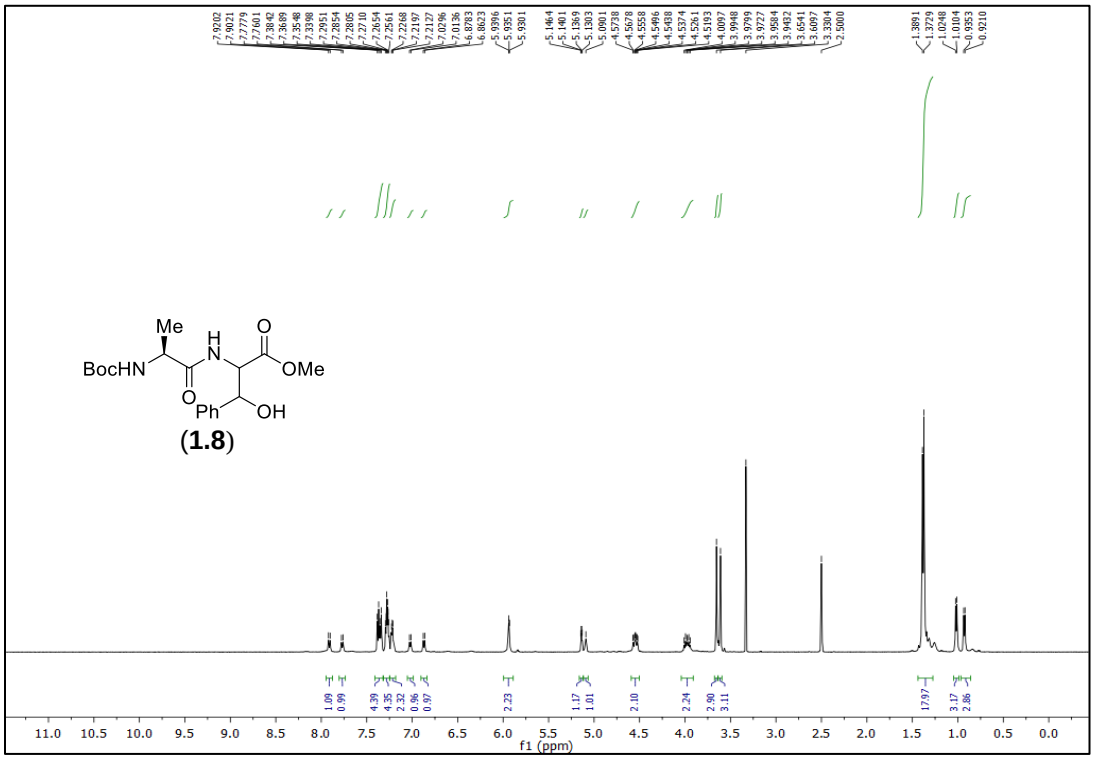

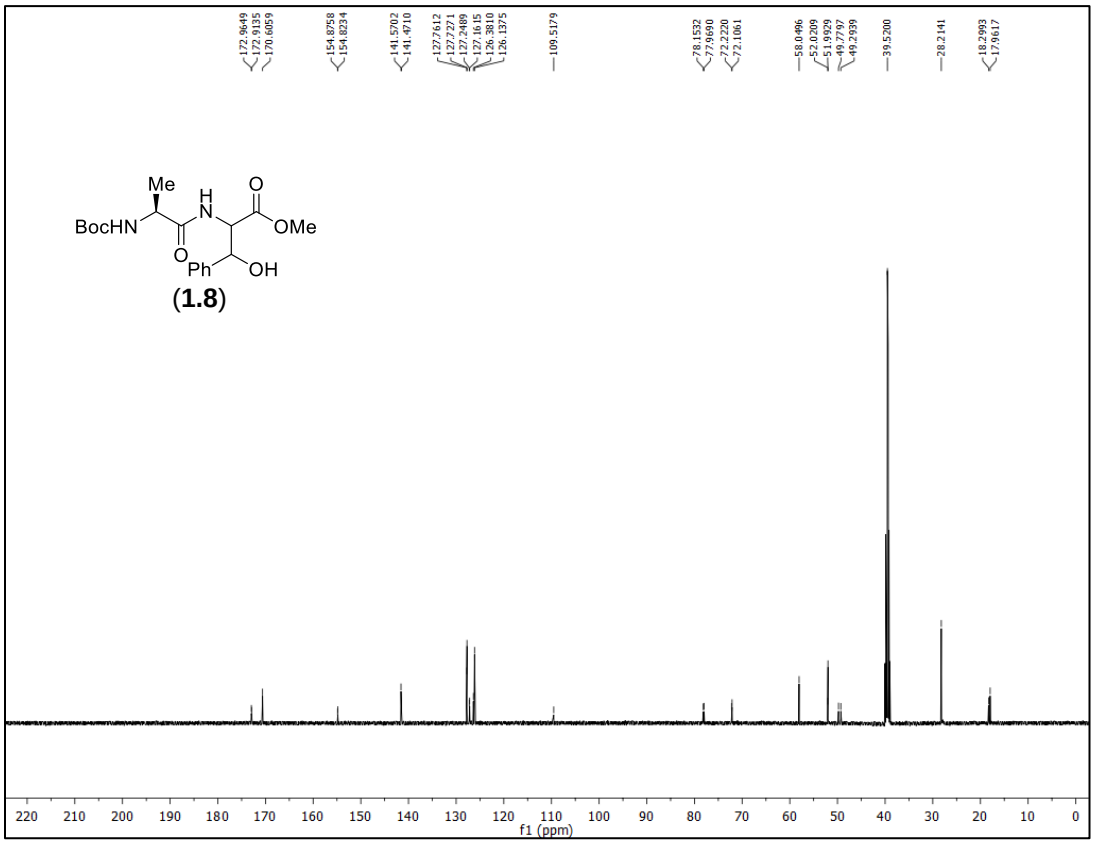

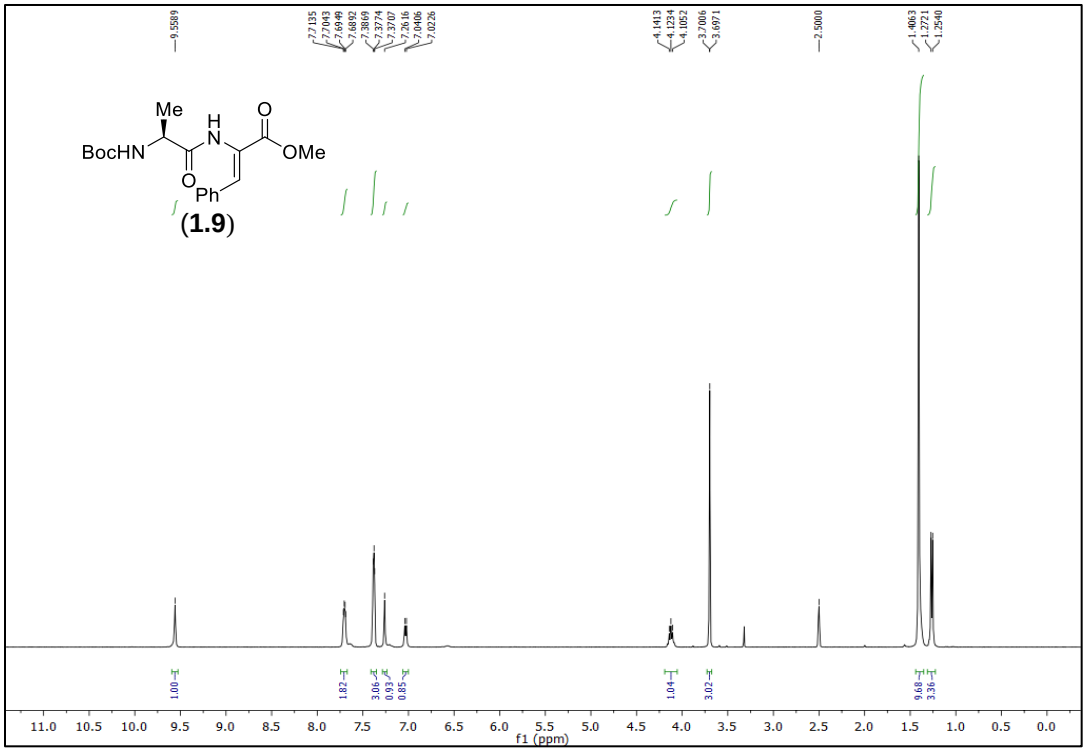
Me
H
N
O
BocHN
OMe
O
Ph
(1.9)
f1 (ppm)

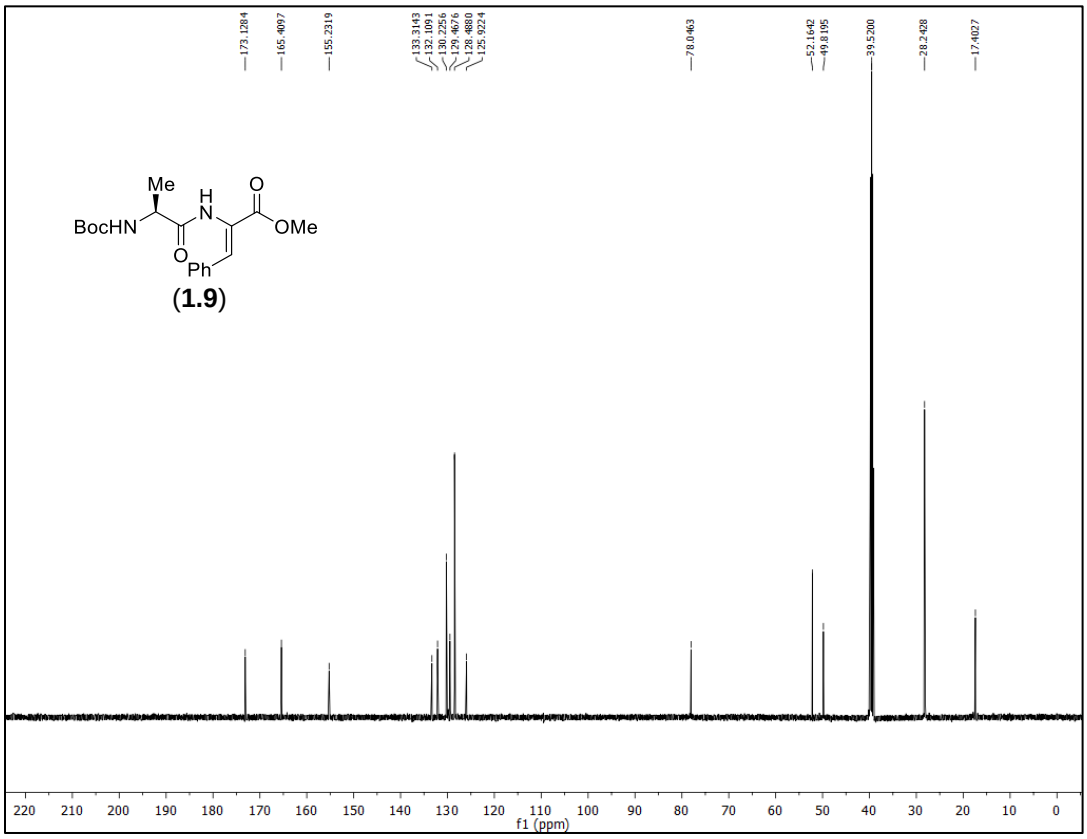
Me
H
N
O
BocHN
OMe
O
Ph
(1.9)
f1 (ppm)

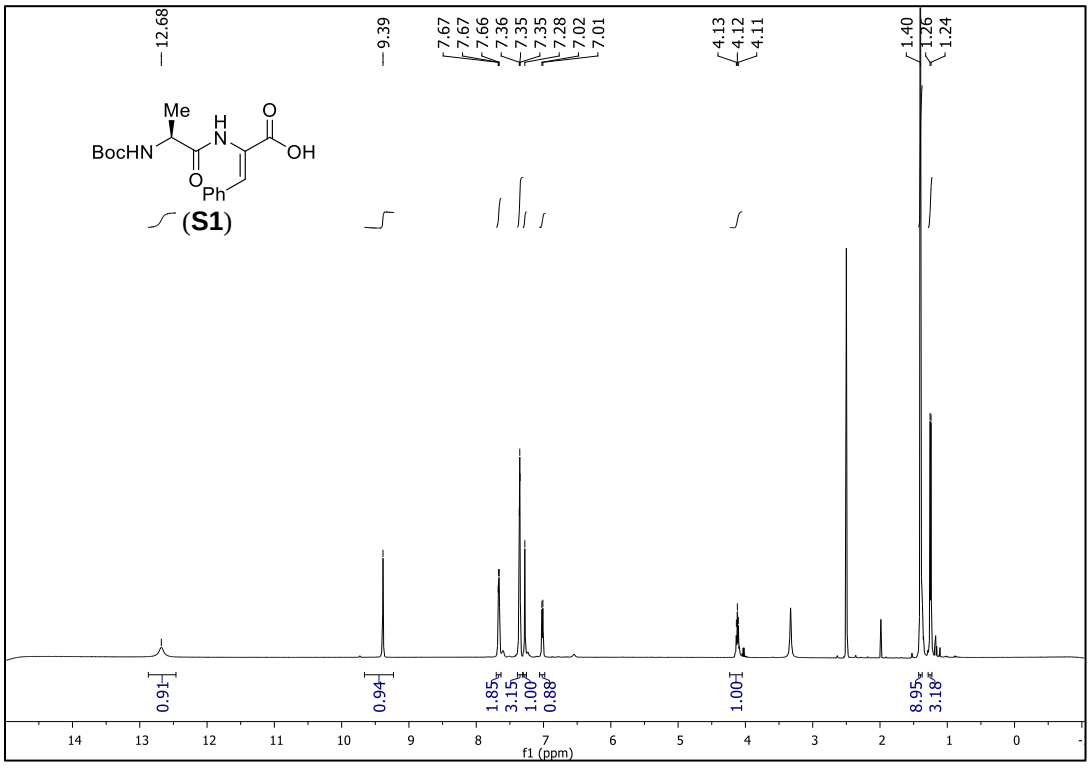
12.68
9.39
7.67
7.67
7.66
7.36
7.35
7.35
7.28
7.02
7.01
4.13
4.12
4.11
1.40
1.26
1.24
Me
H
N
O
BocHN
OH
O
Ph
(S1)
0.91
0.94
1.85
3.15
1.00
0.88
1.00
8.95
3.18
f1 (ppm)

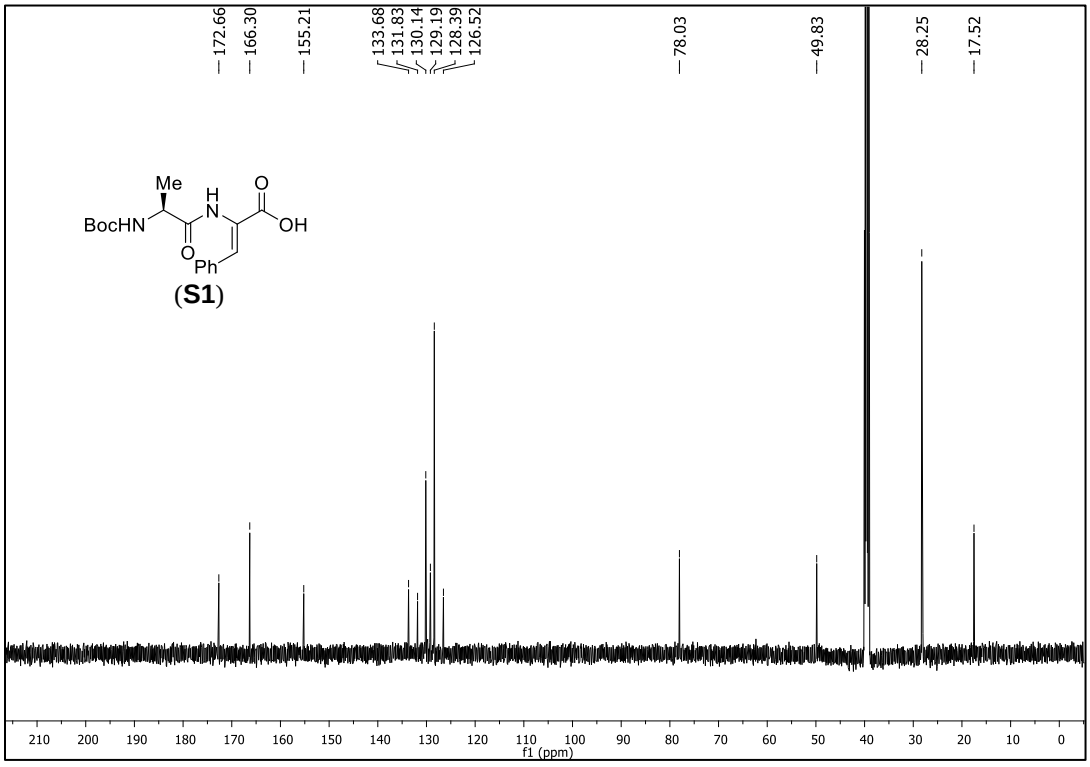
172.66
166.30
155.21
133.68
131.83
130.14
129.19
128.39
126.52
78.03
49.83
28.25
17.52
Me
H
N
O
BocHN
OH
O
Ph
(S1)
f1 (ppm)

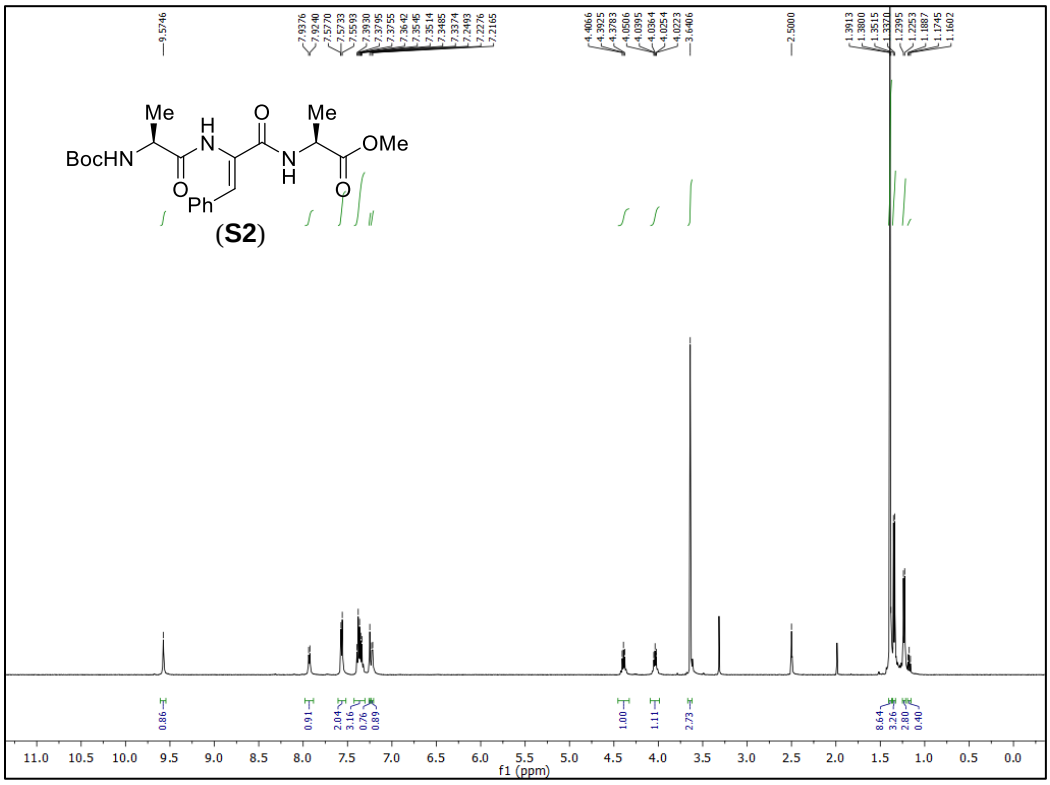
Me
H
N
O
Me
BocHN
N
OMe
H
O
O
Ph
(S2)
f1 (ppm)

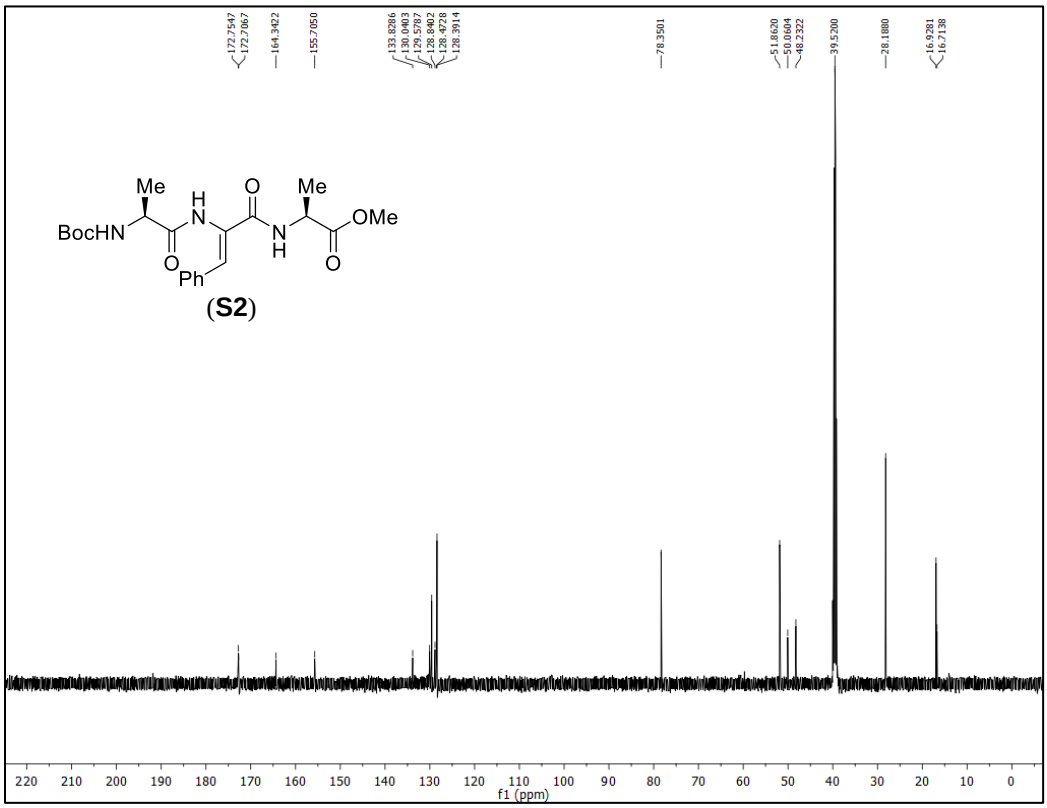
Me
H
N
O
Me
BocHN
N
OMe
H
O
O
Ph
(S2)
f1 (ppm)

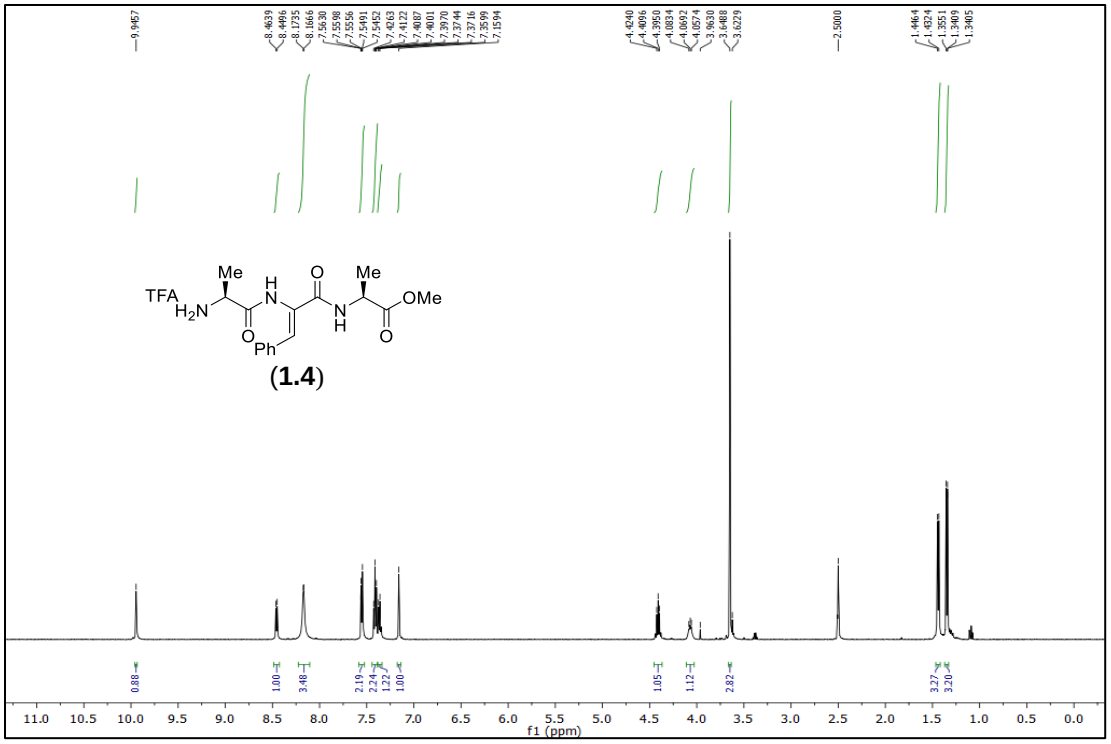
TFA
H2N
Me
H
N
O
Me
N
H
OMe
O
O
Ph
(1.4)
f1 (ppm)

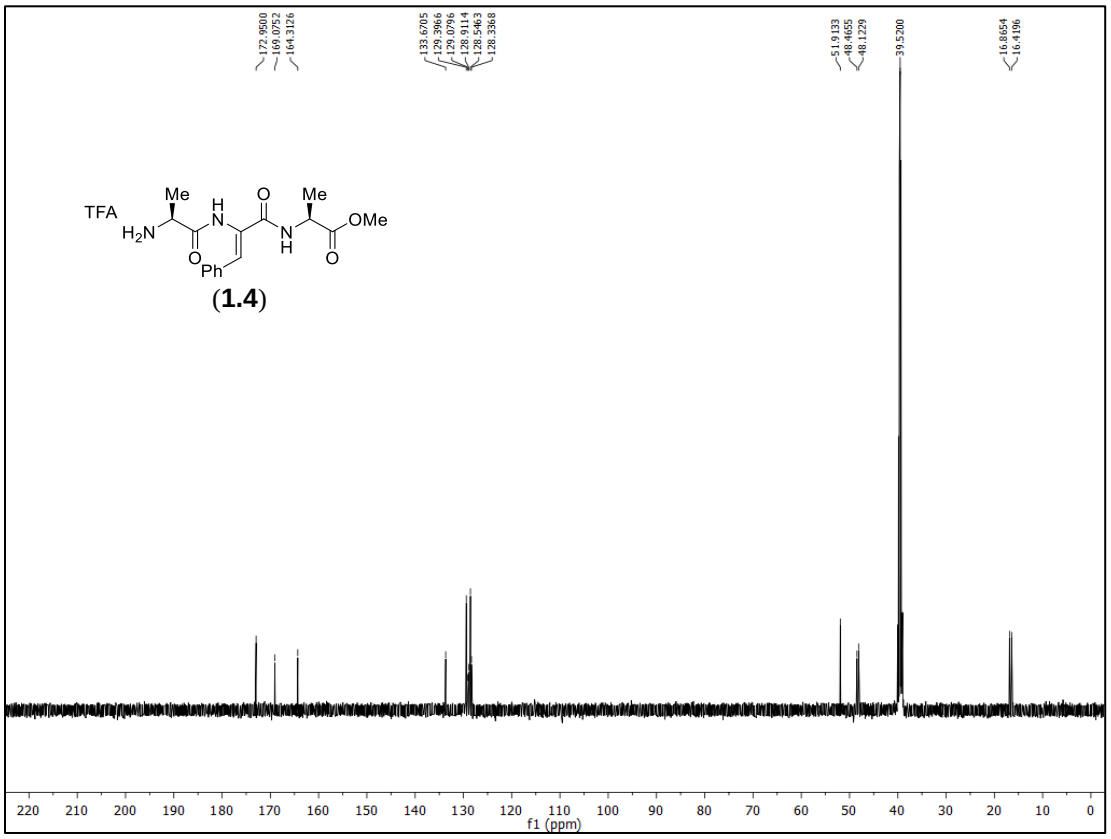
TFA
H2N
Me
H
N
O
Me
N
H
OMe
O
O
Ph
(1.4)
f1 (ppm)

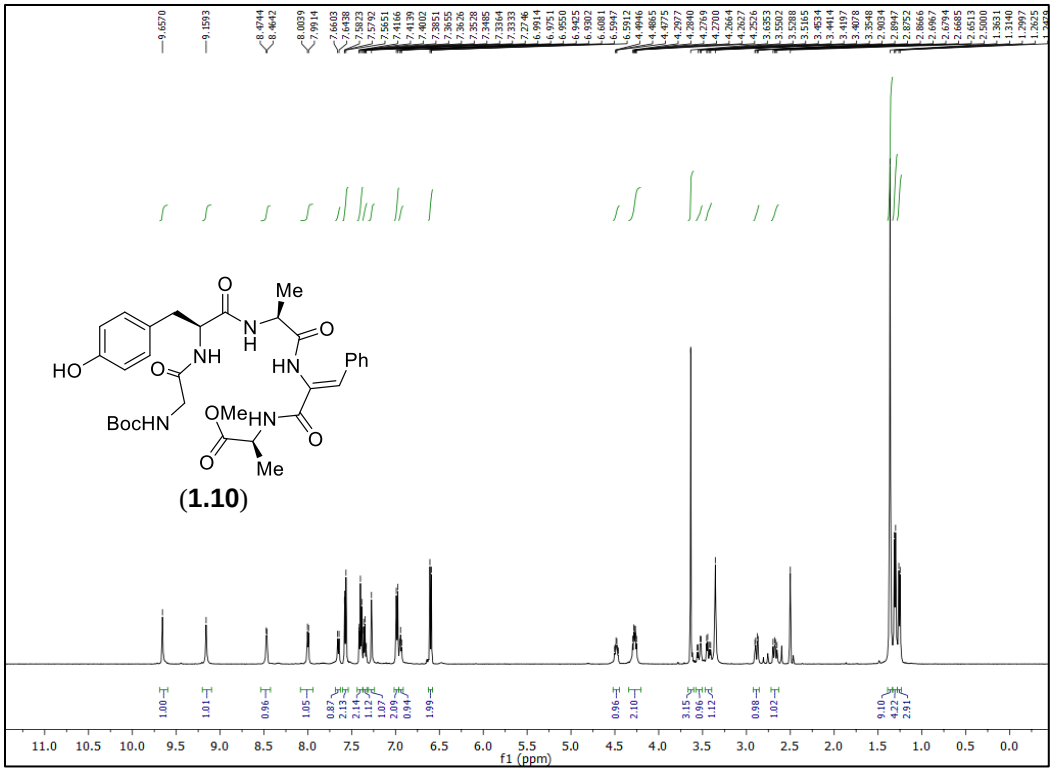
HO
NH
O
N
H
Me
O
HN
Ph
BocHN
OMe
HN
O
O
Me
f1 (ppm)

(**1.10**)

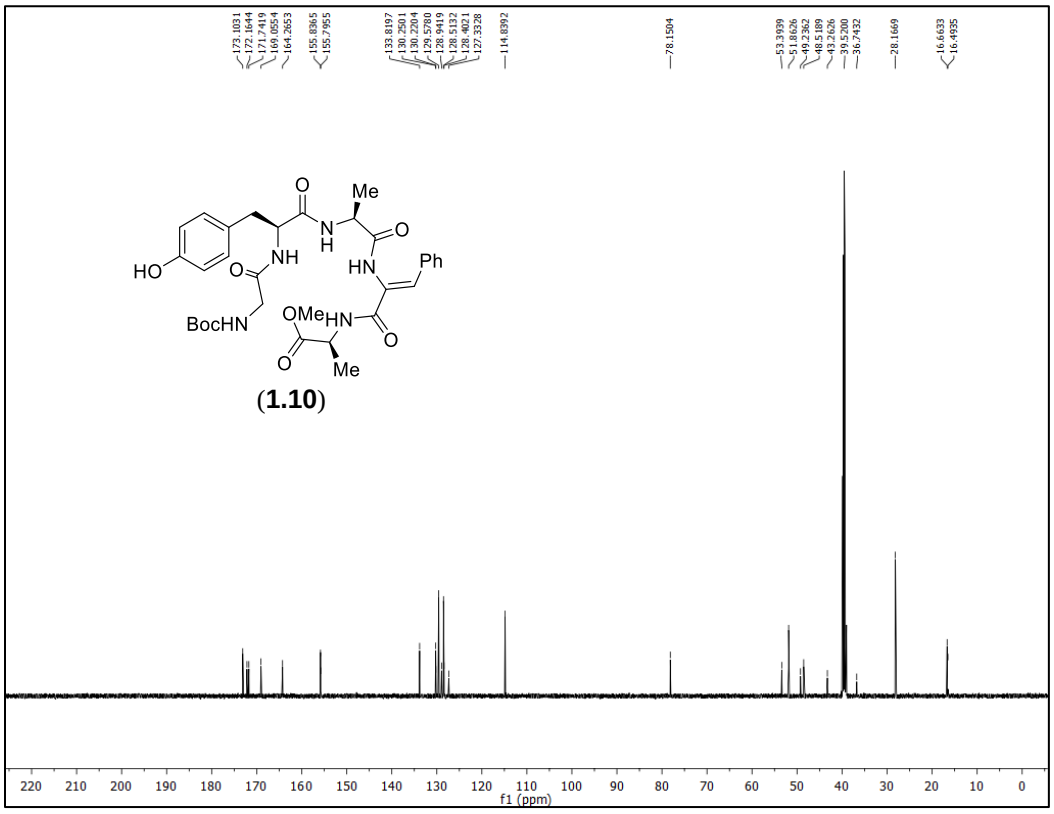
HO
NH
O
N
H
Me
O
HN
Ph
BocHN
OMe
HN
O
O
Me
f1 (ppm)

(**1.10**)

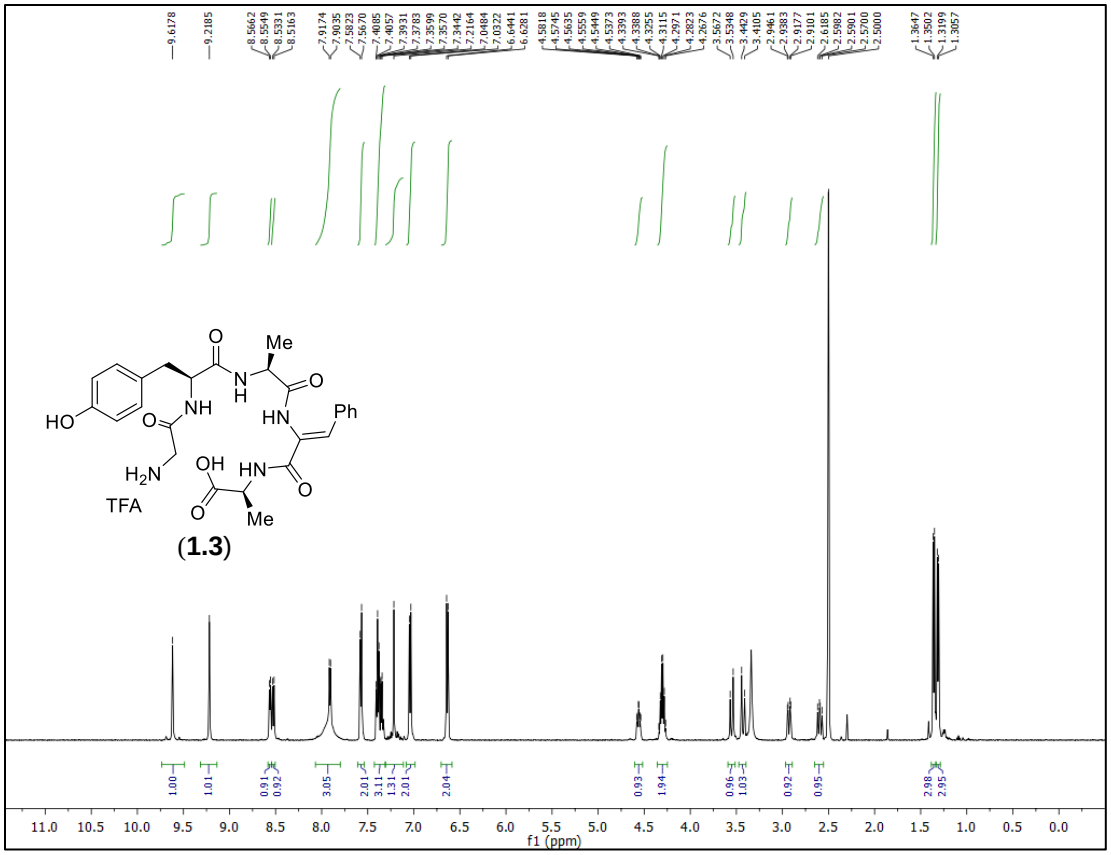
HO
O
N
H
Me
NH
HN
Ph
H2N
TFA
OH
HN
Me
f1 (ppm)

(**1.3**)

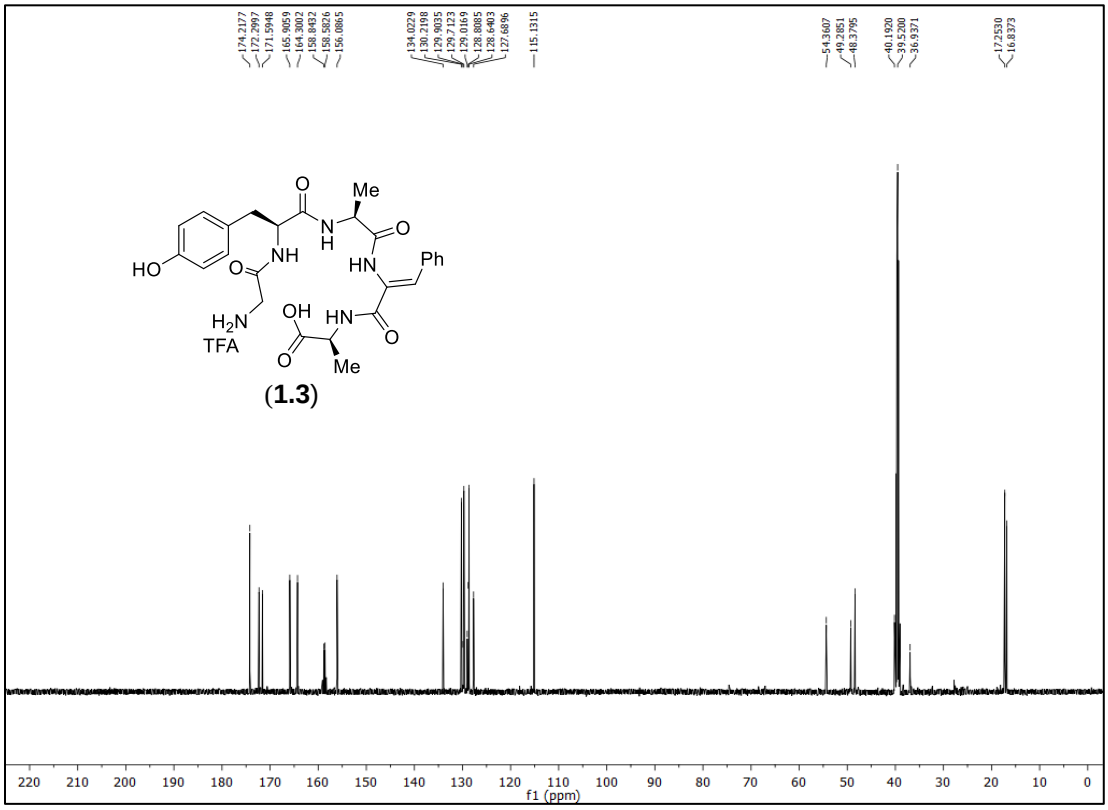
HO
O
N
H
Me
NH
HN
Ph
H2N
TFA
OH
HN
Me
f1 (ppm)

(**1.3**)

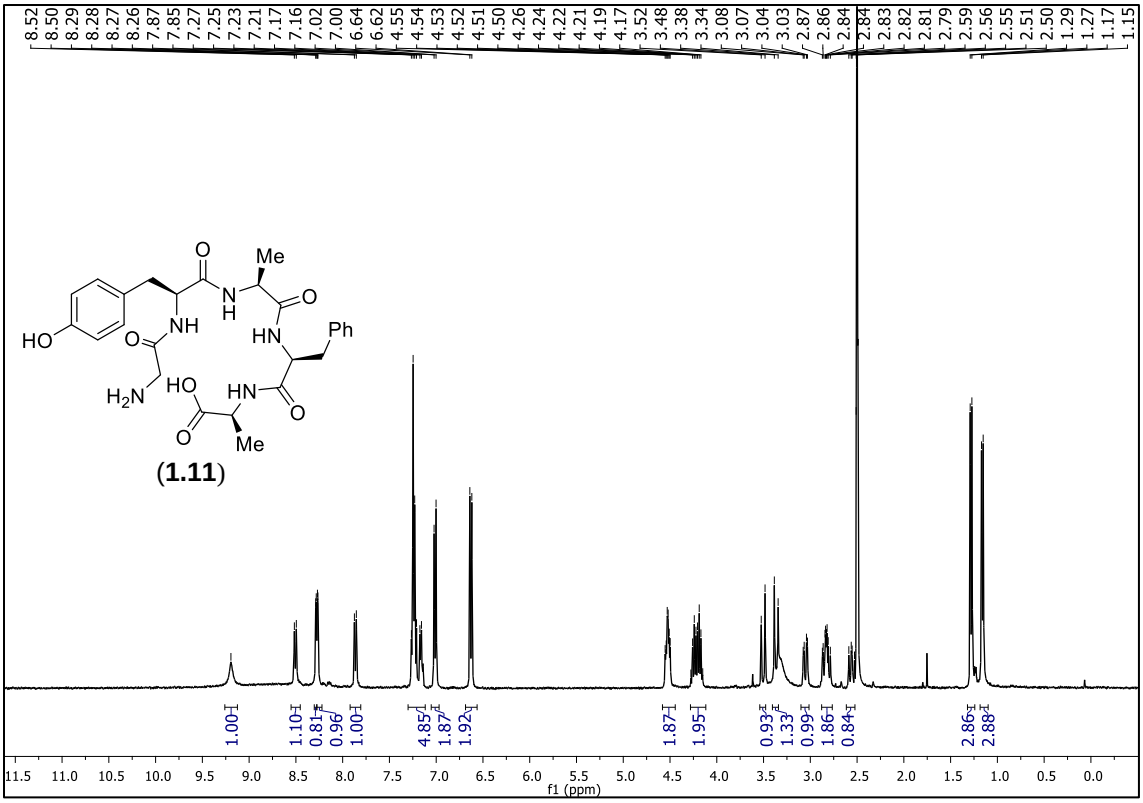
8.52 8.50 8.29 8.28 8.27 8.26 7.87 7.85 7.27 7.25 7.23 7.21 7.17 7.16 7.02 7.00 6.64 6.62 4.55 4.54 4.53 4.52 4.51 4.50 4.26 4.24 4.22 4.21 4.19 4.17 3.52 3.48 3.38 3.34 3.08 3.07 3.04 3.03 2.87 2.86 2.84 2.84 2.83 2.82 2.81 2.79 2.59 2.56 2.55 2.51 2.50 1.29 1.27 1.17 1.15
1.00 1.10 0.81 0.96 1.00 4.85 1.87 1.92 1.87 1.95 0.93 1.33 0.99 1.86 0.84 2.86 2.88
11.5 11.0 10.5 10.0 9.5 9.0 8.5 8.0 7.5 7.0 6.5 6.0 5.5 5.0 4.5 4.0 3.5 3.0 2.5 2.0 1.5 1.0 0.5 0.0
f1 (ppm)

(**1.11**)

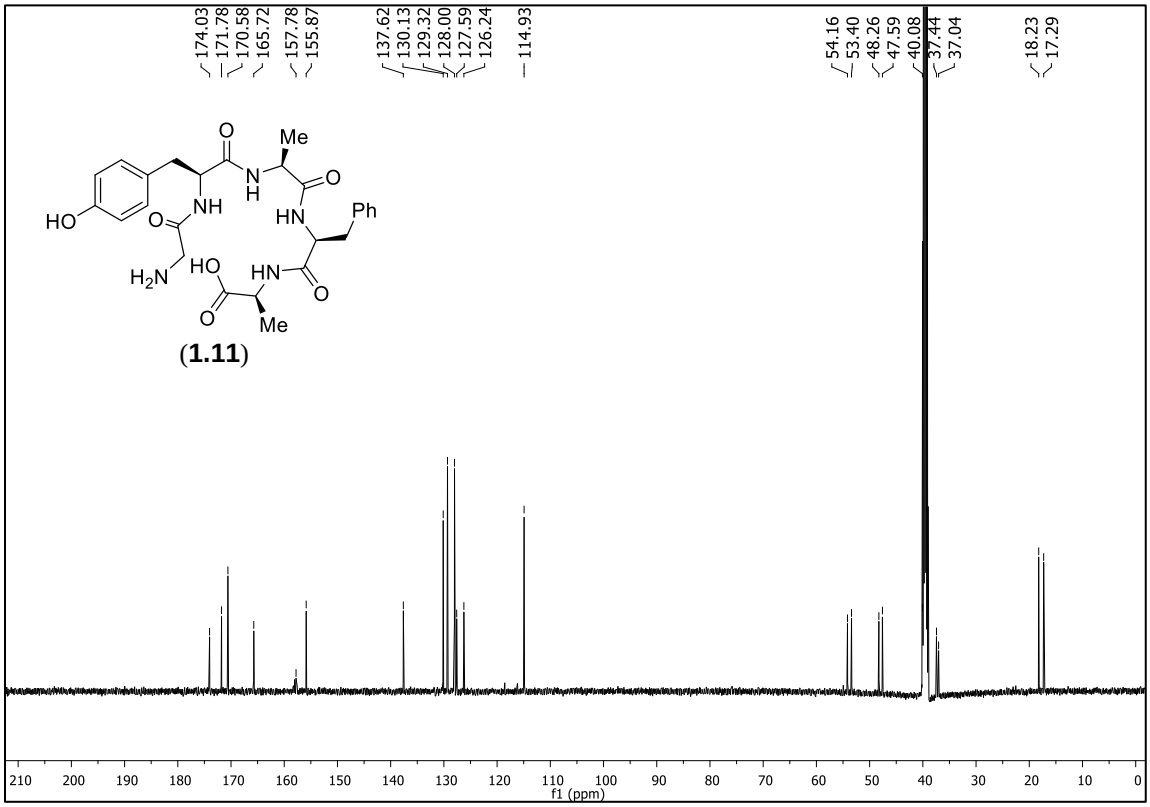
174.03 171.78 170.58 165.72 157.78 155.87 137.62 130.13 129.32 128.00 127.59 126.24 114.93 54.16 53.40 48.26 47.59 40.08 37.44 37.04 18.23 17.29
210 200 190 180 170 160 150 140 130 120 110 100 90 80 70 60 50 40 30 20 10 0
f1 (ppm)

(**1.11**)

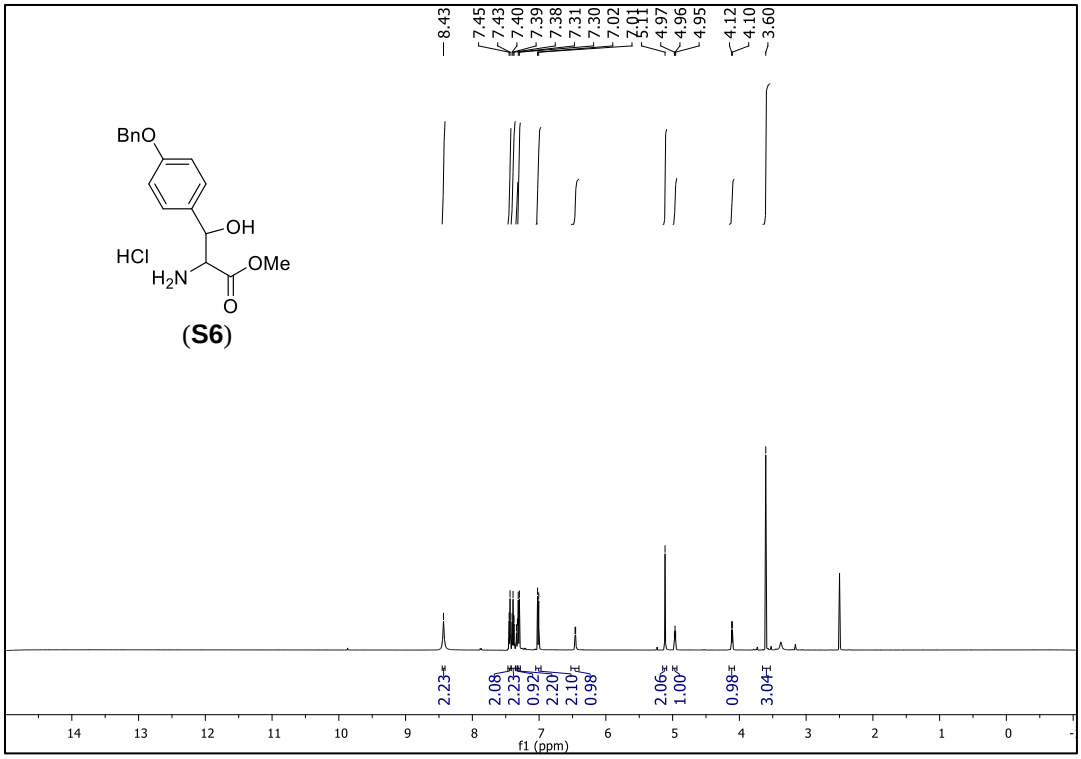
8.43
7.45
7.43
7.40
7.39
7.38
7.31
7.30
7.02
7.01
5.11
4.97
4.96
4.95
4.12
4.10
3.60
BnO
OH
HCl
H2N
OMe
O
(S6)
2.23
2.08
2.23
0.92
2.20
2.10
0.98
2.06
1.00
0.98
3.04
f1 (ppm)

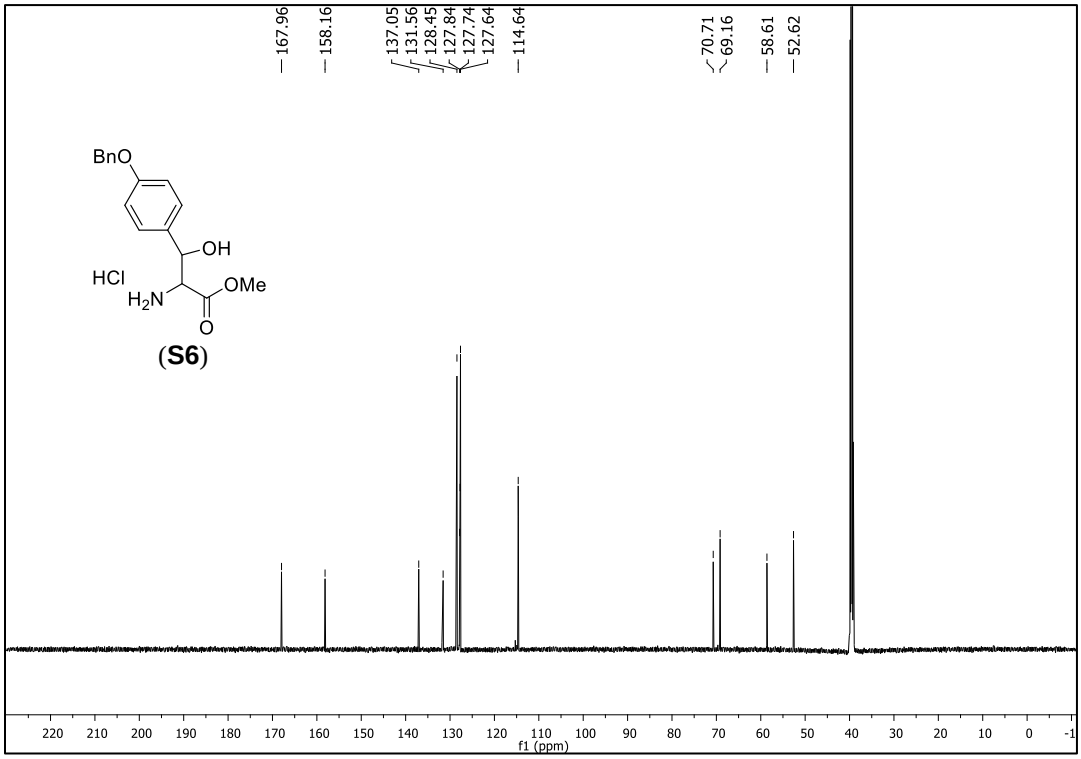
167.96
158.16
137.05
131.56
128.45
127.84
127.74
127.64
114.64
70.71
69.16
58.61
52.62
BnO
OH
HCl
H2N
OMe
O
(S6)
f1 (ppm)

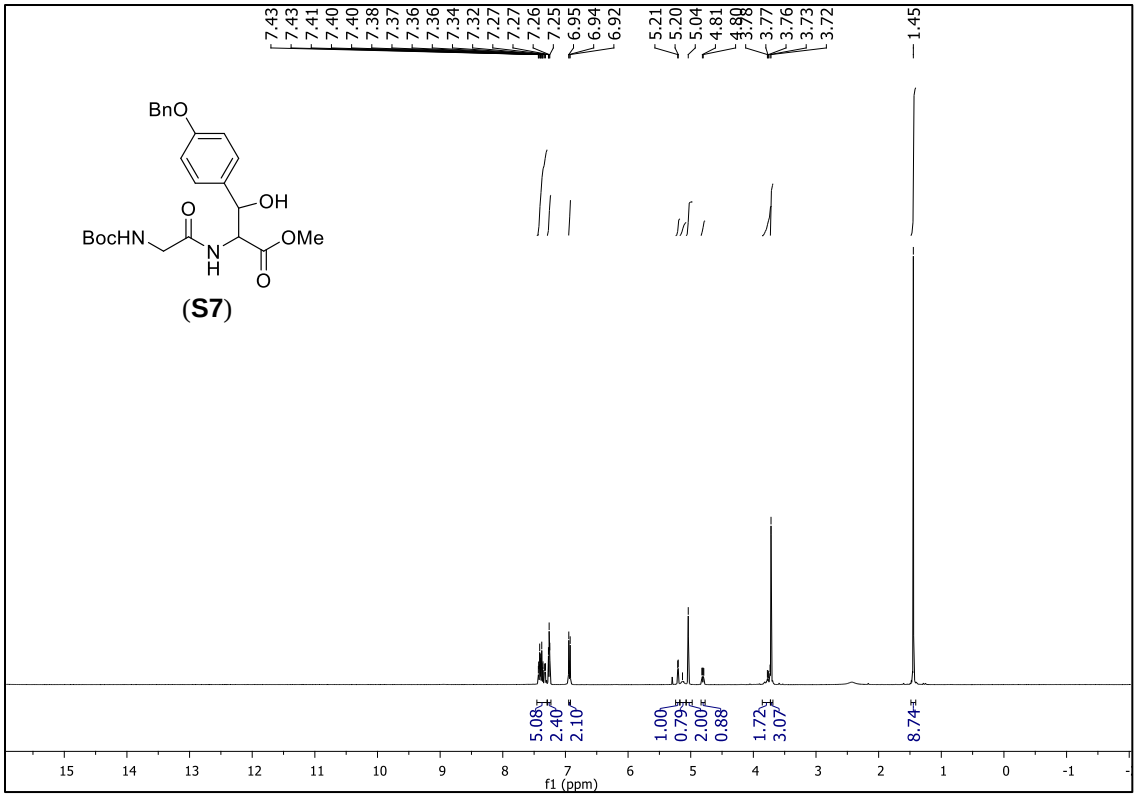
7.43
7.43
7.41
7.40
7.40
7.38
7.37
7.36
7.36
7.34
7.32
7.27
7.27
7.26
7.25
6.95
6.94
6.92
5.21
5.20
5.04
4.81
4.80
3.78
3.77
3.76
3.73
3.72
1.45
BnO
OH
O
BocHN
N
H
OMe
O
O
5.08
2.40
2.10
1.00
0.79
2.00
0.88
1.72
3.07
8.74
15
14
13
12
11
10
9
8
7
6
5
4
3
2
1
0
-1
f1 (ppm)

(**S7**)

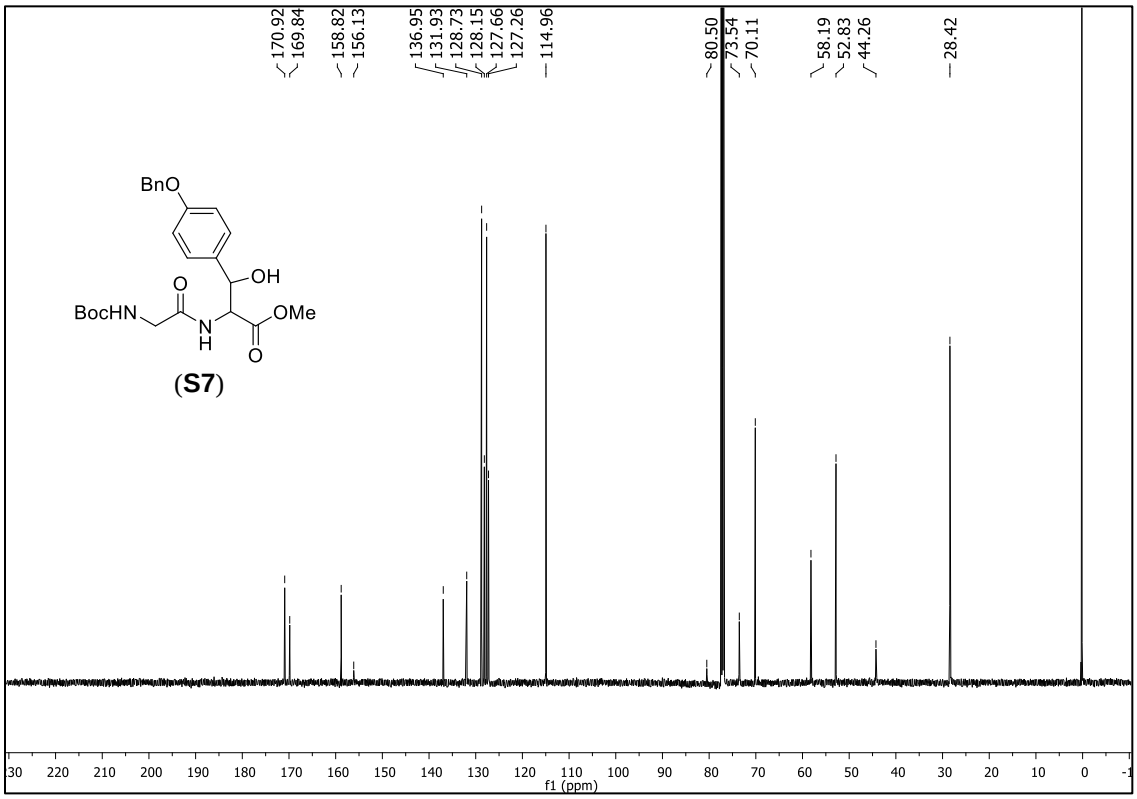
170.92
169.84
158.82
156.13
136.95
131.93
128.73
128.15
127.66
127.26
114.96
80.50
73.54
70.11
58.19
52.83
44.26
28.42
BnO
OH
O
BocHN
N
H
OMe
O
O
220
210
200
190
180
170
160
150
140
130
120
110
100
90
80
70
60
50
40
30
20
10
0
f1 (ppm)

(**S7**)

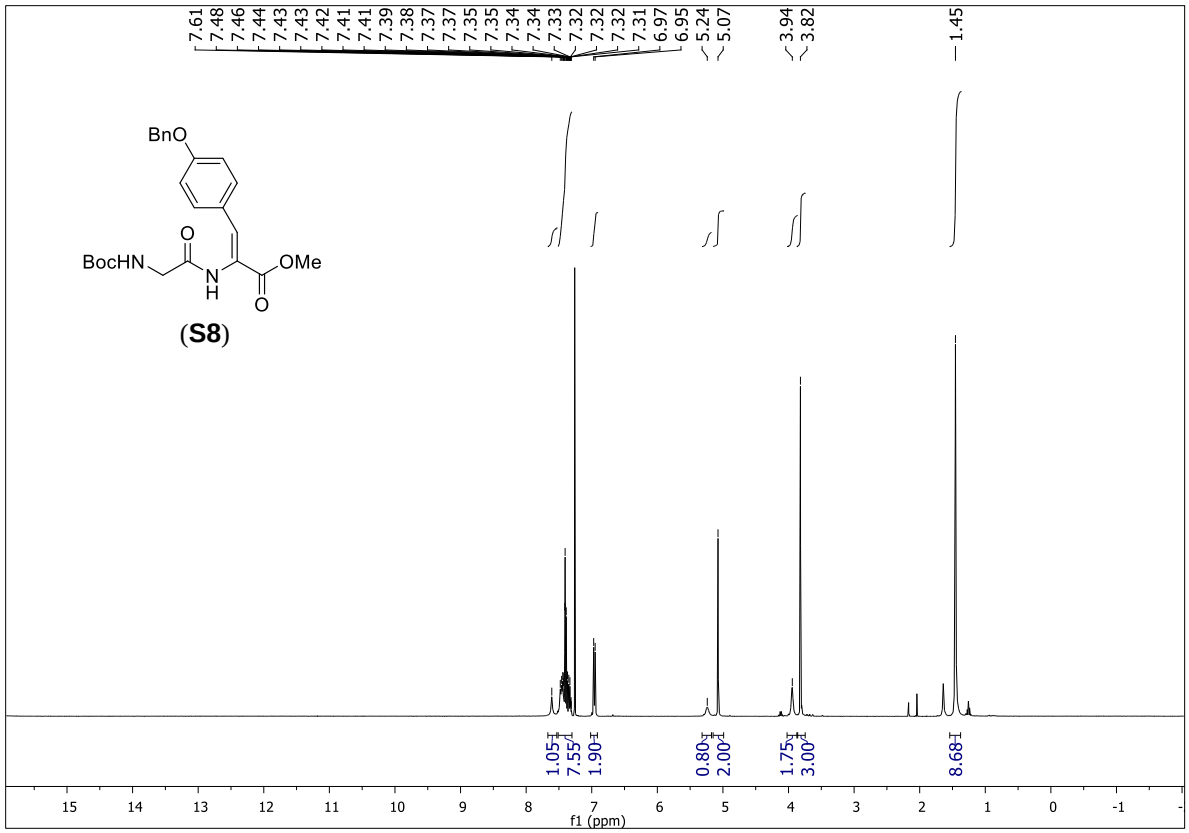
7.61
7.48
7.46
7.44
7.43
7.43
7.42
7.41
7.41
7.39
7.38
7.37
7.37
7.35
7.35
7.34
7.34
7.33
7.32
7.32
7.32
7.31
6.97
6.95
5.24
5.07
3.94
3.82
1.45
BnO
BocHN
O
N
H
OMe
O
O
(S8)
1.05
7.55
1.90
0.80
2.00
1.75
3.00
8.68
f1 (ppm)

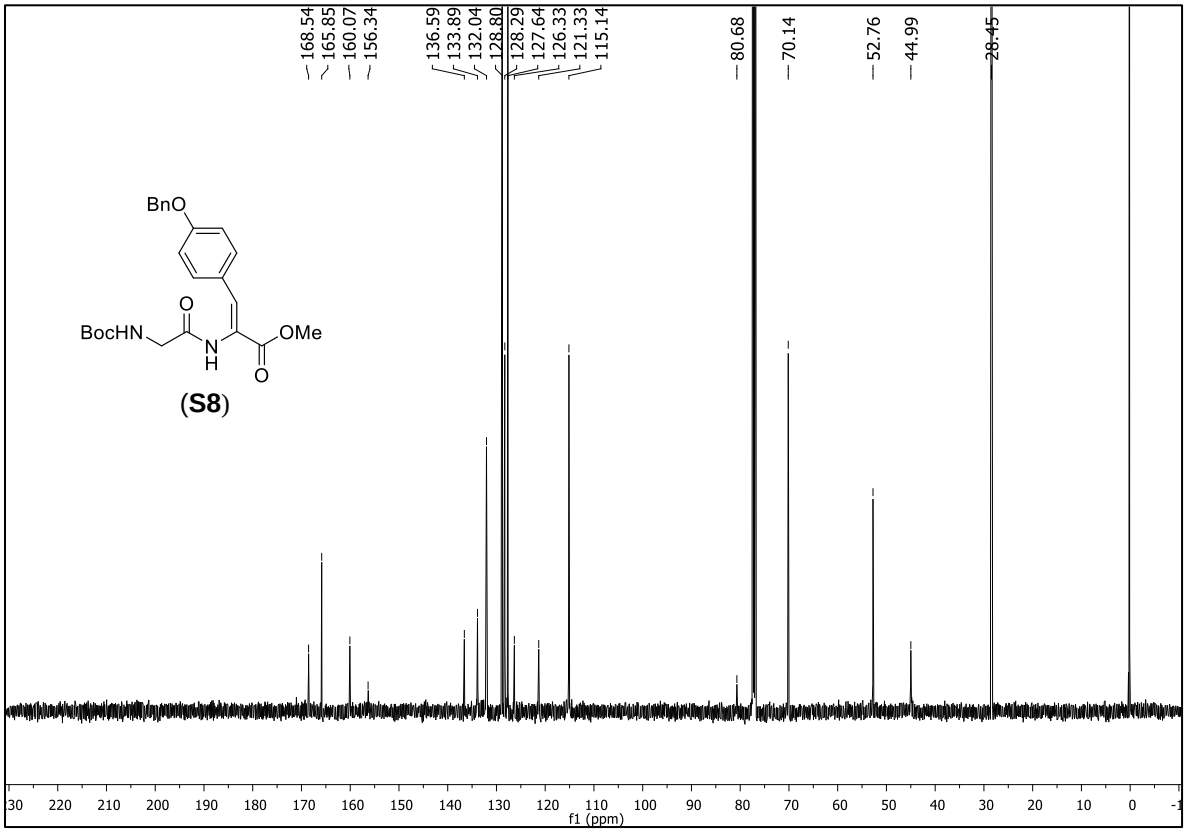
168.54
165.85
160.07
156.34
136.59
133.89
132.04
128.80
128.29
127.64
126.33
121.33
115.14
80.68
70.14
52.76
44.99
28.45
BnO
BocHN
O
N
H
OMe
O
O
(S8)
f1 (ppm)

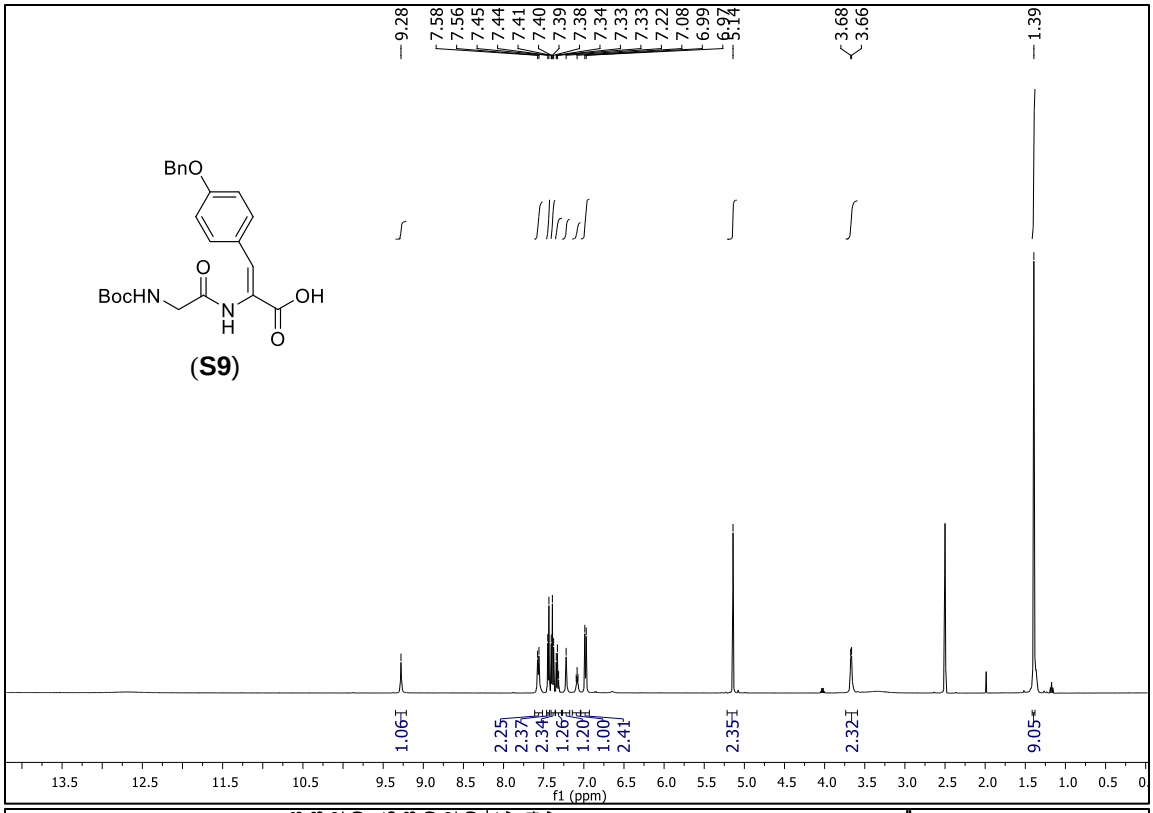
9.28
7.58
7.56
7.45
7.44
7.41
7.40
7.39
7.38
7.34
7.33
7.33
7.22
7.08
6.99
6.97
5.14
3.68
3.66
1.39
BnO
BocHN
O
N
H
OH
O
(S9)
1.06
2.25
2.37
2.34
1.26
1.20
1.00
2.41
2.35
2.32
9.05
f1 (ppm)

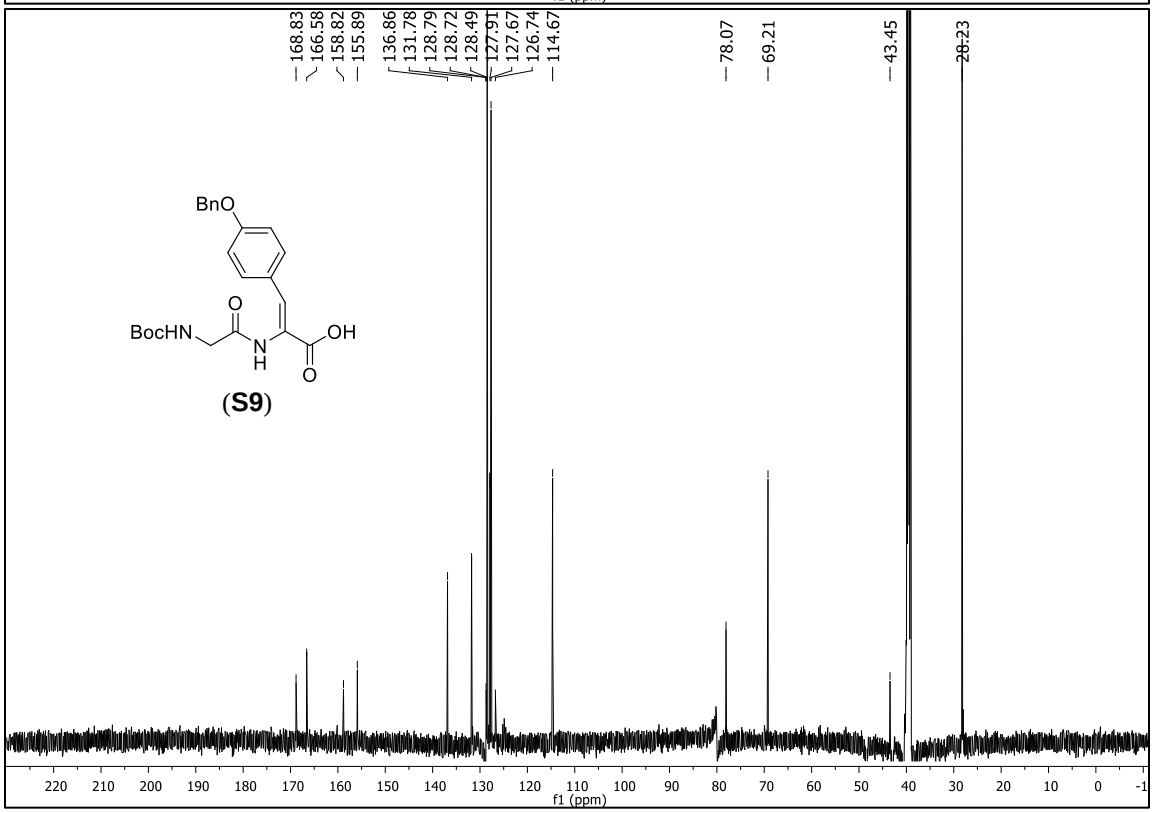
168.83
166.58
158.82
155.89
136.86
131.78
128.79
128.72
128.49
127.91
127.67
126.74
114.67
78.07
69.21
43.45
28.23
BnO
BocHN
O
N
H
OH
O
(S9)
f1 (ppm)

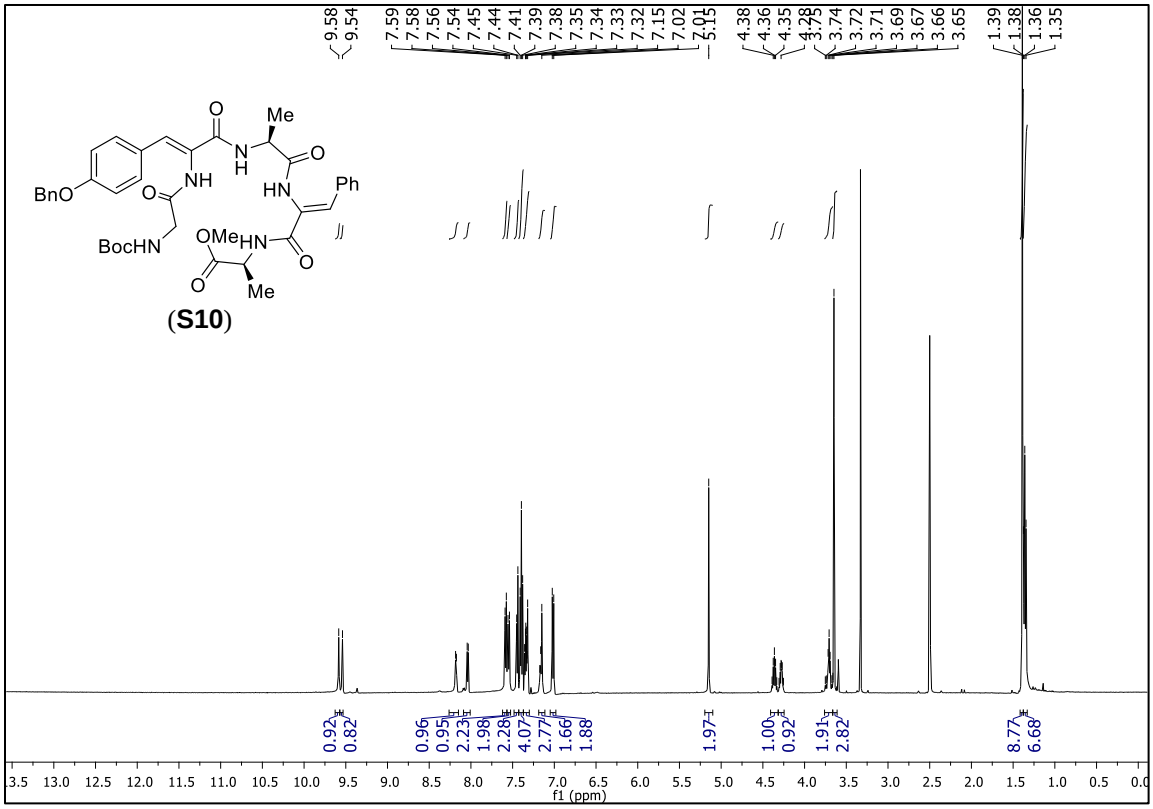
9.58
9.54
7.59
7.58
7.56
7.54
7.45
7.44
7.41
7.39
7.38
7.35
7.34
7.33
7.32
7.15
7.02
7.01
5.15
4.38
4.36
4.35
4.28
4.25
3.74
3.72
3.71
3.69
3.67
3.66
3.65
1.39
1.38
1.36
1.35
0.92
0.82
0.96
0.95
2.23
1.98
2.28
4.07
2.77
1.66
1.88
1.97
1.00
0.92
1.91
2.82
8.77
6.68
f1 (ppm)
(S10)

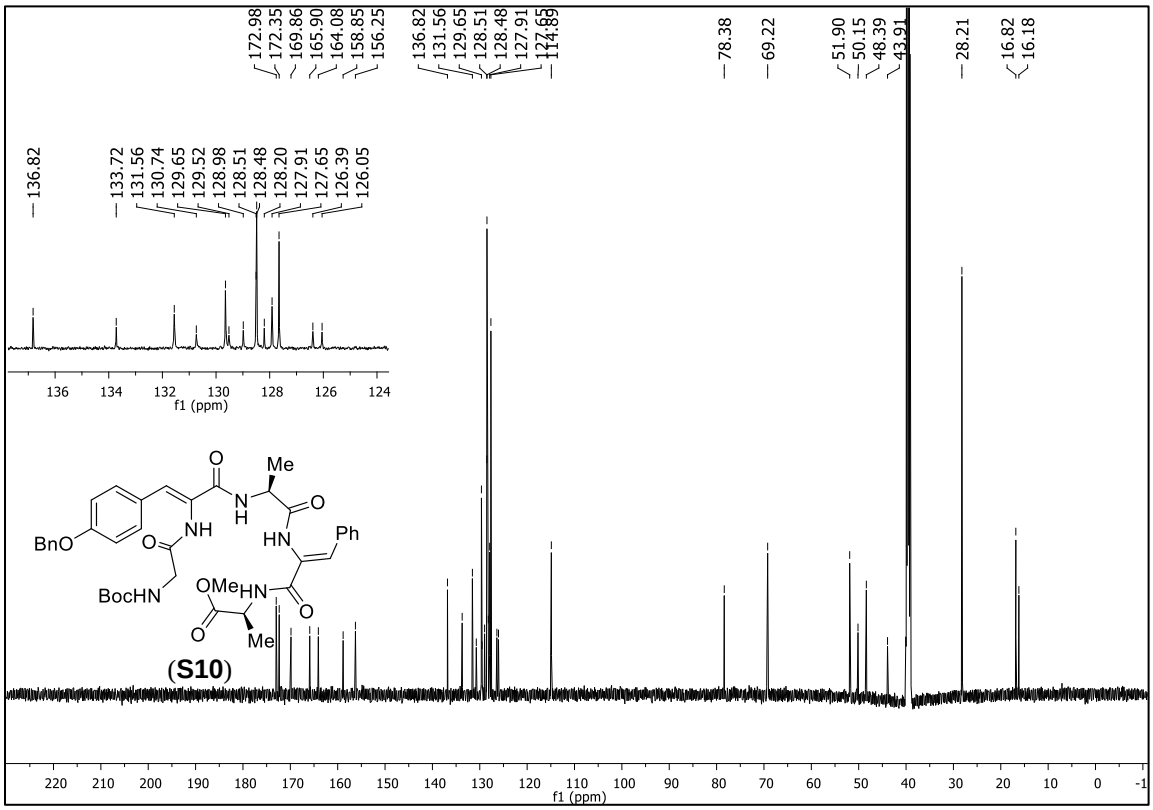
172.98
172.35
169.86
165.90
164.08
158.85
156.25
136.82
131.56
129.65
128.51
128.48
127.91
78.38
69.22
51.90
50.15
48.39
43.91
28.21
16.82
16.18
136.82
133.72
131.56
130.74
129.65
129.52
128.98
128.51
128.48
128.20
127.91
127.65
126.39
126.05
f1 (ppm)
(S10)

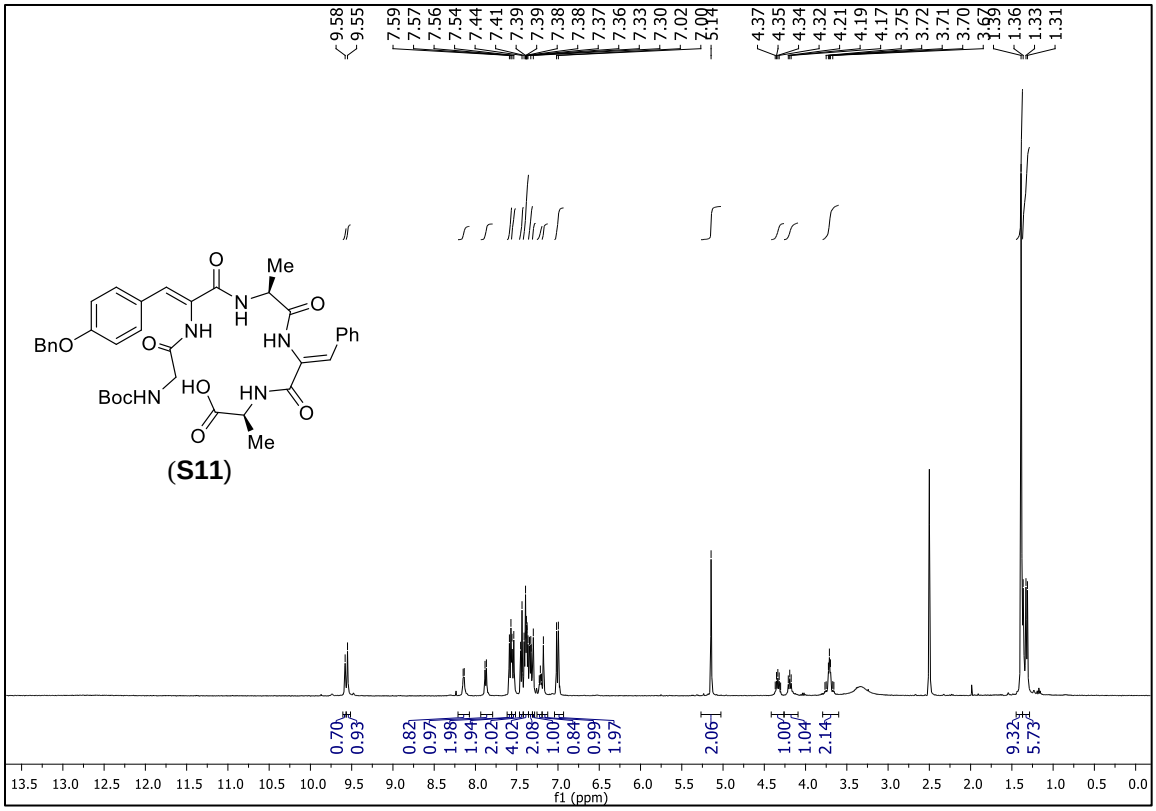
(S11)

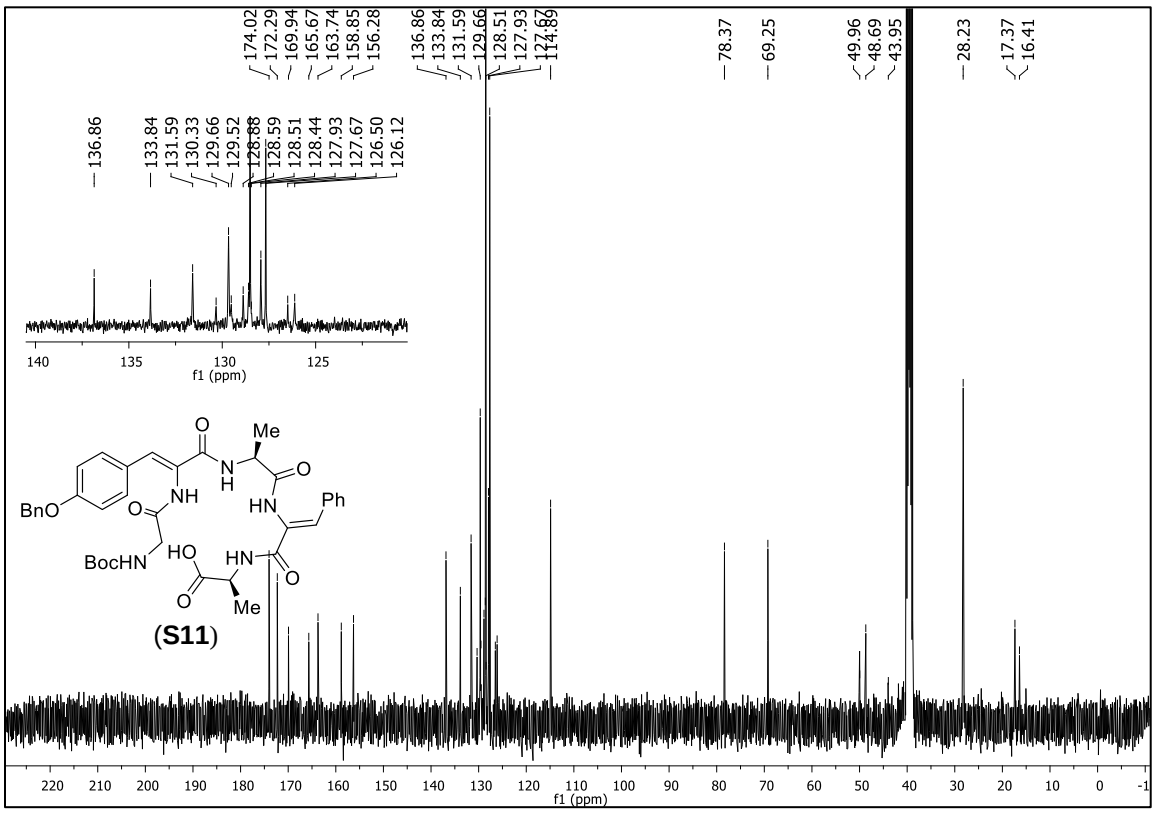
(S11)

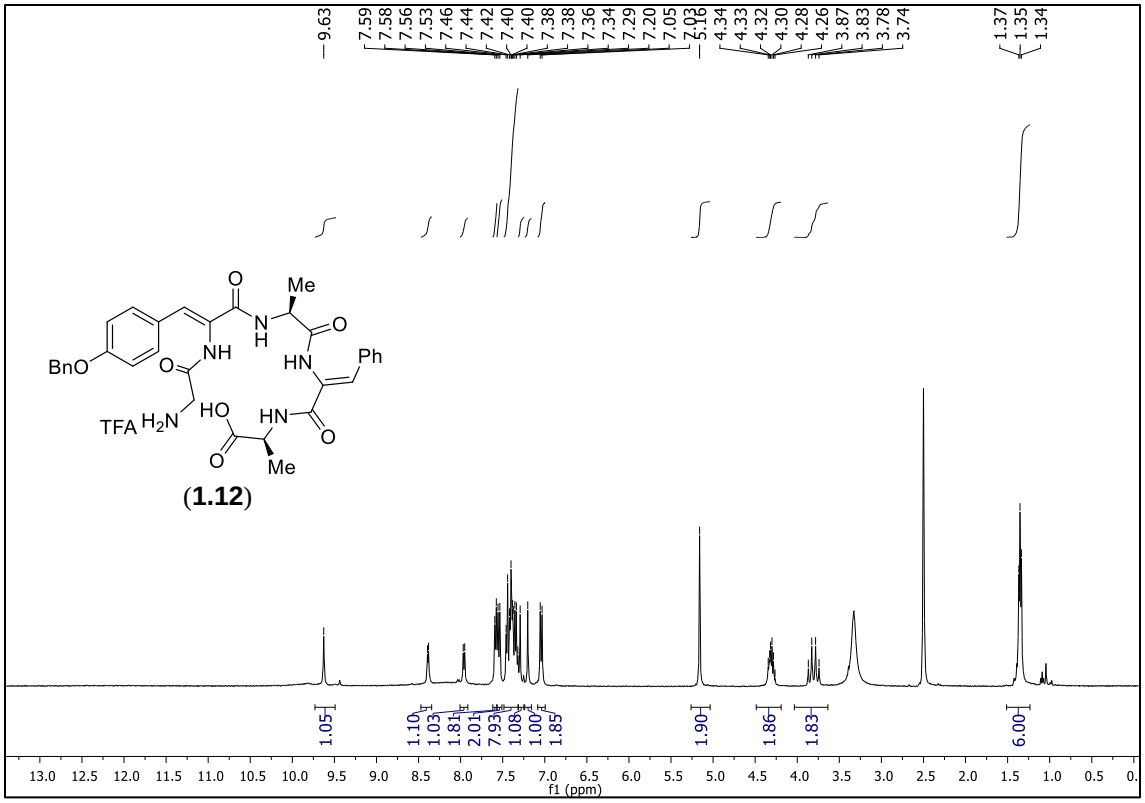
9.63
7.59
7.58
7.56
7.53
7.46
7.44
7.42
7.40
7.40
7.38
7.38
7.36
7.34
7.29
7.20
7.05
7.03
5.16
4.34
4.33
4.32
4.30
4.28
4.26
3.87
3.83
3.78
3.74
1.37
1.35
1.34
1.05
1.10
1.03
1.81
2.01
7.93
1.08
1.00
1.85
1.90
1.86
1.83
6.00
f1 (ppm)

(**1.12**)

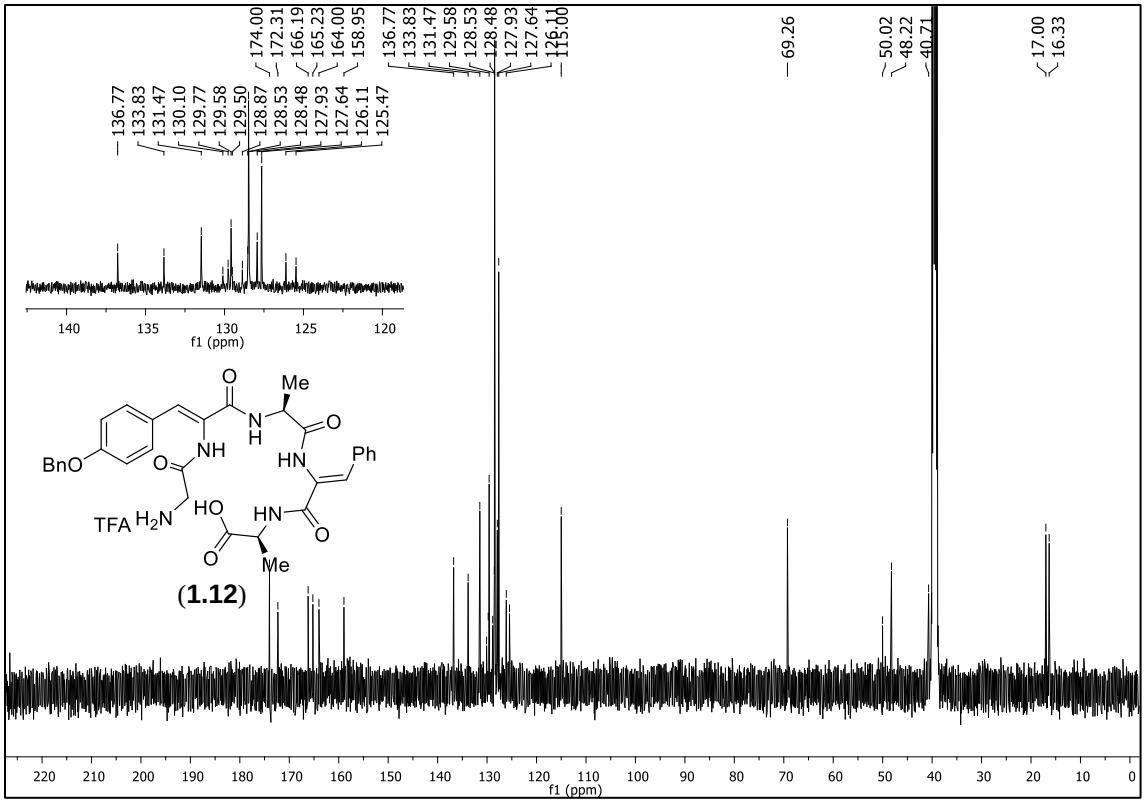
174.00
172.31
166.19
165.23
164.00
158.95
136.77
133.83
131.47
129.58
128.53
128.48
127.93
127.64
126.11
125.00
69.26
50.02
48.22
40.71
17.00
16.33
f1 (ppm)

(**1.12**)

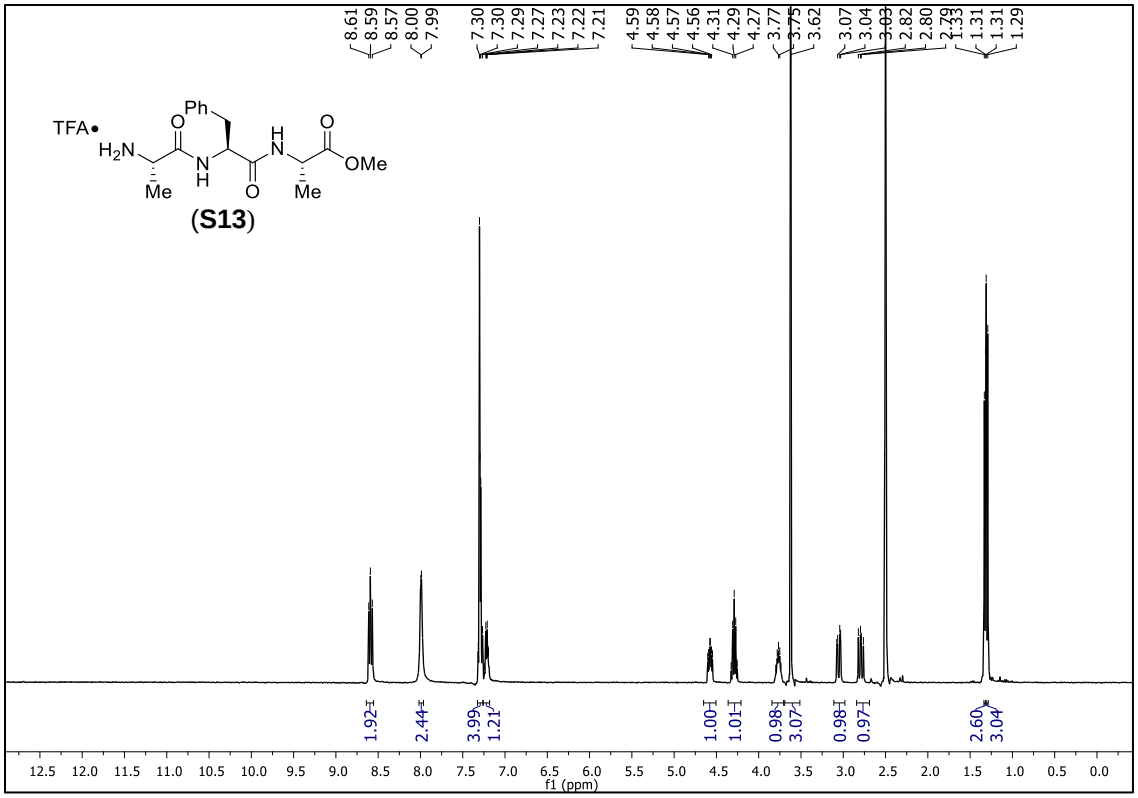
8.61
8.59
8.57
8.00
7.99
7.30
7.30
7.29
7.27
7.23
7.22
7.21
4.59
4.58
4.57
4.56
4.31
4.29
4.27
3.77
3.75
3.62
3.07
3.04
3.03
2.82
2.80
2.79
2.33
1.31
1.31
1.29
TFA•
Ph
O
H2N
N
H
O
H
N
O
OMe
Me
O
Me
(S13)
1.92
2.44
3.99
1.21
1.00
1.01
0.98
3.07
0.98
0.97
2.60
3.04
f1 (ppm)

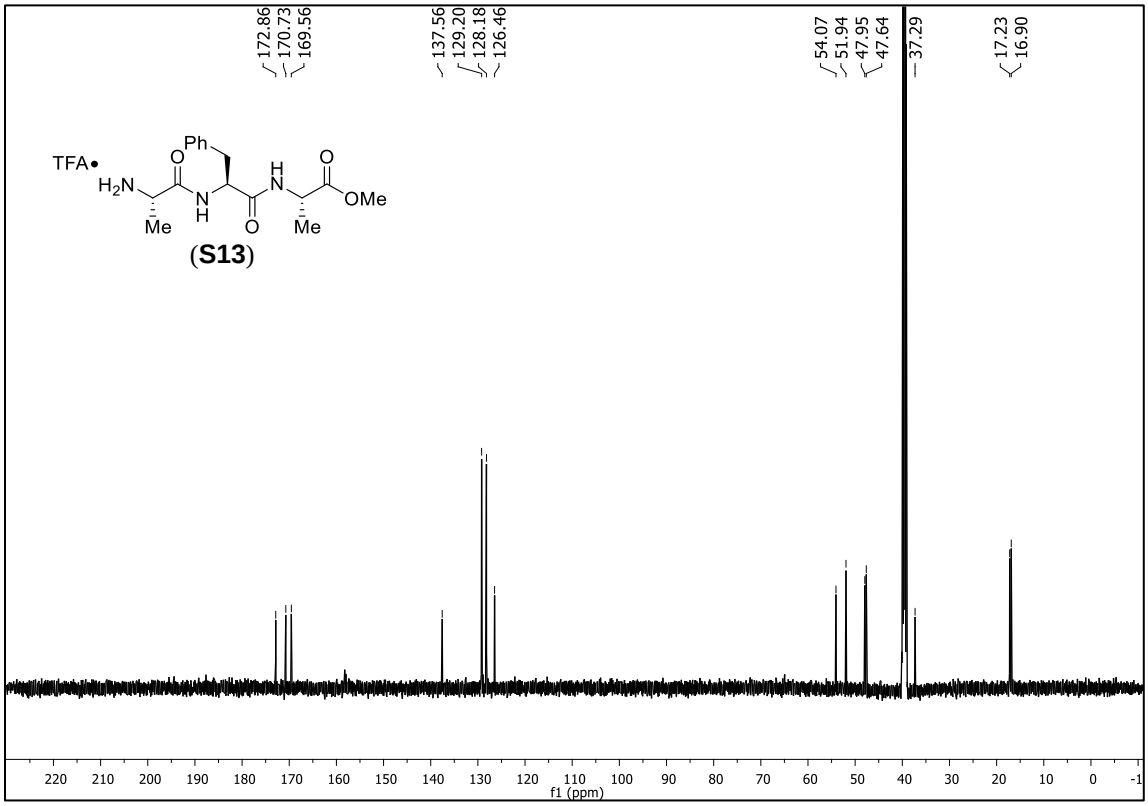
172.86
170.73
169.56
137.56
129.20
128.18
126.46
54.07
51.94
47.95
47.64
37.29
17.23
16.90
TFA•
Ph
O
H2N
N
H
O
H
N
O
OMe
Me
O
Me
(S13)
f1 (ppm)

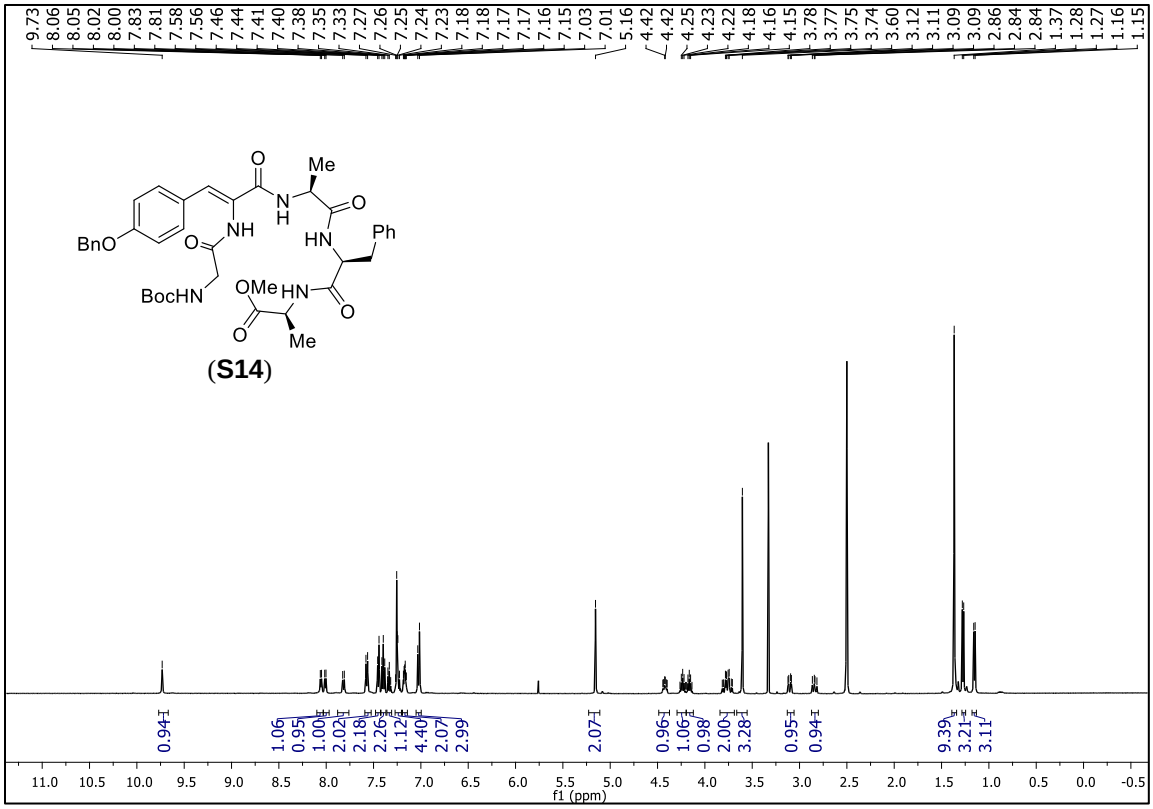
(S14)
f1 (ppm)

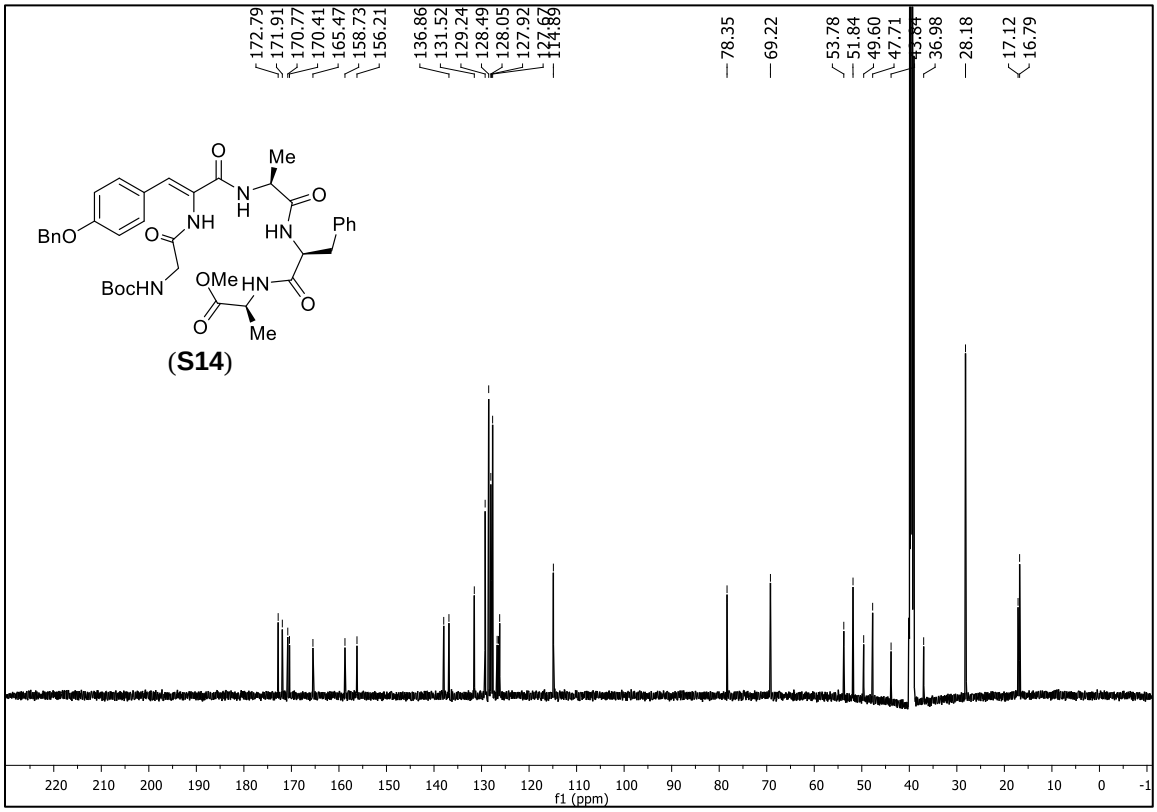
(S14)
f1 (ppm)

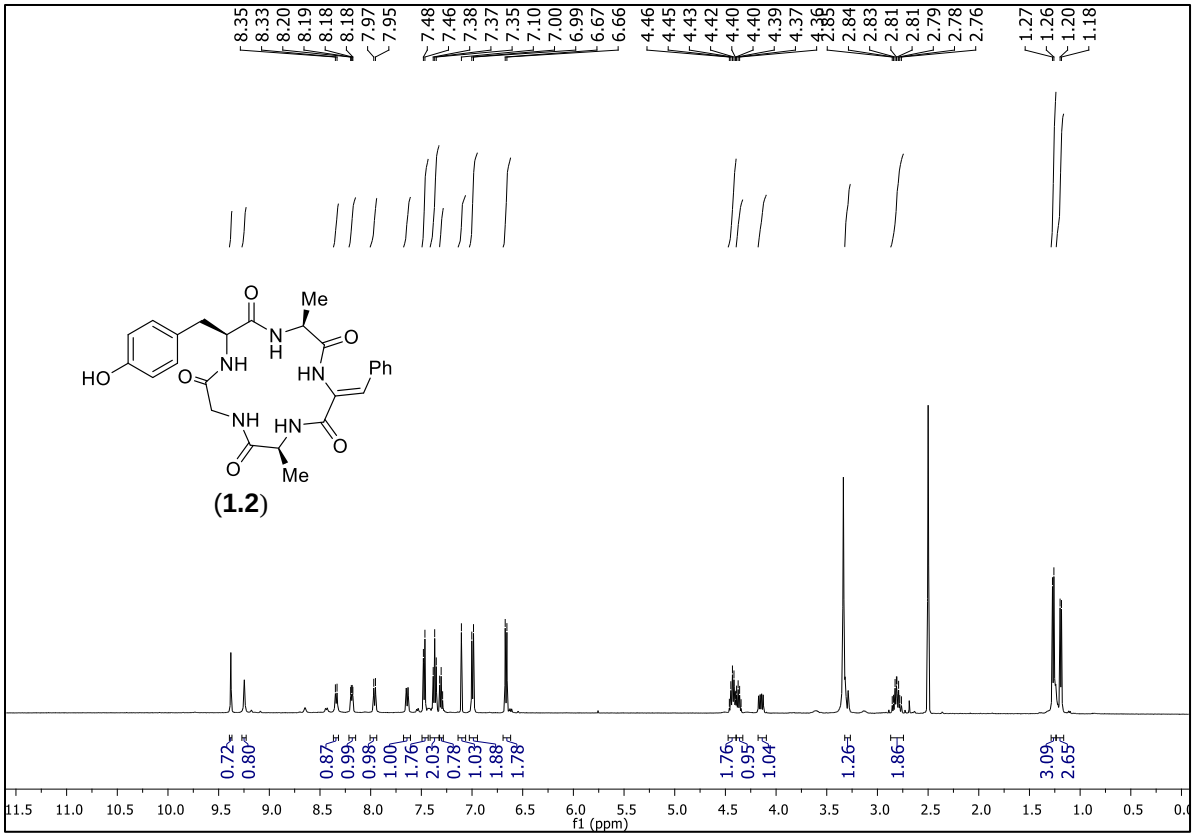
8.35
8.33
8.20
8.19
8.18
8.18
7.97
7.95
7.48
7.46
7.38
7.37
7.35
7.10
7.00
6.99
6.67
6.66
4.46
4.45
4.43
4.42
4.40
4.40
4.39
4.37
4.36
2.84
2.83
2.81
2.81
2.79
2.78
2.76
1.27
1.26
1.20
1.18
HO
NH
O
N
H
Me
O
HN
Ph
NH
HN
O
O
Me
0.72
0.80
0.87
0.99
0.98
1.00
1.76
2.03
0.78
1.03
1.88
1.78
1.76
0.95
1.04
1.26
1.86
3.09
2.65
f1 (ppm)

(**1.2**)

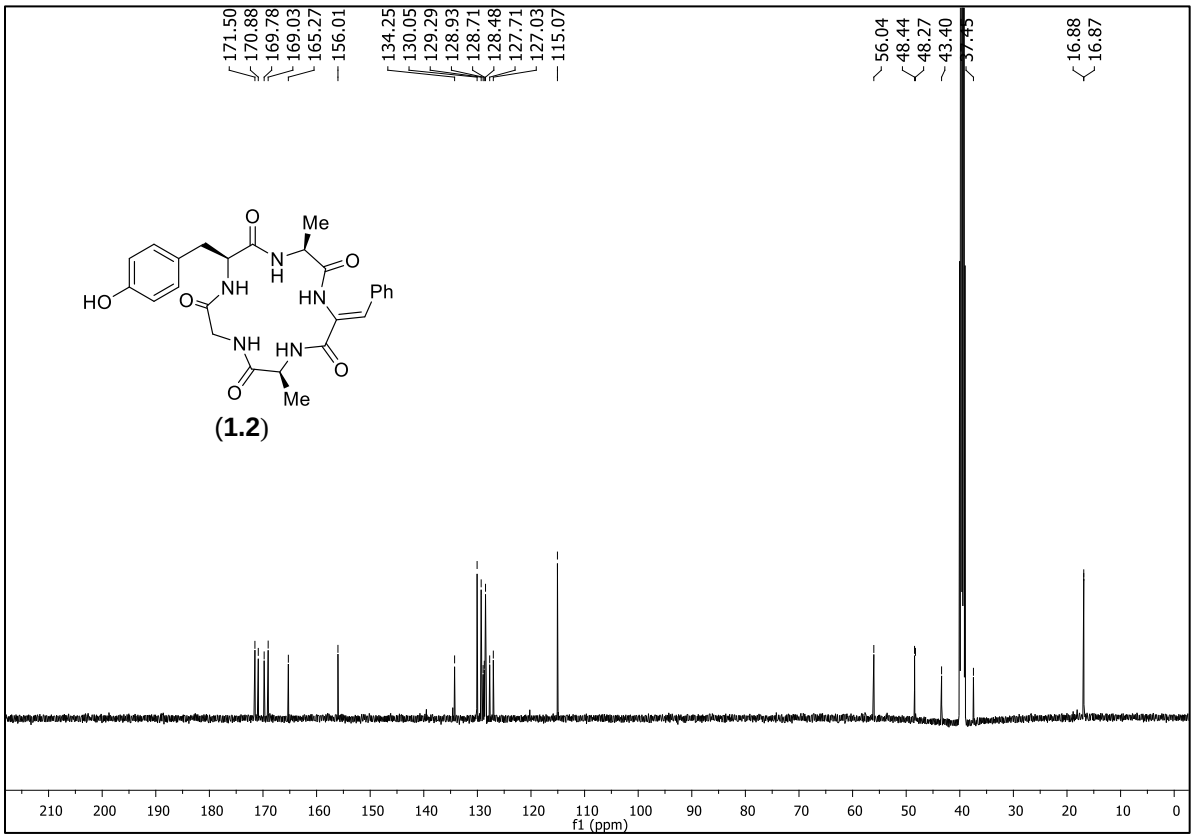
171.50
170.88
169.78
169.03
165.27
156.01
134.25
130.05
129.29
128.93
128.71
128.48
127.71
127.03
115.07
56.04
48.44
48.27
43.40
37.45
16.88
16.87
HO
NH
O
N
H
Me
O
HN
Ph
NH
HN
O
O
Me
f1 (ppm)

(**1.2**)

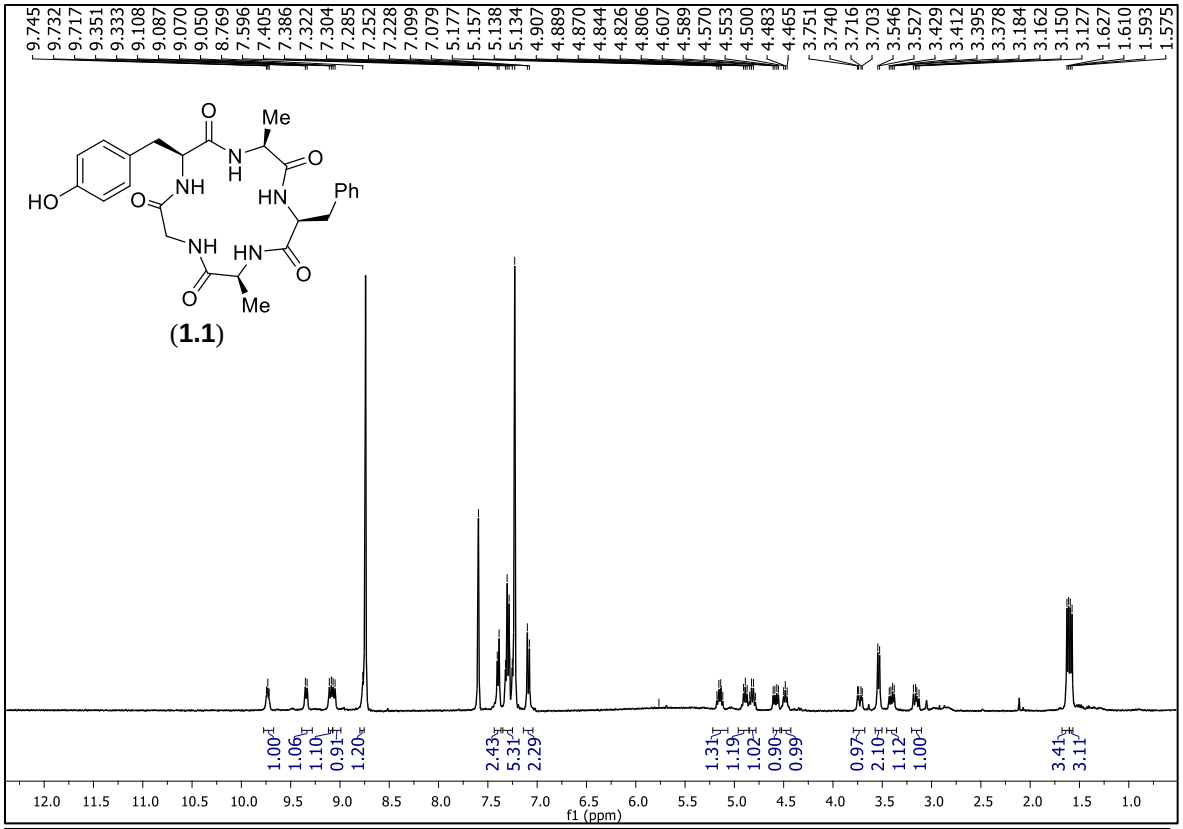
9.745 9.732 9.717 9.351 9.333 9.108 9.087 9.070 9.050 8.769 7.596 7.405 7.386 7.322 7.304 7.285 7.252 7.228 7.099 7.079 5.177 5.157 5.138 5.134 4.907 4.889 4.870 4.844 4.826 4.806 4.607 4.589 4.570 4.553 4.500 4.483 4.465 3.751 3.740 3.716 3.703 3.546 3.527 3.429 3.412 3.395 3.378 3.184 3.162 3.150 3.127 1.627 1.610 1.593 1.575
HO
NH
O
N
H
Me
O
HN
Ph
NH
HN
O
O
Me
1.00 1.06 1.10 0.91 1.20 2.43 5.31 2.29 1.31 1.19 1.02 0.90 0.99 0.97 2.10 1.12 1.00 3.41 3.11
12.0 11.5 11.0 10.5 10.0 9.5 9.0 8.5 8.0 7.5 7.0 6.5 6.0 5.5 5.0 4.5 4.0 3.5 3.0 2.5 2.0 1.5 1.0
f1 (ppm)

(**1.1**)

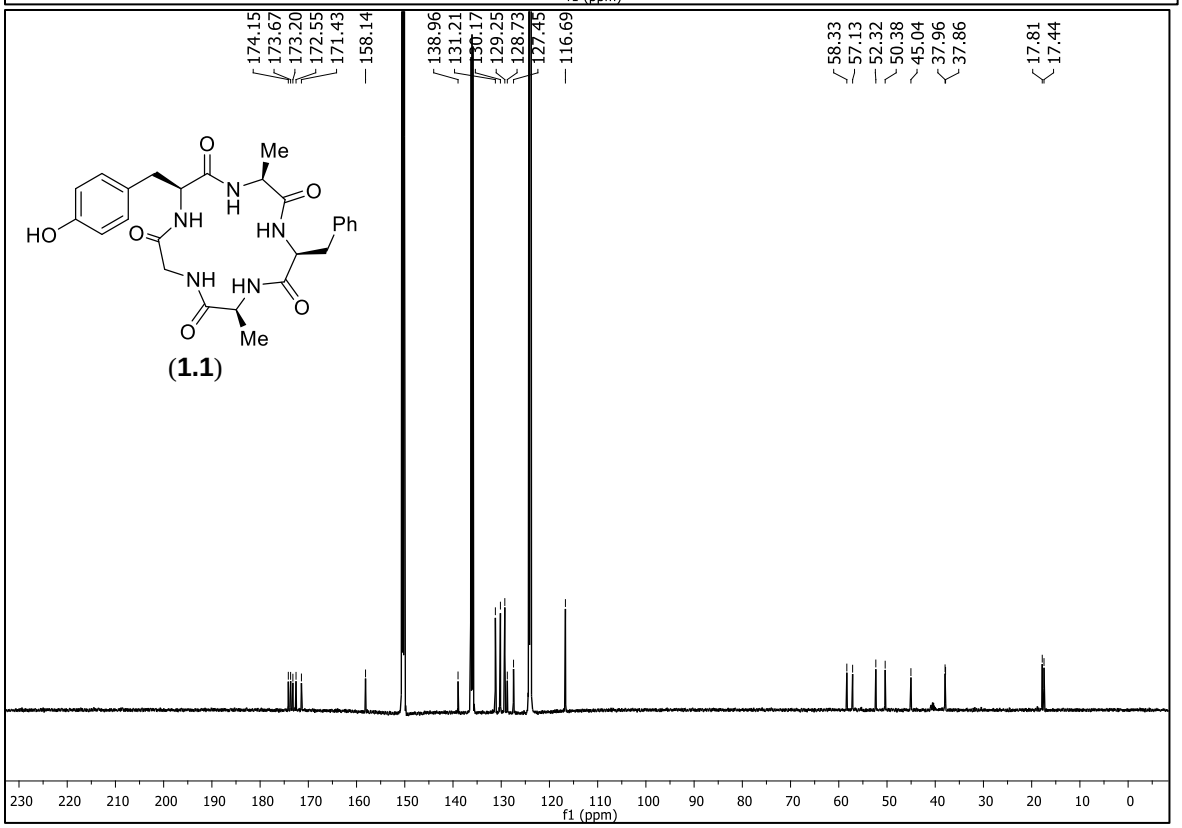
174.15 173.67 173.20 172.55 171.43 158.14 138.96 131.21 130.17 129.25 128.73 127.45 116.69 58.33 57.13 52.32 50.38 45.04 37.96 37.86 17.81 17.44
HO
NH
O
N
H
Me
O
HN
Ph
NH
HN
O
O
Me
230 220 210 200 190 180 170 160 150 140 130 120 110 100 90 80 70 60 50 40 30 20 10 0
f1 (ppm)

(**1.1**)

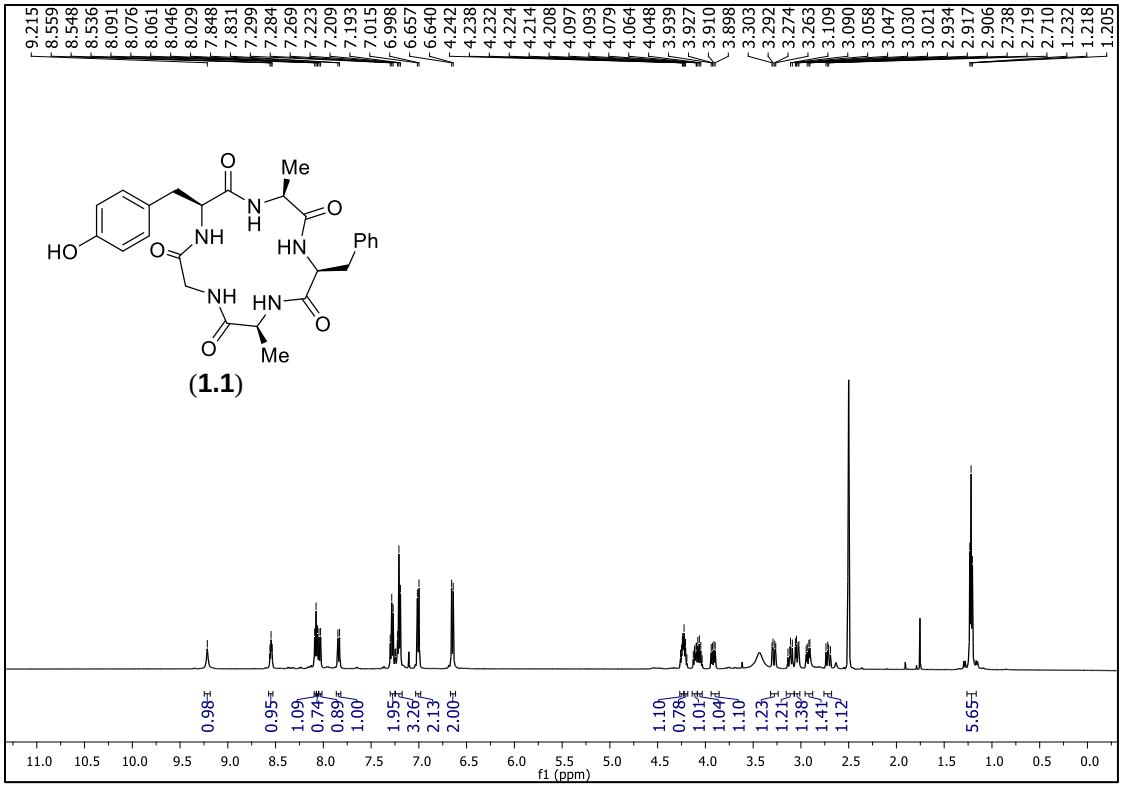
9.215
8.559
8.548
8.536
8.091
8.076
8.061
8.046
8.029
7.848
7.831
7.299
7.284
7.269
7.223
7.209
7.193
7.015
6.998
6.657
6.640
4.242
4.238
4.232
4.224
4.214
4.208
4.097
4.093
4.079
4.064
4.048
3.939
3.927
3.910
3.898
3.303
3.292
3.274
3.263
3.109
3.090
3.058
3.047
3.030
3.021
2.934
2.917
2.906
2.738
2.719
2.710
1.232
1.218
1.205
HO
NH
O
N
H
Me
O
HN
Ph
NH
HN
O
O
Me
(1.1)
0.98
0.95
1.09
0.74
0.89
1.00
1.95
3.26
2.13
2.00
1.10
0.78
1.01
1.04
1.10
1.23
1.21
1.38
1.41
1.12
5.65
11.0
10.5
10.0
9.5
9.0
8.5
8.0
7.5
7.0
6.5
6.0
5.5
5.0
4.5
4.0
3.5
3.0
2.5
2.0
1.5
1.0
0.5
0.0
f1 (ppm)

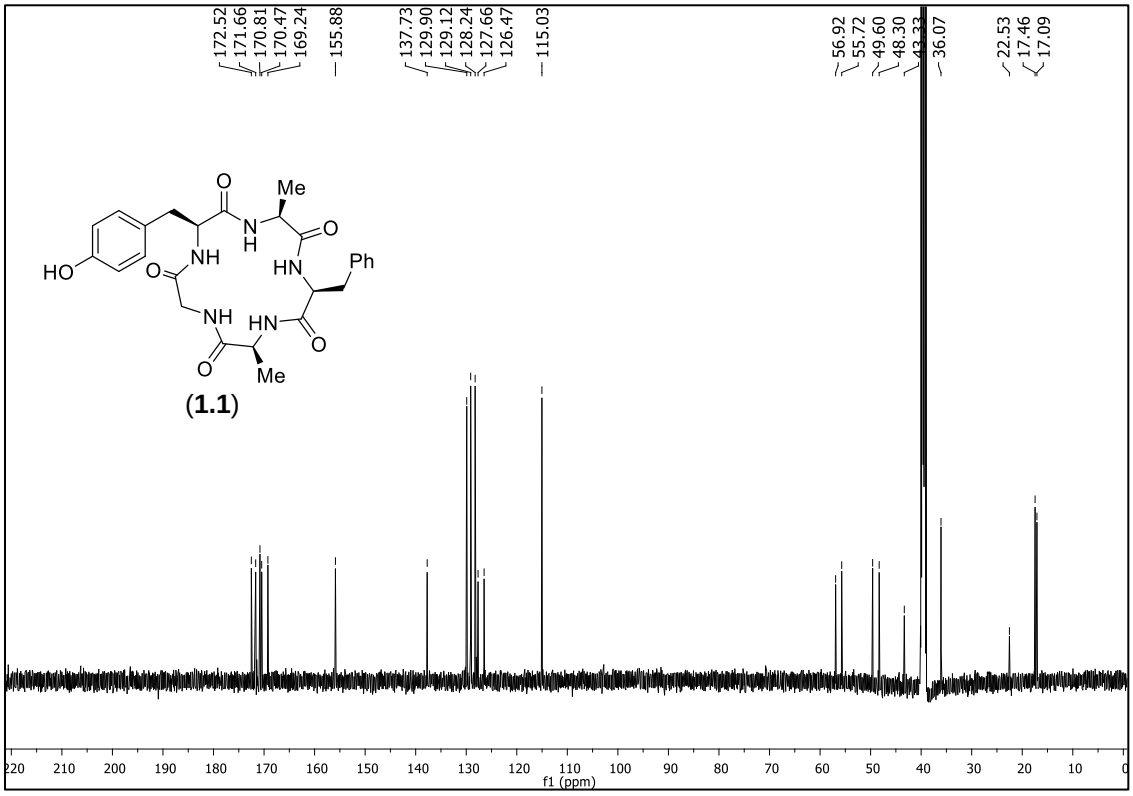
172.52
171.66
170.81
170.47
169.24
155.88
137.73
129.90
129.12
128.24
127.66
126.47
115.03
56.92
55.72
49.60
48.30
43.33
36.07
22.53
17.46
17.09
HO
NH
O
N
H
Me
O
HN
Ph
NH
HN
O
O
Me
(1.1)
220
210
200
190
180
170
160
150
140
130
120
110
100
90
80
70
60
50
40
30
20
10
0
f1 (ppm)

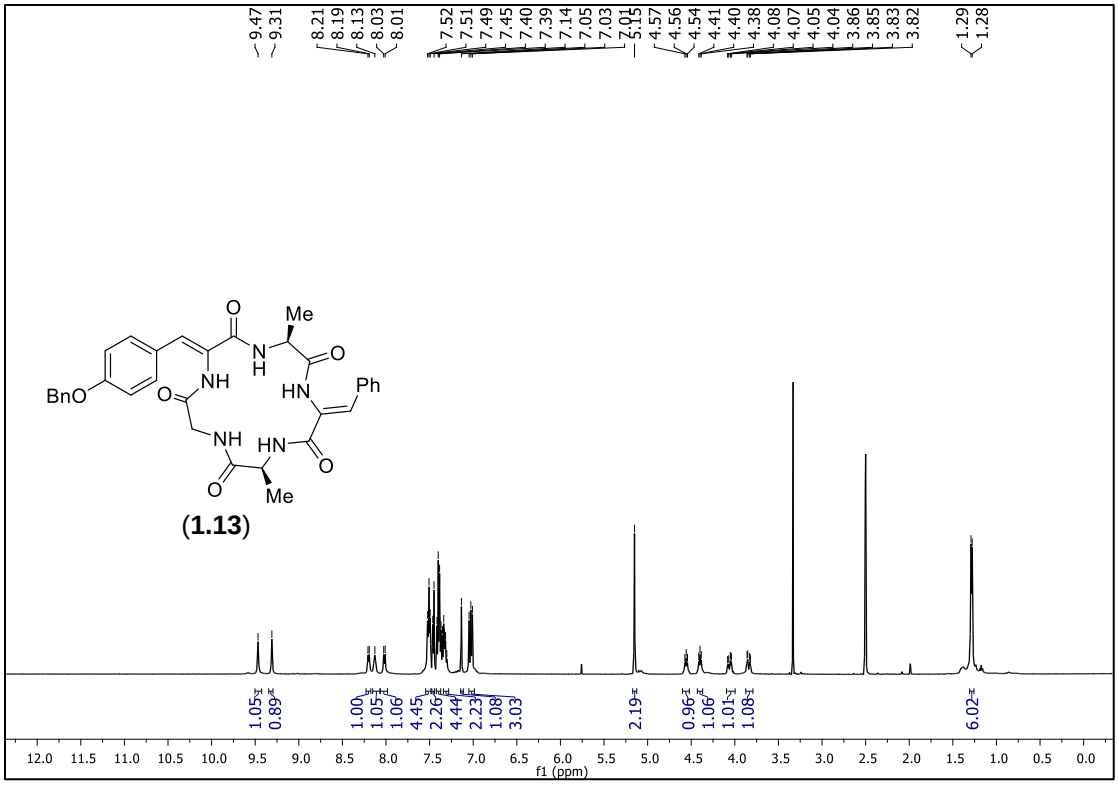
9.47
9.31
8.21
8.19
8.13
8.03
8.01
7.52
7.51
7.49
7.45
7.40
7.39
7.14
7.05
7.03
7.01
5.15
4.57
4.56
4.54
4.41
4.40
4.38
4.08
4.07
4.05
4.04
3.86
3.85
3.83
3.82
1.29
1.28
BnO
Me
Ph
(1.13)
1.05
0.89
1.00
1.05
1.06
4.45
2.26
4.44
2.23
1.08
3.03
2.19
0.96
1.06
1.01
1.08
6.02
f1 (ppm)

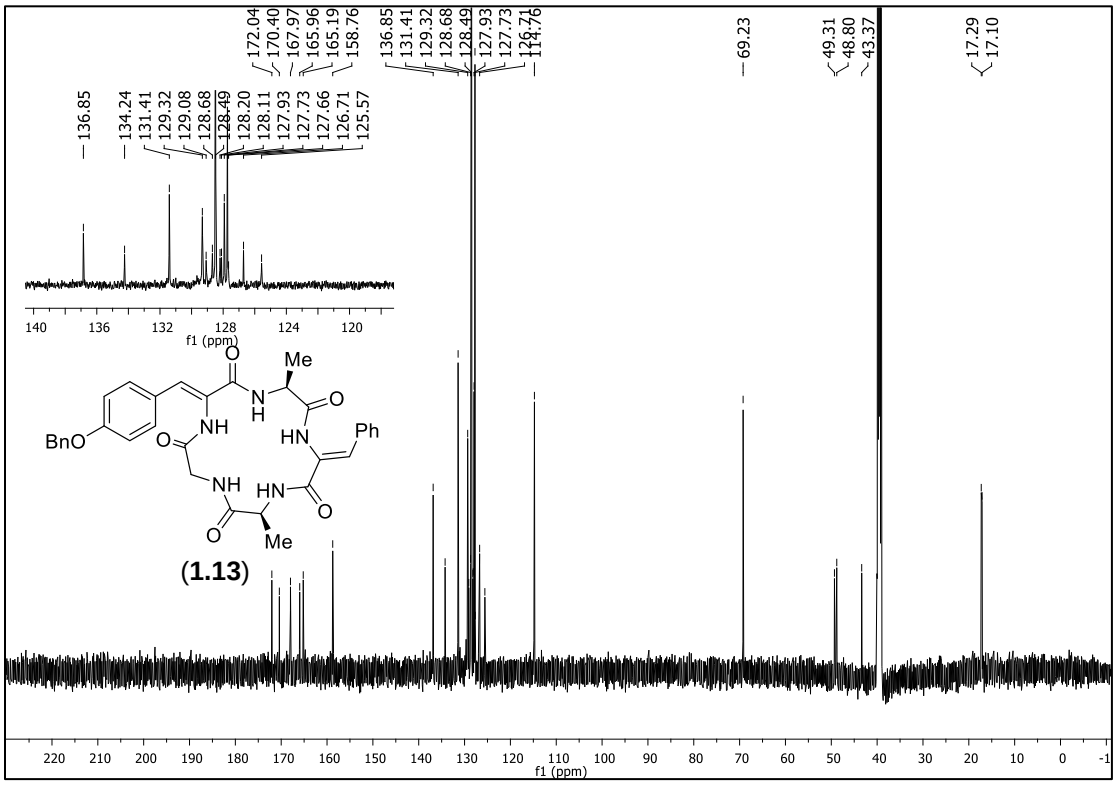
172.04
170.40
167.97
165.96
165.19
158.76
136.85
131.41
129.32
128.68
128.49
127.93
127.73
126.71
114.76
69.23
49.31
48.80
43.37
17.29
17.10
136.85
134.24
131.41
129.32
129.08
128.68
128.49
128.20
128.11
127.93
127.73
127.66
126.71
125.57
f1 (ppm)
BnO
Me
Ph
(1.13)
f1 (ppm)

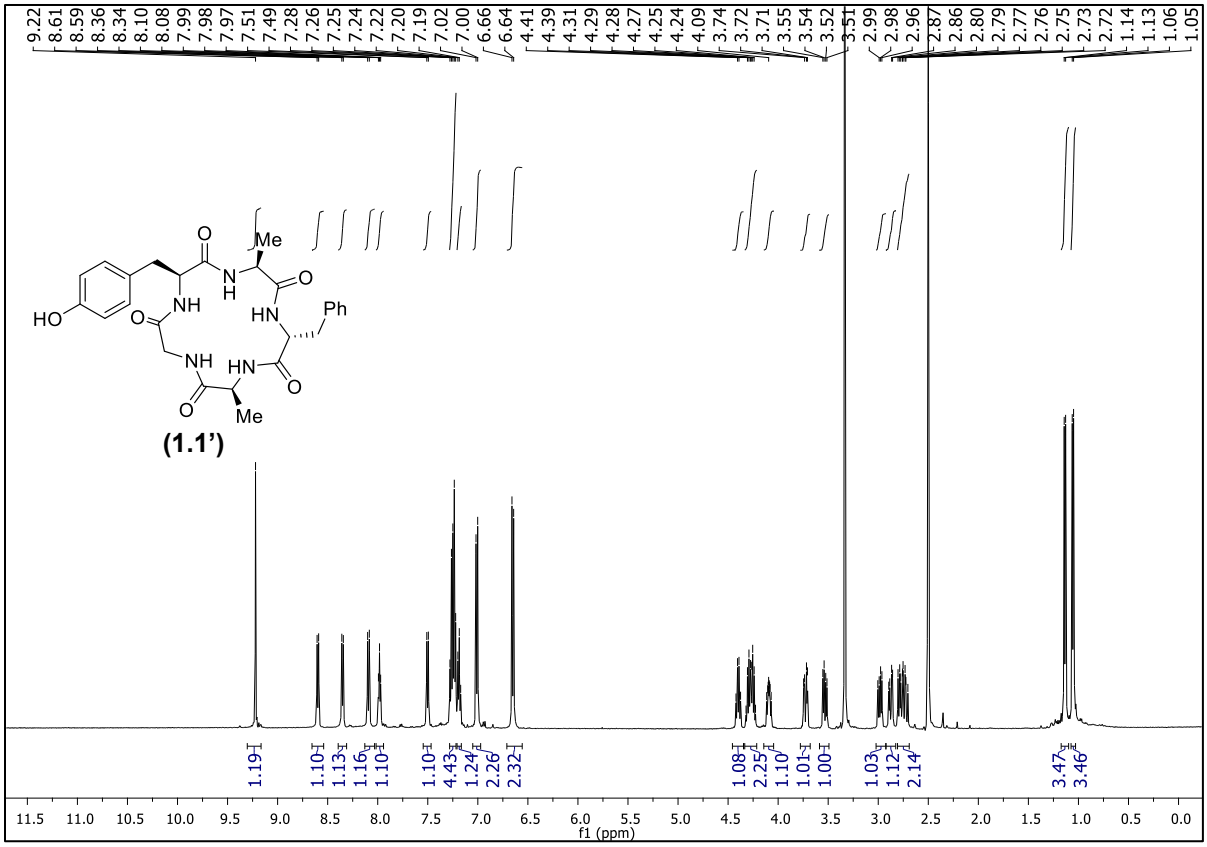
9.22 8.61 8.59 8.36 8.34 8.10 8.08 7.99 7.98 7.97 7.51 7.49 7.28 7.26 7.25 7.24 7.22 7.20 7.19 7.02 7.00 6.66 6.64 4.41 4.39 4.31 4.29 4.28 4.27 4.25 4.24 4.09 3.74 3.72 3.71 3.55 3.54 3.52 3.51 2.99 2.98 2.96 2.87 2.86 2.80 2.79 2.77 2.76 2.75 2.73 2.72 1.14 1.13 1.06 1.05
1.19 1.10 1.13 1.16 1.10 1.10 4.43 1.24 2.26 2.32 1.08 2.25 1.10 1.01 1.00 1.03 1.12 2.14 3.47 3.46
11.5 11.0 10.5 10.0 9.5 9.0 8.5 8.0 7.5 7.0 6.5 6.0 5.5 5.0 4.5 4.0 3.5 3.0 2.5 2.0 1.5 1.0 0.5 0.0
f1 (ppm)
(1.1')

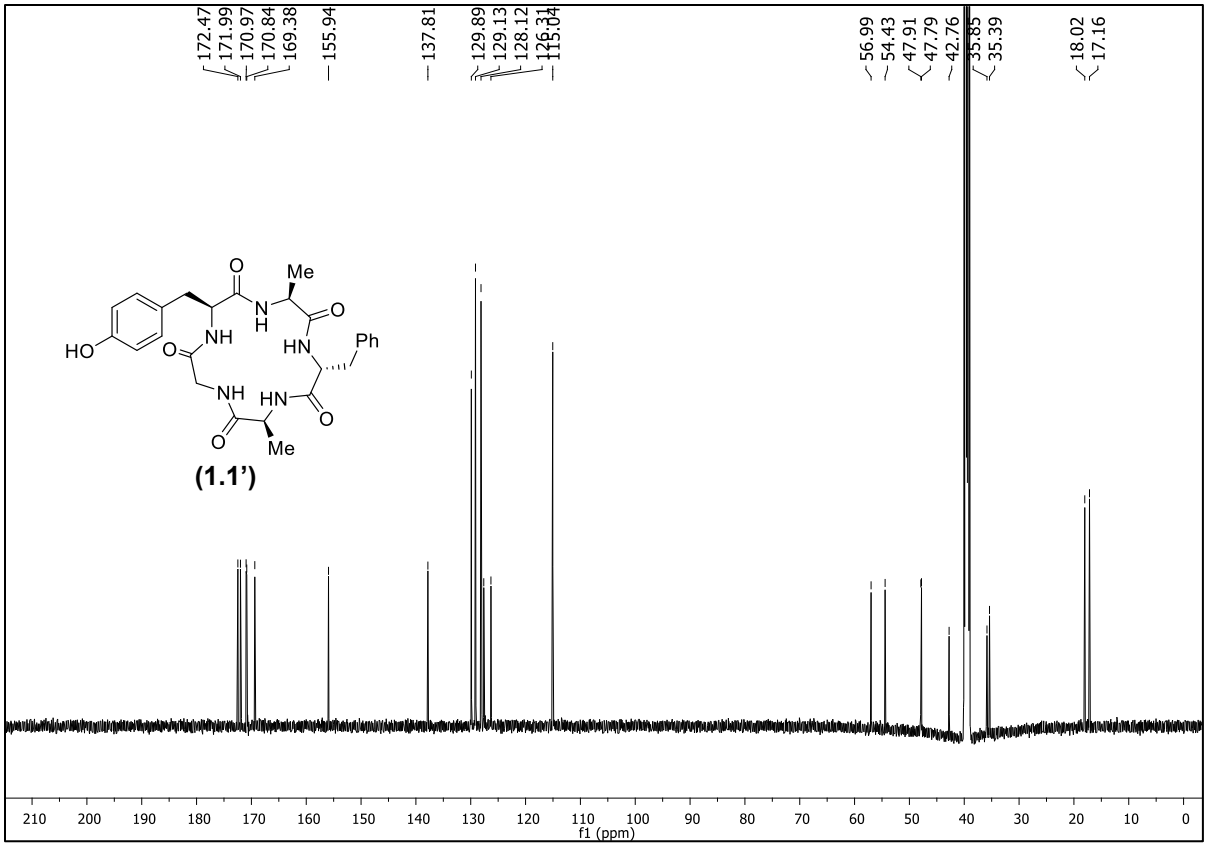
172.47 171.99 170.97 170.84 169.38 155.94 137.81 129.89 129.13 128.12 126.31 115.04 56.99 54.43 47.91 47.79 42.76 35.85 35.39 18.02 17.16
210 200 190 180 170 160 150 140 130 120 110 100 90 80 70 60 50 40 30 20 10 0
f1 (ppm)
(1.1')

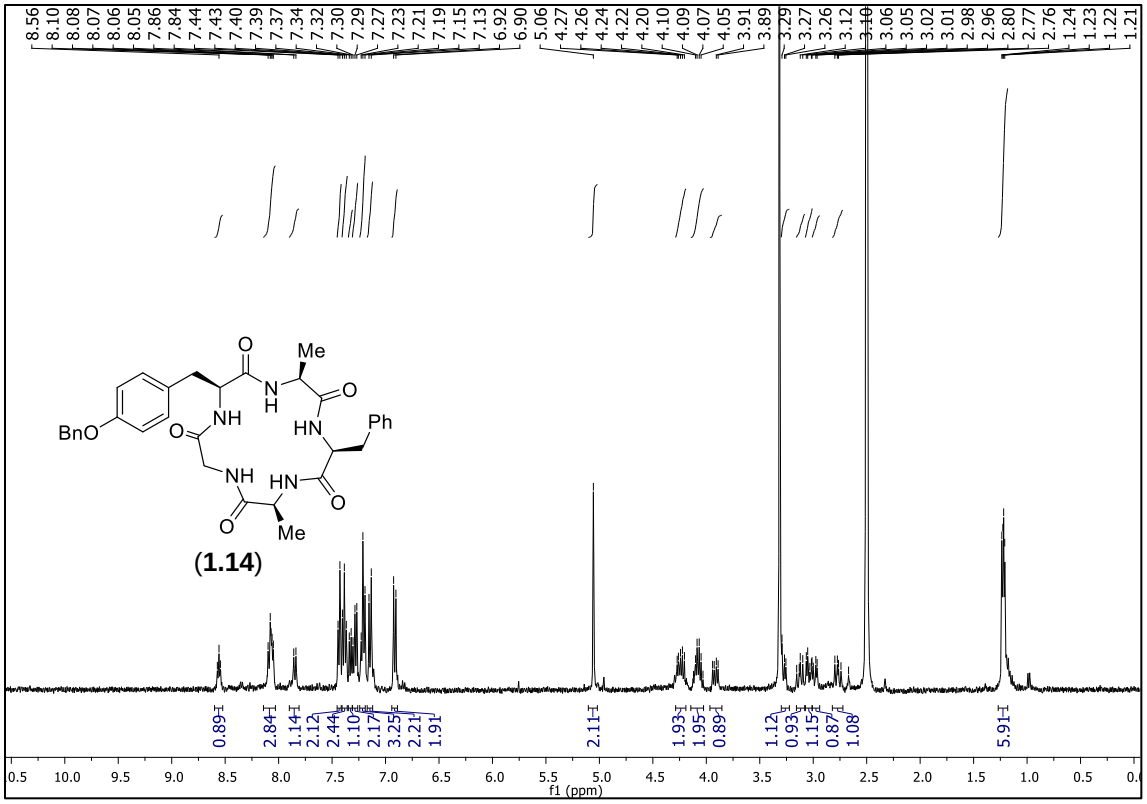
8.56 8.10 8.08 8.07 8.06 8.05 7.86 7.84 7.44 7.43 7.40 7.39 7.37 7.34 7.32 7.30 7.29 7.27 7.23 7.21 7.19 7.15 7.13 6.92 6.90 5.06 4.27 4.26 4.24 4.22 4.20 4.10 4.09 4.07 4.05 3.91 3.89 3.29 3.27 3.26 3.12 3.10 3.06 3.05 3.02 3.01 2.98 2.96 2.80 2.77 2.76 1.24 1.23 1.22 1.21
0.89 2.84 1.14 2.12 2.44 1.10 2.17 3.25 2.21 1.91 2.11 1.93 1.95 0.89 1.12 0.93 1.15 0.87 1.08 5.91
f1 (ppm)
(1.14)

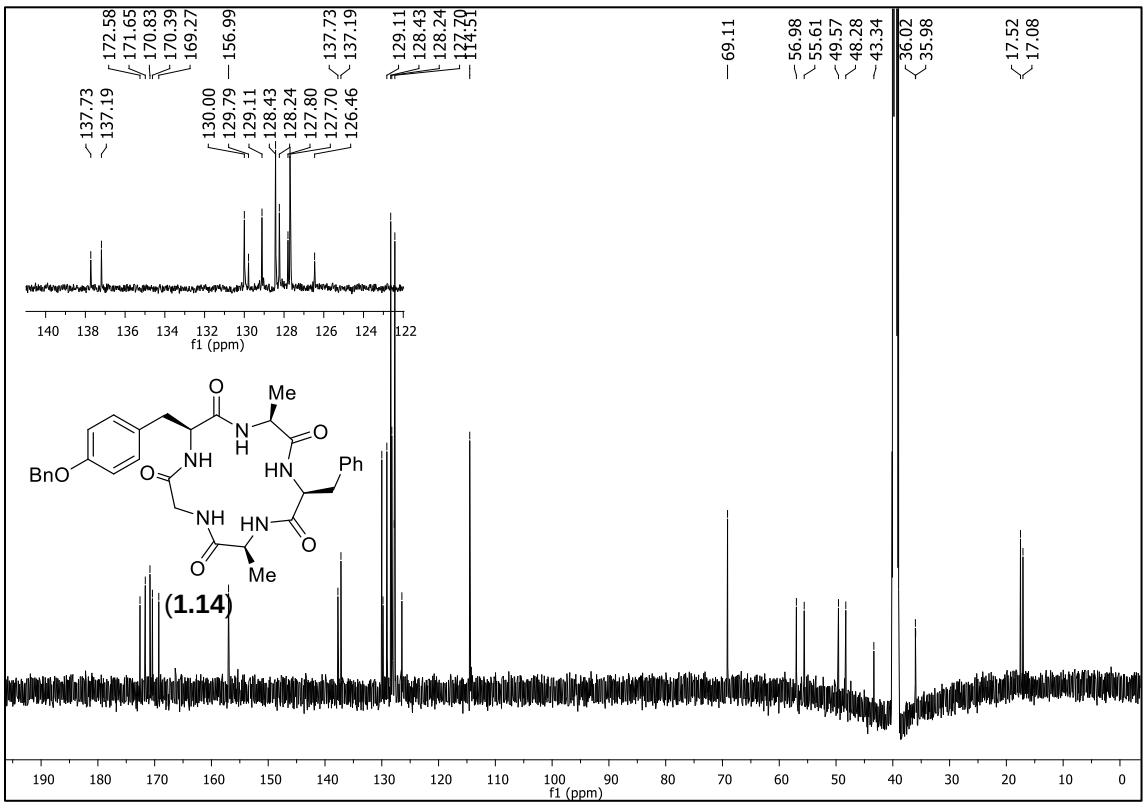
172.58 171.65 170.83 170.39 169.27 156.99 137.73 137.19 129.11 128.43 128.24 127.70 114.51 69.11 56.98 55.61 49.57 48.28 43.34 36.02 35.98 17.52 17.08
137.73 137.19 130.00 129.79 129.11 128.43 128.24 127.80 127.70 126.46
f1 (ppm)
(1.14)

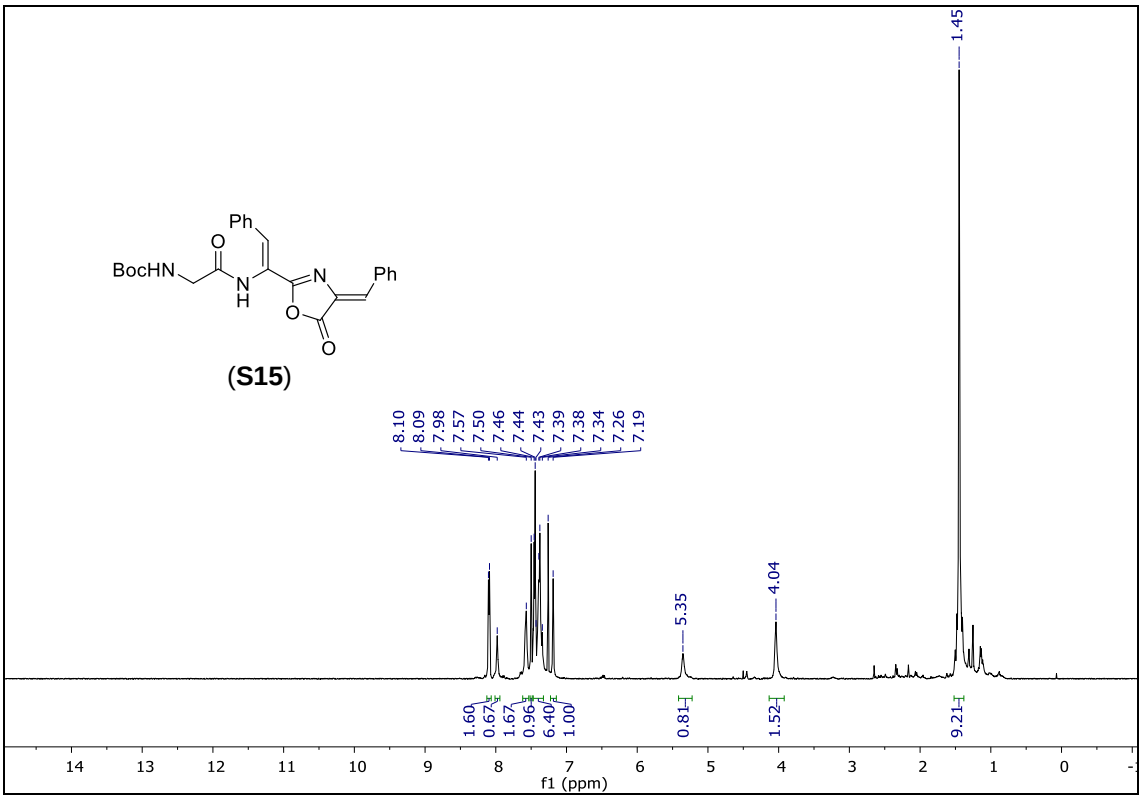
Ph
BocHN
O
N
H
N
Ph
O
O
O
1.45
8.10
8.09
7.98
7.57
7.50
7.46
7.44
7.43
7.39
7.38
7.34
7.26
7.19
5.35
4.04
1.60
0.67
1.67
0.96
6.40
1.00
0.81
1.52
9.21
14
13
12
11
10
9
8
7
6
5
4
3
2
1
0
f1 (ppm)

(**S15**)

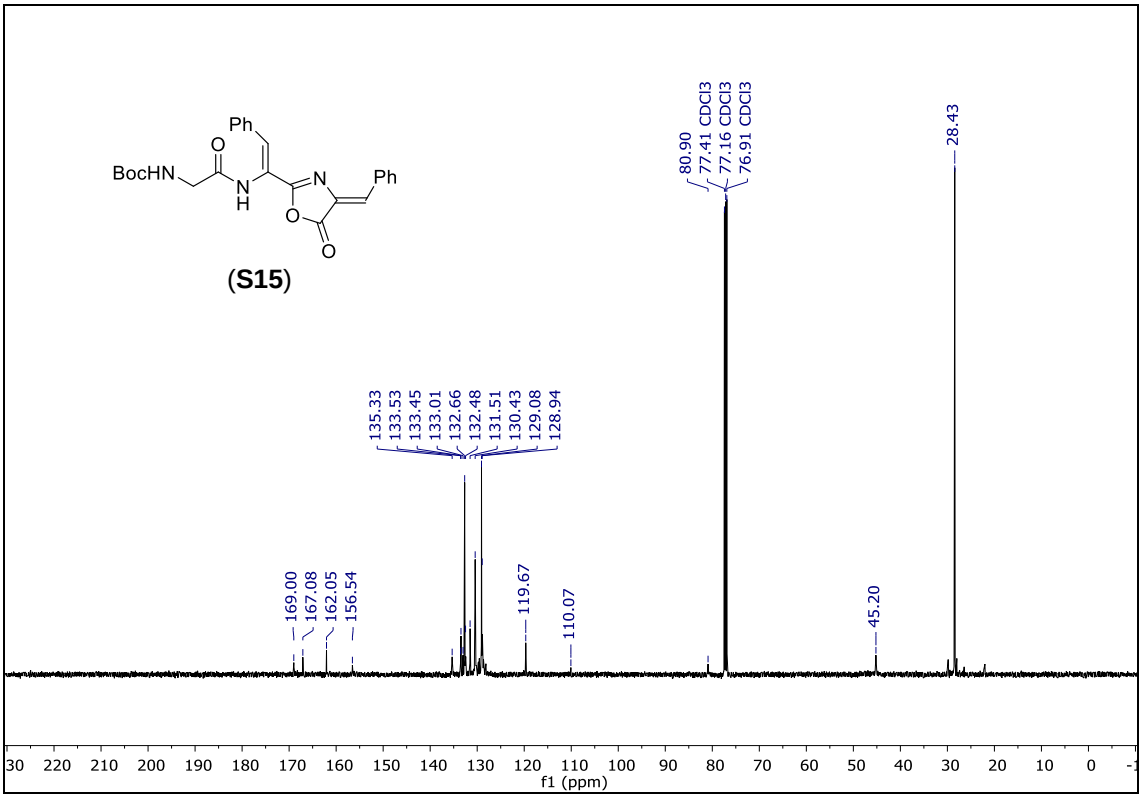
Ph
BocHN
O
N
H
N
Ph
O
O
O
80.90
77.41 CDCl3
77.16 CDCl3
76.91 CDCl3
28.43
135.33
133.53
133.45
133.01
132.66
132.48
131.51
130.43
129.08
128.94
169.00
167.08
162.05
156.54
119.67
110.07
45.20
230
220
210
200
190
180
170
160
150
140
130
120
110
100
90
80
70
60
50
40
30
20
10
0
f1 (ppm)

(**S15**)

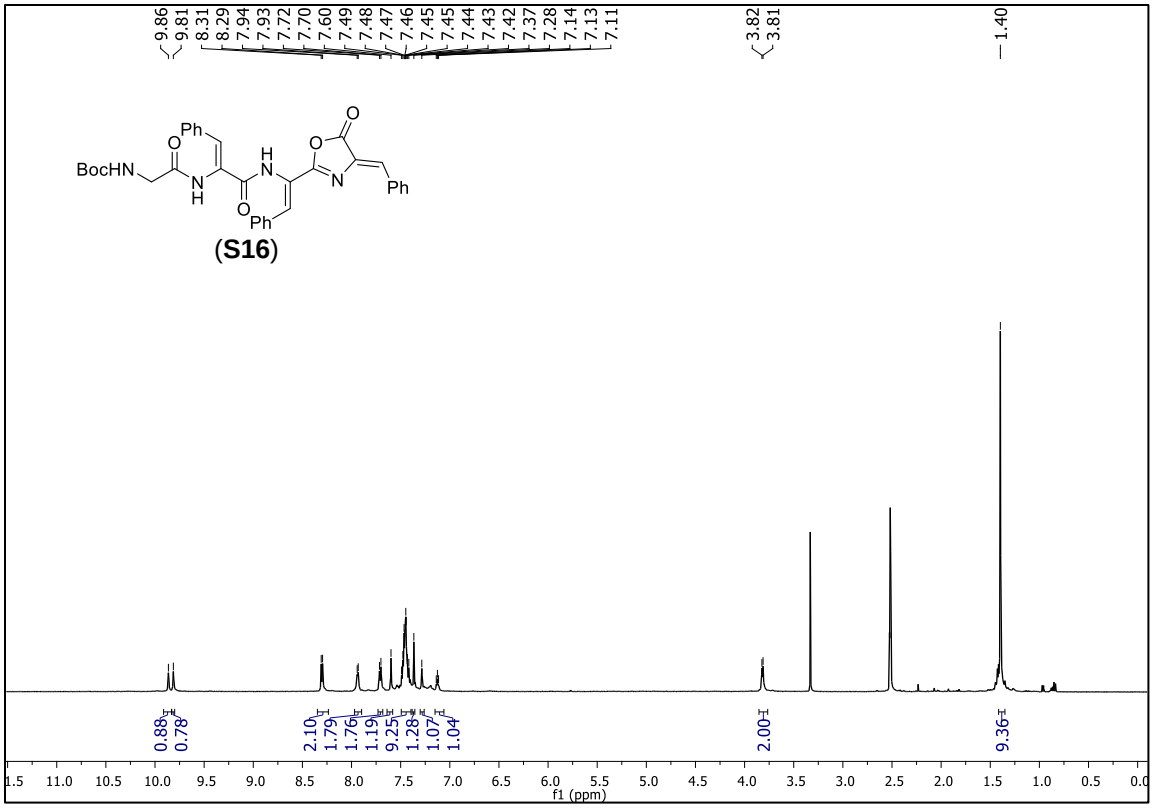
9.86
9.81
8.31
8.29
7.94
7.93
7.72
7.70
7.60
7.49
7.48
7.47
7.46
7.45
7.45
7.44
7.43
7.42
7.37
7.28
7.14
7.13
7.11
3.82
3.81
1.40
BocHN
Ph
O
N
H
Ph
O
N
Ph
0.88
0.78
2.10
1.79
1.76
1.19
9.25
1.28
1.07
1.04
2.00
9.36
f1 (ppm)

(**S16**)

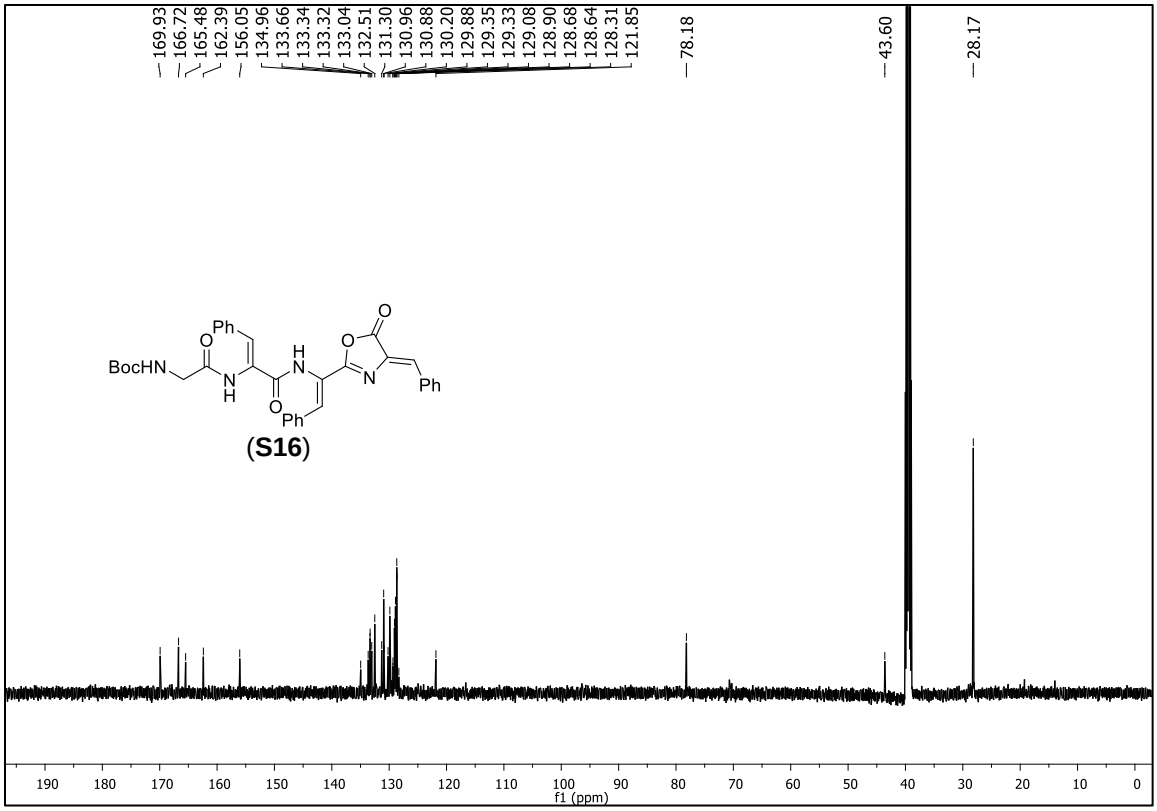
169.93
166.72
165.48
162.39
156.05
134.96
133.66
133.34
133.32
133.04
132.51
131.30
130.96
130.88
130.20
129.88
129.35
129.33
129.08
128.90
128.68
128.64
128.31
121.85
78.18
43.60
28.17
BocHN
Ph
O
N
H
Ph
O
N
Ph
f1 (ppm)

(**S16**)

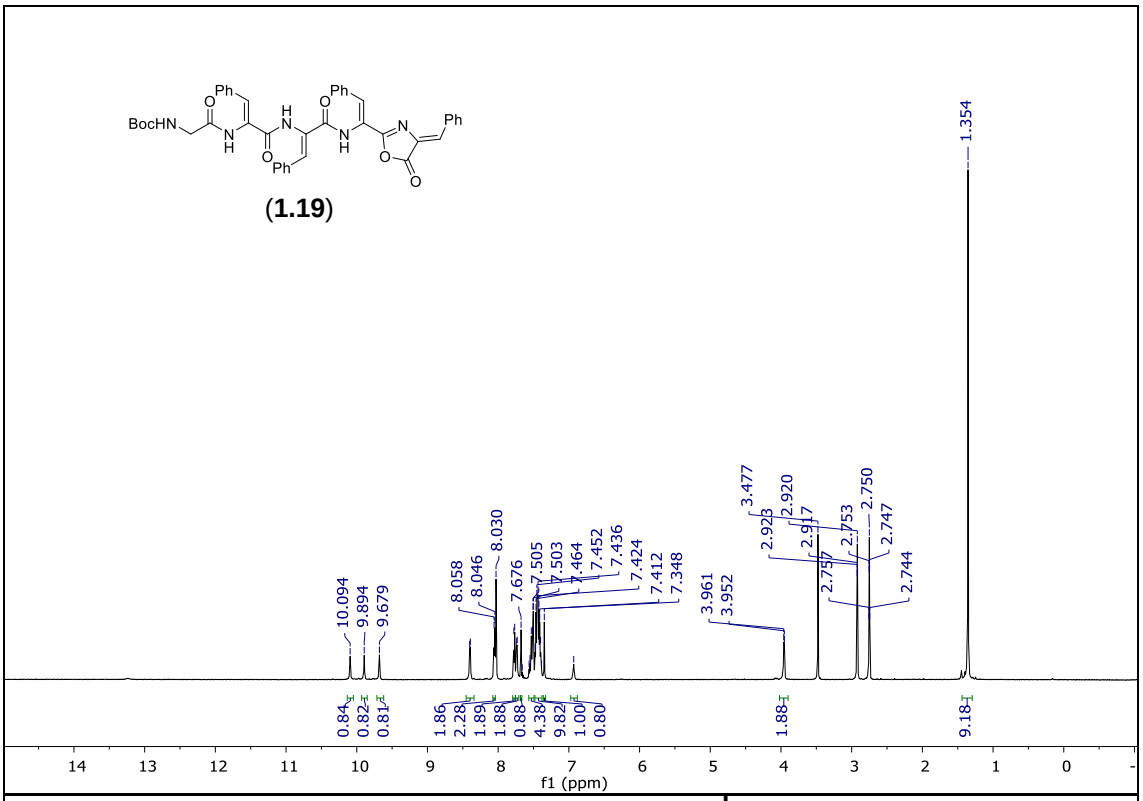
BocHN
Ph
Ph
Ph
Ph
(1.19)
10.094
9.894
9.679
8.058
8.046
8.030
7.676
7.505
7.503
7.464
7.452
7.436
7.424
7.412
7.348
3.961
3.952
3.477
2.928
2.920
2.917
2.757
2.753
2.750
2.747
2.744
1.354
0.84
0.82
0.81
1.86
2.28
1.89
1.88
0.88
4.38
9.82
1.00
0.80
1.88
9.18
f1 (ppm)

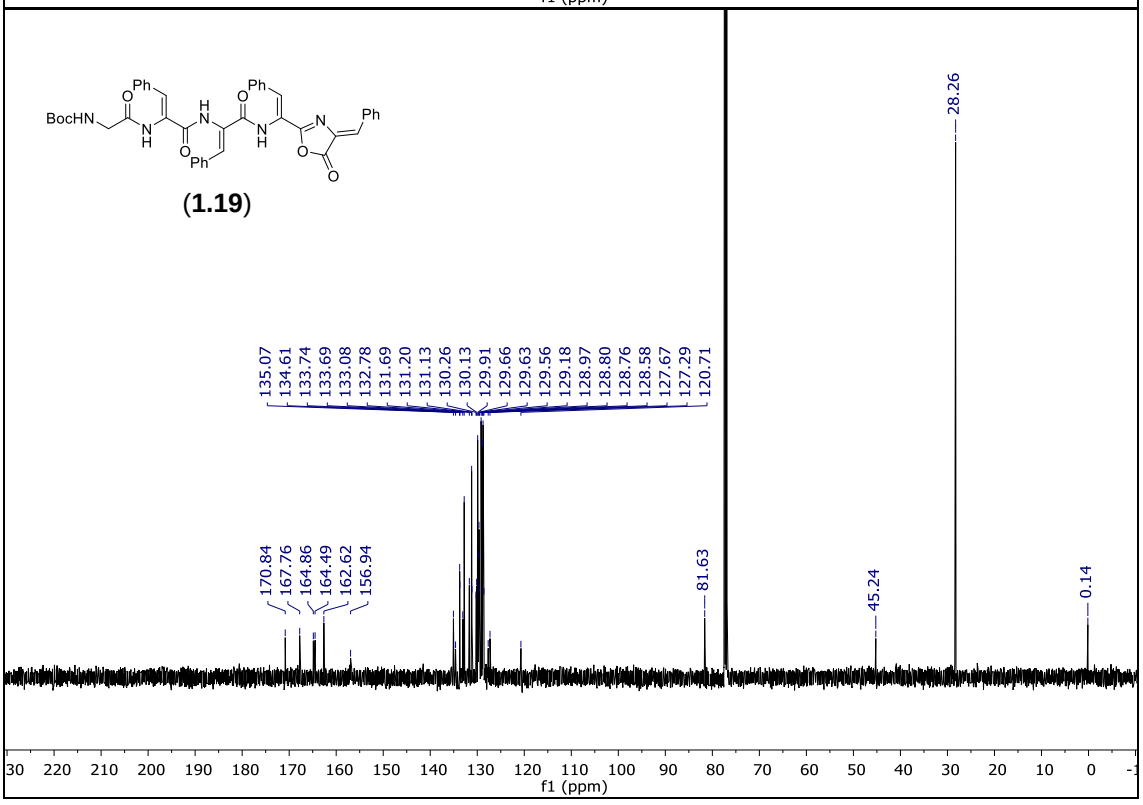
BocHN
Ph
Ph
Ph
Ph
(1.19)
28.26
135.07
134.61
133.74
133.69
133.08
132.78
131.69
131.20
131.13
130.26
130.13
129.91
129.66
129.63
129.56
129.18
128.97
128.80
128.76
128.58
127.67
127.29
120.71
170.84
167.76
164.86
164.49
162.62
156.94
81.63
45.24
0.14
f1 (ppm)

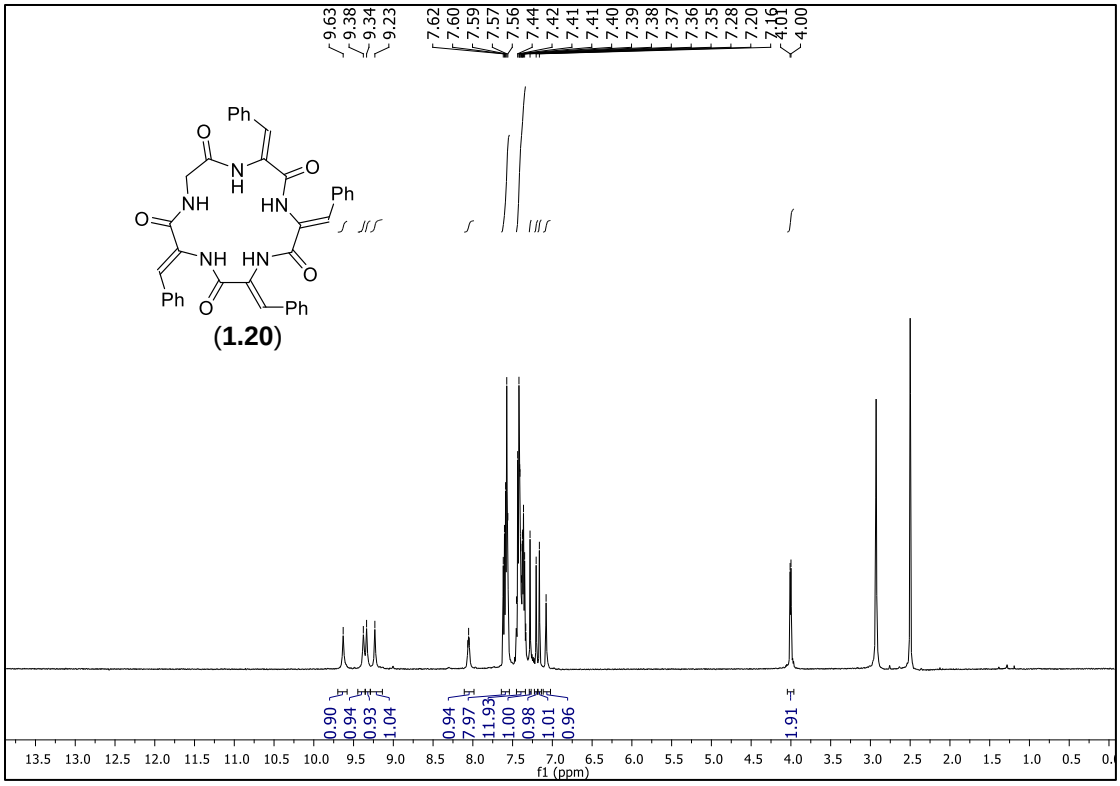
9.63
9.38
9.34
9.23
7.62
7.60
7.59
7.57
7.56
7.44
7.42
7.41
7.41
7.40
7.39
7.38
7.37
7.36
7.35
7.28
7.20
7.16
4.01
4.00
Ph
O
N
H
O
NH
HN
Ph
O
NH
HN
O
Ph
O
Ph
(1.20)
0.90
0.94
0.93
1.04
0.94
7.97
11.93
1.00
0.98
1.01
0.96
1.91
13.5 13.0 12.5 12.0 11.5 11.0 10.5 10.0 9.5 9.0 8.5 8.0 7.5 7.0 6.5 6.0 5.5 5.0 4.5 4.0 3.5 3.0 2.5 2.0 1.5 1.0 0.5
f1 (ppm)

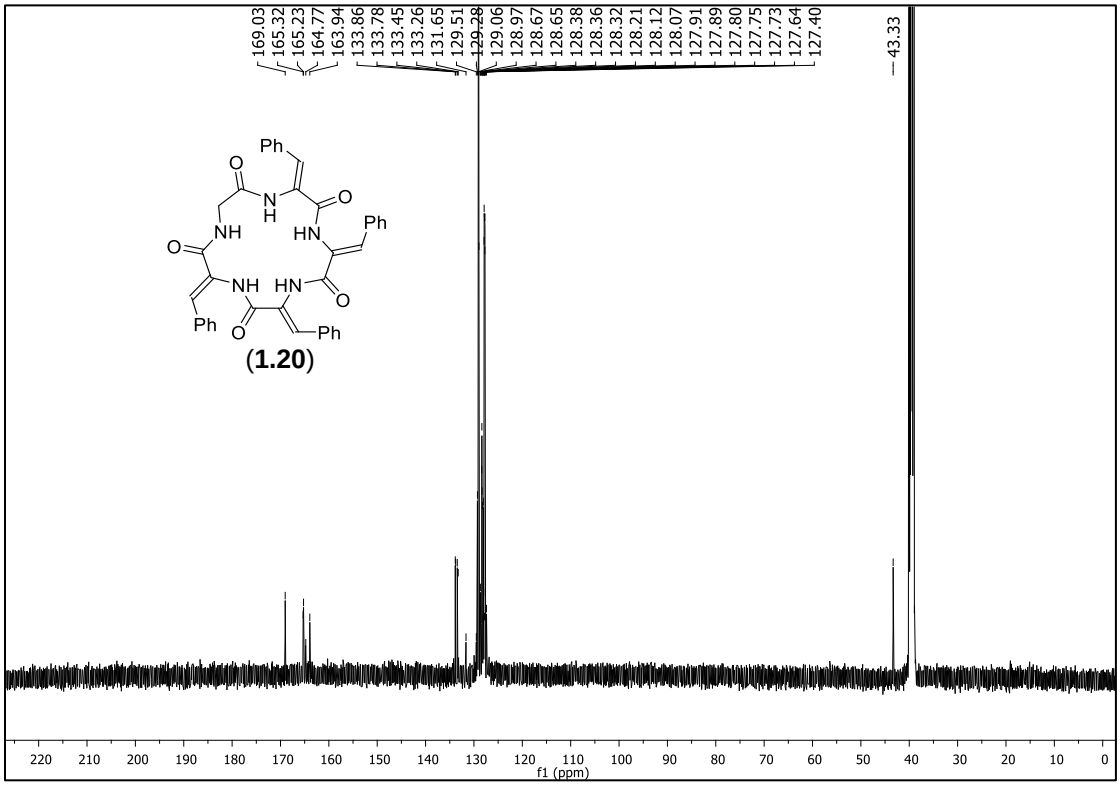
169.03
165.32
165.23
164.77
163.94
133.86
133.78
133.45
133.26
131.65
129.51
129.28
129.06
128.97
128.67
128.65
128.38
128.36
128.32
128.21
128.12
128.07
127.91
127.89
127.80
127.75
127.73
127.64
127.40
43.33
Ph
O
N
H
O
NH
HN
Ph
O
NH
HN
O
Ph
O
Ph
(1.20)
220 210 200 190 180 170 160 150 140 130 120 110 100 90 80 70 60 50 40 30 20 10 0
f1 (ppm)

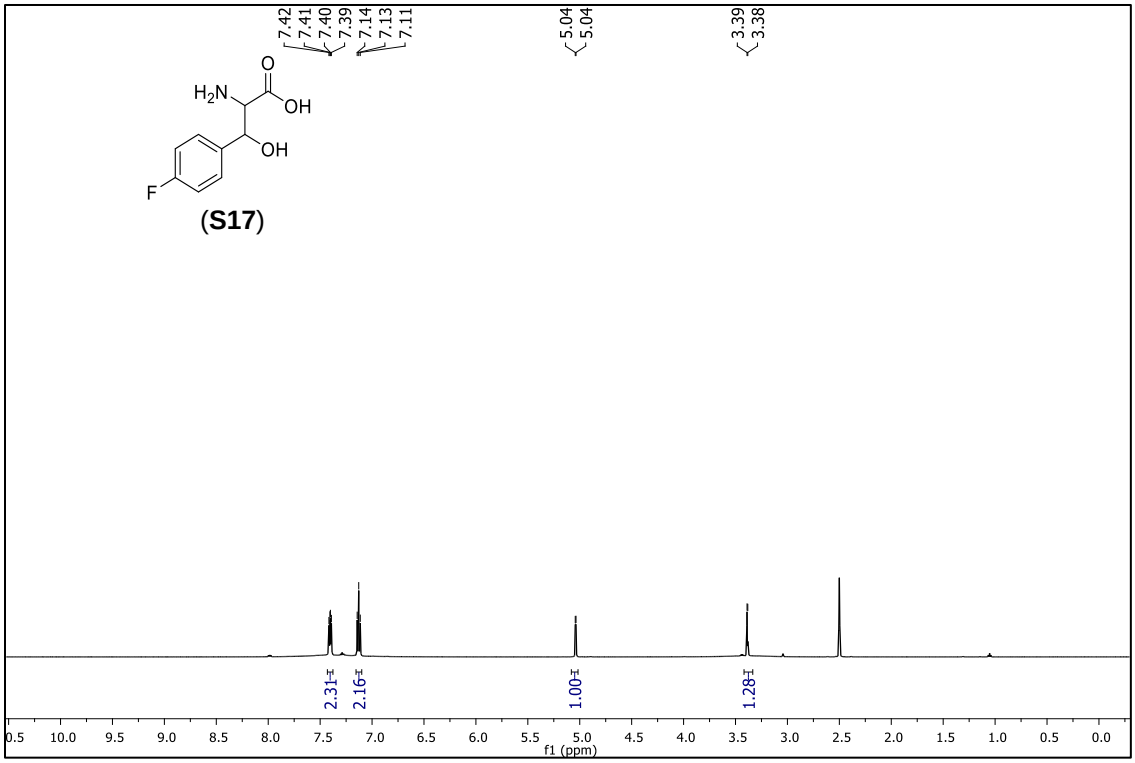
7.42
7.41
7.40
7.39
7.14
7.13
7.11
5.04
5.04
3.39
3.38
O
H2N
OH
OH
F
(S17)
2.31
2.16
1.00
1.28
f1 (ppm)

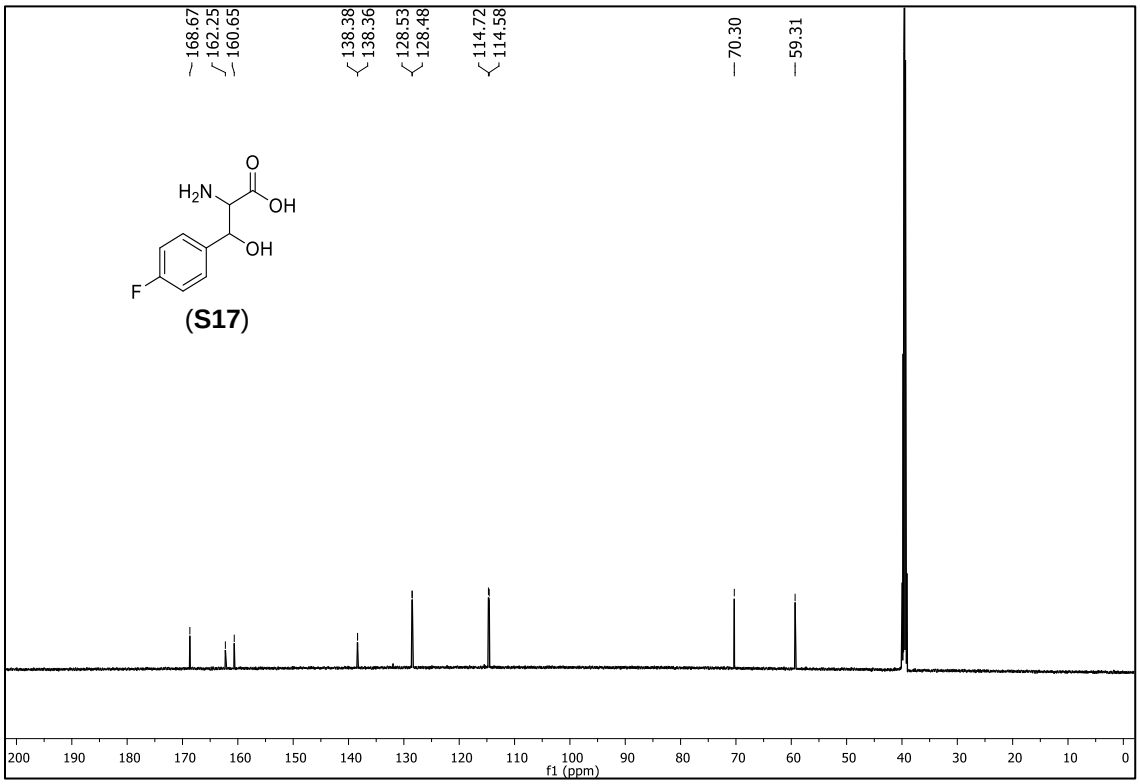
168.67
162.25
160.65
138.38
138.36
128.53
128.48
114.72
114.58
70.30
59.31
O
H2N
OH
OH
F
(S17)
f1 (ppm)

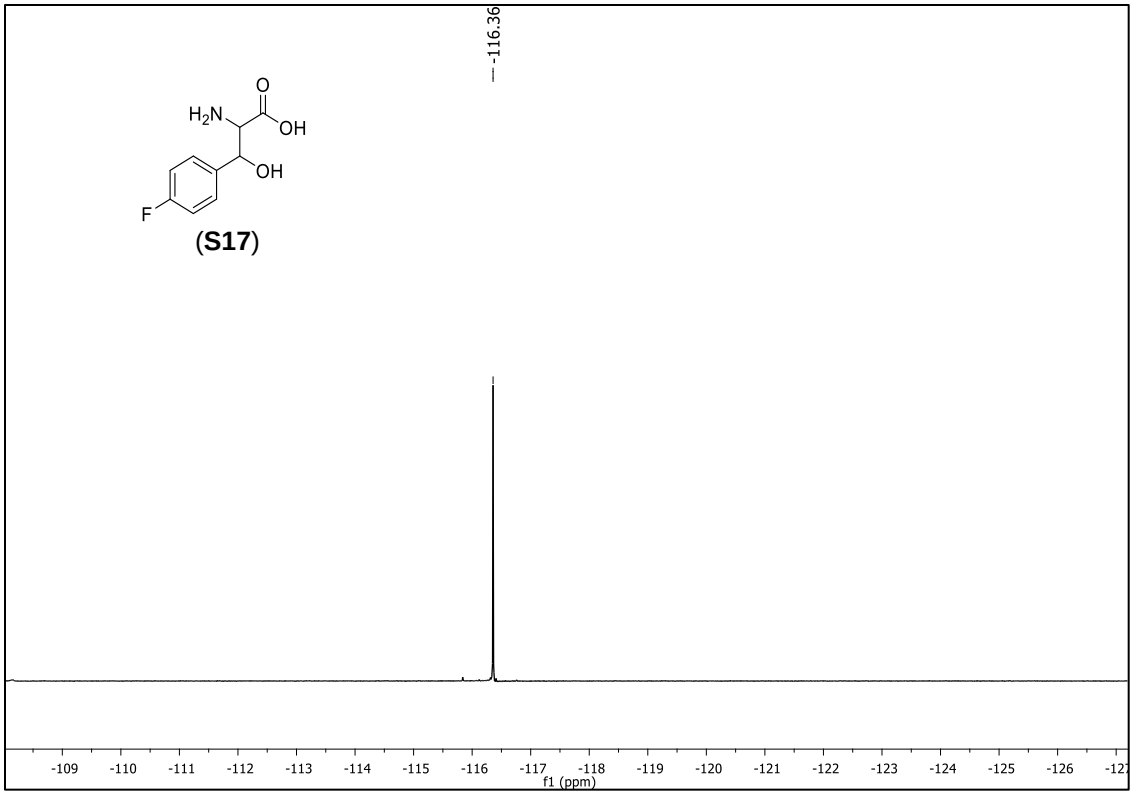
-116.36
O
H2N
OH
OH
F
-109
-110
-111
-112
-113
-114
-115
-116
-117
-118
-119
-120
-121
-122
-123
-124
-125
-126
f1 (ppm)

(**S17**)

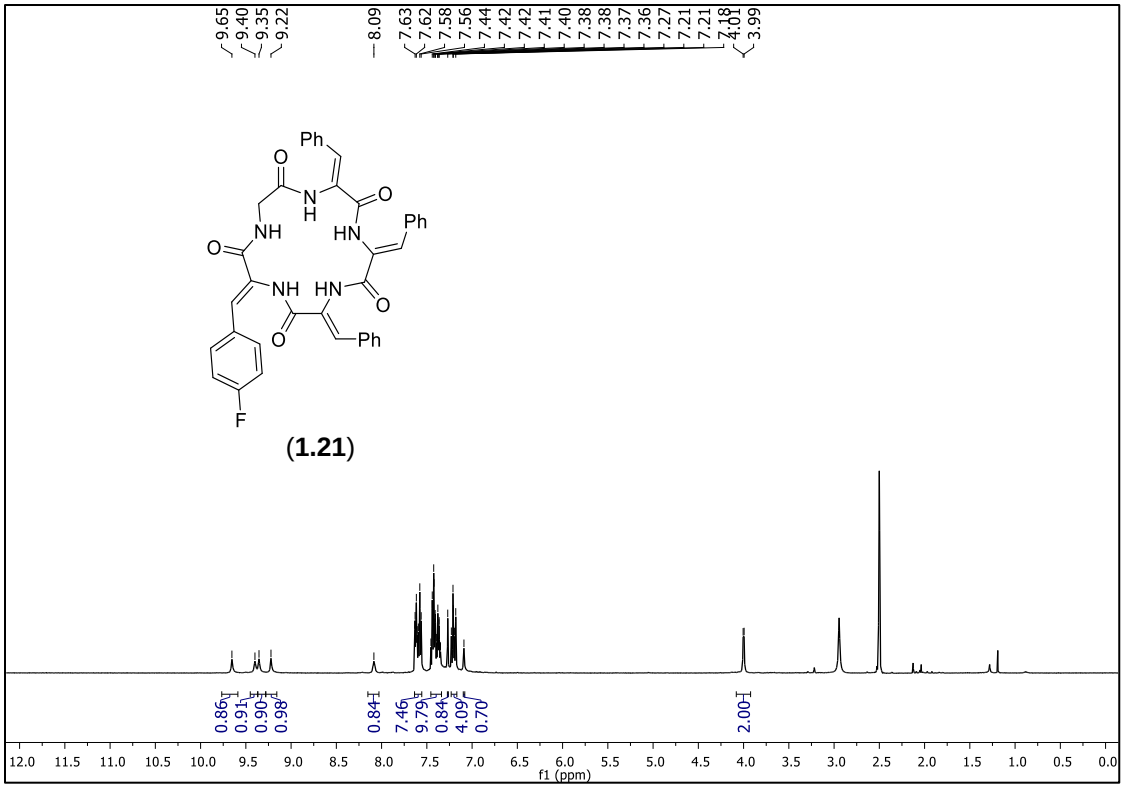
9.65
9.40
9.35
9.22
8.09
7.63
7.62
7.58
7.56
7.44
7.42
7.42
7.41
7.40
7.38
7.38
7.37
7.36
7.27
7.21
7.21
4.18
4.01
3.99
Ph
O
N
H
O
NH
HN
Ph
O
NH
HN
O
O
Ph
F
0.86
0.91
0.90
0.98
0.84
7.46
9.79
0.84
4.09
0.70
2.00
12.0
11.5
11.0
10.5
10.0
9.5
9.0
8.5
8.0
7.5
7.0
6.5
6.0
5.5
5.0
4.5
4.0
3.5
3.0
2.5
2.0
1.5
1.0
0.5
0.0
f1 (ppm)

(**1.21**)

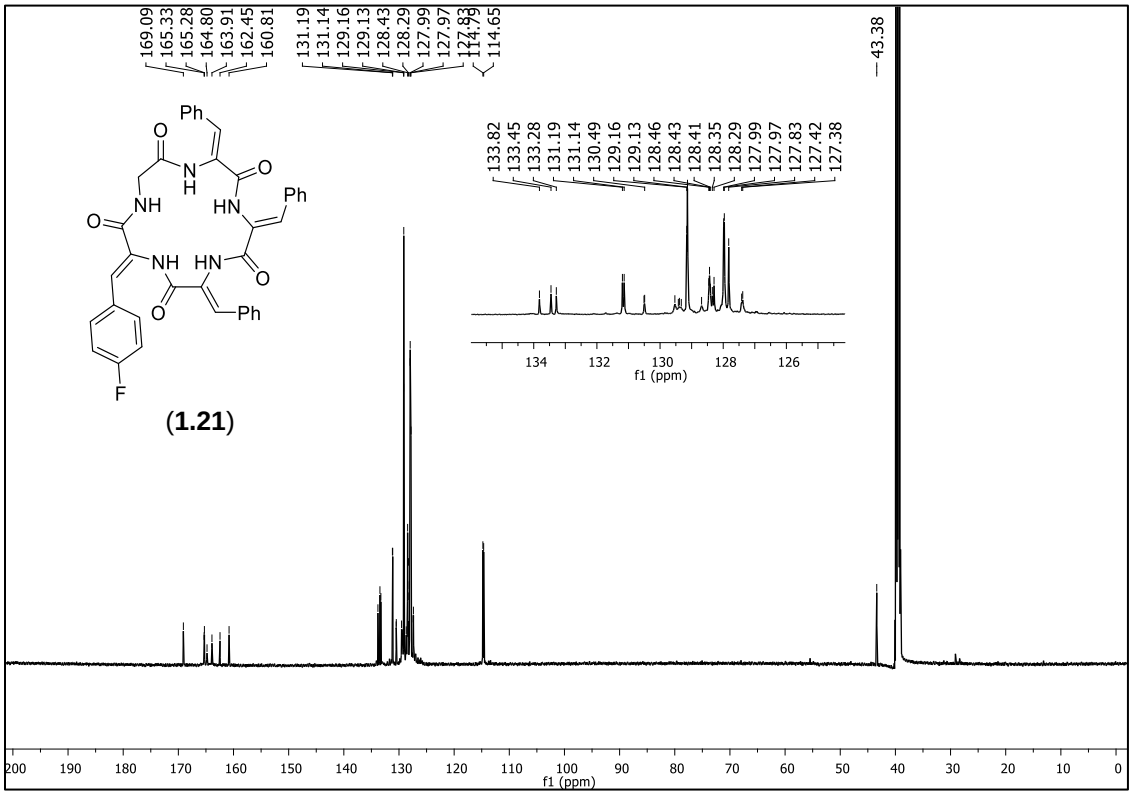
169.09
165.33
165.28
164.80
163.91
162.45
160.81
131.19
131.14
129.16
129.13
128.43
128.29
127.99
127.97
127.83
127.79
114.65
43.38
133.82
133.45
133.28
131.19
131.14
130.49
129.16
129.13
128.46
128.43
128.41
128.35
128.29
127.99
127.97
127.83
127.42
127.38
134
132
130
128
126
f1 (ppm)
Ph
O
N
H
O
NH
HN
Ph
O
NH
HN
O
O
Ph
F
200
190
180
170
160
150
140
130
120
110
100
90
80
70
60
50
40
30
20
10
0
f1 (ppm)

(**1.21**)

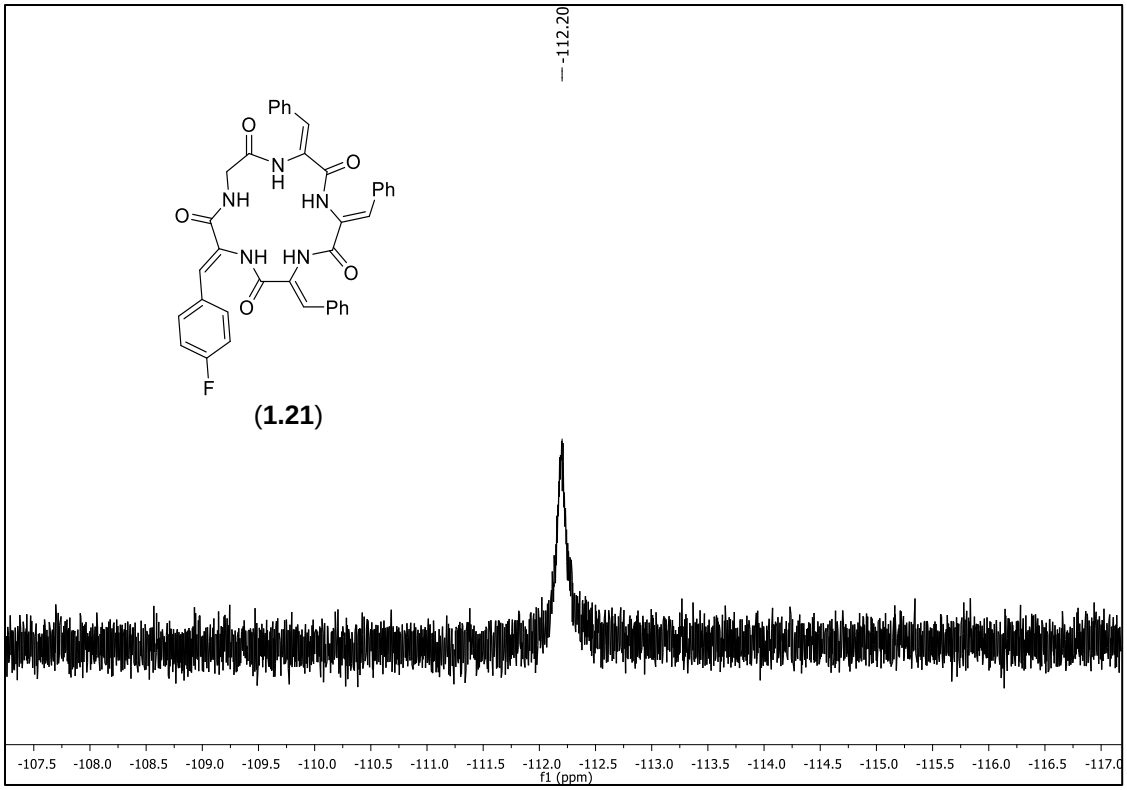
-112.20
Ph
O
N
H
O
NH
HN
Ph
O
NH
HN
O
O
Ph
F
-107.5
-108.0
-108.5
-109.0
-109.5
-110.0
-110.5
-111.0
-111.5
-112.0
-112.5
-113.0
-113.5
-114.0
-114.5
-115.0
-115.5
-116.0
-116.5
-117.0
f1 (ppm)

(**1.21**)

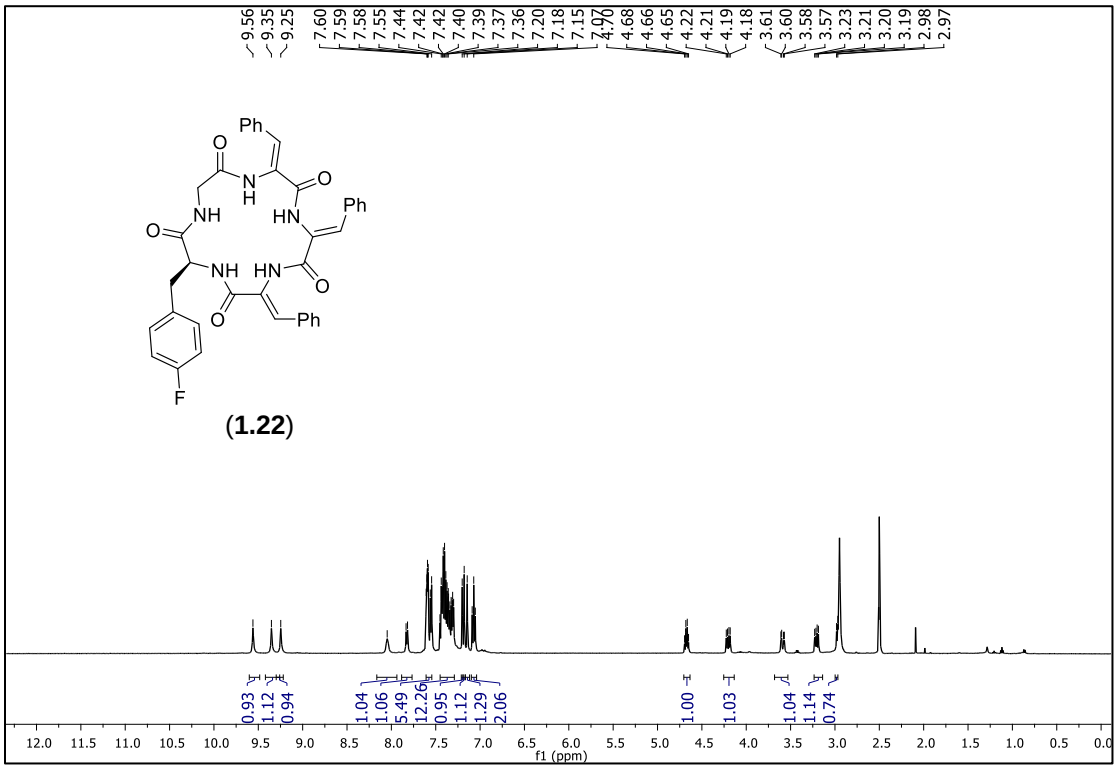
9.56
9.35
9.25
7.60
7.59
7.58
7.55
7.44
7.42
7.42
7.40
7.39
7.37
7.36
7.20
7.18
7.15
4.70
4.68
4.66
4.65
4.22
4.21
4.19
4.18
3.61
3.60
3.58
3.57
3.23
3.21
3.20
3.19
2.98
2.97
Ph
O
N
H
O
NH
HN
Ph
O
NH
HN
O
O
Ph
F
0.93
1.12
0.94
1.04
1.06
5.49
12.26
0.95
1.12
1.29
2.06
1.00
1.03
1.04
1.14
0.74
f1 (ppm)

(**1.22**)

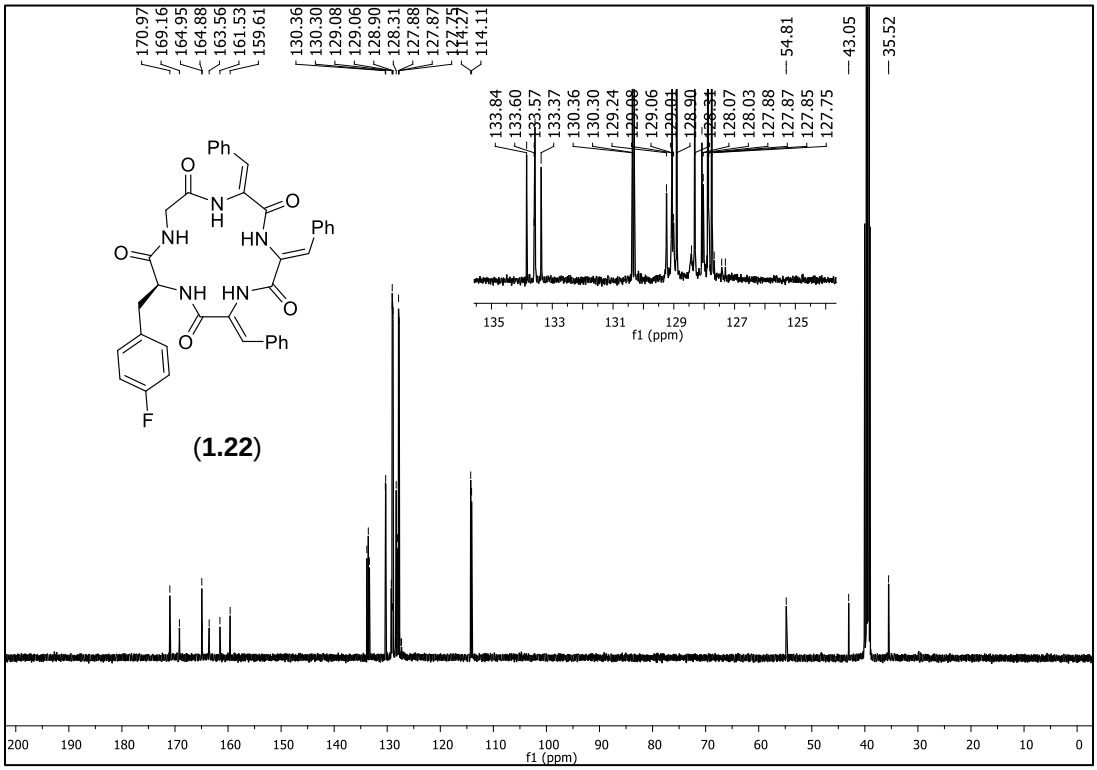
170.97
169.16
164.95
164.88
163.56
161.53
159.61
130.36
130.30
129.08
129.06
128.90
128.31
127.88
127.87
127.75
127.27
114.11
54.81
43.05
35.52
133.84
133.60
133.57
133.37
130.36
130.30
129.24
129.06
129.01
128.90
128.34
128.07
128.03
127.88
127.87
127.85
127.75
Ph
O
N
H
O
NH
HN
Ph
O
NH
HN
O
O
Ph
F
f1 (ppm)

(**1.22**)

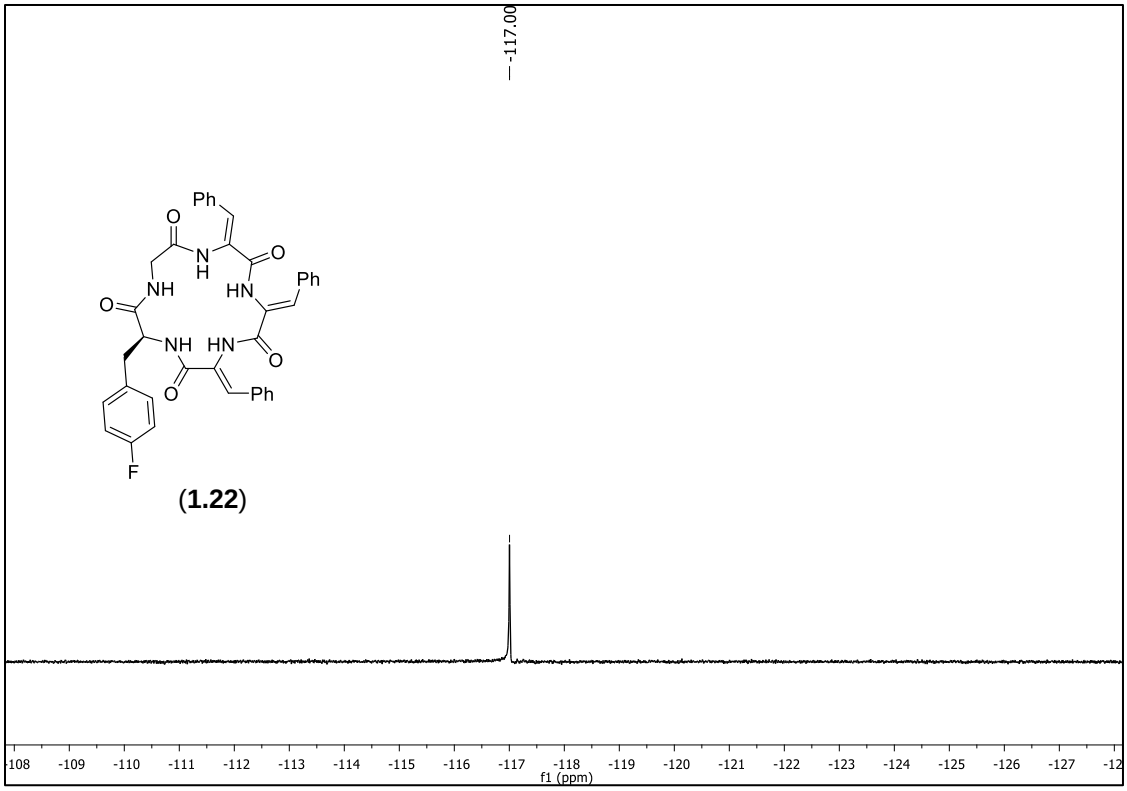
-117.00
Ph
O
N
H
O
HN
Ph
NH
O
NH
HN
O
O
Ph
F
-108
-109
-110
-111
-112
-113
-114
-115
-116
-117
-118
-119
-120
-121
-122
-123
-124
-125
-126
-127
f1 (ppm)

(**1.22**)

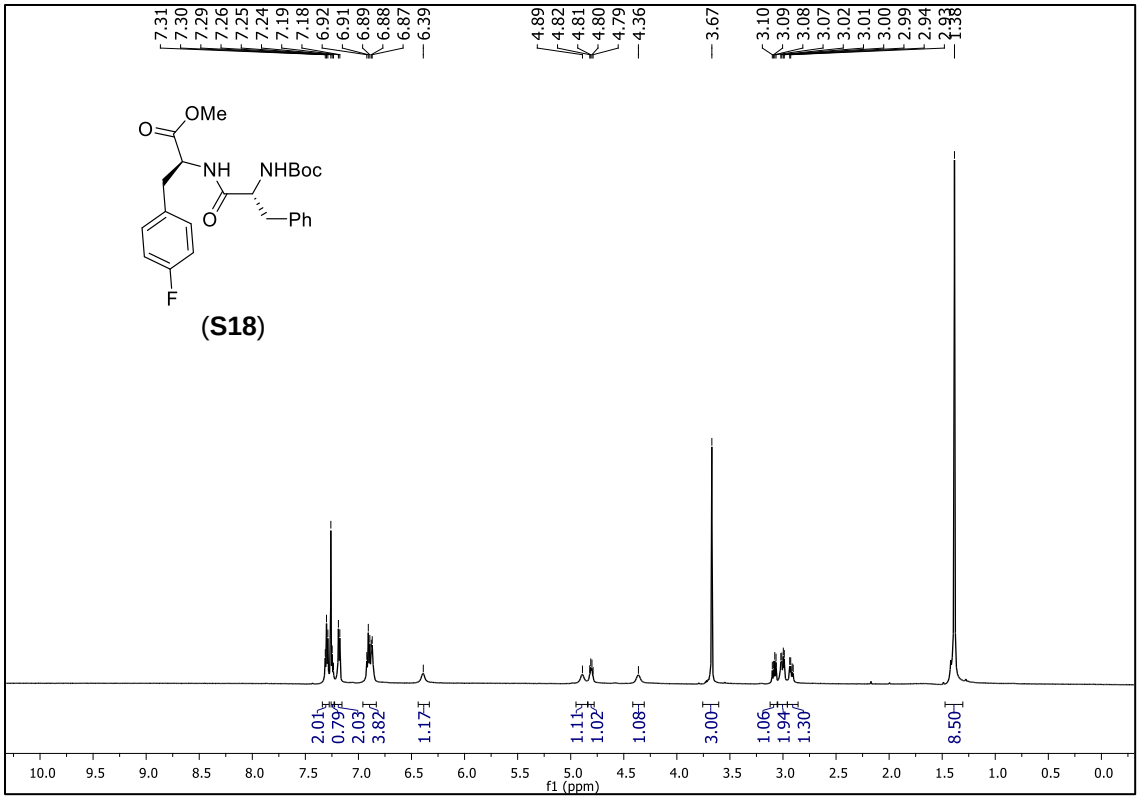
7.31
7.30
7.29
7.26
7.25
7.24
7.19
7.18
6.92
6.91
6.89
6.88
6.87
6.39
4.89
4.82
4.81
4.80
4.79
4.36
3.67
3.10
3.09
3.08
3.07
3.02
3.01
3.00
2.99
2.94
2.93
1.38
OMe
O
NH
NHBoc
O
Ph
F
2.01
0.79
2.03
3.82
1.17
1.11
1.02
1.08
3.00
1.06
1.94
1.30
8.50
f1 (ppm)

(**S18**)

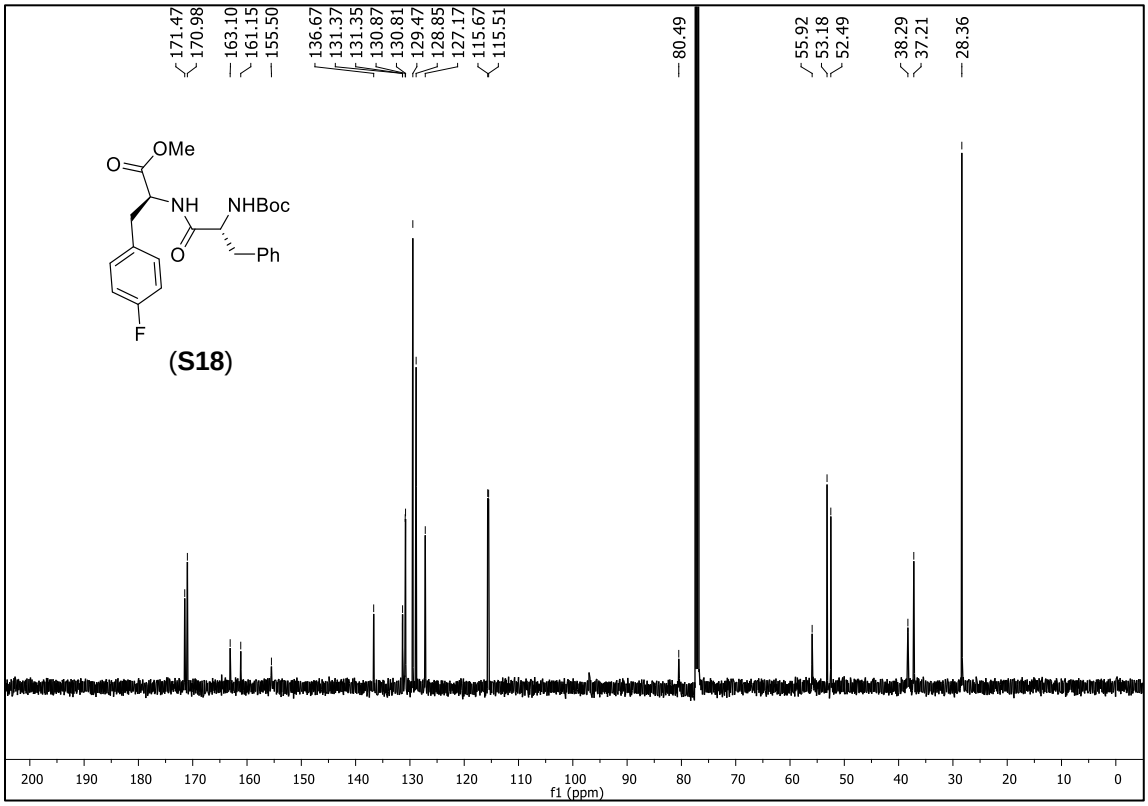
171.47
170.98
163.10
161.15
155.50
136.67
131.37
131.35
130.87
130.81
129.47
128.85
127.17
115.67
115.51
80.49
55.92
53.18
52.49
38.29
37.21
28.36
OMe
O
NH
NHBoc
O
Ph
F
f1 (ppm)

(**S18**)

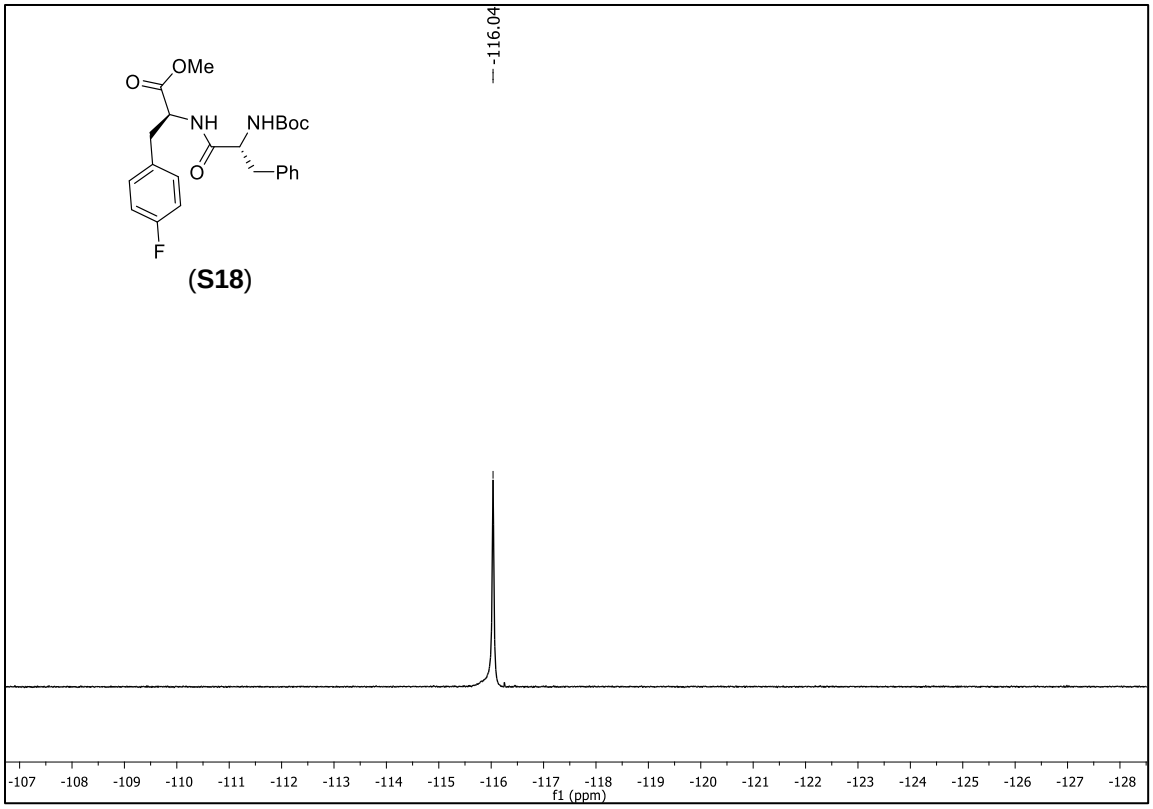
-116.04
OMe
O
NH
NHBoc
O
Ph
F
-107
-108
-109
-110
-111
-112
-113
-114
-115
-116
-117
-118
-119
-120
-121
-122
-123
-124
-125
-126
-127
-128
f1 (ppm)

(**S18**)

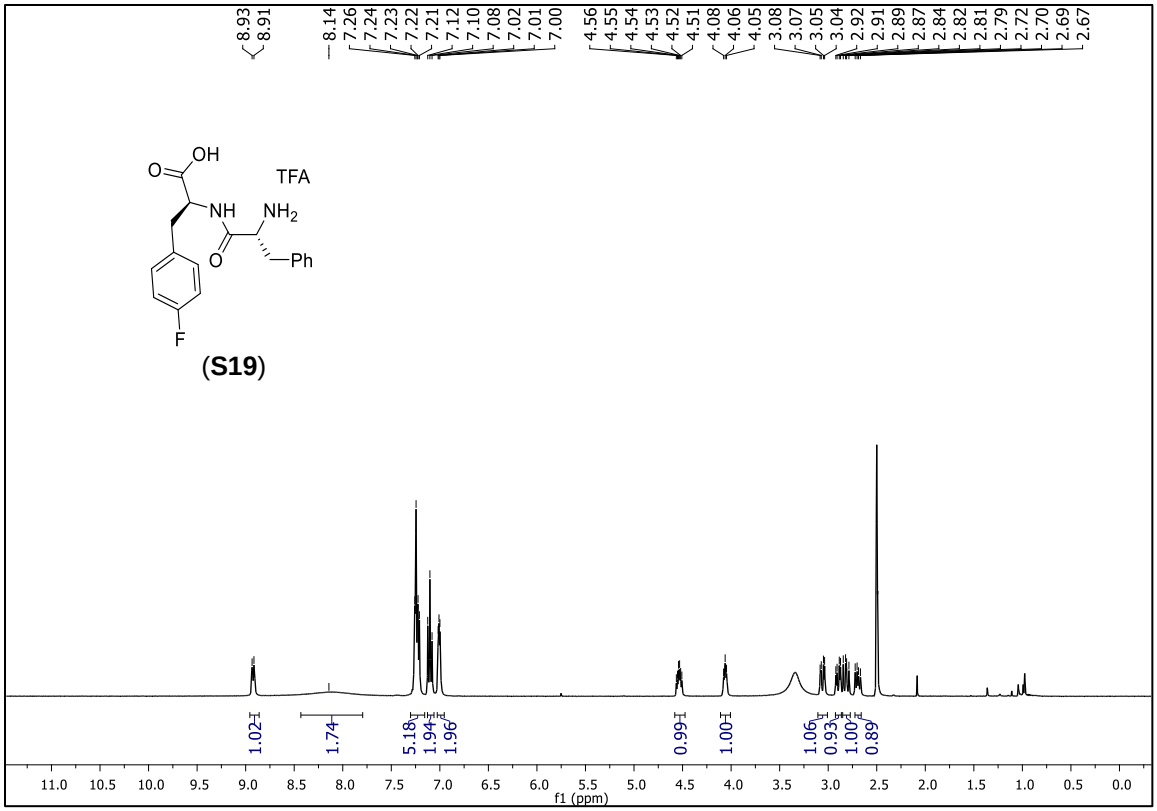
8.93
8.91
8.14
7.26
7.24
7.23
7.22
7.21
7.12
7.10
7.08
7.02
7.01
7.00
4.56
4.55
4.54
4.53
4.52
4.51
4.08
4.06
4.05
3.08
3.07
3.05
3.04
2.92
2.91
2.89
2.87
2.84
2.82
2.81
2.79
2.72
2.70
2.69
2.67
OH
O
NH
NH2
O
Ph
TFA
F
1.02
1.74
5.18
1.94
1.96
0.99
1.00
1.06
0.93
1.00
0.89
11.0
10.5
10.0
9.5
9.0
8.5
8.0
7.5
7.0
6.5
6.0
5.5
5.0
4.5
4.0
3.5
3.0
2.5
2.0
1.5
1.0
0.5
0.0
f1 (ppm)

(**S19**)

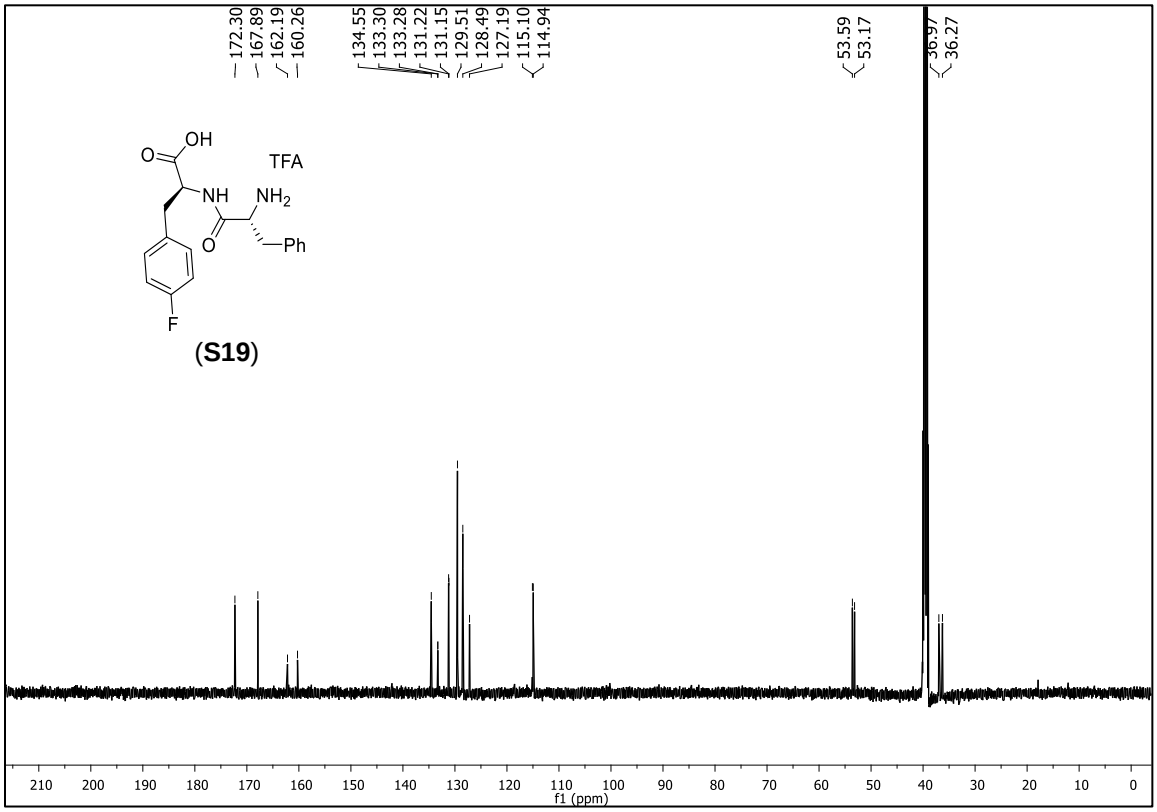
172.30
167.89
162.19
160.26
134.55
133.30
133.28
131.22
131.15
129.51
128.49
127.19
115.10
114.94
53.59
53.17
36.97
36.27
OH
O
NH
NH2
O
Ph
TFA
F
210
200
190
180
170
160
150
140
130
120
110
100
90
80
70
60
50
40
30
20
10
0
f1 (ppm)

(**S19**)

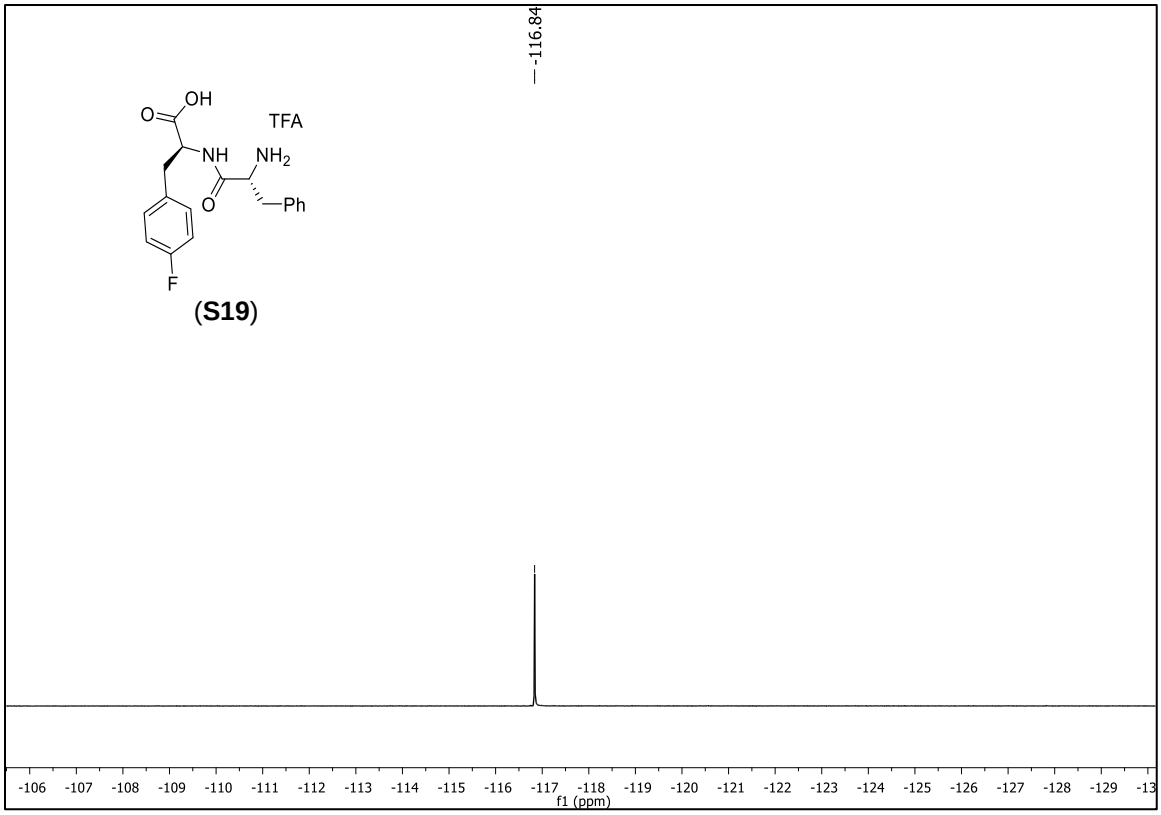
-116.84
OH
O
TFA
NH
NH2
O
Ph
F
-106 -107 -108 -109 -110 -111 -112 -113 -114 -115 -116 -117 -118 -119 -120 -121 -122 -123 -124 -125 -126 -127 -128 -129 -13
f1 (ppm)

(**S19**)

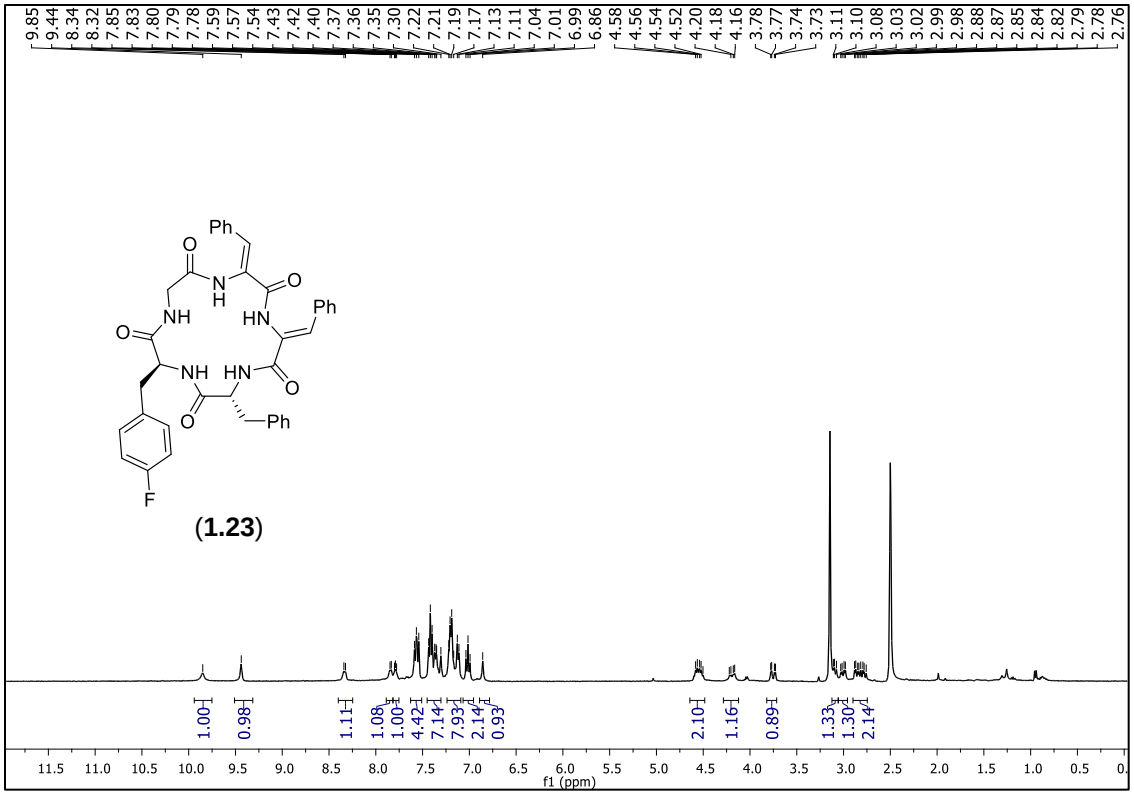
(1.23)
f1 (ppm)

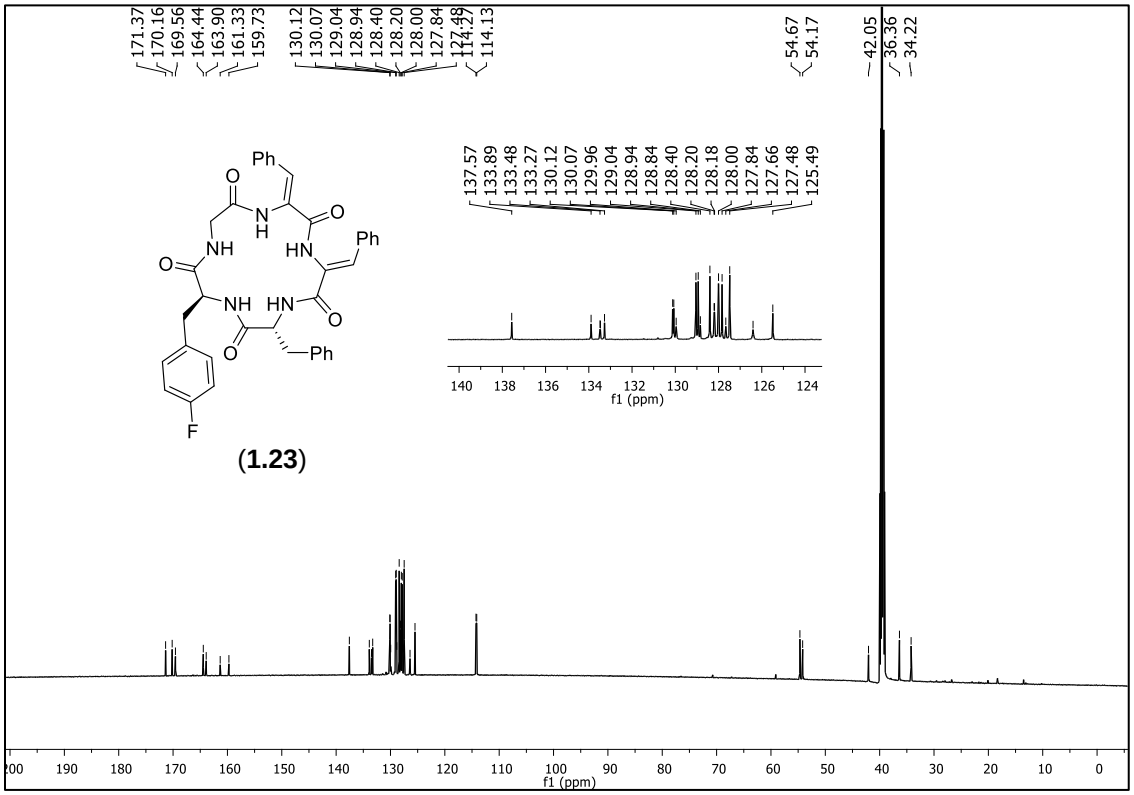
(1.23)
f1 (ppm)
f1 (ppm)

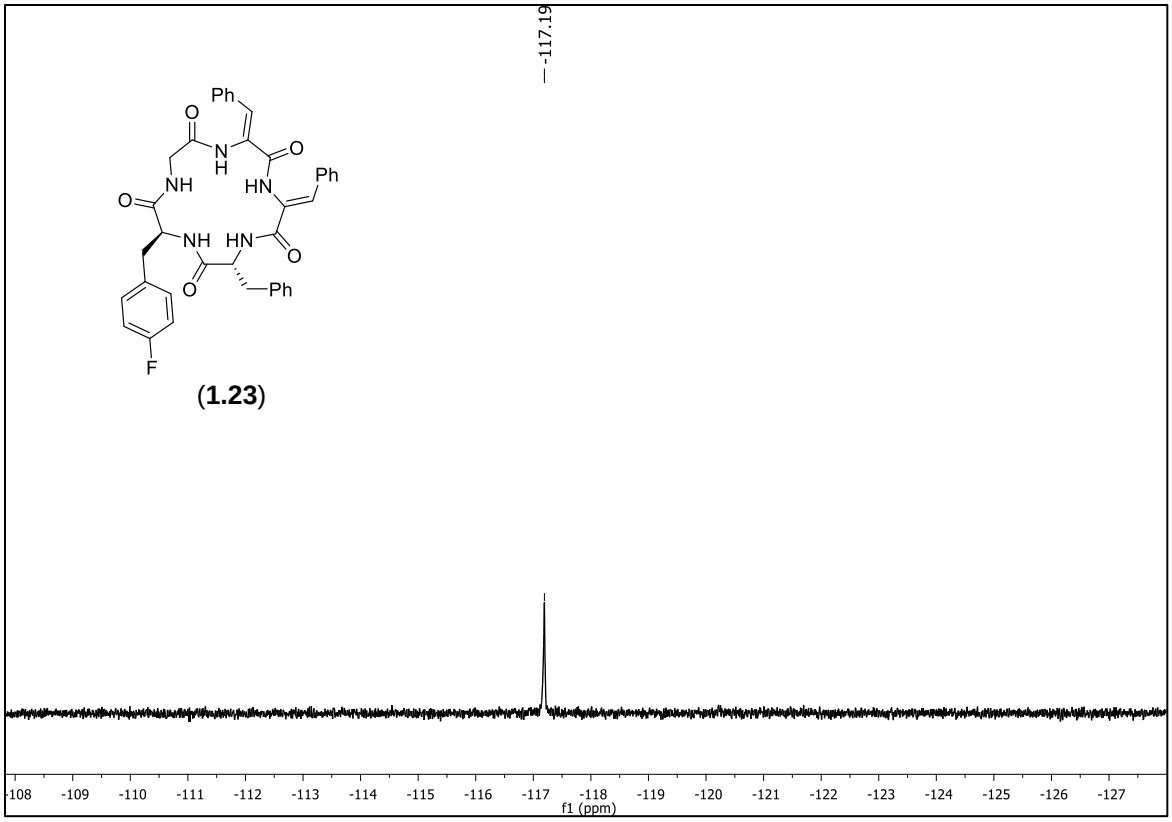
-117.19
Ph
O
N
H
O
NH
HN
Ph
O
NH
HN
O
O
Ph
F
-108
-109
-110
-111
-112
-113
-114
-115
-116
-117
-118
-119
-120
-121
-122
-123
-124
-125
-126
-127
f1 (ppm)

(**1.23**)

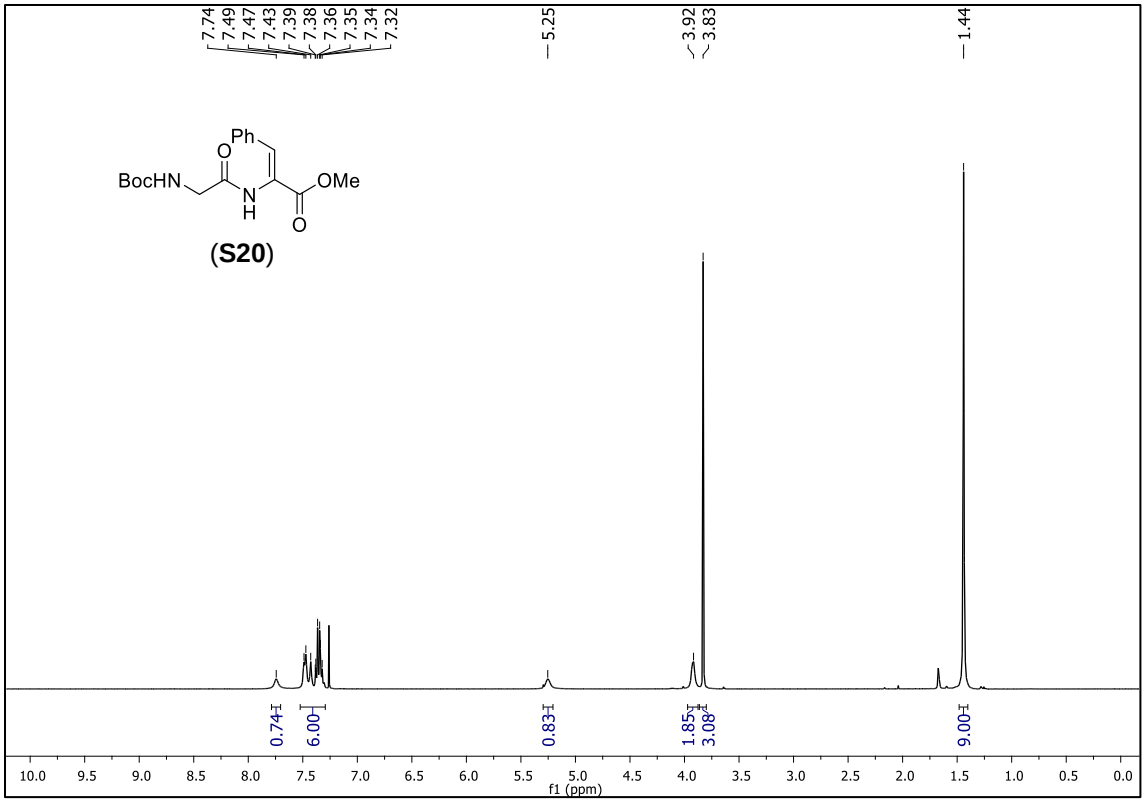
7.74
7.49
7.47
7.43
7.39
7.38
7.36
7.35
7.34
7.32
5.25
3.92
3.83
1.44
Ph
O
BocHN
N
H
OMe
O
(S20)
0.74
6.00
0.83
1.85
3.08
9.00
10.0 9.5 9.0 8.5 8.0 7.5 7.0 6.5 6.0 5.5 5.0 4.5 4.0 3.5 3.0 2.5 2.0 1.5 1.0 0.5 0.0
f1 (ppm)

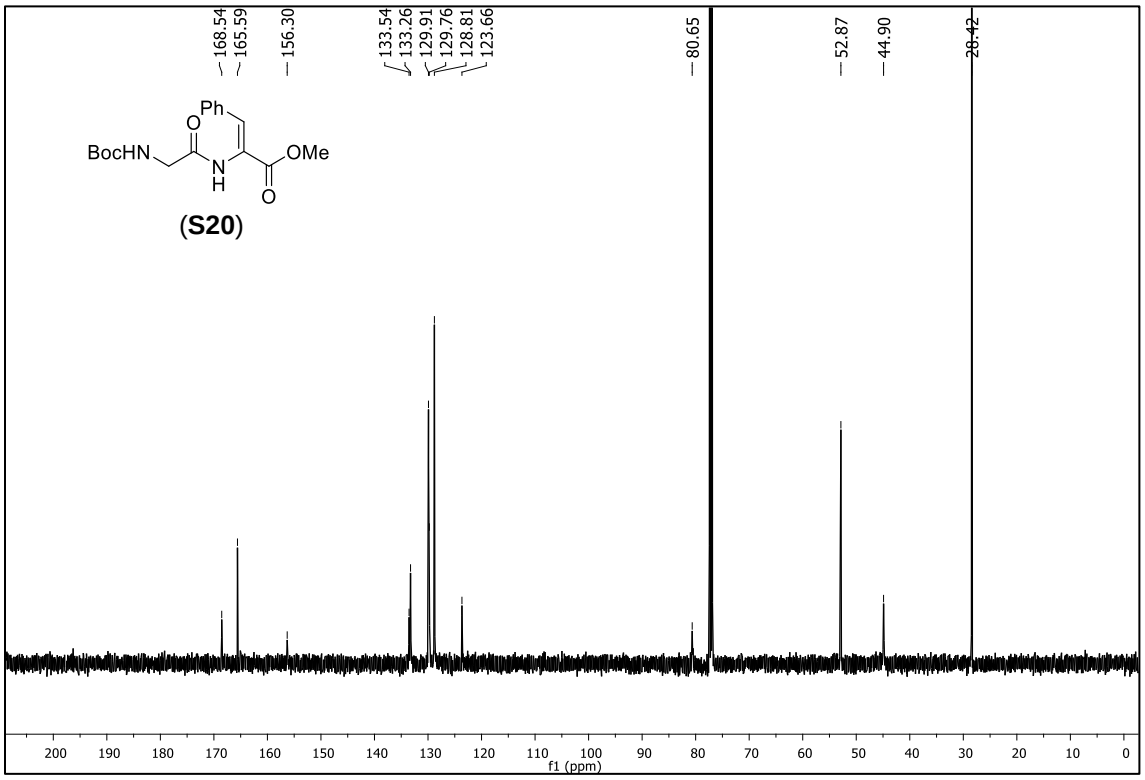
168.54
165.59
156.30
133.54
133.26
129.91
129.76
128.81
123.66
80.65
52.87
44.90
28.42
Ph
O
BocHN
N
H
OMe
O
(S20)
200 190 180 170 160 150 140 130 120 110 100 90 80 70 60 50 40 30 20 10 0
f1 (ppm)

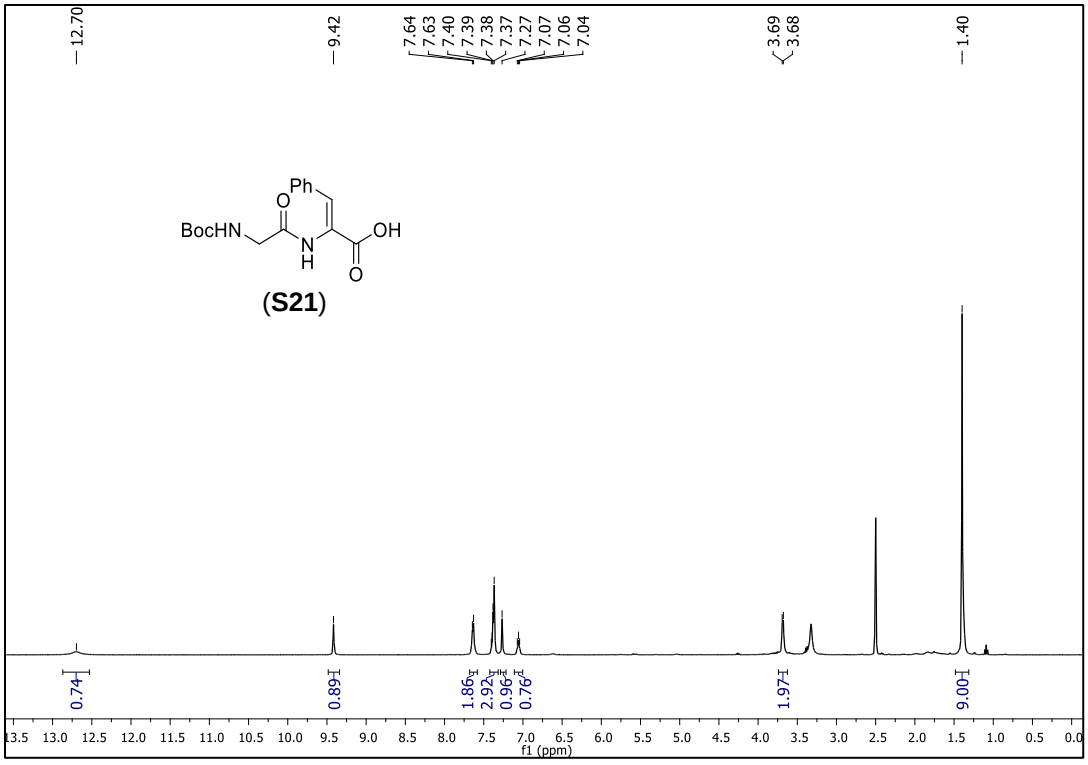
12.70
9.42
7.64
7.63
7.40
7.39
7.38
7.37
7.27
7.07
7.06
7.04
3.69
3.68
1.40
Ph
O
BocHN
N
H
OH
O
0.74
0.89
1.86
2.92
0.96
0.76
1.97
9.00
f1 (ppm)

(**S21**)

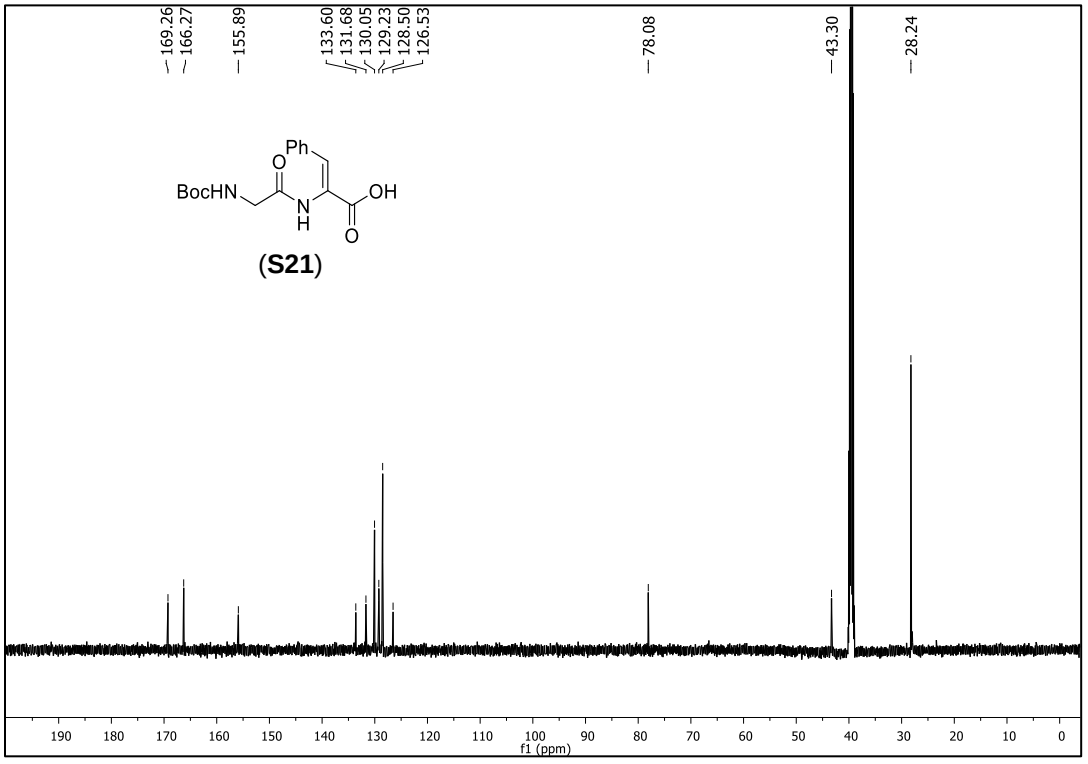
169.26
166.27
155.89
133.60
131.68
130.05
129.23
128.50
126.53
78.08
43.30
28.24
Ph
O
BocHN
N
H
OH
O
f1 (ppm)

(**S21**)

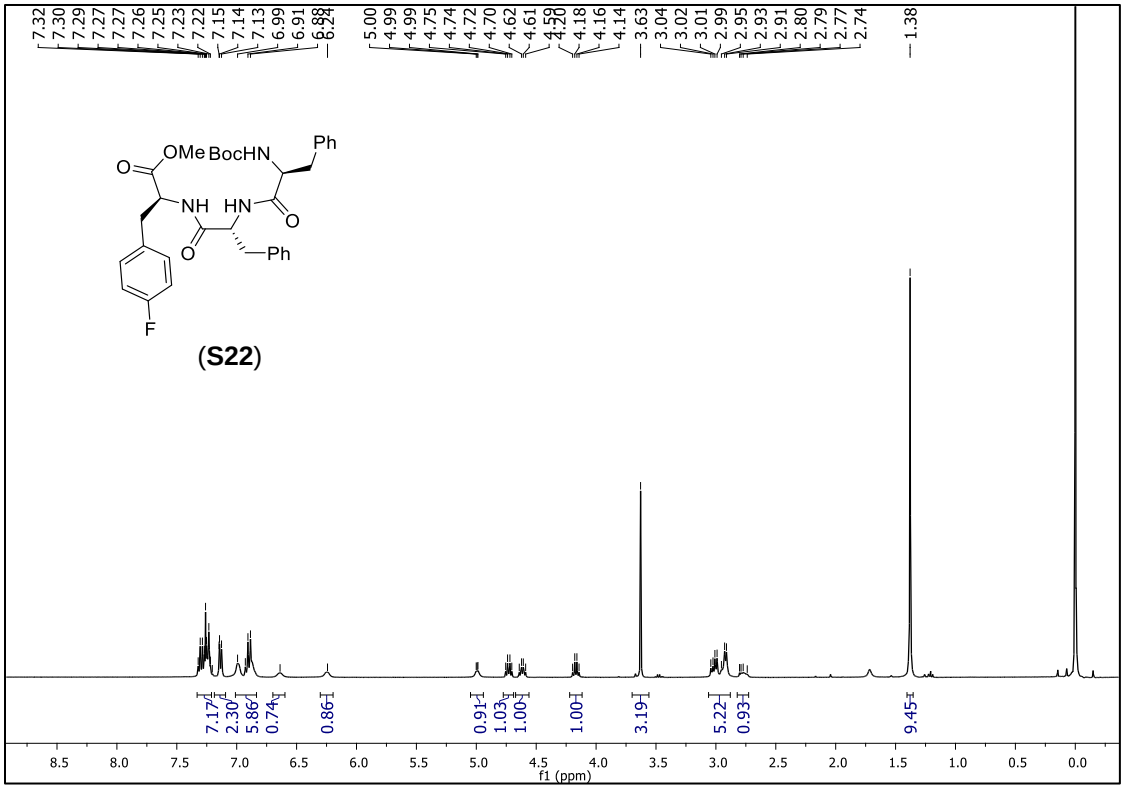
7.32 7.30 7.29 7.27 7.27 7.26 7.25 7.23 7.22 7.15 7.14 7.13 6.99 6.91 6.88 6.24
5.00 4.99 4.99 4.75 4.74 4.72 4.70 4.62 4.61 4.59 4.20 4.18 4.16 4.14
3.63 3.04 3.02 3.01 2.99 2.95 2.93 2.91 2.80 2.79 2.77 2.74
1.38
OMe BocHN Ph
NH HN
Ph
F
(S22)
7.17 2.30 5.86 0.74 0.86 0.91 1.03 1.00 1.00 3.19 5.22 0.93 9.45
f1 (ppm)

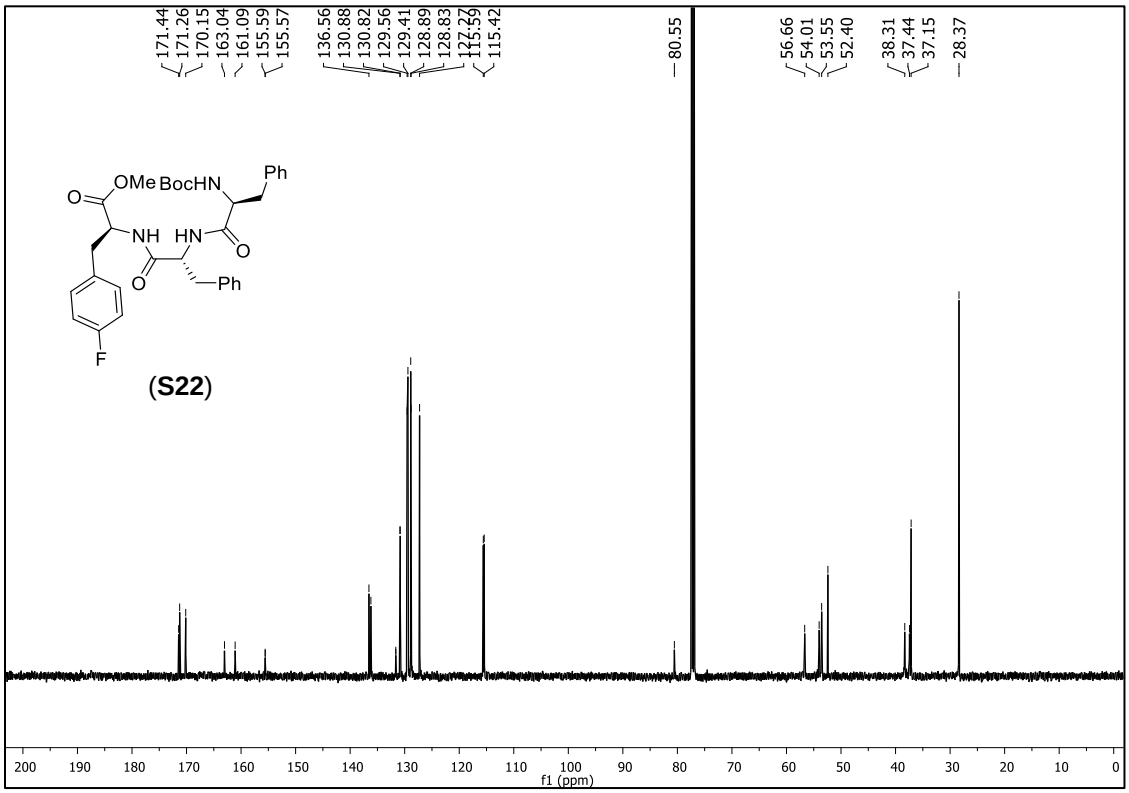
171.44 171.26 170.15 163.04 161.09 155.59 155.57
136.56 130.88 130.82 129.56 129.41 128.89 128.83 127.27 115.59 115.42
80.55
56.66 54.01 53.55 52.40
38.31 37.44 37.15
28.37
OMe BocHN Ph
NH HN
Ph
F
(S22)
f1 (ppm)

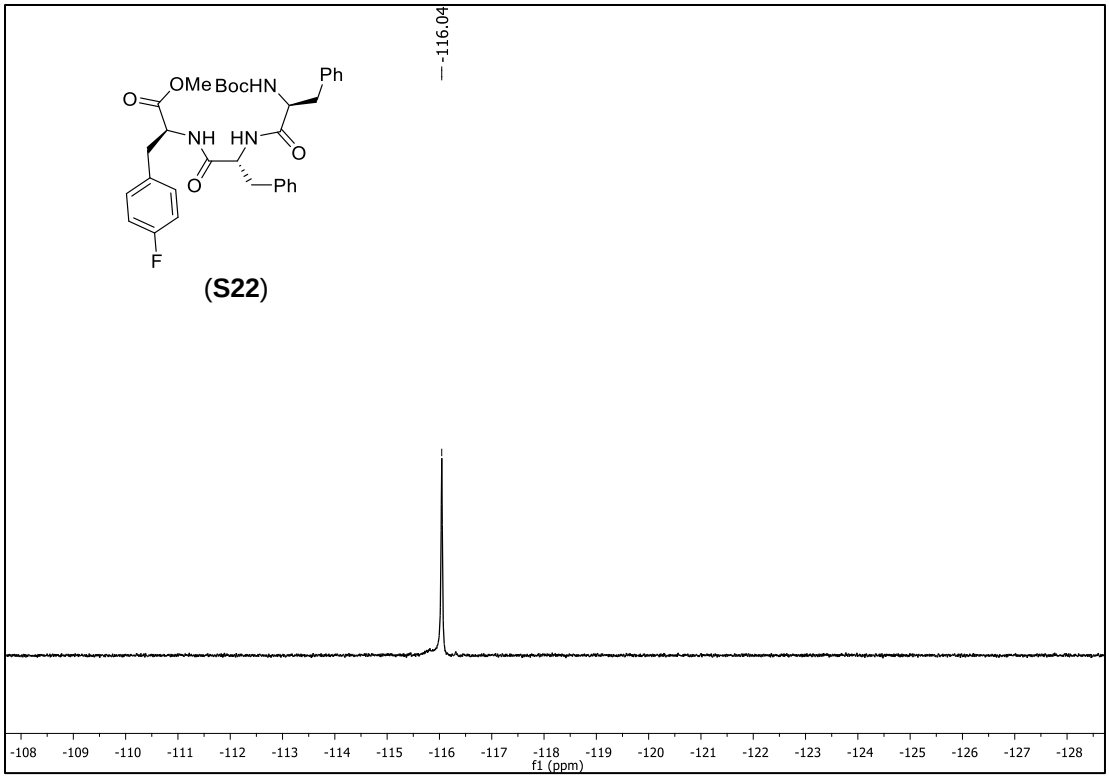
-116.04
OMe
BocHN
Ph
O
NH
HN
O
O
Ph
F
-108
-109
-110
-111
-112
-113
-114
-115
-116
-117
-118
-119
-120
-121
-122
-123
-124
-125
-126
-127
-128
f1 (ppm)

(**S22**)

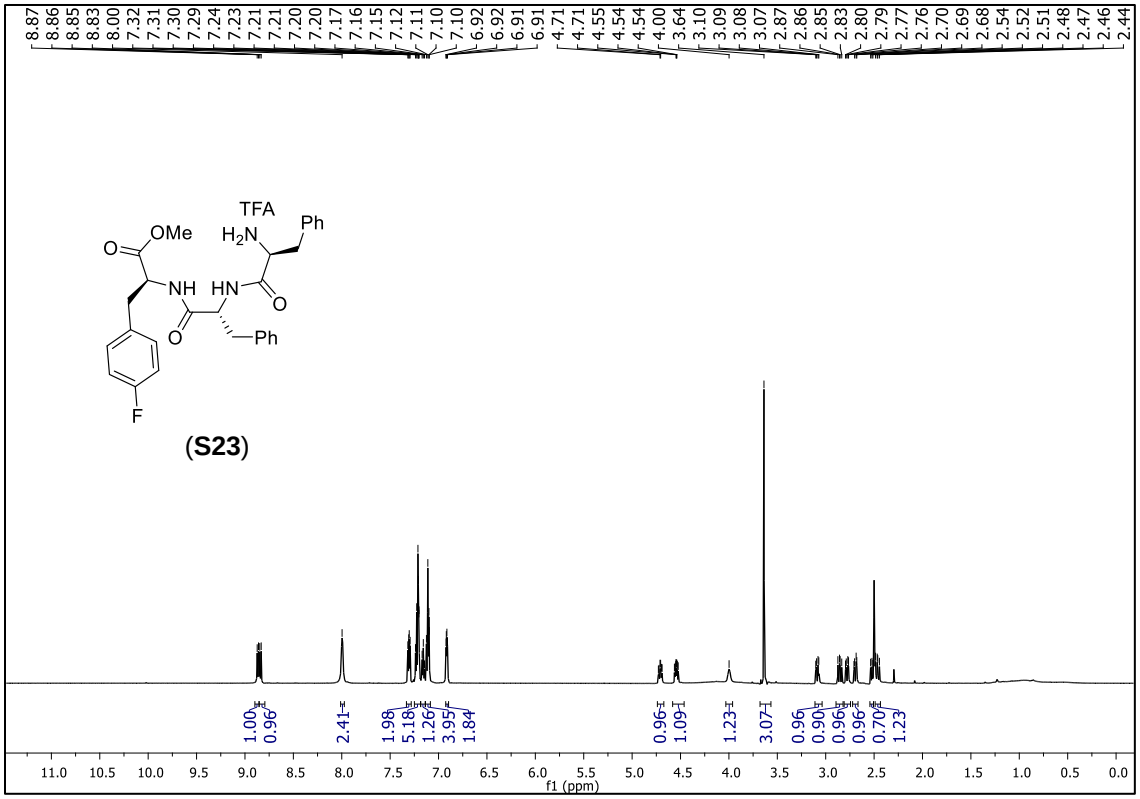
TFA
OMe
H_2N
Ph
O
NH
HN
O
O
Ph
F
(S23)
f1 (ppm)

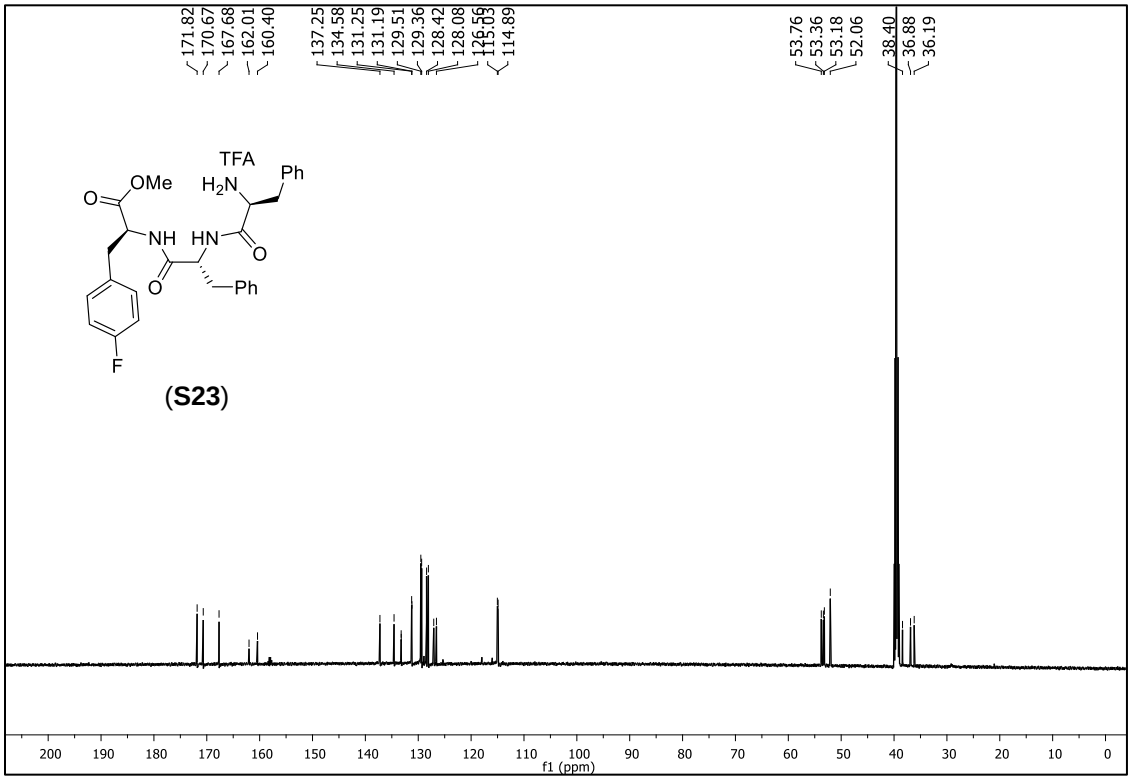
TFA
OMe
H_2N
Ph
O
NH
HN
O
O
Ph
F
(S23)
f1 (ppm)

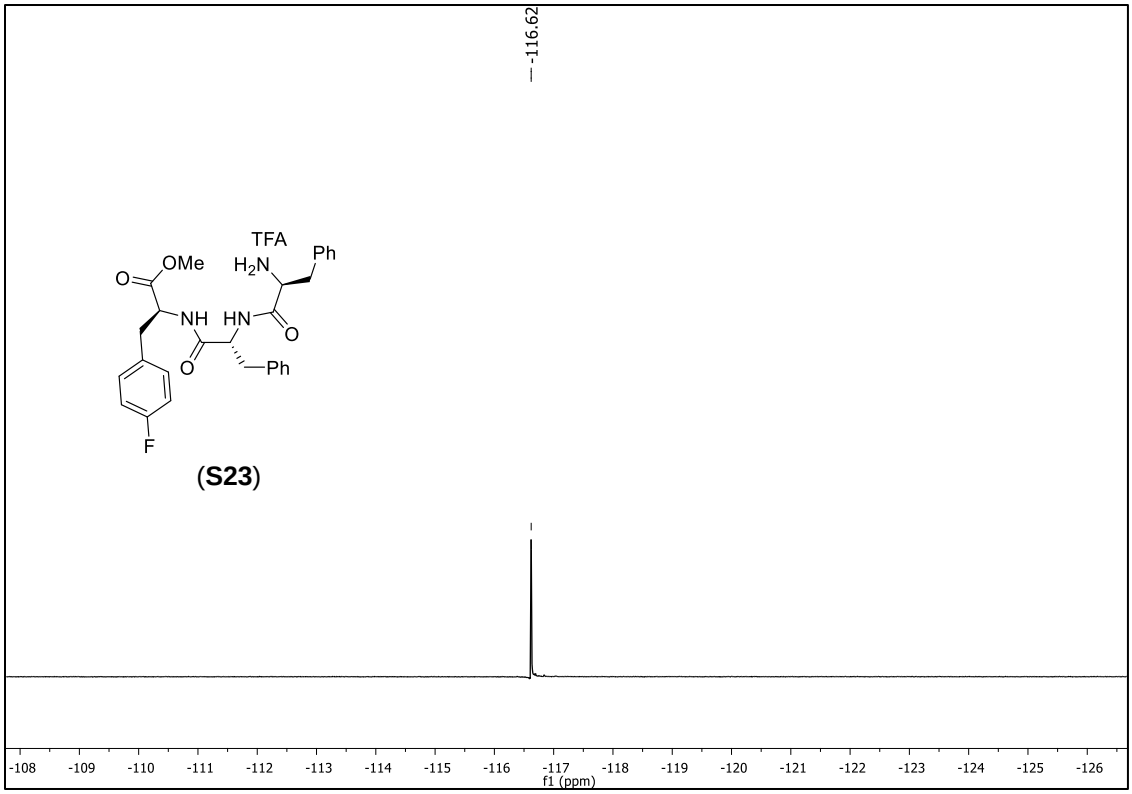
-116.62
TFA
OMe
Ph
NH
HN
Ph
F
-108
-109
-110
-111
-112
-113
-114
-115
-116
-117
-118
-119
-120
-121
-122
-123
-124
-125
-126
f1 (ppm)

(**S23**)

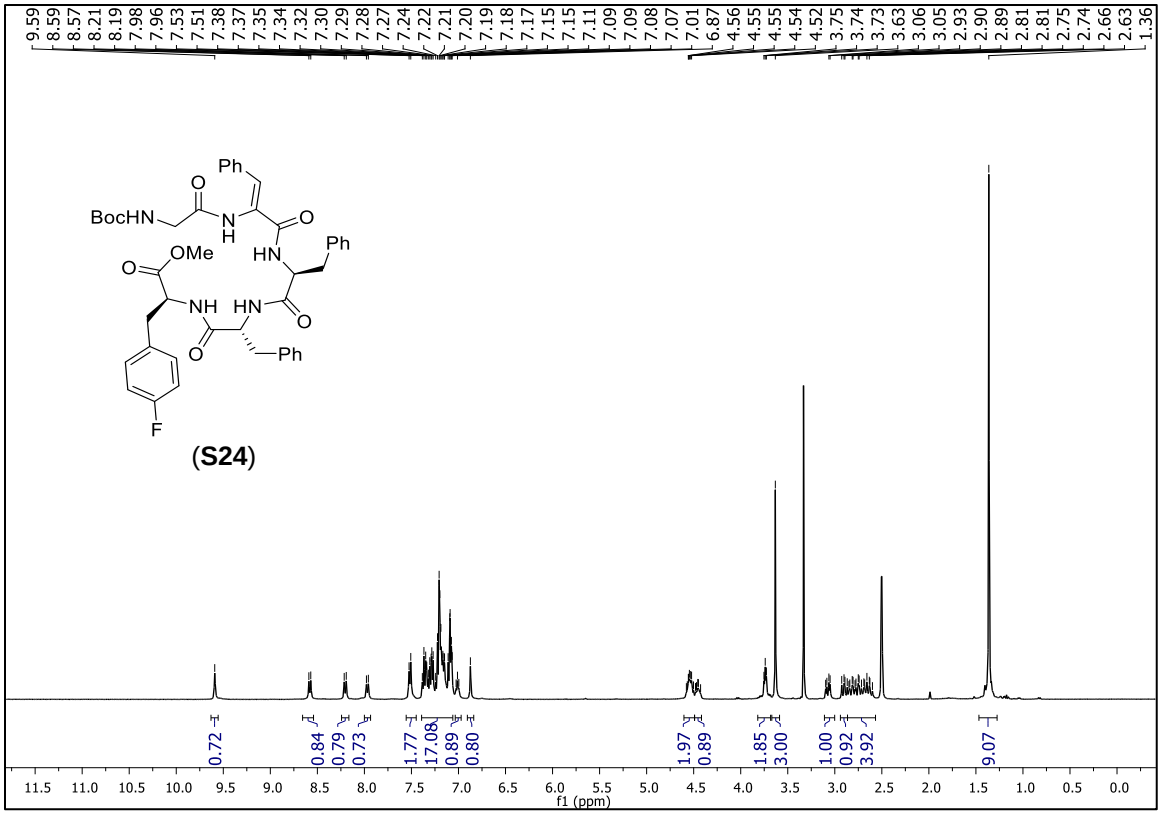
9.59 8.59 8.57 8.21 8.19 7.98 7.96 7.53 7.51 7.38 7.37 7.35 7.34 7.32 7.30 7.29 7.28 7.27 7.24 7.22 7.21 7.20 7.19 7.18 7.17 7.15 7.15 7.11 7.09 7.09 7.08 7.07 7.01 6.87 4.56 4.55 4.55 4.54 4.52 3.75 3.74 3.73 3.63 3.06 3.05 2.93 2.90 2.89 2.81 2.81 2.75 2.74 2.66 2.63 1.36
Ph
BocHN
N
H
O
OMe
HN
Ph
NH
HN
F
0.72 0.84 0.79 0.73 1.77 17.08 0.89 0.80 1.97 0.89 1.85 3.00 1.00 0.92 3.92 9.07
f1 (ppm)

(**S24**)

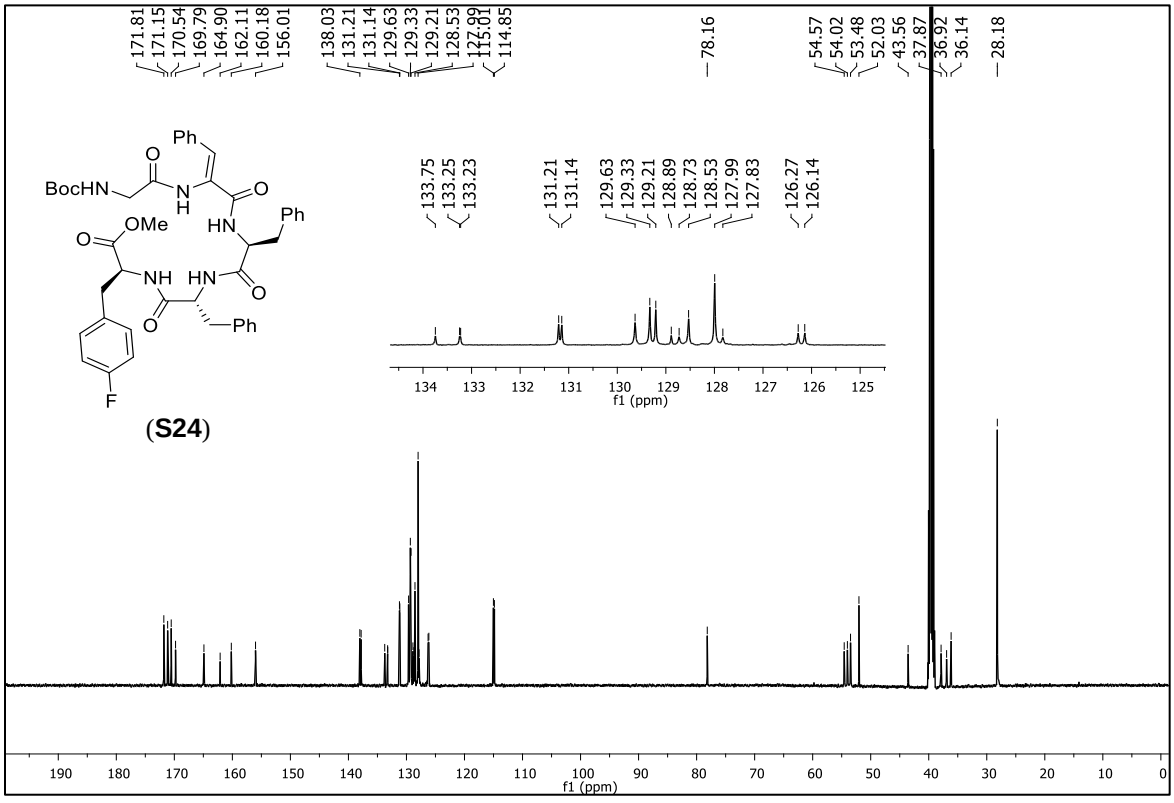
171.81 171.15 170.54 169.79 164.90 162.11 160.18 156.01 138.03 131.21 131.14 129.63 129.33 129.21 128.53 127.99 115.01 114.85 78.16 54.57 54.02 53.48 52.03 43.56 37.87 36.92 36.14 28.18
133.75 133.25 133.23 131.21 131.14 129.63 129.33 129.21 128.89 128.73 128.53 127.99 127.83 126.27 126.14
f1 (ppm)
f1 (ppm)

(**S24**)

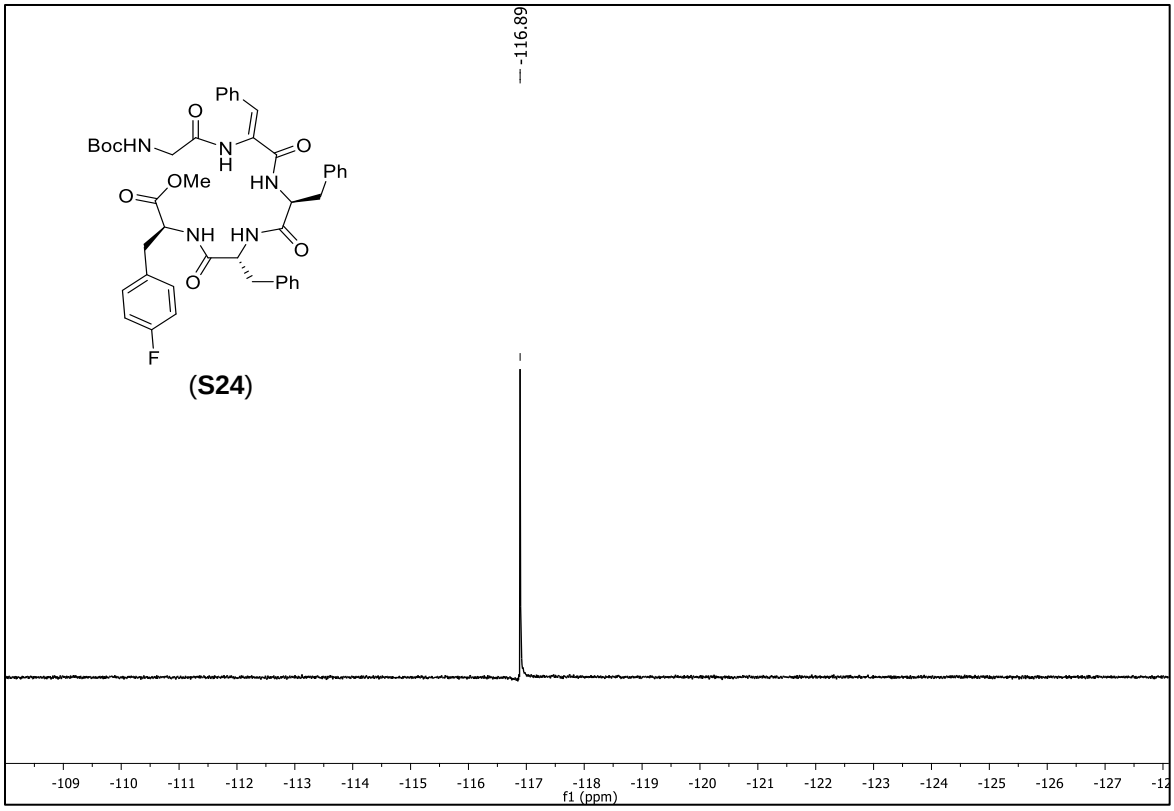
-116.89
Ph
O
BocHN
N
H
O
HN
Ph
OMe
O
NH
HN
O
O
Ph
F
-109
-110
-111
-112
-113
-114
-115
-116
-117
-118
-119
-120
-121
-122
-123
-124
-125
-126
-127
f1 (ppm)

(**S24**)

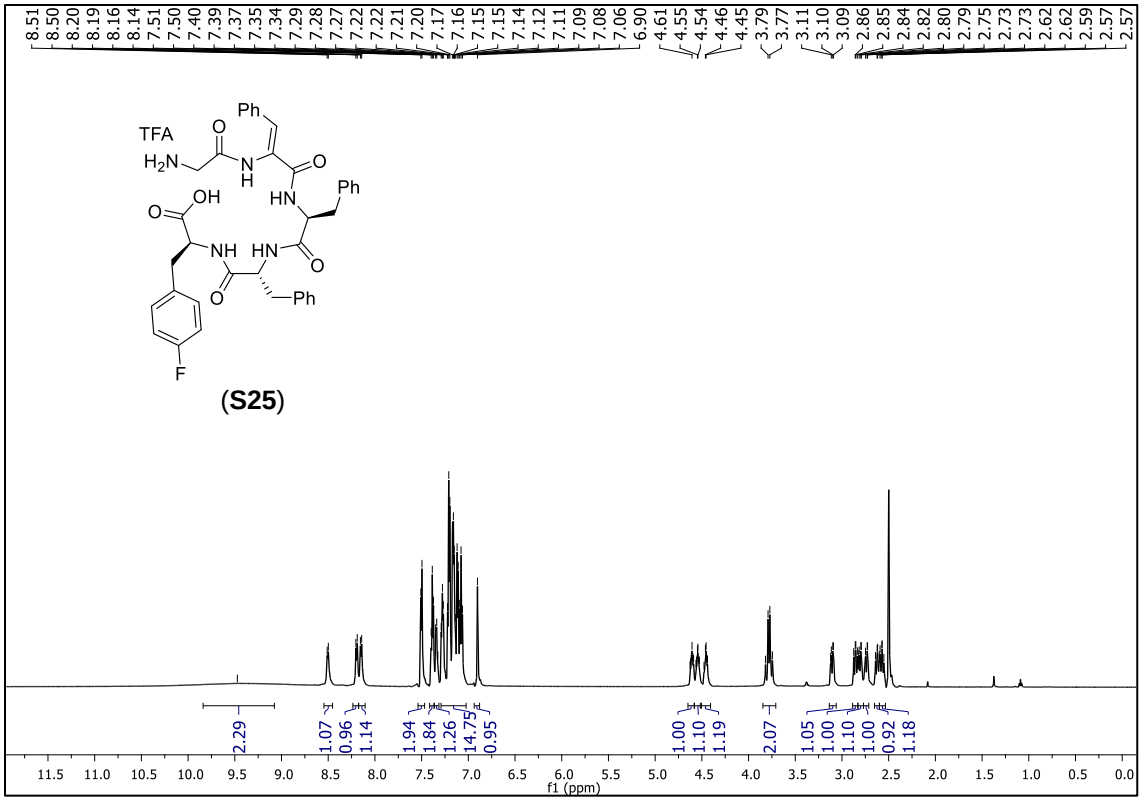

(**S25**)

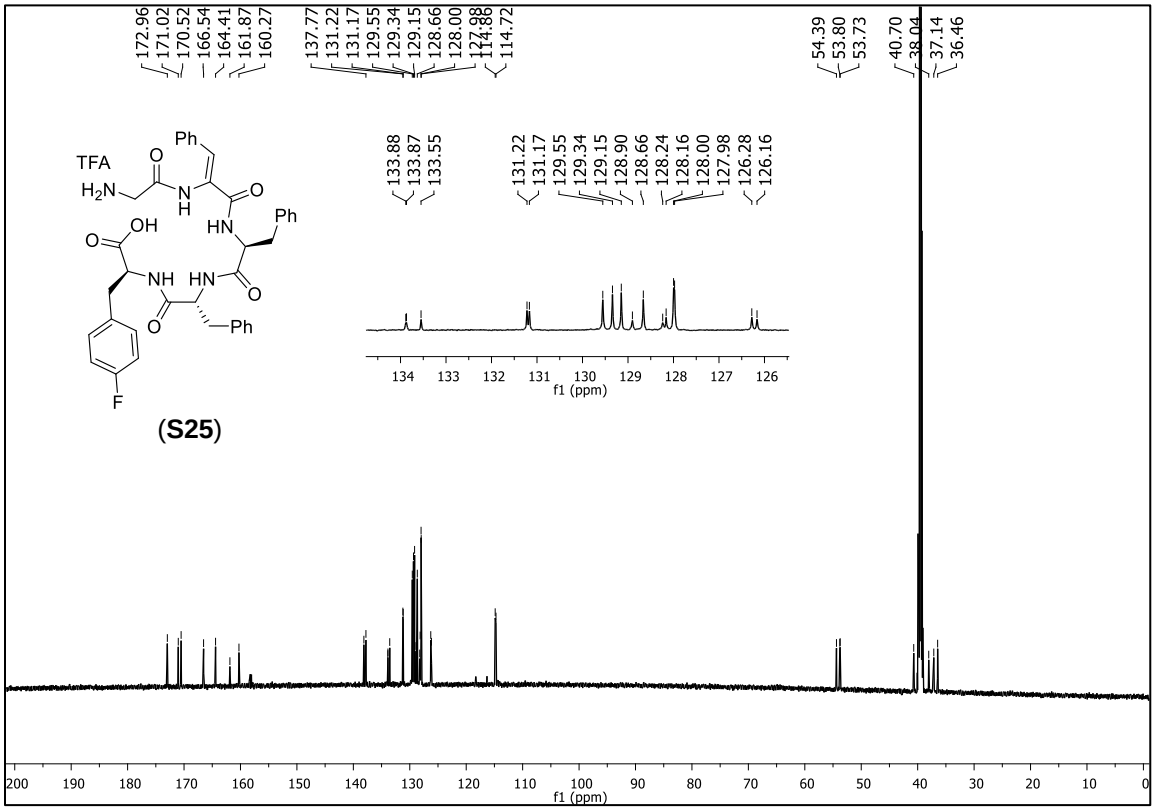

(**S25**)

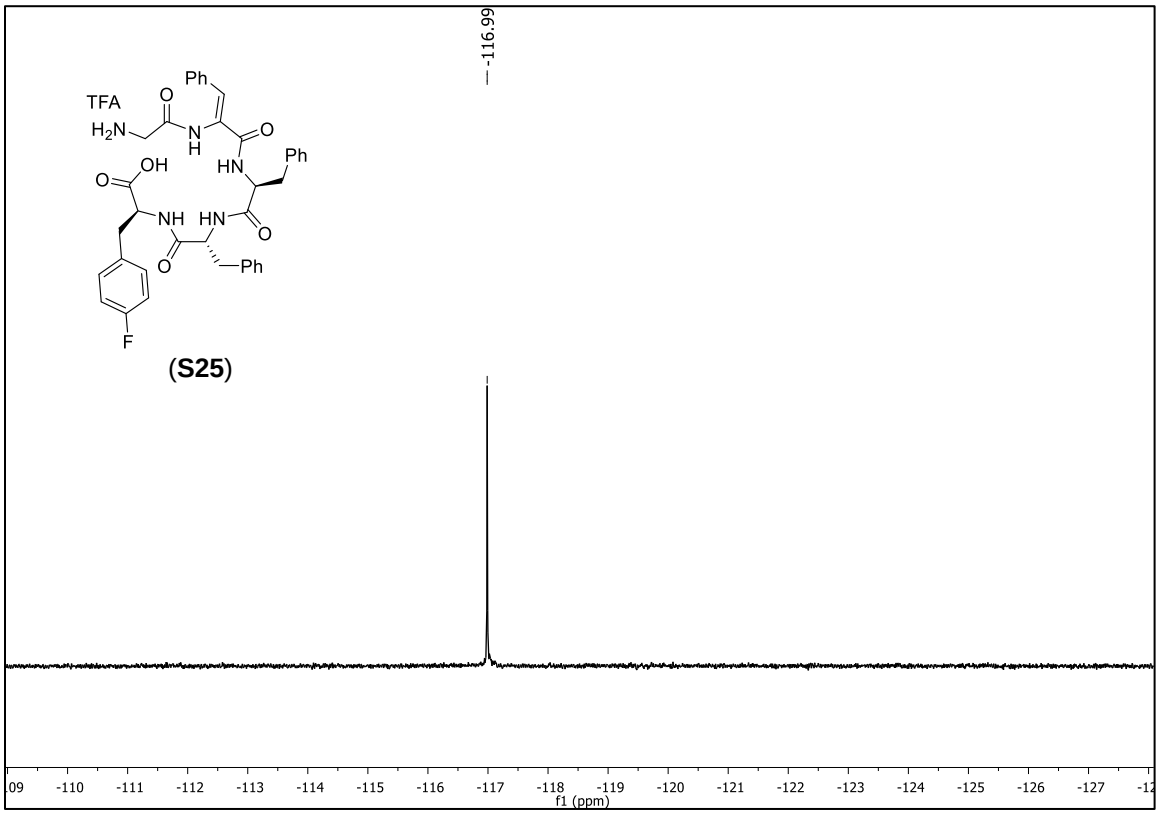
-116.99
TFA
H_2N
O
N
H
O
Ph
HN
Ph
O
OH
NH
HN
O
O
Ph
F
-109
-110
-111
-112
-113
-114
-115
-116
-117
-118
-119
-120
-121
-122
-123
-124
-125
-126
-127
f1 (ppm)

(**S25**)

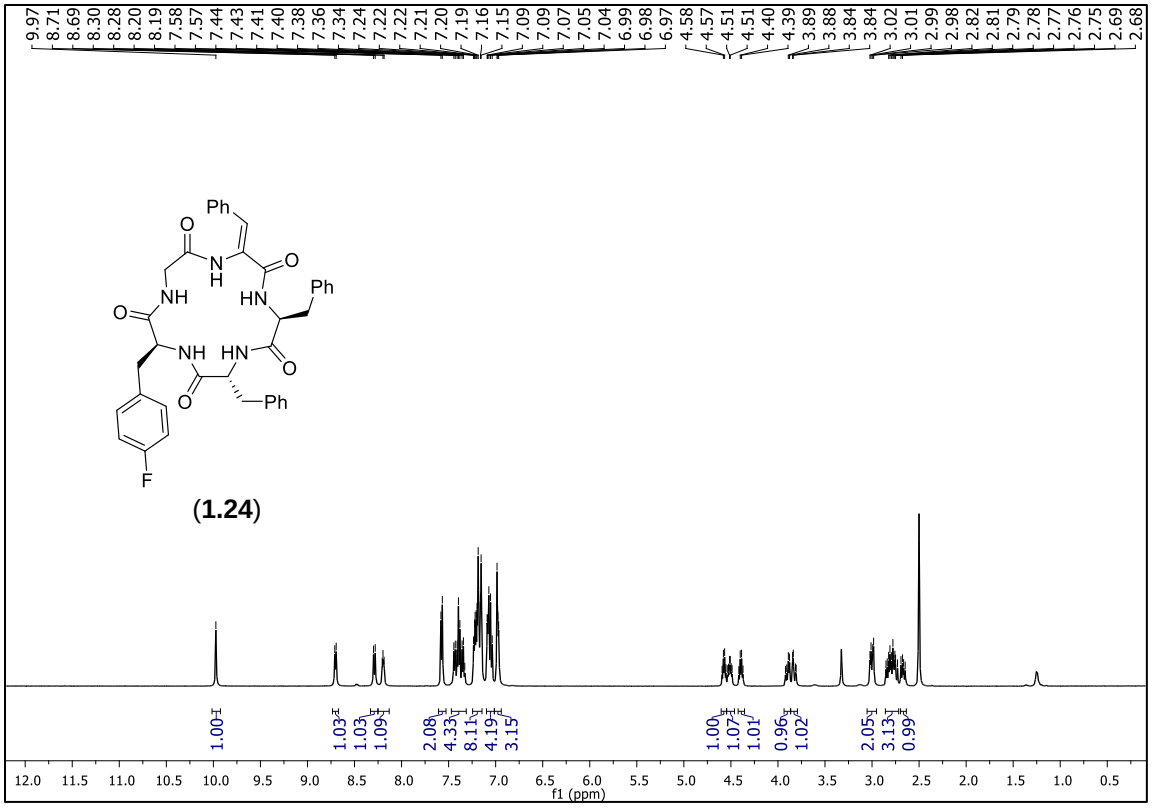
9.97 8.71 8.69 8.30 8.28 8.20 8.19 7.58 7.57 7.44 7.43 7.41 7.40 7.38 7.36 7.34 7.24 7.22 7.22 7.21 7.20 7.19 7.16 7.15 7.09 7.09 7.07 7.05 7.04 6.99 6.98 6.97 4.58 4.57 4.51 4.51 4.40 4.39 3.89 3.88 3.84 3.84 3.02 3.01 2.99 2.98 2.82 2.81 2.79 2.78 2.77 2.76 2.75 2.69 2.68
(1.24)
1.00 1.03 1.03 1.09 2.08 4.33 8.11 4.19 3.15 1.00 1.07 1.01 0.96 1.02 2.05 3.13 0.99
f1 (ppm)

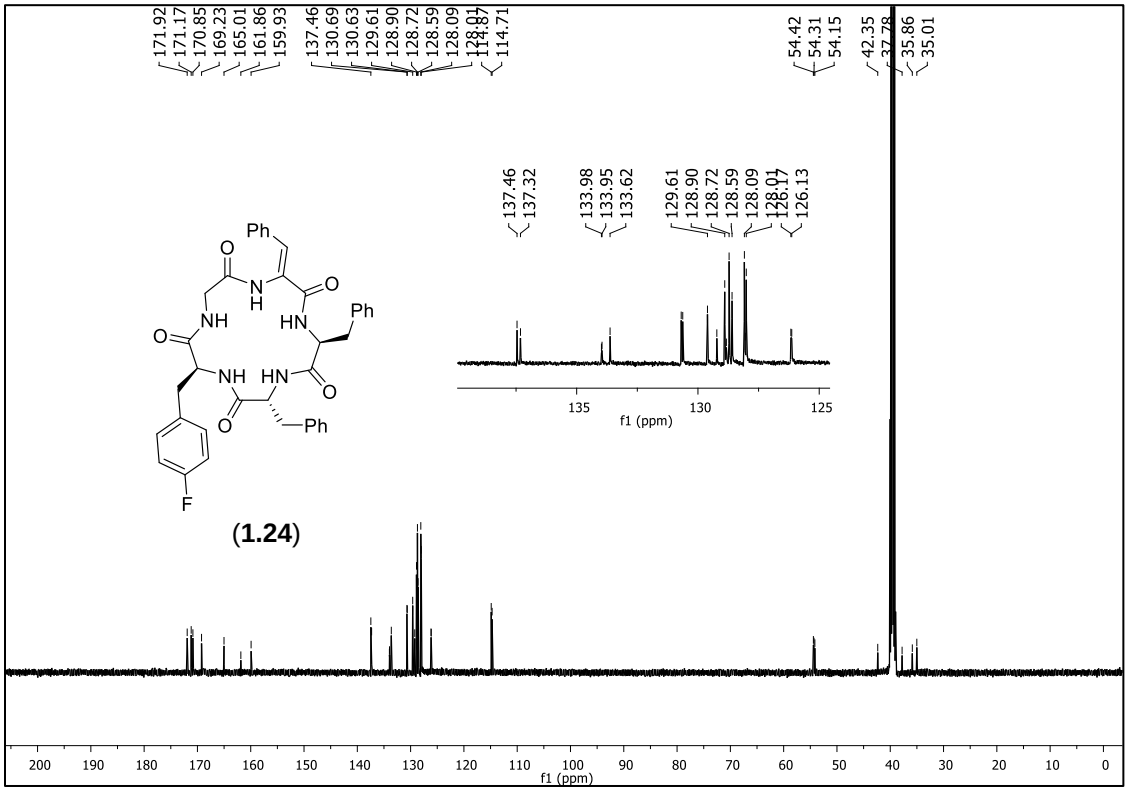
171.92 171.17 170.85 169.23 165.01 161.86 159.93 137.46 130.69 130.63 129.61 128.90 128.72 128.59 128.09 114.71 54.42 54.31 54.15 42.35 35.86 35.01
137.46 137.32 133.98 133.95 133.62 129.61 128.90 128.72 128.59 128.09 126.13
f1 (ppm)
(1.24)
f1 (ppm)

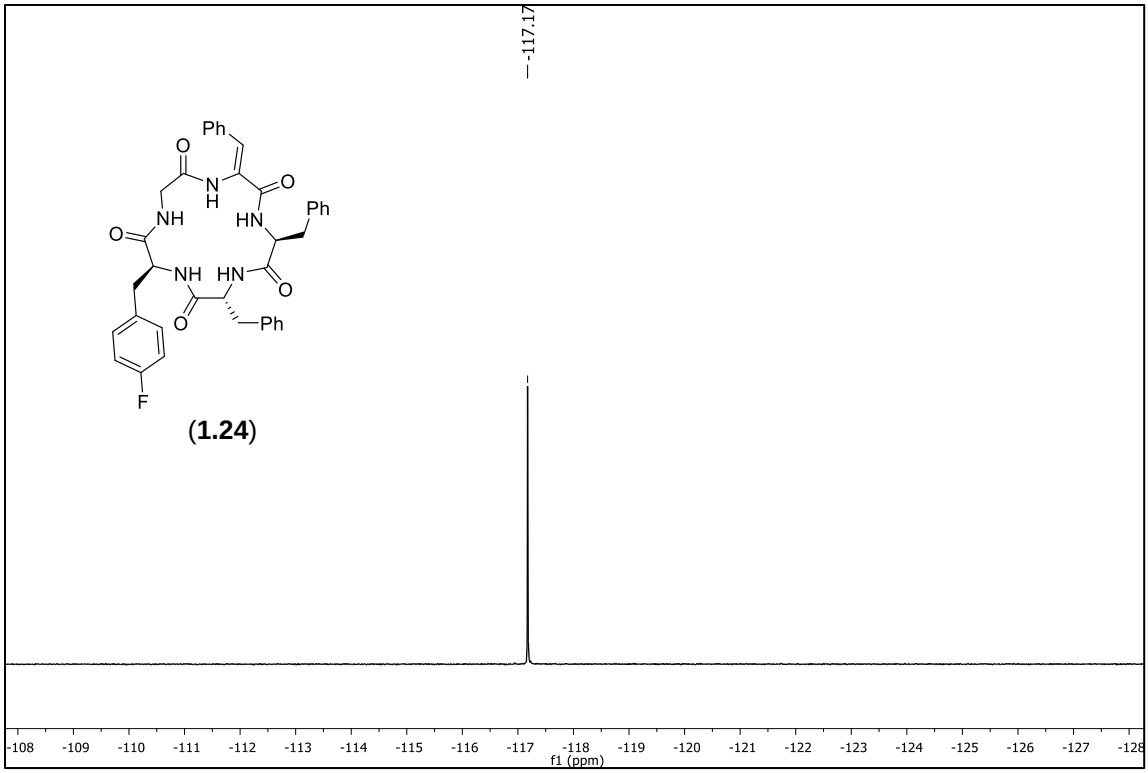
-117.17
Ph
O
N
H
O
NH
HN
Ph
O
NH
HN
O
O
Ph
F
-108
-109
-110
-111
-112
-113
-114
-115
-116
-117
-118
-119
-120
-121
-122
-123
-124
-125
-126
-127
-128
f1 (ppm)

(**1.24**)

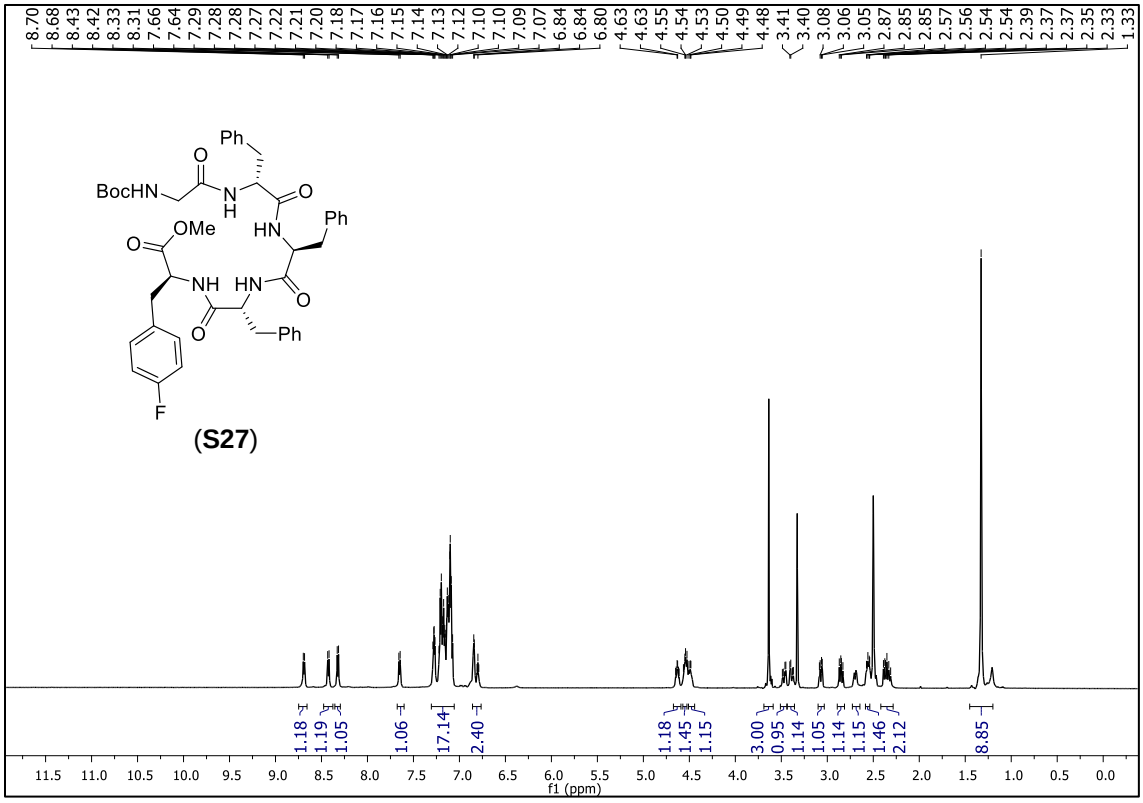
8.70 8.68 8.43 8.42 8.33 8.31 7.66 7.64 7.29 7.28 7.28 7.27 7.22 7.21 7.20 7.18 7.17 7.16 7.15 7.14 7.13 7.12 7.10 7.10 7.09 7.07 6.84 6.84 6.80 4.63 4.63 4.55 4.54 4.53 4.50 4.49 4.48 3.41 3.40 3.08 3.06 3.05 2.87 2.85 2.85 2.57 2.56 2.54 2.54 2.39 2.37 2.37 2.35 2.33 1.33
Ph
O
BocHN
N
H
O
HN
Ph
OMe
O
NH
HN
O
O
Ph
F
(S27)
1.18 1.19 1.05 1.06 17.14 2.40 1.18 1.45 1.15 3.00 0.95 1.14 1.05 1.14 1.15 1.46 2.12 8.85
11.5 11.0 10.5 10.0 9.5 9.0 8.5 8.0 7.5 7.0 6.5 6.0 5.5 5.0 4.5 4.0 3.5 3.0 2.5 2.0 1.5 1.0 0.5 0.0
f1 (ppm)

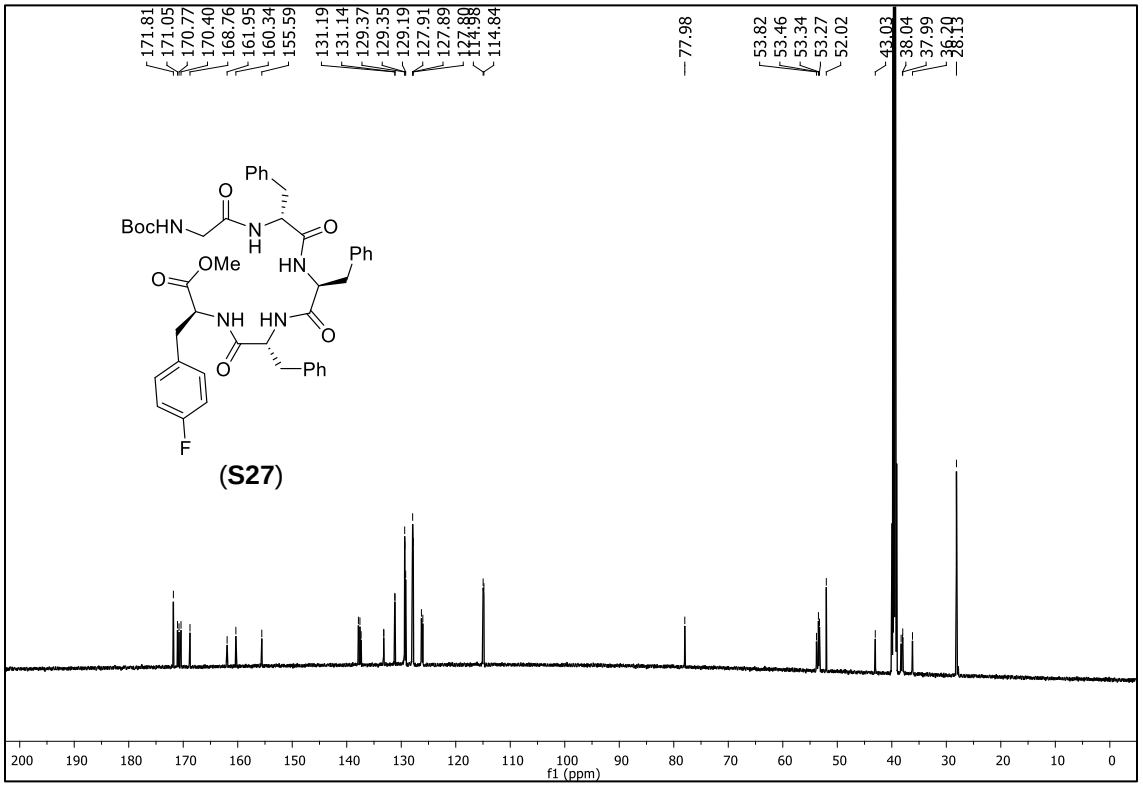
171.81 171.05 170.77 170.40 168.76 161.95 160.34 155.59 131.19 131.14 129.37 129.35 129.19 127.91 127.89 114.84 77.98 53.82 53.46 53.34 53.27 52.02 43.03 38.04 37.99 28.13
Ph
O
BocHN
N
H
O
HN
Ph
OMe
O
NH
HN
O
O
Ph
F
(S27)
200 190 180 170 160 150 140 130 120 110 100 90 80 70 60 50 40 30 20 10 0
f1 (ppm)

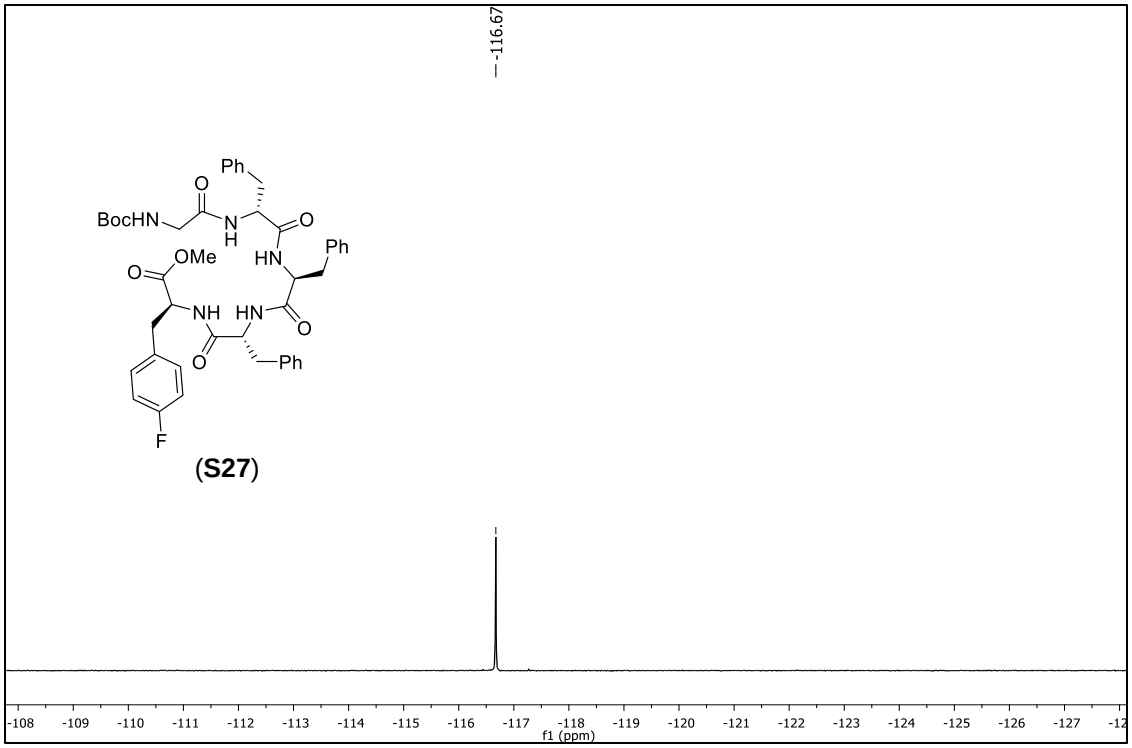
-116.67
Ph
O
BocHN
N
H
O
HN
Ph
OMe
O
NH
HN
O
O
Ph
F
-108
-109
-110
-111
-112
-113
-114
-115
-116
-117
-118
-119
-120
-121
-122
-123
-124
-125
-126
-127
f1 (ppm)

(**S27**)

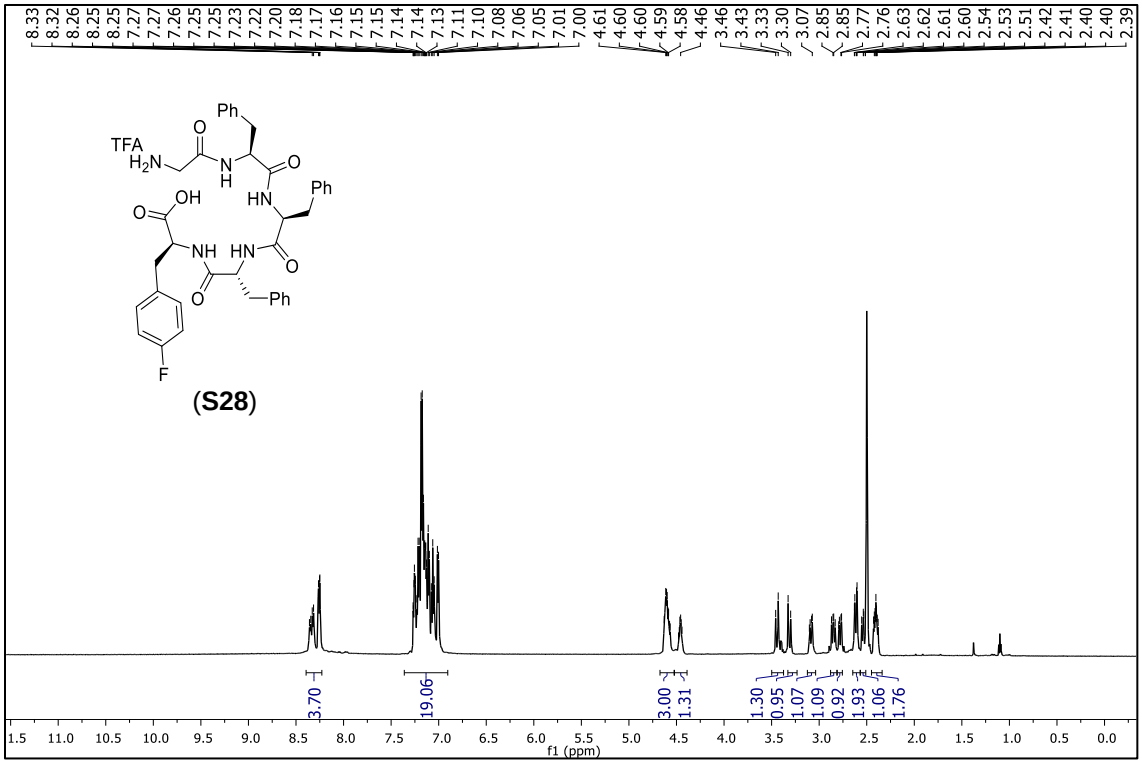
(S28)
f1 (ppm)

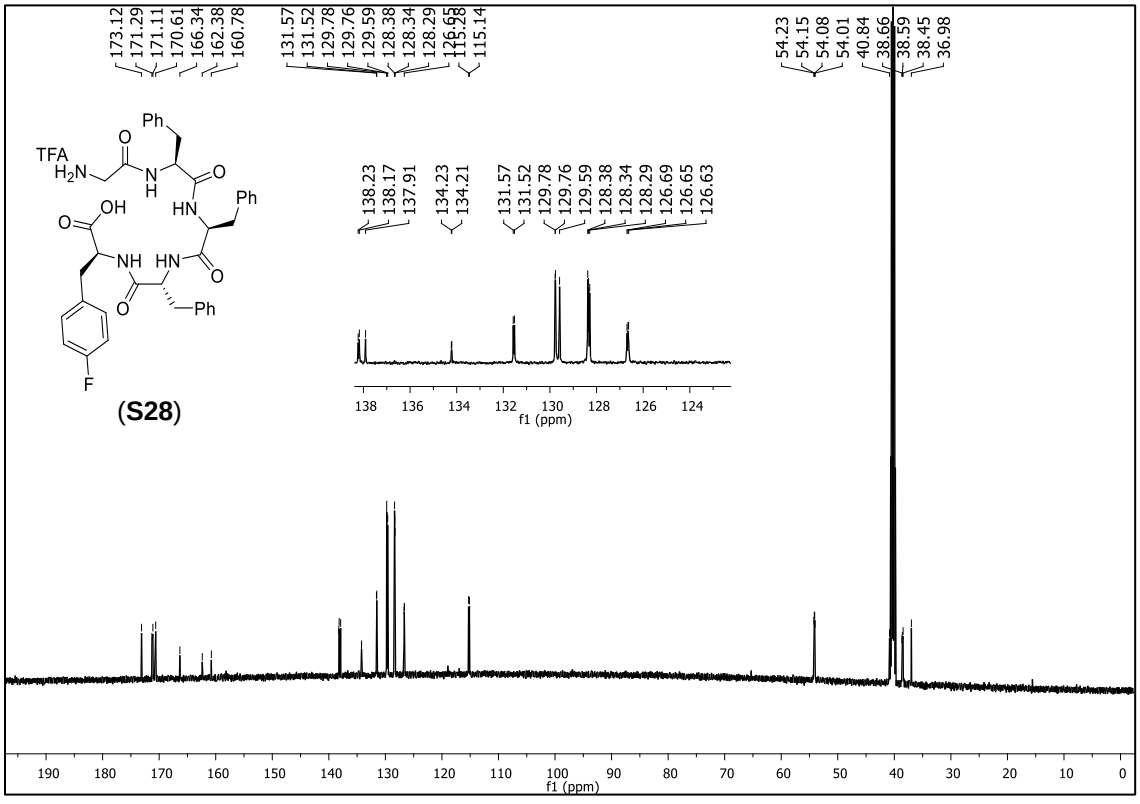
(S28)
f1 (ppm)

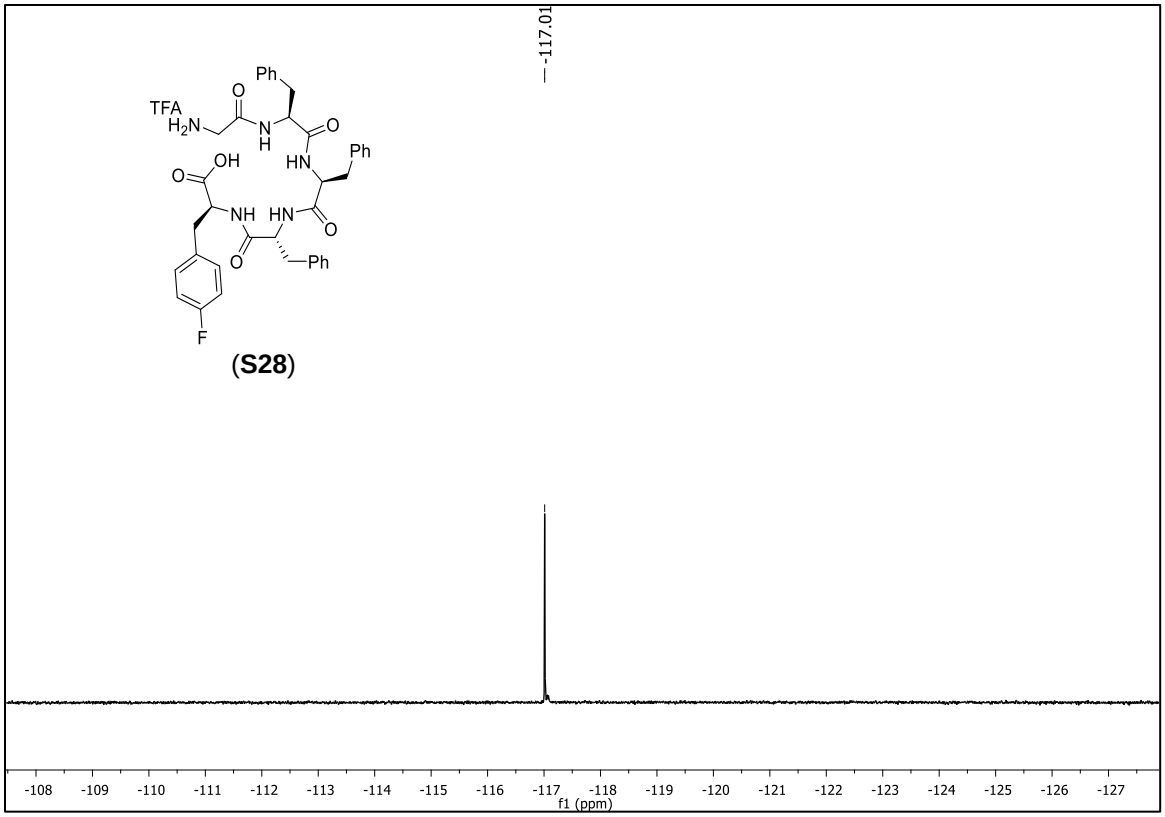
-117.01
TFA
H2N
Ph
O
N
H
O
HN
Ph
OH
O
NH
HN
O
O
Ph
F
-108
-109
-110
-111
-112
-113
-114
-115
-116
-117
-118
-119
-120
-121
-122
-123
-124
-125
-126
-127
f1 (ppm)

(**S28**)

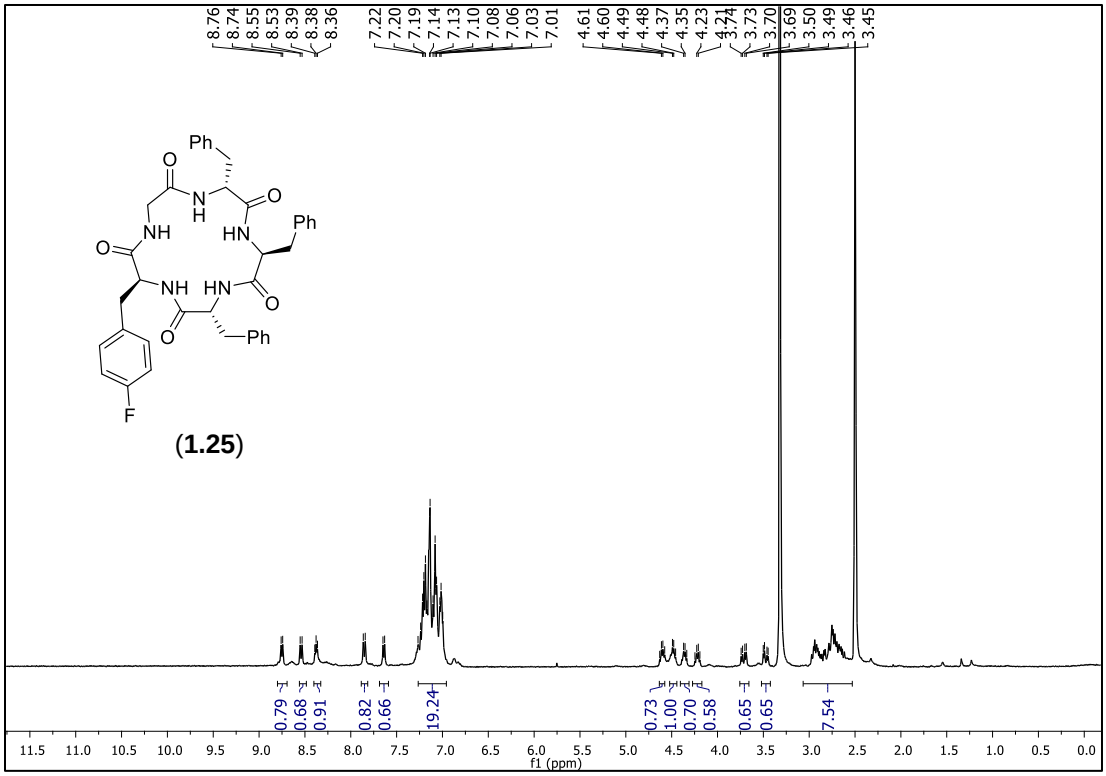
8.76
8.74
8.55
8.53
8.39
8.38
8.36
7.22
7.20
7.19
7.14
7.13
7.10
7.08
7.06
7.03
7.01
4.61
4.60
4.49
4.48
4.37
4.35
4.23
4.21
3.73
3.70
3.69
3.50
3.49
3.46
3.45
Ph
O
N
H
O
HN
Ph
NH
O
NH
HN
O
O
Ph
F
(1.25)
0.79
0.68
0.91
0.82
0.66
19.24
0.73
1.00
0.70
0.58
0.65
0.65
7.54
f1 (ppm)

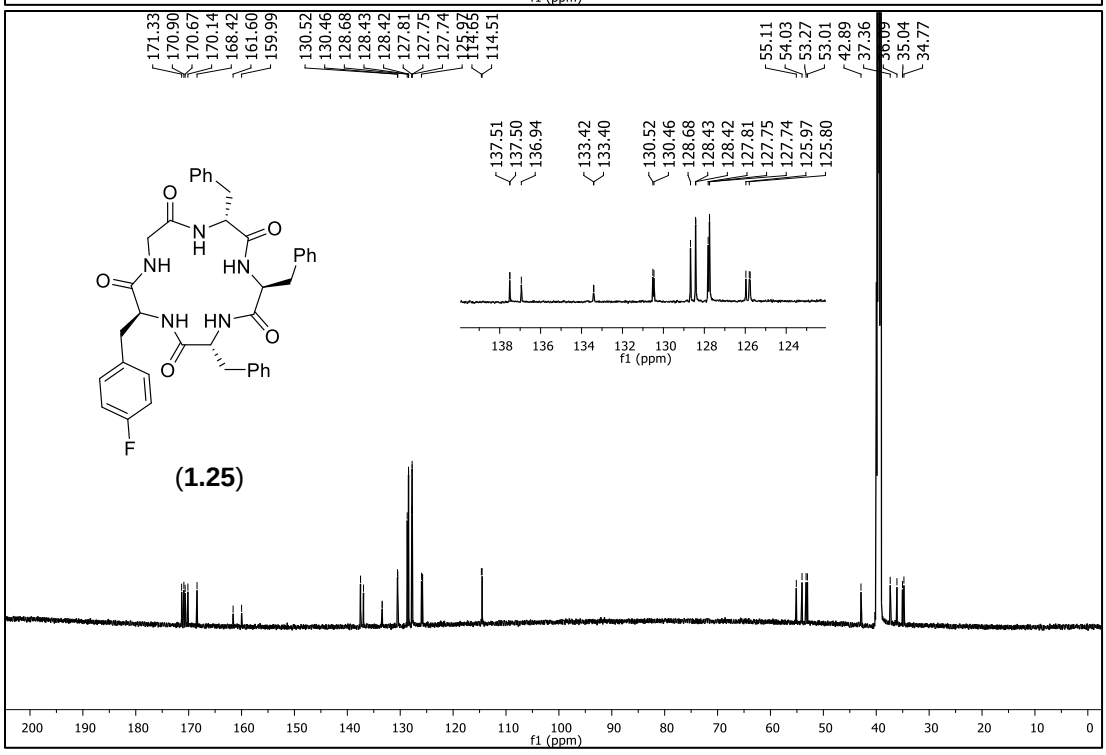
171.33
170.90
170.67
170.14
168.42
161.60
159.99
130.52
130.46
128.68
128.43
128.42
127.81
127.75
127.74
125.97
114.65
114.51
55.11
54.03
53.27
53.01
42.89
37.36
36.09
35.04
34.77
137.51
137.50
136.94
133.42
133.40
130.52
130.46
128.68
128.43
128.42
127.81
127.75
127.74
125.97
125.80
Ph
O
N
H
O
HN
Ph
NH
O
NH
HN
O
O
Ph
F
(1.25)
f1 (ppm)
f1 (ppm)

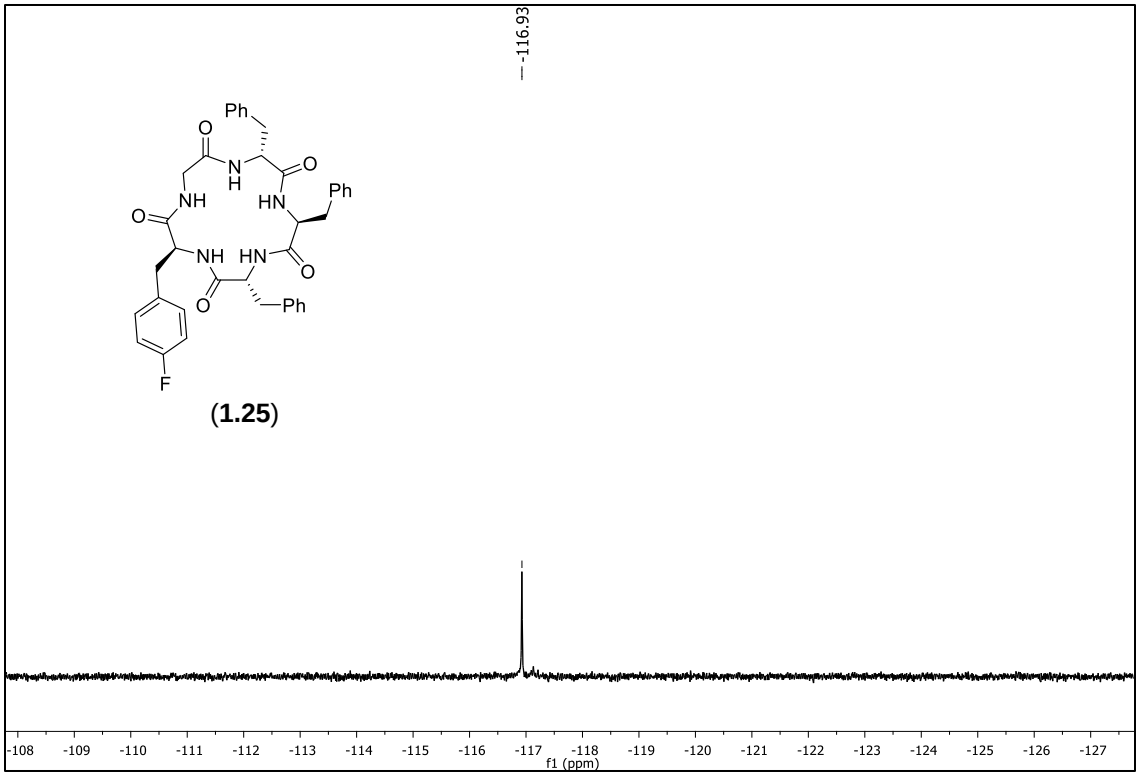
-116.93
Ph
O
N
H
O
NH
HN
Ph
O
NH
HN
O
O
Ph
F
-108
-109
-110
-111
-112
-113
-114
-115
-116
-117
-118
-119
-120
-121
-122
-123
-124
-125
-126
-127
f1 (ppm)

(**1.25**)

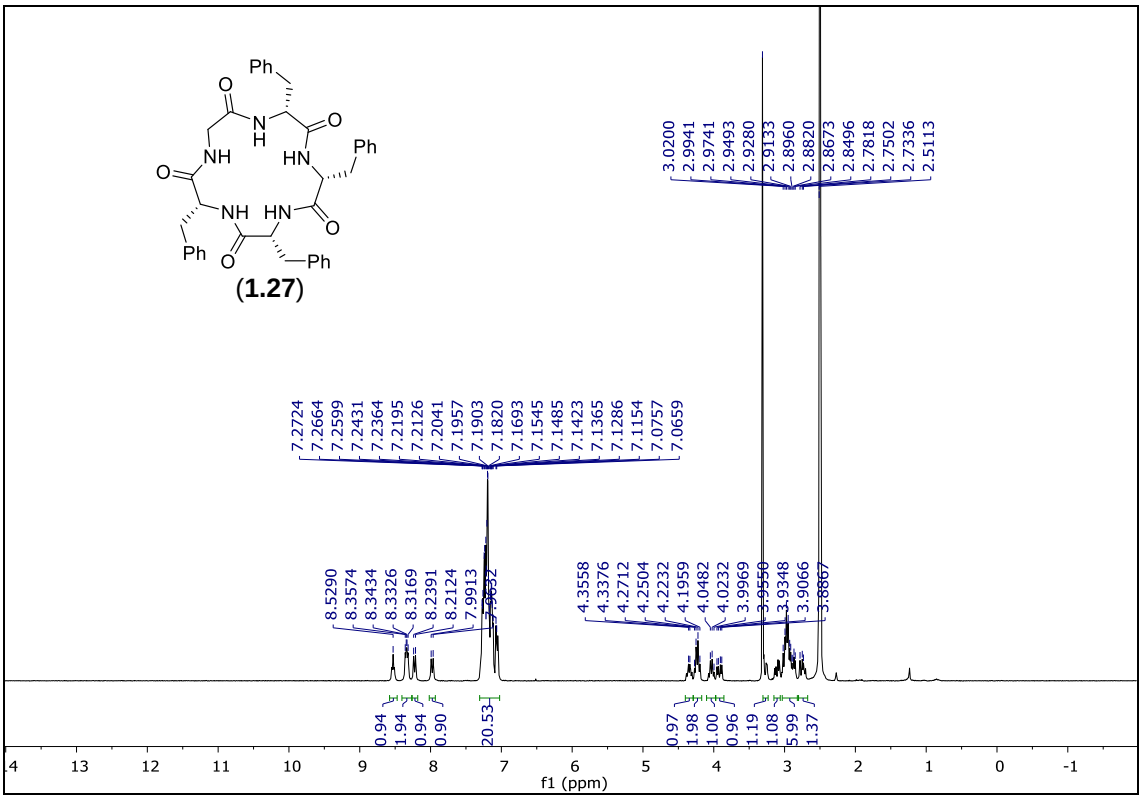
(1.27)
3.0200
2.9941
2.9741
2.9493
2.9280
2.9133
2.8960
2.8820
2.8673
2.8496
2.7818
2.7502
2.7336
2.5113
7.2724
7.2664
7.2599
7.2431
7.2364
7.2195
7.2126
7.2041
7.1957
7.1903
7.1820
7.1693
7.1545
7.1485
7.1423
7.1365
7.1286
7.1154
7.0757
7.0659
8.5290
8.3574
8.3434
8.3326
8.3169
8.2391
8.2124
7.9913
4.3558
4.3376
4.2712
4.2504
4.2232
4.1959
4.0482
4.0232
3.9969
3.9550
3.9348
3.9066
3.8867
0.94
1.94
0.94
0.90
20.53
0.97
1.98
1.00
0.96
1.19
1.08
5.99
1.37
f1 (ppm)

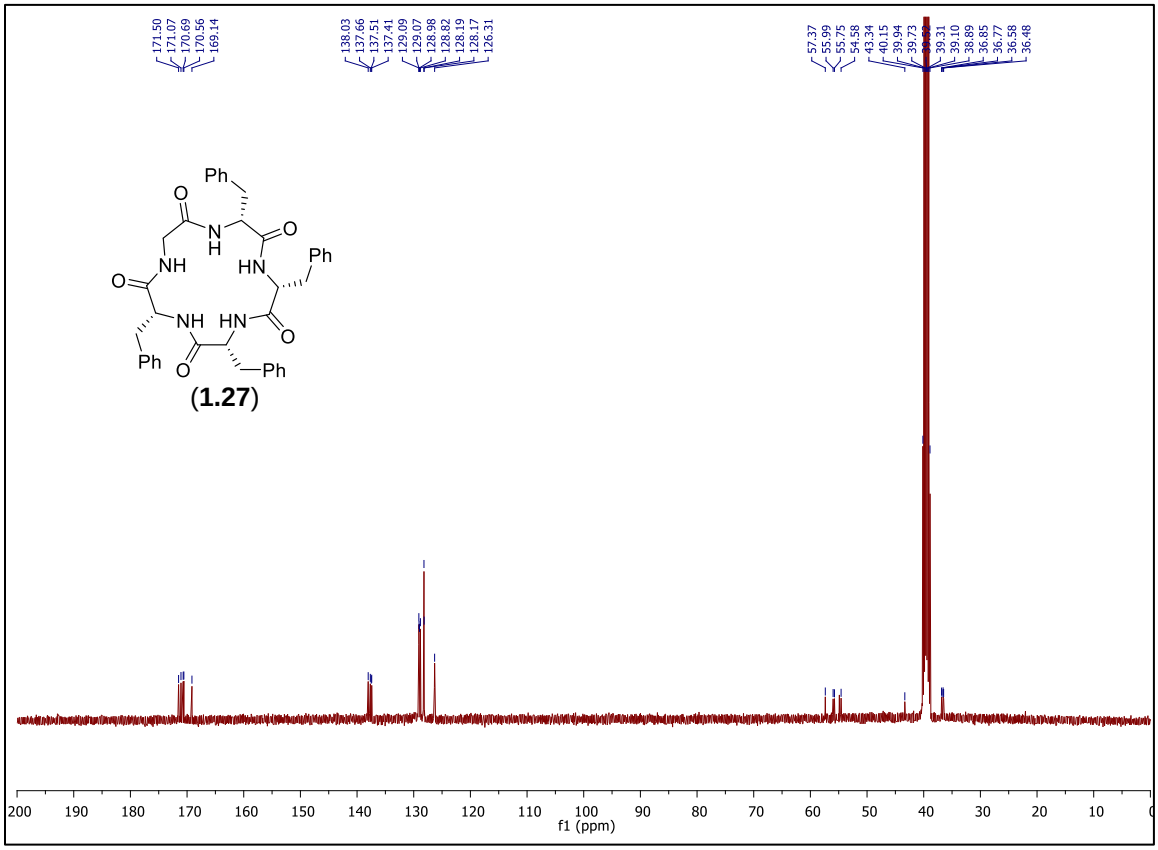
(1.27)
171.50
171.07
170.69
170.56
169.14
138.03
137.66
137.51
137.41
129.09
129.07
128.98
128.82
128.19
128.17
126.31
57.37
55.99
55.75
54.58
43.34
40.15
39.94
39.73
39.52
39.31
39.10
38.89
36.85
36.77
36.58
36.48
f1 (ppm)

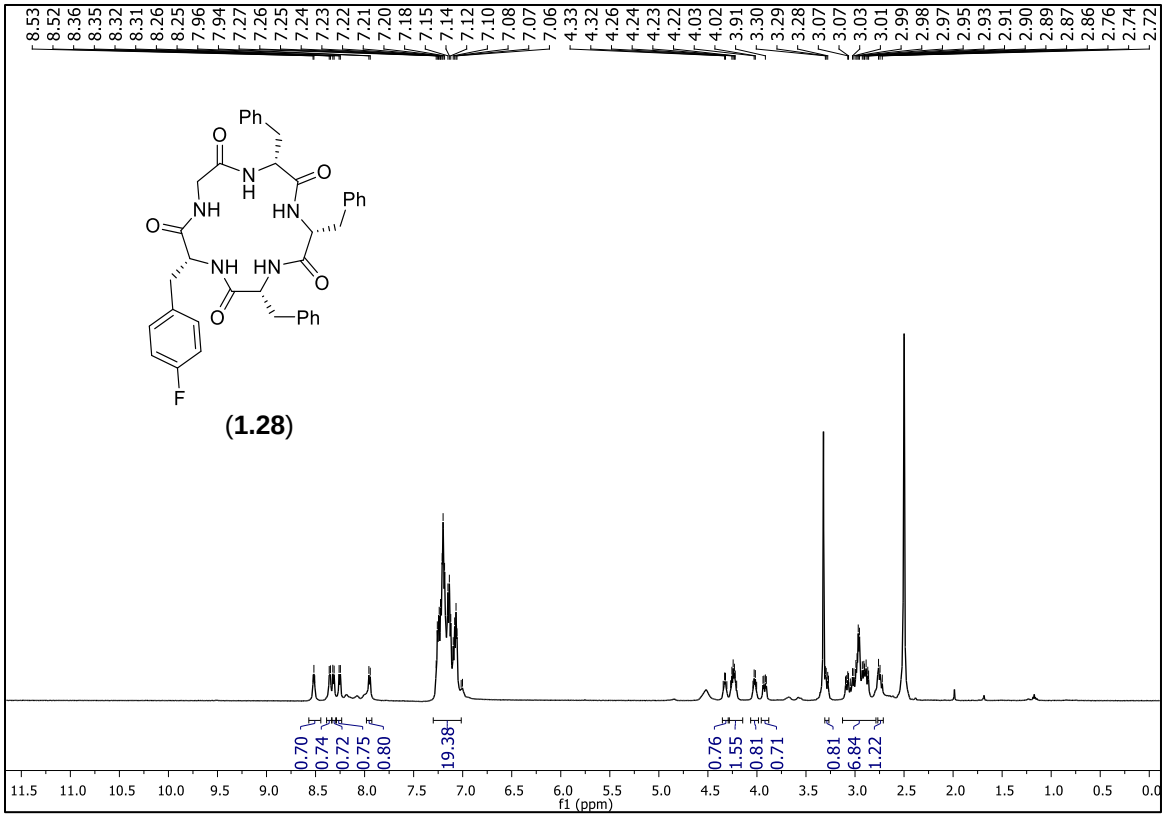
8.53 8.52 8.36 8.35 8.32 8.31 8.26 8.25 7.96 7.94 7.27 7.26 7.25 7.24 7.23 7.22 7.21 7.20 7.18 7.15 7.14 7.12 7.10 7.08 7.07 7.06
4.33 4.32 4.26 4.24 4.23 4.22 4.03 4.02 3.91 3.30 3.29 3.28 3.07 3.07 3.03 3.01 2.99 2.98 2.97 2.95 2.93 2.91 2.90 2.89 2.87 2.86 2.76 2.74 2.72
Ph
O
N
H
O
NH
HN
Ph
O
NH
HN
O
O
Ph
F
0.70 0.74 0.72 0.75 0.80 19.38 0.76 1.55 0.81 0.71 0.81 6.84 1.22
11.5 11.0 10.5 10.0 9.5 9.0 8.5 8.0 7.5 7.0 6.5 6.0 5.5 5.0 4.5 4.0 3.5 3.0 2.5 2.0 1.5 1.0 0.5 0.0
f1 (ppm)

(**1.28**)

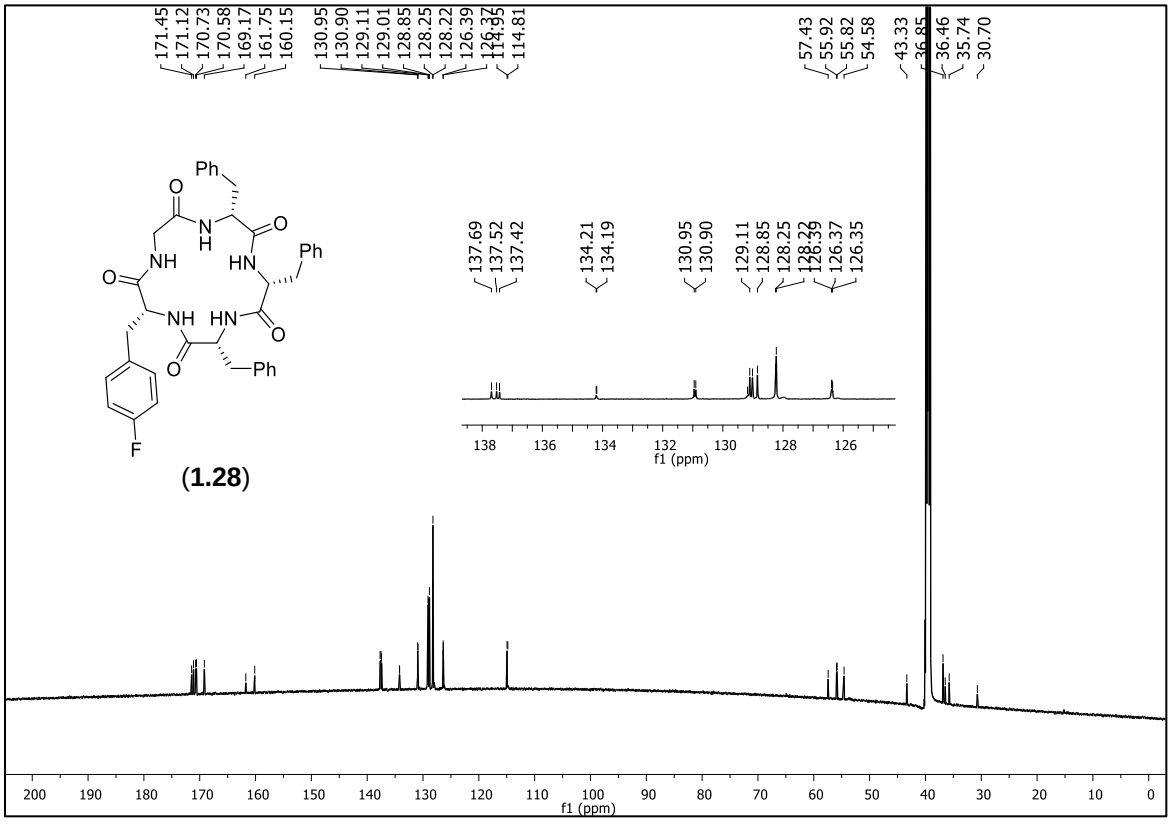
171.45 171.12 170.73 170.58 169.17 161.75 160.15
130.95 130.90 129.11 129.01 128.85 128.25 128.22 126.39 114.95 114.81
57.43 55.92 55.82 54.58 43.33 36.85 36.46 35.74 30.70
Ph
O
N
H
O
NH
HN
Ph
O
NH
HN
O
O
Ph
F
137.69 137.52 137.42 134.21 134.19 130.95 130.90 129.11 128.85 128.25 126.37 126.35
138 136 134 132 130 128 126
f1 (ppm)
200 190 180 170 160 150 140 130 120 110 100 90 80 70 60 50 40 30 20 10 0
f1 (ppm)

(**1.28**)

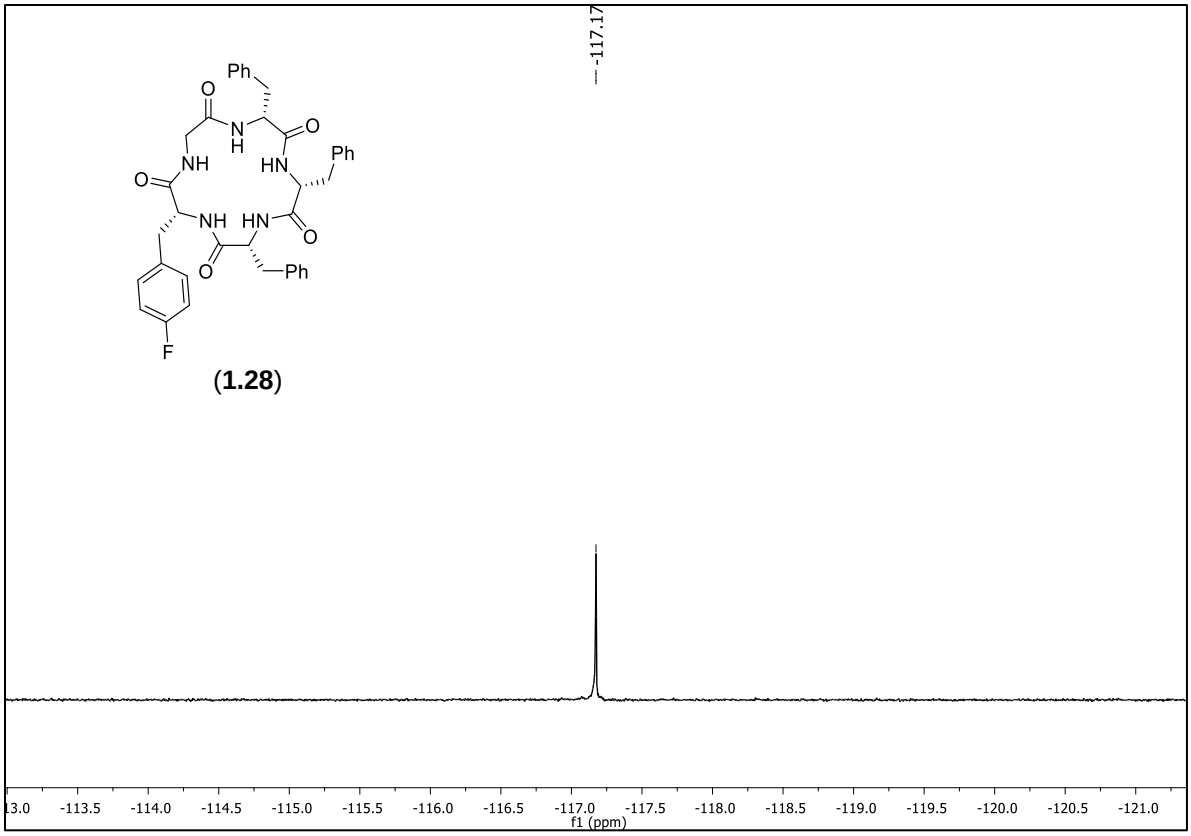
-117.17
Ph
O
N
H
O
NH
HN
Ph
O
NH
HN
O
O
Ph
F
13.0
-113.5
-114.0
-114.5
-115.0
-115.5
-116.0
-116.5
-117.0
-117.5
-118.0
-118.5
-119.0
-119.5
-120.0
-120.5
-121.0
f1 (ppm)

(**1.28**)

CHAPTER 2 – Enantioselective, Rh(I)-Catalyzed Intermolecular Hydroacylation of *α*-Ketoamides

2.1 Rh(I)-Catalyzed Intermolecular Hydroacylation of *α*-Ketoamides*

2.1.1 Introduction

Catalytic hydroacylation is an atom-economical approach to construction of C–O and C–C bonds by adding an aldehyde across an unsaturated bond (*i.e.,* ketone, alkene) (eq 1).

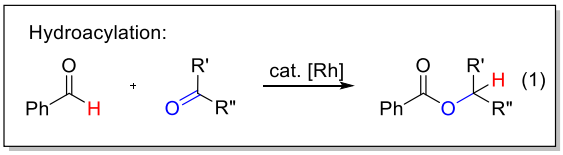

While the alkene hydroacylation has been widely studied,[85,86] ketone hydroacylation remains underdeveloped. In 1990, Bosnich reported the first intramolecular ketone hydroacylation where 1,4-ketoaldehyde **1** reacts with 5 mol% Rh to form lactone **1a** in 59% yield (eq 2).[87] However, ketone **1b** is formed in 40% yield as an undesired byproduct resulting from decarbonylation.

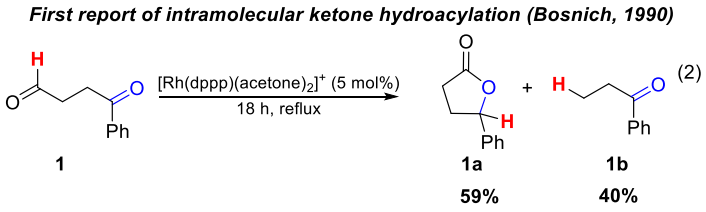

This undesired decarbonylation pathway is one of the challenges associated with transition-metal catalyzed hydroacylation. When aldehyde **2** reacts with the Rh metal, it undergoes C–H activation to form Rh-acyl hydride intermediate **I** (Figure 2.1). The Rh

* Reproduced in part with permission from Kou, K. G. M.; Le, D. N.; Dong, V. M. *J. Am. Chem. Soc*. **2014**, *136*, 9471. Copyright 2017 American Chemical Society

metal is coordinatively unsaturated, so it can undergo deinsertion to form Rh-carbonyl species **II**, which can then undergo reductive elimination to furnish inactive Rh catalyst **2a** and the corresponding alkane **2b**.

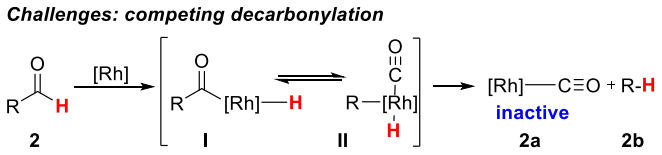

Figure 2.1 Undesired decarbonylation pathway for hydroacylation

Efforts to suppress decarbonylation include studies on the use of a heteroatom directing group to coordinatively saturate the metal center. We reported the use of oxygen and nitrogen directing groups to facilitate the first enantioselective, Rh(I)-catalyzed intramolecular ketone hydroacylations to afford medium-sized lactones in 84-99% yields and up to 99% *ee* (Figure 2.2).[88,89] While there has been much development in intramolecular ketone hydroacylation, *inter*molecular ketone hydroacylation warrants further study.

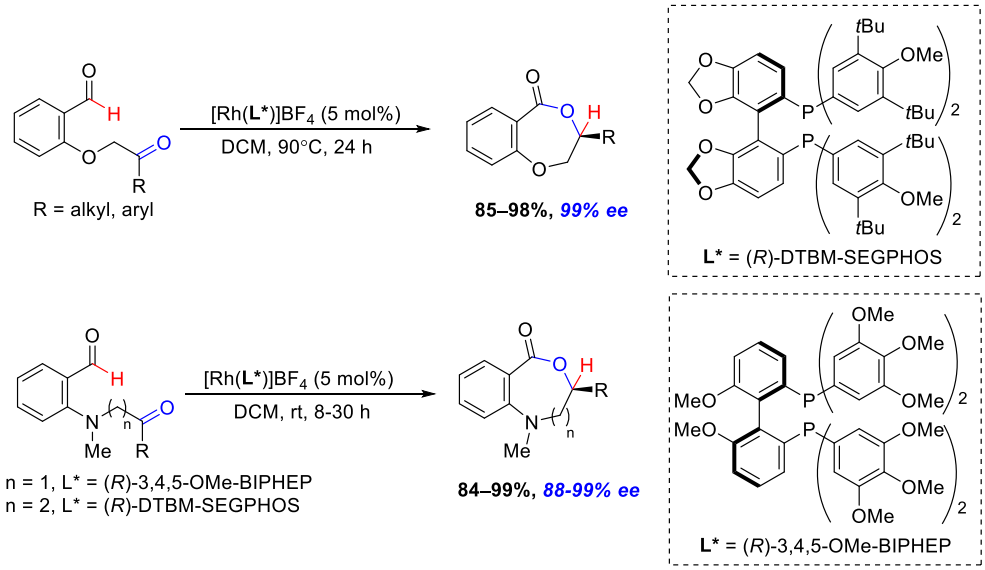

Figure 2.2 Ketone hydroacylation affords medium-sized lactones

Intermolecular ketone hydroacylation using NHC- and organocatalysis has been

reported. Scheidt and coworkers reported an NHC-catalyzed hydroacylation of α-ketoesters and aldehydes, forming esters in 78% yield (eq 3).[90] Moreover, Connon and coworkers uncovered a bio-inspired hydroacylation via thiolate catalysis (eq 4).[91] While these represent the first examples of intermolecular hydroacylation, no asymmetric or transition metal-catalyzed hydroacylations have been reported.

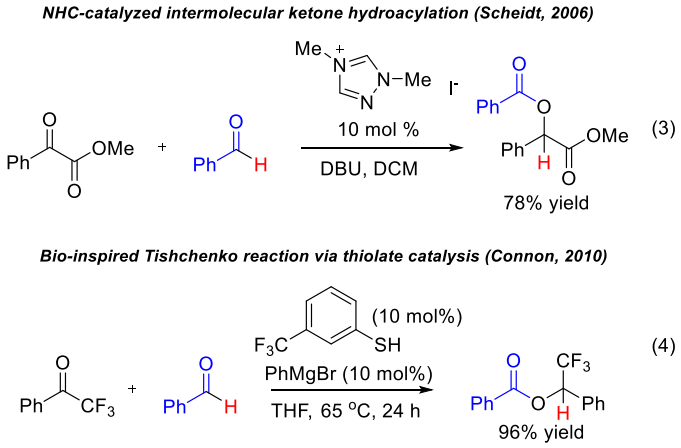

We wondered if the placement of a directing group on ketone coupling partner **3'** would generate fully saturated Rh intermediate **III** and thus disfavor decarbonylation (Figure 2.3a). Hydride insertion to form intermediate **IV** and subsequent reductive elimination would afford ester **4'** and regenerate the Rh(I)-catalyst. We envisioned hydroacylation of *α*-ketoamide **3** with simple aldehyde **2** would afford **4**, an *α*-acyloxyamide containing an ester-amide linkage (Figure 2.3b). These bonds are found in depsipeptides, which are valuable drug therapeutics like their peptide counterparts.[63]

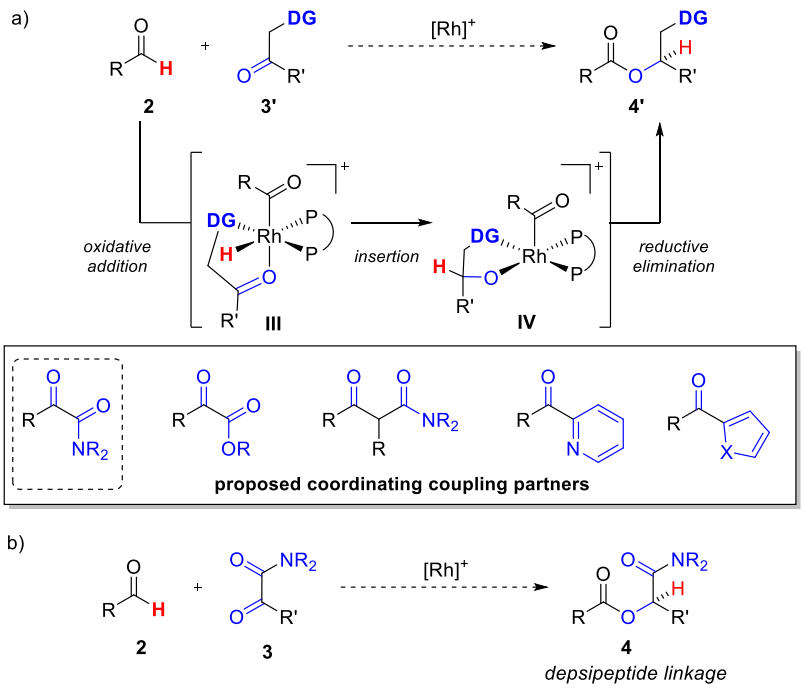

Figure 2.3 Design of a transition metal-catalyzed intermolecular ketone hydroacylation

2.1.2 Development of Rh(I)-Catalyzed Intermolecular Hydroacylation

After evaluating various ligands, Rh(I)-Josiphos catalysts were found to be most promising. Commercially available ligand **L1** provides modest yield and 13% *ee*. Changing to ligand **L2**, which contains a diphenylphosphine and a dialkylphosphine, results in a small improvement in enantioselectivity (21% *ee*). Josiphos **L3** containing a more *π*-accepting difurylphosphine and a *σ*-donating di-*tert*-butylphosphine affords the desired *α*-acyloxyamide in 46% yield and 73% *ee*. We reason that this C1-symmetric ligand may facilitate the product-determining hydride delivery *via* the *trans* effect; the hydride *trans* to the electron-rich dialkylphosphine becomes more hydridic, while the ketone trans to the *π*-acceptor becomes more prone to insertion (Table 2.1). Inspired by **L3**, we created new Josiphos ligands to study the steric influence of the phosphine substituents. Ligand **L4** bears bulkier adamantyl groups and shows inferior performance.

In contrast, **L5**, with bulkier *π*-accepting dibenzofurylphosphines, affords better results than **L3** (65% yield, 87% ee).

Table 2.1 New Josiphos ligand enables high reactivity and enantioselectivity

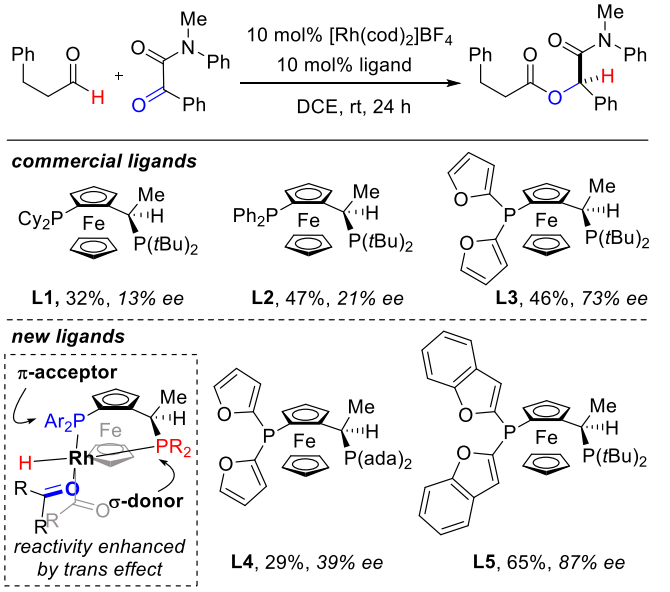

2.1.3 Substrate Scope Evaluation

The substrate scope was investigated on a number of α-ketoamides **3** and nonchelating aliphatic aldehydes **2** to afford enantioenriched esters **4** (Table 2.2). In these select examples, the catalyst loading was optimized to as low as 3.5 mol% Rh. Interestingly, enhanced reactivity is observed as the steric bulk on the aryl ketone is increased; 2-methylphenyl ketone **3b** and mesityl ketone **3c** are coupled to hydrocinnamaldehyde (**2a**) using 5 mol% Rh in 88% and 82% yield and 95% and 96% *ee*, respectively. More sterically demanding 1-naphthyl ketone **3d** undergoes hydroacylation with hydrocinnamaldehyde (**2a**) and 5 mol% Rh to afford α-acyloxyamide **4d** in 86% yield and 95% *ee*. Additionally, 2,5-difluorophenyl ketone **3e**, which is sterically similar to phenyl ketone **3a**, is coupled to hydrocinnamaldehyde **2a** using 10 mol% Rh to generate α-acyloxyamide **4e** in 67% yield and 88% *ee*. Ketones containing diarylamides

promote hydroacylation less effectively, requiring extended reaction times (3 d) and 10 mol% Rh to achieve α-acyloxyamide **4f** in 46% yield with 81% *ee*.

Table 2.2 Substrate scope of hydroacylation of non-chelating aldehydes with α-ketoamides[a]

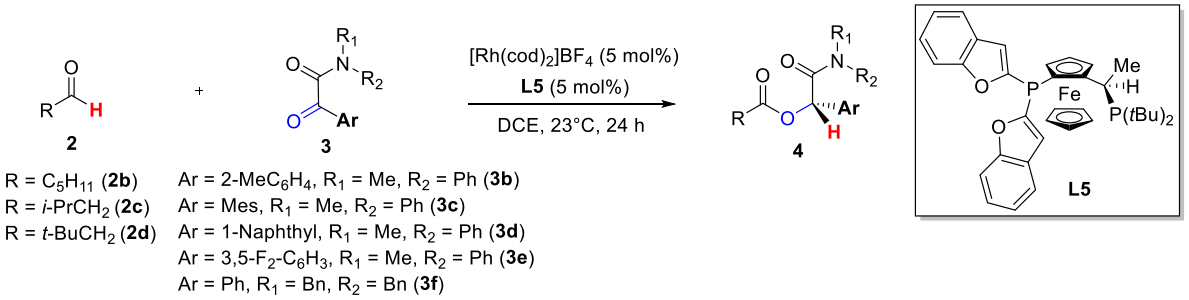

R = C_5H_{11} (**2b**)
R = *i*-$PrCH_2$ (**2c**)
R = *t*-$BuCH_2$ (**2d**)

Ar = 2-MeC_6H_4, R_1 = Me, R_2 = Ph (**3b**)
Ar = Mes, R_1 = Me, R_2 = Ph (**3c**)
Ar = 1-Naphthyl, R_1 = Me, R_2 = Ph (**3d**)
Ar = 3,5-F_2-C_6H_3, R_1 = Me, R_2 = Ph (**3e**)
Ar = Ph, R_1 = Bn, R_2 = Bn (**3f**)

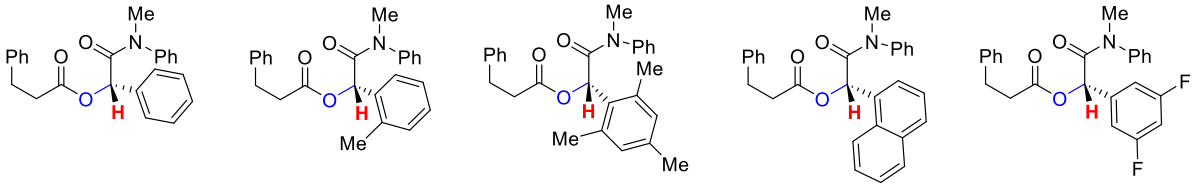

4a: 65%, 87% *ee*[b,g] | **4b**: 88%, 95% *ee*[g] | **4c**: 82%, 96% *ee*[g] | **4d**: 86%, 95% *ee*[g] | **4e**: 67%, 88% *ee*[b,g]

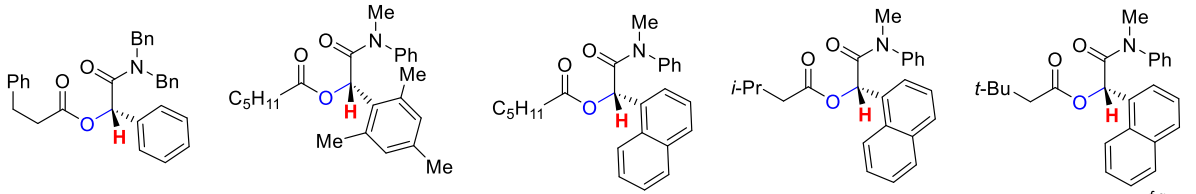

4f: 46%, 81%*ee*[b,c,g] | **4g**: 76%, 96% *ee* 84%, 94% *ee*[d] | **4h**: 73%, 96% *ee* | **4i**: 91%, 94% *ee*[g] | **4j**: 91% 93% *ee*[f,g] 92%, 87% *ee*[d,e,f]

[a] Isolated yield [b] 10 mol% [Rh] [c] 72 h. [d] 60 °C [e] 3.5 mol% [Rh] [f] 1mmol scale [g] synthesized by Kevin Kou

Moreover, the scope of the aldehyde coupling partner was investigated. Using 5 mol% Rh, hexanal (**2b**) is coupled to mesityl ketone **3c** and 1-naphthyl ketone **3d** to give **4g** and **4h** in 76% and 73% yields, respectively, and 96% *ee*. When the temperature is increased to 60 °C, the yield of α-acyloxyamide **4g** is increased to 84% yield (94% *ee*). Isovaleryl aldehyde (**2c**) and 3,3-dimethylbutanal (**2d**) are coupled to 1-naphthyl ketone **3d** using 5 mol% Rh to afford **4i** and **4j** in 91% yields, and 94% and 93% *ee*'s, respectively. I showed that the reaction was scalable by performing the reaction on a 1.0 mmol scale with 3,3-dimethyl-butanal (**2d**) and 1-naphthyl ketone **3d** as substrates. At 60 ˚C and 3.5 mol% catalyst loading, α-acyloxyamide **4j** is obtained in 92% yield and 87% *ee*.

Next, the substrate scope was expanded by coupling non-chelating aliphatic aldehydes with α-ketomorpholine amides, which can be used as a handle for further chemical transformations (Table 2.3).[92] These morpholine amides are effective directing groups, affording α-acyloxyamides in good yields and high enantioselectivities. Similar to the hydroacylation of *N*,*N'*-alkyl-aryl-ketoamides as described above (Table 2.2), the *α*-ketomorpholine amides exhibit higher reactivity and stereoselectivity when the aryl group is bulky. 1-Naphthyl ketone **5a** is coupled to a number of different aliphatic aldehydes in good to high yields (**6a-d**, 71−90% yield) and high enantioselectivities (92−94%). Notably, 1-naphthyl ketone **5a** also couples to α-branched aldehyde (*i.e.*, cyclohexanecarboxaldehyde (**2e**)) to afford α-acyloxyamide **6d** in 59% yield, and 92% *ee*, although slightly elevated temperatures (50 °C) and longer reaction times (72 h) are needed. Mesityl ketone **5b** also requires higher catalyst loadings (10 mol%) to generate α-acyloxyamide **6e** and **6f** in 84% (93% *ee*) and 94% (95% *ee*) yields, respectively. This new methodology tolerates a wide range of aliphatic aldehydes; however, we are unable to employ benzaldehyde as a coupling partner, possibly due to a high barrier to C–H activation for these particular aryl aldehydes in the absence of a directing group.[93]

Table 2.3 Substrate scope of hydroacylation of non-chelating aldehydes with α-ketomorpholine amides[a]

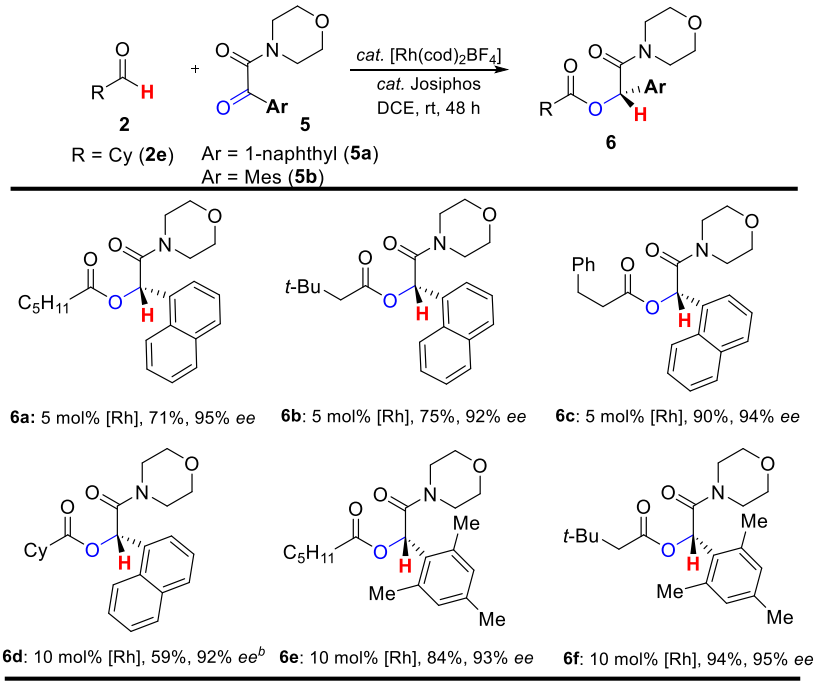

[a] Isolated yield. [b] 50 °C, 72 h

2.1.4 Mechanistic Investigation of Intermolecular Hydroacylation

After expanding the substrate scope, the mechanism of the Rh(I)-catalyzed intermolecular ketone hydroacylation was studied. The coupling of 3,3-dimethyl-butanal (**2d**) and naphthyl ketone **3d** was investigated, which was monitored by ^{1}H NMR (eq 5). The concentrations of 3,3-dimethyl-butanal (**2d**), naphthyl ketone **3d**, and rhodium catalyst were varied and the initial rates were measured. These experiments reveal a first order dependence on the rate of both ketone **3d** (Figure 2.4a) and aldehyde **2d** (Figure 2.4b). Surprisingly, a second order dependence on Rh catalyst was observed (Figure 2.5), suggesting that there are two Rh metals in the turnover-limiting step.

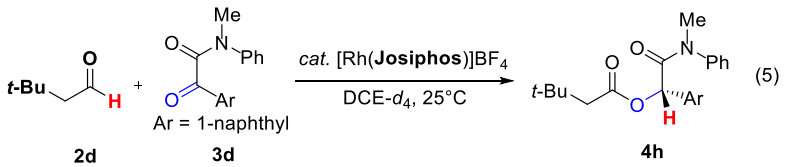

(5)

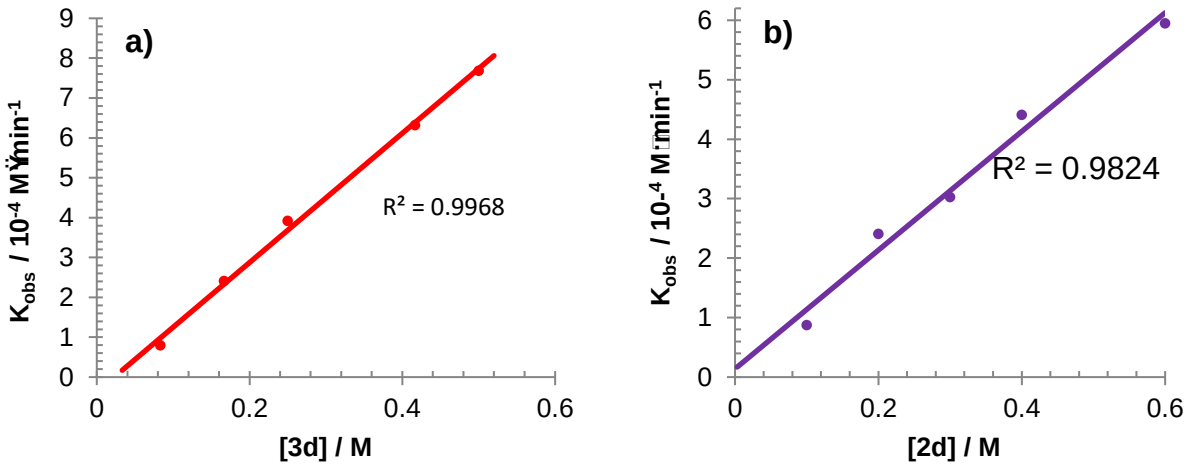

Figure 2.4 a) Plot of initial rates (k_{obs}) with respect to [α-ketoamide **3d**] showing first order dependence. **b)** Plot of initial rates (k_{obs}) with respect to [aldehyde **2d**] showing first order dependence.

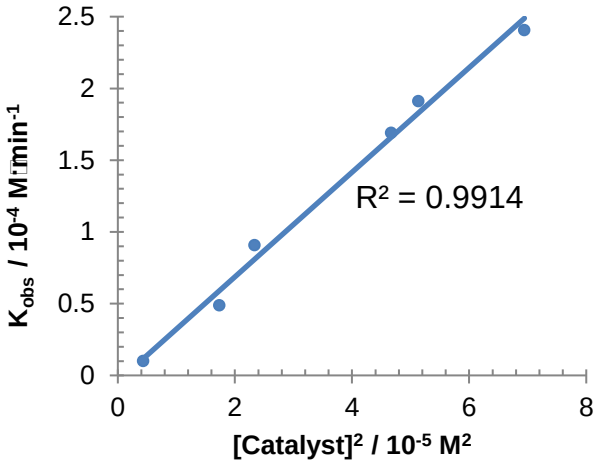

Figure 2.5 Plot of initial rates (k_{obs}) with respect to [catalyst] showing second order dependence.

Subsequently, to gain further insight into the mechanism, a kinetic isotope effect (KIE) experiment was run. Two independent, side-by-side experiments were run using protio-**2a** and deuterated **2a-D** (Figure 2.6).[94] A KIE of 2.6 was observed, which supports C–H activation to be turnover-limiting. Although ketone insertion was previously found to be turnover-limiting in *intra*molecular ketone acylation (KIE = 1.79 ± 0.06),[95] the absence

of a directing group on the aldehyde likely increases the barrier to oxidative addition significantly.[93]

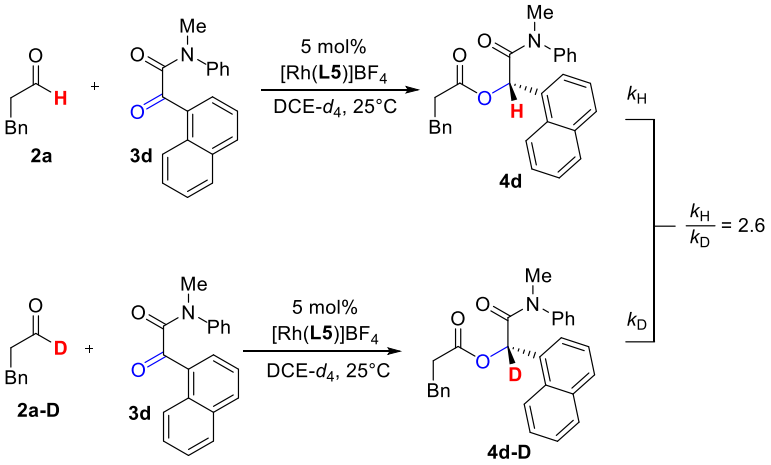

Figure 2.6 Kinetic isotope effect study using method of initial rates

After investigating the kinetic profile of the Rh(I)-catalyzed intermolecular ketone hydroacylation, we propose a mechanism invoking homobimetallic activation[96,97] of the aldehyde where one rhodium catalyst acts as a Lewis acid by coordinating the oxygen atom of the aldehyde, and a second rhodium catalyst participates in the oxidative addition of the formyl C–H bond, producing acyl-Rh(III)-hydride **V** (Figure 2.7). Cationic Rh^+ complexes have previously been used as Lewis acid catalysts.[98] Moreover, Lewis acid additives (*i.e.,* $ZnBr_2$, $ZnCl_2$) have also enhanced reactivity in intermolecular alkene hydroacylations, although their role is unclear.[99] Lastly, after oxidative addition, ketone insertion affords acyl-Rh(III)-alkoxide **VI**, which then undergoes reductive elimination to furnish α-acyloxyamide **4**.

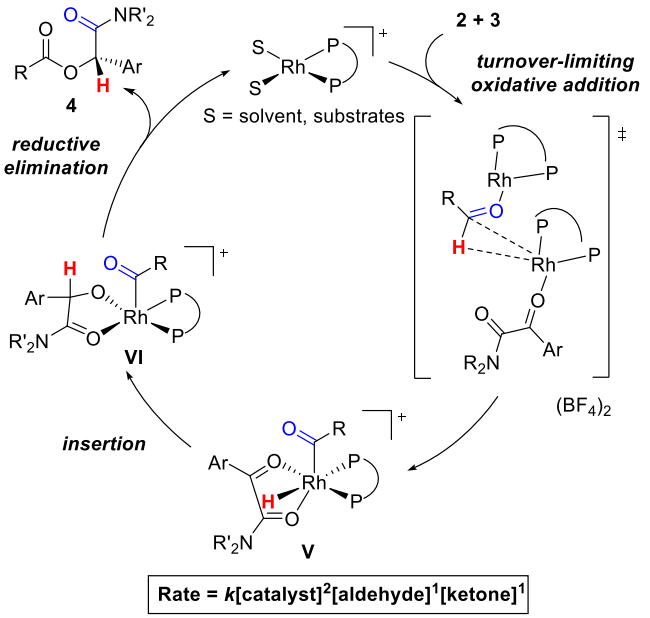

Figure 2.7 Proposed catalytic cycle

2.1.5 Conclusion

In conclusion, we have demonstrated the first enantioselective Rh(I)-catalyzed intermolecular ketone hydroacylation. Non-chelating aliphatic aldehydes are coupled to *α*-ketoamides to afford enantioenriched *α*-acyloxyamides in good to high yields (46-98%) and high enantioselectivities (74-96%) with 3.5−10 mol% catalyst loadings. Mechanistic studies reveal a second order dependence of the rate on Rh and support oxidative addition to be turnover-limiting.

2.2 Experimental Data

2.2.1 Experimental Details

The data shown Table 2.1 and certain substrates in Table 2.2 were obtained by K.G.M.K, and the reader is directed to the Supporting Information of the published manuscript[100] for the details of those experiments. This experimental section will focus on my contributions to the project.

Preparation of α-Ketoamides

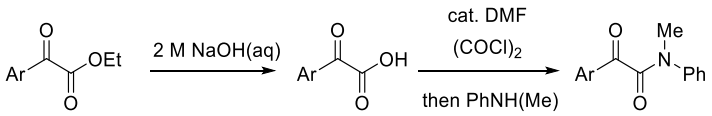

3

2-Mesityl-*N*-methyl-2-oxo-*N*-phenylacetamide (3c)

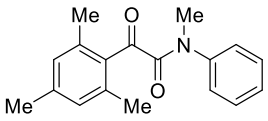

Mesityl glyoxylic acid (1.0 g, 5.2 mmol) was dissolved in DCM (5.2 mL) under a N_2 atmosphere at rt. Oxalyl chloride (0.47 mL, 5.5 mmol) was added in one portion. To the resulting mixture was added anhydrous DMF (2 drops), at which gentle bubbling was observed. The mixture was allowed to stir at rt until gas evolution ceased (12 h). The reaction mixture was then cooled to 0 ˚C in an ice/water bath and successively added Et_3N (0.73 mL, 5.2 mmol) and *N*-methylaniline (0.85 mL, 7.8 mmol). The resulting mixture was stirred at 0 ˚C for an additional 20 min, then warmed to rt. The mixture was maintained at rt for 16 h, then quenched with dH_2O (20 mL). The organic layer was separated, and the aqueous layer was extracted with DCM (2 x 20 mL). The combined organic extract was washed with brine, dried with anhydrous Na_2SO_4, filtered, and concentrated *in vacuo*. Purification of the resulting residue by silica gel chromatography eluting with 4:1 hexanes:EtOAc gave the title product as a pale yellow solid (4:1 mixture of rotamers, 993 mg, 68%, 2 steps). ^{1}H NMR (500 MHz, $CDCl_3$, major rotamer) δ 7.16–7.25 (m, 3H), 7.05 (d, *J* = 7.0 Hz, 2H), 6.69 (s, 2H), 3.37 (s, 3H), 2.21 (s, 3H), 2.18 (s, 6H); ^{13}C NMR (126 MHz, $CDCl_3$, major) δ 184.4, 157.0, 131.6, 131.4, 127.8, 123.1, 119.7, 119.5, 118.2, 117.1, 27.9, 11.3, 10.8. ^{1}H NMR (500 MHz, $CDCl_3$, minor) δ 7.43 (t, *J* = 7.5 Hz, 2H), 7.37 (d, *J* = 7.7 Hz, 2H), 7.30 (t, *J* = 7.1 Hz, 1H), 6.90 (s, 2H), 3.52 (s, 3H), 2.43 (s, 6H), 2.30 (s, 3H); ^{13}C NMR (126 MHz, $CDCl_3$, minor) δ 184.5, 156.7, 132.1, 131.8, 127.9, 123.1, 120.0, 119.4, 117.3, 115.5, 28.7, 11.4, 10.6. IR(ATR): 3065,

2920, 1672, 1659, 1648, 1606, 1594, 1495, 1375, 1220, 856, 799, 771, 703, 651 cm^{-1}. HRMS (ESI-TOF) *m/z* calc'd for $C_{18}H_{19}NO_2Na$ $[M+Na]^+$: 304.1313, found: 304.1316.

1-Mesityl-2-morpholinoethane-1,2-dione (5b)

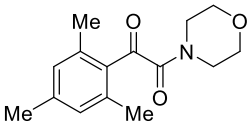

Mesityl glyoxylic acid (2.0 g, 10.4 mmol) was dissolved in DCM (48 mL) under a N_2 atmosphere at rt. Oxalyl chloride (0.93 mL, 11 mmol) was added in one portion. To the resulting mixture was added anhydrous DMF (2 drops), at which gentle bubbling was observed. The mixture was allowed to stir at rt until gas evolution ceased (16 h). The reaction mixture was then cooled to 0 ˚C in an ice/water bath and successively added Et_3N (2.2 mL, 15.8 mmol) and morpholine (1.0 mL, 11.6 mmol). The resulting mixture was gradually warmed to rt over 6 h, then quenched with dH_2O (40 mL). The organic layer was separated, and the aqueous layer was extracted with DCM (2 x 15 mL). The combined organic extract was washed with brine, dried with anhydrous Na_2SO_4, filtered, and concentrated *in vacuo*. The crude material was recrystallized in hot EtOAc/hexanes to give white needles (2.27 g, 84%, 2 steps). ^1H NMR (500 MHz, $CDCl_3$) δ 6.87 (s, 2H), 3.78 (broad s, 4H), 3.70 (dt, *J* = 14.6, 4.2 Hz, 4H), 2.32 (s, 6H), 2.29 (s, 3H); ^{13}C NMR (126 MHz, $CDCl_3$) δ 194.5, 165.6, 141.6, 137.3, 133.5, 129.8, 66.8, 66.7, 46.5, 42.3, 21.4, 20.4. IR (ATR): 2971, 2927, 2856, 1678, 1629, 1604, 1442, 1425, 1267, 1218, 1113, 980, 834, 781, 655, 618, 580. HRMS (ESI-TOF) *m/z* calc'd for $C_{15}H_{19}NO_3Na$ $[M+Na]^+$: 284.1263, found: 284.1252.

Enantioselective Ketone Hydroacylation

i) Standard Procedure

In a N_2-filled glovebox, Josiphos **L5** (3.1 mg, 0.005 mmol, 5 mol %) was dissolved in DCM (0.3 mL) and added to a vial containing $[Rh(cod)_2]BF_4$ (2.0 mg, 0.005 mmol, 5 mol %).

The resulting solution was transferred to a 25 mL Schlenk tube. An additional 0.3 mL DCM was used to rinse the vial containing the ligand, and this liquid was also added to the Schlenk tube. The Schlenk tube was then connected to a Schlenk line (vacuum gas manifold), and the pre-catalyst solution was degassed *via* two cycles of 'freeze-pump-thaw'. The Schlenk tube was backfilled with H_2 gas and the solution was stirred at rt under a gentle flow of H_2 for 45−60 min. The DCM solvent was subsequently removed under reduced pressure to give the rhodium-catalyst as a dark red oil/film. To the catalyst residue was added a solution of α-ketoamide **3** (0.10 mmol) in DCE (0.4 mL), followed by aldehyde **2** (0.11 mmol). The reaction was stirred at rt (23 ˚C) for 24 h. The crude reaction mixture was purified by silica gel chromatography. To demonstrate practicality, a 1.0 mmol scale reaction was performed (product **4j**). In this case, the product was purified by column chromatography.

For the racemic assay/reaction, an achiral catalyst derived from $[Rh(cod)_2]BF_4$ and 1,3-bis(dicyclohexyl)phosphinopropane was used.

ii) Product Characterization

(*S*)-Mesityl-2-(methyl(phenyl)amino)-2-oxoethyl hexanoate (4g)

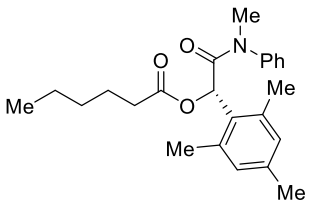

The product was purified by preparative tlc (eluting with 4:1 hexanes:EtOAc, 2 elutions) as a colorless oil (29.1 mg, 76%). ^{1}H NMR (500 MHz, $CDCl_3$) δ 7.05–7.26 (m, 3H), 6.70–7.05 (br. s, 2H), 6.64 (s, 2H), 6.42 (s, 1H), 3.23 (s, 3H), 2.45 (ddd, *J* = 15.3, 8.1, 7.1 Hz, 1H), 2.40–2.29 (m, 1H), 2.21 (s, 3H), 1.75–2.12 (br. s, 5H), 1.61–1.75 (m, 3H), 1.23–1.37 (m, 4H), 0.87 (t, *J* = 7.1 Hz, 3H). ^{13}C NMR (125 MHz, $CDCl_3$) δ 173.7, 169.3, 142.3, 138.8, 138.5,

129.6 (br. s), 129.0, 128.0 (br. s), 70.4, 38.9, 34.1, 31.4, 24.6, 22.4, 21.0, 19.8, 14.0. IR (ATR): 2956, 2928, 2861, 1736, 1677, 1595, 1495, 1377, 1163, 994, 851, 731, 698 cm^{-1}. HRMS (ESI-TOF) *m/z* calc'd for $C_{24}H_{31}NO_3Na$ $[M+Na]^+$: 404.2202, found: 404.2211. SFC analysis: 96% *ee*, 150 mm CHIRALCEL OD-H, 6% *i*PrOH, 3.0 mL/min, 220 nm, 44 °C, nozzle pressure = 200 bar CO_2, t_{R1} (major) = 1.54 min, t_{R2} (minor) = 2.05 min; $[\alpha]^{25}_D$ +188 (*c* = 1.0, $CHCl_3$). The reaction was also performed at 60˚C using 0.24 mmol aldehyde **2b** and 0.20 mmol ketone **3c**, in 0.4 mL DCE (64.3 mg, 84%, 94% ee).

(*S*)-2-(Methyl(phenyl)amino)-1-(naphthalen-1-yl)-2-oxoethyl hexanoate (4h)

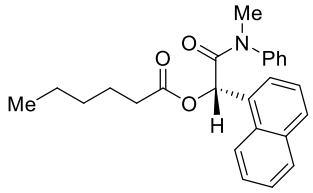

The product was purified by preparative tlc (eluting with 4:1 hexanes:EtOAc) as a colorless oil (28.6 mg, 73%). ^{1}H NMR (500 MHz, $CDCl_3$) δ 7.72–7.87 (m, 2H), 7.52 (d, *J* = 7.8 Hz, 1H) 7.41 (t, *J* = 7.3 Hz, 1H), 7.35 (s, 2H), 7.29 (t, *J* = 7.4 Hz, 1H), 7.05–7.22 (m, 3H), 6.91 (br. s, 2H), 6.66 (s, 1H), 3.27 (s, 3H), 2.47 (dt, *J* = 15.5, 7.5 Hz, 1H), 2.31–2.42 (m, 1H), 1.59–1.75 (m, 2H), 1.23–1.36 (m, 4H), 0.78–0.92 (m, 3H); ^{13}C NMR (125 MHz, $CDCl_3$) δ 173.9, 168.6, 142.4, 133.8, 131.3, 130.1, 129.9, 129.7, 128.6, 128.2, 128.1, 128.0, 126.6, 125.8, 125.2, 123.2, 71.0, 38.1, 34.1, 31.4, 24.6, 22.4, 14.0. IR (ATR): 3062, 2955, 2930, 2870, 1733, 1673, 1595, 1512, 1382, 1238, 1162, 1110, 798, 733, 698, 566 cm^{-1}. HRMS (ESI-TOF) *m/z* calc'd for $C_{25}H_{27}NO_3Na$ $[M+Na]^+$: 412.1889, found: 412.1891. SFC analysis: 96% *ee*, 150 mm CHIRALCEL OJ-H, 5% *i*PrOH, 2.5 mL/min, 220 nm, 44 °C, nozzle pressure = 200 bar CO_2, t_{R1} (major) = 1.15 min, t_{R2} (minor) = 1.77 min; $[\alpha]^{26}_D$ +202 (*c* = 1.4, $CHCl_3$).

(*S*)-2-(methyl(phenyl)amino)-1-(naphthalen-1-yl)-2-oxoethyl 3,3-dimethylbutanoate (4j)

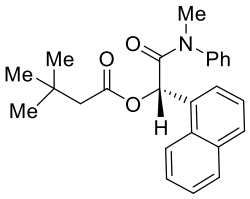

To demonstrate scalability, this reaction was performed on 1.0 mmol scale, 5% Rh-catalyst loading, 3 mL DCE, 36 h reaction time. The product was purified by flash column chromatography (eluting with 0−45% EtOAc in hexanes) to give a pale yellow liquid (353.4 mg, 91%). ^{1}H NMR (500 MHz, $CDCl_3$) δ 7.79 (t, *J* = 7.0 Hz, 2H), 7.51 (d, *J* = 7.5 Hz, 1H), 7.40 (t, *J* = 7.3 Hz, 1H), 7.34 (d, *J* = 4.7 Hz, 2H), 7.28 (t, *J* = 4.5 Hz, 1H), 7.02–7.19 (m, 3H), 6.70–7.05 (br. s, 2H), 6.65 (s, 1H), 3.27 (s, 3H), 2.33 (d, *J* = 13.5 Hz, 1H), 2.27 (d, *J* = 13.5 Hz, 1H), 1.06 (s, 9H); ^{13}C NMR (125 MHz, $CDCl_3$) δ 172.4, 168.5, 142.4, 133.8, 131.3, 130.2, 129.8, 129.7, 128.6, 128.1$_5$, 128.1$_0$, 128.0, 126.5, 125.8, 125.2, 123.2, 70.9, 47.8, 38.2, 31.1, 29.7. IR(ATR): 3061, 2955, 2869,1729, 1673, 1595, 1496, 1384, 1225, 1124, 994, 798, 774, 730, 698 cm^{-1}. HRMS (ESI-TOF) *m/z* calc'd for $C_{25}H_{27}NO_3Na$ $[M+Na]^+$: 412.1889, found: 412.1890. SFC analysis: 93% *ee*, 150 mm CHIRALCEL OD-H, 5% *i*PrOH, 2.0 mL/min, 220 nm, 44 °C, nozzle pressure = 200 bar CO_2, t_{R1} (major) = 4.11 min, t_{R2} (minor) = 4.96 min; $[\alpha]^{27}_D$ +180 (*c* = 1.2, $CHCl_3$).

Also on 1.0 mmol scale, we demonstrate that the catalyst loading can be further reduced to 3.5 mol % by heating the reaction to 60˚C for 24 h in 2 mL DCE (359 mg, 92%, 87% ee).

2-morpholino-1-(naphthalen-1-yl)-2-oxoethyl hexanoate (6a)

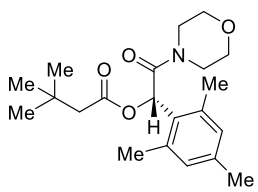

The product was purified by preparative TLC (eluting with 3:2 hexanes:EtOAc) and isolated as a colorless oil (26.2 mg, 71%). ^{1}H NMR (500 MHz, $CDCl_3$) δ 8.03 (d, *J* = 8.4 Hz, 1H), 7.92 (d, *J* = 8.1

Hz, 2H), 7.63 – 7.54 (m, 3H), 7.52 – 7.45 (m, 1H), 6.96 (s, 1H), 3.87 – 3.55 (m, 4H), 3.45 (broad s, 1H), 3.31 (broad s, 1H), 3.16 – 2.97 (m, 2H), 2.44 (dtd, *J* = 31.1, 15.6, 7.6 Hz, 2H), 1.79 – 1.56 (m, 2H), 1.37 – 1.18 (m, 4H), 0.91 – 0.75 (m, 3H); ^{13}C NMR (126 MHz, $CDCl_3$) δ 173.82, 167.02, 134.17, 131.19, 130.59, 129.62, 129.28, 127.57, 127.48, 126.47, 125.47, 122.66, 70.05, 66.86, 66.04, 45.82, 42.74, 34.13, 31.37, 24.63, 22.39, 14.02. IR(ATR): 3049, 2959, 2923, 2853, 1733, 1658, 1459, 1427, 1231, 1157, 1118, 1000, 801, 777, 730 cm^{-1}. HRMS (ESI-TOF) *m/z* calc'd for $C_{22}H_{27}NO_4Na$ $[M+Na]^+$: 392.1838, found: 392.1833. SFC analysis: 95% *ee*, 150 mm CHIRALCEL OD-H, 10% *i*PrOH, 4.0 mL/min, 220 nm, 44 °C, nozzle pressure = 200 bar CO_2, t_{R1} (major) = 1.34 min, t_{R2} (minor) = 2.10 min. $[\alpha]^{25}_D$ +132 (*c* = 1.4, $CHCl_3$).

2-morpholino-1-(naphthalen-1-yl)-2-oxoethyl 3,3-dimethylbutanoate (6b)

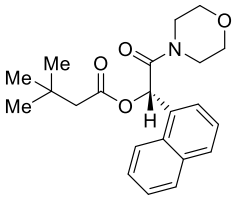

The product was purified by preparative TLC (eluting with 3:2 hexanes:EtOAc) and isolated as a colorless oil (27.7 mg, 75%). ^{1}H NMR (500 MHz, $CDCl_3$) δ 8.04 (d, *J* = 8.5 Hz, 1H), 7.94 – 7.90 (m, 1H), 7.62 – 7.52 (m, 3H), 7.49 (dd, *J* = 8.2, 7.1 Hz, 1H), 6.96 (s, 1H), 3.89 – 3.52 (m, 4H), 3.45 (broad s, 1H), 3.31 (broad s, 1H), 3.13 – 2.94 (m, 2H), 2.39 – 2.25 (m, 2H), 1.05 (s, 9H); ^{13}C NMR (126 MHz, $CDCl_3$) δ 172.23, 166.99, 134.16, 131.12, 130.54, 129.75, 129.28, 127.61, 127.43, 126.45, 125.49, 122.65, 69.88, 66.84, 66.02, 47.65, 45.82, 42.73, 31.06, 29.70. IR(ATR): 3064, 2955, 2853, 1725, 1662, 1455, 1431, 1224, 1118, 1004,

801, 773, 726 cm^{-1}. HRMS (ESI-TOF) *m/z* calc'd for $C_{22}H_{27}NO_4Na$ $[M+Na]^+$: 392.1838, found: 392.1842. SFC analysis: 92% *ee*, 150 mm CHIRALPAK AD-H, 10% *i*PrOH, 3.0 mL/min, 220 nm, 44 °C, nozzle pressure = 200 bar CO_2, t_{R1} (minor) = 1.60 min, t_{R2} (major) = 1.92 min. $[\alpha]^{28}_D$ +124 (*c* = 1.5, $CHCl_3$).

2-morpholino-1-(naphthalen-1-yl)-2-oxoethyl 3-phenylpropanoate (6c)

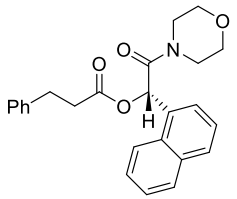

The product was purified by preparative TLC (eluting with 50:40:10 hexanes:EtOAc:Et_2O) and isolated as a colorless oil (36.3 mg, 90%). ^1H NMR (500 MHz, $CDCl_3$) δ 8.03 – 7.85 (m, 3H), 7.62 – 7.53 (m, 3H), 7.50 (dd, *J* = 8.2, 7.1 Hz, 1H), 7.29 – 7.20 (m, 2H), 7.17 (td, *J* = 6.9, 6.5, 1.6 Hz, 3H), 6.97 (s, 1H), 3.92 – 3.50 (m, 4H), 3.45 (broad s, 1H), 3.30 (broad s, 1H), 3.14 – 2.96 (m, 4H), 2.88 – 2.72 (m, 2H); ^{13}C NMR (126 MHz, $CDCl_3$) δ 172.83, 166.92, 140.37, 134.14, 131.15, 130.65, 129.42, 129.26, 128.54, 128.36, 127.58, 127.55, 126.47, 126.30, 125.44, 122.60, 70.30, 66.83, 66.01, 45.79, 42.74, 35.60, 30.84. IR(ATR): 3068, 3025, 2966, 2919, 2861, 1733, 1662, 1451, 1435, 1271, 1228, 1145, 997, 906, 797, 773, 730 cm^{-1}. HRMS (ESI-TOF) *m/z* calc'd for $C_{25}H_{25}NO_4Na$ $[M+Na]^+$: 426.1681, found: 426.1687. SFC analysis: 94% *ee*, 250 mm CHIRALPAK IA, 10% *i*PrOH, 5.0 mL/min, 220 nm, 44 °C, nozzle pressure = 200 bar CO_2, t_{R1} (minor) = 5.69 min, t_{R2} (major) = 6.42 min. $[\alpha]^{28}_D$ +98 (*c* = 1.7, $CHCl_3$).

2-morpholino-1-(naphthalen-1-yl)-2-oxoethyl cyclohexanecarboxylate (6d)

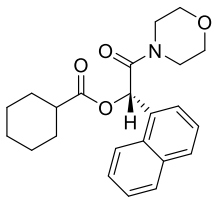

The product was purified by preparative TLC (eluting with 4:1 hexanes:acetone) and isolated as a colorless oil (22.4 mg, 59%). ^1H NMR (500 MHz, $CDCl_3$) δ 8.02 (d, *J* = 8.5, 1.2 Hz, 1H), 7.96 – 7.88 (m,

2H), 7.62 – 7.52 (m, 3H), 7.51 – 7.44 (m, 1H), 6.94 (s, 1H), 3.84 – 3.52 (m, 4H), 3.46 (broad s, 1H), 3.31 (broad s, 1H), 3.07 (d, *J* = 26.3 Hz, 2H), 2.45 (tt, *J* = 11.3, 3.6 Hz, 1H), 2.09 – 2.02 (m, 1H), 1.95 – 1.87 (m, 1H), 1.80 – 1.65 (m, 2H), 1.63 – 1.56 (m, 1H), 1.56 – 1.44 (m, 2H), 1.35 – 1.12 (m, 3H); ^{13}C NMR (126 MHz, $CDCl_3$) δ 176.02, 167.04, 134.19, 131.28, 130.55, 129.75, 129.26, 127.52, 127.46, 126.46, 125.46, 122.76, 69.95, 66.88, 66.07, 45.84, 43.01, 42.74, 29.12, 28.98, 25.82, 25.46, 25.44. IR(ATR): 3005, 2927, 2857, 1729, 1658, 1439, 1247, 1224, 1161, 1114, 1000, 805, 781, 742 cm^{-1}. HRMS (ESI-TOF) *m/z* calc'd for $C_{23}H_{27}NO_4Na$ $[M+Na]^+$: 404.1838, found: 404.1831. SFC analysis: 92% *ee*, 150 mm CHIRALCEL OD-H, 10% *i*PrOH, 3.0 mL/min, 220 nm, 44 °C, nozzle pressure = 200 bar CO_2, t_{R1} (major) = 2.80 min, t_{R2} (minor) = 3.46 min. $[\alpha]^{23}_D$ +96 (*c* = 1.0, $CHCl_3$).

1-mesityl-2-morpholino-2-oxoethyl hexanoate (6e)

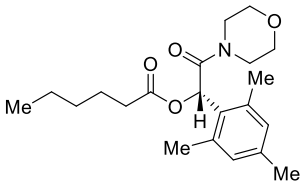

The product was purified by preparative TLC (eluting with 4:1 hexanes:acetone) and isolated as a colorless oil (30.3 mg, 84%). ^{1}H NMR (500 MHz, $CDCl_3$) δ 6.88 (s, 2H), 6.51 (s, 1H), 3.73 (broad s, 2H), 3.49 (broad s, 3H), 3.34 – 2.77 (m, 3H), 2.56 – 2.35 (m, 2H), 2.33 (s, 6H), 2.27 (s, 3H), 1.75 – 1.63 (m, 2H), 1.41 – 1.27 (m, 4H), 0.91 – 0.81 (m, 3H); ^{13}C NMR (126 MHz, $CDCl_3$) δ 173.54, 167.65, 139.19, 137.87, 130.47, 129.15, 69.91, 66.90, 66.10, 45.52, 43.03, 34.25, 31.42, 24.68, 22.42, 21.07, 20.32, 14.04. IR(ATR): 2958, 2923, 2857, 1732, 1662, 1451, 1431, 1271, 1231, 1161, 1110, 1004, 856, 820, 734 cm^{-1}. HRMS (ESI-TOF) *m/z* calc'd for $C_{21}H_{31}NO_4Na$ $[M+Na]^+$: 384.2151, found: 384.2147. SFC analysis: 96% *ee*, 150 mm CHIRALCEL OD-H, 5% *i*PrOH, 3.0 mL/min, 220 nm, 44 °C, nozzle

pressure = 200 bar CO_2, t_{R1} (major) = 1.55 min, t_{R2} (minor) = 2.51 min. $[\alpha]^{28}_D$ +220 (*c* = 0.75, $CHCl_3$).

1-mesityl-2-morpholino-2-oxoethyl 3,3-dimethylbutanoate (6f)

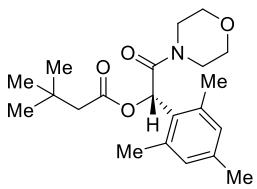

The product was purified by preparative TLC (eluting with 4:1 hexanes:acetone) and isolated as a colorless oil (33.9 mg, 94%). ^{1}H NMR (500 MHz, $CDCl_3$) δ 6.87 (s, 2H), 6.50 (s, 1H), 3.73 (broad s, 2H), 3.47 (broad s, 3H), 3.29 – 2.85 (m, 3H), 2.36 (d, *J* = 13.5 Hz, 1H), 2.32 (s, 6H), 2.29 (d, *J* = 13.6 Hz, 1H), 2.27 (s, 3H), 1.07 (s, 9H); ^{13}C NMR (126 MHz, $CDCl_3$) δ 171.89, 167.63, 139.10, 137.81, 130.45, 129.33, 69.80, 66.81, 66.17, 47.93, 45.49, 43.09, 30.98, 29.74, 21.06, 20.31. IR(ATR): 2959, 2922, 2856, 1728, 1668, 1455, 1425, 1226, 1116, 1000, 863, 820, 726 cm^{-1}. HRMS (ESI-TOF) *m/z* calc'd for $C_{21}H_{31}NO_4Na$ $[M+Na]^+$: 384.2151, found: 384.2140. SFC analysis: 95% *ee*, 150 mm CHIRALCEL OD-H, 5% *i*PrOH, 3.0 mL/min, 220 nm, 44 °C, nozzle pressure = 200 bar CO_2, t_{R1} (major) = 1.35 min, t_{R2} (minor) = 1.83 min. $[\alpha]^{27}_D$ +204 (*c* = 1.3, $CHCl_3$).

(*S*)-(Methyl(phenyl)amino)-1-(naphthalen-1-yl)-2-oxoethyl 3-phenylpropanoate (4d)

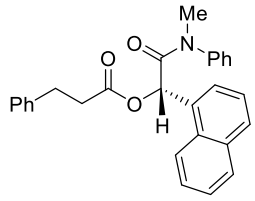

The product was purified by preparative tlc (eluting with 4:1 hexanes/EtOAc) as a colorless oil (36.6 mg, 86%).^{1}H NMR (499 MHz, $CDCl_3$) δ 7.72–7.87 (m, 2H), 7.49 (d, *J* = 7.8 Hz, 1H), 7.40 (t, *J* = 7.3 Hz, 1H), 7.35 (s, 2H), 7.28 (t, *J* = 7.5 Hz, 1H), 7.18–7.26 (m, 2H), 7.04–7.18 (m, 6H), 6.90 (br. s, 2H), 6.68 (s, 1H), 3.28 (s, 3H), 2.92–3.07 (m, 2H), 2.81 (dt, *J* = 15.9, 8.0 Hz, 1H),

2.64–2.75 (m, 1H); ^{13}C NMR (126 MHz, $CDCl_3$) δ 172.9, 168.5, 142.3, 140.5, 133.8, 131.3, 130.0, 129.7, 128.6, 128.5, 128.3, 128.2, 128.1, 127.9, 126.6, 126.3, 125.9, 125.2, 123.2, 71.2, 38.1, 35.6, 30.9. IR (ATR): 3061, 3028, 2929, 1733, 1671, 1595, 1495, 1411, 1237, 1149, 985, 799, 774, 697 cm^{-1}. HRMS (ESI-TOF) *m/z* calc'd for $C_{28}H_{25}NO_3Na$ $[M+Na]^+$: 446.1732, found: 446.1716. SFC analysis: 95% *ee*, 150 mm CHIRALCEL OD-H, 10% *i*PrOH, 2.5 mL/min, 220 nm, 44 °C, nozzle pressure = 200 bar CO_2, t_{R1} (major) = 3.97 min, t_{R2} (minor) = 5.25 min; $[\alpha]^{26}_D$ +90 (*c* = 0.7, $CHCl_3$).

(S)-2-(methyl(phenyl)amino)-1-(naphthalen-1-yl)-2-oxoethyl-1-d 3-phenylpropanoate (4d-D)

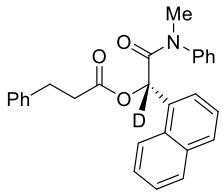

The product was purified by preparative TLC (eluting with 4:1 hexanes:EtOAc). ^{1}H NMR (499 MHz, $CDCl_3$) δ 7.84 – 7.78 (m, 2H), 7.49 (d, *J* = 8.6 Hz, 1H), 7.42 (t, *J* = 7.5 Hz, 1H), 7.39 – 7.34 (m, 2H), 7.29 (t, *J* = 7.7 Hz, 1H), 7.25 – 7.19 (m, 2H), 7.19 – 7.06 (m, 6H), 6.91 (s, 2H), 3.29 (s, 3H), 3.07 – 2.94 (m, 2H), 2.82 (ddd, *J* = 15.9, 8.9, 6.9 Hz, 1H), 2.71 (ddd, *J* = 16.3, 9.5, 6.8 Hz, 1H); ^{13}C NMR (126 MHz, $CDCl_3$) δ 172.93, 168.48, 142.27, 140.49, 133.80, 131.30, 129.97, 129.93, 129.74, 128.60, 128.55, 128.35, 128.20, 128.12, 127.94, 126.63, 126.27, 125.86, 125.23, 123.18, 38.13, 35.65, 30.88. IR (ATR): 3064, 3021, 2919, 1737, 1662, 1600, 1486, 1368, 1298, 1153, 1083, 899, 801, 765, 726, 691 cm^{-1}. HRMS (ESI-TOF) *m/z* calc'd for $C_{28}H_{24}DNO_3Na$ $[M+Na]^+$: 447.1795, found: 447.1791.

Mechanistic Studies

i) Kinetic Experiments

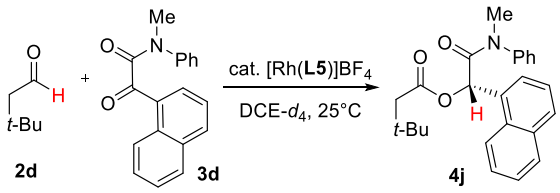

The kinetic profile of the reaction was studied by probing the initial rates of the reactions and varying the concentrations of **2d**, **3d** and Rh-catalyst. No products of decomposition were observed with this system. The rates were monitored by ^{1}H NMR using durene as an internal standard.

Representative procedure:

The catalyst was first prepared by mixing (S_P,*R*)-Josiphos (3.1 mg, 0.005 mmol) and $[Rh(cod)_2]BF_4$ (2.0 mg, 0.005 mmol) in protio-DCE (0.5 mL) in a N_2-filled glovebox and transferring the solution to a J-Young NMR tube. The J-Young NMR tube was connected to a Schlenk/gas line and degassed *via* 'freeze-pump-thaw'. Hydrogen gas was introduced into the J-Young NMR tube, and the content was thoroughly mixed by continuously inverting the tube (~20 min). Upon hydrogenation, the catalyst solution turns from dark red to a very dark brown color. The DCE solvent was then carefully removed under reduced pressure, leaving behind a brown residue. In a separate 1-dram vial, α-ketoamide **3d** (28.9 mg, 0.100 mmol) was dissolved in 0.1 mL DCE-d_4 and transferred to the J-Young NMR tube containing catalyst (in a N_2-filled glovebox). The 1-dram vial was

rinsed with DCE-d_4 (5 × 0.1 mL), and this liquid was also transferred to the J-Young NMR tube (for a total of 0.6 mL solvent). Aldehyde **2d** (15.0 μL, 0.12 mmol) was subsequently added via microsyringe. The J-Young tube was sealed, thoroughly mixed by inverting the sample at least 10 times, and immediately subjected to ^{1}H NMR analysis (T = 298K). Time points were taken every 5 minutes.

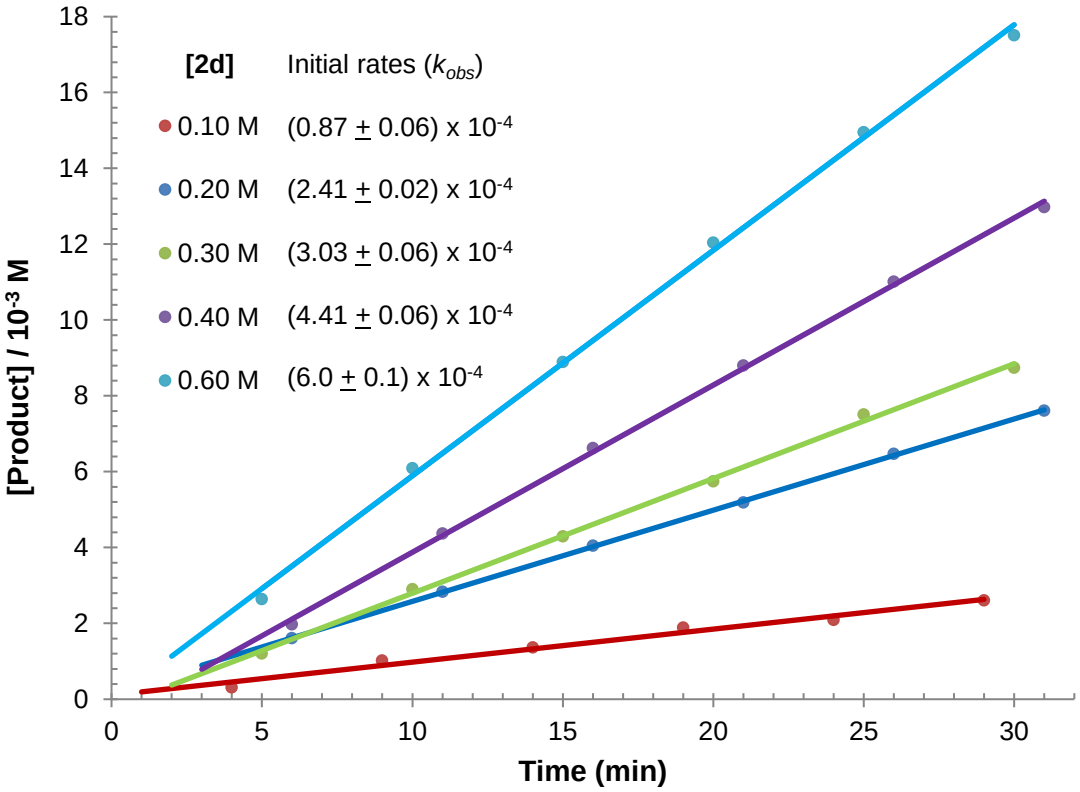

Figure 2.8 Plot of initial rates with various aldehyde concentrations.

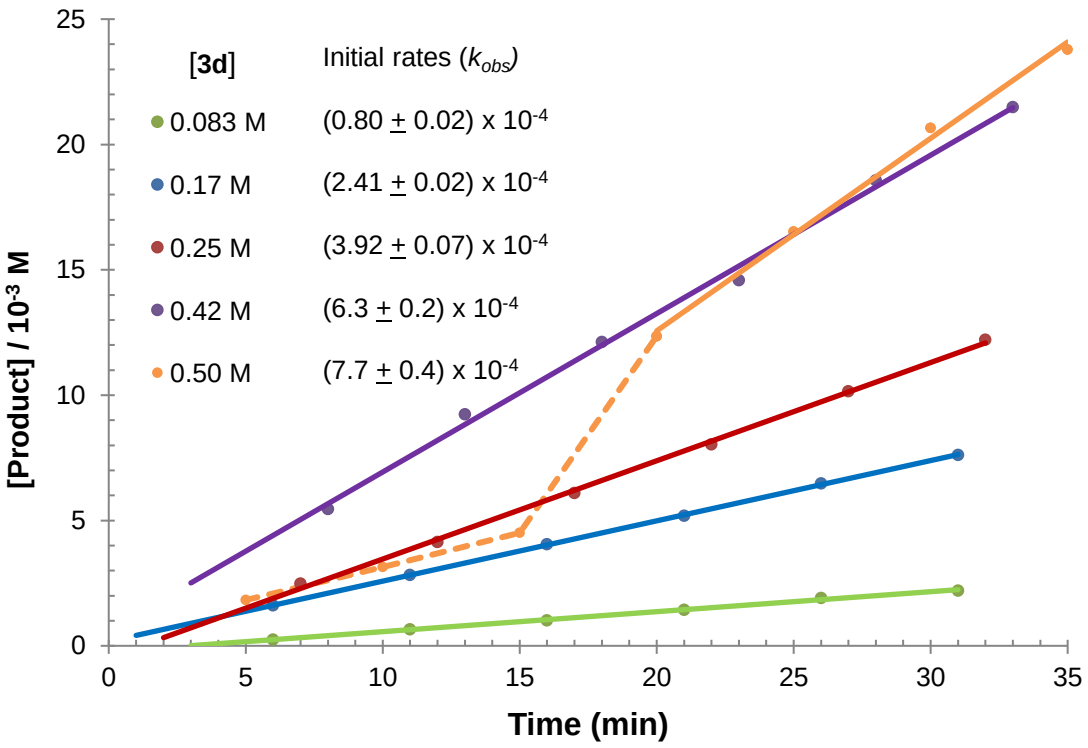

Figure 2.9 Plot of initial rates with various ketone concentrations.
(An induction period is observed when a large excess of ketone **3d** was used (orange line, Figure 2.9). This data was not used in determination of the kinetic order)

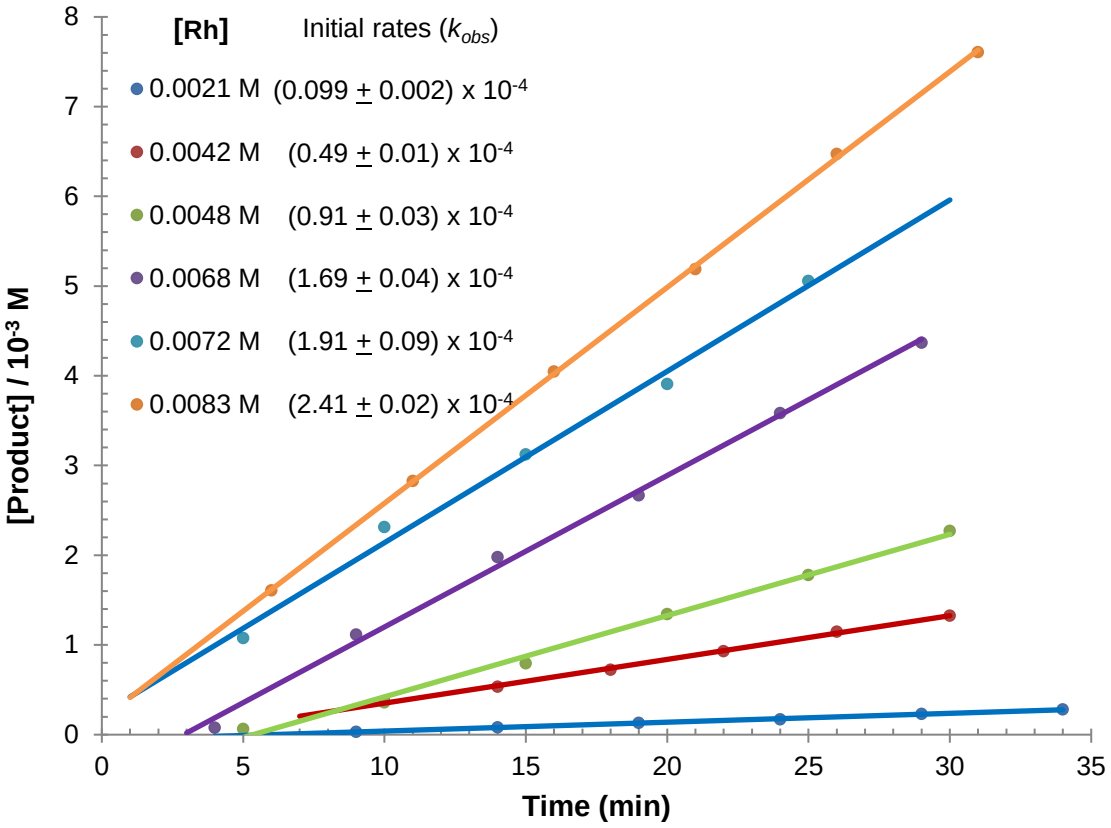

Figure 2.10 Plot of initial rates with various catalyst concentrations.

Second-order dependence of the rate on catalyst order is observed in the regime between 1.25 mol % and 5 mol % [Rh(Josiphos)]BF_4.

Based on this study, the following rate law is obtained:

rate = *k*[aldehyde]^1[α-ketoamide]^1[catalyst]^2

ii) KIE experiment

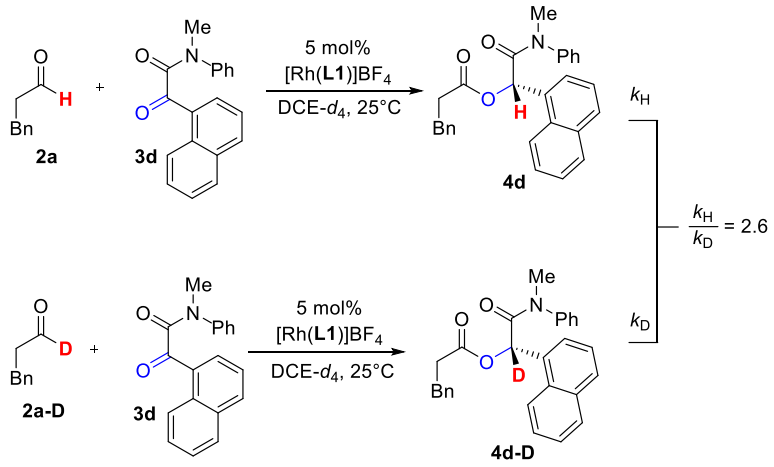

The KIE was obtained by measuring the initial rates of two independent experiments. Hydrocinnamaldehyde **2a** and **2a-D** was chosen for this study because the larger molecular weight of **2a-D**[101] relative to all other aldehydes in this study renders it more convenient to prepare and isolate (*via* distillation). The catalyst was prepared as described in the standard procedure and the reaction was monitored by ^{1}H NMR (T = 298K). The following initial rates were measured: k_{H} = (4.6 ± 0.1) × 10^{-4} M^{-1}·min^{-1}; k_{D} = (1.78 ± 0.05) × 10^{-4} M^{-1}·min^{-1}.

2.2.2 NMR Spectra

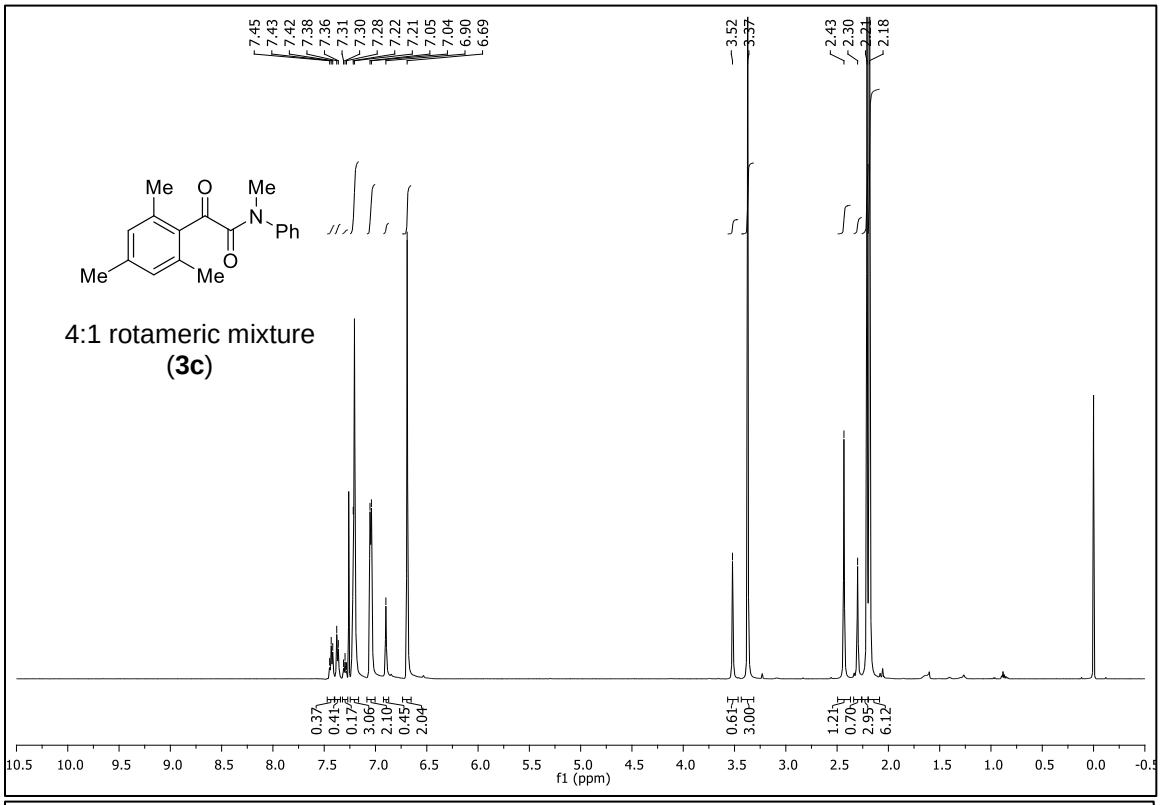

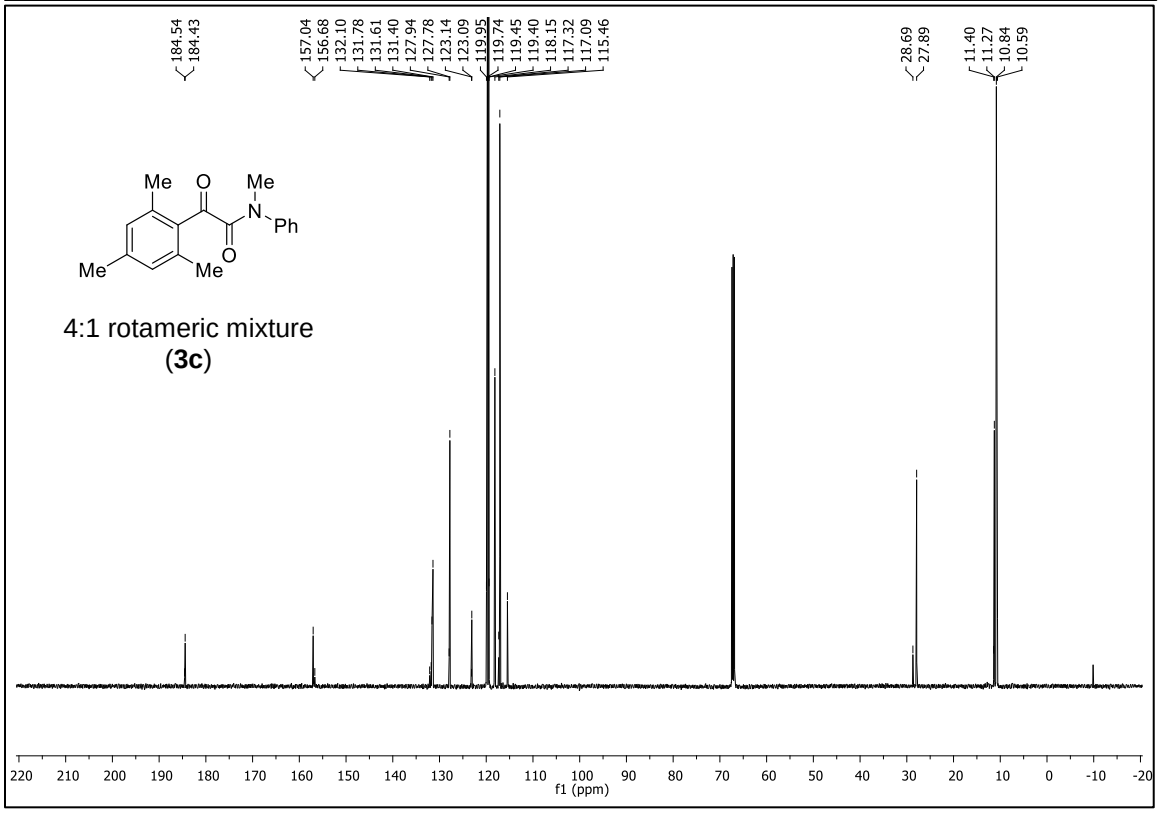

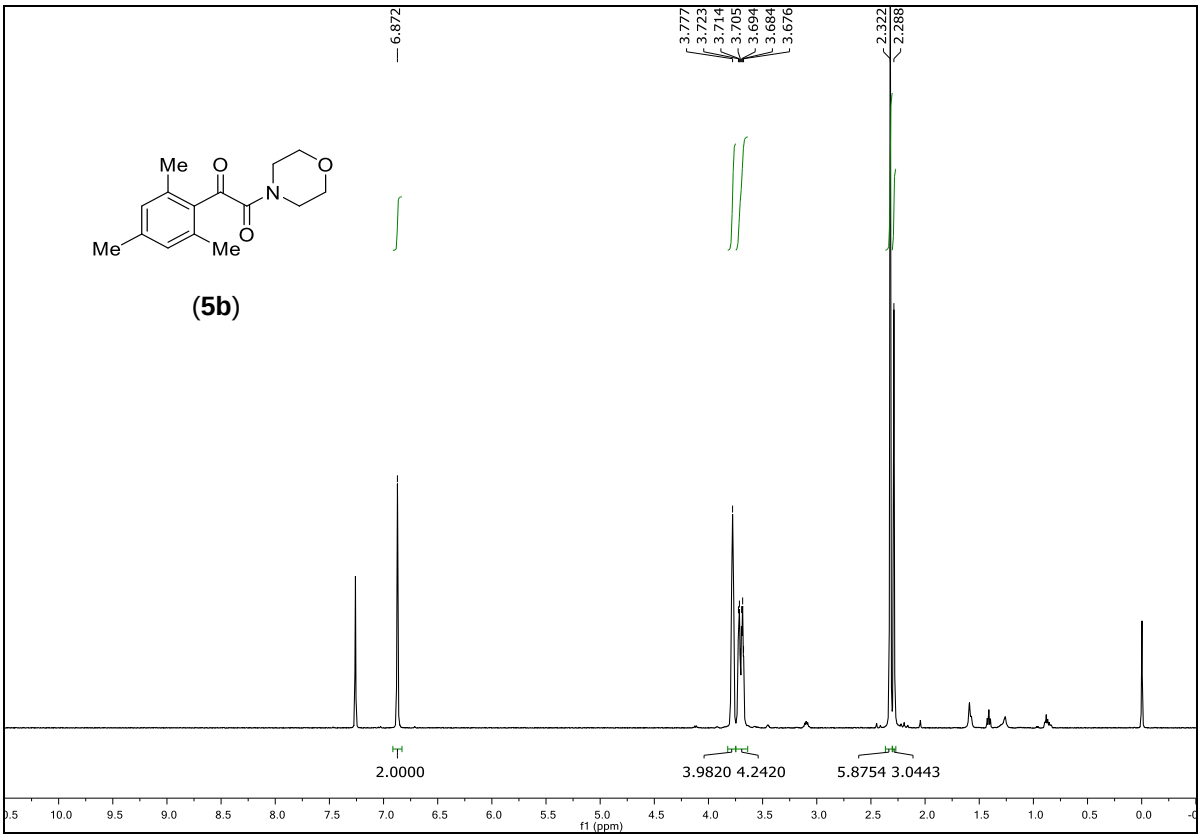
6.872
3.777
3.723
3.714
3.705
3.694
3.684
3.676
2.322
2.288
Me
O
N
O
Me
O
Me
(5b)
2.0000
3.9820 4.2420
5.8754 3.0443
f1 (ppm)

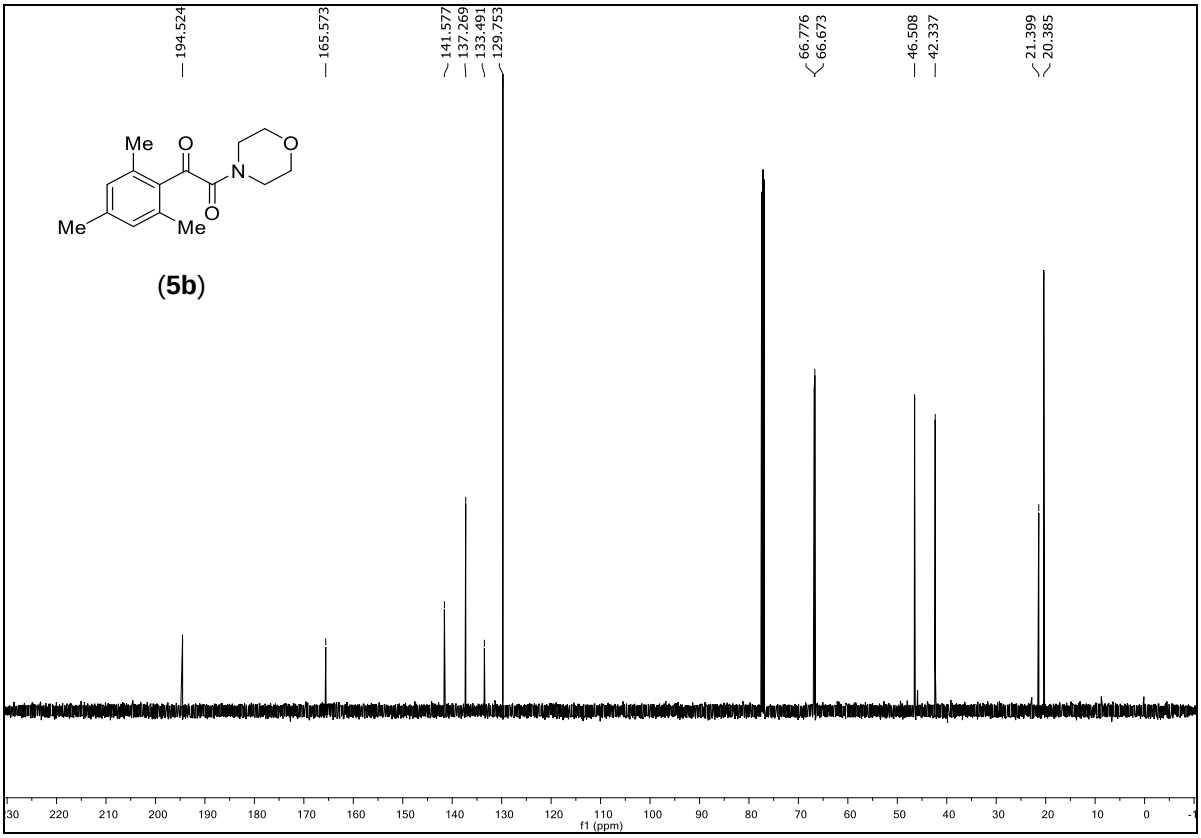
194.524
165.573
141.577
137.269
133.491
129.753
66.776
66.673
46.508
42.337
21.399
20.385
Me
O
N
O
Me
O
Me
(5b)
f1 (ppm)

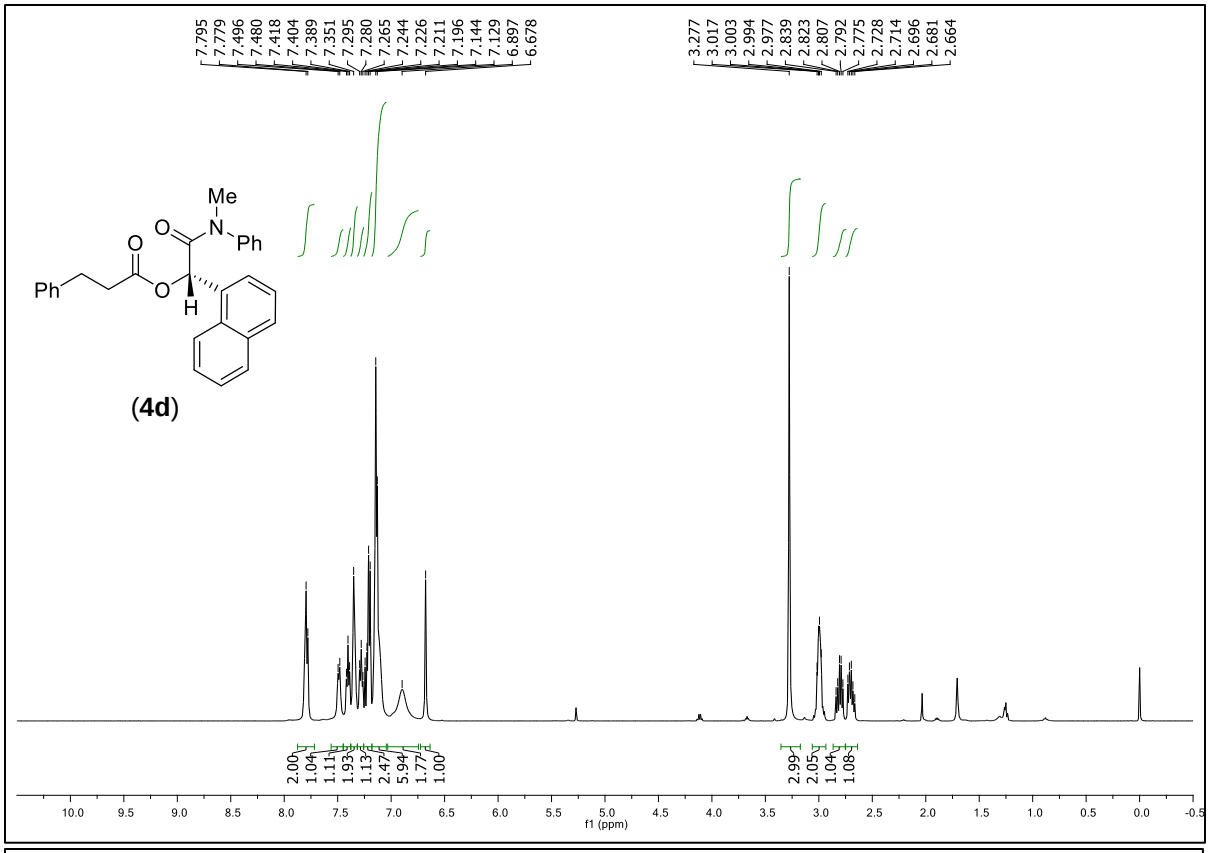
7.795
7.779
7.496
7.480
7.418
7.404
7.389
7.351
7.295
7.280
7.265
7.244
7.226
7.211
7.196
7.144
7.129
6.897
6.678
3.277
3.017
3.003
2.994
2.977
2.839
2.823
2.807
2.792
2.775
2.728
2.714
2.696
2.681
2.664
Me
N
Ph
O
O
Ph
O
H
2.00
1.04
1.11
1.93
1.13
2.47
5.94
1.77
1.00
2.99
2.05
1.04
1.08
f1 (ppm)

(**4d**)

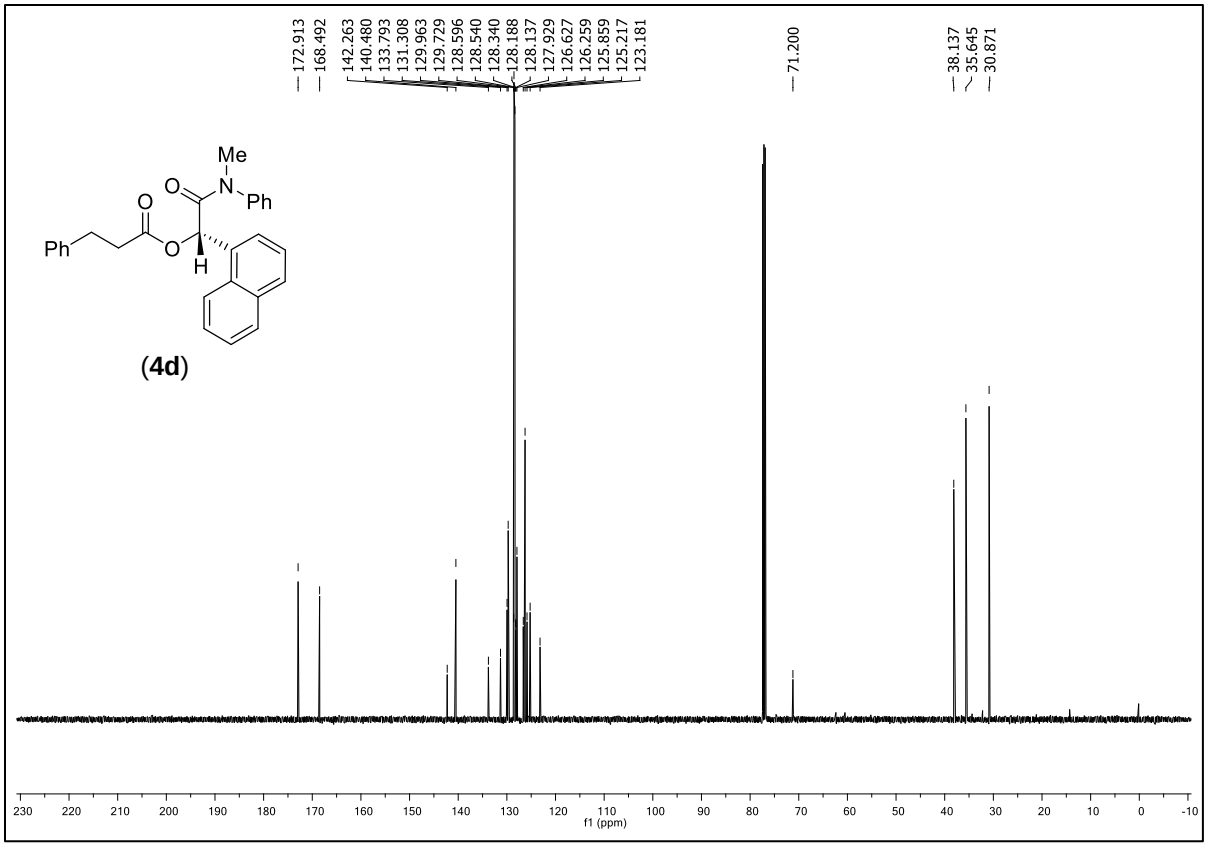
172.913
168.492
142.263
140.480
133.793
131.308
129.963
129.729
128.596
128.540
128.340
128.188
128.137
127.929
126.627
126.259
125.859
125.217
123.181
71.200
38.137
35.645
30.871
Me
N
Ph
O
O
Ph
O
H
f1 (ppm)

(**4d**)

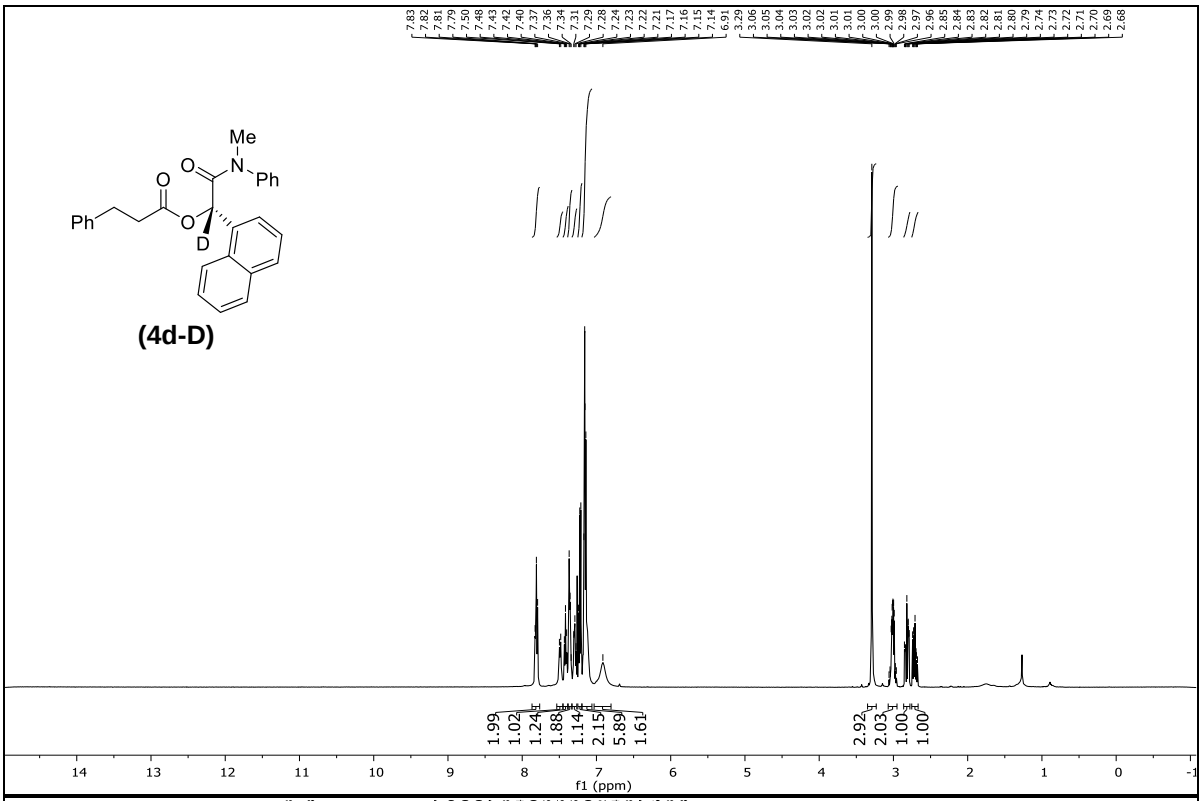
Me
N
Ph
O
O
Ph
O
D
(4d-D)
1.99
1.02
1.24
1.88
1.14
2.15
5.89
1.61
2.92
2.03
1.00
1.00
f1 (ppm)

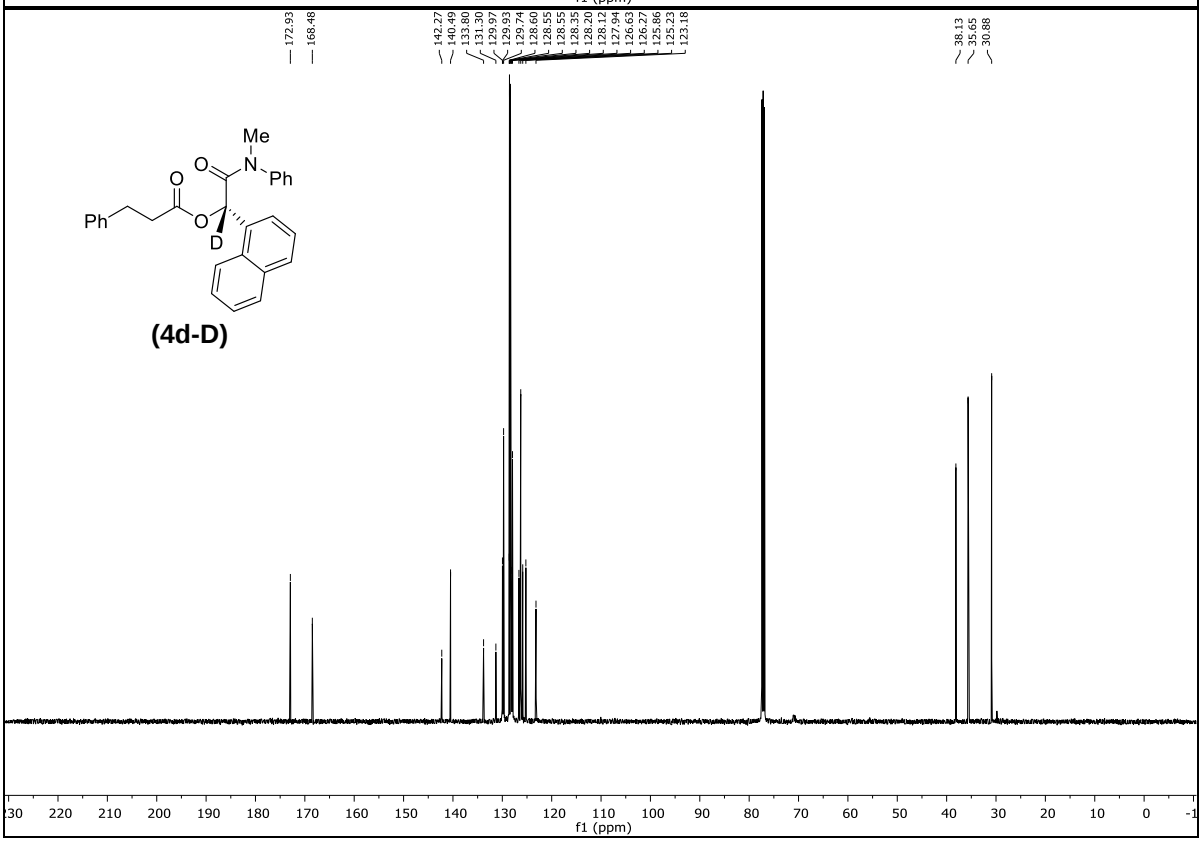
Me
N
Ph
O
O
Ph
O
D
(4d-D)
f1 (ppm)

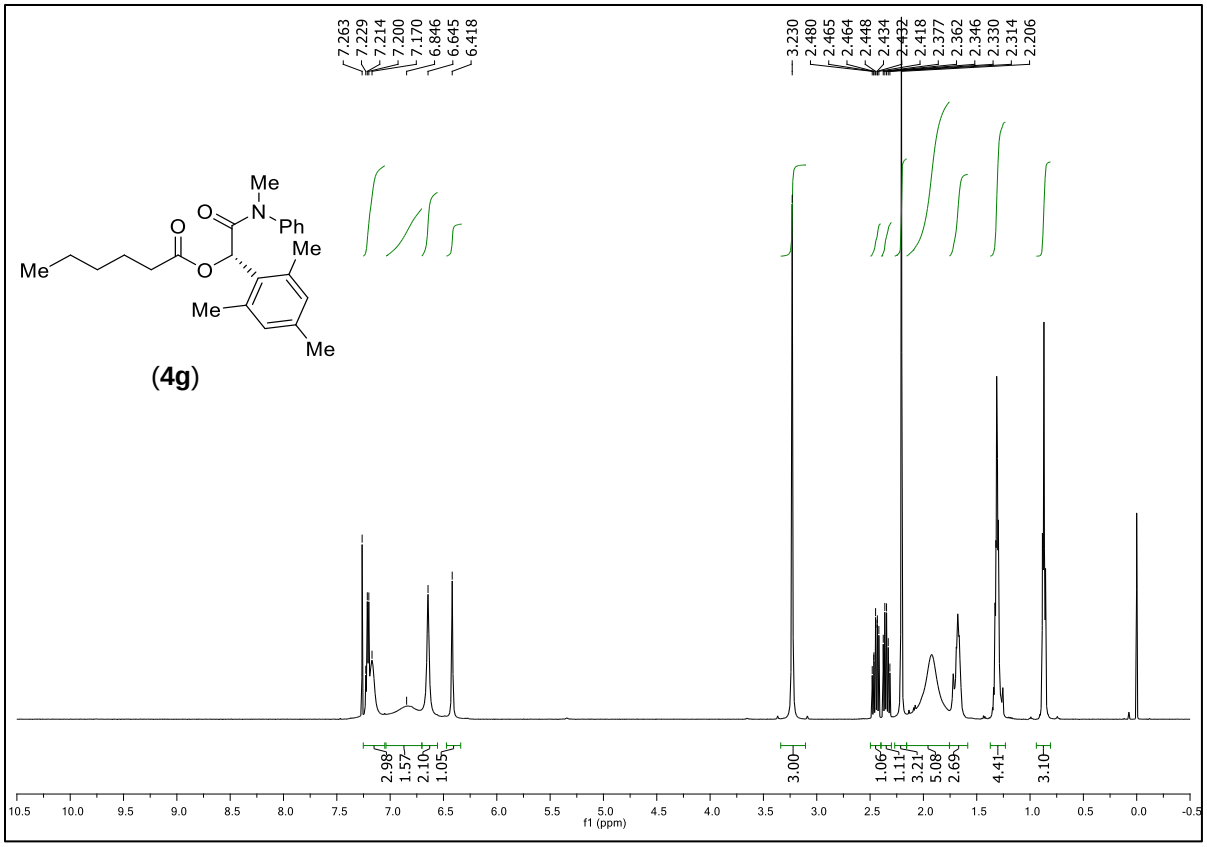
7.263
7.229
7.214
7.200
7.170
6.846
6.645
6.418
3.230
2.480
2.465
2.464
2.448
2.434
2.432
2.418
2.377
2.362
2.346
2.330
2.314
2.206
Me
N
Ph
O
O
Me
Me
Me
Me
(4g)
2.98
1.57
2.10
1.05
3.00
1.06
1.11
3.21
5.08
2.69
4.41
3.10
f1 (ppm)

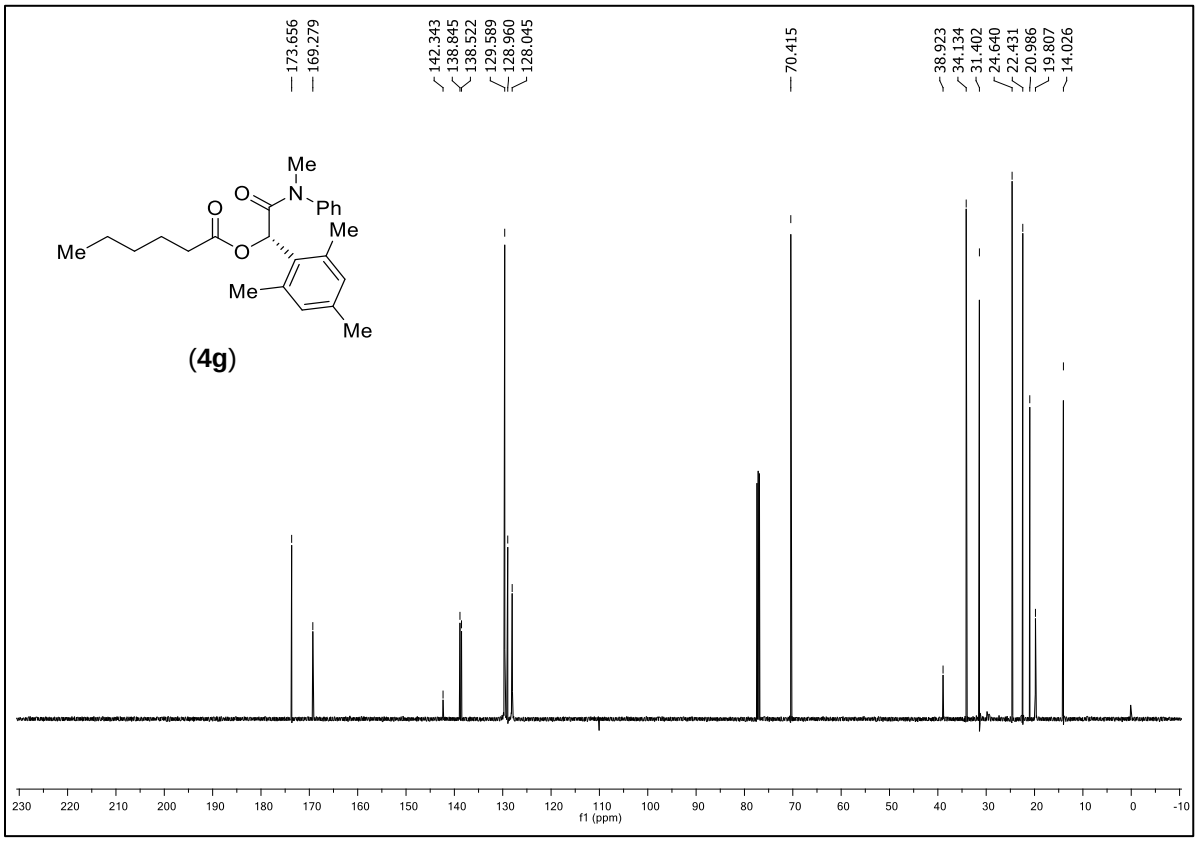
173.656
169.279
142.343
138.845
138.522
129.589
128.960
128.045
70.415
38.923
34.134
31.402
24.640
22.431
20.986
19.807
14.026
Me
N
Ph
O
O
Me
Me
Me
Me
(4g)
f1 (ppm)

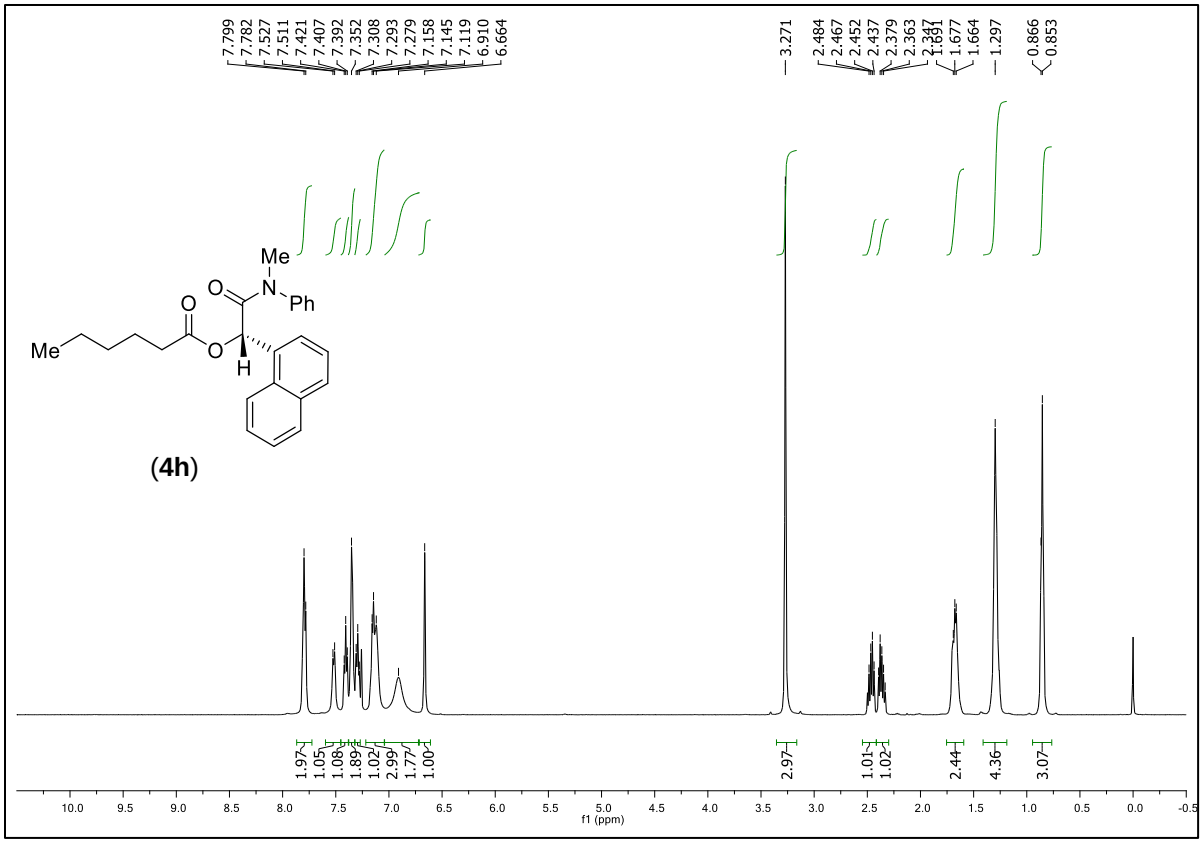
7.799
7.782
7.527
7.511
7.421
7.407
7.392
7.352
7.308
7.293
7.279
7.158
7.145
7.119
6.910
6.664
3.271
2.484
2.467
2.452
2.437
2.379
2.363
2.347
1.691
1.677
1.664
1.297
0.866
0.853
Me
N
Ph
O
O
Me
O
H
1.97
1.05
1.08
1.89
1.02
2.99
1.77
1.00
2.97
1.01
1.02
2.44
4.36
3.07
f1 (ppm)

(**4h**)

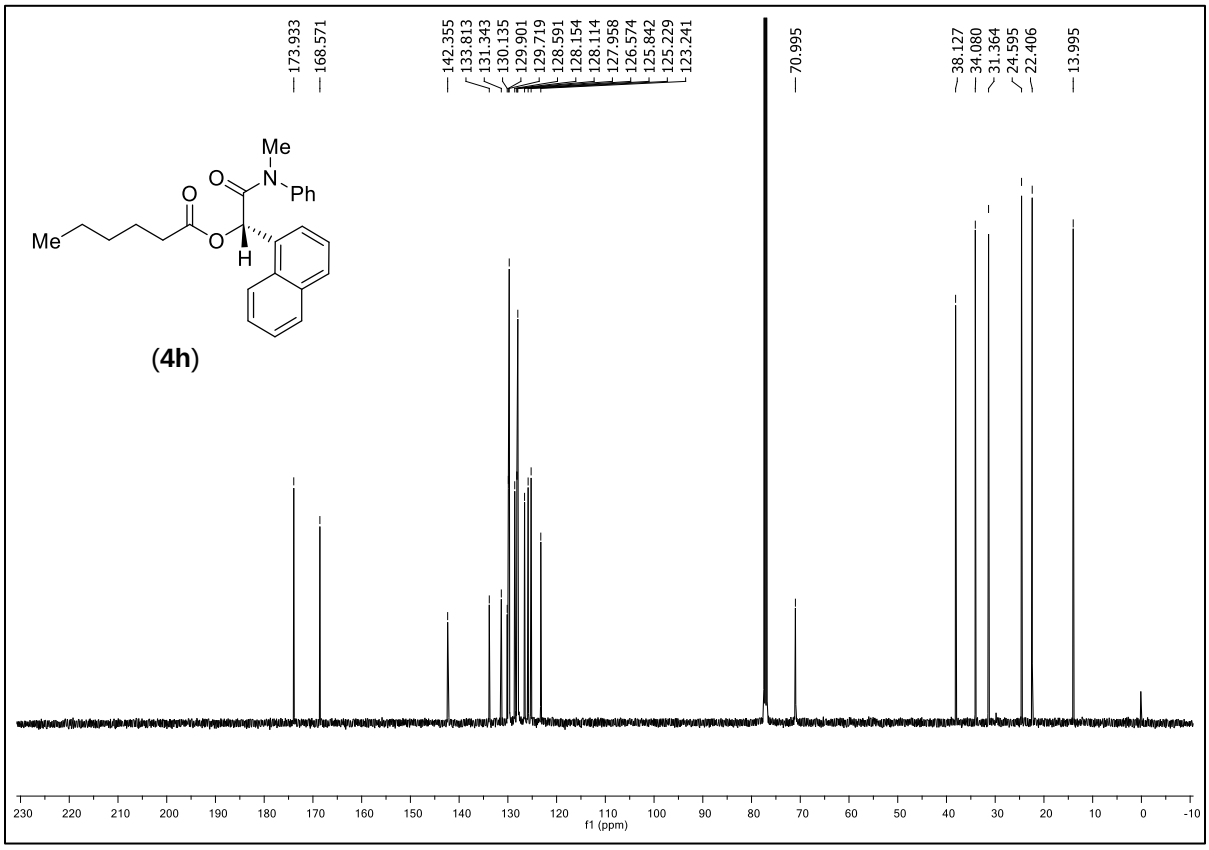
173.933
168.571
142.355
133.813
131.343
130.135
129.901
129.719
128.591
128.154
128.114
127.958
126.574
125.842
125.229
123.241
70.995
38.127
34.080
31.364
24.595
22.406
13.995
Me
N
Ph
O
O
Me
O
H
f1 (ppm)

(**4h**)

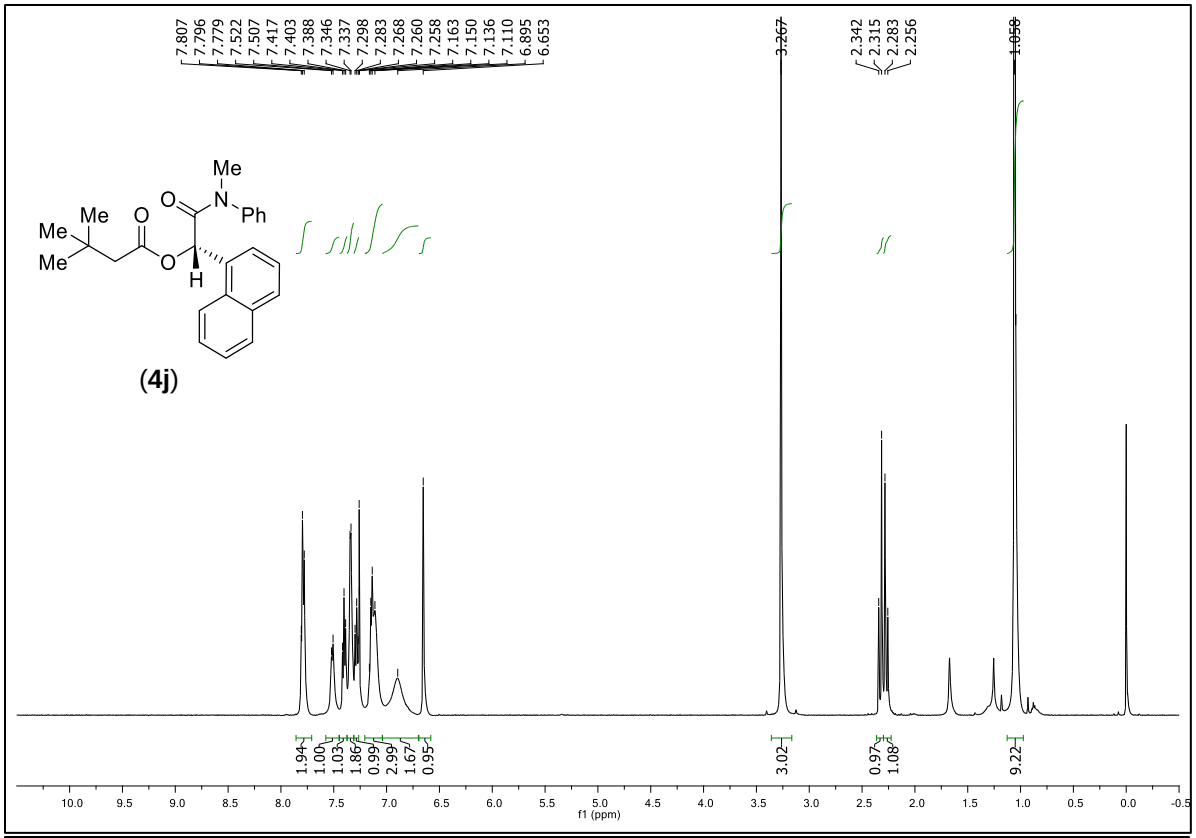
7.807
7.796
7.779
7.522
7.507
7.417
7.403
7.388
7.346
7.337
7.298
7.283
7.268
7.260
7.258
7.163
7.150
7.136
7.110
6.895
6.653
3.267
2.342
2.315
2.283
2.256
1.058
Me
N
Ph
O
Me
Me
O
O
H
(4j)
1.94
1.00
1.03
1.86
0.99
2.99
1.67
0.95
3.02
0.97
1.08
9.22
f1 (ppm)

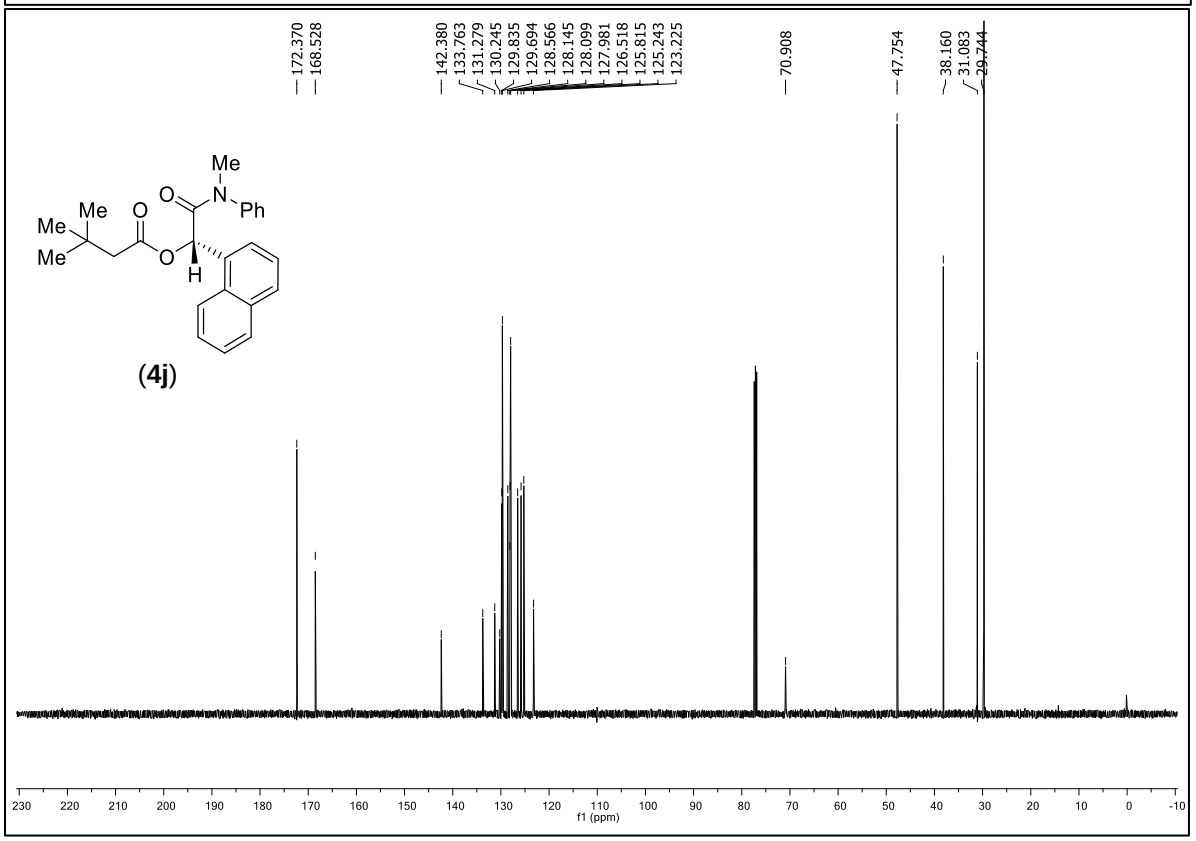
172.370
168.528
142.380
133.763
131.279
130.245
129.835
129.694
128.566
128.145
128.099
127.981
126.518
125.815
125.243
123.225
70.908
47.754
38.160
31.083
29.744
Me
N
Ph
O
Me
Me
O
O
H
(4j)
f1 (ppm)

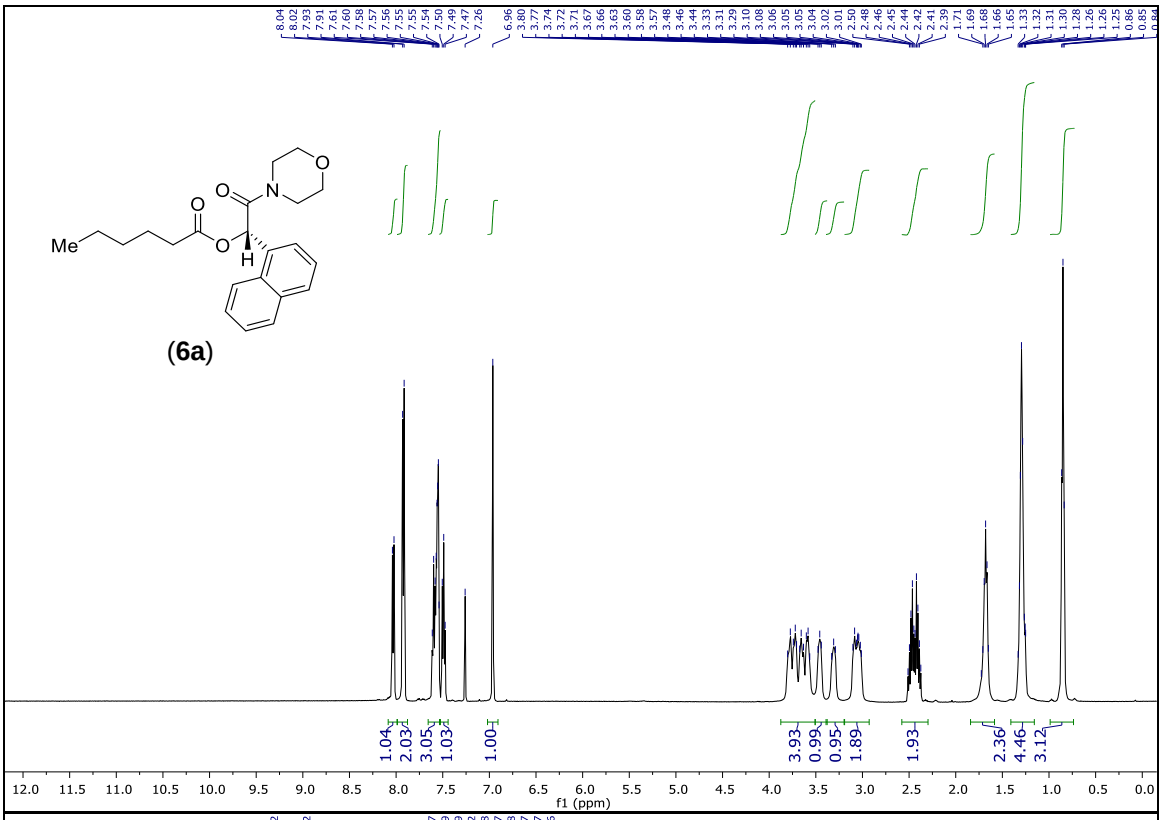
Me
O
O
N
O
O
H
(6a)
f1 (ppm)

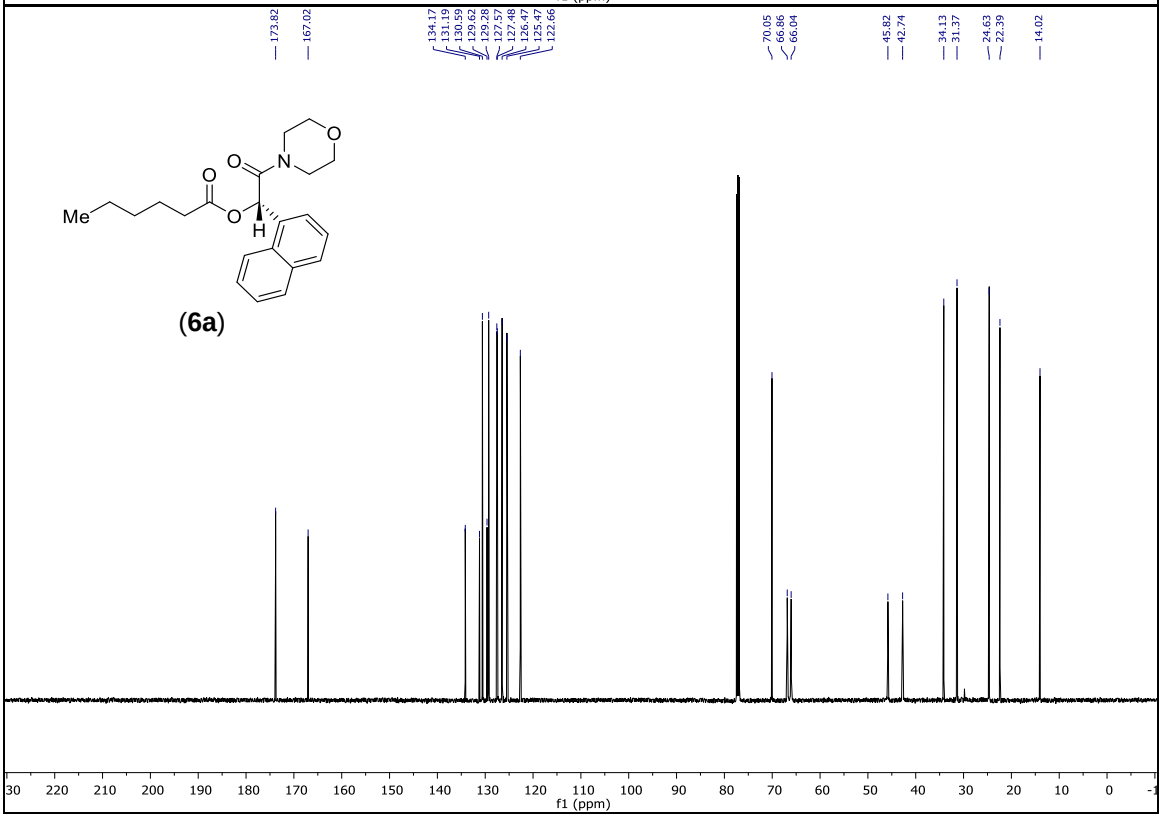
Me
O
O
N
O
O
H
(6a)
f1 (ppm)

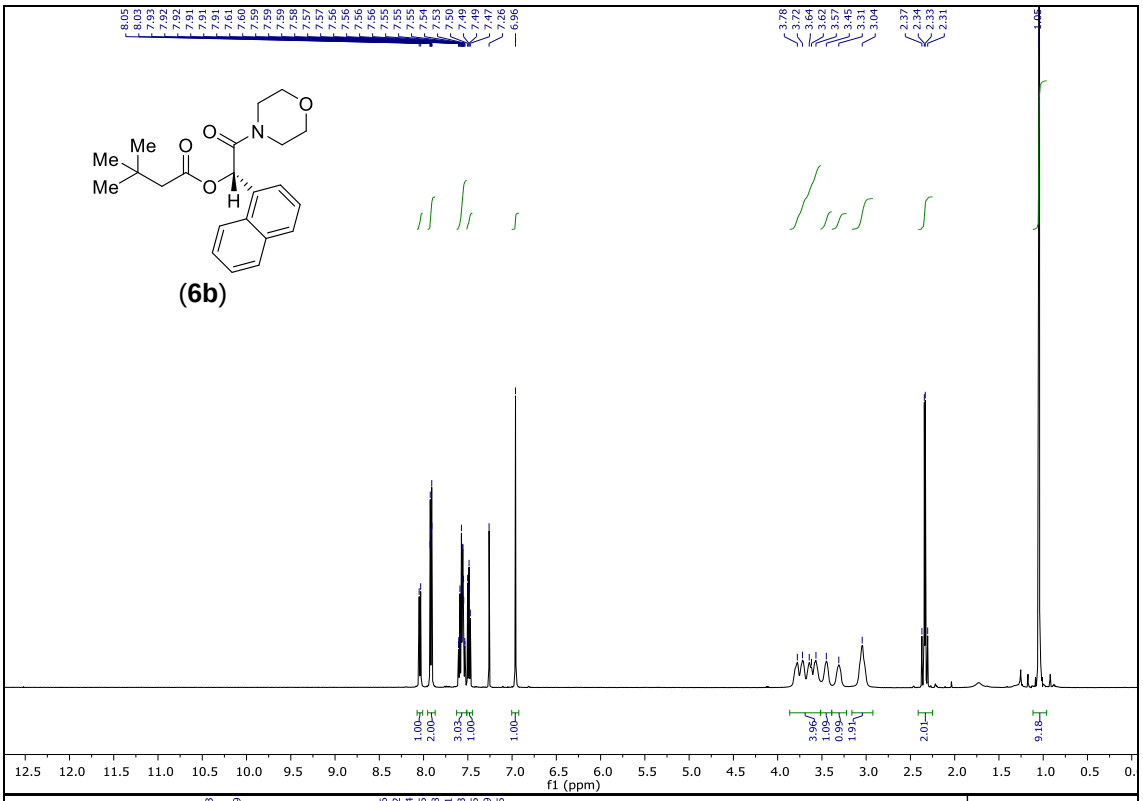
Me
Me
O
O
N
O
O
H
(6b)
f1 (ppm)

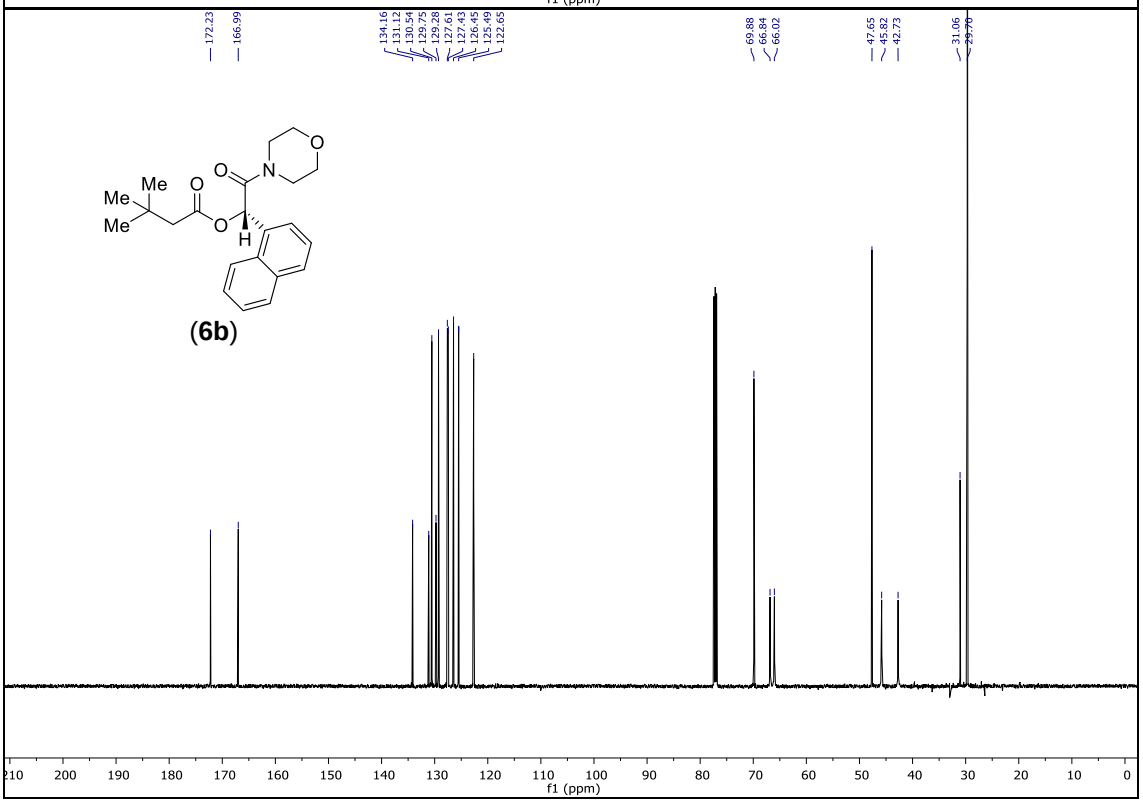
Me
Me
O
O
N
O
O
H
(6b)
f1 (ppm)

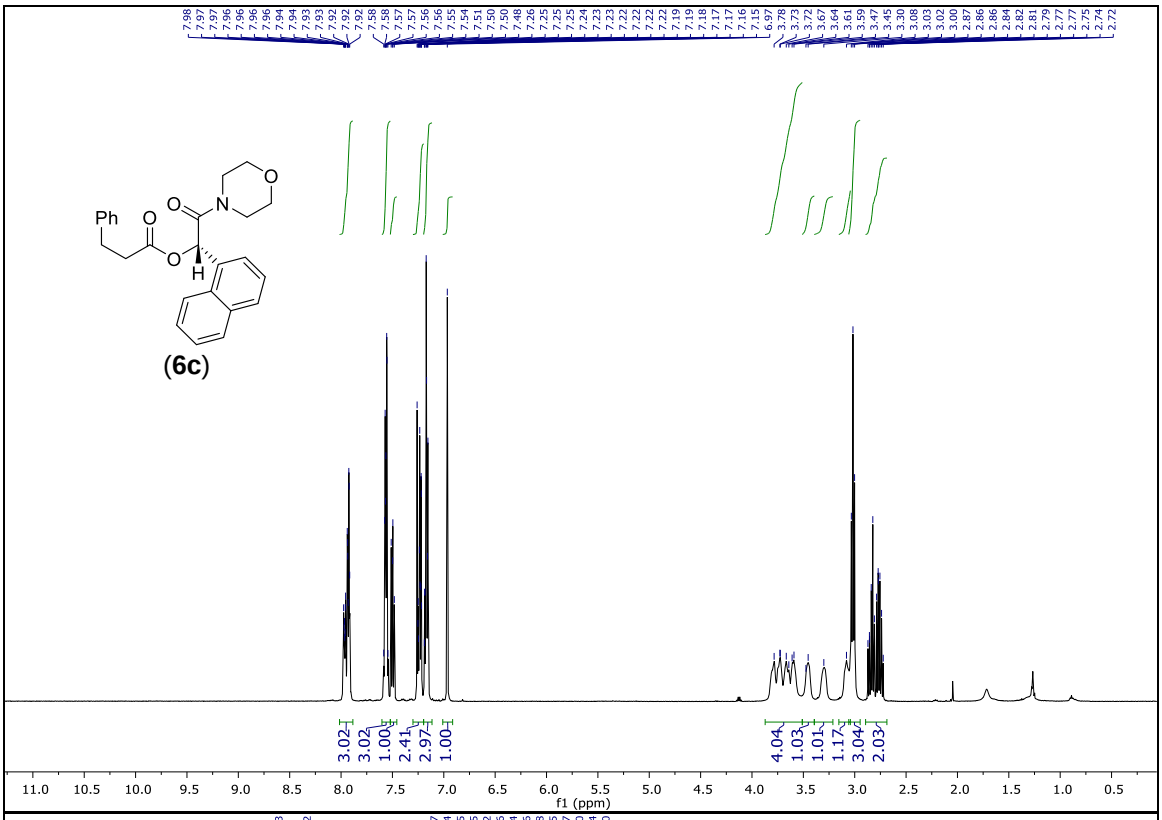
Ph
O
O
N
O
O
H
(6c)
3.02
3.02
1.00
2.41
2.97
1.00
4.04
1.03
1.01
1.17
3.04
2.03
f1 (ppm)

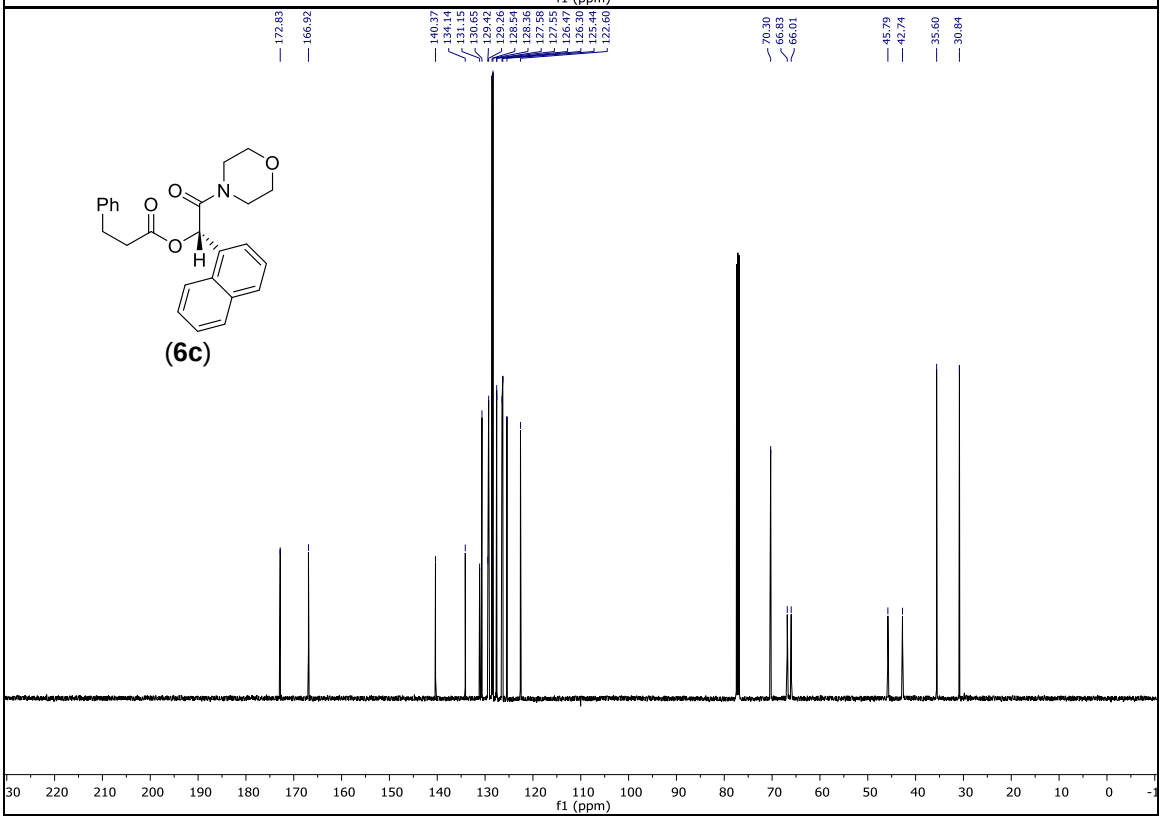
172.83
166.92
140.37
134.14
131.15
130.65
129.42
129.26
128.54
128.36
127.58
127.55
126.47
126.30
125.44
122.60
70.30
66.83
66.01
45.79
42.74
35.60
30.84
Ph
O
O
N
O
O
H
(6c)
f1 (ppm)

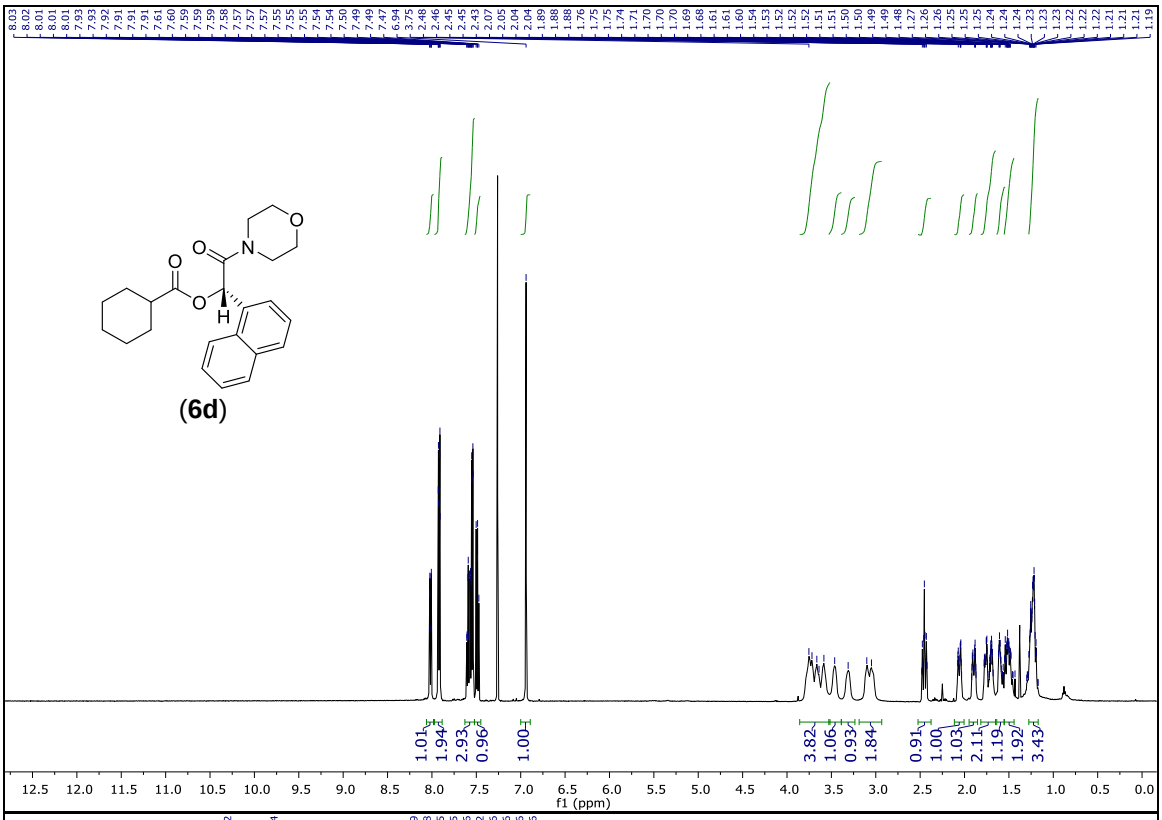
(6d)
f1 (ppm)

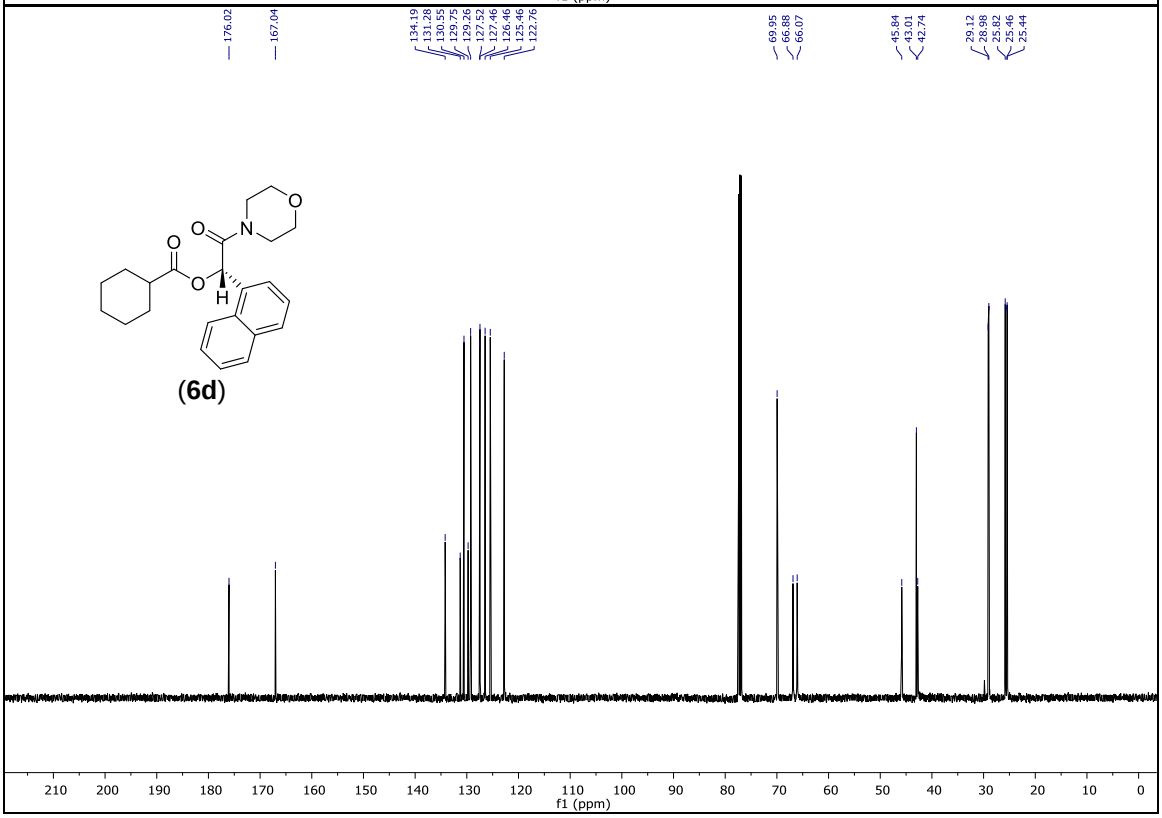
(6d)
f1 (ppm)

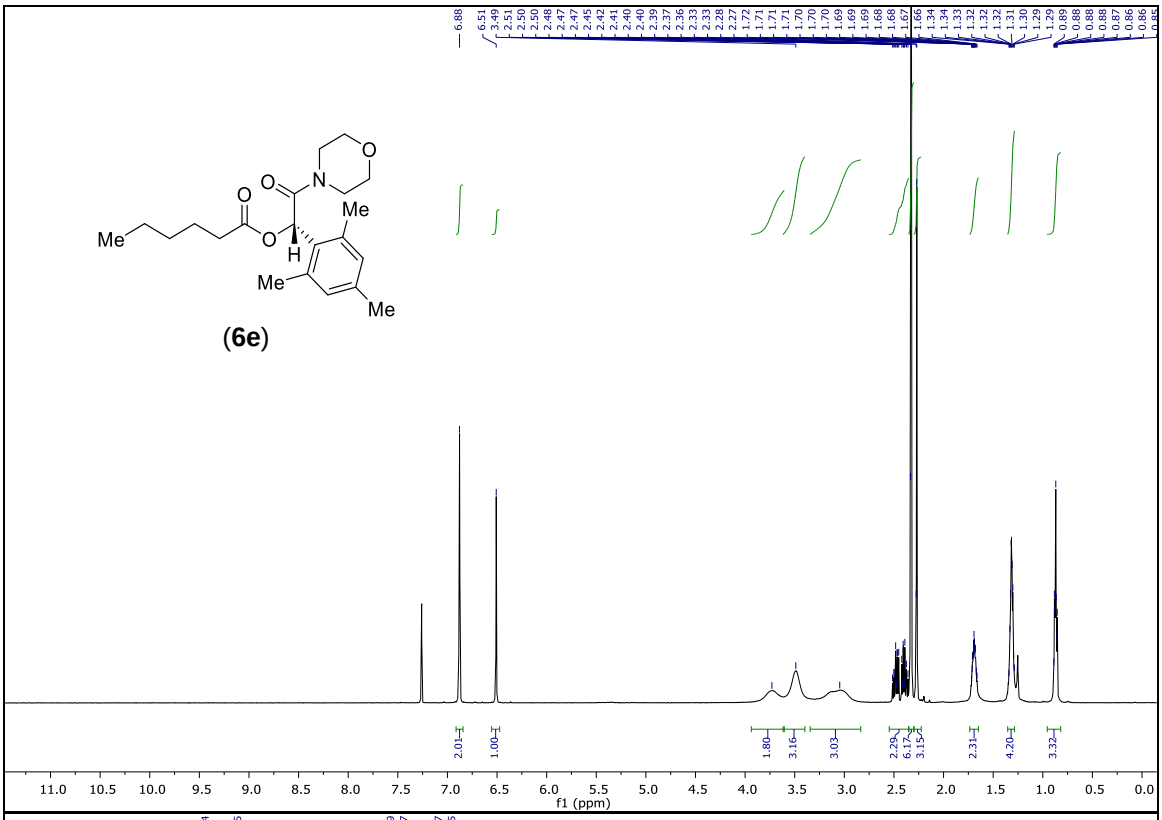
(6e)
f1 (ppm)

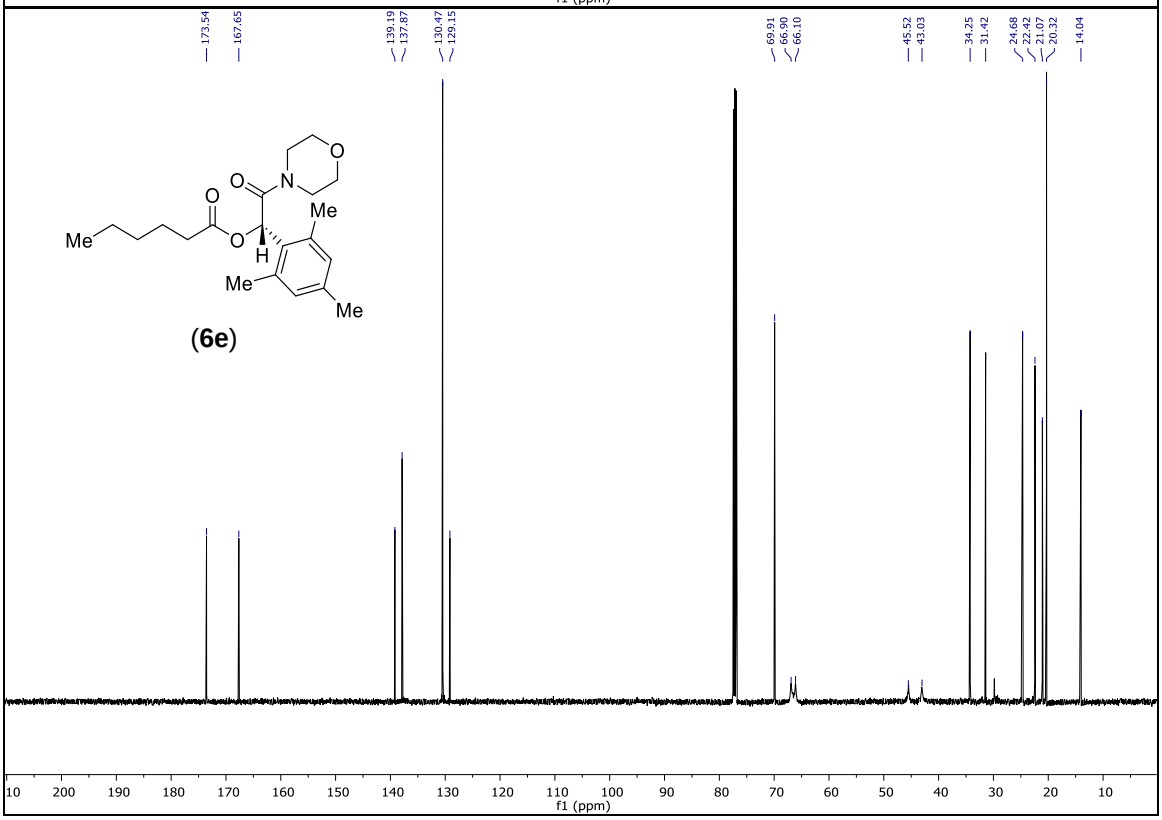
(6e)
f1 (ppm)

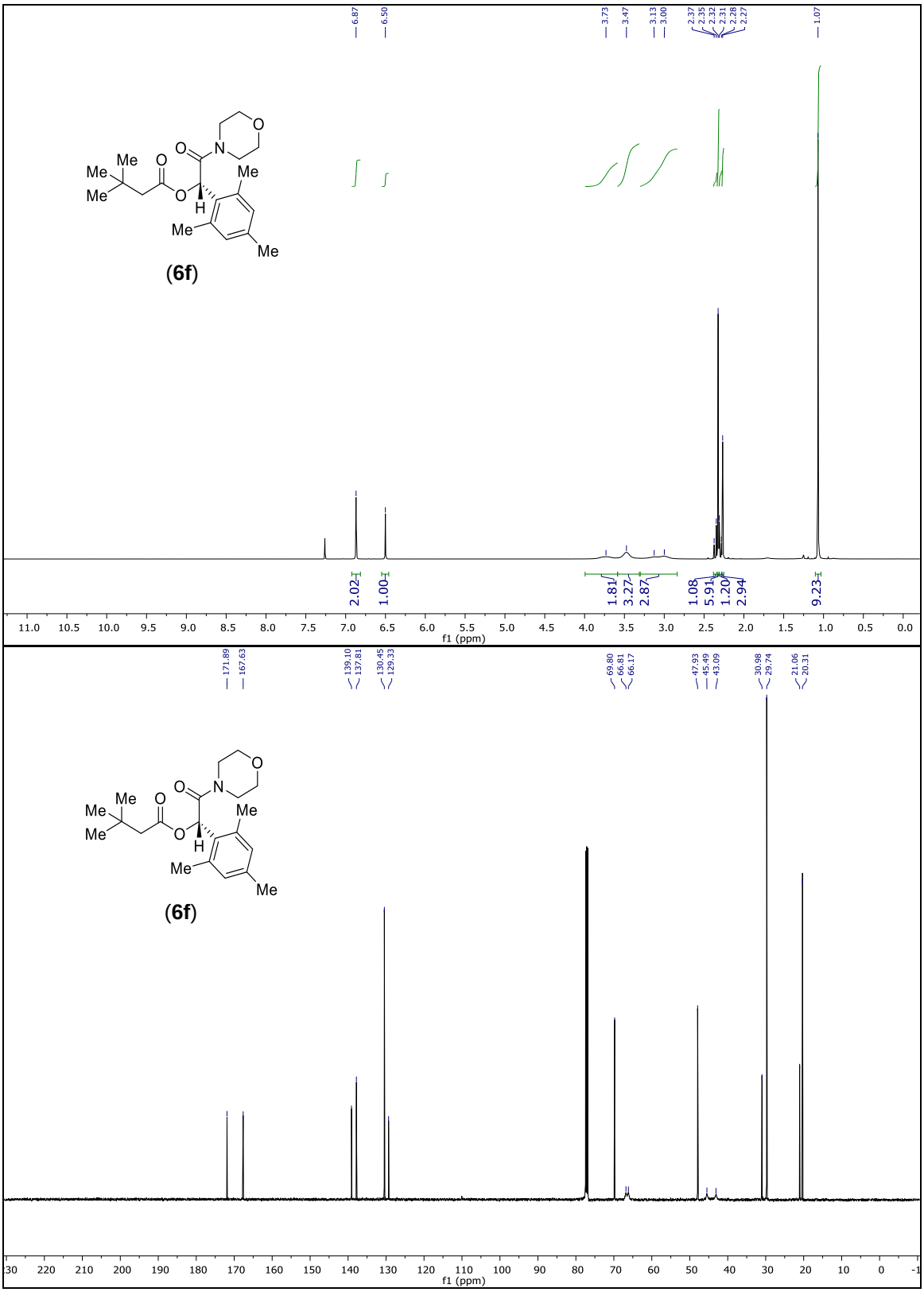

2.2.3 Chiral HPLC Data

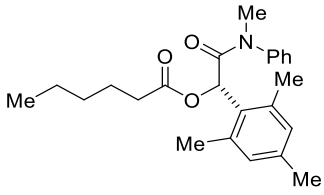

(±)-4g

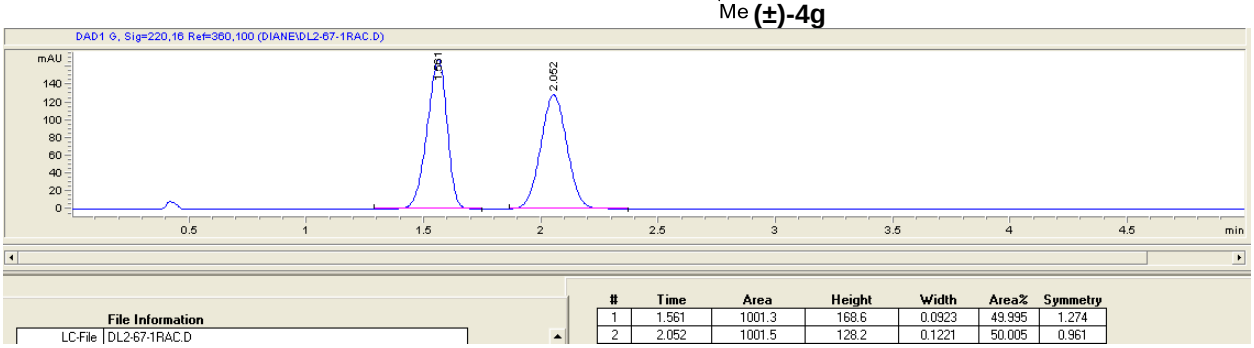

#	Time	Area	Height	Width	Area%	Symmetry
1	1.561	1001.3	168.6	0.0923	49.995	1.274
2	2.052	1001.5	128.2	0.1221	50.005	0.961

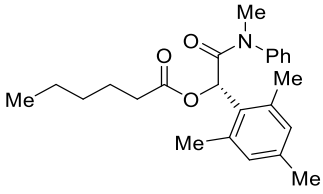

(+)-4g

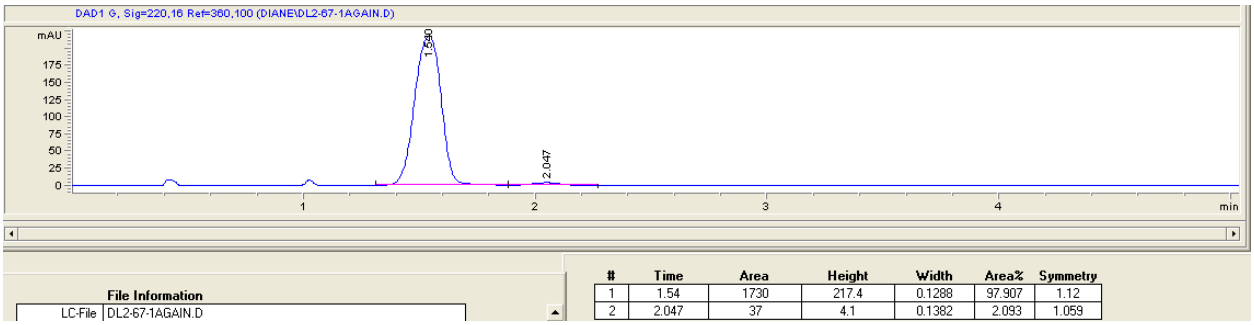

#	Time	Area	Height	Width	Area%	Symmetry
1	1.54	1730	217.4	0.1288	97.907	1.12
2	2.047	37	4.1	0.1382	2.093	1.059

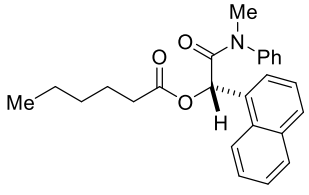

(±)-4h

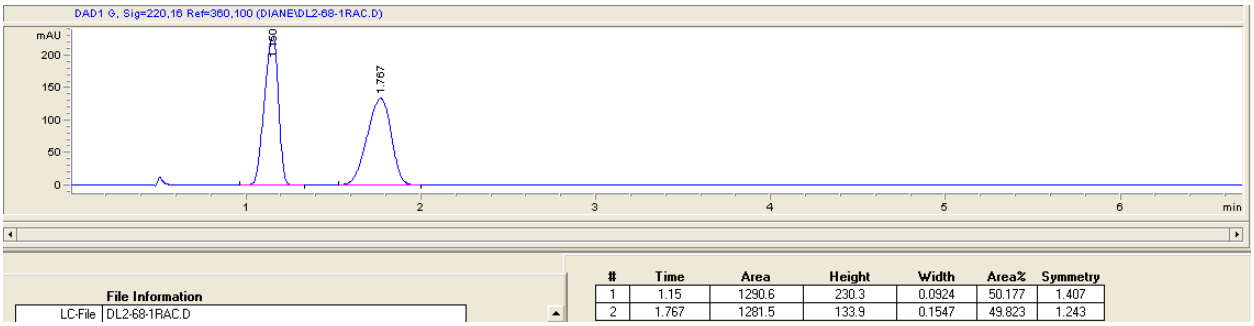

#	Time	Area	Height	Width	Area%	Symmetry
1	1.15	1290.6	230.3	0.0924	50.177	1.407
2	1.767	1281.5	133.9	0.1547	49.823	1.243

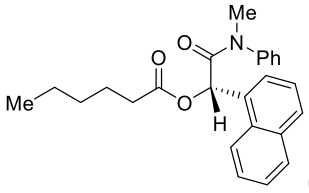

(+)-4h

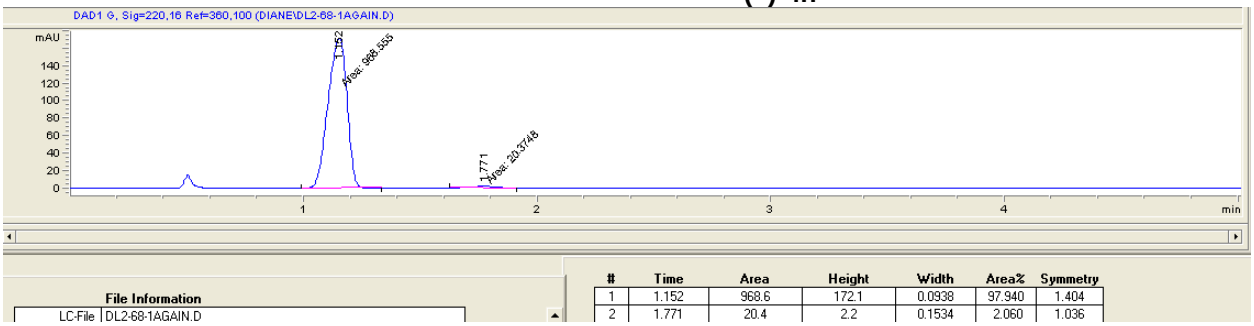

#	Time	Area	Height	Width	Area%	Symmetry
1	1.152	968.6	172.1	0.0938	97.940	1.404
2	1.771	20.4	2.2	0.1534	2.060	1.036

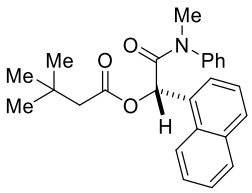

(±)-4j

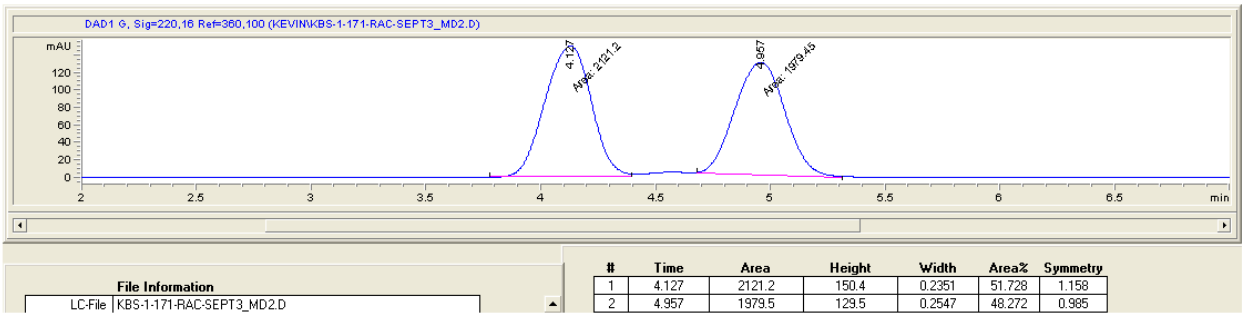

File Information

LC-File	KBS-1-171-RAC-SEPT3_MD2.D

#	Time	Area	Height	Width	Area%	Symmetry
1	4.127	2121.2	150.4	0.2351	51.728	1.158
2	4.957	1979.5	129.5	0.2547	48.272	0.985

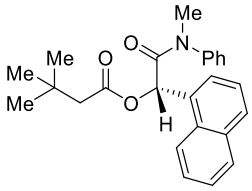

(+)-4j

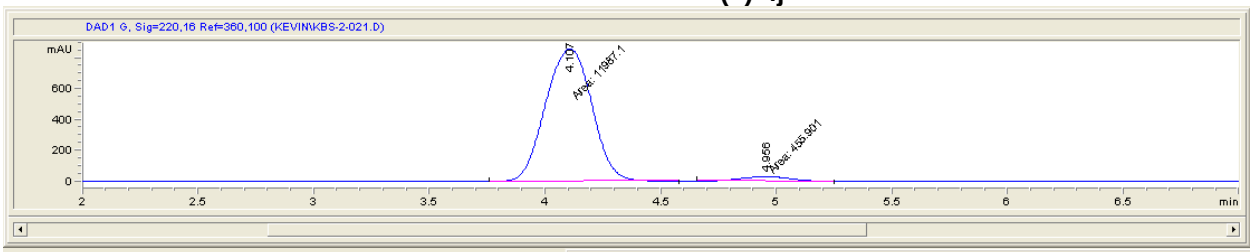

File Information

LC-File	KBS-2-021.D

#	Time	Area	Height	Width	Area%	Symmetry
1	4.107	11987.1	858.6	0.2327	96.336	1.078
2	4.956	455.9	30.1	0.2526	3.664	1.1

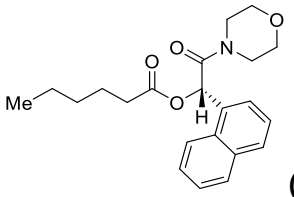

(±)-6a

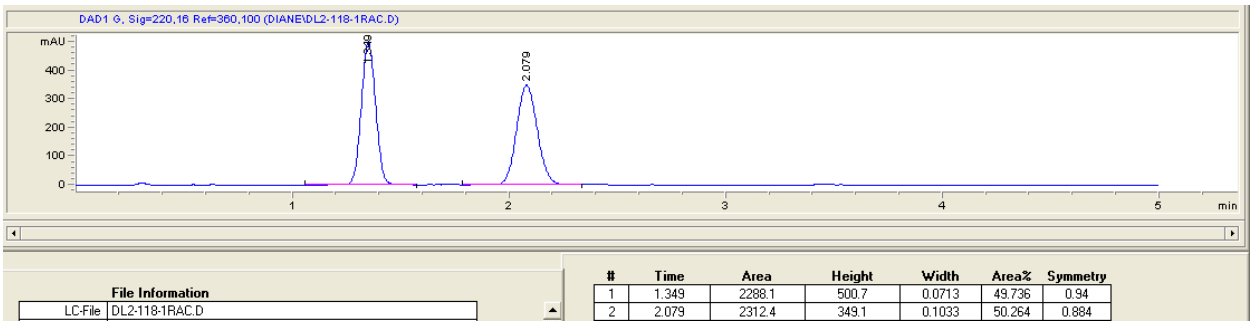

File Information

LC-File	DL2-118-1RAC.D

#	Time	Area	Height	Width	Area%	Symmetry
1	1.349	2288.1	500.7	0.0713	49.736	0.94
2	2.079	2312.4	349.1	0.1033	50.264	0.884

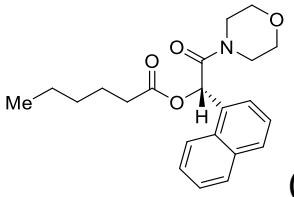

(+)-6a

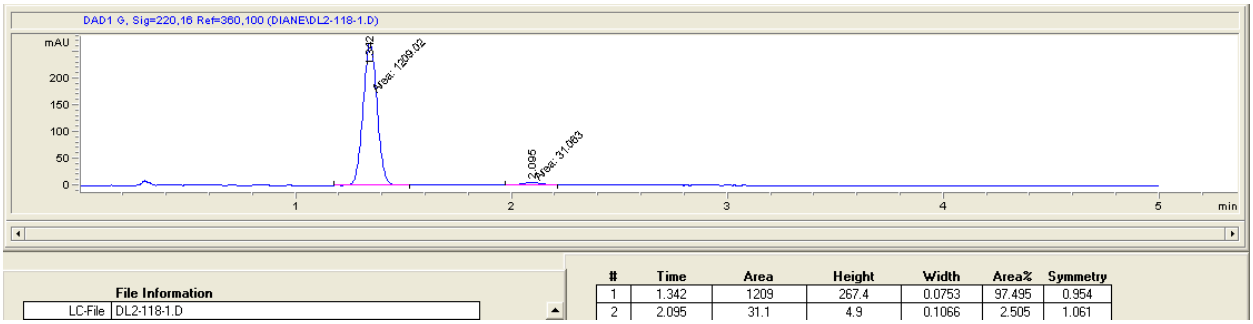

File Information

LC-File	DL2-118-1.D

#	Time	Area	Height	Width	Area%	Symmetry
1	1.342	1209	267.4	0.0753	97.495	0.954
2	2.095	31.1	4.9	0.1066	2.505	1.061

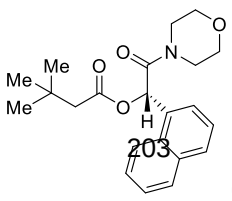

(±)-6b

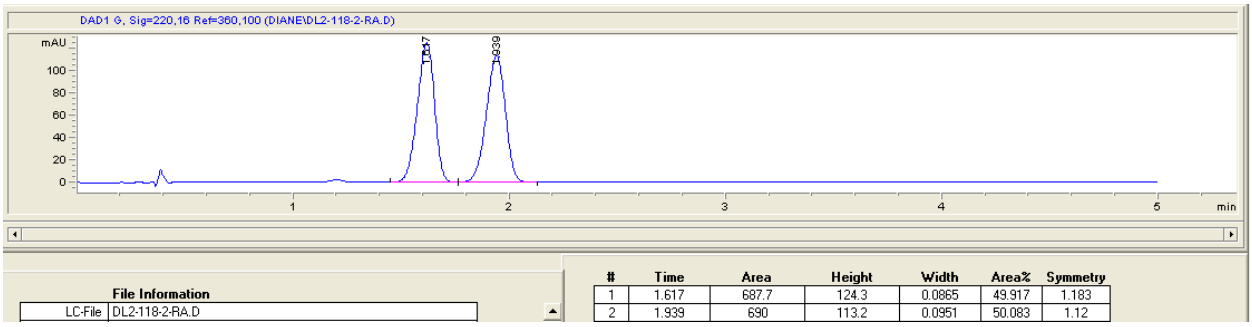

File Information

LC-File	DL2-118-2-RA.D

#	Time	Area	Height	Width	Area%	Symmetry
1	1.617	687.7	124.3	0.0865	49.917	1.183
2	1.939	690	113.2	0.0951	50.083	1.12

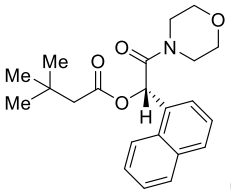

(+)-6b

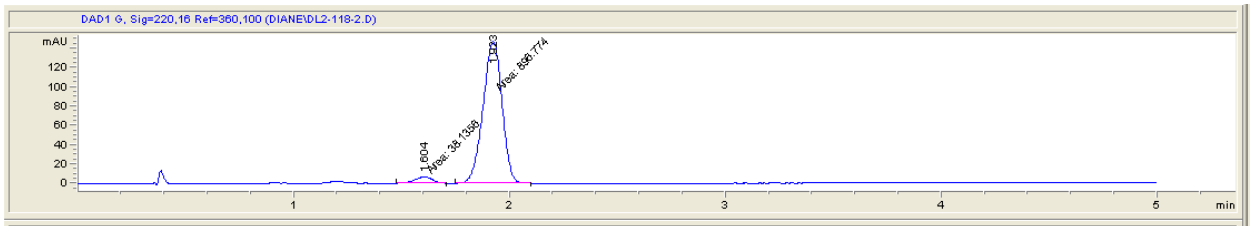

File Information

LC-File	DL2-118-2.D

#	Time	Area	Height	Width	Area%	Symmetry
1	1.604	38.1	6.7	0.0949	4.079	1.206
2	1.923	896.8	146.8	0.1018	95.921	1.117

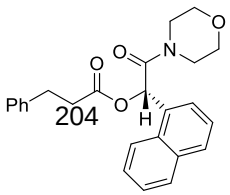

(±)-6c

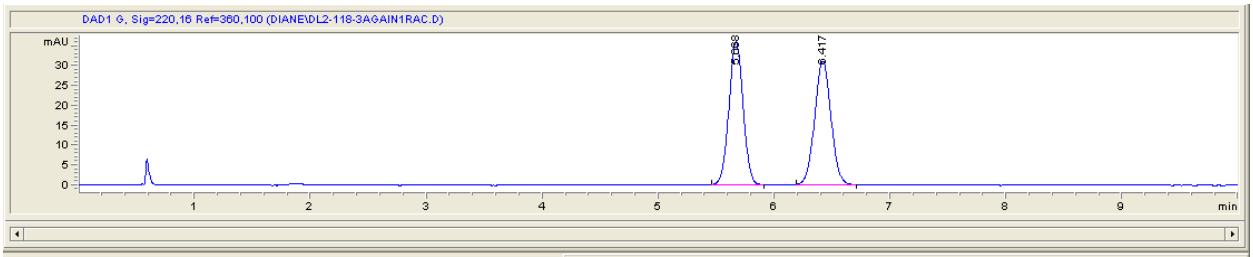

File Information

LC-File	DL2-118-3AGAIN1RAC.D

#	Time	Area	Height	Width	Area%	Symmetry
1	5.668	307.5	36	0.1305	50.049	0.962
2	6.417	306.9	31.1	0.153	49.951	0.963

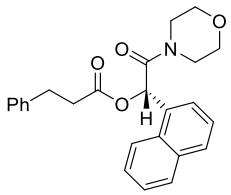

(+)-6c

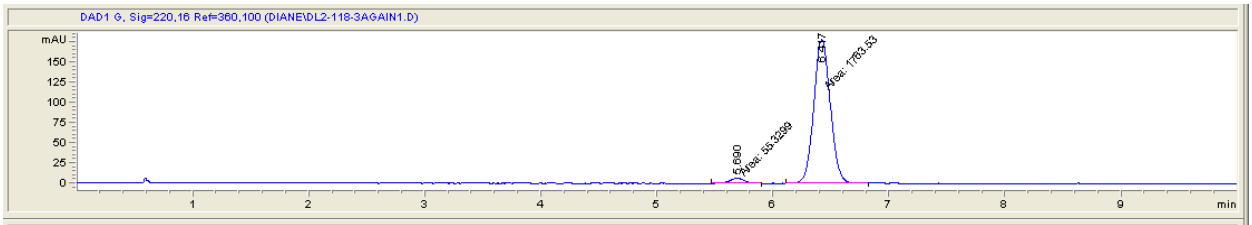

File Information

LC-File	DL2-118-3AGAIN1.D

#	Time	Area	Height	Width	Area%	Symmetry
1	5.69	55.3	6.3	0.1453	3.042	0.959
2	6.417	1763.5	177.8	0.1653	96.958	0.895

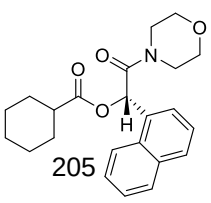

(+)-6d

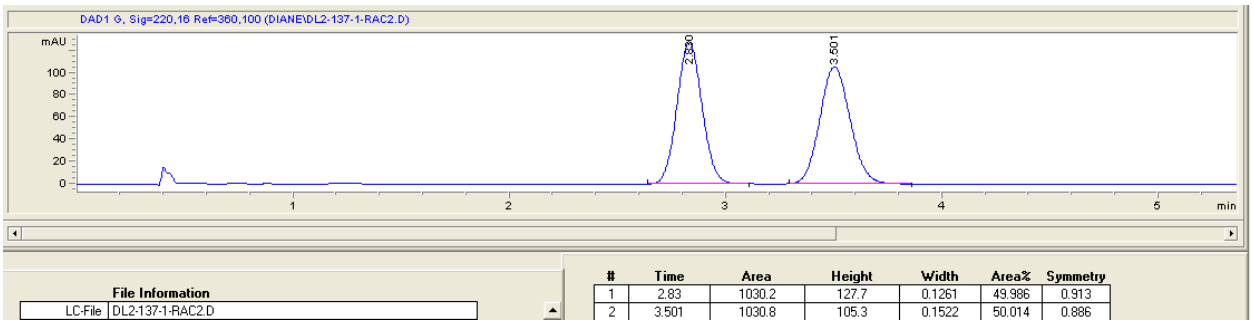

#	Time	Area	Height	Width	Area%	Symmetry
1	2.83	1030.2	127.7	0.1261	49.986	0.913
2	3.501	1030.8	105.3	0.1522	50.014	0.886

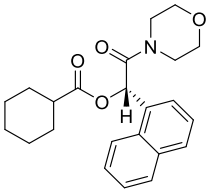

(+)-6d

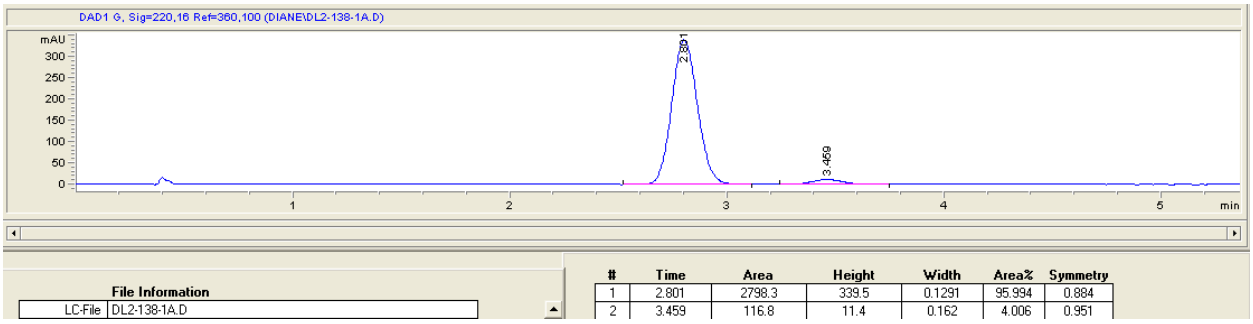

#	Time	Area	Height	Width	Area%	Symmetry
1	2.801	2798.3	339.5	0.1291	95.994	0.884
2	3.459	116.8	11.4	0.162	4.006	0.951

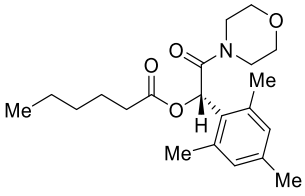

(±)-6e

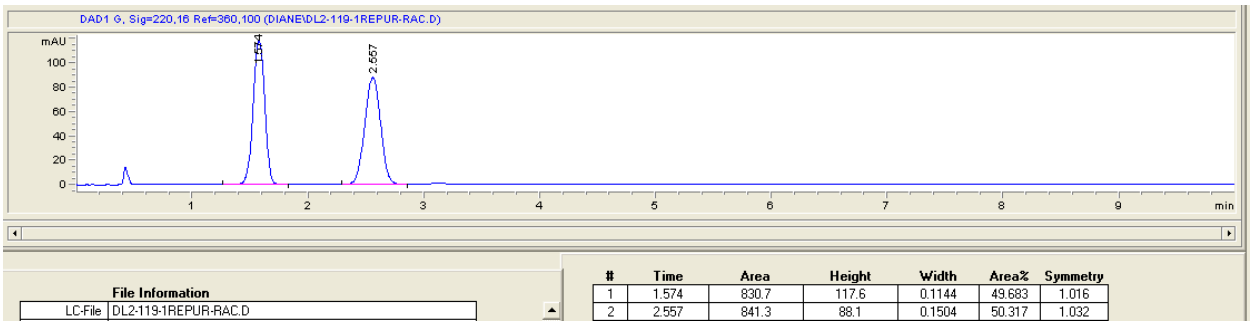

#	Time	Area	Height	Width	Area%	Symmetry
1	1.574	830.7	117.6	0.1144	49.683	1.016
2	2.557	841.3	88.1	0.1504	50.317	1.032

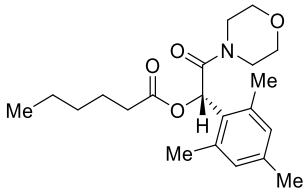

(+)-6e

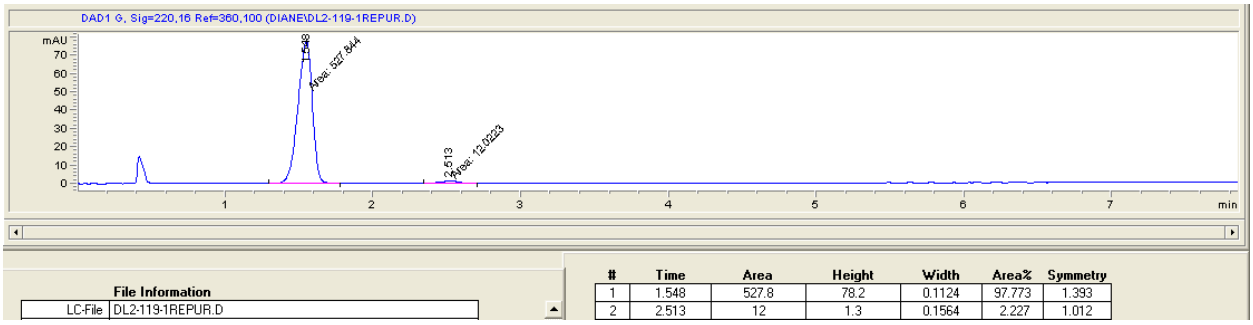

#	Time	Area	Height	Width	Area%	Symmetry
1	1.548	527.8	78.2	0.1124	97.773	1.393
2	2.513	12	1.3	0.1564	2.227	1.012

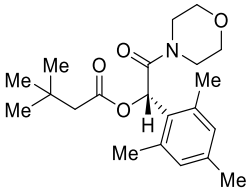

(±)-6f

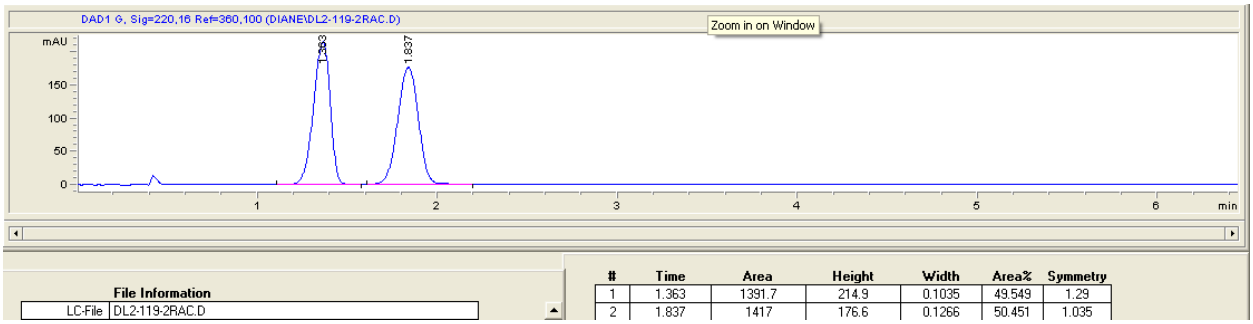

#	Time	Area	Height	Width	Area%	Symmetry
1	1.363	1391.7	214.9	0.1035	49.549	1.29
2	1.837	1417	176.6	0.1266	50.451	1.035

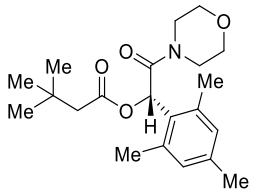

(±)-6f

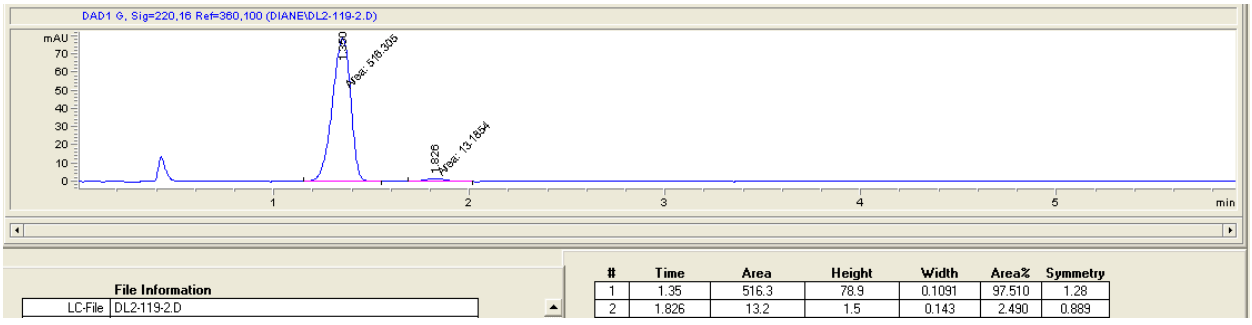

#	Time	Area	Height	Width	Area%	Symmetry
1	1.35	516.3	78.9	0.1091	97.510	1.28
2	1.826	13.2	1.5	0.143	2.490	0.889

CHAPTER 3 – Regioselective Functionalization of Carbohydrates

3.1 Cu(II)-Catalyzed Regioselective Functionalization of Monosaccharides*

3.1.1 Introduction

As an abundant natural resource, monosaccharides appear to be ideal feedstocks for constructing medicines,[102] fuels,[103] and polymers.[104] In particular, they find importance in cellular communication,[105] structural recognition,[106] and cancer treatment.[107] The majority of these oligosaccharides are generated through chemical synthesis.[108] These sugars are generally difficult to derivatize, however, due to their many reactive hydroxyl sites. Organotin-based methods can be used to achieve selective transformation of various sugars[109] en route to valuable oligosaccharides, including anti-cancer vaccines.[108,110] To replace these toxic stoichiometric reagents, catalytic strategies have emerged, featuring Lewis acid-catalysis (e.g., Matsumura's organotin chloride and Taylor's borinic acids)[111,112] (Figure 3.1) and organocatalysis (e.g., Kawabata's chiral DMAP, Miller's peptides, Tan's scaffolding imidazole, and Nagorny's phosphoric acid).[113-116] Designing catalytic methods for site-selective transformations with carbohydrates represents a valuable goal that promises to streamline access to oligosaccharides.

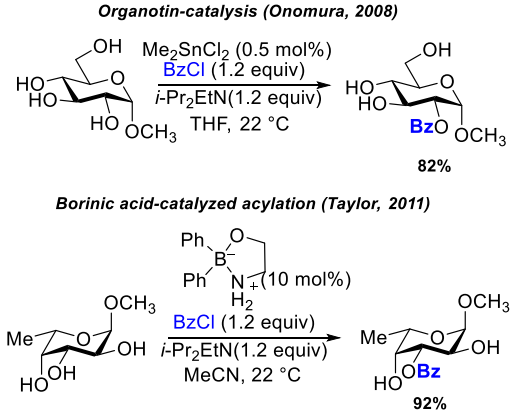

Figure 3.1 Catalytic advances to functionalize carbohydrate derivatives

* Adapted from Chen, I.-H.; Kou, K. G. M.; Le, D. N.; Rathbun C. M.; Dong, V. M. *Chem. Eur. J.* **2014**, *20*, 5013 with permission from John Wiley & Sons.

Herein, we report that chiral copper complexes are versatile catalysts for the regioselective functionalization of monosaccharides. Our findings complement and corroborate Allen and Miller's independent report.[117] In comparison to current strategies, copper-catalysis allows easy tailoring of the catalyst to (a) transform a wide range of sugars and (b) control site-selectivity by ligand choice.

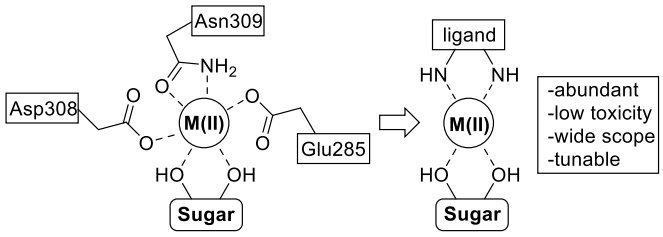

Figure 3.2 Inspiration from lectin

Our study draws inspiration from lectins, proteins that recognize sugars with high specificity through diol coordination to a metal center (*e.g.*, Ca, Mn, and Cu).[118-120] By analogy to these natural metallopeptides, we reasoned that synthetic metal complexes bearing a chiral ligand, would similarly bind and possibly activate sugars for selective functionalization (Figure 3.2). We chose to investigate copper on the basis of reports where stoichiometric salts (*e.g.*, $Cu(acac)_2$ and $Cu(TFA)_2$) were used to promote acylation of sugars.[121,122] As summarized in Figure 3.3, we imagined that the appropriate ligands ($\mathbf{L^n}$) on copper would allow selective activation of hydroxyl groups in a wide range of sugars, including both pyranosides and furanosides.[123] Besides enhancing regiocontrol, the ligand should promote catalysis. Indeed, Onomura has reported chiral copper(II) catalysts for desymmetrization of *meso*-1,2-vicinal diols.[124] While widely applied in enantioselective catalysis, the use of chiral copper complexes for site-selective transformations warrants study.

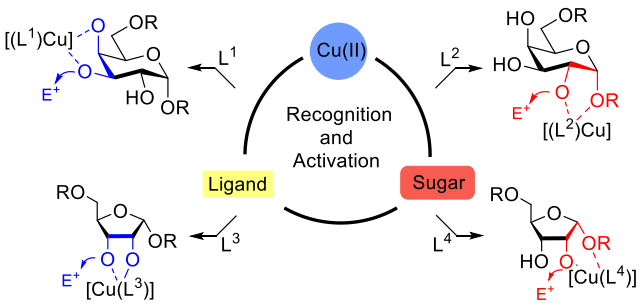

Figure 3.3 Proposed ligand-controlled site-selective binding with Cu(II) complexes

3.1.2 Development of Cu(II)-Catalyzed Regioselective Functionalization

Inspired by solution studies,[118] that demonstrate copper complexes are capable of coordinating to sugars, we studied the benzoylation of α-glucopyranoside **1a** (Table 3.1). The silyl group protects the primary alcohol leaving three secondary hydroxyl groups for possible functionalization. A control experiment in the absence of copper salts displayed no reactivity. In the absence of ligand, no catalyst turnover is observed: use of 10 mol% copper(II) triflate yields less than 10% benzoylation after 16 hours. Nitrogen-based ligands known to coordinate well to copper(II) (e.g., bipyridine, terpyridine and 1,10-phenanthroline) do not promote catalysis. The privileged chiral bisoxazoline (Box, **L1**–**L3**) and pyridine bisoxazoline (PyBox, **L4** and **L5**) structures, however, enable catalyst turnover (33 to 90% yields).[125,126] In all cases, the 2-*O*-acylated isomer **2aa** is formed as the major product with regiocontrol (3:1 to >20:1, Table 3.1). The minor products include 4-*O*-acylated **2aa'** and dibenzoylated **3a**. The absolute configuration of the ligand impacts

selectivity. For example, (*R,R*)-Ph-PyBox **L4** yields benzoylation with 7:1 selectivity in favor of 2-*O*-benzoylated **2aa**, while its enantiomer (**L5**) gives >20:1 selectivity.

Table 3.1 Selective acylation of α-glucopyranosides

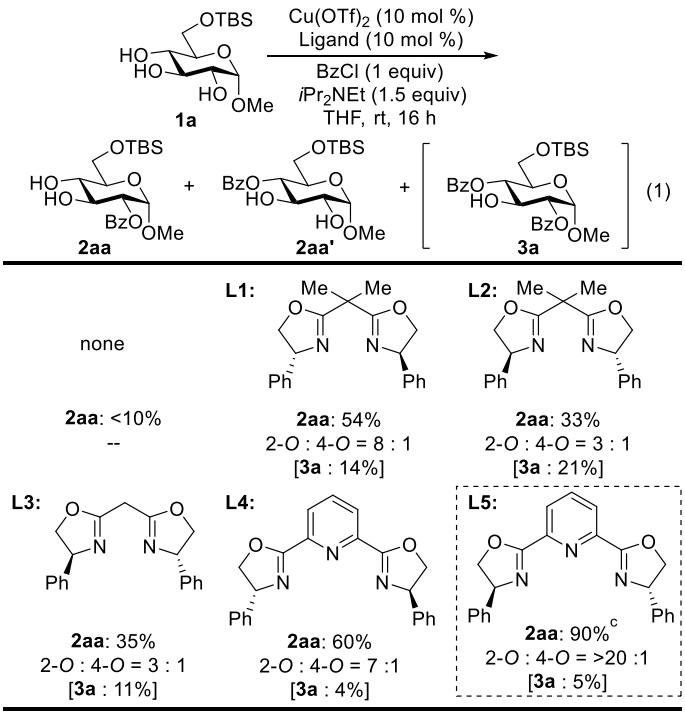

[a] Yields for **2aa** and **3a** determined by ^{1}H NMR spectroscopy. [b] The selectivity between **2aa** and **2aa'** was determined by ^{1}H NMR. The 3-*O* acylated product was not observed by ^{1}H NMR. [c] DCM used instead of THF; In THF, 87% yield and 16:1 selectivity is obtained.

With copper-**L5** catalyst in hand, we found that α-glucopyranosides undergo acylation with a wide range of electrophiles (Table 3.2). Both aromatic and aliphatic acid chlorides are effective electrophiles (74–84% yields, entries 1–4). Commonly used protecting groups such as Cbz and Fmoc can be incorporated (83% and 71% yields, entries 5–6). Glucose derivative **1b** containing a 4,6-*O*-benzylidene acetal undergoes acylation to provide 2-*O*-benzoylated **2b** in 83% yield and >20:1 regioselectivity.

Table 3.2 Substrate scope evaluation for selective acylation of *α*-glucopyranosides [a][b]

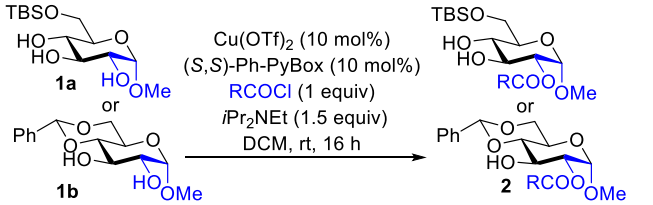

Entry	Substrate	Acyl Chloride	Product	Yield(%)	2-*O* : 4-*O*
1	**1a**	BzCl	**2aa**	84	>20:1
2	**1a**	2-NO_2−C_6H_4COCl	**2ab**	80	>20:1
3	**1a**	*i*PrCOCl	**2ac**	82	9:1
4	**1a**	Piv−Cl	**2ad**	74	>20:1
5	**1a**	Cbz−Cl	**2ae**	83	15:1
6	**1a**	Fmoc−Cl	**2af**	71	7:1
7	**1b**	BzCl	**2b**	83	>20:1

[a] Isolated yields. [b] Selectivity ratios determined by ^{1}H NMR spectroscopy.

The site-selective benzoylation of pyranoside derivatives containing *cis*-diol motifs was also examined. In particular, subjecting α-mannopyranoside **2** and α-rhamnopyranoside **3** to catalytic amounts (10 mol%) of $Cu(OTf)_2$ and (*S,S*)-Ph-PyBox or *(S,S)*-PhBox to benzoylate gives 3-*O* acylated **2a** and **3a** in high yields (74% to 94%) and regioselectivity (9:1 to >20:1) (eq 1 and 2).

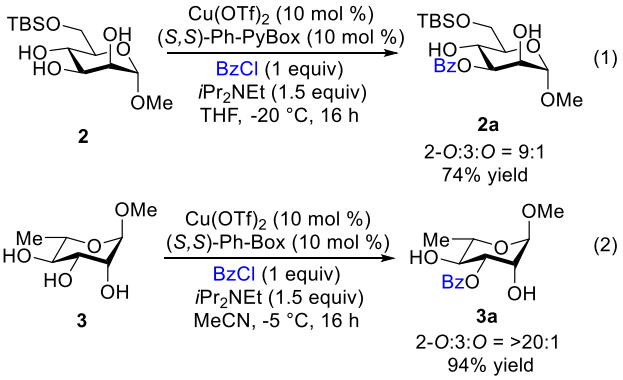

Although glucopyranosides do not contain a *cis*-diol, this transformation occurs presumably through copper activation at the anomeric ether and the adjacent 2-hydroxyl group to form a five-membered metallacycle, analogous to previously proposed organotin

complexes.[127] This binding renders the 2-hydroxyl group more acidic and thus more prone to deprotonation. The activated 2-hydroxyl group reacts with benzoyl chloride to form the 2-*O*-acylated product.

In the cases where 3-*O* acylated **2a** and **3a** are formed, the copper also coordinates to the *cis*-diol motif to form five-membered metallacycles (Figure 3.4). We hypothesize that the equatorial hydroxyl group of the copper metallacycle to be the most sterically accessible and therefore undergoes nucleophilic attack to provide the major regioisomer, which is in agreement with previous work by Evtushenko using stoichiometric $Cu(TFA)_2$ salts.[122]

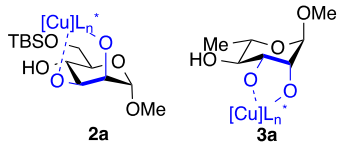

Figure 3.4 Copper(II) activation of *cis*-diol motifs

3.1.3 Expansion of Methodology to Furanosides

Subsequently, this copper(II)-catalyzed methodology was extended to the site-selective functionalization of furanosides. Model substrate β-ribofuranoside **5** is obtained in 20% yield over two steps from D-ribose **4** (eq 3). The primary alcohol is protected with a trityl group to aid solubility in organic solvents.

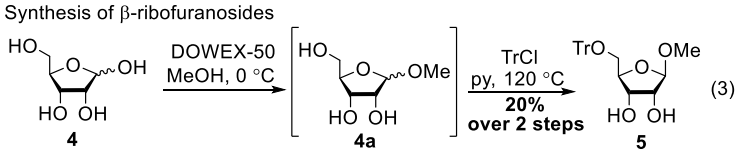

Initial experiments were performed with benzoyl chloride as the electrophile (Table 3.3). In the presence of $Cu(OTf)_2$ and (*S,S*)-Ph-PyBox, low regioselectivies are observed between the 3-*O*-acylated **5a** and 2-*O*-acylated **5a'** (entry 1). In the absence of $Cu(OTf)_2$ and ligand, background reactivity gave 66% conversion to a 1:1 regiomeric mixture of acylated product (entry 2).

Table 3.3 Benzoylation of β-ribofuranoside **5**

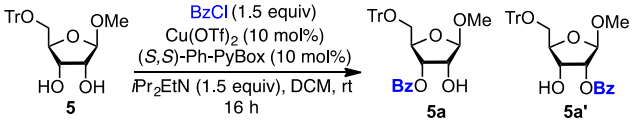

Entry	Catalyst/ligand	Temperature(°C)	% conversion[a]	3-*O*:2-*O*[a]
1	$Cu(OTf)_2$/(*S,S*)-Ph-PyBox	-30	100	2:1
2	——	-30	66	1:1

[a] Conversions and regiomeric ratios determined by ^{1}H-NMR analysis of the unpurified reaction mixture

The use of tosyl chloride as the electrophile was subsequently investigated for this transformation (Table 3.4). Under the conditions of catalytic $Cu(OTf)_2$ and (*S,S)*-Ph-PyBox (10 mol%), at −18 ˚C, >20:1 regioselectivity is observed and 3-*O*-tosylated **5b** is isolated in 75% yield (entry 1). At 0 ˚C, tosylation occurs to give 3-*O*-tosylated **5b** as the major regioisomer (18:1 regioselectivity and 67% yield, entry 2). When the temperature is increased to 22 ˚C and 40 ˚C, the regioselectivity decreases to 15:1 and 10:1, respectively (entries 3 and 4). Notably, the background reaction proceeds with low conversion (16%) at −10 ˚C and a 1:1 regiomeric mixture is obtained in the absence of Cu-Ph-PyBox catalyst.

Table 3.4 Copper(II)-catalyzed regioselective tosylation of β-ribofuranoside 5

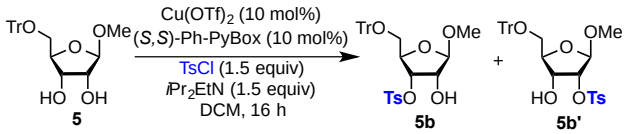

Entry	Temperature (°C)	Yield (%)[a]	3-*O*:2-*O*[b,c]
1	-18	75	>20:1
2	0	67	18:1
3	22	75	15:1
4	40	68	10:1

[a] Isolated yield of **5b**. [b] Ratios determined by ^{1}H-NMR analysis of the unpurified reaction mixture. [c] In the absence of $Cu(OTf)_2$ and (*S,S*)-Ph-PyBox, 1:1 regiomeric mixture observed.

With the optimized reaction conditions, preliminary studies were carried out on the scope of the sulfonylation (Table 3.5). When the electrophile is switched to 2-nitrobenzenesulfonyl chloride, 3-*O*-tosylated **5c** is formed in >20:1 regioselectivity and 49% yield (entry 1). Pentafluorobenzene sulfonyl chloride also furnishes 3-*O*-tosylated **5d** in 5:1 selectivity and 65% yield (entry 2). However, when methanesulfonyl chloride or trifylsulfonyl chloride are used, no product formation occurs and decomposition of the starting material to a mixture of products that were not identified is observed (entries 3 and 4).

Table 3.5 Copper(II)-catalyzed tosylation of β-ribofuranoside **5** using various sulfonyl chloride

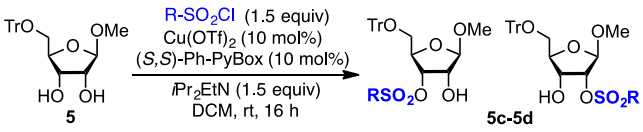

Entry	R=	Product	Yield (%)[a]	3-*O*:2-*O*[b]
1		**5c**	49%	>20:1
2	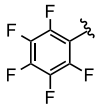	**5d**	65%	5:1
3		—	—	—
4		—	—	—

[a] Isolated yield of 3-*O* tosylated product. [b] Ratios determined by ^{1}H-NMR analysis of the unpurified reaction mixture.

Next, the effect of the chiral ligand on regioselectivity was investigated. We were particularly interested in studying α-ribofuranoside **6** because it contains two *cis*-dioxygen motifs, both of which can bind copper. This renders the system potentially amenable to a ligand-controlled switch in regioselectivity. Various reaction conditions were examined and a variety of nitrogen-based ligands were surveyed to test the hypothesis of reversing regioselectivity (Table 3.6). When (*S,S)*-Ph-PyBox **L6** is used as ligand, 1:3.8

regioselectivity is observed in favor of the 3-*O*-acylated **6b** in DCM, while (*R,R*)-Ph-PyBox **L5** affords 2-*O*-acylated **6a** as the major regioisomer with 5.5:1 regioselectivity in THF (86% yield). Moreover, the choice of solvent (either DCM or THF) is important to achieve the desired regioselectivity. The use of (*S,S*)-Ph-Box **L2** gives 3-*O*-acylated **6b** in increased 6:1 regioselectivity and 69% yield when DCM is used as solvent.

However, no reversal of regioselectivity is observed when enantiomeric (*R,R*)-PhBox **L1** is used, and 3-*O*-acylated **6b** is obtained as the major regioisomer in a modest 3.2:1 regioselectivity. Moreover, a switch in regioselectivity is also observed for the benzoylation process using (*S,S*)-Ph-EtPyBox **L7** to afford 3-*O* acylated **6b** in 3.2:1 regioselectivity and (*R,R*)-Ph-EtPyBox **L8** to give 2-*O* acylated **6a** in 3:1 regioselectivity.

Table 3.6 Ligand-controlled switch in regioselectivity using copper(II) catalysis [a,b]

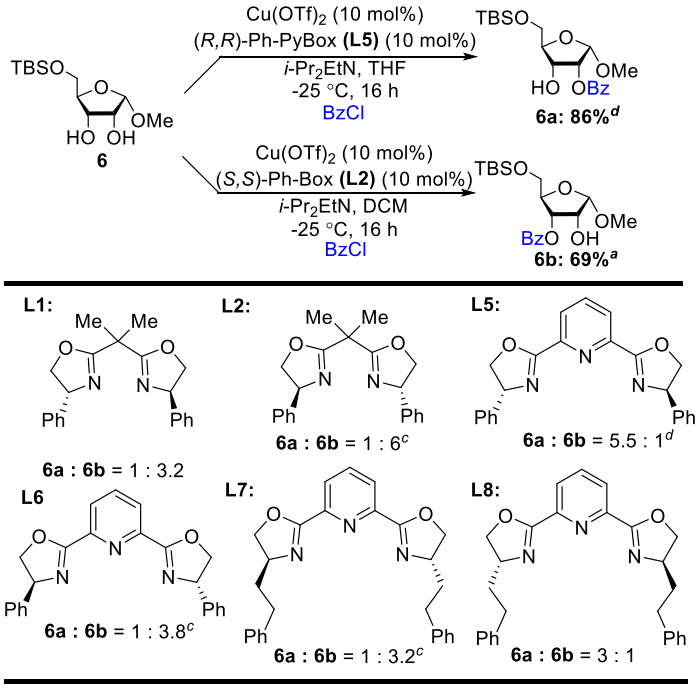

[a] Isolated yield. [b] Ratios determined by ^{1}H-NMR analysis of the unpurified reaction mixture. [c] DCM used instead of THF [d] Isolated as a mixture of isomers

Next, a switch in regioselectivity was observed when $Ca(OTf)_2$ was used in place of $Cu(OTf)_2$. The reaction proceeds to furnish 2-*O*-tosylated **5b'** in moderate conversion (38%) and regioselectivity (2.3:1) in THF solvent (Table 3.7, entry 1). Furthermore, using 2-nitrobenzene sulfonyl chloride gives the 2-*O*-tosylated **5c'** in 44% and 2:1 regioselectivity (entry 2), while pentafluorobenzene sulfonyl chloride gives 2-*O*-tosylated **5d'** in 56% conversion and 5.5:1 regioselectivity (entry 3).

Table 3.7 Switch in regioselectivity using $Ca(OTf)_2$

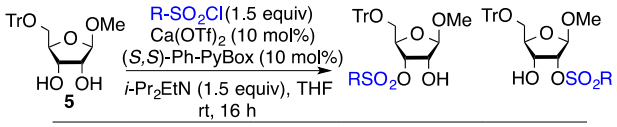

Entry	R	Product	% conversion[a]	3-*O*:2-*O*[a]
1	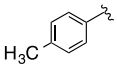	**5b'**	38	1:2.3
2		**5c'**	44	1:2
3	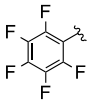	**5d'**	56	1:5.5

[a] Conversions and ratios were determined by ^{1}H-NMR analysis of the unpurified reaction mixture.

Overall, site-selective transformation of furanosides via copper(II)-catalysis forms functionalized sugars in high yields and regioselectivities. Although there have been extensive conformational studies on furanosides,[128] there has been little development in the study of their overall reactivity and selectivity. Furanosides exist in a puckered form, where they can interconvert between two different conformations: C2 and C3 endo (Figure 3.5). Because of this equilibrium, we speculate that the observed

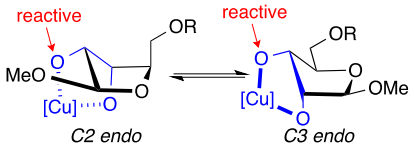

Figure 3.5 Interconversion between C2 and C3 endo

regioselectivity is due to a combination of metal, ligand, and solvent effects, which will influence the favorability of one conformation over the other. This hypothesis is consistent with the observed switch in regioselectivity when a calcium(II) salt is used instead of copper(II). In addition, the electrophile has a significant effect on regioselectivity. When more reactive electrophiles such as benzoyl chloride are employed, low regioselectivity is observed (2:1, Table 3.3, entry 1). In contrast, the use of weaker electrophiles such as sulfonyl chloride derivatives furnishes tosylated sugars in high regioselectivity (>20:1, table 3.4, entry 1). Similar to our explanation for achieving regioselectivity in the pyranoside examples, we believe that the 2-*O* and 3-*O* regioselectivity of the furanosides arises from copper activation of the more accessible equatorial hydroxyl group in either the C2 or C3 endo conformations to furnish the functionalized product.

3.1.4 Expansion of Methodology to Regioselective Alkylation

Alkyl ethers, such as benzyl- or 4-methoxybenzyl ethers are extensively used as protecting groups for carbohydrates. However, alkyl halides are less electrophilic than acyl chlorides and tosyl chlorides, thereby rendering site-selective alkylations considerably more difficult. Nonselective- and/or over-alkylation occur under harsh conditions. Although organotin-mediated alkylations[129] have been developed to address this problem, alternative strategies that do not rely on the use of stochiometric amounts of toxic dibutyltin oxide are needed. In addition to derivatizing sugar building blocks, these new catalysts would be applicable to site-selective alkylation or phosphorylation of complex nucleotide derivatives and natural products. Thus, we envision that alkylating monosaccharides in a site-selective fashion will be especially impactful.

In accordance with our goal, rhamnopyranoside **7** was treated with various metal catalysts to afford a site selective benzylation of *cis*-1,2-dioxy motifs. When 20 mol% $Ca(OTf)_2$ was used with NaHMDS in THF solvent, the desired benzylated sugar **7a** was obtained in 39% yield (Figure 3.6). Alternatively, $SrBr_2$ also afforded the desired product in 44% yield. The key to this reaction was the use of NaHMDS as base. When organic bases such as *i*Pr_2EtN, DBU, or Et_3N were used, no reaction was observed. In the absence of metal catalyst, the desired product was only observed in only 14% yield.

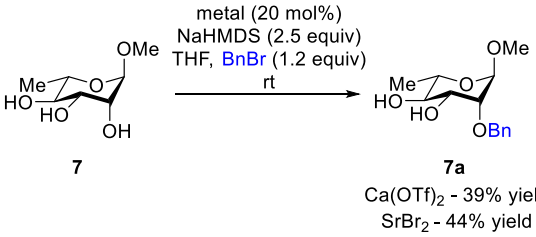

Figure 3.6 Site selective alkylation of carbohydrate derivatives

We also looked at developing a site-selective benzylation using Cu or Ni catalysis in combination with chiral ligands (Figure 3.7). Currently, when pyranoside **8** is submitted to 10 mol% $NiCl_2$ and 10 mol% (*R,R*)-DACH ligand, the 2-*O* isomer **8a** is observed in 17% yield and >20:1 selectivity for the desired isomer. Current efforts are focused on improving the conversion and exploring the conditions to obtain a switch in regioselectivity toward a site-selective benzylation.

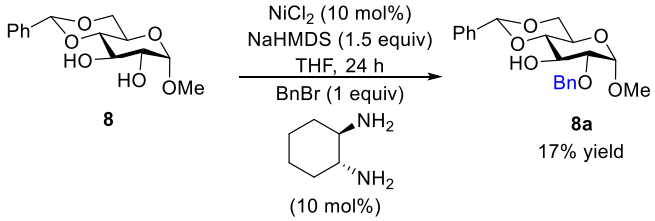

Figure 3.7 Application of Sr-catalyzed benzylation and efforts towards building block synthesis

3.1.5 Conclusion

In summary, we have demonstrated a site-selective, copper(II)-catalyzed regioselective acylation and tosylation of monosaccharides. Using this new method, various pyranosides and furanoside derivatives were functionalized in good yields and regioselectivities (up to >20:1). Moreover, the site of acylation can be controlled by choosing the proper ligand. Extension of this methodology to site-selective alkylation using earth-abundant catalysts is currently underway.

3.2 Experimental Data

3.2.1 Experimental Details

The data shown in Table 3.1 and certain substrates in Table 3.2 were obtained by I-H.C and K.G.M.K, and the reader is directed to the Supporting Information of the published manuscript[130] for the details of those experiments. This experimental section will focus on my contributions to the project.

Copper Catalyzed Acylation of Pyranoside Derivatives

i) General Procedure for the Copper Catalyzed Acylation of Pyranoside Derivatives

A 1-dram vial fitted with a septum cap was charged with copper(II) trifluoromethanesulfonate (3.6 mg, 0.01 mmol, 0.1 equiv), (*S,S*)-Ph-PyBox (3.7 mg, 0.01 mmol 0.1 equiv), pyranoside **2** or **3** (0.1 mmol, 1 equiv), and dichloromethane (0.5 mL) in a N_2-filled glovebox. To the resulting mixture was added diisopropylethylamine (26 µL, 0.15 mmol, 1.5 equiv) and this mixture was stirred at ambient temperature for 5 minutes and subsequently taken outside of the glovebox. Benzoyl chloride (12 µL, 0.100 mmol, 1 equiv) was then added via syringe and the reaction mixture was maintained at rt for 16 h.

The reaction mixture quenched with 100 μL saturated sodium bicarbonate solution. After eluting the crude through a plug of silica with ethyl acetate, the resulting solution was concentrated in vacuo. The regioselectivity for the transformation was measured by performing a ^{1}H NMR analysis of the unpurified reaction mixture. The resulting residue was purified by preparative thin layer chromatography (eluting with hexanes:EtOAc = 2:1) to give the acylated products **2a-3a**. The assignment of the regioisomers was determined by COSY NMR spectroscopy.

Methyl 6-(tert-butyldimethylsilyloxy)-3-*O*-(benzoyl)-α-*D*-mannopyranoside (2a)

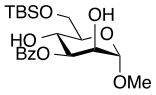

Mannopyranoside **2a** was synthesized according to general procedure for acylation. Colorless oil, 59.4 mg, 72% yield, 9:1 regioselectivity. Spectroscopic data was consistent with reported literature.[112]

Methyl-3-*O*-(benzoyl)-α-*L*-rhamnopyranoside (3a)

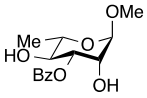

Rhamnopyranoside **3a** was synthesized according to general procedure for acylation. Colorless oil, 26.5 mg, 94% yield, >20:1 regioselectivity. Spectroscopic data was consistent with reported literature.[112]

Copper Catalyzed Tosylation of Ribofuranoside Derivatives

i) Synthesis of Methyl 5-(trityl)-β-D-ribofuranoside (**5**)

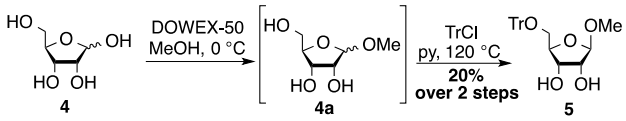

To a flame-dried 250-mL round bottom flask was added D-ribose **4** (10 g, 66.6 mmol, 1 equiv), Dowex-50 (H^+, 10 g, 10–20% w/w), and 150 mL anhydrous MeOH at 0 °C. The reaction mixture was stirred at 4 °C for 16 h. The mixture was quenched with Na_2CO_3, filtered, and concentrated in vacuo to give methoxy ribose **4a** as colorless oil in quantitative yield. Methoxy **4a** was used without further purification. Subsequently, to a flame-dried 100-mL round bottom flask under N_2 was added methoxy ribose **4a** (6.8 g, 41.4 mmol, 1 equiv), trityl chloride (13.4 g, 48.1 mmol, 1.16 equiv), and 33mL dry pyridine at 120 ˚C for 4 h. The pyridine was concentrated in vacuo and the resultant oil was dissolved in chloroform. The oil was washed with water and 0.5 M HCl, dried over Na_2SO_4 and concentrated in vacuo. Column chromatography was performed (0–5% MeOH: $CHCl_3$) to give β-ribofuranoside **5** as a white solid in 20% yield (3.4 g, 8.35 mmol). Spectroscopic data was consistent with reported literature.[131,132]

ii) General Procedure for the Copper Catalyzed Tosylation of Ribofuranoside Derivatives

A 1-dram vial fitted with a septum cap was charged with copper(II) trifluoromethanesulfonate (3.6 mg, 0.01 mmol), (*S,S*)-Ph-PyBox (3.7 mg, 0.01 mmol), β-ribofuranoside **5** (40.6 mg, 0.1 mmol), and dichloromethane (0.5 mL) in a N_2-filled glovebox. To the resulting mixture was added diisopropylethylamine (26 uL, 0.15 mmol) and this mixture was stirred at ambient temperature for 5 minutes. Tosyl chloride (28.6 mg, 0.150 mmol) in 0.5mL dichloromethane was then added and the reaction mixture was maintained at rt for 16 h. The reaction mixture was quenched with 100 µL saturated sodium bicarbonate solution. This mixture was filtered through a plug of silica gel (eluting with ethyl acetate), then the filtrate was concentrated in vacuo. The regioselectivity for the

transformation was measured by ^{1}H NMR analysis of the unpurified reaction mixture. The resulting residue was purified by preparative thin layer chromatography (eluting with hexanes:EtOAc) to give the tosylated products **5b-6b**. The assignment of the regioisomers was determined by COSY NMR spectroscopy.

Methyl 5-(trityl)-3-*O*-(*p*-toluenesulfonyl)-β-*D*-ribofuranoside (5b)

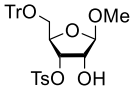

Colorless oil, 20.9 mg, 75% yield, >20:1 regioselectivity. ^{1}H NMR (500 MHz, $CDCl_3$) δ 7.69 (d, *J* = 8.1 Hz, 2H), 7.44-7.32 (m, 6H), 7.25 (m, 9H), 7.16 (d, *J* = 8.1 Hz, 2H), 4.91 (s, 1H), 4.87 (dd, *J* = 6.8, 4.4 Hz, 1H), 4.30 (d, *J* = 4.4 Hz, 1H), 4.26 (dt, *J* = 7.3, 4.3 Hz, 1H), 3.33 (s, 3H), 3.19 (dd, *J* = 10.3, 3.8 Hz, 1H), 2.95 (dd, *J* = 10.3, 4.5 Hz, 1H), 2.63 (s, 1H), 2.35 (s, 3H); ^{13}C NMR (126 MHz, $CDCl_3$) δ 145.55, 143.85, 132.08, 130.10, 128.74, 128.20, 127.88, 127.13, 107.98, 86.64, 79.63, 79.25, 74.24, 63.32, 55.55, 21.77. IR (ATR, neat): 3475, 3061, 3027, 2923, 2848, 1596, 1488, 1439, 1367, 1220, 1193, 1177, 1113, 1017, 969, 902 cm^{-1}. HRMS (ESI^{+}) calc'd for $[C_{32}H_{32}O_7S+Na]^{+}$: 583.1766; found: 583.1757. $[\alpha]^{29}_{D}$ = –1.8° (*c* 1.39, $CHCl_3$).

Methyl 5-(trityl)-2-*O*-(*p*-toluenesulfonyl)-β-*D*-ribofuranoside (5b')

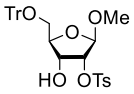

Colorless oil, 1.6 mg, 6% yield. ^{1}H NMR (400 MHz, $CDCl_3$) δ 7.83 (d, *J* = 8.3 Hz, 2H), 7.48 – 7.43 (m, 6H), 7.36 (d, *J* = 8.1 Hz, 2H), 7.32 – 7.20 (m, 9H), 4.91 (d, *J* = 0.8 Hz, 1H), 4.75 (dd, *J* = 4.6, 0.9 Hz, 1H), 4.40 (td, *J* = 7.3, 4.7 Hz, 1H), 4.05 (dt, *J* = 7.0, 4.4 Hz, 1H), 3.33 (dd, *J* = 10.2, 3.6 Hz, 1H), 3.30 (s, 3H), 3.17 (dd, *J* = 10.2, 4.8 Hz, 1H), 2.46 (s, 3H), 2.06 (d, *J* = 7.9 Hz, 1H).^{13}C NMR (126 MHz, $CDCl_3$) δ 145.6, 143.9, 133.0, 130.2, 128.8, 128.2, 128.0, 127.2, 105.4, 86.8, 82.6, 82.3, 71.0, 64.1, 55.7,

21.9. IR (ATR, neat): 3521, 3057, 3025, 2928, 2853, 1598, 1496, 1372, 1212, 1193, 1181, 1093, 1049, 965, 906 cm^{-1}. HRMS (ESI^+) calc'd for $[C_{32}H_{32}O_7S+Na]^+$: 583.1766; found: 583.1758. $[\alpha]^{28}_D$ = +11.6° (*c* 1.61, $CHCl_3$).

Methyl 5-(trityl)-3-*O*-(*o*-nitrobenzenesulfonyl)-β-*D*-ribofuranoside (5c)

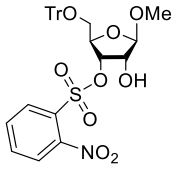

Colorless oil, 28.2 mg, 48% yield, >20:1 regioselectivity. ^1H NMR (600 MHz, $CDCl_3$) δ 8.07 (d, *J* = 8.0 Hz, 1H), 7.79 – 7.75 (m, 2H), 7.68 – 7.63 (m, 1H), 7.43 (d, *J* = 7.7 Hz, 6H), 7.26 (ddd, *J* = 21.7, 14.8, 7.3 Hz, 9H), 5.25 – 5.17 (m, 1H), 4.93 (s, 1H), 4.40 (dd, *J* = 9.9, 4.1 Hz, 1H), 4.22 (t, *J* = 3.4 Hz, 1H), 3.38 (s, 3H), 3.37 (dd, *J* = 10.2, 4.2 Hz, 1H), 3.17 (dd, *J* = 10.3, 4.3 Hz, 1H), 2.65 (d, *J* = 4.3 Hz, 1H). ^{13}C NMR (126 MHz, $CDCl_3$) δ 143.8, 135.5, 132.6, 131.8, 128.9, 128.82, 128.79, 128.0, 127.2, 125.3, 107.9, 86.8, 81.3, 79.5, 74.3, 63.1, 55.9. IR (ATR, neat): 3534, 3070, 2934, 1542, 1491, 1449, 1374, 1195 cm^{-1}. HRMS (ESI^+) calc'd for $[C_{31}H_{29}NO_9S+Na]^+$: 614.1461; found: 614.1458. $[\alpha]^{25}_D$ = –1.1° (*c* 1.1, $CHCl_3$).

Methyl 5-(trityl)-3-*O*-(pentafluorobenzenesulfonyl)-β-*D*-ribofuranoside (5d)

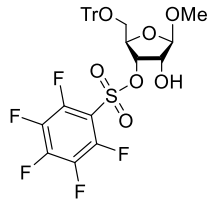

Colorless oil, 20.7 mg, 65% yield, 5:1 regioselectivity. ^1H NMR (500 MHz, $CDCl_3$) δ 7.41 (m, 6H), 7.27 (m, 9H), 5.20 (t, *J* = 5.1 Hz, 1H), 4.93 (s, 1H), 4.35 (d, *J* = 5.2 Hz, 2H), 3.41 (s, 3H), 3.35 (dd, *J* = 10.4, 4.0 Hz, 1H), 3.13 (dd, *J* = 10.4, 4.3 Hz, 1H), 2.27 (d, *J* = 5.2 Hz, 1H). ^{13}C NMR (126 MHz, $CDCl_3$) δ 146.2, 144.1, 143.6, 139.1, 137.0, 128.7, 128.0, 127.3, 108.1, 87.0, 82.4, 79.4, 74.4, 63.2, 56.1. IR (ATR, neat): 3533, 3061, 2928, 1523, 1501, 1450, 1401, 1316, 1193, 1098,

1003 cm^{-1}. HRMS (ESI^+) calc'd for $[C_{31}H_{25}F_5O_7S+Na]^+$: 659.1139; found: 659.1138. $[\alpha]^{25}_D$ = +11.6° (*c* 0.98, $CHCl_3$).

Methyl 5-(*tert*-butyldimethylsilyloxy)-3-*O*-(benzoyl)-α-*D*-ribofuranoside (6b)

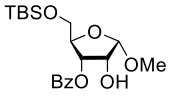

Colorless oil, 26.3 mg, 69% yield, 6:1 regioselectivity. ^1H NMR (500 MHz, $CDCl_3$) δ 8.05 (d, *J* = 8.0 Hz, 2H), 7.57 (t, *J* = 7.5 Hz, 1H), 7.45 (t, *J* = 7.8 Hz, 2H), 5.34 (dd, *J* = 6.6, 2.1 Hz, 1H), 4.98 (d, *J* = 4.8 Hz, 1H), 4.36 (ddd, *J* = 11.4, 6.6, 4.7 Hz, 1H), 4.22 (q, *J* = 2.3 Hz, 1H), 3.92 (dd, *J* = 11.2, 2.6 Hz, 1H), 3.78 (dd, *J* = 11.2, 2.6 Hz, 1H), 3.52 (s, 3H), 2.71 (d, *J* = 11.3 Hz, 1H), 0.90 (s, 9H), 0.08 (d, *J* = 8.2 Hz, 6H). ^{13}C NMR (126 MHz, $CDCl_3$) δ 166.19, 133.33, 130.03, 129.88, 128.55, 102.78, 84.01, 72.68, 72.07, 63.47, 55.68, 26.02, 18.44, -5.22, -5.35. IR (ATR, neat): 3536, 2954, 2927, 2859, 1730, 1266, 1115, 1098, 1064, 1036, 824 cm^{-1}. HRMS (ESI^+) calc'd $[C_{19}H_{30}O_6Si+Na]^+$: 405.1709; found 405.1699. $[\alpha]^{25}_D$ = +30.8° (*c* 1.1, $CHCl_3$).

Methyl 5-(*tert*-butyldimethylsilyloxy)-2-*O*-(benzoyl)-α-*D*-ribofuranoside + Methyl 5-(*tert*-butyldimethylsilyloxy)-3-*O*-(benzoyl)-α-*D*-ribofuranoside (6a major) + (6b minor)

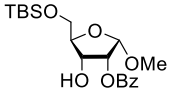

6a: Colorless oil, 33.0 mg, 86% combined yield, 3.5:1 regioselectivity. TLC: 45:50:5 dichloromethane:hexanes:acetone, R_f=0.3 (visualized with anisaldehyde stain). ^1H NMR (400 MHz, $CDCl_3$) δ 8.12–8.10 (m, 2H), 7.59–7.55 (m, 1H), 7.47–7.43 (m, 2H), 5.24 (d, *J* = 4.1 Hz, 2H), 5.05 (dd, *J* = 5.9, 4.1 Hz, 1H), 4.35 (m, 1H), 4.23–4.22 (m, 1H), 3.82 (dd, *J* = 11.3, 2.9 Hz, 1H), 3.74 (dd, *J* = 11.2, 3.3 Hz, 1H), 3.44

(s, 1H), 2.94 (s, 1H), 0.91 (s, 9H), 0.08 (d, *J* = 5.2 Hz, 6H). HRMS (ESI$^+$) calc'd $[C_{19}H_{30}O_6Si+Na]^+$: 405.1709; found 405.1697.

Site-Selective Alkylation of Pyranoside Derivatives

i) Procedure for the Sr- or Ca-Catalyzed Alkylation of Pyranoside Derivatives

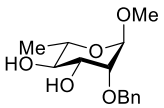

A 1-dram vial fitted with a septum cap was charged with $SrBr_2$ (0.02 mmol), pyranoside **7** (29.2 mg, 0.1 mmol), and NaHMDS (45.9 mg, 0.250 mmol) and THF (1 mL) in a N_2-filled glovebox. This mixture was stirred at ambient temperature for 5 minutes. Benzyl bromide (15 µL, 0.126 mmol) was then added and the reaction mixture was maintained at rt for 16 h. The reaction mixture was quenched with 100 µL saturated sodium bicarbonate solution. This mixture was filtered through a plug of silica gel (eluting with ethyl acetate), then the filtrate was concentrated in vacuo. The resulting residue was purified by preparative thin layer chromatography (eluting with hexanes:EtOAc) to give the benzylated product **7a** as a colorless oil (11.8 mg, 44%). When $Ca(OTf)_2$ was used instead of $SrBr_2$, **7a** was isolated as a colorless oil (10.4 mg, 39%). Spectroscopic data was consistent with reported literature.[133]

ii) Procedure for the Ni-Catalyzed Alkylation of Pyranoside Derivatives

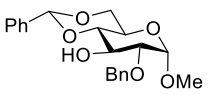

A 1-dram vial fitted with a septum cap was charged with $NiCl_2$ (0.01 mmol), (*R,R*)-DACH (0.01 mmol), and THF (1 mL) in a N_2-filled glovebox. This mixture was stirred at ambient temperature for 5 minutes. Then NaHMDS (13.8 mg, 0.075 mmol) followed by pyranoside **8** (14.1 mg, 0.05 mmol) was added. This mixture was stirred at ambient temperature for 5 minutes. Benzyl bromide (6 µL, 0.100 mmol) was then added and the reaction mixture was maintained at rt for 24 h. The reaction

mixture was quenched with 100 µL saturated ammonium chloride solution. This mixture was then extracted with EtOAc (2 x 5 mL). The organic layers were combined and then washed with brine. The organic layer was then dried with Na_2SO_4, filtered, and concentrated in vacuo. The regioselectivity for the transformation was measured by ^1H NMR analysis of the unpurified reaction mixture. Pyranoside **8a** was observed in 17% NMR yield and >20:1 regioselectivity for the 2-*O* isomer. Spectroscopic data was consistent with reported literature.[134]

3.2.2 NMR Spectra

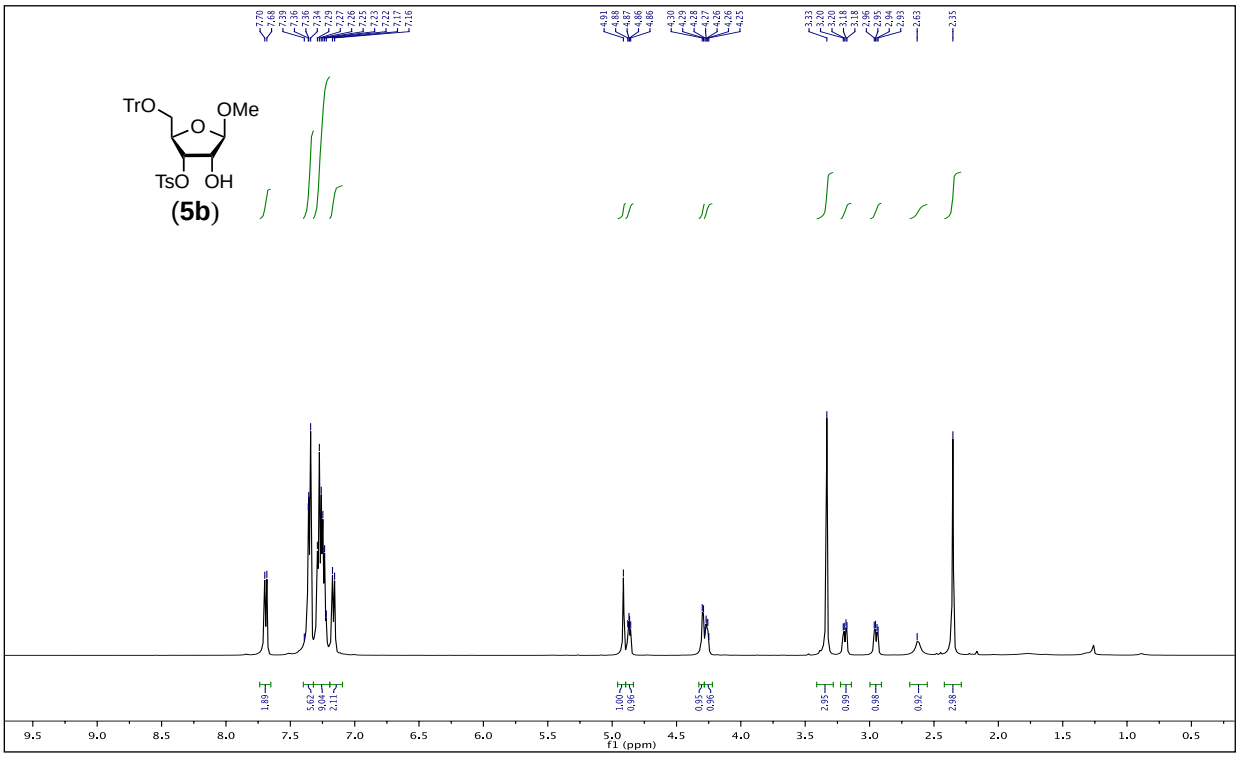

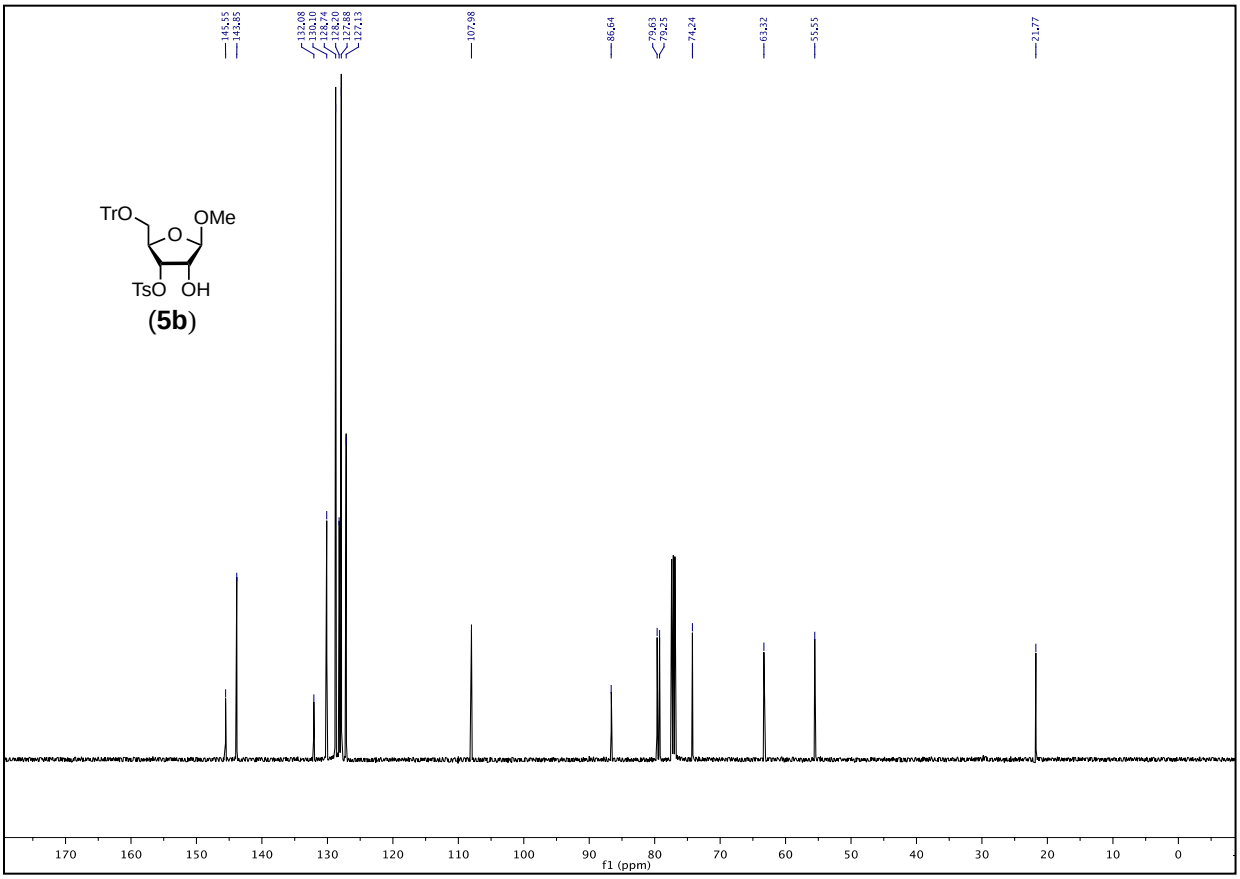

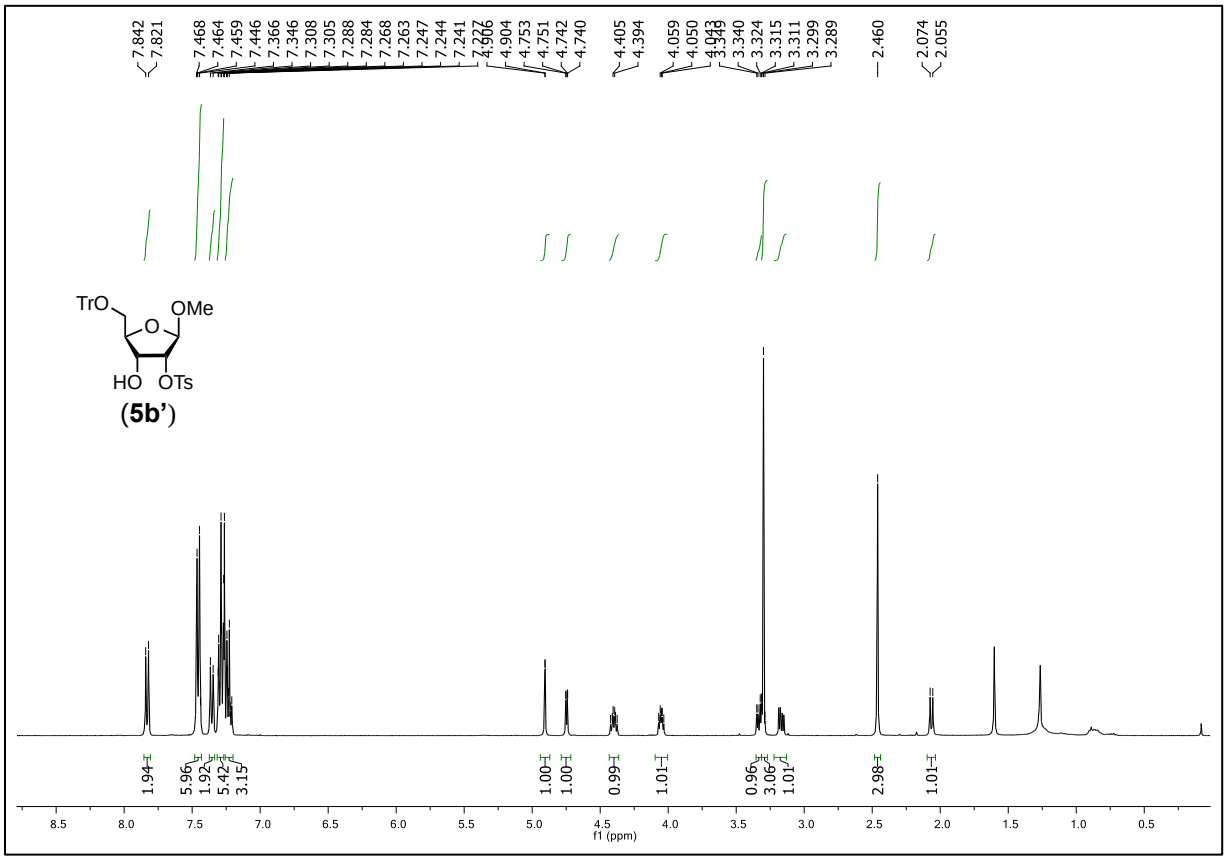
7.842
7.821
7.468
7.464
7.459
7.446
7.366
7.346
7.308
7.305
7.288
7.284
7.268
7.263
7.247
7.244
7.241
4.906
4.904
4.753
4.751
4.742
4.740
4.405
4.394
4.059
4.050
4.043
3.343
3.340
3.324
3.315
3.311
3.299
3.289
2.460
2.074
2.055
TrO
OMe
O
HO
OTs
(5b')
1.94
5.96
1.92
5.42
3.15
1.00
1.00
0.99
1.01
0.96
3.06
1.01
2.98
1.01
f1 (ppm)

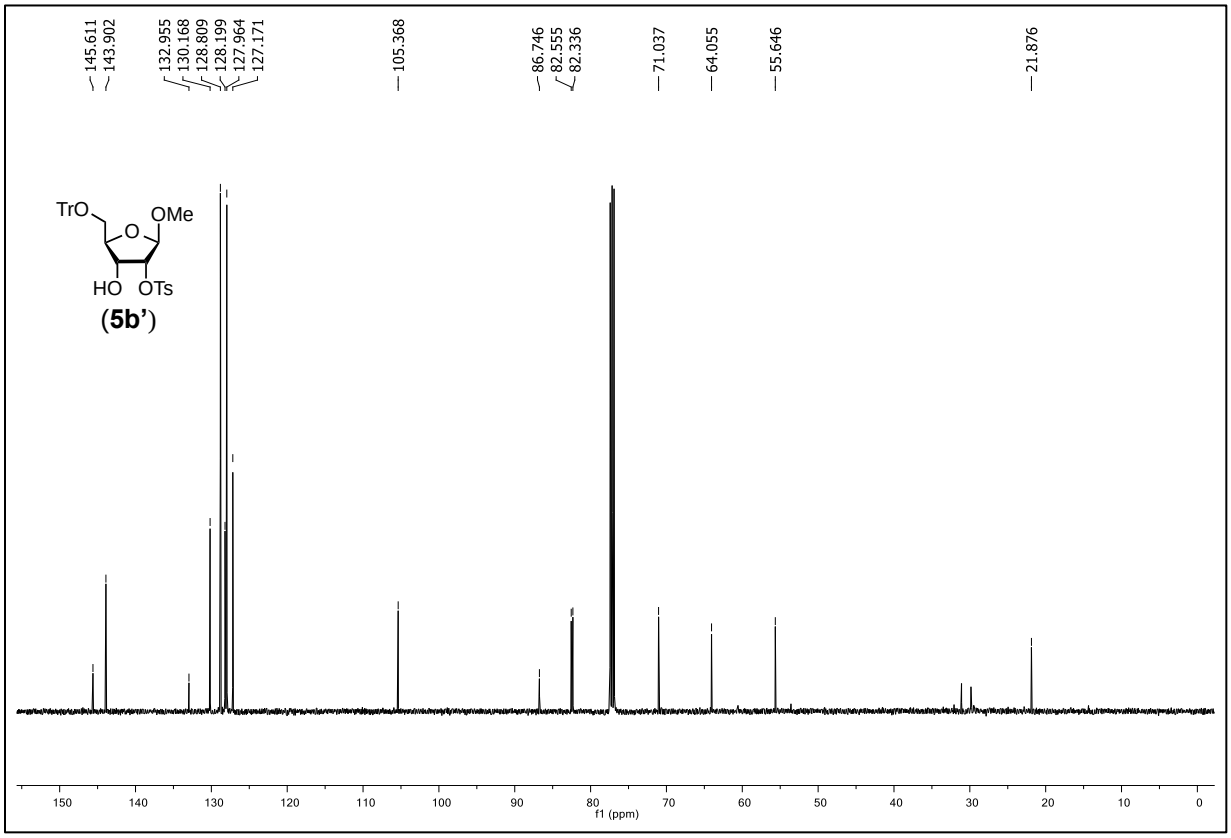
145.611
143.902
132.955
130.168
128.809
128.199
127.964
127.171
105.368
86.746
82.555
82.336
71.037
64.055
55.646
21.876
TrO
OMe
O
HO
OTs
(5b')
f1 (ppm)

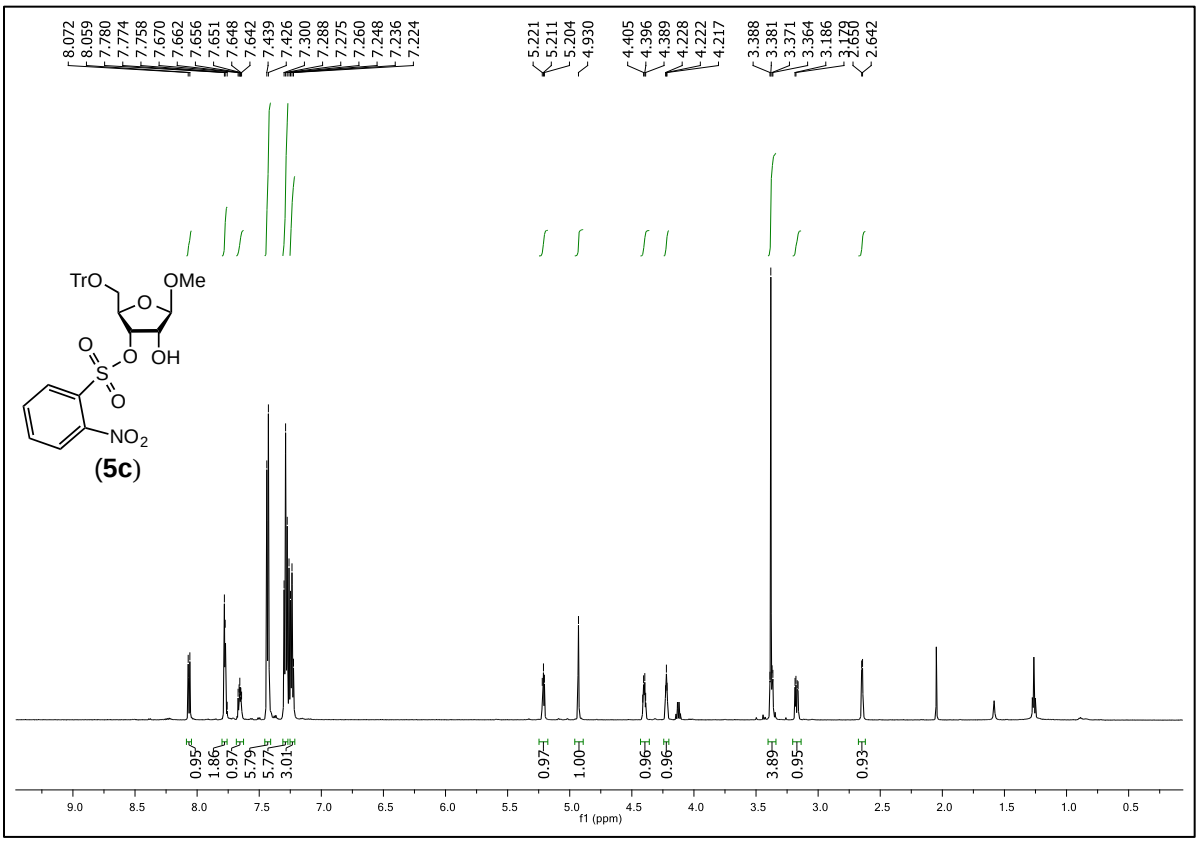
8.072
8.059
7.780
7.774
7.758
7.670
7.662
7.656
7.651
7.648
7.642
7.439
7.426
7.300
7.288
7.275
7.260
7.248
7.236
7.224
5.221
5.211
5.204
4.930
4.405
4.396
4.389
4.228
4.222
4.217
3.388
3.381
3.371
3.364
3.186
3.179
2.650
2.642
TrO
OMe
O
O
OH
O
S
O
NO2
(5c)
0.95
1.86
0.97
5.79
5.77
3.01
0.97
1.00
0.96
0.96
3.89
0.95
0.93
9.0
8.5
8.0
7.5
7.0
6.5
6.0
5.5
5.0
4.5
4.0
3.5
3.0
2.5
2.0
1.5
1.0
0.5
f1 (ppm)

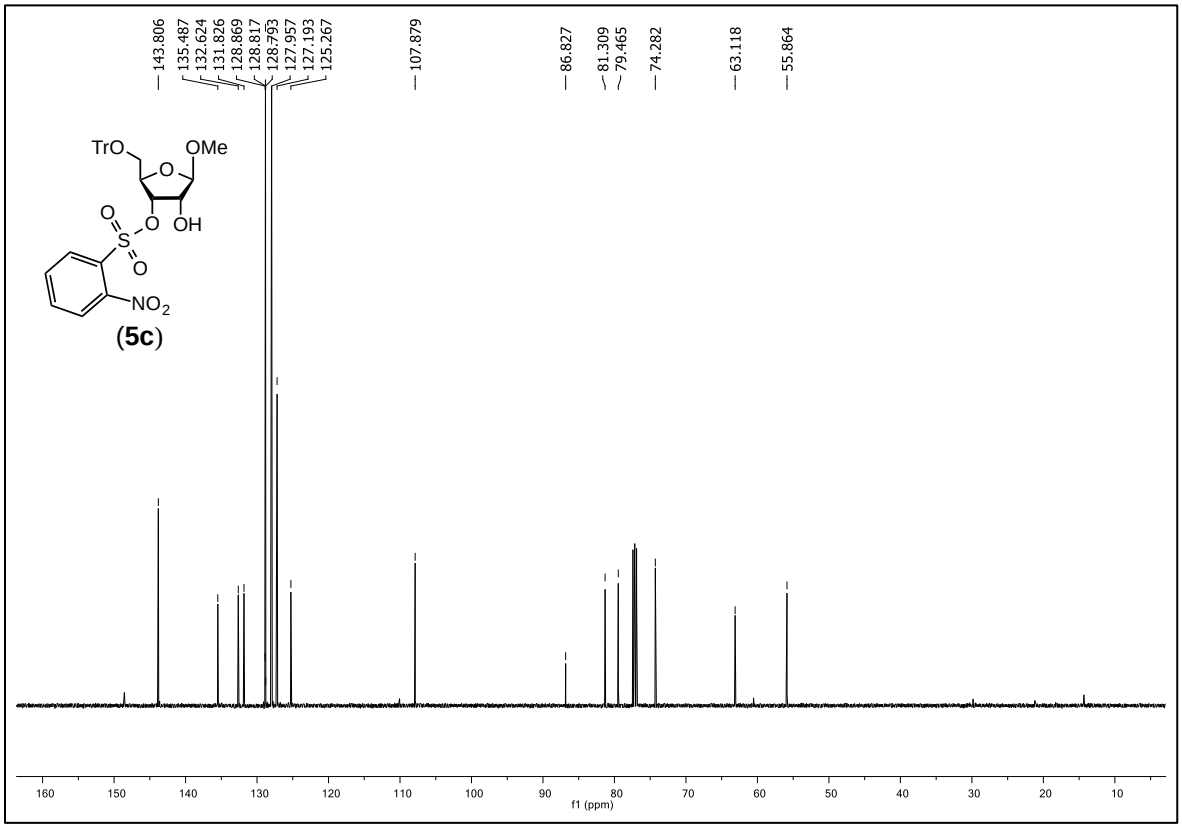
143.806
135.487
132.624
131.826
128.869
128.817
128.793
127.957
127.193
125.267
107.879
86.827
81.309
79.465
74.282
63.118
55.864
TrO
OMe
O
O
OH
O
S
O
NO2
(5c)
160
150
140
130
120
110
100
90
80
70
60
50
40
30
20
10
f1 (ppm)

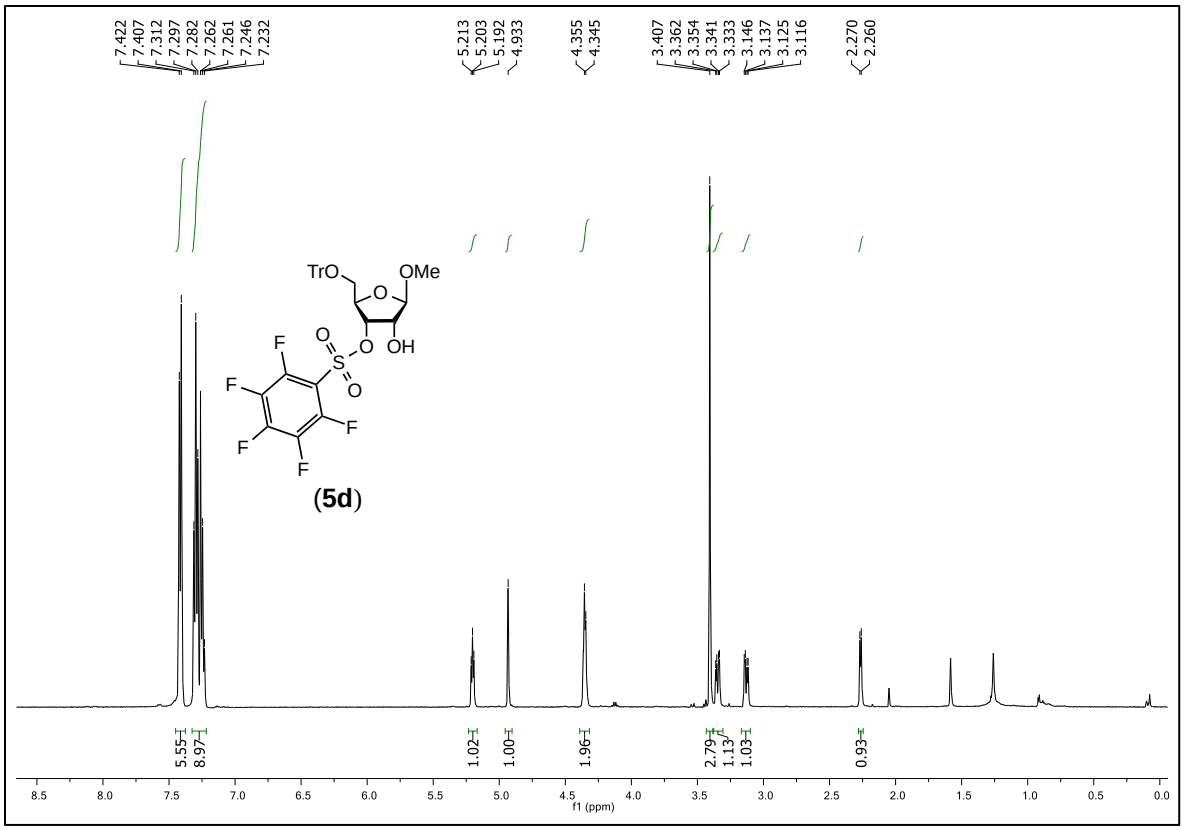
7.422
7.407
7.312
7.297
7.282
7.262
7.261
7.246
7.232
5.213
5.203
5.192
4.933
4.355
4.345
3.407
3.362
3.354
3.341
3.333
3.146
3.137
3.125
3.116
2.270
2.260
TrO
OMe
O
O
S
O
O
OH
F
F
F
F
F
(5d)
5.55
8.97
1.02
1.00
1.96
2.79
1.13
1.03
0.93
f1 (ppm)

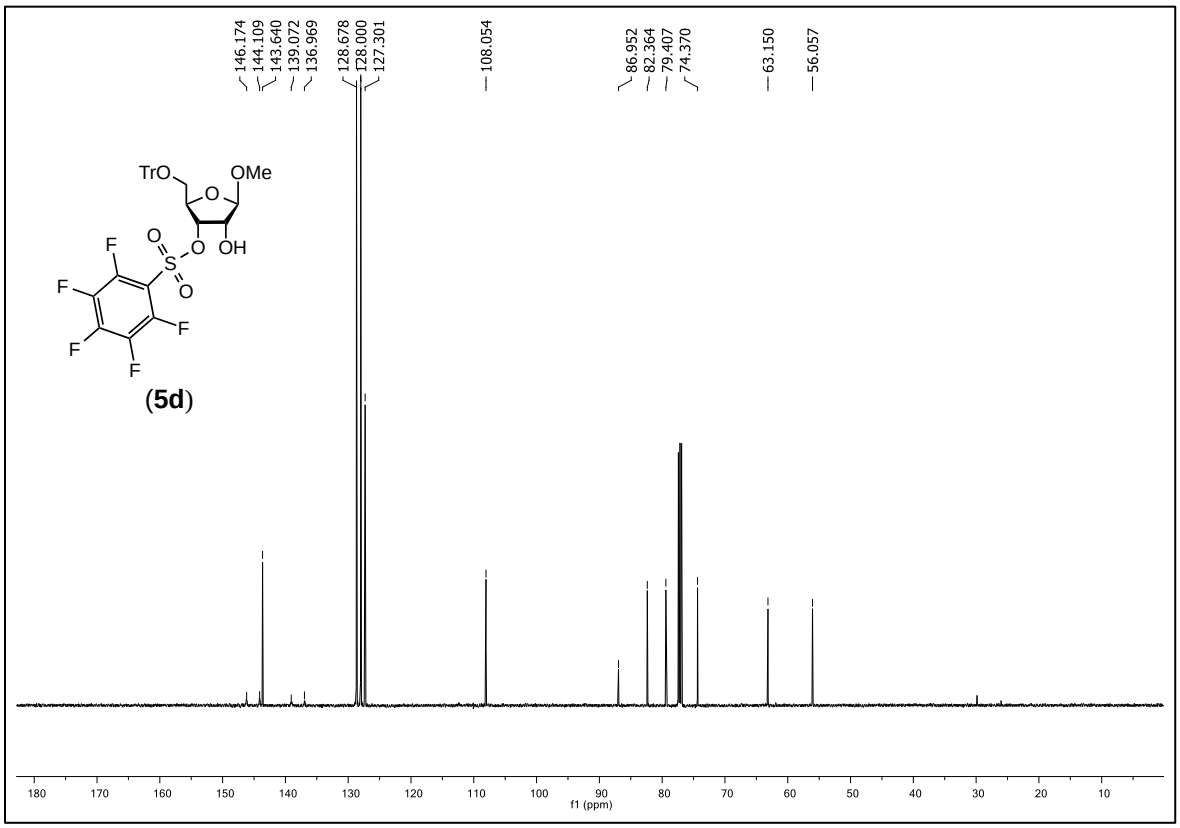
146.174
144.109
143.640
139.072
136.969
128.678
128.000
127.301
108.054
86.952
82.364
79.407
74.370
63.150
56.057
TrO
OMe
O
O
S
O
O
OH
F
F
F
F
F
(5d)
f1 (ppm)

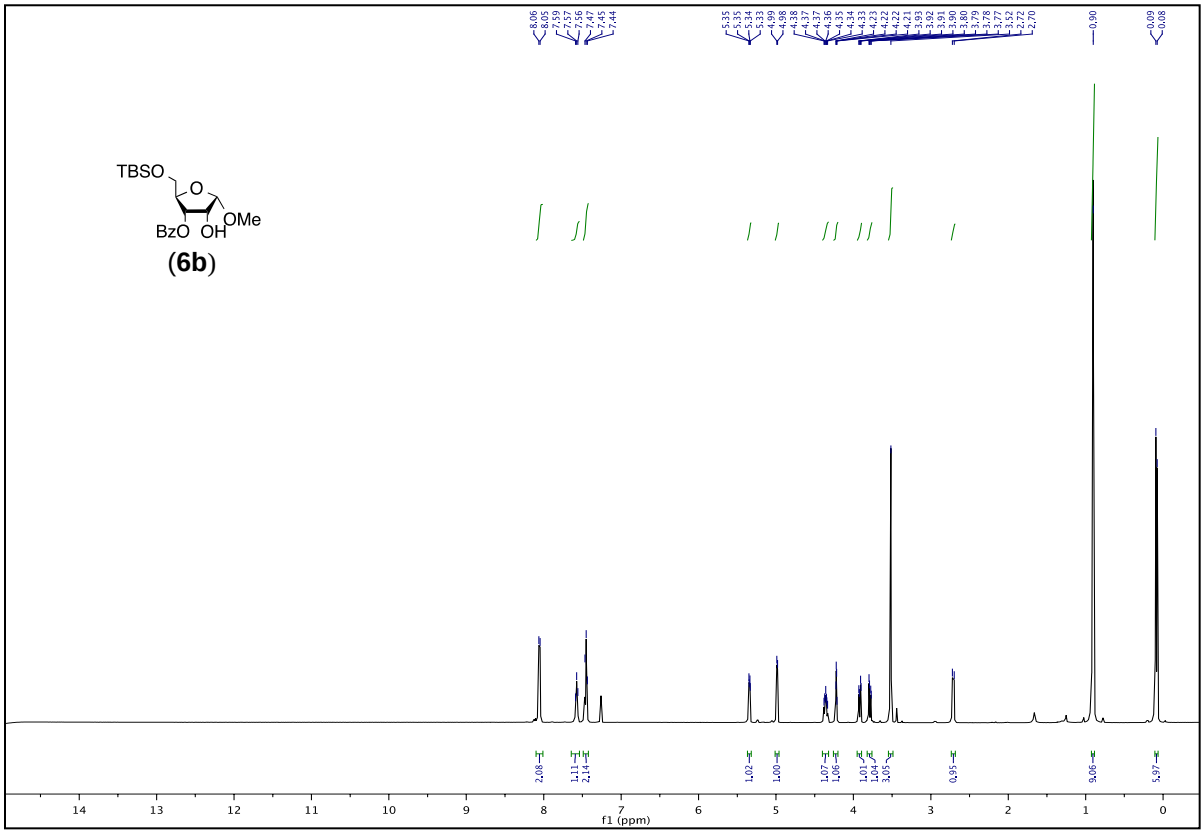
TBSO
O
OMe
BzO OH
(6b)
f1 (ppm)

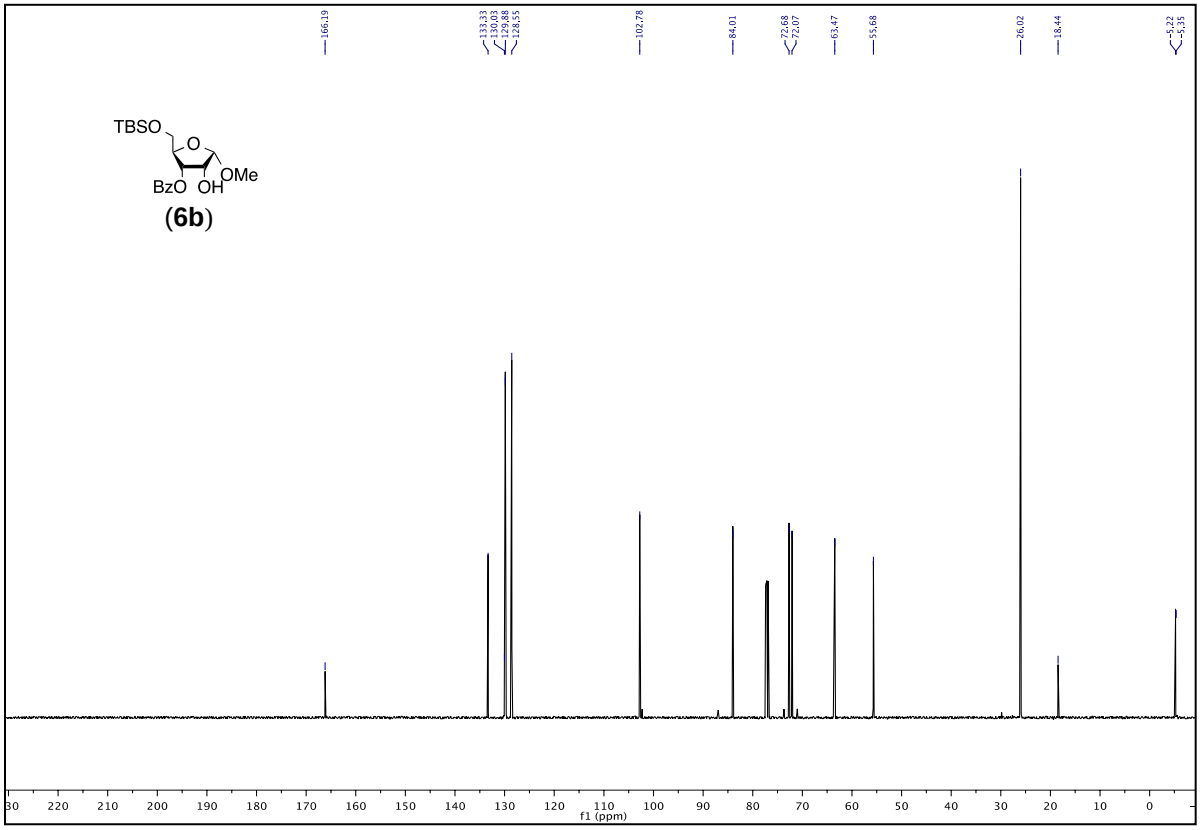
TBSO
O
OMe
BzO OH
(6b)
f1 (ppm)

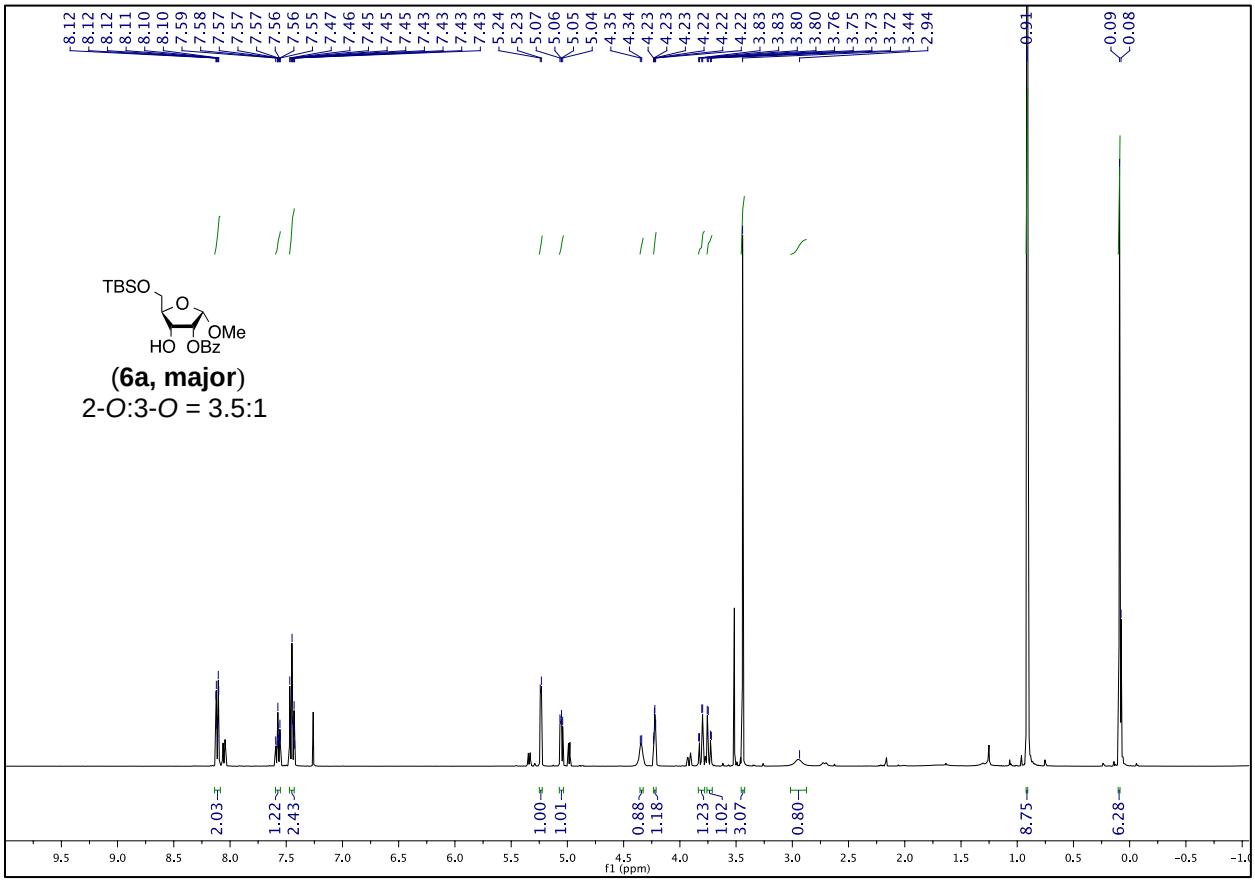
TBSO
O
OMe
HO OBz
(6a, major)
2-O:3-O = 3.5:1
f1 (ppm)

CHAPTER 4 – Approach to Stereodefined All-Carbon Tetrasubstituted Alkenes Mediated by Lithium Hexamethyldisilazide[a]

4.1 Synthesis of All-Carbon Tetrasubstituted Alkenes Mediated by Lithium Hexamethyldisilazide[*]

4.1.1 Introduction

Alkenes are valuable feedstocks commonly found in natural products,[135] medicines,[136] and petrochemicals[137] in chemical industry. Because they are versatile functional groups,[138] the synthesis of alkenes represents an important endeavor in organic synthesis. While methods to synthesize di- and trisubstituted alkenes have been reported,[139] methods toward synthesis of all-carbon tetrasubstituted alkenes are underdeveloped. The synthesis of all-carbon tetrasubstituted alkenes is most challenging due to issues with regio- and stereoselectivity. For example, one way to synthesize tetrasubstituted alkenes is through an alkyne functionalization (Figure 4.1a). However, in this approach, regioselectivity becomes an issue due to unselective alkyne carbometallation plus unselective trapping of the resulting metal-vinyl species. Moreover, there are classical approaches to all-carbon tetrasubstituted alkenes via Julia,[140] Peterson,[141] Horner-Wadsworth-Emmons,[142] Wittig,[143] and McMurry reactions.[144] However, these reactions often result in poor stereoselectivities. To circumvent these selectivity issues, directing groups have been employed (Figure 4.1b).[145] However, this method limits the scope of alkynes that can be used and is often undesirable due to the additional synthetic manipulations required to install and remove the directing group.

[a] As a part of continued training in pursuit of my doctoral studies at UC Irvine, this work was completed during a summer internship with Genentech in the Small Molecule Process Chemistry Department from June 2016-August 2016.

[*] Reproduced in part with permission from Li, B. X.; Le, D. N.; Mack, K. A.; McClory, A.; Lim, N.-K.; Cravillion, T.; Savage, S.; Han, C.; Collum, D. B.; Zhang, H.; Gosselin, F. *J. Am. Chem. Soc.* **2017**, *139*, 10777.

Considering these challenges, developing a general protocol toward the synthesis of all-carbon tetrasubstituted alkenes warrants further study.

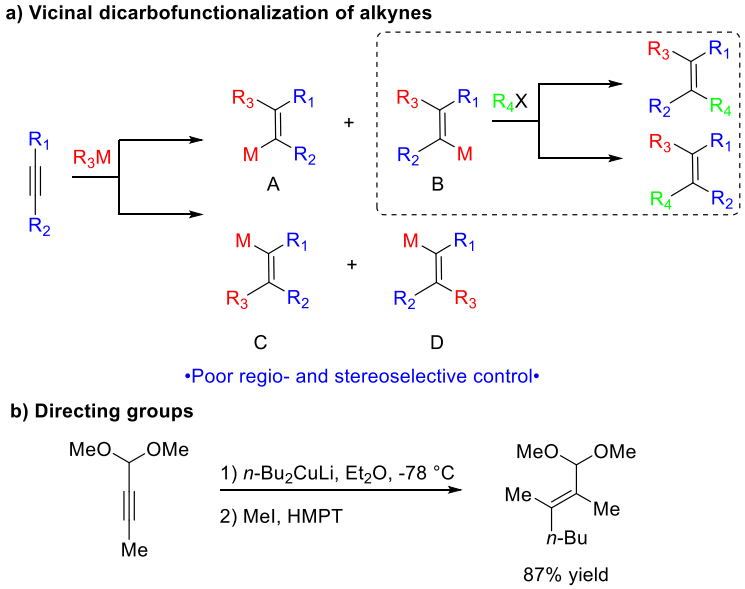

Figure 4.1 Synthesizing tetrasubstituted alkenes

Tetrasubstituted alkenes are found in important pharmaceuticals such as Tamoxifen,[146] Afimoxifene,[136] and Etacstil (Figure 4.2).[147] These drugs are selective estrogen receptor modulators (SERM) with activity against breast cancer. Seragon Pharmaceuticals previously identified a new drug, GDC-0810, a selective estrogen receptor down regulator (SERD), with robust activity against Tamoxifen-resistant breast cancer cell lines.[136] In Seragon's approach, they were able synthesize GDC-0810 in 20% overall yield (Figure 4.3). However, there were still limitations associated with this route. One of the problems was in the

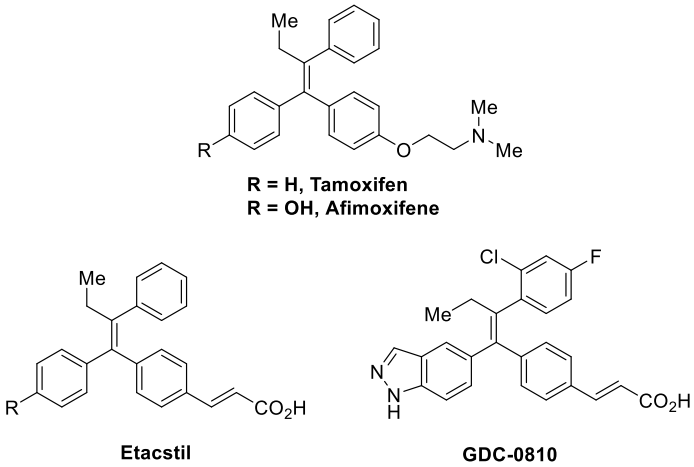

Figure 4.2 Drug therapeutics containing all-carbon tetrasubstituted alkenes

Suzuki reaction, where there were issues of low alkene chemoselectivity (4:1) in the cross-coupling of the vinyl diboronate. In addition, there was only one isolation in the entire process during the final step, thereby decreasing the overall yield in the reaction.

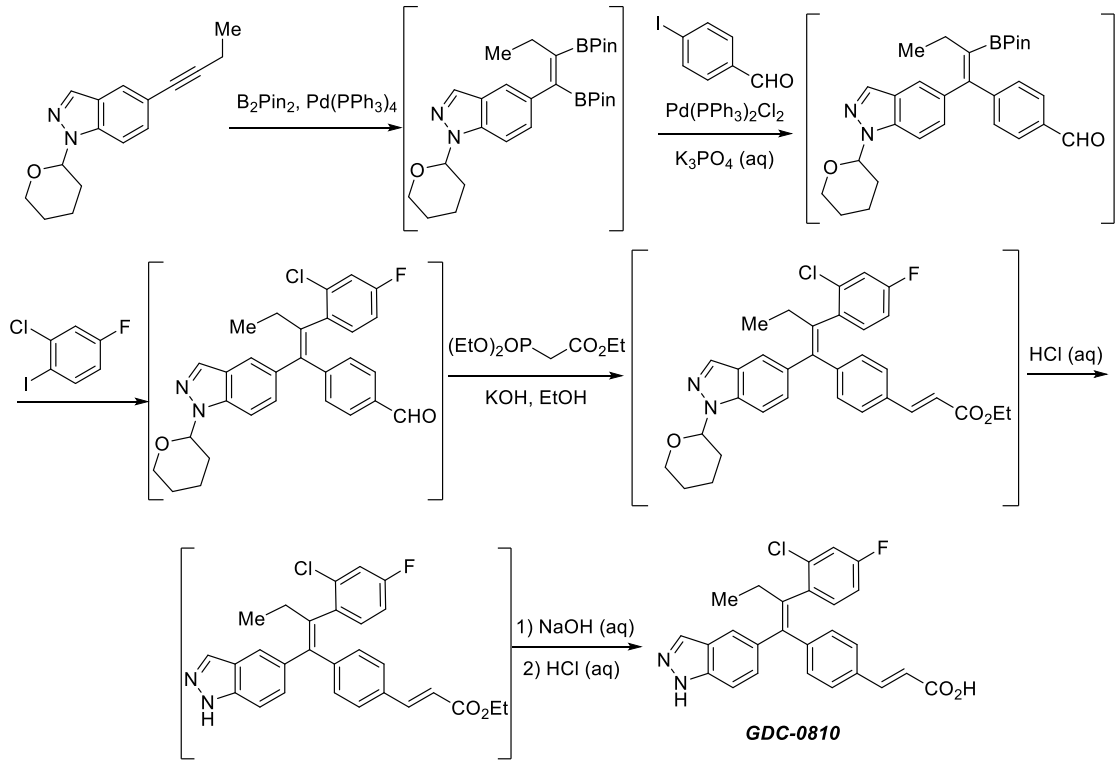

Figure 4.3 Synthetic route toward GDC-0810

To circumvent issues presented in the Suzuki cross-coupling of the vinyl diboronate, an alternative approach to access all-carbon tetrasubstituted alkenes was investigated involving the stereoselective formation of a lithium enolate. Thus, a collaboration with Professor David Collum (Cornell University) was initiated. Collum originally reported the stereoselective formation of lithium enolates using lithium hexamethyldisilazide (LiHMDS), where an additive effect was observed upon adding triethylamine (Et_3N) to the reaction mixture.[148,149] A 3000-fold increase in the rate was observed (Figure 4.4). The formation of a dimeric 8-membered transition state was proposed. Subsequently in 2008, this LiHMDS/Et_3N effect was also noted in the case of

acyclic ketones.[150] After the lithium enolate was formed, it was trapped with TMS-Cl to afford the *E*-silyl enol ether in 110:1 selectivity.

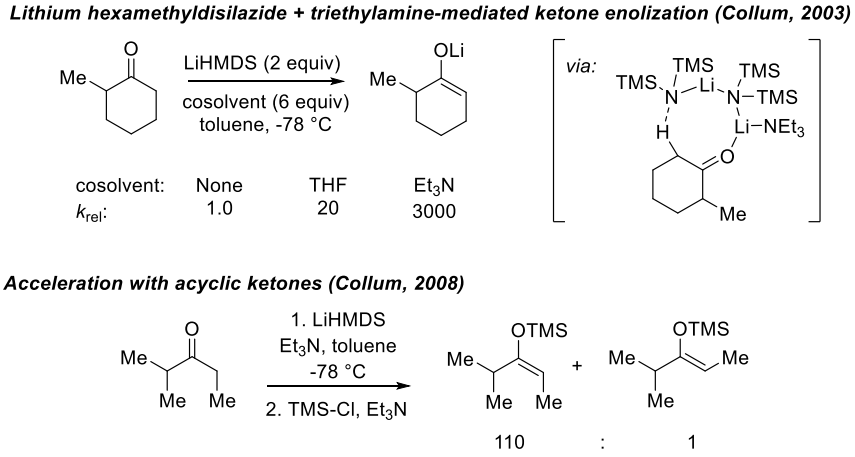

Figure 4.4 Lithium enolates using LiHMDS and trialkylamine additives

Thus, we wondered if we could use a similar approach to stereoselectively access the analogous enol tosylate from readily accessible ketones (Figure 4.5). We reasoned if we could obtain the enol tosylates, we could then perform a stereospecific Suzuki-Miyaura cross coupling to afford a variety of all-carbon tetrasubstituted alkenes.

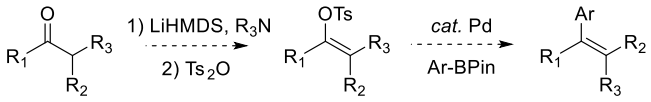

Figure 4.5 Proposed route to all-carbon tetrasubstituted alkenes

4.1.2 Development of Stereoselective Enolate Formation and Tosylation

To test out the model system, aryl ketone **1a** was subjected to two equivalents of LiHMDS and an excess of dimethylethylamine (DMEA) additive for 30 min. Then, a solution of tosyl anhydride (Ts_2O) in toluene was added to the enolate. After 30 min, desired enol tosylate **2a** was observed in 62% conversion and >95:5 *E/Z* (eq 1).

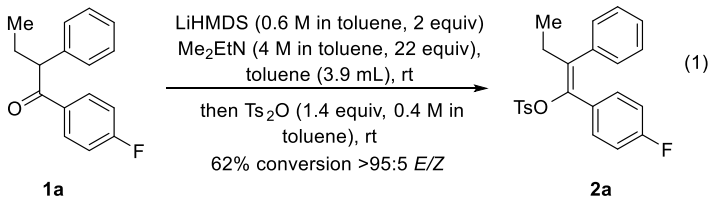

With these promising results in hand, different conditions were evaluated to improve the conversion in the reaction (Table 4.1). First, a reverse addition of the enolate to the Ts_2O solution was examined. However, this resulted in a decrease in reactivity (entry 1). Then, the Ts_2O solution was changed from toluene to DCM and an increase to 73% conversion was observed (entry 2). By using two equivalents of Ts_2O, the conversion increased to 87% and >95:5 *E/Z* (entry 4). Switching the amine additive resulted in an overall decrease in reactivity and selectivity (entries 5 and 6).

Table 4.1 Reaction optimization

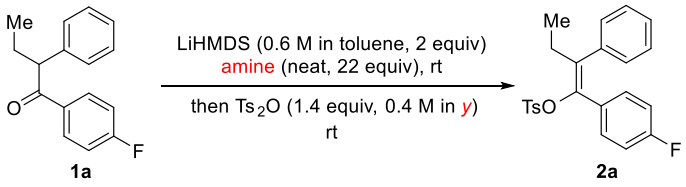

Entry	*y* (solvent)	amine	Conversion to **2** (%)	*E/Z*[d]
1[a]	toluene	Me_2EtN	29	>95:5
2	DCM	Me_2EtN	73	>95:5
3[b]	DCM	Me_2EtN	77	>95:5
4[c]	**DCM**	**Me_2EtN**	**87**	**>95:5**
5	DCM	Et_3N	25	89:11
6	DCM	iPr_2EtN	79	87:13

[a] Reverse addition of enolate into Ts_2O. [b] New batch of Ts_2O. [c] Increase to 2 equiv Ts_2O [d] *E/Z* ratio determined by HPLC of unpurified reaction mixture.

After titrating the bottle of LiHMDS, full conversion for desired enol tosylate **2a** was observed with >95:5 *E/Z* (Table 4.2, entry 1). With this result in hand, the next thing to do was to optimize the base equivalence in the reaction. The reaction was optimized down to as low as two equivalents of base (entry 7) to afford the desired product in 78% isolated yield and >95:5 *E/Z*. The 1:1 ratio of LiHMDS:DMEA was also important, because when less than two equivalents were evaluated, there was more side product formation in the reaction profile. Thus, the conditions noted in entry 7 were used to evaluate the substrate scope.

Table 4.2 Optimizing base equivalence

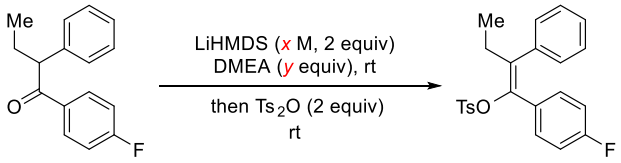

1a **2a**

Entry	*x* (mol/L)	y (equiv)	Conversion to **2** (%)	*E/Z*[d]
1[a]	0.42	22	full	>95:5
2	0.82	22	full	>95:5
3	0.82	10	full	>95:5
4	0.82	5	full	>95:5
5	0.82	4	full	>95:5
6	0.82	3	full	>95:5
7	**0.82**	**2**	**full (78)[b]**	**>95:5**
8	0.82	1	full[c]	nd
9	0.82	0	full[c]	nd

[a] 0.5 M ketone [b] Isolated yield on 2 mmol scale. [c] More side product formation in reaction profile. [d] *E/Z* ratio determined by HPLC of unpurified reaction mixture.

4.1.3 Substrate Scope Evaluation

With the optimized conditions in hand, the substrate scope was evaluated with variation in R_1 in aryl ketone **1** to form the desired enol tosylates **2** (Table 4.3). Electron

withdrawing groups (e.g., 4-F, 4-Cl, 4-CF_3, 3-OMe, 4-CO_2Et, and 4-CO_2tBu) are tolerated in up to >99:1 *E/Z* and up to 87% yield. Moreover, electron donating groups such as 4-Me and 4-OMe are tolerated in 82% and 66% yields, respectively and 98:2 *E*/*Z* selectivity. When the aryl group is substituted with 2-Me, there is a decrease in selectivity (82:18 *E*/*Z*). When a substrate containing thiophene was evaluated, there was no desired product formation and decomposition of the starting material is observed.

Table 4.3 Substrate scope evaluation with variation at R_1

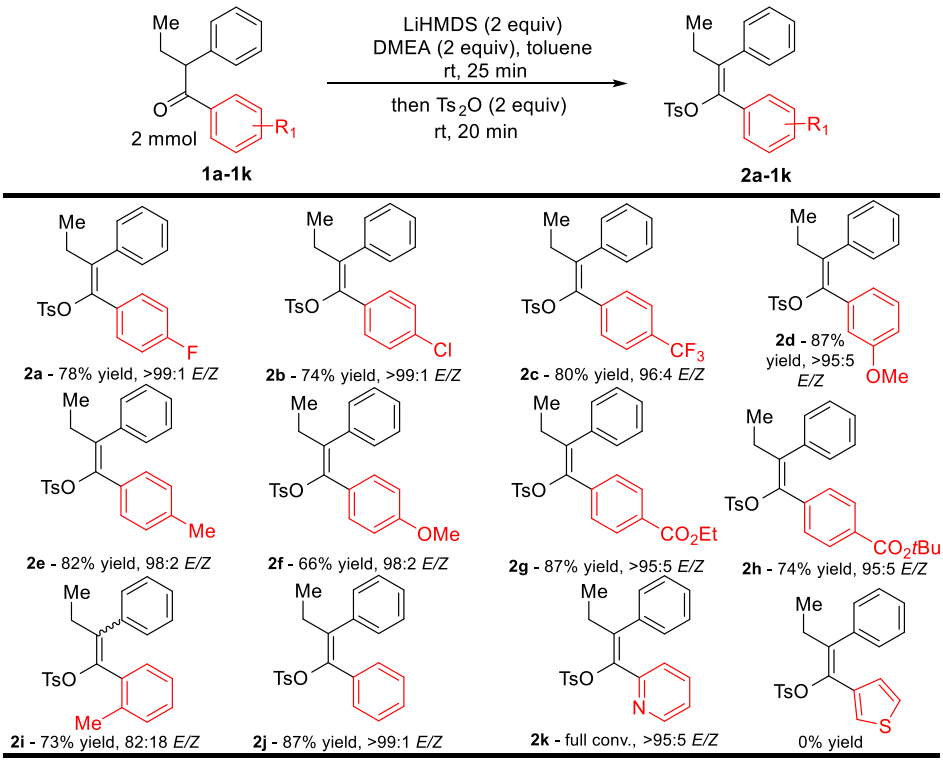

Next, different substrates were evaluated with variation at R_2 (Table 4.4). Various electron withdrawing (e.g., 4-F, 4-Cl, 4-CF_3, 3-OMe) are tolerated in up to 87% yield and >99:1 *E/Z*. Electron donating groups (e.g., 4-OMe and 4-Me) also work well in 75% and 84% yields, respectively and >95:5 *E/Z* selectivity. A substrate containing an indole also is tolerated to afford the desired product in 65% yield and 93:7 *E/Z* selectivity.

Subsequently, a crystal structure of **2r** was obtained to confirm the *E*-selectivity observed in the reaction.

Table 4.4 Substrate scope evaluation with variation at R_2

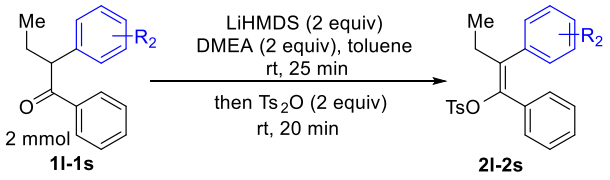

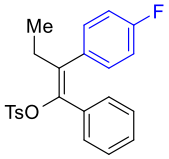

2l - 76% yield, >99:1 *E/Z*

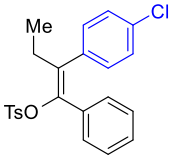

2m - 80% yield, >99:1 *E/Z*

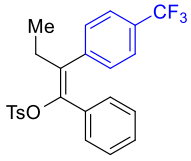

2n - 87% yield, 97:3 *E/Z*

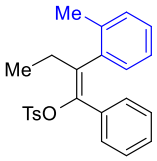

2o - 50% yield, >95:5 *E/Z*

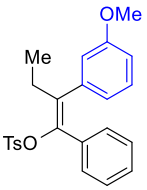

2p - 78% yield, >95:5 *E/Z*

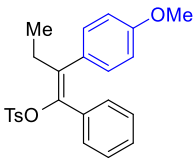

2q - 75% yield, >95:5 *E/Z*

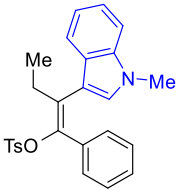

2r - 65% yield, 93:7 *E/Z*

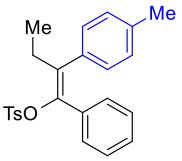

2s - 84% yield, >95:5 *E/Z*

Finally, the pendant ethyl group was changed to different alkyl substituents. There was a steric effect on the reactivity and selectivity of the reaction (Table 4.5). When R_3 = H, only 44% yield for enol tosylate **2t** is observed with a 67:33 *E/Z* mixture of isomers. As the steric bulk was increased (R_3 = Me), there is a slight increase in yield and selectivity. Thus, we found when R_3 = Et, high reactivity and selectivity is achieved. Accordingly, R_3 was varied with allyl or cyclopropyl substituents to afford the desired products in 81% and 82% yields, respectively, with >95:5 *E/Z* selectivity. When R_3 = *i*Pr or *t*Bu, no reaction is observed and only starting material remains.

Table 4.5 Substrate scope evaluation with variation at R_3

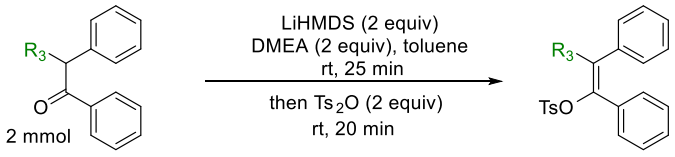

1t-1w **2t-2w**

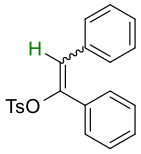

2t - 44% yield, 67:33 *E/Z*

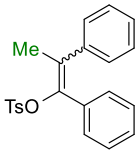

2u - 56% yield, 83:17 *E/Z*

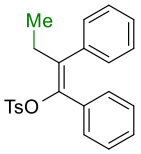

2j - 87% yield, >99:1 *E/Z*

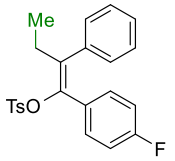

2a - 78% yield, >99:1 *E/Z*

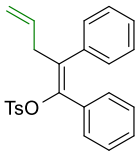

2v - 81% yield, >95:5 *E/Z*

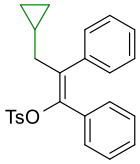

2w - 82% yield, >95:5 *E/Z*

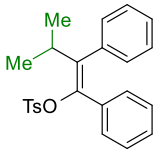

no reaction

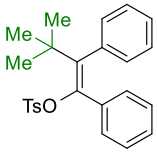

no reaction

4.1.4 Stereospecific Suzuki-Miyaura Cross-Coupling

Next, the Suzuki–Miyaura coupling of enol tosylate **2** and 4-fluorophenyl pinacol boronic ester was examined. High-throughput screening led to the optimal conditions using 1.0 equiv of enol tosylate **2**, 1.1 equiv of boronic ester, 1 mol% of $Pd(OAc)_2$, 2 mol% of RuPhos, and 1.5 equiv of K_3PO_4•H2O in PhMe/H_2O (0.5 M, 3:1) at 70 °C (Table 4.6). In select examples, enol tosylates with electron donating (4-Me) or withdrawing groups (4-F, 4-CF_3) are all tolerated in high yields (up to 96%) and selectivities (up to >99:1 *E/Z*). A 2-pyridyl group is also tolerated to afford the all-carbon tetrasubstituted alkene in 65% yield and 96:4 *E/Z.*

Table 4.6 Stereospecific Suzuki-Miyaura Cross Coupling

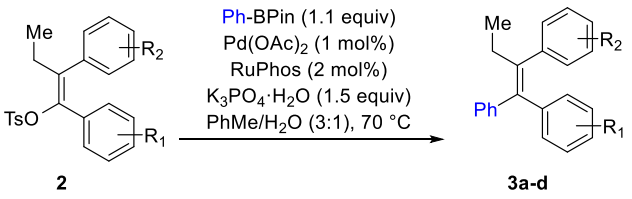

2 **3a-d**

Select scope

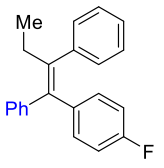

3a - 93% yield, 98:2 *E/Z*

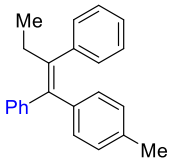

3b - 96% yield, 96:4 *E/Z*

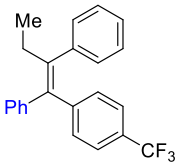

3c - 96% yield, >99:1 *E/Z*

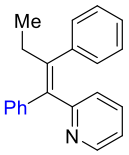

3d - 65% yield, 96:4

4.1.5 Conclusion

In conclusion, we developed a new route to all-carbon tetrasubstituted alkenes via a stereoselective enol tosylation followed by a Suzuki-Miyaura cross coupling. By using LiHMDS and a DMEA additive, we could access stereodefined enol tosylates in high yields (up to 95%) and selectivities (up to >99:1 *E/Z*). Using high throughput screening, we found optimized conditions to perform a stereospecific Suzuki-Miyaura cross coupling with the enol tosylates to afford the all-carbon tetrasubstituted alkene with high yields (up to 99%) and stereochemical fidelity (up to >99:1 *E/Z*).

4.2 Experimental Data

4.2.1 Experimental Details

The data shown Table 4.6 and certain substrates in Tables 4.1-4.5 were obtained by B.X.L and coworkers, and the reader is directed to the Supporting Information of the published manuscript[151] for the details of those experiments. This experimental section will focus on my contributions to the project.

Enol tosylate formation via LiHMDS (representative example):

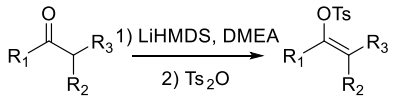

1-(4-fluorophenyl)-2-phenylbut-1-en-1-yl 4-methylbenzenesulfonate (2a)

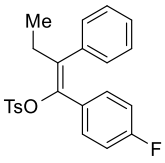

To a flame dried round bottom flask equipped with a stir bar under N_2 was added LiHMDS (1 M in toluene, 4 mmol, 2 equiv) and DMEA (0.434 mL, 4 mmol, 2 equiv). The reaction mixture was placed in a rt water bath and a solution of 1-(4-fluorophenyl)-2-phenyl-butan-1-one (**1a**, 484.6 mg in 2 mL toluene, 2.0 mmol, 1 equiv) was added and the reaction stirred at rt. After 20 min, the reaction mixture was placed in a rt water bath and Ts_2O (1.31 g in 10 mL DCM, 4 mmol, 2 equiv) was added dropwise over 1 min. The reaction mixture then stirred at rt for 20 min. An aliquot was taken and via HPLC analysis, the reaction went to full conversion and the *E/Z* ratio was determined to be >99:1. MTBE (10 mL) and NaOH (0.25 M aq, 4 mL) was added to quench the reaction and the mixture then transferred to a separatory funnel. The organic layer was separated from the aqueous layer (pH = 13), washed with brine, dried over Na_2SO_4, filtered, and concentrated under reduced pressure. The crude reaction mixture was then purified by silica gel column chromatography using heptane/isopropyl acetate and compound **2a** was obtained as a white solid (617 mg, 78%). ^{1}H NMR (400 MHz, $CDCl_3$) δ 7.53 – 7.41 (m, 2H), 7.20 – 7.09 (m, 5H), 7.04 – 6.94 (m, 2H), 6.89 – 6.79 (m, 2H), 6.64 – 6.49 (m, 2H), 2.67 (q, *J* = 7.5 Hz, 2H), 2.37 (s, 3H), 0.91 (t, *J* = 7.5 Hz, 3H). ^{13}C NMR (101 MHz, $CDCl_3$) δ 161.89 (d, *J* = 248.6 Hz), 144.58, 141.54, 138.07, 137.13, 134.35, 131.68 (d, *J* = 8.4 Hz), 130.09 (d, *J* = 3.6 Hz), 129.31, 129.28, 128.22, 127.96, 127.16, 114.39 (d, *J* = 21.9 Hz), 26.10, 21.55, 11.89; ^{19}F NMR (376 MHz, $CDCl_3$) δ -

113.10; mp 71 °C; IR (ATR) 3045, 2988, 2924, 1598, 1506, 1368, 1163 cm^{-1}; HRMS (ESI−) *m/z* calculated for $C_{23}H_{21}FO_3S$ ($[M–H]^-$), 395.1117; found, 395.1154.

(*E*)-1-(4-chlorophenyl)-2-phenylbut-1-en-1-yl 4-methylbenzenesulfonate (2b)

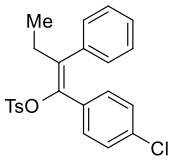

1-(4-chlorophenyl)-2-phenyl-butan-1-one (**1b**, 517 mg, 2.0 mmol) was employed. The *E/Z* ratio before workup via HPLC was determined to be >99:1. After silica gel column chromatography, compound **2b** was obtained as a white solid (611.5 mg, 74%). ^1H NMR (400 MHz, $CDCl_3$) δ 7.48 (d, *J* = 8.4 Hz, 2H), 7.18 (dd, *J* = 5.1, 1.9 Hz, 3H), 7.12 (dt, *J* = 7.8, 0.7 Hz, 2H), 7.05 – 6.96 (m, 2H), 6.85 (d, *J* = 8.7 Hz, 2H), 6.78 (d, *J* = 8.6 Hz, 2H), 2.67 (q, *J* = 7.5 Hz, 2H), 2.39 (s, 3H), 0.91 (t, *J* = 7.5 Hz, 3H); ^{13}C NMR (101 MHz, $CDCl_3$) δ 144.74, 141.35, 137.91, 137.70, 134.22, 133.51, 132.48, 131.08, 129.31, 129.27, 128.29, 127.99, 127.59, 127.29, 26.16, 21.57, 11.85; mp 75 °C; IR (ATR) 3050, 2987, 2923, 2874, 1598, 1487, 1347, 1177 cm^{-1}; HRMS (ESI−) *m/z* calculated for $C_{23}H_{21}ClO_3S$ ($[M–H]^-$), 411.0822; found, 411.0853.

(*E*)-1-(3-methoxyphenyl)-2-phenylbut-1-en-1-yl 4-methylbenzenesulfonate (2d)

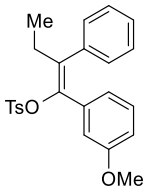

1-(3-methoxyphenyl)-2-phenyl-butan-1-one (**1d**, 509 mg, 2.0 mmol) was employed. The *E/Z* ratio before workup was determined via HPLC to be >95:5. After silica gel column chromatography, compound **2d** was obtained as a white solid (711.5 mg, 87%). ^1H NMR (400 MHz, $CDCl_3$) δ 7.52 – 7.42 (m, 2H), 7.23 – 7.12 (m, 3H), 7.12 – 6.99 (m, 4H), 6.79 (t, *J* = 7.9 Hz, 1H), 6.58 – 6.44 (m, 2H), 6.34 (dd, *J* = 2.6, 1.6 Hz, 1H), 3.42 (s, 3H), 2.70 (q, *J* = 7.5 Hz, 2H), 2.35 (s, 3H), 0.93 (t, *J* =

7.5 Hz, 3H); ^{13}C NMR (101 MHz, $CDCl_3$) δ 158.46, 144.32, 142.42, 138.41, 137.02, 134.92, 134.40, 129.29, 129.13, 128.28, 128.15, 128.01, 127.06, 122.54, 114.38, 114.31, 54.80, 26.20, 21.52, 11.91; mp 105 °C; IR (ATR) 3075, 2980, 2932, 2872, 2836, 1598, 1577, 1487, 1362, 1174 cm^{-1}; HRMS (ESI−) *m/z* calculated for $C_{22}H_{21}NO_3S$ ($[M–H]^-$), 407.1317; found, 407.1317.

(*E*)-2-phenyl-1-(*p*-tolyl)but-1-en-1-yl 4-methylbenzenesulfonate (2e)

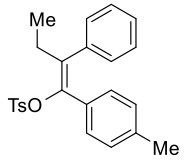

2-phenyl-1-(*p*-tolyl)butan-1-one (**1e**, 477 mg, 2.0 mmol) was employed. The *E/Z* ratio before workup was determined via HPLC to be 98:2. After silica gel column chromatography, compound **2e** was obtained as a white solid (645 mg, 82%). ^{1}H NMR (400 MHz, $CDCl_3$) δ 7.53 – 7.43 (m, 2H), 7.16 (dd, *J* = 6.0, 1.5 Hz, 3H), 7.08 (d, *J* = 8.1 Hz, 2H), 7.05 – 6.98 (m, 2H), 6.76 (d, *J* = 8.2 Hz, 2H), 6.69 (d, *J* = 8.0 Hz, 2H), 2.65 (q, *J* = 7.5 Hz, 2H), 2.36 (s, 3H), 2.16 (s, 3H), 0.90 (t, *J* = 7.5 Hz, 3H). ^{13}C NMR (101 MHz, $CDCl_3$) δ 144.20, 142.76, 138.47, 137.44, 136.12, 134.45, 130.98, 129.73, 129.38, 129.12, 128.08, 128.02, 126.91, 26.10, 21.55, 21.15, 11.95; mp 86 °C; IR (ATR) 2972, 2924, 2872, 2855, 1595, 1363, 1189 cm^{-1}; HRMS (ESI−) *m/z* calculated for $C_{24}H_{24}O_3S$ ($[M–H]^-$), 391.1368; found, 391.1368.

(*E*)-1-(4-methoxyphenyl)-2-phenylbut-1-en-1-yl 4-methylbenzenesulfonate (2f)

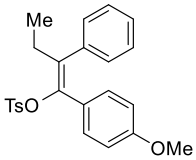

1-(4-methoxyphenyl)-2-phenyl-butan-1-one (**1f**, 509 mg, 2.0 mmol) was employed. The *E/Z* ratio before workup was determined via HPLC to be 98:2. After silica gel column chromatography, compound **2f** was obtained as a white solid (542 mg, 66%). ^{1}H NMR (400 MHz, $CDCl_3$) δ 7.52 – 7.45 (m, 2H), 7.20 – 7.12 (m, 3H), 7.10 (d, J = 8.2 Hz, 2H), 7.08 – 6.98 (m, 2H), 6.84 – 6.75 (m, 2H), 6.47 –

6.36 (m, 2H), 3.66 (s, 3H), 2.66 (q, *J* = 7.5 Hz, 2H), 2.36 (s, 3H), 0.91 (t, *J* = 7.5 Hz, 3H); ^{13}C NMR (101 MHz, $CDCl_3$) δ 158.87, 144.14, 142.56, 138.50, 135.60, 134.52, 131.19, 129.38, 129.14, 128.09, 127.99, 126.85, 126.30, 112.76, 55.04, 26.04, 21.53, 11.97; mp 89 °C; IR (ATR) 3016, 2960, 2932, 1608, 1492, 1363, 1172 cm^{-1}; HRMS (ESI−) *m/z* calculated for $C_{24}H_{24}O_4S$ ($[M–H]^-$), 407.1317; found, 407.1327.

Ethyl (*E*)-4-(2-phenyl-1-(tosyloxy)but-1-en-1-yl)benzoate (2g)

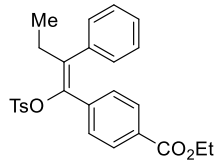

ethyl 4-(2-phenylbutanoyl)benzoate (**1g**, 593 mg, 2.0 mmol) was employed. The *E/Z* ratio before workup was determined via HPLC to be >95:5. After silica gel column chromatography, compound **2g** was obtained as a white solid (780 mg, 87%). ^{1}H NMR (400 MHz, $CDCl_3$) δ 7.59 – 7.54 (m, 2H), 7.52 – 7.45 (m, 2H), 7.17 (ddt, *J* = 5.5, 4.0, 2.4 Hz, 3H), 7.09 (d, *J* = 8.1 Hz, 2H), 7.05 – 6.97 (m, 2H), 6.97 – 6.87 (m, 2H), 4.31 (q, *J* = 7.1 Hz, 2H), 2.68 (q, *J* = 7.5 Hz, 2H), 2.35 (s, 3H), 1.34 (t, *J* = 7.1 Hz, 3H), 0.91 (t, *J* = 7.5 Hz, 3H); ^{13}C NMR (101 MHz, $CDCl_3$) δ 166.21, 144.93, 141.56, 138.99, 138.65, 137.94, 134.20, 129.79, 129.48, 129.41, 129.34, 128.67, 128.47, 128.17, 127.58, 61.08, 26.44, 21.67, 14.45, 11.96; mp 84 °C; IR (ATR) 3054, 2980, 2923, 1713, 1362, 1275, 1191 cm^{-1}; HRMS (ESI−) *m/z* calculated for $C_{26}H_{26}O_5S$ ($[M–H]^-$), 449.1423; found, 449.1461.

***tert*-butyl (*E*)-4-(1-phenyl-1-(tosyloxy)but-1-en-2-yl)benzoate (2h)**

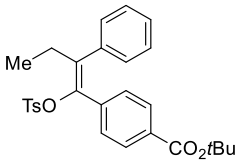

tert-butyl 4-(2-phenylbutanoyl)benzoate (**1h**, 649 mg, 2.0 mmol) was employed. The *E/Z* ratio before workup was determined via HPLC to be >95:5. After silica gel column chromatography, compound **2h** was obtained as a white

solid (710 mg, 74%). ^{1}H NMR (400 MHz, $CDCl_3$) δ 7.49 (dd, *J* = 8.2, 1.7 Hz, 4H), 7.23 – 7.13 (m, 3H), 7.08 (d, *J* = 8.1 Hz, 2H), 7.00 (dd, *J* = 6.6, 3.0 Hz, 2H), 6.97 – 6.81 (m, 2H), 2.68 (q, *J* = 7.5 Hz, 2H), 2.35 (s, 3H), 1.54 (s, 9H), 0.91 (t, *J* = 7.5 Hz, 3H); ^{13}C NMR (101 MHz, $CDCl_3$) δ 165.17, 144.70, 141.55, 138.55, 138.07, 137.84, 134.04, 130.73, 129.54, 129.31, 129.27, 128.41, 128.32, 128.03, 127.38, 80.98, 28.14, 26.25, 21.53, 11.82; mp 110 °C; IR (ATR) 3066, 2965, 2932, 2874, 1711, 1606, 1371, 1294, 1188, 1111 cm^{-1}.

(*E*)-2-phenyl-1-(*o*-tolyl)but-1-en-1-yl 4-methylbenzenesulfonate (2i) 1-(*o*-tolyl)-2-phenyl-butan-1-one (**1i**, 477 mg, 2.0 mmol) was employed. The *E/Z* ratio before workup was determined via HPLC to be 82:18. After silica gel column chromatography, compound **2i** was obtained as a white solid (480 mg, 61%).

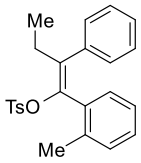

^{1}H NMR (400 MHz, $CDCl_3$) δ 7.34 (d, J = 8.4 Hz, 2H), 7.13 – 7.07 (m, 3H), 7.03 – 6.99 (m, 2H), 6.99 – 6.89 (m, 4H), 6.81 – 6.74 (m, 2H), 2.88 (dq, *J* = 14.9, 7.5 Hz, 1H), 2.69 (dq, *J* = 14.8, 7.5 Hz, 1H), 2.32 (s, 3H), 2.01 (s, 3H), 1.00 (t, *J* = 7.5 Hz, 3H); ^{13}C NMR (101 MHz, $CDCl_3$) δ 144.10, 142.74, 138.21, 137.74, 137.67, 134.58, 133.07, 132.33, 129.68, 129.14, 129.07, 128.47, 127.98, 127.72, 127.08, 125.02, 25.67, 21.66, 19.91, 12.66; mp 97 °C; IR (ATR) 3055, 2976, 2922, 2863, 1596, 1442, 1356, 1158 cm^{-1}; HRMS (ESI−) *m/z* calculated for $C_{24}H_{24}O_3S$ ($[M–H]^-$), 391.1368; found, 391.1408.

(*Z*)-2-phenyl-1-(o-tolyl)but-1-en-1-yl 4-methylbenzenesulfonate (2i')

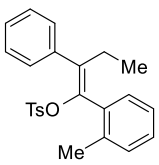

1-(*o*-tolyl)-2-phenyl-butan-1-one (**1i**, 477 mg, 2.0 mmol) was employed. Compound **2i'** was obtained as a white solid (90 mg, 12%). ^{1}H NMR (400 MHz, $CDCl_3$) δ 7.41 (dd, *J* = 7.3, 1.7 Hz, 1H), 7.37 – 7.27 (m, 5H), 7.23 – 7.16 (m, 2H), 7.16 – 7.12 (m, 2H), 7.06 – 7.02 (m, 1H), 6.94 (d, *J* = 8.1 Hz, 2H), 2.31 (s,

3H), 2.30 – 2.24 (m, 1H), 2.23 (s, 3H), 2.21 – 2.15 (m, 1H), 0.78 (t, *J* = 7.4 Hz, 3H); ^{13}C NMR (101 MHz, $CDCl_3$) δ 143.66, 140.98, 137.85, 137.21, 135.85, 134.27, 132.82, 131.44, 129.97, 129.08, 128.88, 128.77, 128.05, 127.47, 127.18, 125.27, 26.48, 21.49, 19.57, 12.52; mp 115 °C; FTIR (ATR) 3068, 2970, 2930, 2872, 1597, 1361, 1173 cm^{-1}.

(*E*)-2-(4-fluorophenyl)-1-phenylbut-1-en-1-yl 4-methylbenzenesulfonate (2l)

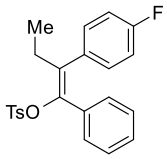

2-(4-fluorophenyl)-1-phenyl-butan-1-one (**1l**, 485 mg, 2.0 mmol) was employed. The *E/Z* ratio before workup was determined via HPLC to be >99:1. After silica gel column chromatography, compound **2l** was obtained as a white solid (600 mg, 76%). ^{1}H NMR (400 MHz, $CDCl_3$) δ 7.49 – 7.42 (m, 2H), 7.10 – 7.04 (m, 2H), 7.03 – 6.95 (m, 3H), 6.93 – 6.82 (m, 6H), 2.68 (q, *J* = 7.5 Hz, 2H), 2.35 (s, 3H), 0.92 (t, *J* = 7.5 Hz, 3H); ^{13}C NMR (101 MHz, $CDCl_3$) δ 161.80 (d, *J* = 246.4 Hz), 144.35, 142.83, 135.90, 134.32, 134.14 (d, *J* = 3.6 Hz), 133.70, 131.03 (d, *J* = 8.0 Hz), 129.87, 129.20, 127.96, 127.68, 127.44, 115.16 (d, *J* = 21.3 Hz), 26.11, 21.55, 11.91; ^{19}F NMR (376 MHz, $CDCl_3$) δ -114.93; mp 121 °C; IR (ATR) 3041, 2973, 2939, 2876, 1598, 1507, 1446, 1347, 1173 cm^{-1}; HRMS (ESI−) *m/z* calculated for $C_{23}H_{21}FO_3S$ ($[M–H]^-$), 395.1117; found, 395.1202.

(*E*)-2-(4-chlorophenyl)-1-phenylbut-1-en-1-yl 4-methylbenzenesulfonate (2m):

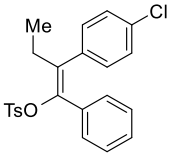

2-(4-chlorophenyl)-1-phenyl-butan-1-one (**1m**, 517 mg, 2.0 mmol) was employed. The *E/Z* ratio before workup was determined via HPLC to be >99:1. After silica gel column chromatography, compound **2m** was obtained as a white solid (600 mg, 80%). ^{1}H NMR (400 MHz, $CDCl_3$) δ 7.50 – 7.39 (m, 2H), 7.17 – 7.10 (m, 2H), 7.07 (d, *J* = 8.1 Hz, 2H), 7.04 – 6.82 (m, 7H), 2.68 (q, *J* = 7.5 Hz, 2H), 2.35 (s, 3H),

0.91 (t, *J* = 7.5 Hz, 3H). ^{13}C NMR (101 MHz, $CDCl_3$) δ 144.38, 142.98, 136.79, 135.73, 134.29, 133.54, 132.94, 130.77, 129.88, 129.22, 129.20, 128.40, 127.95, 127.81, 127.51, 25.98, 21.55, 11.93; mp 125 °C; IR (ATR) 2975, 2961, 2932, 1596, 1487, 1444, 1347, 1172 cm^{-1}; HRMS (ESI−) *m/z* calculated for $C_{23}H_{21}ClO_3S$ ($[M–H]^-$), 411.0822; found, 411.0883.

(*E*)-1-phenyl-2-(4-(trifluoromethyl)phenyl)but-1-en-1-yl 4-methylbenzenesulfonate (2n)

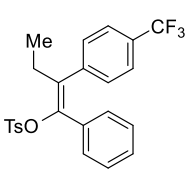

1-phenyl-2-[4-(trifluoromethyl)phenyl]butan-1-one (**1n**, 585 mg, 2.0 mmol) was employed. The *E/Z* ratio before workup was determined via HPLC to be 97:3. After silica gel column chromatography, compound **2n** was obtained as a white solid (790 mg, 88%). ^{1}H NMR (400 MHz, $CDCl_3$) δ 7.43 (dd, *J* = 11.5, 8.3 Hz, 4H), 7.19 – 6.98 (m, 5H), 6.96 – 6.83 (m, 4H), 2.73 (q, *J* = 7.5 Hz, 2H), 2.35 (s, 3H), 0.92 (t, *J* = 7.5 Hz, 3H); ^{13}C NMR (101 MHz, DMSO) δ 145.03, 142.97, 142.14, 134.95, 133.06, 132.92, 130.02, 129.72, 129.55, 128.27, 127.62, 127.55, 127.65 (q, *J* = 31.2 Hz), 125.09 (q, *J* = 3.8 Hz), 124.03 (q, *J* = 271.7 Hz), 25.13, 21.04, 11.62; ^{19}F NMR (376 MHz, $CDCl_3$) δ -62.61; mp 94 °C; IR (ATR) 3061, 2996, 2969, 2937, 1597, 1324, 1171 cm^{-1}; HRMS (ESI−) *m/z* calculated for $C_{24}H_{21}F_3O_3S$ ($[M–H]^-$), 445.1085; found, 445.1114.

(*E*)-1-phenyl-2-(*o*-tolyl)but-1-en-1-yl 4-methylbenzenesulfonate (2o)

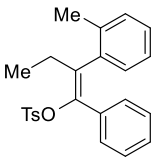

2-(*o*-tolyl)-1-phenyl-butan-1-one (**1o**, 477 mg, 2.0 mmol) was employed. The *E/Z* ratio before workup was determined via HPLC to be >95:5. After silica

gel column chromatography, compound **2o** was obtained as a white solid (390 mg, 50%). ^{1}H NMR (400 MHz, $CDCl_3$) δ 7.52 (d, *J* = 8.3 Hz, 2H), 7.18 – 6.79 (m, 11H), 2.82 – 2.59 (m, 1H), 2.59 – 2.44 (m, 1H), 2.35 (s, 3H), 2.05 (s, 3H), 0.91 (t, *J* = 7.5 Hz, 3H); ^{13}C NMR (101 MHz, $CDCl_3$) δ 144.38, 142.33, 137.43, 136.17, 135.89, 134.17, 134.05, 130.10, 129.65, 129.22, 128.79, 128.10, 127.48, 127.28, 127.21, 125.48, 26.20, 21.54, 19.36, 11.39; mp 89 °C; IR (ATR) 3023, 2973, 2933, 1597, 1492, 1443, 1360, 1174 cm^{-1}; HRMS (ESI−) *m/z* calculated for $C_{24}H_{24}O_3S$ ($[M–H]^-$), 391.1368; found, 391.1441.

(*E*)-2-(1-methyl-1*H*-indol-3-yl)-1-phenylbut-1-en-1-yl 4-methylbenzenesulfonate (2r)

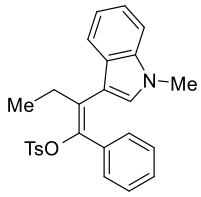

2-(1-methylindol-3-yl)-1-phenyl-butan-1-one (**1r**, 555 mg, 2.0 mmol) was employed. The *E/Z* ratio before workup was determined via HPLC to be 93:7. After silica gel column chromatography, compound **2r** was obtained as a light yellow solid (560 mg, 65%). ^{1}H NMR (400 MHz, $CDCl_3$) δ 7.51 (d, *J* = 8.3 Hz, 2H), 7.26 – 7.05 (m, 5H), 7.00 – 6.89 (m, 4H), 6.82 (t, *J* = 7.6 Hz, 2H), 6.66 (s, 1H), 3.65 (s, 3H), 2.71 (q, *J* = 7.5 Hz, 2H), 2.36 (s, 3H), 0.93 (t, *J* = 7.5 Hz, 3H); ^{13}C NMR (101 MHz, $CDCl_3$) δ 144.19, 142.53, 136.80, 134.73, 134.42, 130.28, 129.22, 129.15, 128.29, 128.10, 127.21, 127.15, 121.52, 120.09, 119.24, 111.96, 109.08, 32.75, 26.22, 21.55, 12.41; mp 135 °C; IR (ATR) 3024, 2969, 2922, 2855, 1612, 1597, 1530, 1446 ,1362, 1176 cm^{-1}.

(*E*)-2-(3-methoxyphenyl)-1-phenylbut-1-en-1-yl 4-methylbenzenesulfonate (2p)

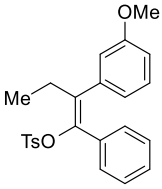

2-(3-methoxyphenyl)-1-phenyl-butan-1-one (**1p**, 509 mg, 2.0 mmol) was employed. The *E/Z* ratio before workup was determined via HPLC to be >95:5. After silica gel column chromatography, compound **2p** was obtained as a white solid (640 mg, 78%). ^{1}H NMR (400 MHz, $CDCl_3$) δ 7.53 – 7.42 (m, 2H), 7.07

(dd, *J* = 8.1, 5.9 Hz, 3H), 7.03 – 6.96 (m, 1H), 6.90 (d, *J* = 4.4 Hz, 4H), 6.69 (ddd, *J* = 8.3, 2.7, 0.9 Hz, 1H), 6.60 (dd, *J* = 7.7, 1.3 Hz, 1H), 6.55 (dd, *J* = 2.6, 1.5 Hz, 1H), 3.63 (s, 3H), 2.67 (q, *J* = 7.5 Hz, 2H), 2.35 (s, 3H), 0.93 (t, *J* = 7.5 Hz, 3H); ^{13}C NMR (101 MHz, $CDCl_3$) δ 159.26, 144.30, 142.60, 139.63, 136.74, 134.33, 133.93, 129.75, 129.19, 129.09, 128.00, 127.59, 127.34, 121.91, 114.90, 112.81, 55.10, 26.06, 21.55, 11.98; mp 86 °C; IR (ATR) 3054, 2977, 2933, 2874, 1712, 1594, 1366, 1173 cm^{-1}; HRMS (ESI−) *m/z* calculated for $C_{24}H_{24}O_4S$ ([M–H]$^-$), 407.1317; found, 407.1200.

(*E*)-2-(4-methoxyphenyl)-1-phenylbut-1-en-1-yl 4-methylbenzenesulfonate (2q)

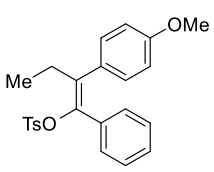

2-(4-methoxyphenyl)-1-phenyl-butan-1-one (**1q**, 509 mg, 2.0 mmol) was employed. The *E/Z* ratio before workup was determined via HPLC to be >99:1. After silica gel column chromatography, compound **2q** was obtained as a light yellow solid (610 mg, 75%); ^{1}H NMR (400 MHz, $CDCl_3$) δ 7.46 (d, *J* = 8.4 Hz, 2H), 7.07 (d, *J* = 8.1 Hz, 2H), 7.02 – 6.85 (m, 7H), 6.77 – 6.66 (m, 2H), 3.74 (s, 3H), 2.66 (q, *J* = 7.5 Hz, 2H), 2.35 (s, 3H), 0.91 (t, *J* = 7.5 Hz, 3H); ^{13}C NMR (101 MHz, $CDCl_3$) δ 158.56, 144.22, 142.28, 136.44, 134.42, 134.10, 130.53, 130.35, 129.87, 129.17, 127.97, 127.39, 127.35, 113.57, 55.11, 26.12, 21.54, 11.99; mp 105 °C; IR (ATR) 2995, 2967, 2922, 1606, 1508, 1346, 1172 cm^{-1}; HRMS (ESI−) *m/z* calculated for $C_{22}H_{21}NO_3S$ ([M–H]$^-$), 407.1317; found, 407.1284.

(*E*)-1-phenyl-2-(*p*-tolyl)but-1-en-1-yl 4-methylbenzenesulfonate (2s)

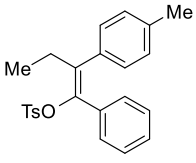

1-phenyl-2-(*p*-tolyl)butan-1-one (**1s**, 477 mg, 2.0 mmol) was employed. The *E/Z* ratio before workup was determined via HPLC to be >95:5. After silica gel column chromatography, compound **2s** was obtained as a light

yellow solid (660 mg, 84%); ^{1}H NMR (400 MHz, $CDCl_3$) δ 7.49 – 7.44 (m, 2H), 7.07 (d, *J* = 8.1 Hz, 2H), 7.02 – 6.94 (m, 3H), 6.93 – 6.83 (m, 6H), 2.66 (q, *J* = 7.5 Hz, 2H), 2.35 (s, 3H), 2.26 (s, 3H), 0.91 (t, *J* = 7.5 Hz, 3H); ^{13}C NMR (101 MHz, $CDCl_3$) δ 144.22, 142.35, 136.81, 136.68, 135.17, 134.41, 134.06, 129.87, 129.24, 129.17, 128.82, 127.98, 127.43, 127.30, 26.14, 21.54, 21.14, 11.96; mp 117 °C; IR (ATR) 3046, 2970, 2931, 2895, 1595, 1365, 1175 cm^{-1}; HRMS (ESI−) *m/z* calculated for $C_{24}H_{24}O_3S$ ($[M–H]^-$), 391.1368; found, 391.1388.

1,2-diphenylvinyl 4-methylbenzenesulfonate (2t)

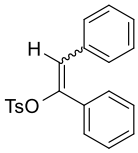

1,2-diphenylethanone (**1t**, 392 mg, 2.0 mmol) was employed. The *E/Z* ratio before workup was determined via HPLC to be 67:33. After silica gel column chromatography, compound **2t** was obtained as a white solid as an inseparable 1.2:1 mixture (310 mg, 44%); ^{1}H NMR (400 MHz, $CDCl_3$) δ 7.75 – 7.59 (m, 2H), 7.55 – 7.40 (m, 6H), 7.32 – 7.25 (m, 5H), 7.22 – 7.11 (m, 12H), 7.07 – 6.97 (m, 4H), 6.57 (s, 1H), 6.48 (s, 1H), 2.40 (s, 3H), 2.32 (s, 3H).

(*E*)-1,2-diphenylprop-1-en-1-yl 4-methylbenzenesulfonate (2u):

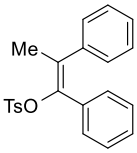

1,2-diphenylpropan-1-one (**1u**, 421 mg, 2.0 mmol) was employed. The *E/Z* ratio before workup was determined via HPLC to be 83:17. After silica gel column chromatography, compound **2u** was obtained as a white solid (341 mg, 47%). ^{1}H NMR (400 MHz, $CDCl_3$) δ 7.55 – 7.45 (m, 2H), 7.20 – 6.85 (m, 11H), 2.35 (s, 3H), 2.20 (s, 3H); ^{13}C NMR (101 MHz, $CDCl_3$) δ 144.35, 143.33, 139.97, 134.36, 133.95, 130.97, 129.82, 129.23, 128.75, 128.15, 128.00, 127.66, 127.43, 127.09, 21.55, 19.92; mp 92 °C;

IR (ATR) 3060, 3029, 2919, 2870, 1650, 1597, 1372, 1172 cm^{-1}; HRMS (ESI−) *m/z* calculated for $C_{22}H_{20}O_3S$ ($[M–H]^-$), 363.1055; found, 363.1112.

(*Z*)-1,2-diphenylprop-1-en-1-yl 4-methylbenzenesulfonate (2u')

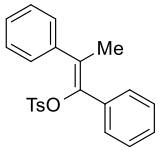

1,2-diphenylpropan-1-one (**1u**, 421 mg, 2.0 mmol) was employed. Compound **2u** was obtained as a white solid (70 mg, 10%). ^{1}H NMR (400 MHz, $CDCl_3$) δ 7.44 – 7.36 (m, 2H), 7.32 – 7.27 (m, 6H), 7.25 – 7.21 (m, 1H), 7.21 – 7.15 (m, 2H), 6.96 (d, *J* = 8.1 Hz, 2H), 2.33 (s, 3H), 2.02 (s, 3H); ^{13}C NMR (101 MHz, $CDCl_3$) δ 143.83, 141.49, 139.31, 134.10, 133.99, 129.77, 128.98, 128.54, 128.17, 127.99, 127.92, 127.70, 127.13, 21.51, 20.57; mp 103 °C; IR (ATR) 3060, 2983, 2921, 1598, 1491, 1444, 1365, 1172 cm^{-1}.

(*E*)-1,2-diphenylpenta-1,4-dien-1-yl 4-methylbenzenesulfonate (2v)

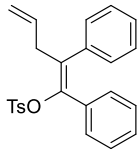

1,2-diphenylpent-4-en-1-one (**1v**, 473 mg, 2.0 mmol) was employed. The *E/Z* ratio before workup was determined via HPLC to be >95:5. After silica gel column chromatography, compound **2v** was obtained as a white solid (630 mg, 81%). ^{1}H NMR (400 MHz, $CDCl_3$) δ 7.55 – 7.43 (m, 2H), 7.20 – 7.11 (m, 3H), 7.11 – 7.05 (m, 2H), 7.05 – 6.97 (m, 3H), 6.89 (d, *J* = 4.4 Hz, 4H), 5.70 (ddt, *J* = 16.8, 10.0, 6.7 Hz, 1H), 5.03 (dq, *J* = 17.1, 1.6 Hz, 1H), 4.97 (dq, *J* = 10.0, 1.5 Hz, 1H), 3.44 (dt, *J* = 6.7, 1.5 Hz, 2H), 2.35 (s, 3H); ^{13}C NMR (101 MHz, $CDCl_3$) δ 144.38, 143.67, 138.21, 134.34, 134.05, 133.66, 132.91, 129.92, 129.49, 129.23, 128.05, 127.98, 127.75, 127.37, 127.11, 116.84, 37.53, 21.55; mp 73 °C; IR (ATR) 3057, 2982, 2893, 1641, 1597, 1347, 1171 cm^{-1}; HRMS (ESI−) *m/z* calculated for $C_{24}H_{22}O_3S$ ($[M–H]^-$), 389.1212; found, 389.1254.

(*E*)-3-cyclopropyl-1,2-diphenylprop-1-en-1-yl 4-methylbenzenesulfonate (2w)

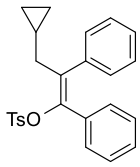

3-cyclopropyl-1,2-diphenyl-propan-1-one (**1w**, 501 mg, 2.0 mmol) was employed. The *E/Z* ratio before workup was determined via HPLC to be >95:5. After silica gel column chromatography, compound **2w** was obtained as a white solid (660 mg, 82%). ^{1}H NMR (400 MHz, $CDCl_3$) δ 7.51 – 7.42 (m, 2H), 7.22 – 7.12 (m, 3H), 7.12 – 7.03 (m, 4H), 7.03 – 6.93 (m, 1H), 6.88 (d, *J* = 4.4 Hz, 4H), 2.57 (d, *J* = 7.0 Hz, 2H), 2.35 (s, 3H), 0.71 – 0.55 (m, 1H), 0.40 – 0.27 (m, 2H), 0.13 – 0.03 (m, 2H); ^{13}C NMR (101 MHz, $CDCl_3$) δ 144.29, 142.81, 138.87, 135.49, 134.33, 133.85, 129.88, 129.45, 129.18, 128.00, 127.53, 127.29, 126.93, 37.53, 21.55, 9.30, 4.58; mp 113 °C; IR (ATR) 3066, 2981, 2920, 1597, 1362, 1167 cm^{-1}; HRMS (ESI−) *m/z* calculated for $C_{25}H_{24}O_3S$ ($[M–H]^-$), 403.1368; found, 403.1414.

4.2.2 NMR Spectra

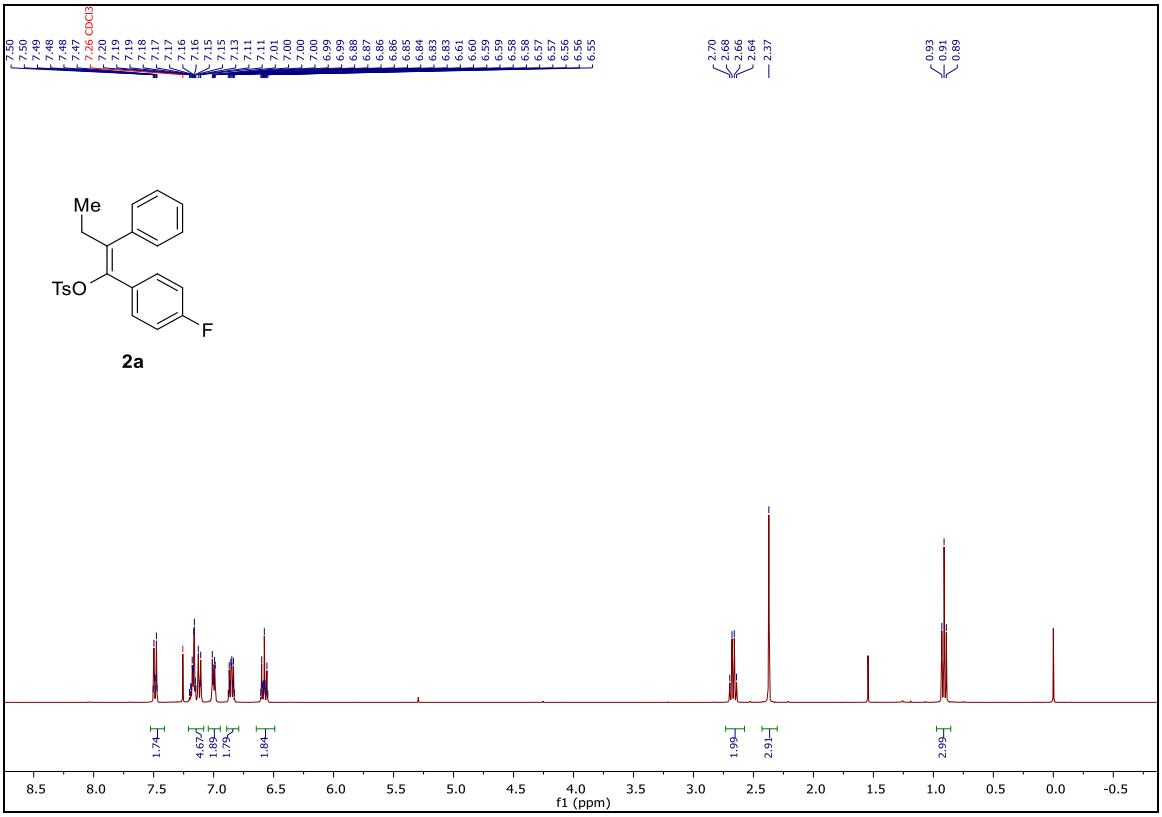

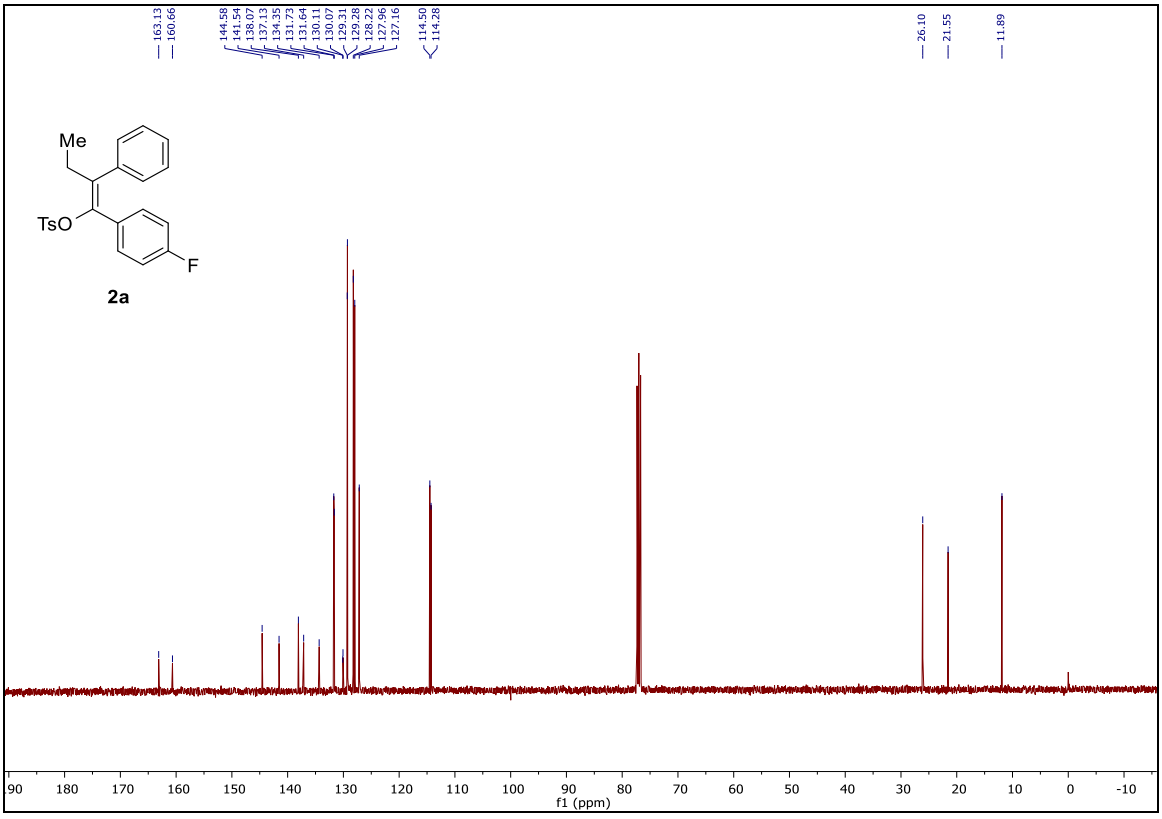

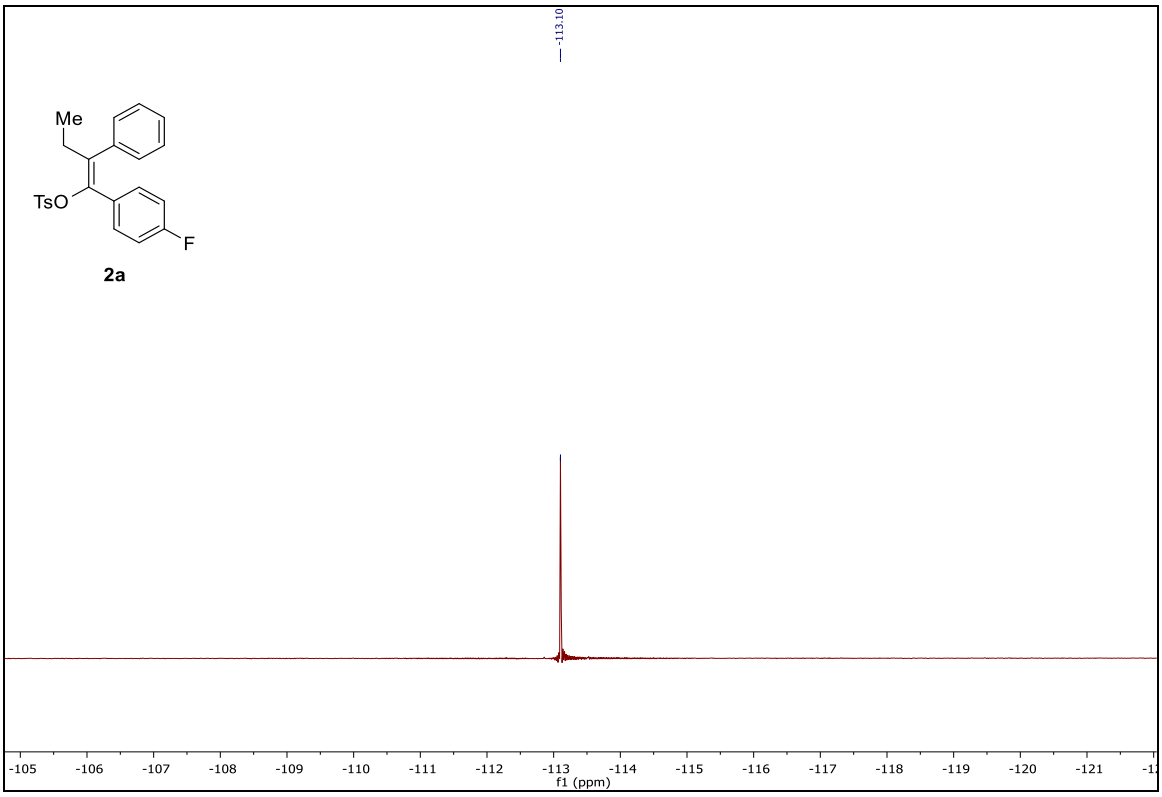
-113.10
Me
TsO
F
2a
-105
-106
-107
-108
-109
-110
-111
-112
-113
-114
-115
-116
-117
-118
-119
-120
-121
f1 (ppm)

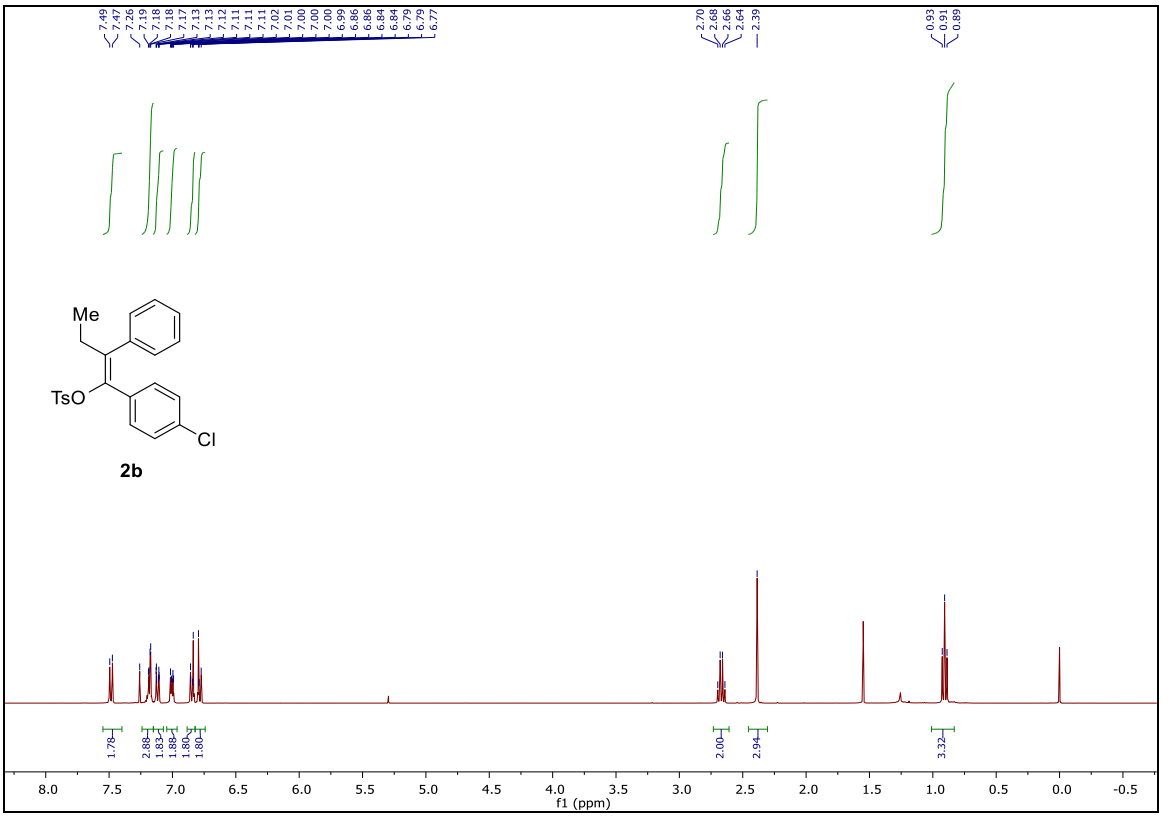
Me
TsO
Cl
2b
f1 (ppm)

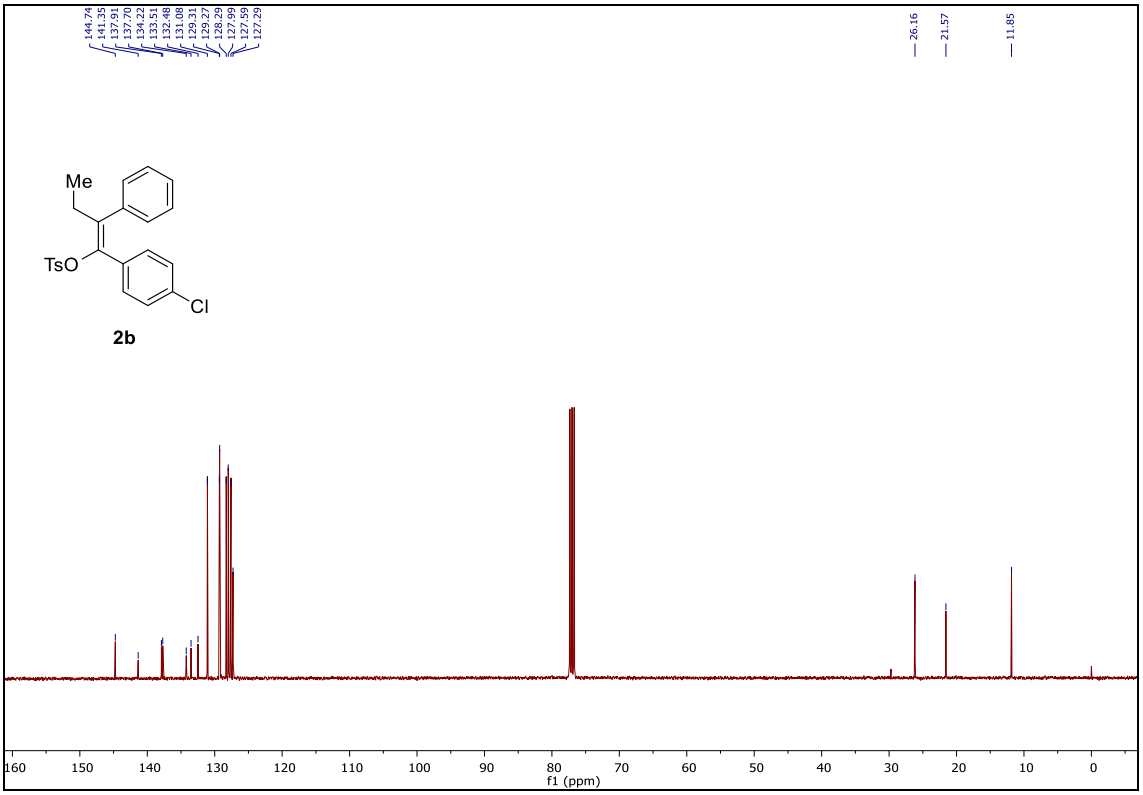
Me
TsO
Cl
2b
f1 (ppm)

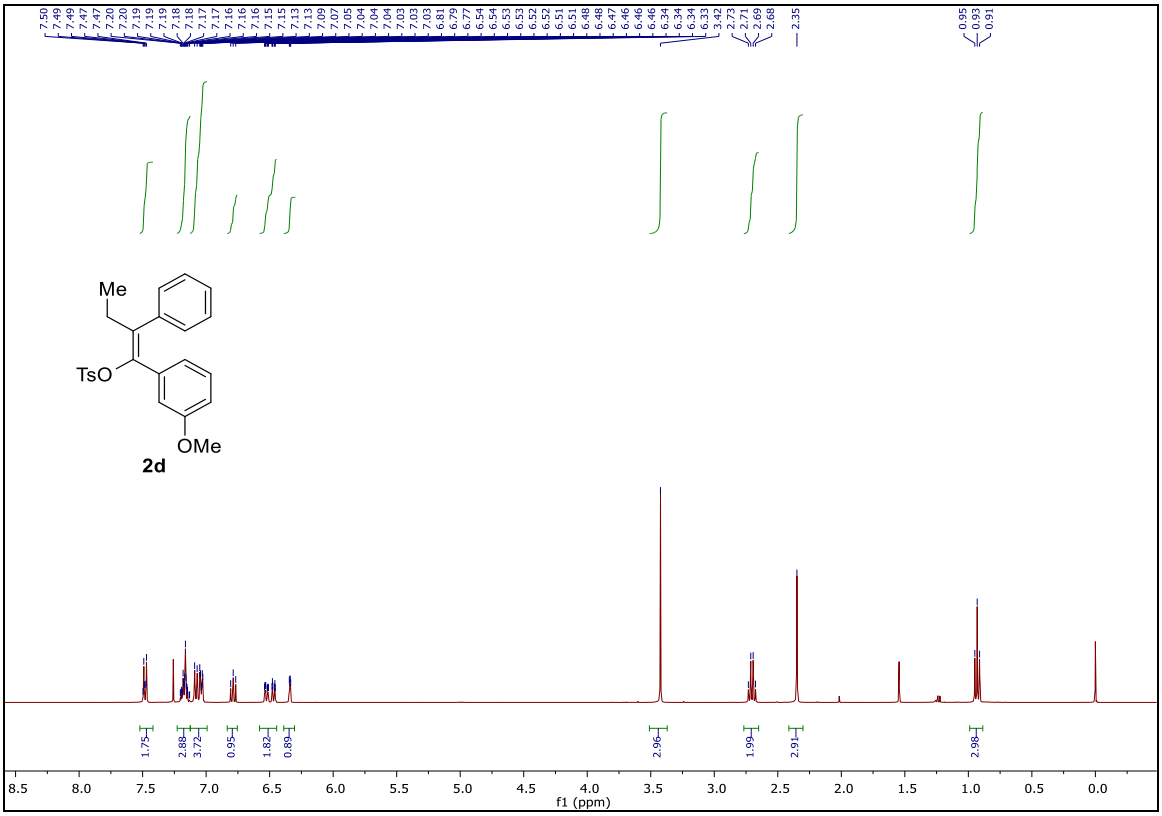
Me
TsO
OMe
2d
f1 (ppm)

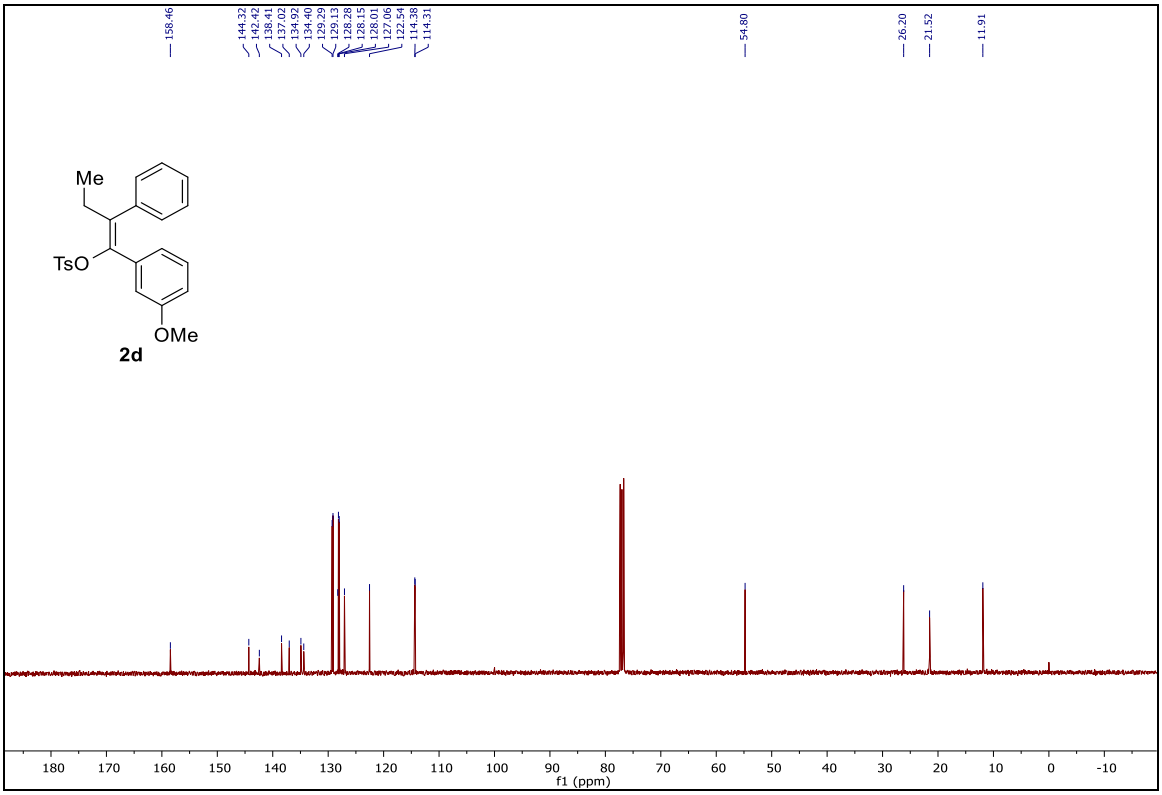
Me
TsO
OMe
2d
f1 (ppm)

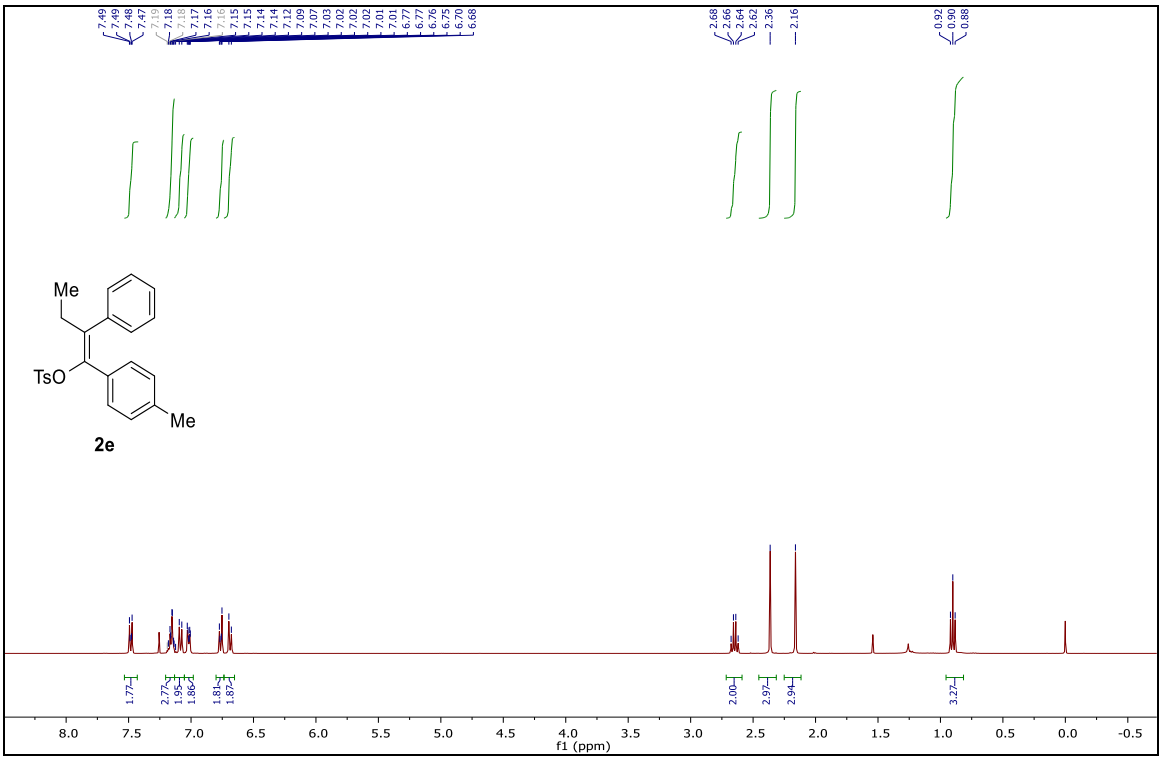
Me
TsO
Me
2e
f1 (ppm)

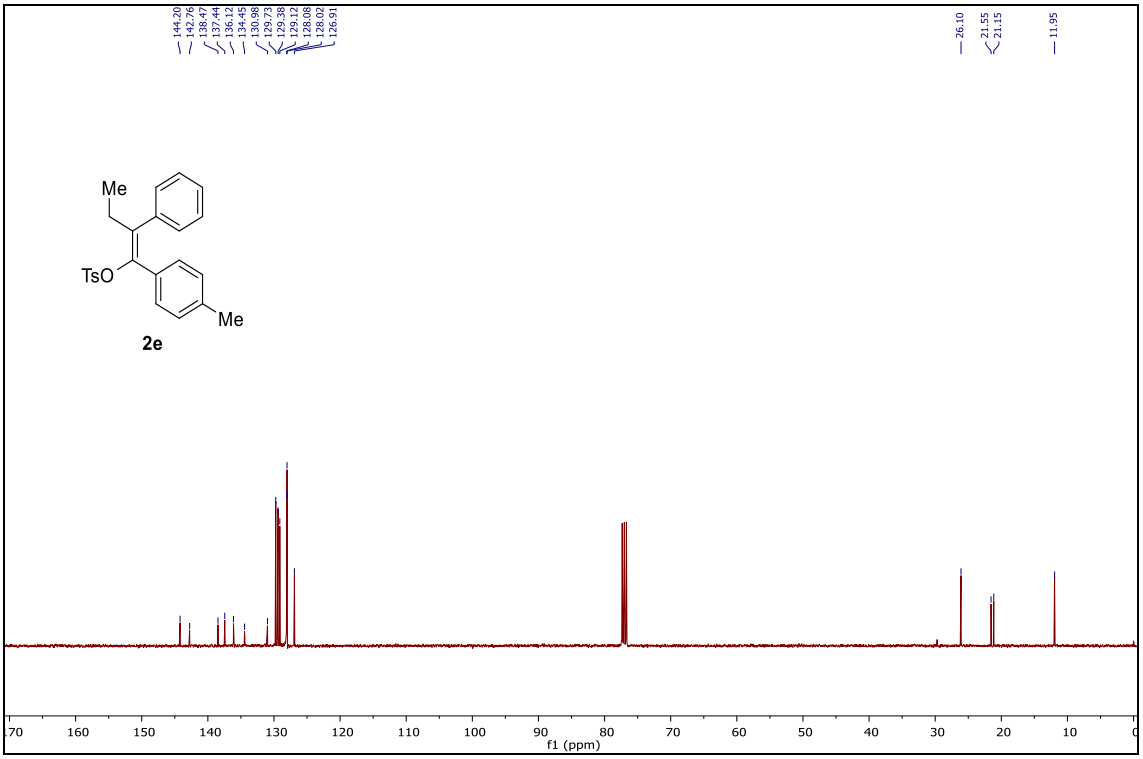
Me
TsO
Me
2e
f1 (ppm)

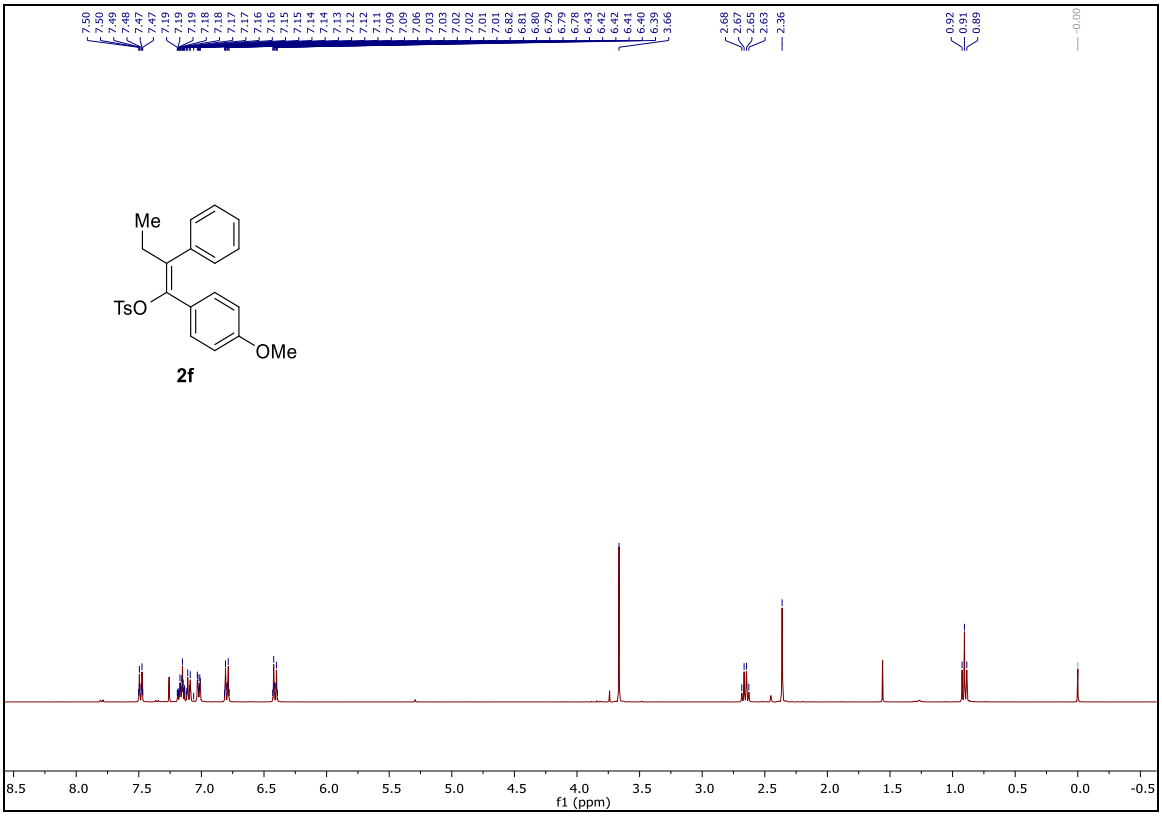
Me
TsO
OMe
2f
f1 (ppm)

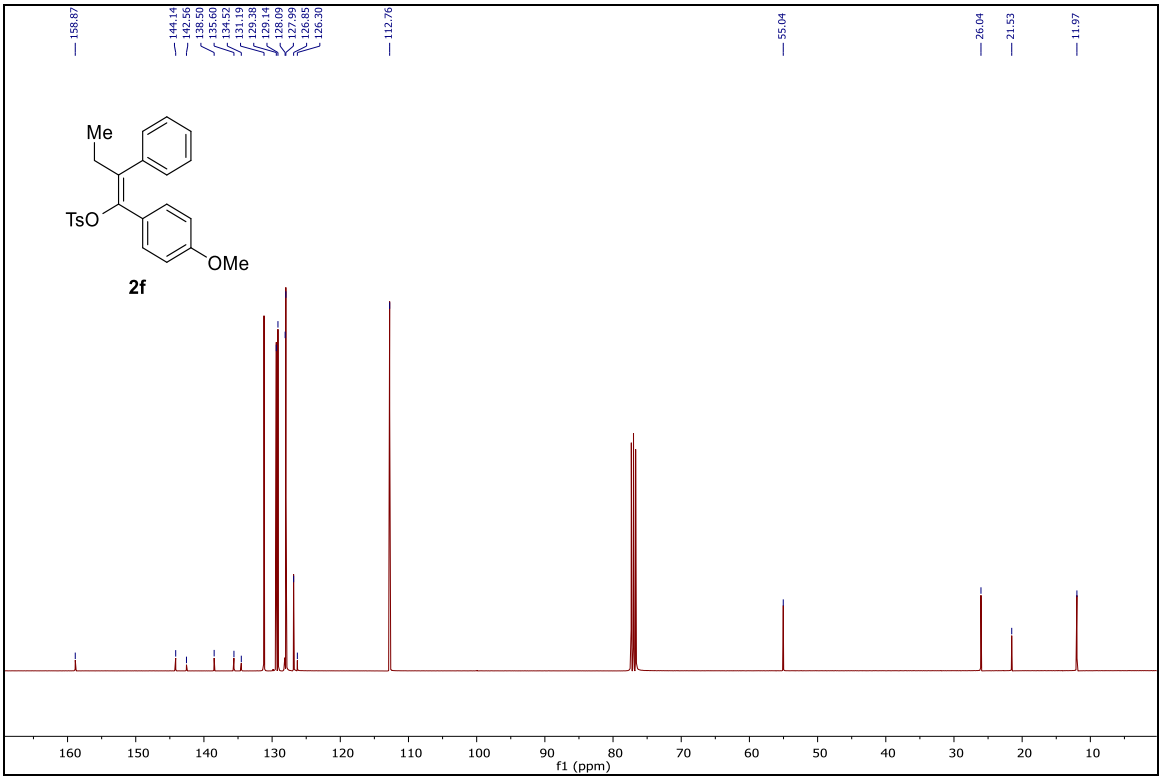
Me
TsO
OMe
2f
f1 (ppm)

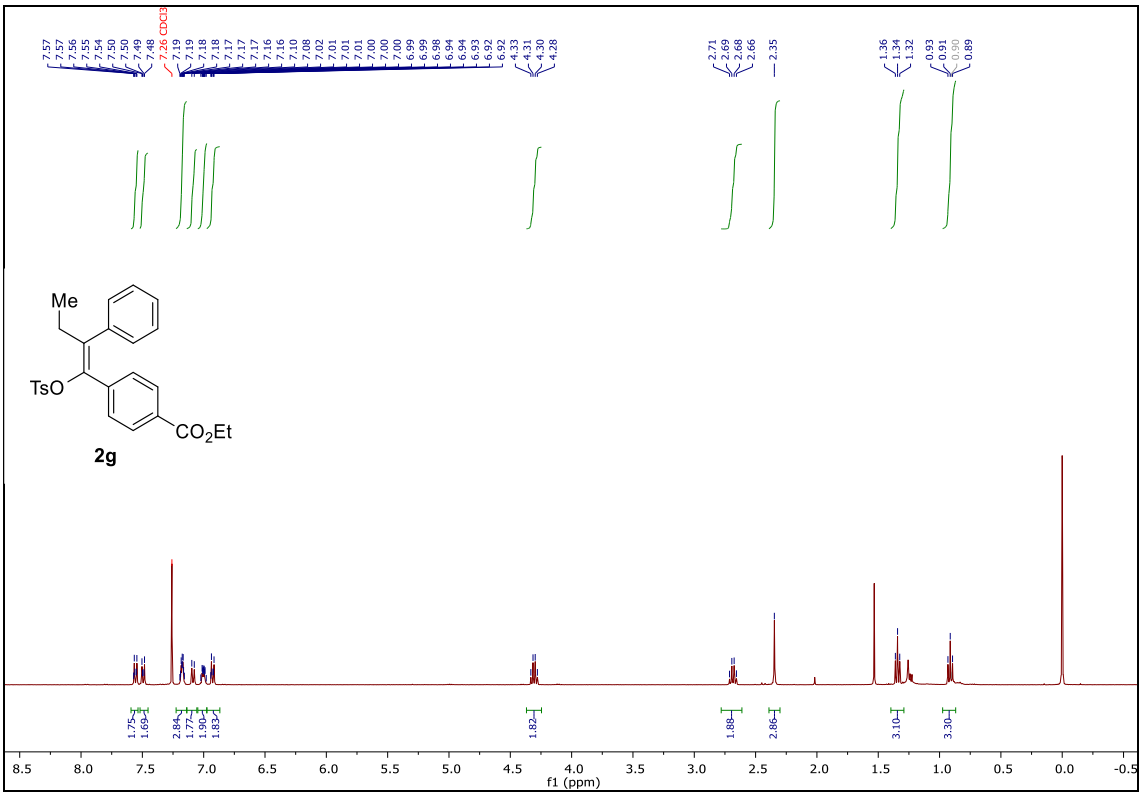
Me
TsO
CO2Et
2g
f1 (ppm)

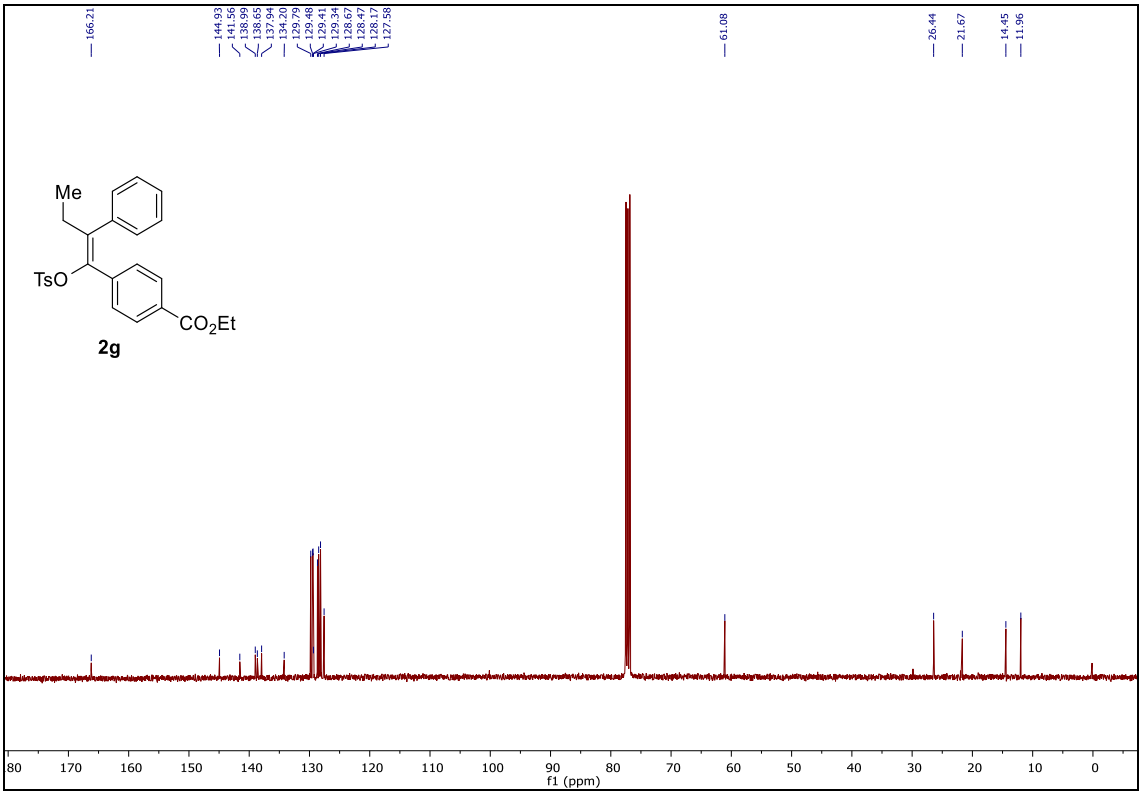
Me
TsO
CO2Et
2g
f1 (ppm)

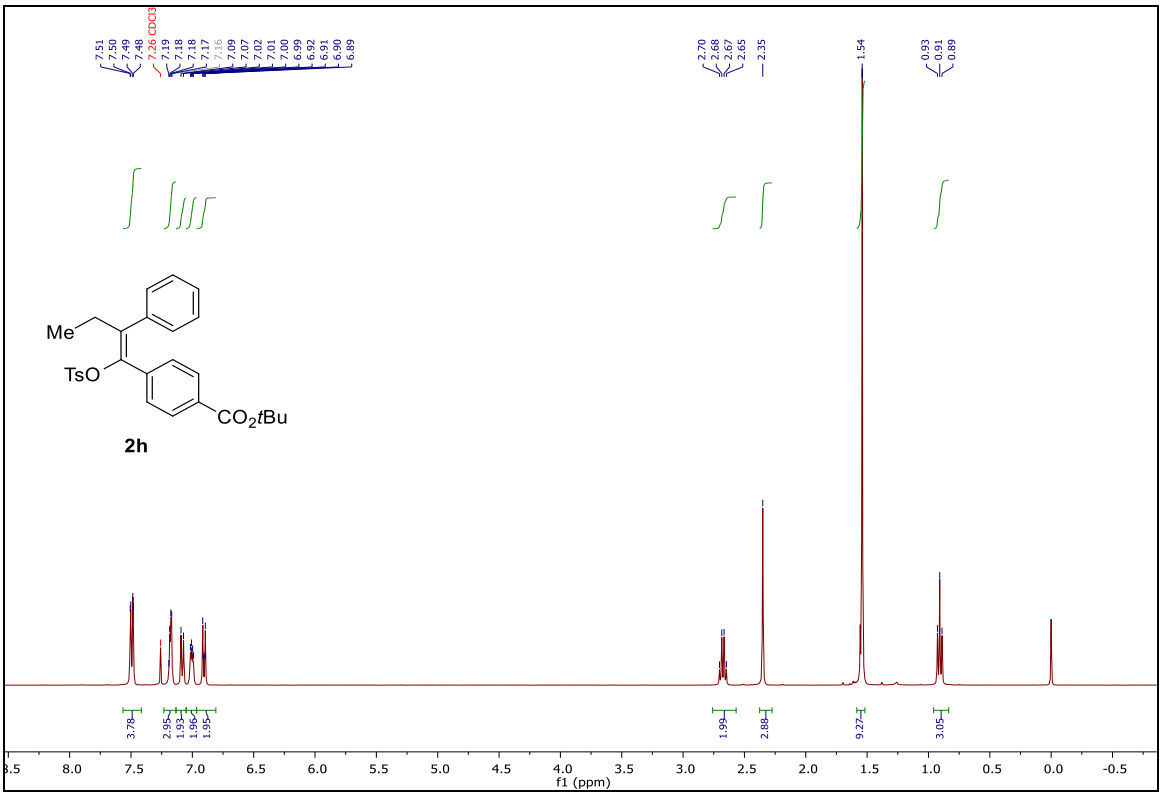
Me
TsO
CO2tBu
2h
f1 (ppm)

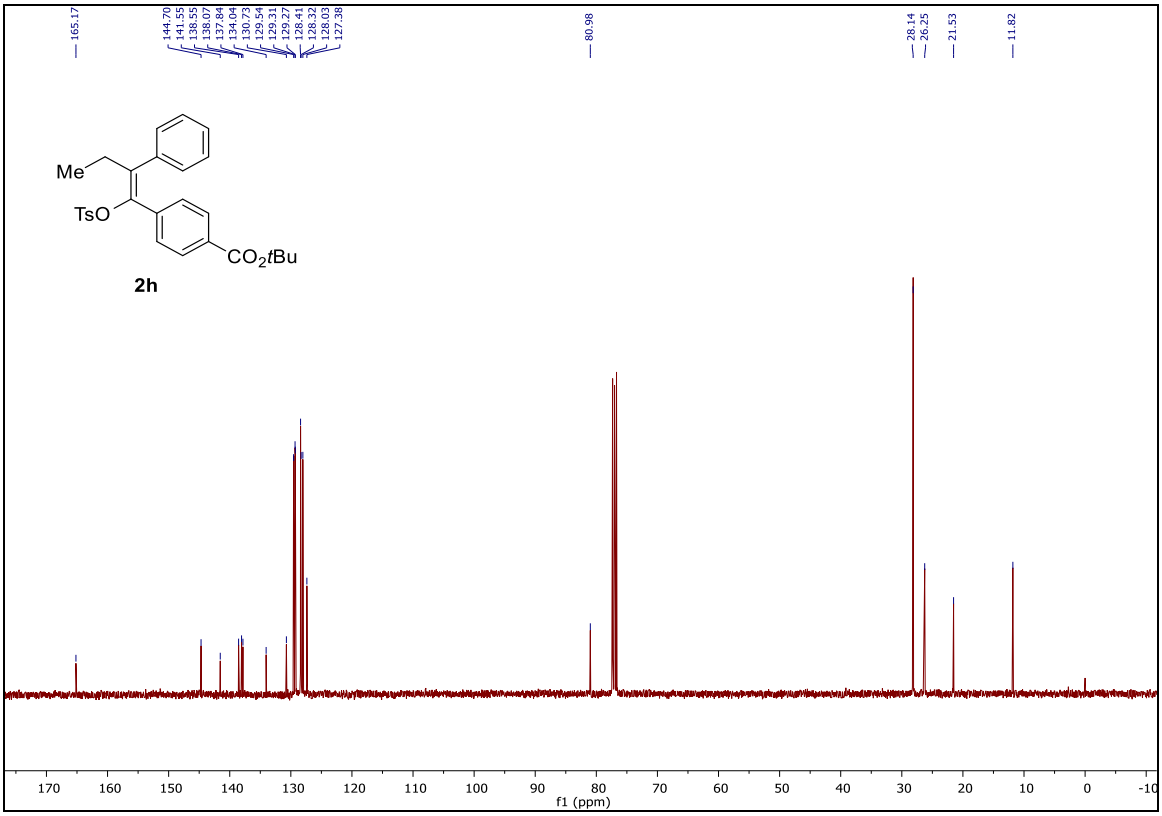
Me
TsO
CO2tBu
2h
f1 (ppm)

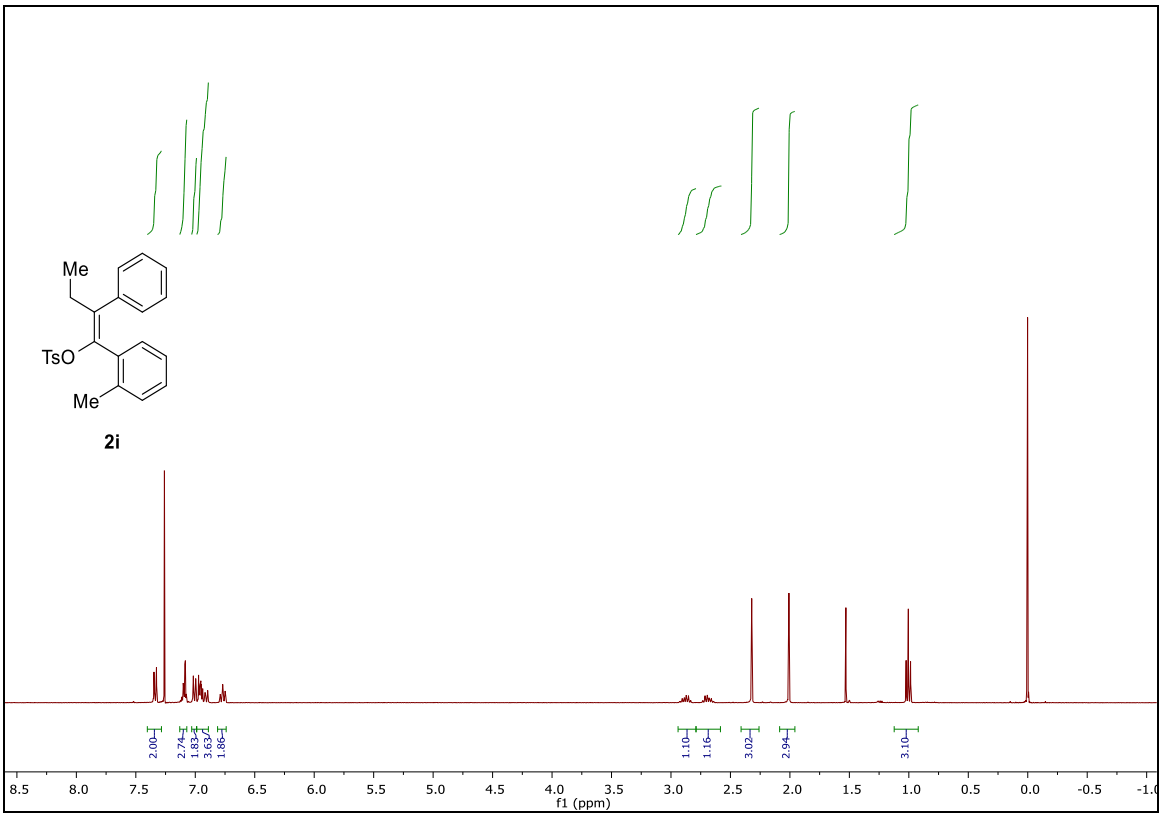
Me
TsO
Me
2i
2.00
2.74
1.83
3.63
1.86
1.10
1.16
3.02
2.94
3.10
8.5 8.0 7.5 7.0 6.5 6.0 5.5 5.0 4.5 4.0 3.5 3.0 2.5 2.0 1.5 1.0 0.5 0.0 -0.5
f1 (ppm)

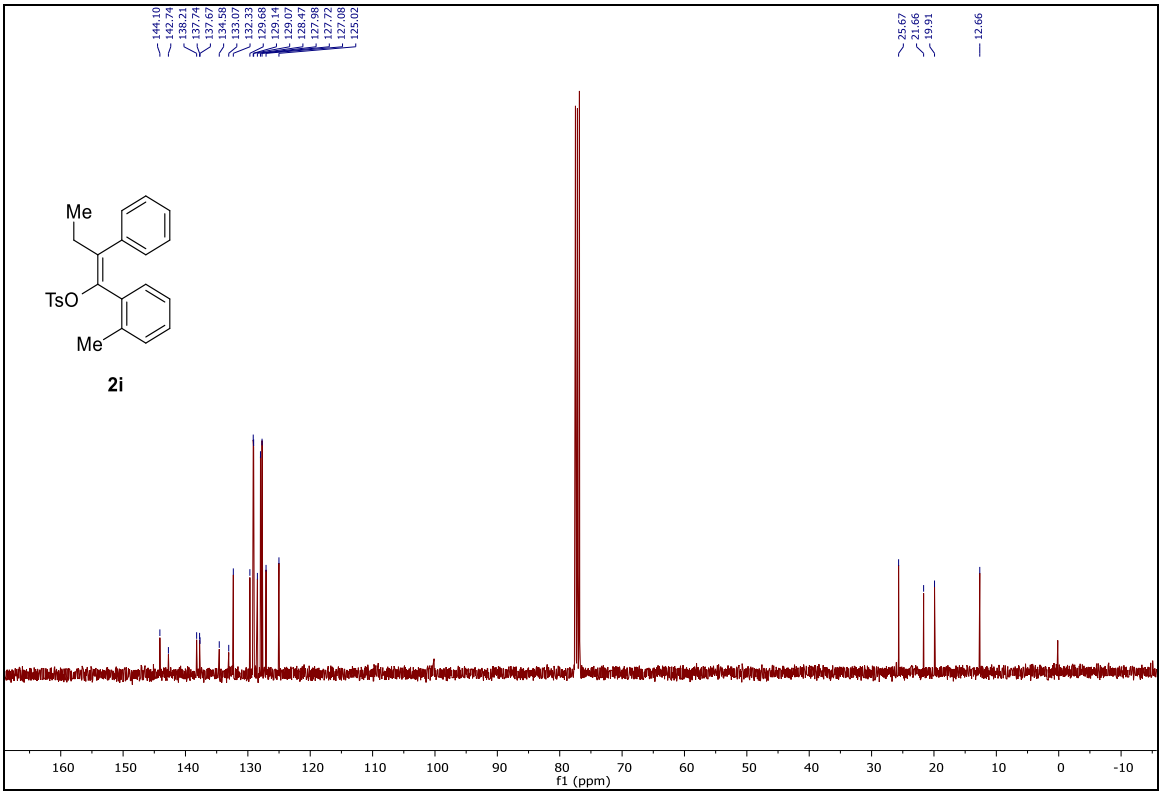
144.10
142.74
138.21
137.74
137.67
134.58
133.07
132.33
129.68
129.14
129.07
128.47
127.99
127.72
127.08
125.02
25.67
21.66
19.91
12.66
Me
TsO
Me
2i
160 150 140 130 120 110 100 90 80 70 60 50 40 30 20 10 0 -10
f1 (ppm)

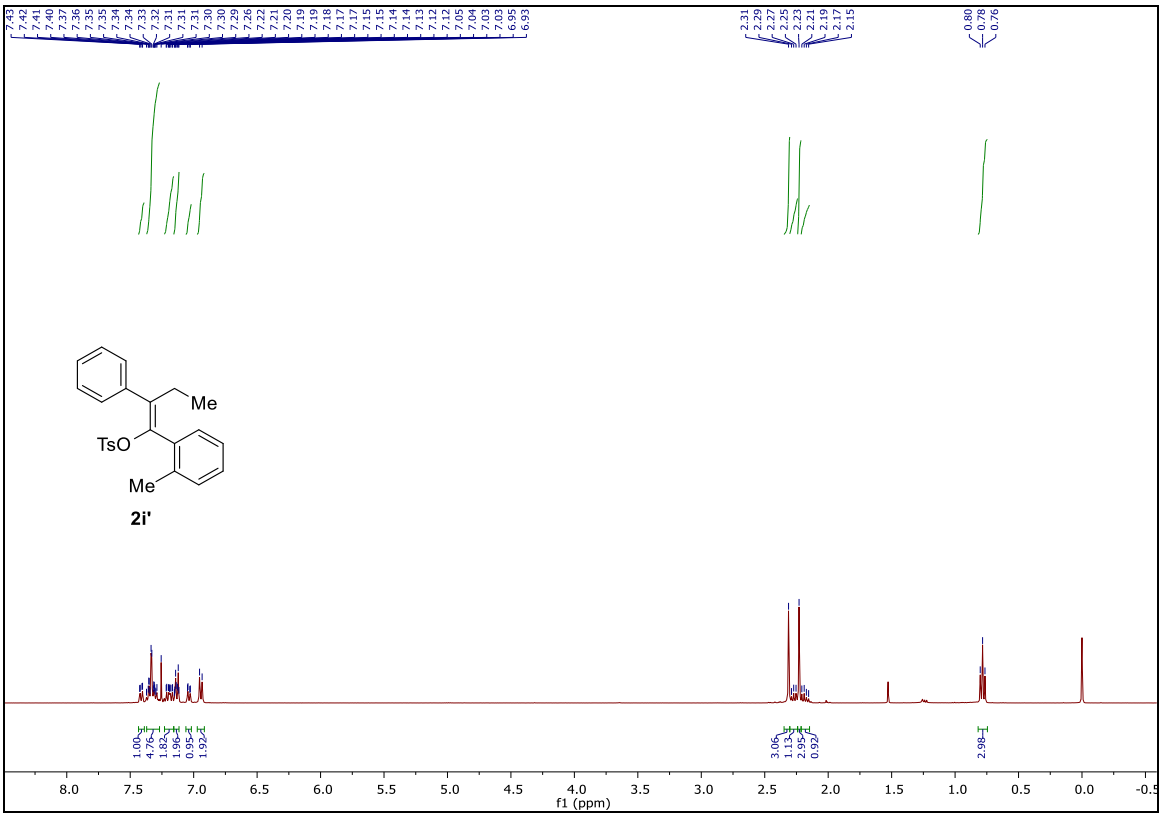
Me
TsO
Me
2i'
f1 (ppm)

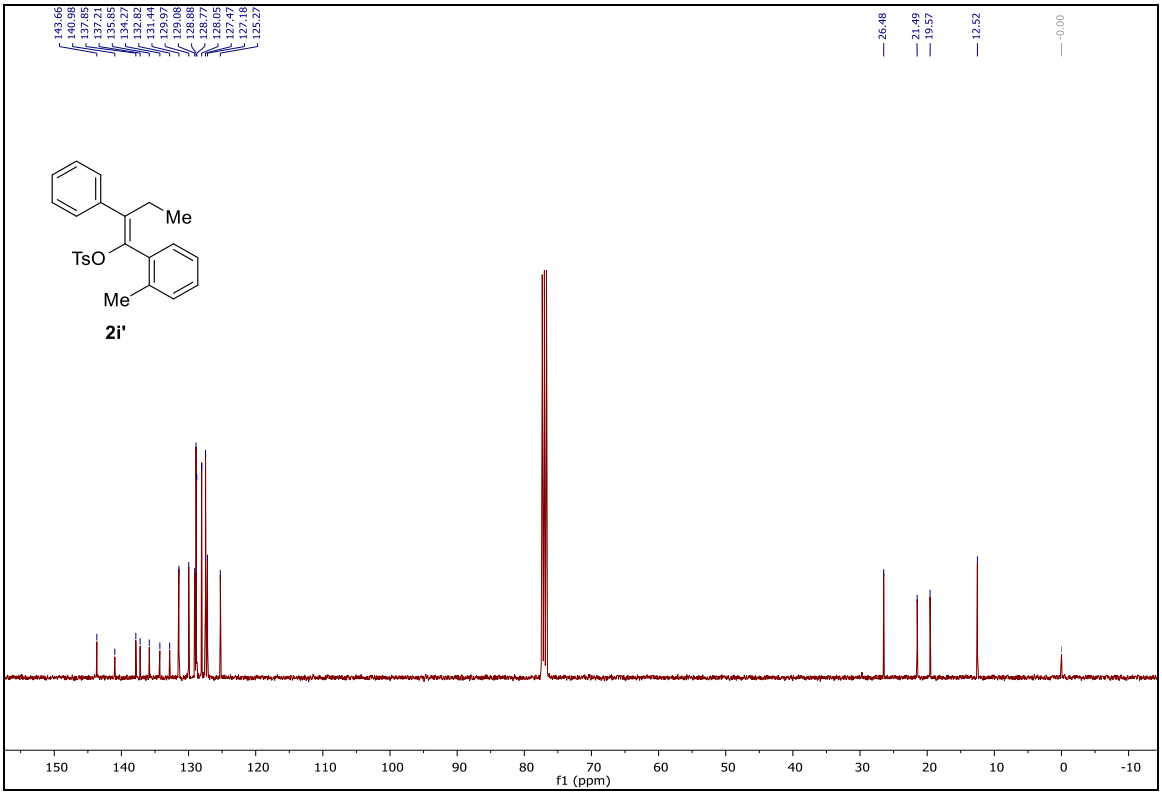
Me
TsO
Me
2i'
f1 (ppm)

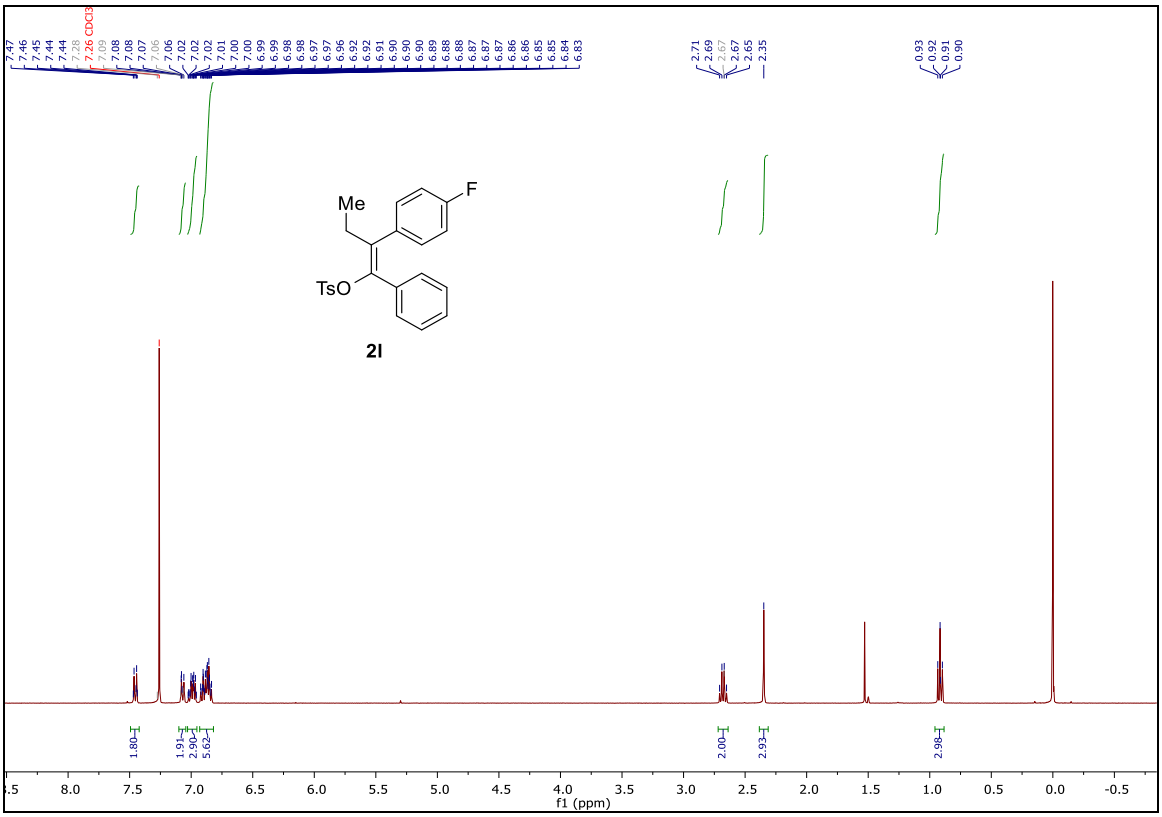
Me
F
TsO
2l
f1 (ppm)

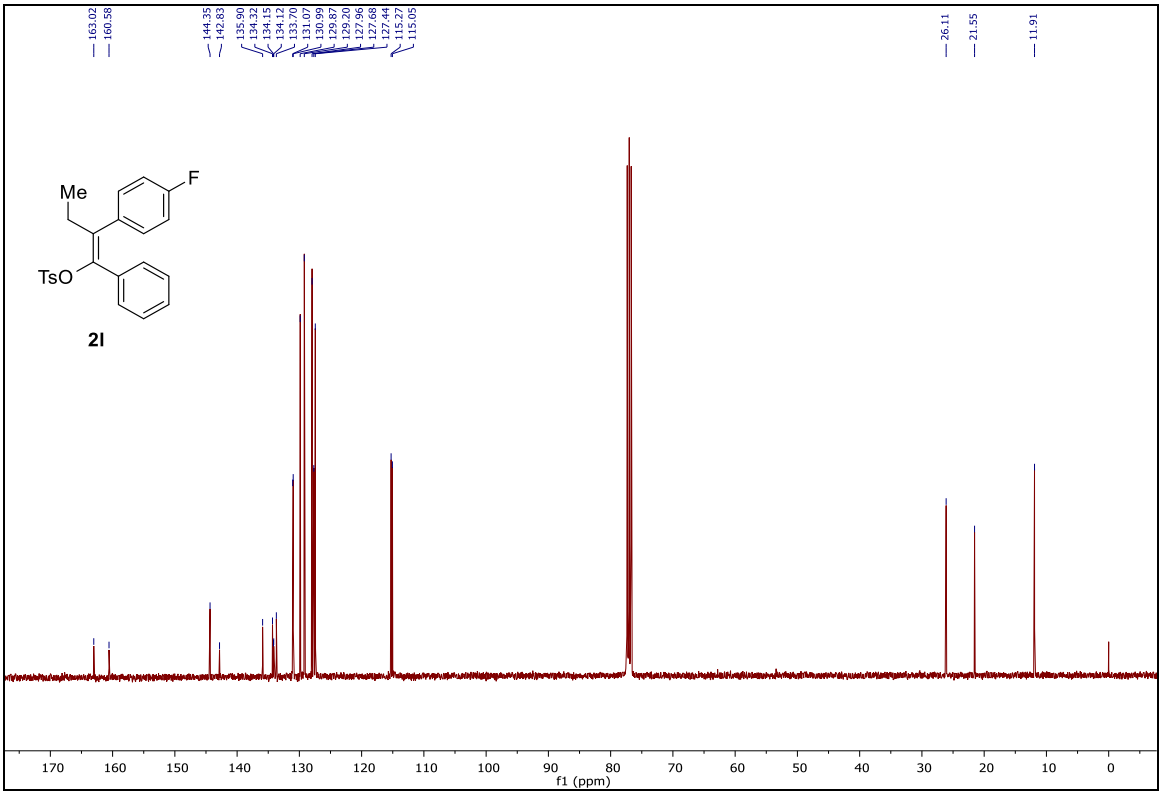
Me
F
TsO
2l
f1 (ppm)

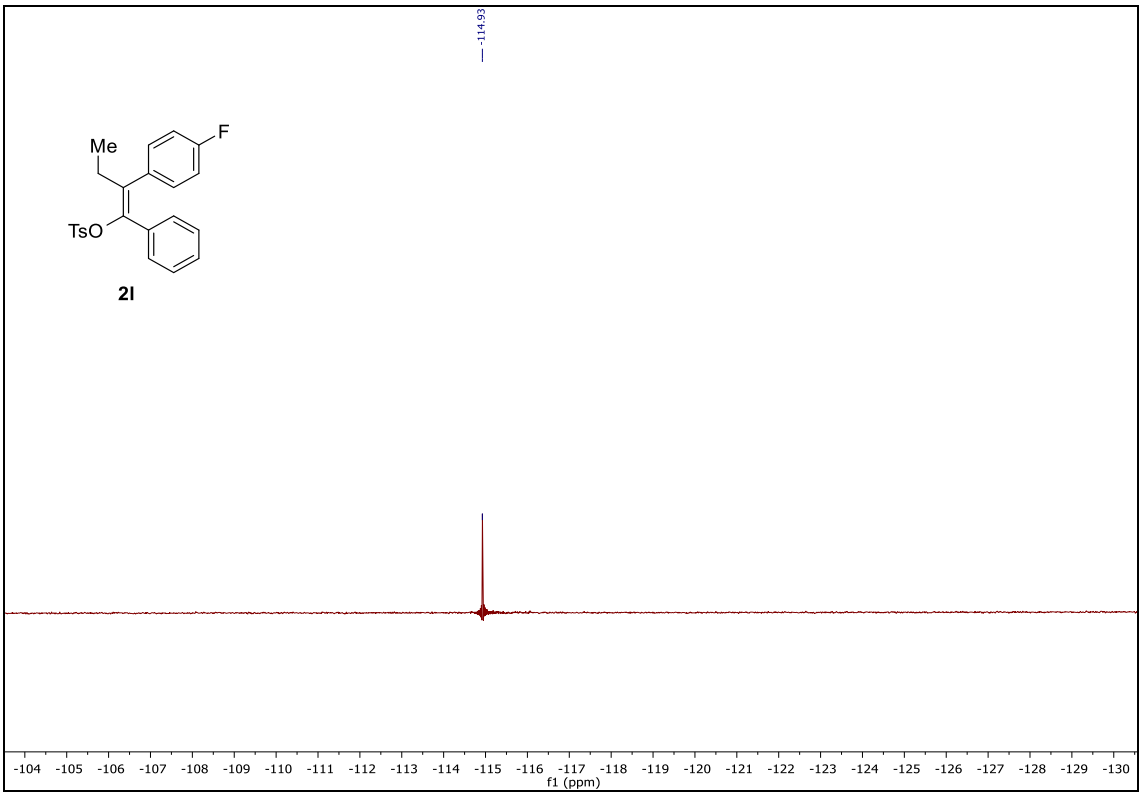
-114.93
Me
F
TsO
2l
-104 -105 -106 -107 -108 -109 -110 -111 -112 -113 -114 -115 -116 -117 -118 -119 -120 -121 -122 -123 -124 -125 -126 -127 -128 -129 -130
f1 (ppm)

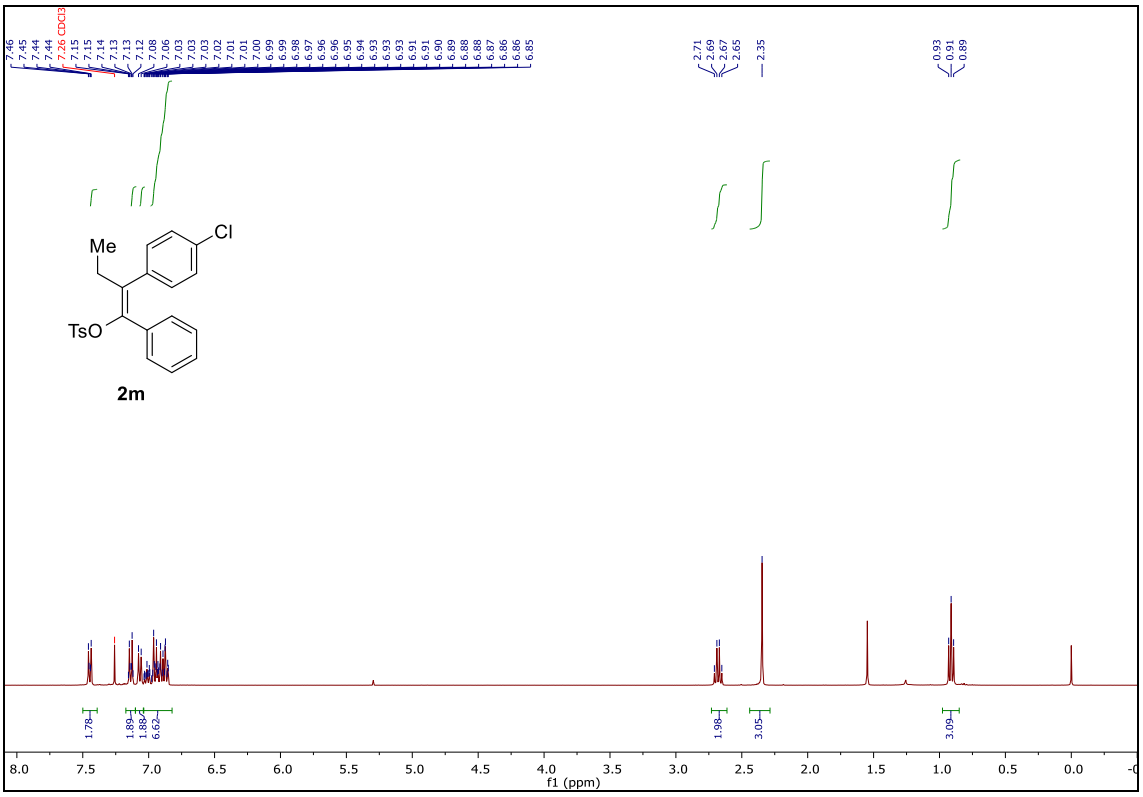
Me
Cl
TsO
2m
f1 (ppm)

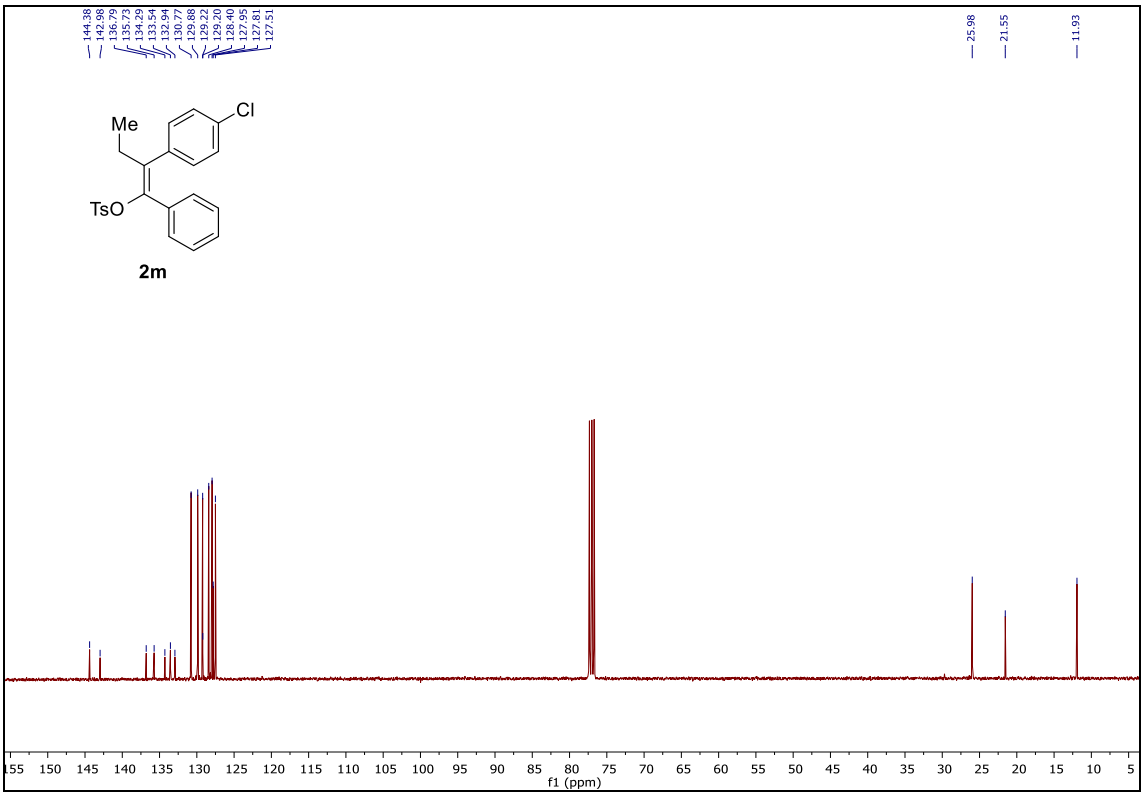
Me
Cl
TsO
2m
f1 (ppm)

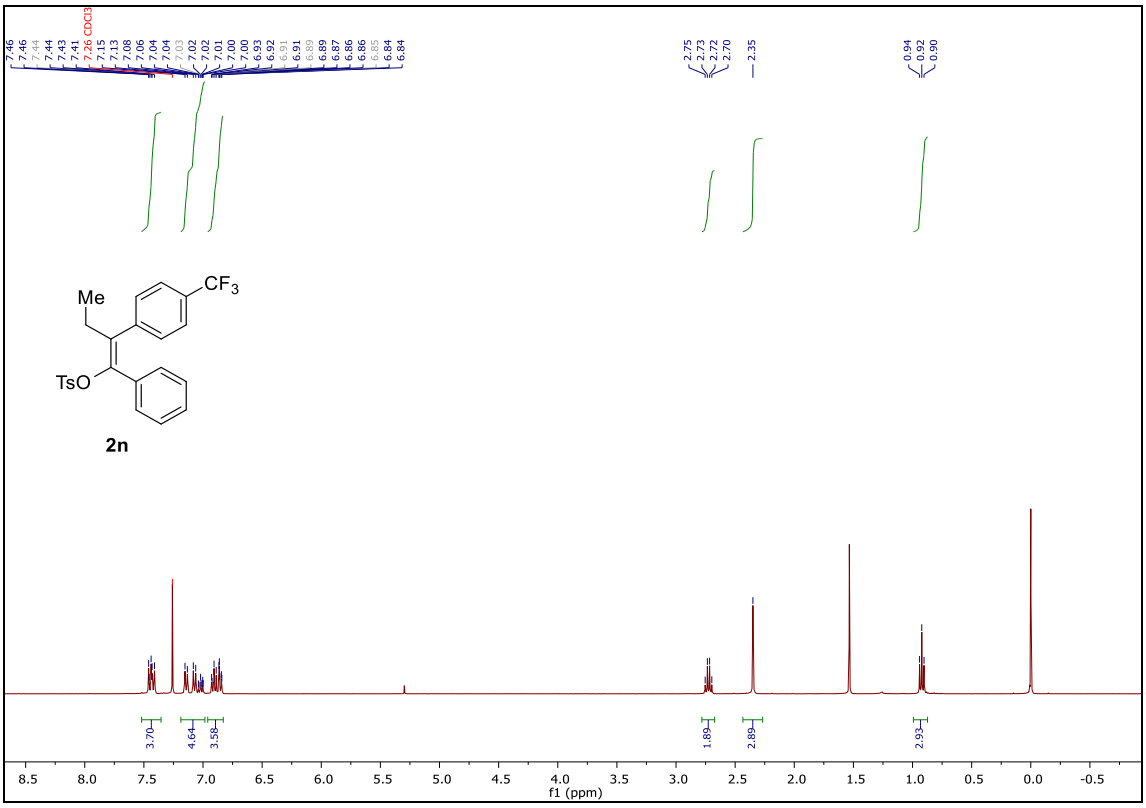
Me
CF3
TsO
2n
f1 (ppm)

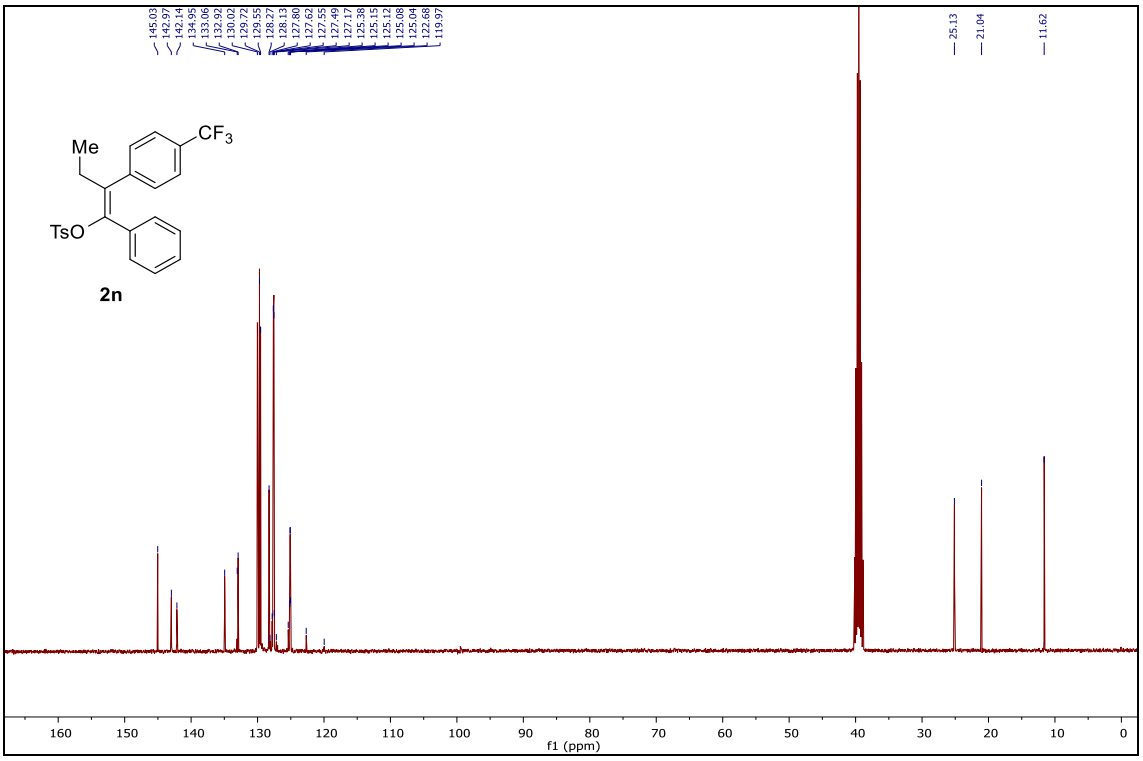
Me
CF3
TsO
2n
f1 (ppm)

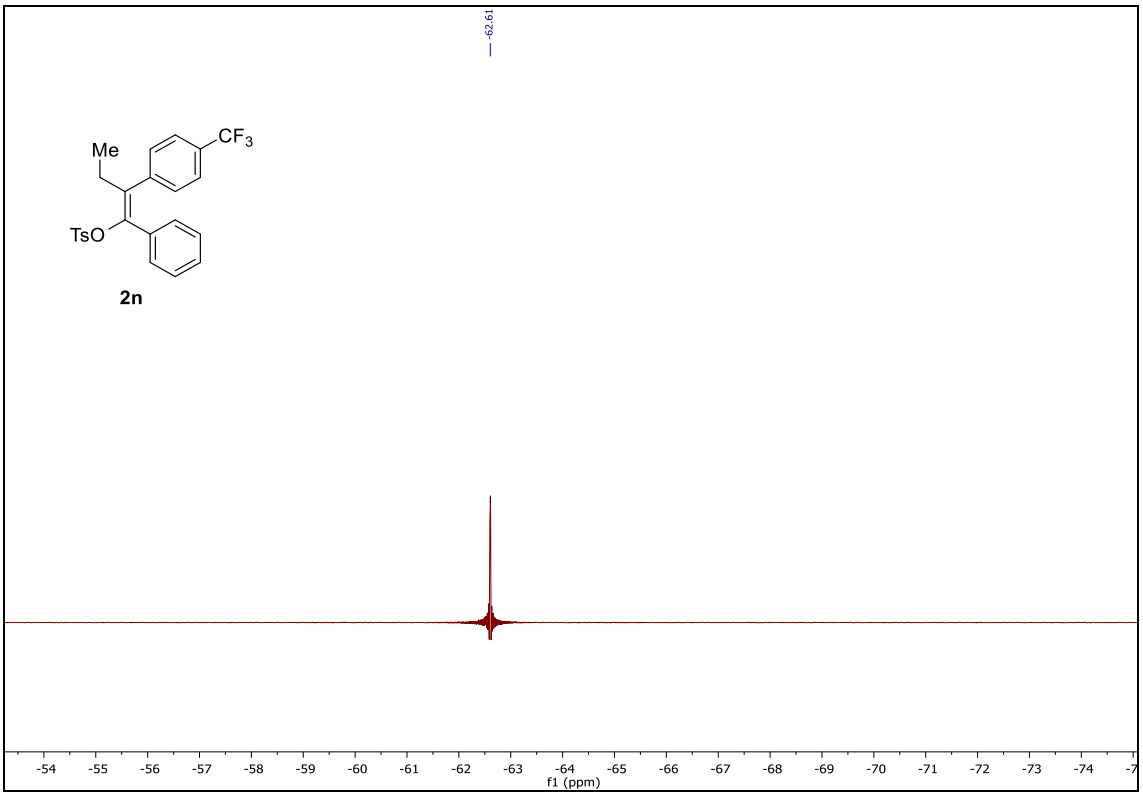
-62.61
Me
CF3
TsO
2n
-54
-55
-56
-57
-58
-59
-60
-61
-62
-63
-64
-65
-66
-67
-68
-69
-70
-71
-72
-73
-74
f1 (ppm)

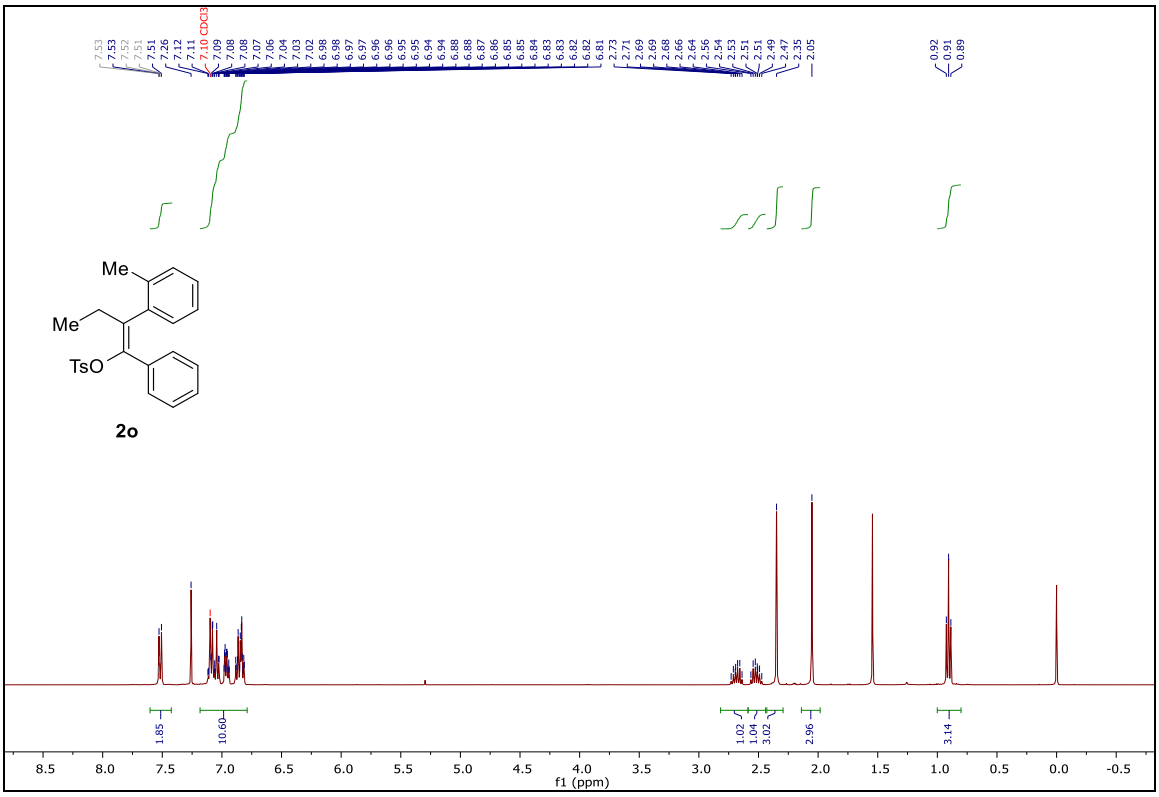
Me
Me
TsO
2o
f1 (ppm)

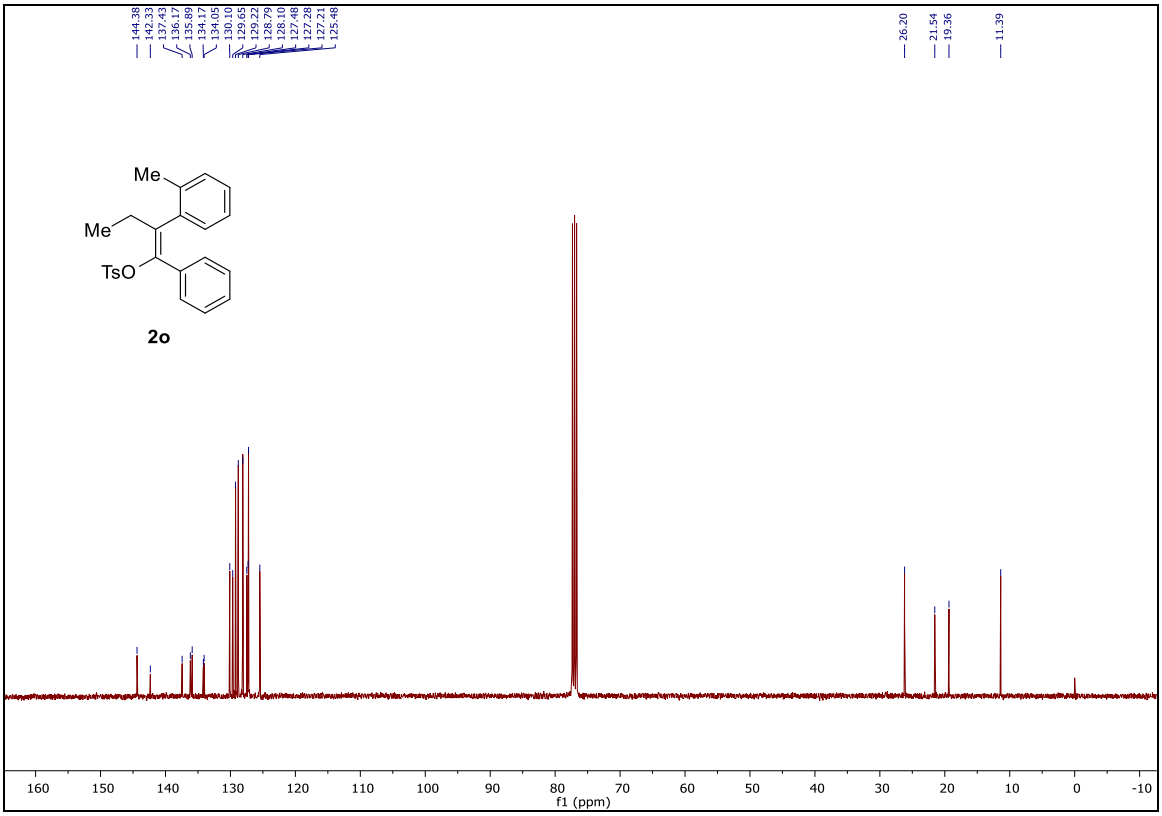
Me
Me
TsO
2o
f1 (ppm)

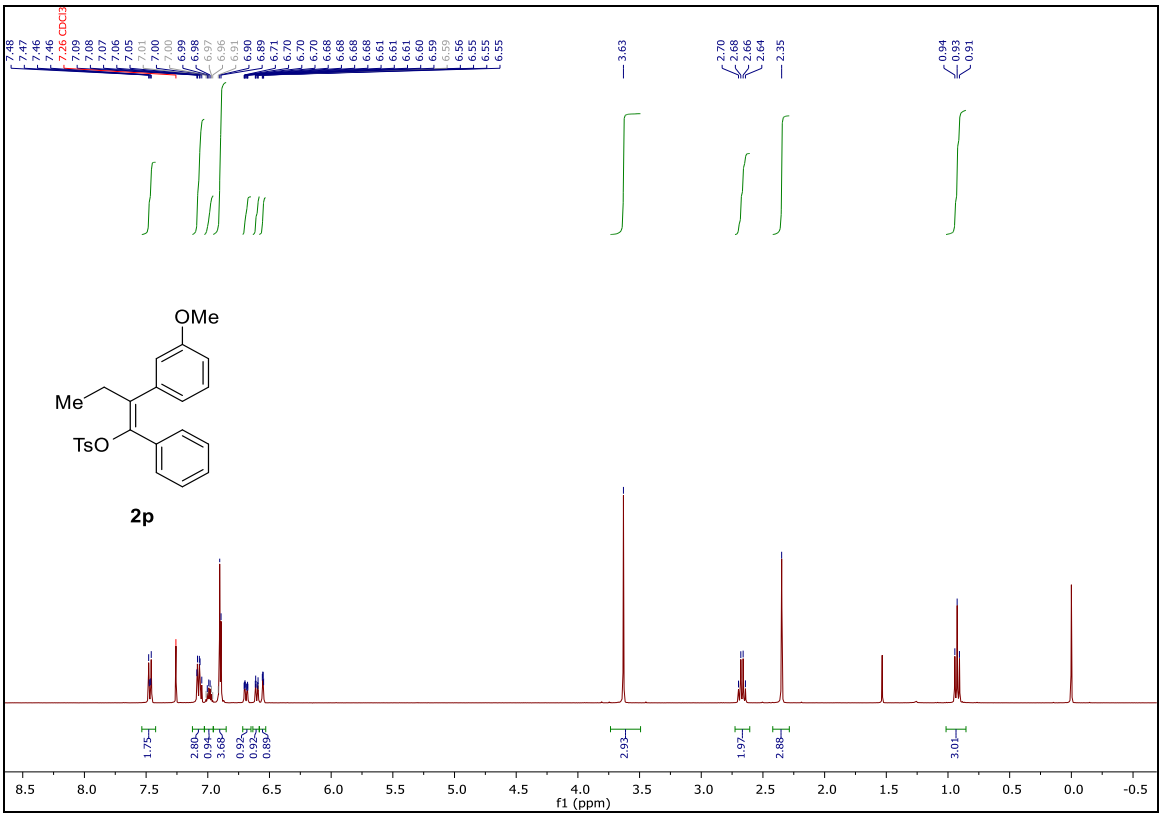
OMe
Me
TsO
2p
f1 (ppm)

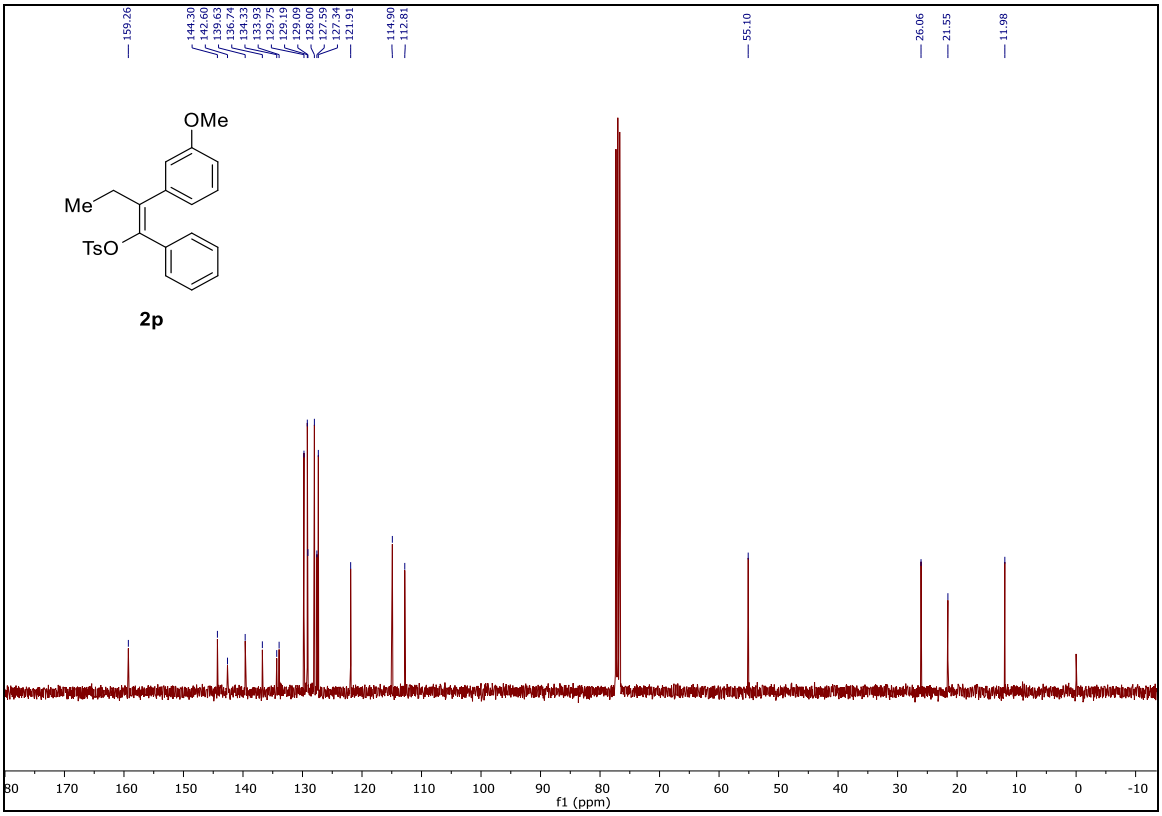
OMe
Me
TsO
2p
f1 (ppm)

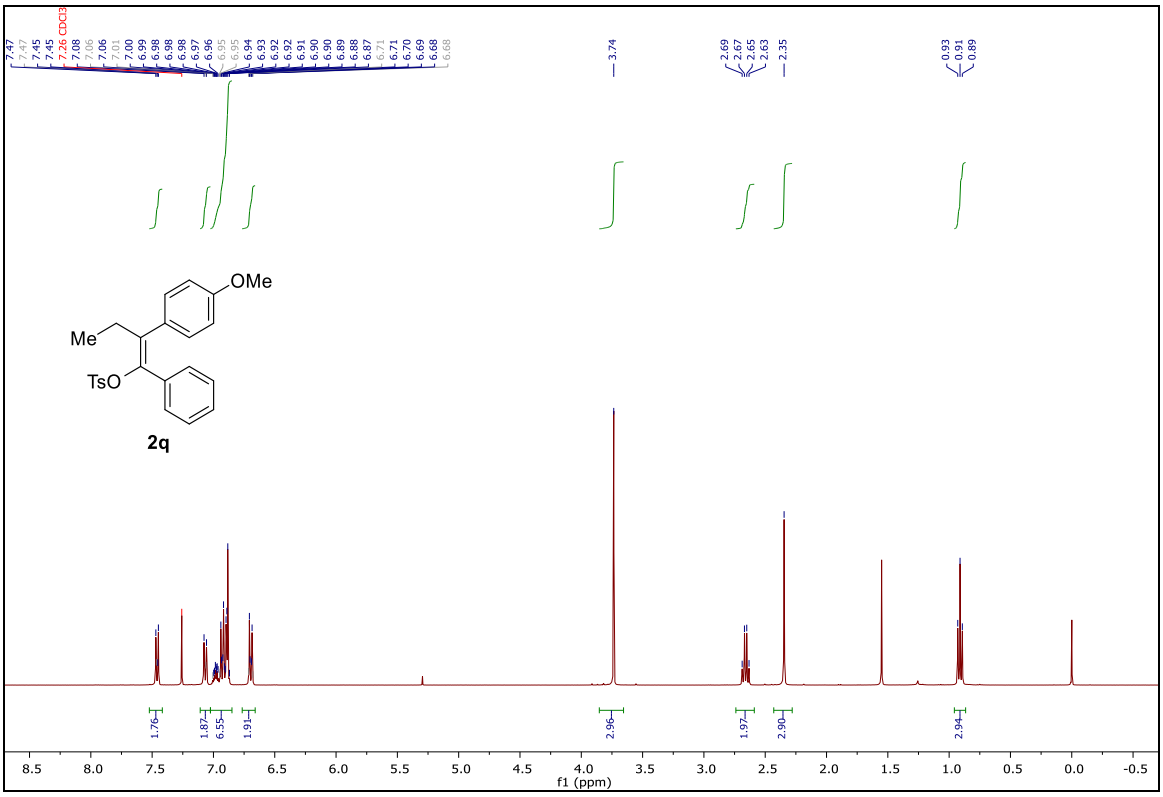
OMe
Me
TsO
2q
f1 (ppm)

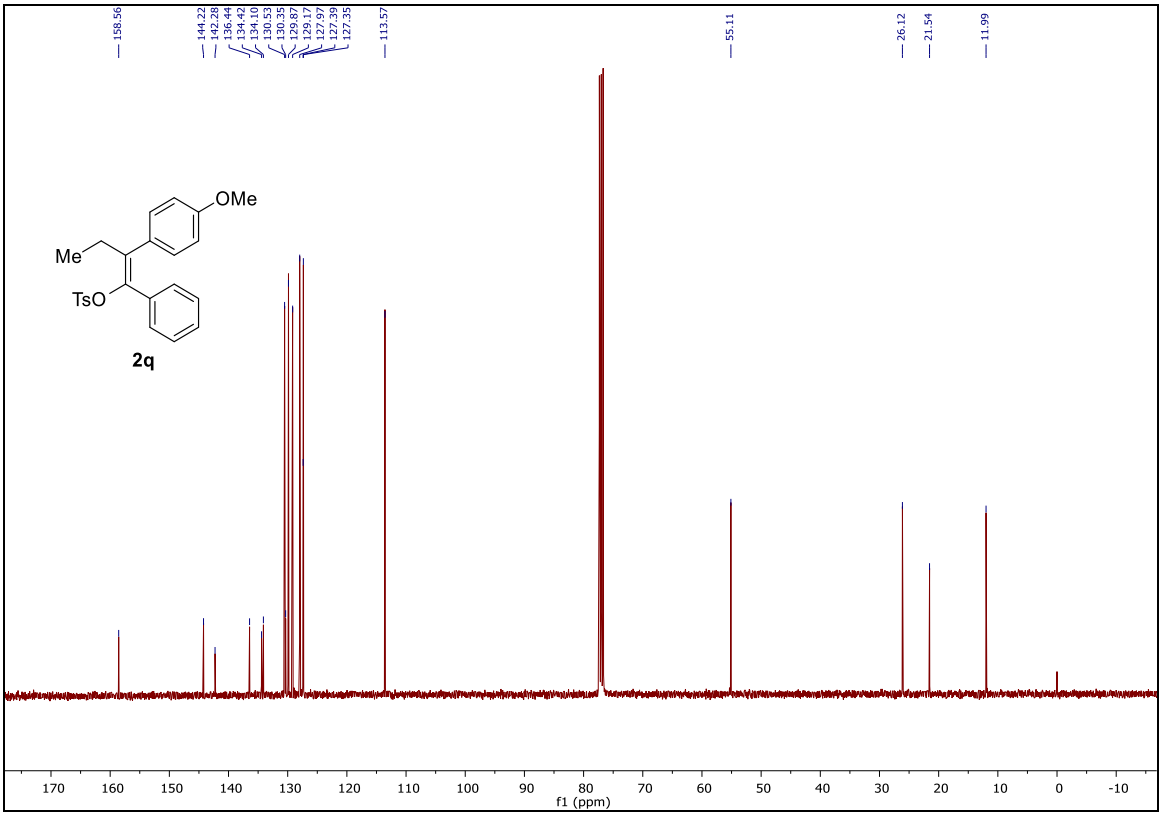
OMe
Me
TsO
2q
f1 (ppm)

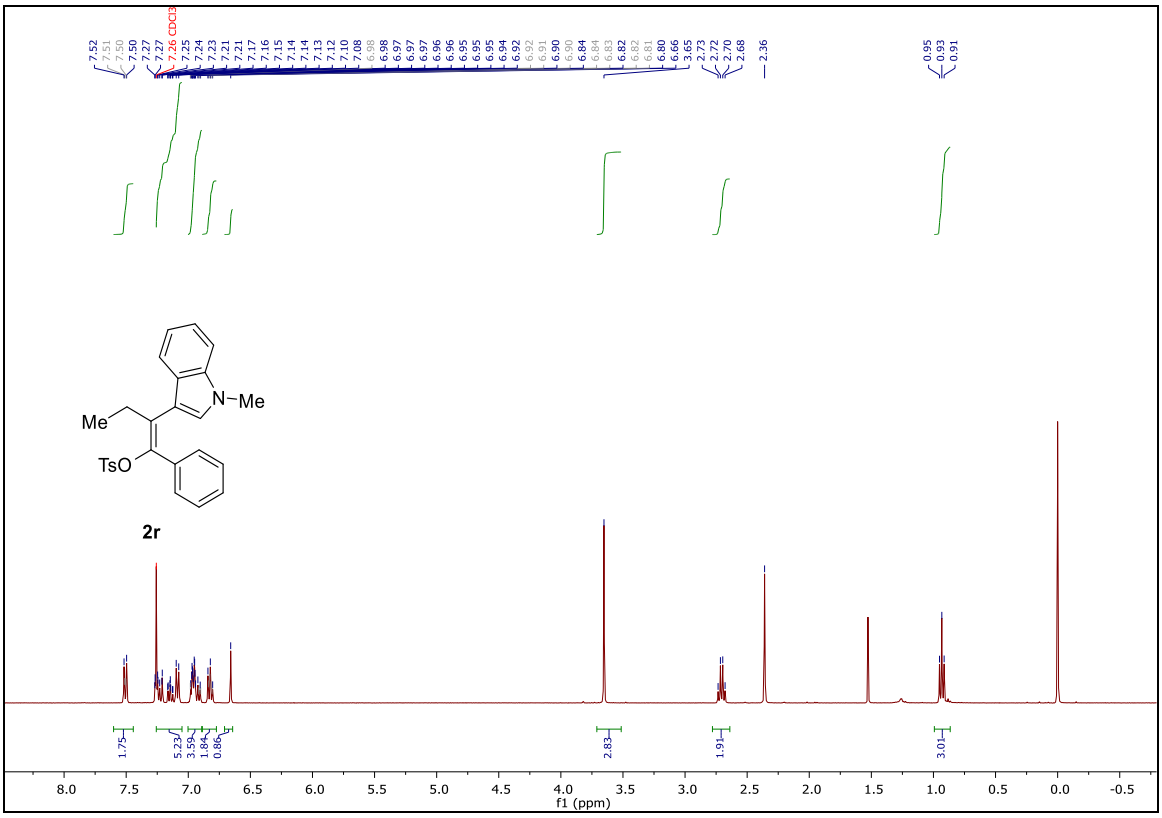
7.52
7.51
7.50
7.50
7.27
7.26 CDCl3
7.25
7.24
7.23
7.21
7.21
7.17
7.16
7.15
7.14
7.14
7.13
7.12
7.10
7.08
6.98
6.97
6.97
6.97
6.96
6.96
6.95
6.95
6.95
6.94
6.92
6.92
6.91
6.90
6.90
6.84
6.84
6.83
6.82
6.82
6.81
6.80
6.66
3.65
2.73
2.72
2.70
2.68
2.36
0.95
0.93
0.91
N–Me
Me
TsO
2r
1.75
5.23
3.59
1.84
0.86
2.83
1.91
3.01
8.0
7.5
7.0
6.5
6.0
5.5
5.0
4.5
4.0
3.5
3.0
2.5
2.0
1.5
1.0
0.5
0.0
-0.5
f1 (ppm)

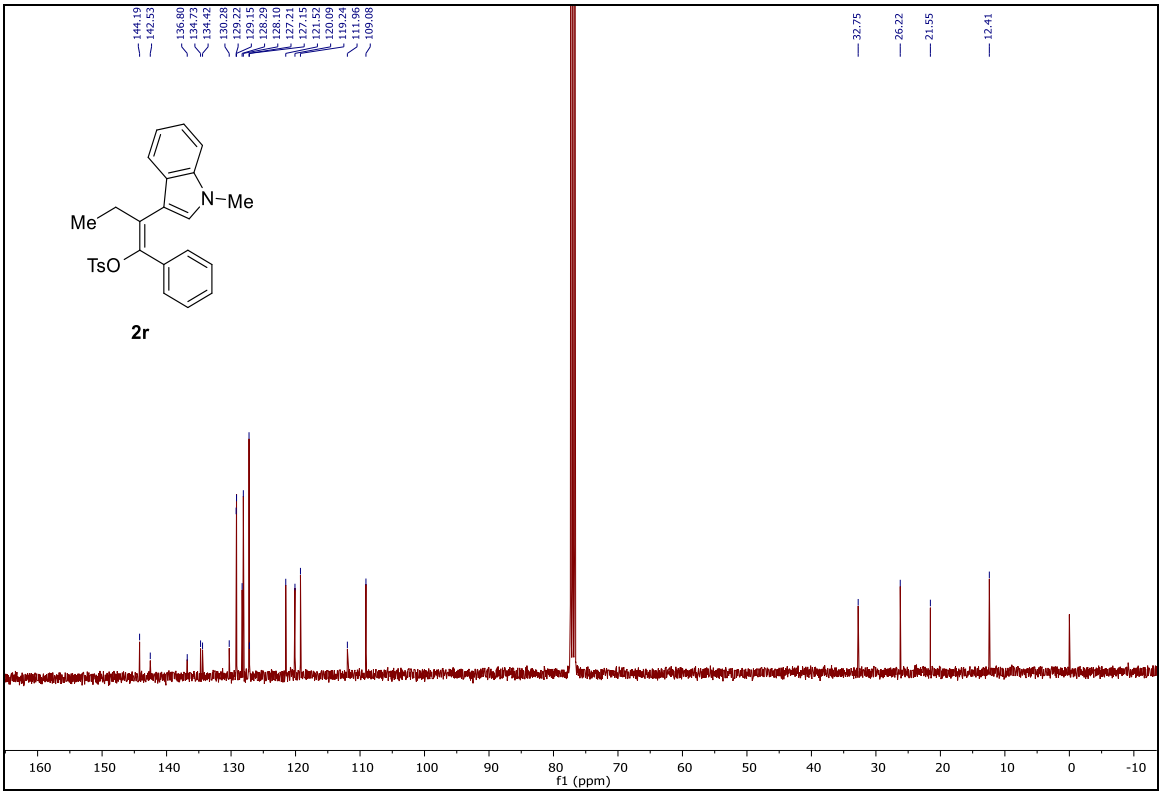
144.19
142.53
136.80
134.73
134.42
130.28
129.22
129.15
128.29
128.10
127.21
127.15
121.52
120.09
119.24
111.96
109.08
32.75
26.22
21.55
12.41
N–Me
Me
TsO
2r
160
150
140
130
120
110
100
90
80
70
60
50
40
30
20
10
0
-10
f1 (ppm)

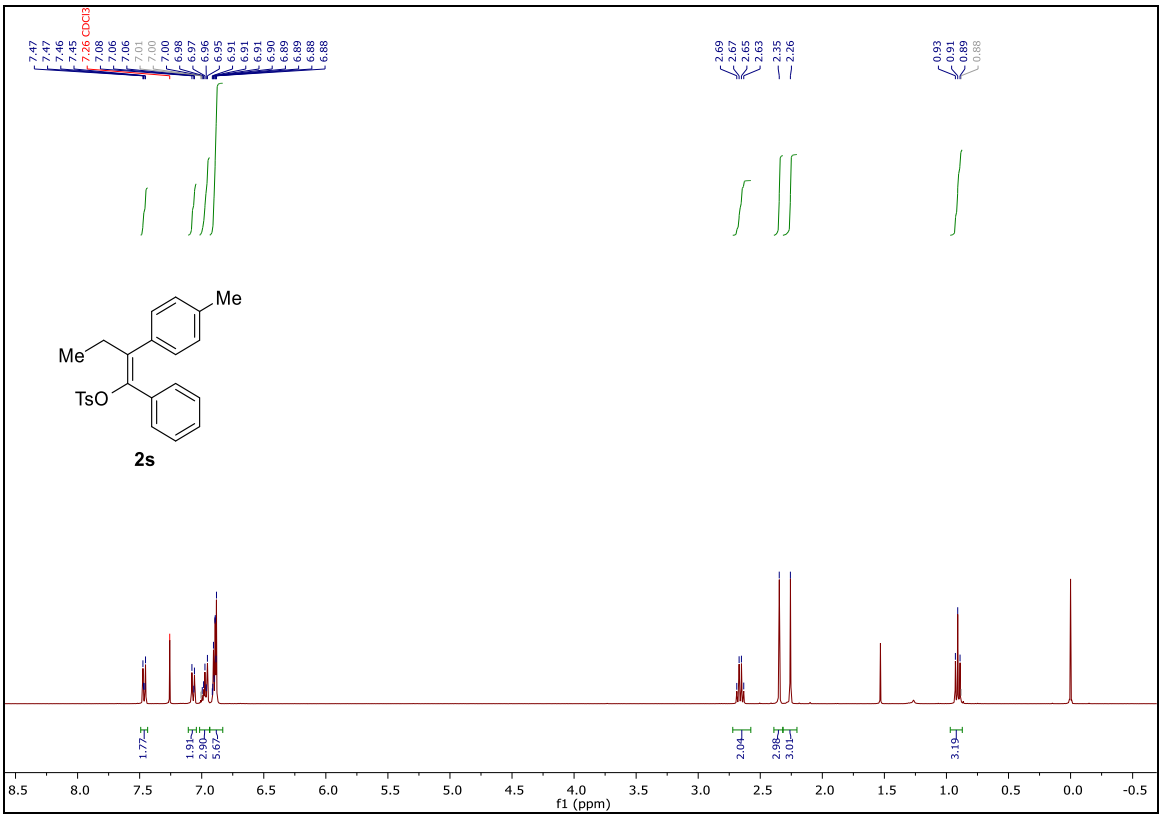
Me
Me
TsO
2s
f1 (ppm)

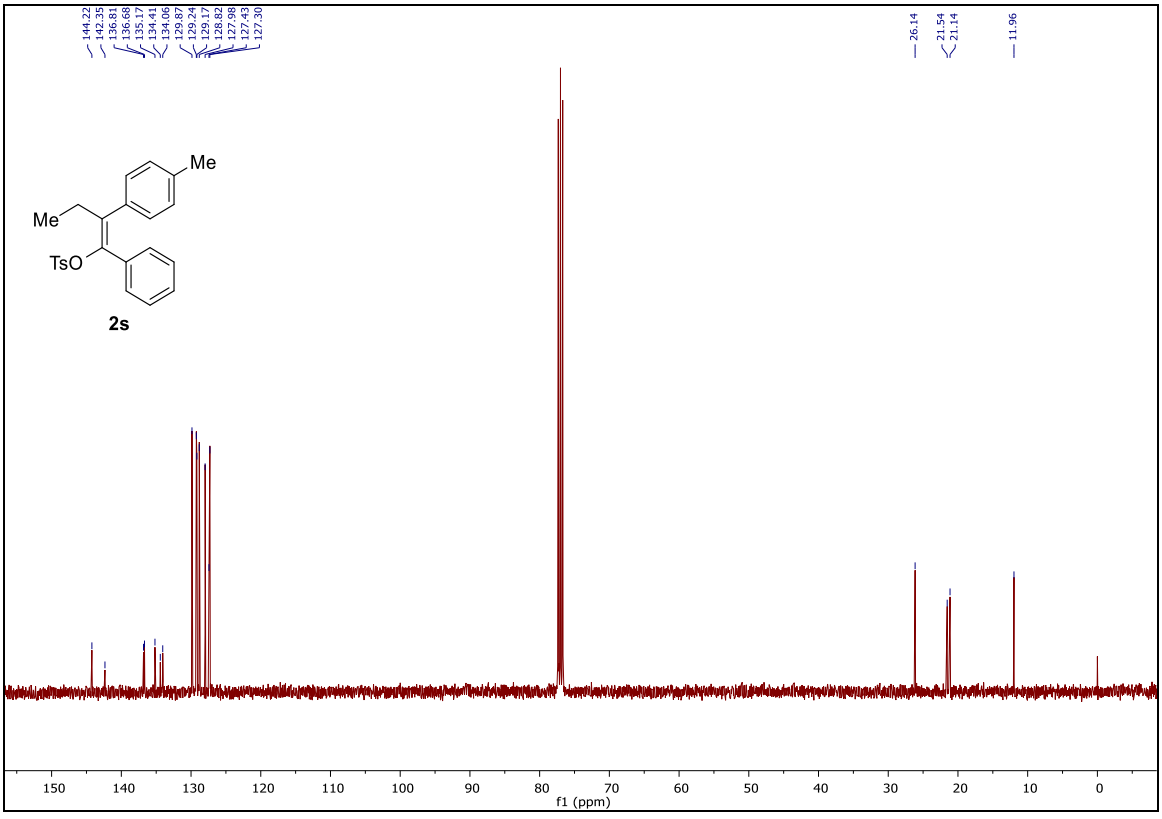
Me
Me
TsO
2s
f1 (ppm)

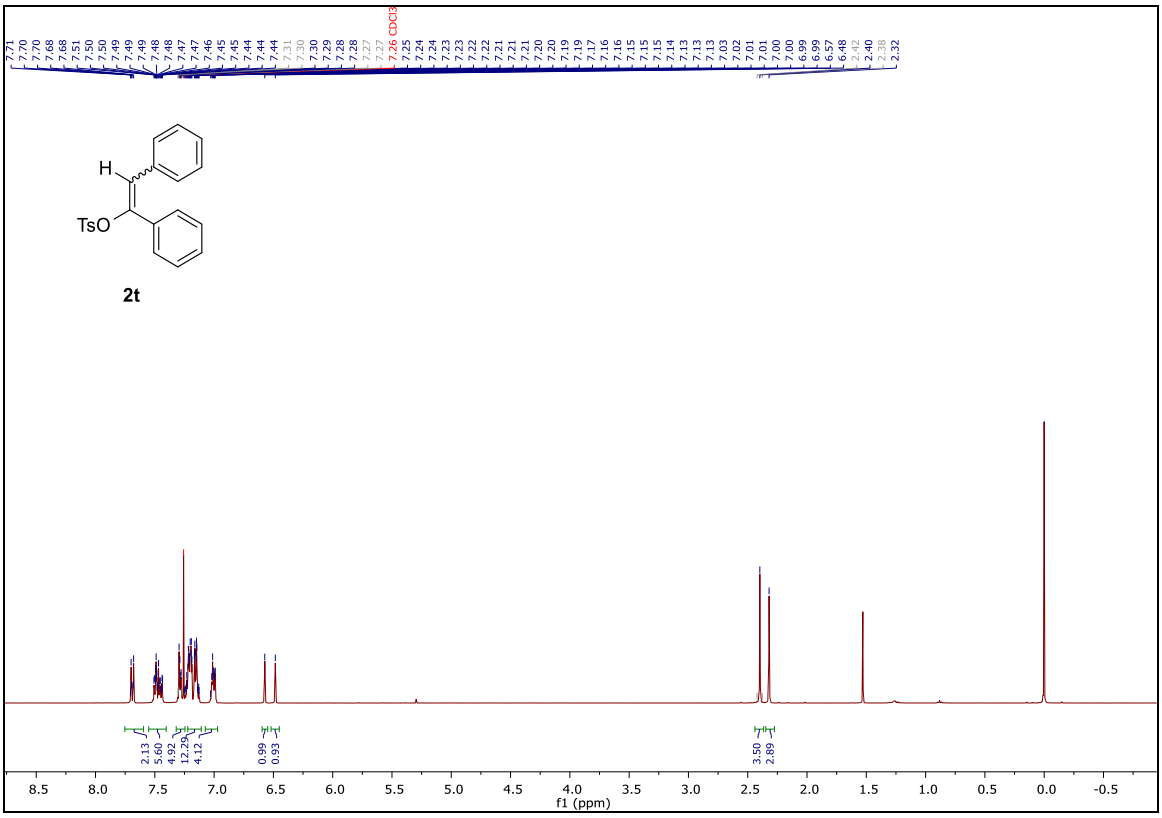
H
TsO
2t
f1 (ppm)

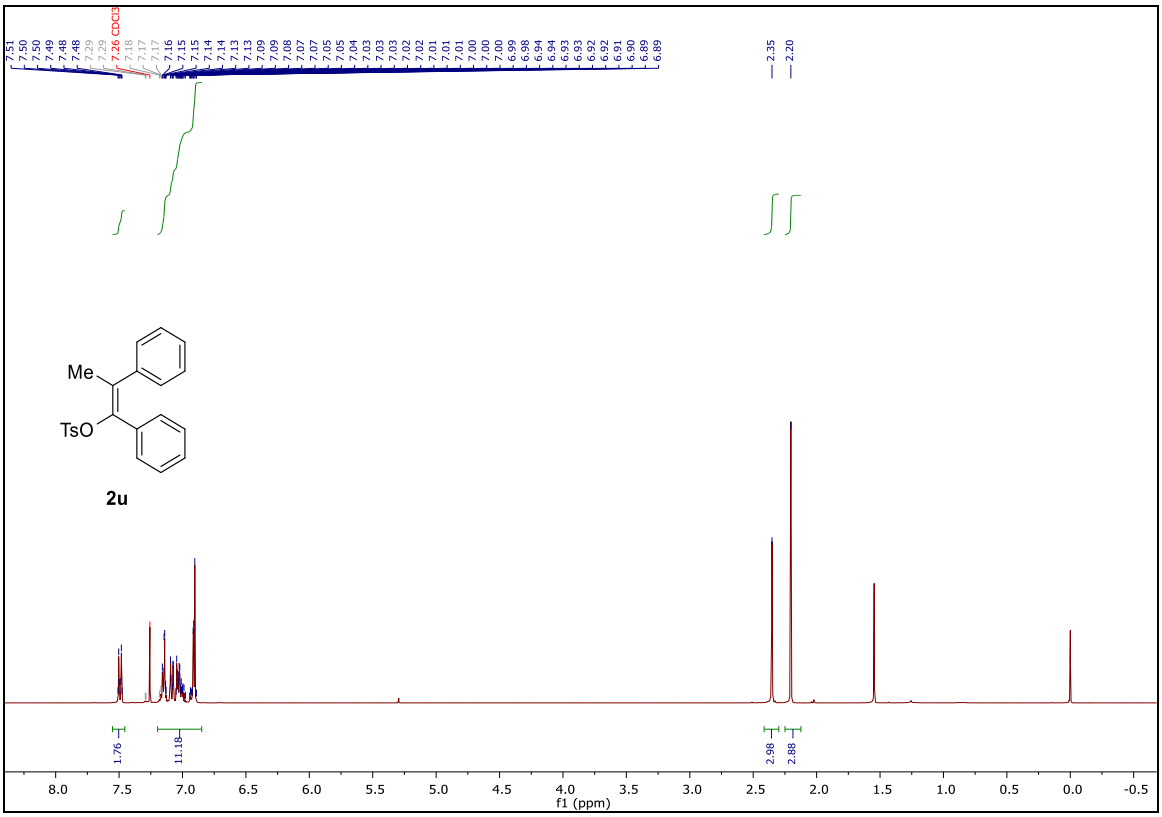
Me
TsO
2u
f1 (ppm)

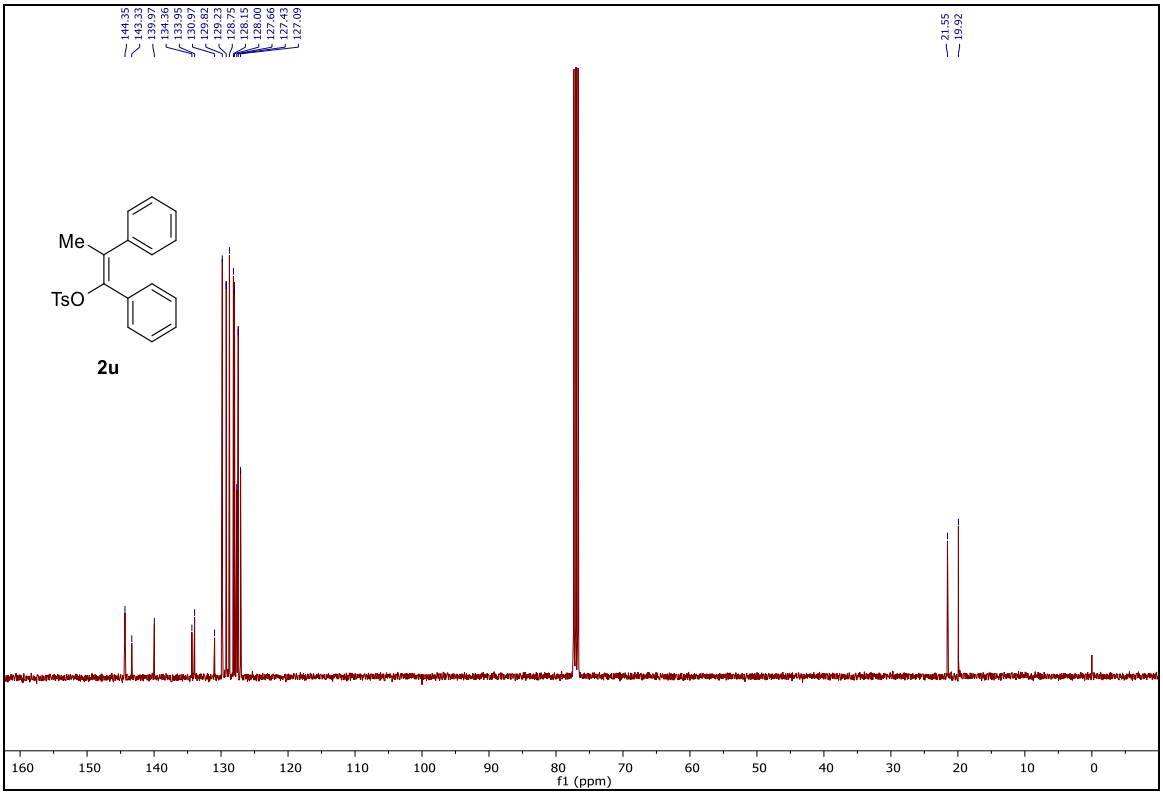
Me
TsO
2u
f1 (ppm)

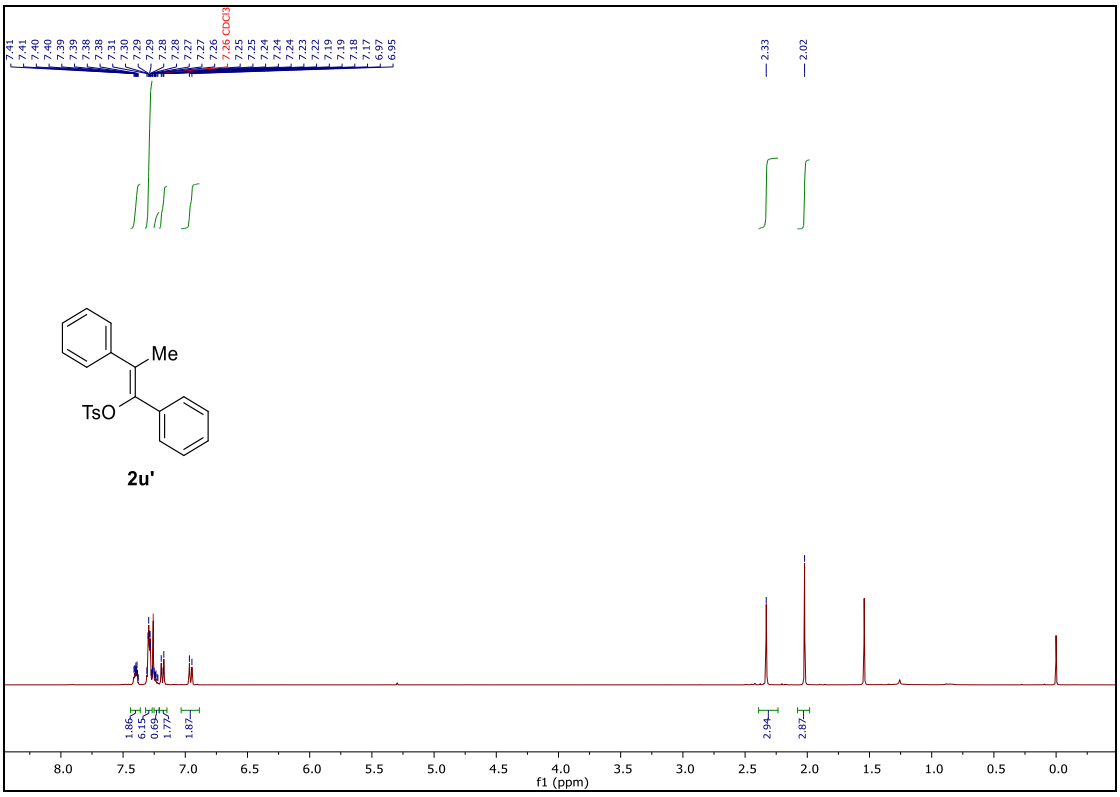
Me
TsO
2u'
f1 (ppm)

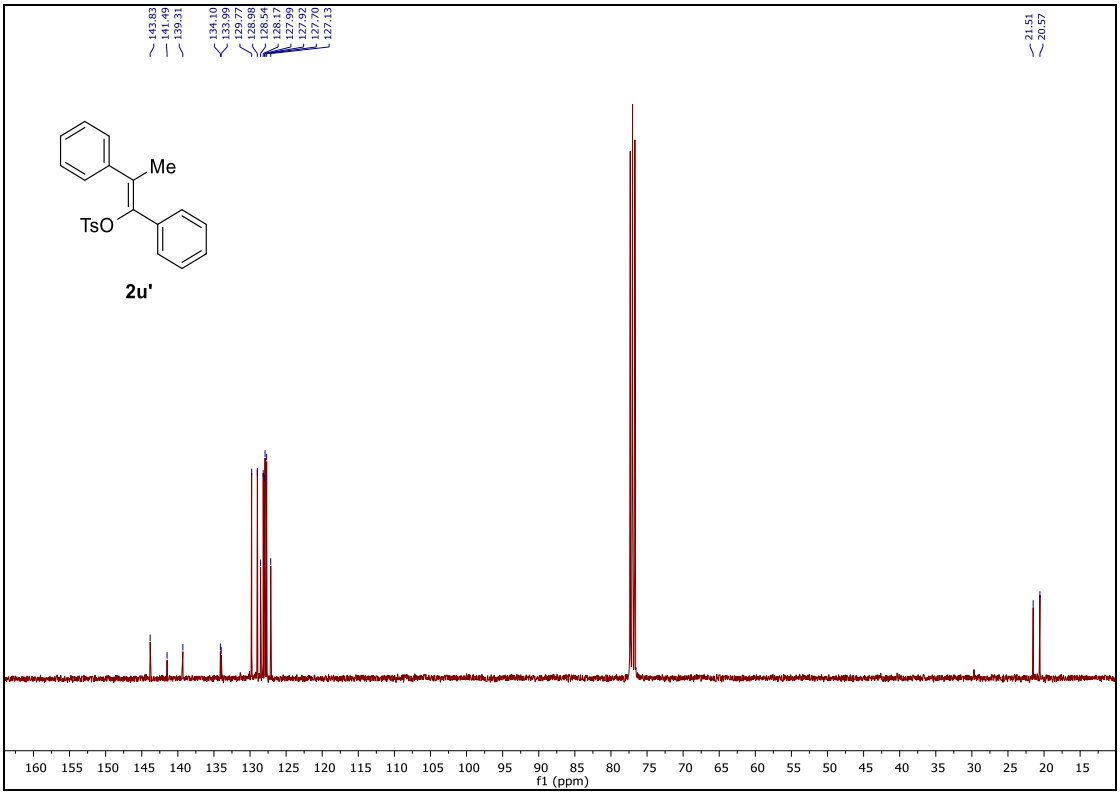
Me
TsO
2u'
f1 (ppm)

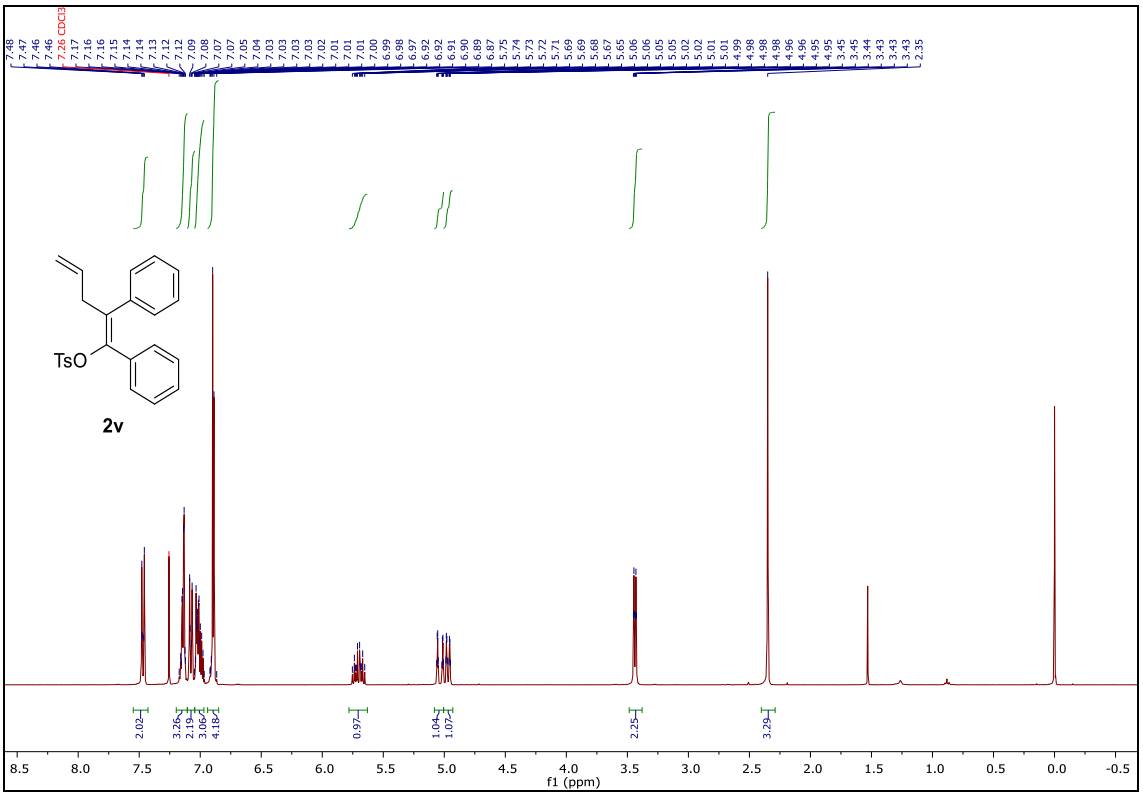
TsO
2v
f1 (ppm)

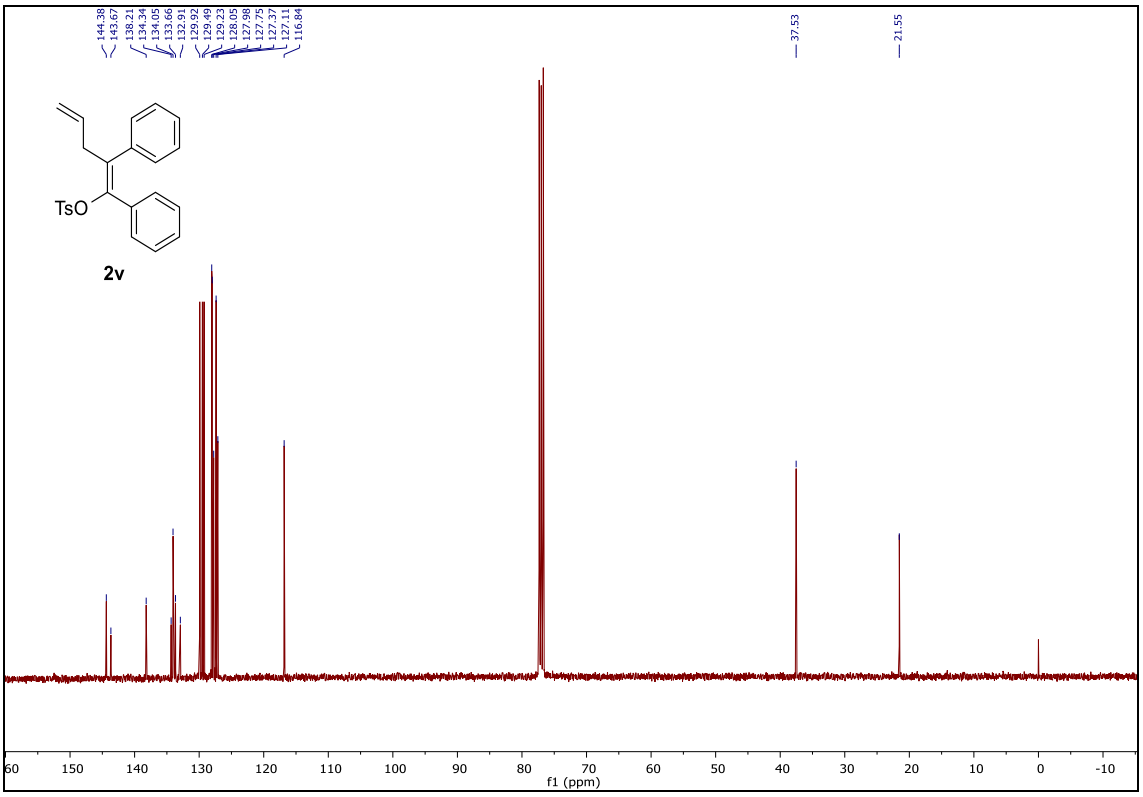
TsO
2v
f1 (ppm)

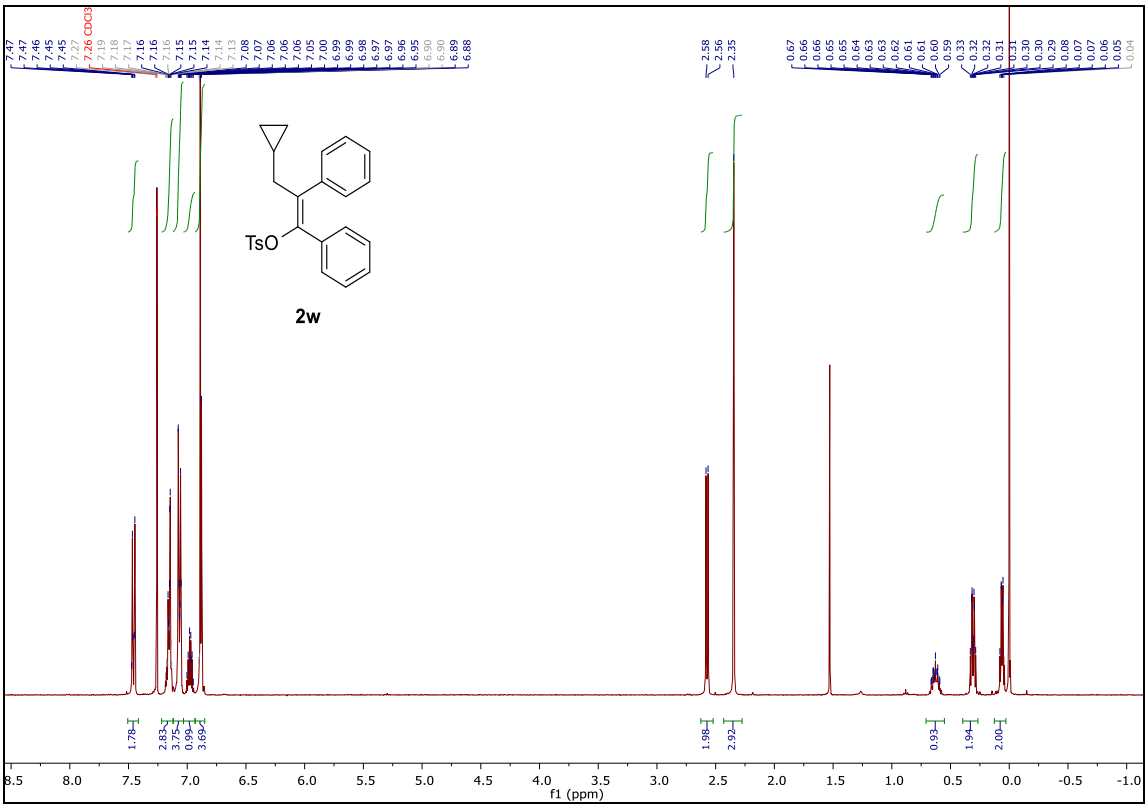
TsO
2w
f1 (ppm)

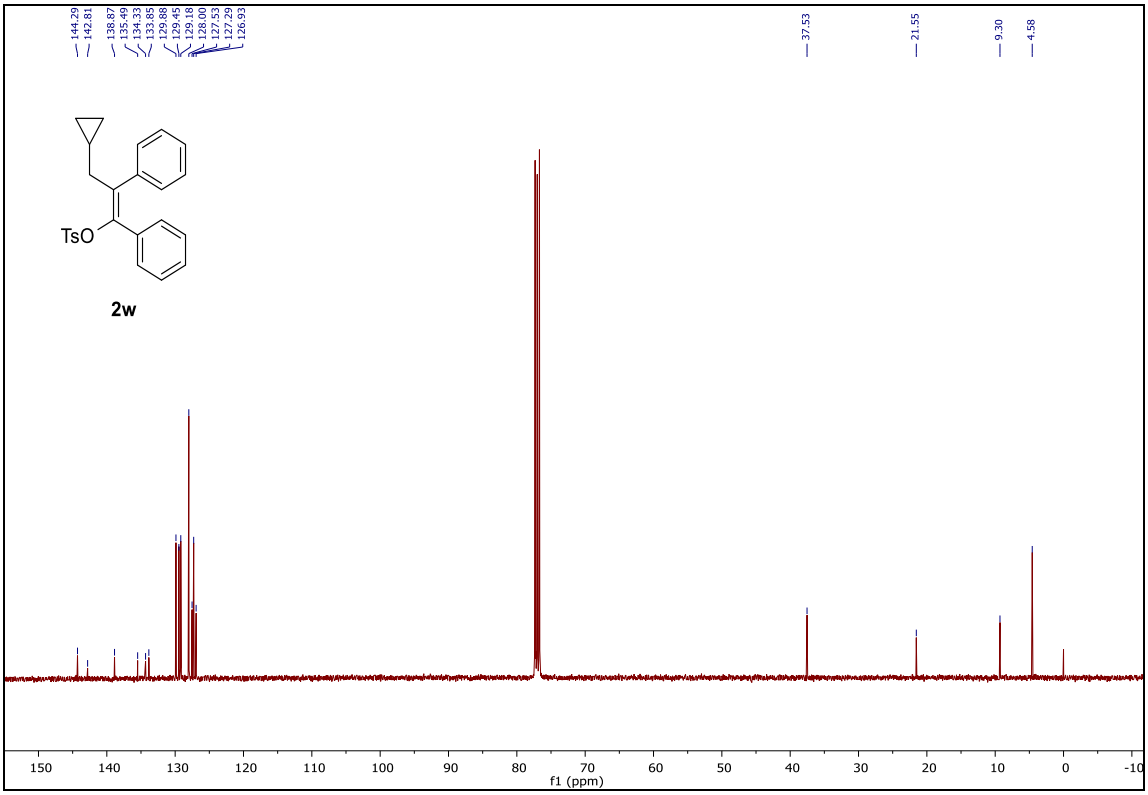
TsO
2w
f1 (ppm)

REFERENCES

(1) Miller, S. J.; Blackwell, H. E.; Grubbs, R. H. *J. Am. Chem. Soc.* **1996**, *118*, 9606.

(2) White, C. J.; Hickey, J. L.; Scully, C. C. G.; Yudin, A. K. *J. Am. Chem. Soc.* **2014**, *136*, 3728.

(3) Illesinghe, J.; Guo, C. X.; Garland, R.; Ahmed, A.; van Lierop, B.; Elaridi, J.; Jackson, W. R.; Robinson, A. J. *Chem. Commun.* **2009**, *3*, 295.

(4) Hili, R.; Rai, V.; Yudin, A. K. *J. Am. Chem. Soc.* **2010**, *132*, 2889.

(5) White, C. J.; Yudin, A. K. *Nat. Chem.* **2011**, *3*, 509.

(6) Levine, D. P. *Clin. Infect. Dis.* **2006**, *42*, S5.

(7) Fernandez-Lopez, S.; Kim, H. S.; Choi, E. C.; Delgado, M.; Granja, J. R.; Khasanov, A.; Kraehenbuehl, K.; Long, G.; Weinberger, D. A.; Wilcoxen, K. M.; Ghadiri, M. R. *Nature* **2001**, *412*, 452.

(8) Tang, Y. Q.; Yuan, J.; Ösapay, G.; Ösapay, K.; Tran, D.; Miller, C. J.; Ouellette, A. J.; Selsted, M. E. *Science* **1999**, *286*, 498.

(9) Laupacis, A.; Keown, P. A.; Ulan, R. A.; McKenzie, N.; Stiller, C. R. *Can. Med. Assoc. J.* **1982**, *126*, 1041.

(10) Craik, D. J. *Science* **2006**, *311*, 1563.

(11) Fairlie, D. P.; Abbenante, G.; March, D. R. *Curr. Med. Chem.* **1995**, *2*, 654.

(12) Mas-Moruno, C.; Rechenmacher, F.; Kessler, H. *Anti-Cancer Agents Med. Chem.* **2010**, *10*, 753.

(13) Thakkar, A.; Trinh, T. B.; Pei, D. *ACS Comb. Sci.* **2013**, *15*, 120.

(14) Haas, K.; Ponikwar, W.; Nöth, H.; Beck, W. *Angew. Chem., Int. Ed.* **1998**, *37*, 1086.

(15) Ye, Y. h.; Gao, X. m.; Liu, M.; Tang, Y. c.; Tian, G. l. *Lett. Pept. Sci.* **2003**, *10*, 571.

(16) Meutermans, W. D. F.; Bourne, G. T.; Golding, S. W.; Horton, D. A.; Campitelli, M. R.; Craik, D.; Scanlon, M.; Smythe, M. L. *Org. Lett.* **2003**, *5*, 2711.

(17) Bock, V. D.; Perciaccante, R.; Jansen, T. P.; Hiemstra, H.; van Maarseveen, J. H. *Org. Lett.* **2006**, *8*, 919.

(18) Bruckdorfer, T.; Marder, O.; Albericio, F. *Current Pharmaceutical Biotechnology* **2004**, *5*, 29.

(19) Bray, B. L. *Nat. Rev. Drug Discovery* **2003**, *2*, 587.

(20) Mulder, K. C. L.; Viana, A. A. B.; Xavier, M.; Parachin, N. S. *Curr. Protein Pept. Sci.* **2013**, *14*, 556.

(21) Skropeta, D.; Jolliffe, K. A.; Turner, P. *J. Org. Chem.* **2004**, *69*, 8804.

(22) Fairweather, K. A.; Sayyadi, N.; Luck, I. J.; Clegg, J. K.; Jolliffe, K. A. *Org. Lett.* **2010**, *12*, 3136.

(23) Robinson, J. A. *Acc. Chem. Res.* **2008**, *41*, 1278.

(24) Rückle, T.; de Lavallaz, P.; Keller, M.; Dumy, P.; Mutter, M. *Tetrahedron* **1999**, *55*, 11281.

(25) Ehrlich, A.; Heyne, H. U.; Winter, R.; Beyermann, M.; Haber, H.; Carpino, L. A.; Bienert, M. *J. Org. Chem.* **1996**, *61*, 8831.

(26) Schmidt, U.; Langner, J. *J. Pept. Res.* **1997**, *49*, 67.

(27) Busetti, V.; Crisma, M.; Toniolo, C.; Salvadori, S.; Balboni, G. *Int. J. Biol. Macromol.* **1992**, *14*, 23.

(28) Broda, M. A.; Siodłak, D.; Rzeszotarska, B. *J. Pept. Sci.* **2005**, *11*, 546.

(29) Bhandary, K. K.; Chauhan, V. S. *Biopolymers* **1993**, *33*, 209.

(30) Tang, W.; Jiménez-Osés, G.; Houk, K. N.; van der DonkWilfred, A. *Nat. Chem.* **2015**, *7*, 57.

(31) Jiang, J.; Luo, S.; Castle, S. L. *Tetrahedron Lett.* **2015**, *56*, 3311.

(32) Gupta, M.; Chauhan, V. S. *Biopolymers* **2011**, *95*, 161.

(33) Mathur, P.; Ramakumar, S.; Chauhan, V. S. *Pept. Sci.* **2004**, *76*, 150.

(34) Ramagopal, U. A.; Ramakumar, S.; Joshi, R. M.; Chauhan, V. S. *J. Pept. Res.* **1998**, *52*, 208.

(35) Somvanshi, R. K.; Goel, V. K.; Dey, S.; Singh, T. P. *J. Chem. Crystallogr.* **2005**, *35*, 761.

(36) Bonauer, C.; Walenzyk, T.; König, B. *Synthesis* **2006**, *2006*, 1.

(37) Hill, T. A.; Shepherd, N. E.; Diness, F.; Fairlie, D. P. *Angew. Chem., Int. Ed.* **2014**, *53*, 13020.
(38) Holder, J. R.; Haskell-Luevano, C. *Med. Res. Rev.* **2004**, *24*, 325.
(39) Morita, H.; Kayashita, T.; Shishido, A.; Takeya, K.; Itokawa, H.; Shiro, M. *Tetrahedron* **1996**, *52*, 1165.
(40) Nitz, T. J.; Holt, E. M.; Rubin, B.; Stammer, C. H. *J. Org. Chem.* **1981**, *46*, 2667.
(41) Patel, H. C.; Singh, T. P.; Chauhan, V. S.; Kaur, P. *Biopolymers* **1990**, *29*, 509.
(42) Zhang, L.; Tam, J. P. *J. Am. Chem. Soc.* **1999**, *121*, 3311.
(43) Kopple, K. D. *J. Pharm. Sci.* **1972**, *61*, 1345.
(44) Monteiro, L. S.; Andrade, J. J.; Suárez, A. C. *Eur. J. Org. Chem.* **2011**, *2011*, 6764.
(45) Shultz, C. S.; Krska, S. W. *Acc. Chem. Res.* **2007**, *40*, 1320.
(46) Liu, D.; Zhang, X. *Eur. J. Org. Chem.* **2005**, *2005*, 646.
(47) Woody, R. W. *Methods Enzymol.* **1995**, *246*, 34.
(48) Mutzenhardt, P.; Guenneau, F.; Canet, D. *J. Magn. Reson.* **1999**, *141*, 312.
(49) Karplus, M. *J. Am. Chem. Soc.* **1963**, *85*, 2870.
(50) Kessler, H. *Angew. Chem., Int. Ed. Engl.* **1982**, *21*, 512.
(51) Menting, J. G.; Yang, Y.; Chan, S. J.; Phillips, N. B.; Smith, B. J.; Whittaker, J.; Wickramasinghe, N. P.; Whittaker, L. J.; Pandyarajan, V.; Wan, Z. l.; Yadav, S. P.; Carroll, J. M.; Strokes, N.; Roberts, C. T.; Ismail-Beigi, F.; Milewski, W.; Steiner, D. F.; Chauhan, V. S.; Ward, C. W.; Weiss, M. A.; Lawrence, M. C. *Proc. Natl. Acad. Sci. U. S. A.* **2014**, *111*, E3395.
(52) Crisma, M.; Formaggio, F.; Toniolo, C.; Yoshikawa, T.; Wakamiya, T. *J. Am. Chem. Soc.* **1999**, *121*, 3272.
(53) Merrifield, R. B. *J. Am. Chem. Soc.* **1963**, *85*, 2149.
(54) Steitz, T. A. *Angew. Chem. Int. Ed.* **2010**, *49*, 4381.
(55) Ramakrishnan, V. *Angew. Chem. Int. Ed.* **2010**, *49*, 4355.
(56) Yonath, A. *Angew. Chem. Int. Ed.* **2010**, *49*, 4340.
(57) Steitz, T. A. *Nat. Rev. Mol. Cell Biol.* **2008**, *9*, 242.
(58) Lewandowski, B.; De Bo, G.; Ward, J. W.; Papmeyer, M.; Kuschel, S.; Aldegunde, M. J.; Gramlich, P. M. E.; Heckmann, D.; Goldup, S. M.; D'Souza, D. M.; Fernandes, A. E.; Leigh, D. A. *Science* **2013**, *339*, 189.
(59) Fogg, D. E.; dos Santos, E. N. *Coord. Chem. Rev.* **2004**, *248*, 2365.
(60) Fairlie, D. P.; Abbenante, G.; March, D. R. *Curr. Med. Chem.* **1995**, *2*, 654.
(61) Carlos, M.-M.; Florian, R.; Horst, K. *Anticancer Agents Med. Chem.* **2010**, *10*, 753.
(62) Merrifield, B. *Science* **1986**, *232*, 341.
(63) Davies, J. S. *J. Pept. Sci.* **2003**, *9*, 471.
(64) Le, D. N.; Riedel, J.; Kozlyuk, N.; Martin, R. W.; Dong, V. M. *Org. Lett.* **2017**, *19*, 114.
(65) Doherty, D. G.; Tietzman, J. E.; Bergmann, M. *J. Biol. Chem.* **1943**, *147*, 617.
(66) (±) Diastereomer **5** was observed as the major product (20:2:1:1:1). Four additional minor diastereomers were observed by ^{19}F-NMR spectroscopy. The other three possible diastereomers were not observed.
(67) Fernandez-Lopez, S.; Kim, H.-S.; Choi, E. C.; Delgado, M.; Granja, J. R.; Khasanov, A.; Kraehenbuehl, K.; Long, G.; Weinberger, D. A.; Wilcoxen, K. M.; Ghadiri, M. R. *Nature* **2001**, *412*, 452.
(68) Goldberg, J. *Trends Biotechnol* **2001**, *19*, 379.
(69) 1.0:1.5:3.3:1.8:1.4:2.7:2.0:2.5 *dr* observed via ^{19}F-NMR spectroscopy.
(70) Donoghue, P. J.; Helquist, P.; Norrby, P.-O.; Wiest, O. *J. Chem. Theory Comput.* **2008**, *4*, 1313.
(71) Hansen, E.; Rosales, A. R.; Tutkowski, B.; Norrby, P.-O.; Wiest, O. *Acc. Chem. Res.* **2016**, *49*, 996.
(72) Donoghue, P. J.; Helquist, P.; Norrby, P.-O.; Wiest, O. *J. Am. Chem. Soc.* **2009**, *131*, 410.
(73) Weiss, M. S.; Jabs, A.; Hilgenfeld, R. *Nat. Struct. Mol. Biol.* **1998**, *5*, 676.
(74) Tang, W.; Zhang, X. *Chem. Rev.* **2003**, *103*, 3029.
(75) Osberger, T. J.; Rogness, D. C.; Kohrt, J. T.; Stepan, A. F.; White, M. C. *Nature* **2016**, *537*, 214.
(76) Shiraiwa, T.; Saijoh, R.; Suzuki, M.; Yoshida, K.; Nishimura, S.; Nagasawa, H. *Chem. Pharm. Bull.* **2003**, *51*, 1363.

(77) Miyata, O.; Asai, H.; Naito, T. *Chem. Pharm. Bull.* **2005**, *53*, 355.
(78) Naskar, J.; Drew, M. G. B.; Deb, I.; Das, S.; Banerjee, A. *Org. Lett.* **2008**, *10*, 2625.
(79) Hardee, D. J.; Kovalchuke, L.; Lambert, T. H. *J. Am. Chem. Soc.* **2010**, *132*, 5002.
(80) Ray, S.; Das, A. K.; Banerjee, A. *Chem. Commun.* **2006**, 2816.
(81) Ferreira, P. M. T.; Monteiro, L. S.; Pereira, G.; Ribeiro, L.; Sacramento, J.; Silva, L. *Eur. J. Org. Chem.* **2007**, *2007*, 5934.
(82) Guo, Y.-M.; Oike, H.; Aida, T. *J. Am. Chem. Soc.* **2004**, *126*, 716.
(83) Balachandra, C.; Sharma, N. K. *Tetrahedron* **2014**, *70*, 7464.
(84) Carpino, L. A.; Chao, H. G.; Nowshad, F.; Shroff, H. *J. Org. Chem.* **1988**, *53*, 6139.
(85) Sakai, K.; Ide, J.; Oda, O.; Nakamura, N. *Tetrahedron Lett.* **1972**, *13*, 1287.
(86) Willis, M. C. *Chem. Rev.* **2010**, *110*, 725.
(87) Bergens, S. H.; Fairlie, D. P.; Bosnich, B. *Organometallics* **1990**, *9*, 566.
(88) Shen, Z.; Khan, H. A.; Dong, V. M. *J. Am. Chem. Soc.* **2008**, *130*, 2916.
(89) Khan, H. A.; Kou, K. G. M.; Dong, V. M. *Chemical Science* **2011**, *2*, 407.
(90) Chan, A.; Scheidt, K. A. *J. Am. Chem. Soc.* **2006**, *128*, 4558.
(91) Cronin, L.; Manoni, F.; O' Connor, C. J.; Connon, S. J. *Angew. Chem. Int. Ed.* **2010**, *49*, 3045.
(92) Kurosu, M.; Kishi, Y. *Tetrahedron Lett.* **1998**, *39*, 4793.
(93) Chung, L. W.; Wiest, O.; Wu, Y.-D. *J. Org. Chem.* **2008**, *73*, 2649.
(94) Simmons, E. M.; Hartwig, J. F. *Angew. Chem. Int. Ed.* **2012**, *51*, 3066.
(95) Shen, Z.; Dornan, P. K.; Khan, H. A.; Woo, T. K.; Dong, V. M. *J. Am. Chem. Soc.* **2009**, *131*, 1077.
(96) Martinez, L. E.; Leighton, J. L.; Carsten, D. H.; Jacobsen, E. N. *J. Am. Chem. Soc.* **1995**, *117*, 5897.
(97) Sammis, G. M.; Danjo, H.; Jacobsen, E. N. *J. Am. Chem. Soc.* **2004**, *126*, 9928.
(98) Dias, E. L.; Brookhart, M.; White, P. S. *Chem. Commun.* **2001**, 423.
(99) Inui, Y.; Tanaka, M.; Imai, M.; Tanaka, K.; Suemune, H. *Chem. Pharm. Bull.* **2009**, *57*, 1158.
(100) Kou, K. G. M.; Le, D. N.; Dong, V. M. *J. Am. Chem. Soc.* **2014**, *136*, 9471.
(101) Campaña, A. G.; Carlone, A.; Chen, K.; Dryden, D. T. F.; Leigh, D. A.; Lewandowska, U.; Mullen, K. M. *Angew. Chem. Int. Ed.* **2012**, *51*, 5480.
(102) Sames, D.; Chen, X.-T.; Danishefsky, S. J. *Nature* **1997**, *389*, 587.
(103) Anbarasan, P.; Baer, Z. C.; Sreekumar, S.; Gross, E.; Binder, J. B.; Blanch, H. W.; Clark, D. S.; Toste, F. D. *Nature* **2012**, *491*, 235.
(104) Xu, Y.; Masuko, S.; Takieddin, M.; Xu, H.; Liu, R.; Jing, J.; Mousa, S. A.; Linhardt, R. J.; Liu, J. *Science* **2011**, *334*, 498.
(105) Brandley, B. K.; Schnaar, R. L. *Journal of Leukocyte Biology* **1986**, *40*, 97.
(106) Leonidas, D. D.; Vatzaki, E. H.; Vorum, H.; Celis, J. E.; Madsen, P.; Acharya, K. R. *Biochemistry* **1998**, *37*, 13930.
(107) Wang, C.-C.; Huang, Y.-L.; Ren, C.-T.; Lin, C.-W.; Hung, J.-T.; Yu, J.-C.; Yu, A. L.; Wu, C.-Y.; Wong, C.-H. *Proc. Natl. Acad. Sci. U.S.A.* **2008**, *105*, 11661.
(108) Danishefsky, S. J.; Bilodeau, M. T. *Angewandte Chemie International Edition in English* **1996**, *35*, 1380.
(109) Zhang, Z.; Ollmann, I. R.; Ye, X.-S.; Wischnat, R.; Baasov, T.; Wong, C.-H. *J. Am. Chem. Soc.* **1999**, *121*, 734.
(110) Tsai, T.-I.; Lee, H.-Y.; Chang, S.-H.; Wang, C.-H.; Tu, Y.-C.; Lin, Y.-C.; Hwang, D.-R.; Wu, C.-Y.; Wong, C.-H. *J. Am. Chem. Soc.* **2013**, *135*, 14831.
(111) Demizu, Y.; Kubo, Y.; Miyoshi, H.; Maki, T.; Matsumura, Y.; Moriyama, N.; Onomura, O. *Org. Lett.* **2008**, *10*, 5075.
(112) Lee, D.; Taylor, M. S. *J. Am. Chem. Soc.* **2011**, *133*, 3724.
(113) Kawabata, T.; Muramatsu, W.; Nishio, T.; Shibata, T.; Schedel, H. *J. Am. Chem. Soc.* **2007**, *129*, 12890.
(114) Griswold, K. S.; Miller, S. J. *Tetrahedron* **2003**, *59*, 8869.
(115) Sun, X.; Lee, H.; Lee, S.; Tan, K. L. *Nat. Chem.* **2013**, *5*, 790.
(116) Mensah, E.; Camasso, N.; Kaplan, W.; Nagorny, P. *Angew. Chem. Int. Ed.* **2013**, *52*, 12932.

(117) Allen, C. L.; Miller, S. J. *Org. Lett.* **2013**, *15*, 6178.
(118) Chatwell, L.; Holla, A.; Kaufer, B. B.; Skerra, A. *Molecular Immunology* **2008**, *45*, 1981.
(119) Yamamoto, K.; Konami, Y.; Osawa, T.; Irimura, T. *The Journal of Biochemistry* **1992**, *111*, 436.
(120) Gilbride, K. J.; Pistole, T. G. *Developmental & Comparative Immunology* **1981**, *5*, 347.
(121) Osborn, H. M. I.; Brome, V. A.; Harwood, L. M.; Suthers, W. G. *Carbohydrate Research* **2001**, *332*, 157.
(122) Evtushenko, E. V. *Carbohydrate Research* **2012**, *359*, 111.
(123) Klüfers, P.; Kunte, T. *European Journal of Inorganic Chemistry* **2002**, *2002*, 1285.
(124) Matsumura, Y.; Maki, T.; Murakami, S.; Onomura, O. *J. Am. Chem. Soc.* **2003**, *125*, 2052.
(125) Evans, D. A.; Rovis, T.; Johnson, J. S. In *Pure and Applied Chemistry* 1999; Vol. 71, p 1407.
(126) Nishiyama, H.; Sakaguchi, H.; Nakamura, T.; Horihata, M.; Kondo, M.; Itoh, K. *Organometallics* **1989**, *8*, 846.
(127) Grindley, T. B.; Thangarasa, R. *Canadian Journal of Chemistry* **1990**, *68*, 1007.
(128) Olson, W. K.; Sussman, J. L. *J. Am. Chem. Soc.* **1982**, *104*, 270.
(129) David, S.; Hanessian, S. *Tetrahedron* **1985**, *41*, 643.
(130) Chen, I. H.; Kou, K. G. M.; Le, D. N.; Rathbun, C. M.; Dong, V. M. *Chemistry - A European Journal* **2014**, *20*, 5013.
(131) Buchini, S.; Leumann, C. J. *Eur. J. Org. Chem.* **2006**, *2006*, 3152.
(132) Hird, G. S.; McIntosh, T. J.; Ribeiro, A. A.; Grinstaff, M. W. *J. Am. Chem. Soc.* **2002**, *124*, 5983.
(133) Crich, D.; Vinogradova, O. *J. Org. Chem.* **2007**, *72*, 3581.
(134) Matwiejuk, M.; Thiem, J. *Chem. Commun.* **2011**, *47*, 8379.
(135) Wilson, M. R.; Taylor, R. E. *Angew. Chem. Int. Ed.* **2013**, *52*, 4078.
(136) Lai, A.; Kahraman, M.; Govek, S.; Nagasawa, J.; Bonnefous, C.; Julien, J.; Douglas, K.; Sensintaffar, J.; Lu, N.; Lee, K.-j.; Aparicio, A.; Kaufman, J.; Qian, J.; Shao, G.; Prudente, R.; Moon, M. J.; Joseph, J. D.; Darimont, B.; Brigham, D.; Grillot, K.; Heyman, R.; Rix, P. J.; Hager, J. H.; Smith, N. D. *Journal of Medicinal Chemistry* **2015**, *58*, 4888.
(137) In *Alkenes and Aromatics*; Taylor, P., Ed.; The Royal Society of Chemistry: 2002, p 144.
(138) In *Organometallic Chemistry and Catalysis*; Springer Berlin Heidelberg: Berlin, Heidelberg, 2007, p 367.
(139) Negishi, E.-i.; Huang, Z.; Wang, G.; Mohan, S.; Wang, C.; Hattori, H. *Acc. Chem. Res.* **2008**, *41*, 1474.
(140) Julia, M.; Paris, J.-M. *Tetrahedron Lett.* **1973**, *14*, 4833.
(141) Brown, P. A.; Bonnert, R. V.; Jenkins, P. R.; Selim, M. R. *Tetrahedron Lett.* **1987**, *28*, 693.
(142) Wadsworth, W. S. In *Organic Reactions*; John Wiley & Sons, Inc.: 2004.
(143) Maryanoff, B. E.; Reitz, A. B. *Chem. Rev.* **1989**, *89*, 863.
(144) Takeda, T.; Tsubouchi, A. In *Organic Reactions*; John Wiley & Sons, Inc.: 2004.
(145) Alexakis, A.; Commerčon, A.; Coulentianos, C.; Normant, J. F. *Tetrahedron* **1984**, *40*, 715.
(146) Osborne , C. K. *New England Journal of Medicine* **1998**, *339*, 1609.
(147) Connor, C. E.; Norris, J. D.; Broadwater, G.; Willson, T. M.; Gottardis, M. M.; Dewhirst, M. W.; McDonnell, D. P. *Cancer Research* **2001**, *61*, 2917.
(148) Zhao, P.; Collum, D. B. *J. Am. Chem. Soc.* **2003**, *125*, 4008.
(149) Zhao, P.; Collum, D. B. *J. Am. Chem. Soc.* **2003**, *125*, 14411.
(150) Godenschwager, P. F.; Collum, D. B. *J. Am. Chem. Soc.* **2008**, *130*, 8726.
(151) Li, B. X.; Le, D. N.; Mack, K. A.; McClory, A.; Lim, N.-K.; Cravillion, T.; Savage, S.; Han, C.; Collum, D. B.; Zhang, H.; Gosselin, F. *J. Am. Chem. Soc.* **2017**, *139*, 10777.